

DYNAMIC PROPERTIES OF REINFORCED SAND

A THESIS

*submitted in fulfilment of the
requirements for the award of the degree*

of

DOCTOR OF PHILOSOPHY

in

EARTHQUAKE ENGINEERING

By

RAVI KUMAR SHARMA



DEPARTMENT OF EARTHQUAKE ENGINEERING
UNIVERSITY OF ROORKEE
ROORKEE-247 667 (INDIA)

SEPTEMBER, 1997

Goat's

CANDIDATE'S DECLARATION

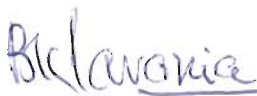
I hereby certify that the work which is being presented in the thesis entitled **DYNAMIC PROPERTIES OF REINFORCED SAND** in fulfilment of the requirement for the award of the degree of **Doctor of Philosophy** and submitted in the **Department of Earthquake Engineering** of the University of Roorkee, is an authentic record of my own work carried out during a period from Aug. 1992 to September, 1997 under the supervision of **Dr. Swami Saran** and **Dr. B.V.K. Lavania**.


The matter presented in this thesis has not been submitted by me for the award of any other degree of this or any other University.

Dated : September 12, 1997

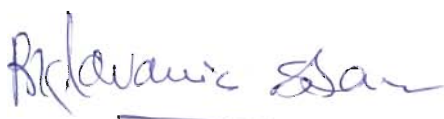

(Ravi Kumar Sharma)


This is to certify that the above statement made by the candidate is correct to the best of our knowledge.

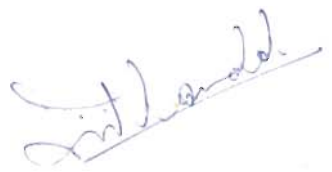

Dr. B.V.K. Lavania 12/9/97
Professor
Earthquake Engineering Department
University of Roorkee
Roorkee - 247 667, INDIA


Dr. Swami Saran 12.9.97
Professor
Civil Engineering Department
University of Roorkee
Roorkee - 247 667, INDIA

The Ph.D. viva-voce examination of **Mr. Ravi Kumar Sharma**, Research Scholar, has been held on 8.3.97


Signatures of Supervisors


Signature of Head,
EQED


Signature of
External Examiner

ABSTRACT

The dynamic stiffness properties of soils must be determined for the purpose of analyzing machine foundations and substructures subjected to earthquakes. The significant advances in mathematical techniques for analyzing dynamic soil-structure interaction problems necessitate a realistic determination of pertinent stiffness properties. This determination can be quite involved because of the dependence of these properties on a large number of parameters. During the past three decades, reinforced earth has been extensively used to improve the static strength characteristics of soils. The study of dynamic response of foundations on reinforced sand beds and the dynamic properties, however, has not received the needed quantum of attention.

The present research work has been carried out to study the dynamic response of foundations on reinforced sand beds experimentally and to interpret the dynamic stiffness properties of reinforced sand on the basis of experimental data and analytical analysis. It is anticipated that the study would help in better understanding of the dynamic behaviour of foundations on reinforced sand beds and lead to realistic and safe design.

In India, the cyclic plate load and block vibration tests are generally used for the determination of dynamic stiffness properties of soils. A large number of reinforcement parameters are likely to influence the dynamic behaviour of soil; the present study, however, has been undertaken to investigate the following aspects :

- (1) The effect of size & number of reinforcement layers, density of sand and size of footing on the coefficient of elastic uniform compression, C_u of the sand by performing cyclic plate load tests in the laboratory.
- (2) To perform vertical and horizontal forced vibration tests on reinforced sand beds in the laboratory to study the effect of size and number of reinforcement

layers on the dynamic response, coefficient of elastic uniform compression C_u , the coefficient of elastic uniform shear C_τ and the damping ratio.

- (3) Analysis and interpretation of experimental data for developing non-dimensional plots and correlations.
- (4) To develop an analytical approach for determining the coefficient of elastic uniform compression C_u and coefficient of elastic uniform shear C_τ of reinforced sand, treating it macro-homogeneous.

The experimental investigation includes the determination of physical and mechanical properties of sand and geogrid reinforcement. The cyclic plate load tests have been performed on unreinforced and reinforced sand beds at relative densities of 50% and 70%. The sizes of the plates used in the tests are 0.15m square and 0.3m square and thickness 20 mm each. The sand beds are prepared in rigid steel tanks of sizes 0.9m×0.9m×1.0m and 1.5m×1.5m×1.0m for conducting tests on the two plates respectively. The sand beds are reinforced with 2 to 8 layers of geogrid Netlon CE-121, having size one to five times the width of the plate. A total of 38 cyclic plate load tests were conducted for different combinations of the above mentioned parameters affecting the behaviour.

Considering the cyclic plate load tests as the static tests, the data has been analyzed to determine the coefficient of elastic uniform compression C_u and damping capacity ratio. The static strength characteristics like, the bearing capacity ratio and settlement ratio are also determined. The pressure versus elastic rebound plots are bilinear; the two straight lines meet at a pressure value close to the ultimate bearing capacity of the sand bed. The slope of the first line gives C_u , and that of the other showing post-failure behaviour has been represented by symbol C'_u . The confining pressure and area corrections have been applied to determine the standard values of C_u and C'_u for unreinforced and reinforced sand beds.

A comparison of the damping capacities of the reinforced and the unreinforced sand beds has been made by measuring the areas of the hysteresis loops of the first ten cycles of loading and unloading (till the failure of the unreinforced sand bed

occurred) from the pressure-settlement plots.

The second part of the experimental investigation consists of performing vertical and horizontal block vibration tests (total number 200) on unreinforced and reinforced sand beds. A rigid steel tank of size 1.5m×1.5m×1.0m was used to prepare the sand beds reinforced with 2 to 6 geogrid layers of different sizes. An M-20 concrete block of size 0.8m×0.4m×0.4m was cast for performing the block vibration tests. The frequency and amplitude observations were recorded at four force levels using the equipment specified in IS:5249-1977 and the soil data logger NE-4201.

The vertical and horizontal vibration test data have been analyzed to determine the coefficient of elastic uniform compression C_u and the coefficient of elastic uniform shear C_τ respectively. The corrections for confining pressure and area of foundation are applied to obtain the standard values of C_u and C_τ . The ratio of dynamic force F to weight of block W , and the strain levels associated with different tests have been determined. The values of C_u and C_τ are interpreted at various F/W ratios and strain levels. In vertical vibration tests, the damping ratio ξ has been determined by the bandwidth method. The damping ratios ξ_1 and ξ_2 corresponding to the first and second modes of vibration in the horizontal vibration tests have also been determined by the bandwidth method and their values are found to differ, while the values of C_τ obtained in both the modes of vibration are almost the same.

Non-dimensional plots and correlations have been obtained for the coefficient of elastic uniform compression C_u , damping capacity ratio, bearing capacity ratio and the settlement ratio using the cyclic plate load test data. Non-dimensional plots and correlations have also been developed for the coefficient of elastic uniform compression C_u , the coefficient of elastic uniform shear C_τ , damping ratios ξ and ξ_1 and the amplitude reduction factors with reference to the number and sizes of geogrid layers from the vertical and horizontal vibration test data.

An equivalent parameter analysis has been developed to determine the coefficient of elastic uniform compression and coefficient of elastic uniform shear of reinforced sand from the coefficient of elastic uniform compression and coefficient of elastic

uniform shear respectively of the unreinforced sand and the elastic modulus of the geogrid reinforcements. The composite material is assumed to be homogeneous and elastic with negligible mobilization of interface friction between the soil and geogrid at low strain levels. The analytically predicted values of coefficient of elastic uniform compression and coefficient of elastic uniform shear are compared with the experimental values and a reasonable agreement is obtained.

Based upon the experimental and analytical studies, the following conclusions are drawn :

- (1) In cyclic plate load tests, the values of coefficient of elastic uniform compression of reinforced sand decrease, with the maximum decrease being 45%. This decrease is more with the increase in number and decrease in size of geogrid layers. However, the pressure range for validity of C_u value of reinforced sand bed is higher than that for the unreinforced sand bed. The damping capacity is increased, the improvement being more with increase in number and size of reinforcement layers. The ultimate bearing capacity values are increased upto about four times and the total settlements are reduced to less than half as compared to those of unreinforced sand, depending upon the size and number of geogrid layers.
- (2) In vertical vibration tests, the maximum amplitudes are reduced maximum by 43% for reinforced sand beds. The decrease in amplitudes is generally more with the increase in size and number of geogrid layers. The resonant frequency is reduced by a maximum of 14%, the decrease being dependent upon the size and number of geogrid reinforcements. The damping ratio, ξ increases depending upon the size and number of reinforcements. The coefficient of elastic uniform compression C_u decreases by a maximum of about 26% depending upon the size and number of the reinforcement layers. The C_u -values of reinforced sand beds are less than the C_u -values of unreinforced sand bed for strain levels less than 3%; whereas for strain levels higher than this, C_u values for reinforced sand beds are more. This shows that for strain levels less than 3%, the mobilization of interface

friction between sand and geogrid is not significant to contribute to the coefficient of elastic uniform compression of reinforced sand.

- (3) In horizontal vibration tests on reinforced sand beds, the maximum amplitudes corresponding to both the modes of vibration are reduced upto about 50% depending upon the size and number of geogrid layers. The resonant frequencies corresponding to the first and second modes of vibration decrease by a maximum of 28% and 20%, the decrease being more with the increase in size and number of reinforcement layers. The damping ratios ξ_1 and ξ_2 , for the two modes of vibration increase depending upon the configuration of the reinforcement and are found to be different. The coefficient of elastic uniform shear is reduced by a maximum of 48%, the decrease being dependent upon the size and number of reinforcement layers. A comparison of the values of coefficient of elastic uniform compression, $(C_{u100})_{10}$ with the corresponding values of coefficient of elastic uniform shear, $(C_{\tau 100})_{10}$ shows that $(C_{u100})_{10}/(C_{\tau 100})_{10}$ ratio is 2.8 to 2.95 for unreinforced sand bed whereas it is 3.2 to 3.9 for the reinforced sand beds. Thus, the decrease in C_{τ} is more than the decrease in C_u for the similar geogrid reinforced sand beds.

The results of this study are especially useful in the design of foundations of machines, where the natural frequency of the soil-foundation system may lie close to the operating frequency of machine otherwise and the maximum amplitude exceeds permissible limits. The maximum amplitudes can be brought under control and the disturbance during the starting and stopping of the machine can be reduced.

Another important conclusion drawn on the basis of test results is that though the static strength characteristics of the sand are considerably improved upon reinforcing with geogrid layers, but the coefficient of elastic uniform compression is marginally reduced at low strain levels till the mobilization of interface friction effectively contributes to the modulus of reinforced sand.

ACKNOWLEDGEMENTS

The author wishes to express his sincere gratitude and indebtedness to **Dr. Swami Saran**, Professor of Civil Engineering and **Dr. B.V.K. Lavania**, Professor of Earthquake Engineering, University of Roorkee, Roorkee for their valuable guidance, support and encouragement throughout this work. Their painstaking efforts in editing the manuscript and giving useful suggestions for its improvement are gratefully and humbly acknowledged.

The author wishes to gratefully acknowledge the encouragement and help, **Dr. S. Basu**, Head of Earthquake Engineering Department, University of Roorkee, Roorkee, provided during this work.


The author would like to thank all those at his parent institution Regional Engineering College, Hamirpur (Himachal Pradesh), who helped in one way or the other during the period of this research work.

The author thanks his colleagues Mr. Sushil Chauhan, Mr. Janak Raj Sharma, Mr. Mahesh Sharma, Mr. N.S. Thakur, Mr. R.N. Sharma and others for their cooperation and help during all stages of this work.

The help of the laboratory staff of Geotechnical Engineering Laboratory during the experimentation is acknowledged. Heartful thanks are due to Mr. J.K. Yadav and Mr. Gian Chand for extending their help and cooperation throughout. Thanks are also due to Mr. Raju for careful typing, printing and transforming the manuscript in its present shape.

The author expresses his sincere gratitude for the blessings and moral support of his parents and brother-in-law, Dr. L.D. Hill. It is a distinct pleasure for the author to acknowledge and express heartfelt gratitude to his wife Urmil, daughter Nikita and son Rachit for their forbearance and personal sacrifices during the course of this work.

Finally, my salutations to All-pervading Almighty, whose Divine Light provided me faith, inspiration, guidance and strength to carry on with this research work.


(RAVI KUMAR SHARMA)

CONTENTS

	Page No.
<i>Candidate's Declaration</i>	
<i>Abstract</i>	i
<i>Acknowledgements</i>	vii
<i>Table of Contents</i>	ix
<i>List of Figures</i>	xv
<i>List of Tables</i>	xxxix
<i>List of Notations</i>	xxxiii
<i>List of Papers</i>	xxxxi

Chapter 1 : Introduction

1.1 General	1
1.2 Basic Mechanism of Reinforced Earth	2
1.3 Brief Review of Literature	3
1.4 Scope of Work	6
1.4.1 Cyclic Plate Load Tests	6
1.4.2 Block Vibration Tests	7
1.4.3 Analysis of Experimental Data	7
1.4.4 Analytical Investigation	7
1.5 Concluding Remarks	8

Chapter 2 : Review of Literature

2.1 General	9
2.2 Dynamic Response of Block Foundation on Unreinforced Soil	9
2.2.1 Analytical Formulations	9
2.2.1.1 Dynamic Winkler Model	10
2.2.1.2 Elastic Half Space Theory	11
2.2.1.3 Lumped Parameter Approach	17
2.2.1.4 Approaches Based On Numerical Techniques	20
2.2.2 Experimental Investigations	24
2.2.2.1 Experimental Studies on Large Blocks	24
2.2.2.2 Model Tests in Laboratory	27

2.3 Determination of Dynamic Soil Properties	30
2.4 Strength Characteristics of Reinforced Earth Slabs Under Static Load	36
2.5 Dynamic Characteristics of Reinforced Earth	41
2.6 Concluding Remarks	44

Chapter 3 : Experimental Investigations

3.1 General	45
3.2 Soil Used	46
3.3 Reinforcing Material	47
3.4 Cyclic Plate Load Tests	47
3.4.1 Test Tanks	48
3.4.2 Loading Arrangement	48
3.4.3 Load Measuring Device	50
3.4.4 Settlement Measuring Arrangement	50
3.4.5 Preparation of Sand Bed	50
3.4.6 Arrangement of Reinforcement Layers	51
3.4.7 Test Procedure	51
3.4.8 Tests Performed	52
3.5 Block Vibration Tests	54
3.5.1 Test Tank	54
3.5.2 Foundation Block	55
3.5.3 Characteristics of Foundation Block	55
3.5.4 Frequency Measuring Device	55
3.5.5 Amplitude Measuring Device	57
3.5.6 Preparation of Sand bed	58
3.5.7 Arrangement of Reinforcement Layers	58
3.5.8 Testing Equipment	58
3.5.9 Test Procedure	61
3.5.10 Tests Performed	62
3.6 Test Results	62
3.6.1 Cyclic Plate Load Tests	62
3.6.2 Vertical Vibration Tests	63
3.6.3 Horizontal Vibration Tests	63
3.7 Concluding Remarks	63

Chapter 4 : Interpretation and Analysis

4.1 General	137
4.2 Cyclic Plate Load Tests	138
4.2.1 General	138
4.2.2 Pressure-Settlement Characteristics	139
4.2.3 Bearing Capacity Ratio	143
4.2.4 Settlement Ratio	144
4.2.5 Damping Capacity	145
4.2.6 Coefficient of Elastic Uniform Compression	146
4.2.6.1 Corrections for Confining Pressure and Area of Footing	149
4.2.6.2 Strain Level	153
4.2.6.3 Coefficient of Elastic Uniform Compression versus Strain level	153
4.2.6.4 Coefficient of Elastic Uniform Compression versus Number of Geogrid Layers	155
4.2.6.5 Coefficient of Elastic Uniform Compression versus Size of Reinforcement	156
4.2.6.6 C_u versus Relative Density of Sand and Size of Footing	157
4.2.7 Discussion Summary	157
4.3 Vertical Vibration Tests	158
4.3.1 General	158
4.3.2 Amplitude-Frequency Plots	159
4.3.3 Analysis of the Amplitude-Frequency Data	162
4.3.4 Effect of F/W on Resonant Frequency and Damping Ratio ξ	164
4.3.5 Effect of Reinforcement on Damping Ratio ξ	165
4.3.6 Strain Level versus F/W Ratio	165
4.3.7 Amplitude Reduction Factor versus Number of Reinforcement Layers	166
4.3.8 Coefficient of Elastic Uniform Compression $(C_{u100})_{10}$ versus Number of Reinforcement Layers	166
4.3.9 Coefficient of Elastic Uniform Compression $(C_{u100})_{10}$ versus F/W Ratio	169
4.3.10 Coefficient of Elastic Uniform Compression versus Reinforcement Area	169

4.3.11	Coefficient of Elastic Uniform Compression – Vertical Vibration Tests vis-a-vis Cyclic Plate Tests	170
4.3.12	Discussion Summary	170
4.4	Horizontal Vibration Tests	171
4.4.1	General	171
4.4.2	Amplitude-Frequency Curves	172
4.4.3	Analysis of Amplitude-Frequency Data	176
4.4.4	Effect of F_1/W on Resonant Frequencies and Damping Ratios	178
4.4.5	Effect of Reinforcement on Damping Ratios ξ_1 and ξ_2	179
4.4.6	Amplitude/Width Ratio versus F_1/W	179
4.4.7	Amplitude Reduction Factor versus Number of Reinforcement Layers	180
4.4.8	Coefficient of Elastic Uniform Shear $(C_{1100})_{10}$ versus Number of Reinforcement Layers	180
4.4.9	Coefficient of Elastic Uniform Shear $(C_{1100})_{10}$ versus F_1/W	182
4.4.10	Coefficient of Elastic Uniform Shear versus Size of Reinforcement	183
4.4.11	Comparison of $(C_{u100})_{10}$ and $(C_{1100})_{10}$	184
4.4.12	Discussion Summary	184
4.5	Non-dimensional Correlations	185
4.5.1	General	185
4.5.2	Cyclic Plate Load Tests	185
4.5.2.1	Coefficient of Elastic Uniform Compression	185
4.5.2.2	Damping Capacity Ratio	186
4.5.2.3	Ultimate Bearing Capacity Ratio, BCR	186
4.5.2.4	Settlement Ratio (SR)	187
4.5.3	Vertical Vibration Tests	187
4.5.3.1	Coefficient of Elastic Uniform Compression $(C_{u100})_{10}$	187
4.5.3.2	Damping Ratio ξ	188
4.5.3.3	Amplitude Reduction Factor	188
4.5.4	Horizontal Vibration Tests	189
4.5.4.1	Coefficient of Elastic Uniform Shear $(C_{1100})_{10}$	189
4.5.4.2	Damping Ratio ξ_1	189
4.5.4.3	Amplitude Reduction Factor	189
4.5.5	Discussion Summary	190
4.6	Equivalent Parameter Analysis	190
4.6.1	General	190

4.6.2	Analysis	192
4.6.2.1	Assumptions	192
4.6.2.2	Justification of Assumptions	193
4.6.2.3	Analytical Formulation	194
4.6.3	Application of the Analysis to Vertical Vibration Tests	196
4.6.4	Application of the Analysis to Cyclic Plate Load Tests	198
4.6.5	Application of Analysis to Horizontal Vibration Tests	200
4.6.6	Concluding Remarks	204
4.7	Design Problem	204
Chapter 5 : Conclusious		268
Chapter 6 : Recommendations for Further Research		273
References		274

LIST OF FIGURES

Fig. No.	Description	Page No.
3.1	Grain Size Distribution Curve of Amanantgarh Sand	65
3.2	Direct Shear Tests on Amanantgarh Sand	65
3.3	Stress-Strain Curve of Geogrid Netlon CE-121	65
3.4	Experimental Set-up of Cyclic Plate Load Test on 150mm Square Footing	66
3.5	Experimental Set-up for Cyclic Plate Load Test.	67
3.6	Lever Arm Loading Arrangement for Cyclic Plate Load Tests	68
3.7	Experimental Set-up for Cyclic Plate Load Test on 300mm Square Footing	68
3.8	Settlement Pattern in Cyclic Plate Load Test on Reinforced Sand Bed	69
3.9	Cyclic Plate Load Test in Progress	69
3.10	Height of Fall versus Relative Density for Amanantgarh Sand	70
3.11	Sand Filling by Rainfall Technique	71
3.12	Laying of Reinforcement Layer in Sand Bed	72
3.13	Experimental Set-up for Vertical Block Vibration Test	72
3.14	Experimental Set-up for Block Vibration Tests	73
3.15	Experimental Set-up for Horizontal Block Vibration Tests	74
3.16	Soil Data Logger-4201.	74
3.17	Dynamic Force versus Frequency of Oscillator	75
3.18	Placing the Block over Sand Bed	76
3.19	Block Diagram of Testing Equipment for Block Vibration Tests	75
3.20(a)	Cyclic Plate Load Test-Pressure versus Total Settlement Plot for Unreinforced Sand ($D_r=70\%$, 150mm Square Footing)	77
3.20(b)	Cyclic Plate Load Test-Pressure versus Total Settlement Log-Log Plot for Unreinforced Sand ($D_r=70\%$, 150mm Square Footing)	77

3.21 Cyclic Plate Load Test-Pressure versus Total Settlement Plot for Geogrid Reinforced Sand ($D_r=70\%$, 150mm Square Footing, $B_r/B=1$, $n=2$)	78
3.22 Cyclic Plate Load Test-Pressure versus Total Settlement Plot for Reinforced Sand ($D_r=70\%$, 150mm Square Footing, $B_r/B=1$, $n=3$)	78
3.23 Cyclic Plate Load Test-Pressure versus Total Settlement Plot for Reinforced Sand ($D_r=70\%$, 150mm Square Footing, $B_r/B=1$, $n=4$)	79
3.24 Cyclic Plate Load Test-Pressure versus Total Settlement Plot for Reinforced Sand ($D_r=70\%$, 150mm Square Footing, $B_r/B=1$, $n=6$)	79
3.25 Cyclic Plate Load Test-Pressure versus Total Settlement Plot for Reinforced Sand ($D_r=70\%$, 150mm Square Footing, $B_r/B=1$, $n=8$)	80
3.26 Cyclic Plate Load Test-Pressure versus Total Settlement Plot for Reinforced Sand ($D_r=70\%$, 150mm Square Footing, $B_r/B=2$, $n=2$)	80
3.27 Cyclic Plate Load Test-Pressure versus Total Settlement Plot for Reinforced Sand ($D_r=70\%$, 150mm Square Footing, $B_r/B=2$, $n=3$)	81
3.28 Cyclic Plate Load Test-Pressure versus Total Settlement Plot for Reinforced Sand ($D_r=70\%$, 150mm Square Footing, $B_r/B=2$, $n=4$)	81
3.29 Cyclic Plate Load Test-Pressure versus Total Settlement Plot for Reinforced Sand ($D_r=70\%$, 150mm Square Footing, $B_r/B=2$, $n=6$)	82
3.30 Cyclic Plate Load Test-Pressure versus Total Settlement Plot for Reinforced Sand ($D_r=70\%$, 150mm Square Footing, $B_r/B=2$, $n=8$)	82
3.31 Cyclic Plate Load Test-Pressure versus Total Settlement Plot for Reinforced Sand ($D_r=70\%$, 150mm Square Footing, $B_r/B=3$, $n=2$)	83
3.32 Cyclic Plate Load Test-Pressure versus Total Settlement Plot for Reinforced Sand ($D_r=70\%$, 150mm Square Footing, $B_r/B=3$, $n=3$)	83
3.33 Cyclic Plate Load Test-Pressure versus Total Settlement Plot for Reinforced Sand ($D_r=70\%$, 150mm Square Footing, $B_r/B=3$, $n=4$)	84
3.34 Cyclic Plate Load Test-Pressure versus Total Settlement Plot for Reinforced Sand ($D_r=70\%$, 150mm Square Footing, $B_r/B=3$, $n=6$)	84

3.35 Cyclic Plate Load Test-Pressure versus Total Settlement Plot for Reinforced Sand ($D_r=70\%$, 150mm Square Footing, $B_r/B=3$, $n=8$)	85
3.36 Cyclic Plate Load Test-Pressure versus Total Settlement Plot for Reinforced Sand ($D_r=70\%$, 150mm Square Footing, $B_r/B=4$, $n=2$)	85
3.37 Cyclic Plate Load Test-Pressure versus Total Settlement Plot for Reinforced Sand ($D_r=70\%$, 150mm Square Footing, $B_r/B=4$, $n=3$)	86
3.38 Cyclic Plate Load Test-Pressure versus Total Settlement Plot for Reinforced Sand ($D_r=70\%$, 150mm Square Footing, $B_r/B=4$, $n=4$)	86
3.39 Cyclic Plate Load Test-Pressure versus Total Settlement Plot for Reinforced Sand ($D_r=70\%$, 150mm Square Footing, $B_r/B=4$, $n=6$)	87
3.40 Cyclic Plate Load Test-Pressure versus Total Settlement Plot for Reinforced Sand ($D_r=70\%$, 150mm Square Footing, $B_r/B=4$, $n=8$)	87
3.41 Cyclic Plate Load Test-Pressure versus Total Settlement Plot for Reinforced Sand ($D_r=70\%$, 150mm Square Footing, $B_r/B=5$, $n=2$)	88
3.42 Cyclic Plate Load Test-Pressure versus Total Settlement Plot for Reinforced Sand ($D_r=70\%$, 150mm Square Footing, $B_r/B=5$, $n=3$)	88
3.43 Cyclic Plate Load Test-Pressure versus Total Settlement Plot for Reinforced Sand ($D_r=70\%$, 150mm Square Footing, $B_r/B=5$, $n=4$)	89
3.44 Cyclic Plate Load Test-Pressure versus Total Settlement Plot for Reinforced Sand ($D_r=70\%$, 150mm Square Footing, $B_r/B=5$, $n=6$)	89
3.45 Cyclic Plate Load Test-Pressure versus Total Settlement Plot for Reinforced Sand ($D_r=70\%$, 150mm Square Footing, $B_r/B=5$, $n=8$)	90
3.46 Cyclic Plate Load Test-Pressure versus Total Settlement Plot for Unreinforced Sand ($D_r=50\%$, 150mm Square Footing)	90
3.47 Cyclic Plate Load Test - Pressure versus Total Settlement Plot for Reinforced Sand ($D_r=50\%$, 150mm Square Footing, $n=4$, $B_r/B=1$)	91
3.48 Cyclic Plate Load Test - Pressure versus Total Settlement Plot for Reinforced Sand ($D_r=50\%$, 150mm Square Footing, $n=4$, $B_r/B=2$).	91

3.49 Cyclic Plate Load Test - Pressure versus Total Settlement Plot for Reinforced Sand ($D_r=50\%$, 150mm Square Footing, $n=4$, $B_r/B=3$).	92
3.50 Cyclic Plate Load Test - Pressure versus Total Settlement Plot for Reinforced Sand ($D_r=50\%$, 150mm Square Footing, $n=4$, $B_r/B=4$).	92
3.51 Cyclic Plate Load Test - Pressure versus Total Settlement Plot for Reinforced Sand ($D_r=50\%$, 150mm Square Footing, $n=4$, $B_r/B=5$).	93
3.52 Cyclic Plate Load Test-Pressure versus Total Settlement Plot for Unreinforced sand ($D_r=70\%$, 300 mm Square Footing).	93
3.53 Cyclic Plate Load Test-pressure versus Total Settlement Plot for Reinforced Sand ($D_r=70\%$, 300 mm Square Footing, $n=4$, $B_r/B=1$)	94
3.54 Cyclic Plate Load Test-pressure versus Total Settlement Plot for Reinforced Sand ($D_r=70\%$, 300 mm Square Footing, $n=4$, $B_r/B=2$)	94
3.55 Cyclic Plate Load Test-pressure versus Total Settlement Plot for Reinforced Sand ($D_r=70\%$, 300 mm Square Footing, $n=4$, $B_r/B=3$)	95
3.56 Cyclic Plate Load Test-pressure versus Total Settlement Plot for Reinforced Sand ($D_r=70\%$, 300 mm Square Footing, $n=4$, $B_r/B=4$)	95
3.57 Cyclic Plate Load Test-pressure versus Total Settlement Plot for Reinforced Sand ($D_r=70\%$, 300 mm Square Footing, $n=4$, $B_r/B=5$)	96
3.58 Cyclic Plate Load Test-Pressure Versus Elastic Settlement Plot for Unreinforced Sand ($D_r=70\%$, 150mm Square Footing).	96
3.59 Cyclic Plate Load Test-Pressure versus Elastic Settlement Plot for Reinforced Sand ($D_r=70\%$, 150mm Square Footing, $B_r/B=1$, $n=2$ and 3)	97
3.60 Cyclic Plate Load Test-Pressure versus Elastic Settlement Plot for Reinforced Sand ($D_r=70\%$, 150mm Square Footing, $B_r/B=1$, $n=4$)	97
3.61 Cyclic Plate Load Test-Pressure versus Elastic Settlement Plot for Reinforced Sand ($D_r=70\%$, 150mm Square Footing, $B_r/B=1$, $n=6$)	98
3.62 Cyclic Plate Load Test-Pressure versus Elastic Settlement Plot for Reinforced Sand ($D_r=70\%$, 150mm Square Footing, $B_r/B=1$, $n=8$)	98

3.63	Cyclic Plate Load Test-Pressure versus Elastic Settlement Plot for Reinforced Sand ($D_r=70\%$, 150mm Square Footing, $B_r/B=2$, $n=2$ and 3)	99
3.64	Cyclic Plate Load Test-Pressure versus Elastic Settlement Plot for Reinforced Sand ($D_r=70\%$, 150mm Square Footing, $B_r/B=2$, $n=4$)	99
3.65	Cyclic Plate Load Test-Pressure versus Elastic Settlement Plot for Reinforced Sand ($D_r=70\%$, 150mm Square Footing, $B_r/B=2$, $n=6$)	100
3.66	Cyclic Plate Load Test-Pressure versus Elastic Settlement Plot for Reinforced Sand ($D_r=70\%$, 150mm Square Footing, $B_r/B=2$, $n=8$)	100
3.67	Cyclic Plate Load Test-Pressure versus Elastic Settlement Plot for Reinforced Sand ($D_r=70\%$, 150mm Square Footing, $B_r/B=3$, $n=2$ and 3)	101
3.68	Cyclic Plate Load Test-Pressure versus Elastic Settlement Plot for Reinforced Sand ($D_r=70\%$, 150mm Square Footing, $B_r/B=3$, $n=4$)	101
3.69	Cyclic Plate Load Test-Pressure versus Elastic Settlement Plot for Reinforced Sand ($D_r=70\%$, 150mm Square Footing, $B_r/B=3$, $n=6$)	102
3.70	Cyclic Plate Load Test-Pressure versus Elastic Settlement Plot for Reinforced Sand ($D_r=70\%$, 150mm Square Footing, $B_r/B=3$, $n=8$)	102
3.71	Cyclic Plate Load Test-Pressure versus Elastic Settlement Plot for Reinforced Sand ($D_r=70\%$, 150mm Square Footing, $B_r/B=4$, $n=2$ and 3)	103
3.72	Cyclic Plate Load Test-Pressure versus Elastic Settlement Plot for Reinforced Sand ($D_r=70\%$, 150mm Square Footing, $B_r/B=4$, $n=4$)	103
3.73	Cyclic Plate Load Test-Pressure versus Elastic Settlement Plot for Reinforced Sand ($D_r=70\%$, 150mm Square Footing, $B_r/B=4$, $n=6$)	104
3.74	Cyclic Plate Load Test-Pressure versus Elastic Settlement Plot for Reinforced Sand ($D_r=70\%$, 150mm Square Footing, $B_r/B=4$, $n=8$)	104
3.75	Cyclic Plate Load Test-Pressure versus Elastic Settlement Plot for Reinforced Sand ($D_r=70\%$, 150mm Square Footing, $B_r/B=5$, $n=2$ and 3)	105
3.76	Cyclic Plate Load Test-Pressure versus Elastic Settlement Plot for Reinforced Sand ($D_r=70\%$, 150mm Square Footing, $B_r/B=5$, $n=4$)	105

3.77	Cyclic Plate Load Test-Pressure versus Elastic Settlement Plot for Reinforced Sand ($D_r=70\%$, 150mm Square Footing, $B_r/B=5$, $n=6$)	106
3.78	Cyclic Plate Load Test-Pressure versus Elastic Settlement Plot for Reinforced Sand ($D_r=70\%$, 150mm Square Footing, $B_r/B=5$, $n=8$)	106
3.79	Cyclic Plate Load Test-Pressure versus Elastic Settlement Plot for Unreinforced Sand ($D_r=50\%$, 150 mm Square Footing).	107
3.80	Cyclic Plate Load Test-Pressure versus Elastic Settlement Plot for Reinforced Sand ($D_r=50\%$, 150mm Square Footing, $n=4$, $B_r/B=1$ and 2)	107
3.81	Cyclic Plate Load Test-Pressure versus Elastic Settlement Plot for Reinforced Sand ($D_r=50\%$, 150mm Square Footing, $n=4$, $B_r/B=3$)	108
3.82	Cyclic Plate Load Test-Pressure versus Elastic Settlement Plot for Reinforced Sand ($D_r=50\%$, 150mm Square Footing, $n=4$, $B_r/B=4$)	108
3.83	Cyclic Plate Load Test-Pressure versus Elastic Settlement Plot for Reinforced Sand ($D_r=50\%$, 150mm Square Footing, $n=4$, $B_r/B=5$)	109
3.84	Cyclic Plate Load Test-Pressure versus Elastic Settlement Plot for Unreinforced Sand ($D_r=70\%$, 300 mm Square Footing).	109
3.85	Cyclic Plate Load Test-Pressure versus Elastic Settlement Plot for Reinforced Sand ($D_r=70\%$, 300 mm Square Footing, $n=4$, $B_r/B=1$ and 2)	110
3.86	Cyclic Plate Load Test-Pressure versus Elastic Settlement Plot for Reinforced Sand ($D_r=70\%$, 300 mm Square Footing, $n=4$, $B_r/B=3$)	110
3.87	Cyclic Plate Load Test-Pressure versus Elastic Settlement Plot for Reinforced Sand ($D_r=70\%$, 300 mm Square Footing, $n=4$, $B_r/B=4$)	111
3.88	Cyclic Plate Load Test-Pressure versus Elastic Settlement Plot for Reinforced Sand ($D_r=70\%$, 300 mm Square Footing, $n=4$, $B_r/B=5$)	111
3.89	Vertical Vibration Test on Unreinforced Sand, $D_r=70\%$, Amplitude versus Frequency Plot	112
3.90	Vertical Vibration Test on Geogrid Reinforced Sand, $D_r=70\%$, Amplitude versus Frequency Plot ($L_r/L=B_r/B=1$, $n=2$)	112

3.91	Vertical Vibration Test on Geogrid Reinforced Sand, $D_r=70\%$, Amplitude versus Frequency Plot ($L_r/L=B_r/B=1$, $n=3$)	113
3.92	Vertical Vibration Test on Geogrid Reinforced Sand, $D_r=70\%$, Amplitude versus Frequency Plot ($L_r/L=B_r/B=1$, $n=4$)	113
3.93	Vertical Vibration Test on Geogrid Reinforced Sand, $D_r=70\%$, Amplitude versus Frequency Plot ($L_r/L=B_r/B=1$, $n=6$)	114
3.94	Vertical Vibration Test on Geogrid Reinforced Sand, $D_r=70\%$, Amplitude versus Frequency Plot ($L_r/L=B_r/B=1.5$, $n=2$)	114
3.95	Vertical Vibration Test on Geogrid Reinforced Sand, $D_r=70\%$, Amplitude versus Frequency Plot ($L_r/L=B_r/B=1.5$, $n=3$)	115
3.96	Vertical Vibration Test on Geogrid Reinforced Sand, $D_r=70\%$, Amplitude versus Frequency Plot ($L_r/L=B_r/B=1.5$, $n=4$)	115
3.97	Vertical Vibration Test on Geogrid Reinforced Sand, $D_r=70\%$, Amplitude versus Frequency Plot ($L_r/L=B_r/B=1.5$, $n=6$)	116
3.98	Vertical Vibration Test on Geogrid Reinforced Sand, $D_r=70\%$, Amplitude versus Frequency Plot ($L_r/L=B_r/B=1.875$, $n=2$)	116
3.99	Vertical Vibration Test on Geogrid Reinforced Sand, $D_r=70\%$, Amplitude versus Frequency Plot ($L_r/L=B_r/B=1.875$, $n=3$)	117
3.100	Vertical Vibration Test on Geogrid Reinforced Sand, $D_r=70\%$, Amplitude versus Frequency Plot ($L_r/L=B_r/B=1.875$, $n=4$)	117
3.101	Vertical Vibration Test on Geogrid Reinforced Sand, $D_r=70\%$, Amplitude versus Frequency Plot ($L_r/L=B_r/B=1.875$, $n=6$)	118
3.102	Vertical Vibration Test on Geogrid Reinforced Sand, $D_r=70\%$, Amplitude versus Frequency Plot ($L_r/L=1.25$, $B_r/B=2.50$, $n=2$)	118
3.103	Vertical Vibration Test on Geogrid Reinforced Sand, $D_r=70\%$, Amplitude versus Frequency Plot ($L_r/L=1.25$, $B_r/B=2.50$, $n=3$)	119
3.104	Vertical Vibration Test on Geogrid Reinforced Sand, $D_r=70\%$, Amplitude versus Frequency Plot ($L_r/L=1.25$, $B_r/B=2.50$, $n=4$)	119

3.105 Vertical Vibration Test on Geogrid Reinforced Sand, $D_r=70\%$, Amplitude versus Frequency Plot ($L_r/L=1.25$, $B_r/B=2.50$, $n=6$)	120
3.106 Vertical Vibration Test on Geogrid Reinforced Sand, $D_r=70\%$, Amplitude versus Frequency Plot ($L_r/L=1.50$, $B_r/B=3.00$, $n=2$)	120
3.107 Vertical Vibration Test on Geogrid Reinforced Sand, $D_r=70\%$, Amplitude versus Frequency Plot ($L_r/L=1.50$, $B_r/B=3.00$, $n=3$)	121
3.108 Vertical Vibration Test on Geogrid Reinforced Sand, $D_r=70\%$, Amplitude versus Frequency Plot ($L_r/L=1.50$, $B_r/B=3.00$, $n=4$)	121
3.109 Vertical Vibration Test on Geogrid Reinforced Sand, $D_r=70\%$, Amplitude versus Frequency Plot ($L_r/L=1.50$, $B_r/B=3.00$, $n=6$)	122
3.110 Vertical Vibration Test on Geogrid Reinforced Sand, $D_r=70\%$, Amplitude versus Frequency Plot ($L_r/L=1.875$, $B_r/B=3.75$, $n=2$)	122
3.111 Vertical Vibration Test on Geogrid Reinforced Sand, $D_r=70\%$, Amplitude versus Frequency Plot ($L_r/L=1.875$, $B_r/B=3.75$, $n=3$)	123
3.112 Vertical Vibration Test on Geogrid Reinforced Sand, $D_r=70\%$, Amplitude versus Frequency Plot ($L_r/L=1.875$, $B_r/B=3.75$, $n=4$)	123
3.113 Vertical Vibration Test on Geogrid Reinforced Sand, $D_r=70\%$, Amplitude versus Frequency Plot ($L_r/L=1.875$, $B_r/B=3.75$, $n=6$)	124
3.114 Horizontal Vibration Test on Unreinforced Sand, $D_r=70\%$, Amplitude versus Frequency Plot	124
3.115 Horizontal Vibration Test on Geogrid Reinforced Sand, $D_r=70\%$, Amplitude versus Frequency Plot ($L_r/L=B_r/B=1$, $n=2$)	125
3.116 Horizontal Vibration Test on Geogrid Reinforced Sand, $D_r=70\%$, Amplitude versus Frequency Plot ($L_r/L=B_r/B=1$, $n=3$)	125
3.117 Horizontal Vibration Test on Geogrid Reinforced Sand, $D_r=70\%$, Amplitude versus Frequency Plot ($L_r/L=B_r/B=1$, $n=4$)	126
3.118 Horizontal Vibration Test on Geogrid Reinforced Sand, $D_r=70\%$, Amplitude versus Frequency Plot ($L_r/L=B_r/B=1$, $n=6$)	126

3.119 Horizontal Vibration Test on Geogrid Reinforced Sand, $D_r=70\%$, Amplitude versus Frequency Plot ($L_r/L=B_r/B=1.5$, $n=2$)	127
3.120 Horizontal Vibration Test on Geogrid Reinforced Sand, $D_r=70\%$, Amplitude versus Frequency Plot ($L_r/L=B_r/B=1.5$, $n=3$)	127
3.121 Horizontal Vibration Test on Geogrid Reinforced Sand, $D_r=70\%$, Amplitude versus Frequency Plot ($L_r/L=B_r/B=1.5$, $n=4$)	128
3.122 Horizontal Vibration Test on Geogrid Reinforced Sand, $D_r=70\%$, Amplitude versus Frequency Plot ($L_r/L=B_r/B=1.5$, $n=6$)	128
3.123 Horizontal Vibration Test on Geogrid Reinforced Sand, $D_r=70\%$, Amplitude versus Frequency Plot ($L_r/L=B_r/B=1.875$, $n=2$)	129
3.124 Horizontal Vibration Test on Geogrid Reinforced Sand, $D_r=70\%$, Amplitude versus Frequency Plot ($L_r/L=B_r/B=1.875$, $n=3$)	129
3.125 Horizontal Vibration Test on Geogrid Reinforced Sand, $D_r=70\%$, Amplitude versus Frequency Plot ($L_r/L=B_r/B=1.875$, $n=4$)	130
3.126 Horizontal Vibration Test on Geogrid Reinforced Sand, $D_r=70\%$, Amplitude versus Frequency Plot ($L_r/L=B_r/B=1.875$, $n=6$)	130
3.127 Horizontal Vibration Test on Geogrid Reinforced Sand, $D_r=70\%$, Amplitude versus Frequency Plot ($L_r/L=1.25$, $B_r/B=2.50$, $n=2$)	131
3.128 Horizontal Vibration Test on Geogrid Reinforced Sand, $D_r=70\%$, Amplitude versus Frequency Plot ($L_r/L=1.25$, $B_r/B=2.50$, $n=3$)	131
3.129 Horizontal Vibration Test on Geogrid Reinforced Sand, $D_r=70\%$, Amplitude versus Frequency Plot ($L_r/L=1.25$, $B_r/B=2.50$, $n=4$)	132
3.130 Horizontal Vibration Test on Geogrid Reinforced Sand, $D_r=70\%$, Amplitude versus Frequency Plot ($L_r/L=1.25$, $B_r/B=2.50$, $n=6$)	132
3.131 Horizontal Vibration Test on Geogrid Reinforced Sand, $D_r=70\%$, Amplitude versus Frequency Plot ($L_r/L=1.50$, $B_r/B=3.00$, $n=2$)	133
3.132 Horizontal Vibration Test on Geogrid Reinforced Sand, $D_r=70\%$, Amplitude versus Frequency Plot ($L_r/L=1.50$, $B_r/B=3.00$, $n=3$)	133

3.133 Horizontal Vibration Test on Geogrid Reinforced Sand, $D_r=70\%$, Amplitude versus Frequency Plot ($L_r/L=1.50$, $B_r/B=3.00$, $n=4$)	134
3.134 Horizontal Vibration Test on Geogrid Reinforced Sand, $D_r=70\%$, Amplitude versus Frequency Plot ($L_r/L=1.50$, $B_r/B=3.00$, $n=6$)	134
3.135 Horizontal Vibration Test on Geogrid Reinforced Sand, $D_r=70\%$, Amplitude versus Frequency Plot ($L_r/L=1.875$, $B_r/B=3.75$, $n=2$)	135
3.136 Horizontal Vibration Test on Geogrid Reinforced Sand, $D_r=70\%$, Amplitude versus Frequency Plot ($L_r/L=1.875$, $B_r/B=3.75$, $n=3$)	135
3.137 Horizontal Vibration Test on Geogrid Reinforced Sand, $D_r=70\%$, Amplitude versus Frequency Plot ($L_r/L=1.875$, $B_r/B=3.75$, $n=4$)	136
3.138 Horizontal Vibration Test on Geogrid Reinforced Sand, $D_r=70\%$, Amplitude versus Frequency Plot ($L_r/L=1.875$, $B_r/B=3.75$, $n=6$)	136
4.1 Cyclic Plate Load Tests - Bearing Capacity Ratio versus Number of Reinforcement Layers (Factor of Safety=1)	244
4.2 Cyclic Plate Load Tests - Settlement Ratio versus Number of Reinforcement Layers (Factor of Safety=1)	244
4.3 Cyclic Plate Load Tests - Damping Capacity Ratio versus Number of Reinforcement Layers.	245
4.4 Cyclic Plate Load Tests - Coefficient of Elastic Uniform Compression (C_{u100}) ₁₀ versus Normal Strain [Effect of Geogrid Reinforcement]	245
4.5 Cyclic Plate Load Tests-Coefficient of Elastic Uniform Compression (C_{u100}) ₁₀ versus Number of Reinforcement Layers (Strain Level- 2×10^{-3})	246
4.6 Cyclic Plate Load Tests-Coefficient of Elastic Uniform Compression (C_{u100}) ₁₀ versus Number of Reinforcement Layers (Strain Level- 4×10^{-3})	246
4.7 Cyclic Plate Load Tests-Coefficient of Elastic Uniform Compression (C_{u100}) ₁₀ versus Number of Reinforcement Layers (Strain Level- 6×10^{-3})	247
4.8 Cyclic Plate Load Tests-Coefficient of Elastic Uniform Compression (C'_{u100}) ₁₀ versus Number of Reinforcement Layers (Strain Level- 1×10^{-2})	247

4.9 Cyclic Plate Load Tests-Coefficient of Elastic Uniform Compression (C_{u100}) ₁₀ versus Reinforcement Size (Strain Level- 4×10^{-3})	248
4.10 Cyclic Plate Load Tests-Coefficient of Elastic Uniform Compression (C_{u100}) ₁₀ versus Reinforcement Size (Strain Level- 6×10^{-3})	248
4.11 Cyclic Plate Load Tests-Effect of Soil Density and Footing Size on C_u (Strain Level- 4×10^{-3})	249
4.12 Vertical Vibration Tests-Damping Ratio versus F/W, ($L_r/L=B_r/B=1.0$)	250
4.13 Vertical Vibration Tests - Damping Ratio versus F/W, ($L_r/L=B_r/B=1.5$)	250
4.14 Vertical Vibration Tests-Damping Ratio versus F/W, ($L_r/L=B_r/B=1.875$)	250
4.15 Vertical Vibration Tests - Damping Ratio versus F/W, ($L_r/L=1.25$, $B_r/B=2.50$).	250
4.16 Vertical Vibration Tests - Damping Ratio versus F/W, ($L_r/L=1.5$, $B_r/B=3.0$).	251
4.17 Vertical Vibration Tests - Damping Ratio versus F/W, ($L_r/L=1.875$, $B_r/B=3.75$).	251
4.18 Vertical Vibration Tests-Strain Amplitude Ratio versus F/W, ($L_r/L=B_r/B=1.0$).	251
4.19 Vertical Vibration Tests - Strain Amplitude Ratio versus F/W, ($L_r/L=B_r/B=1.5$).	251
4.20 Vertical Vibration Tests - Strain Amplitude Ratio versus F/W, ($L_r/L=B_r/B=1.875$).	252
4.21 Vertical Vibration Tests - Strain Amplitude Ratio versus F/W, ($L_r/L=1.25$, $B_r/B=2.50$).	252
4.22 Vertical Vibration Tests - Strain Amplitude Ratio versus F/W, ($L_r/L=1.50$, $B_r/B=3.00$).	252
4.23 Vertical Vibration Tests - Strain Amplitude Ratio versus F/W, ($L_r/L=1.875$, $B_r/B=3.75$).	252

4.24 Vertical Vibration Tests - Amplitude Reduction Factor versus n, ($L_r/L=B_r/B=1, 1.5, 1.875; \theta=4^\circ$)	253
4.25 Vertical Vibration Tests - Amplitude Reduction Factor versus n, ($L_r/L=1.25, 1.50, 1.875; B_r/B=2.50, 3.0, 3.75; \theta=4^\circ$)	253
4.26 Vertical Vibration Tests - Amplitude Reduction Factor versus n, ($L_r/L=B_r/B=1, 1.50, 1.875; \theta=12^\circ$)	253
4.27 Vertical Vibration Tests - Amplitude Reduction Factor versus n, ($L_r/L=B_r/B=1, 1.50, 1.875; \theta=20^\circ$)	253
4.28 Vertical Vibration Tests - Amplitude Reduction Factor versus n, ($L_r/L=B_r/B=1, 1.50, 1.875; \theta=28^\circ$)	254
4.29 Vertical Vibration Tests - Amplitude Reduction Factor versus n, ($L_r/L=1.25, 1.50, 1.875; B_r/B=2.5, 3.0, 3.75; \theta=12^\circ$)	254
4.30 Vertical Vibration Tests - Amplitude Reduction Factor versus n, ($L_r/L=1.25, 1.50, 1.875; B_r/B=2.5, 3.0, 3.75; \theta=20^\circ$)	254
4.31 Vertical Vibration Tests - Amplitude Reduction Factor versus n, ($L_r/L=1.25, 1.50, 1.875; B_r/B=2.50, 3.0, 3.75; \theta=28^\circ$)	254
4.32 Vertical Vibration Tests- $(C_{u100})_{10}$ versus F/W, ($L_r/L=B_r/B=1.0$)	255
4.33 Vertical Vibration Tests- $(C_{u100})_{10}$ versus F/W, ($L_r/L=B_r/B=1.5$)	255
4.34 Vertical Vibration Tests- $(C_{u100})_{10}$ versus F/W, ($L_r/L=B_r/B=1.875$)	255
4.35 Vertical Vibration Tests- $(C_{u100})_{10}$ versus F/W, ($L_r/L=1.25, B_r/B=2.50$)	255
4.36 Vertical Vibration Tests- $(C_{u100})_{10}$ versus F/W, ($L_r/L=1.50, B_r/B=3.00$)	256
4.37 Vertical Vibration Tests- $(C_{u100})_{10}$ versus F/W, ($L_r/L=1.875, B_r/B=3.75$)	256
4.38 Vertical Vibration Tests- $(C_{u100})_{10R}/(C_{u100})_{10U}$ Ratio versus Number of Reinforcement Layers n	256
4.39 Vertical Vibration Tests - C_u -Ratio versus Ratio of Reinforcement Area to Area of Block	257
4.40 Vertical Vibration Tests - $(C_{u100})_{10}$ versus Number of Reinforcement Layers n.	257

4.41 Coefficient of Elastic Uniform Compression C_u (or C'_u) versus Normal Strain - Effect of Geogrid Reinforcement on C_u	258
4.42 Horizontal Vibration Tests - Strain Amplitude Ratio versus F_1/W , ($L_r/L=B_r/B=1.0$)	259
4.43 Horizontal Vibration Tests - Strain Amplitude Ratio versus F_1/W , ($L_r/L=B_r/B=1.5$)	259
4.44 Horizontal Vibration Tests - Strain Amplitude Ratio versus F_1/W , ($L_r/L=B_r/B=1.875$)	259
4.45 Horizontal Vibration Tests - Strain Amplitude Ratio versus F_1/W , ($L_r/L=1.875, B_r/B=3.75$)	259
4.46 Horizontal Vibration Tests - Strain Amplitude Ratio versus F_1/W , ($L_r/L=1.25, B_r/B=2.50$)	260
4.47 Horizontal Vibration Tests - Strain Amplitude Ratio versus F_1/W , ($L_r/L=1.5, B_r/B=3.0$)	260
4.48 Horizontal Vibration Tests - $(C_{\tau 100})_{10}$ versus F_1/W , ($L_r/L = B_r/B = 1.0$)	260
4.49 Horizontal Vibration Tests - $(C_{\tau 100})_{10}$ versus F_1/W , ($L_r/L = B_r/B = 1.5$)	260
4.50 Horizontal Vibration Tests - $(C_{\tau 100})_{10}$ versus F_1/W , ($L_r/L = B_r/B = 1.875$)	261
4.51 Horizontal Vibration Tests - $(C_{\tau 100})_{10}$ versus F_1/W , ($L_r/L = 1.25, B_r/B = 2.50$)	261
4.52 Horizontal Vibration Tests - $(C_{\tau 100})_{10}$ versus F_1/W , ($L_r/L = 1.50, B_r/B = 3.0$)	261
4.53 Horizontal Vibration Tests - $(C_{\tau 100})_{10}$ versus F_1/W , ($L_r/L = 1.875, B_r/B = 3.75$)	261
4.54 Horizontal Vibration Tests - Damping Ratio ζ_1 versus F_1/W , ($L_r/L=B_r/B=1.0$)	262

4.55 Horizontal Vibration Tests - Damping Ratio ζ_1 versus F_1/W , ($L_r/L=B_r/B=1.50$)	262
4.56 Horizontal Vibration Tests - Damping Ratio ζ_1 versus F_1/W , ($L_r/L=B_r/B=1.875$)	262
4.57 Horizontal Vibration Tests - Damping Ratio ζ_1 versus F_1/W , ($L_r/L=1.25, B_r/B=2.50$)	262
4.58 Horizontal Vibration Tests - Damping Ratio ζ_1 versus F_1/W , ($L_r/L=1.50, B_r/B=3.0$)	263
4.59 Horizontal Vibration Tests - Damping Ratio ζ_1 versus F_1/W , ($L_r/L=1.875, B_r/B=3.75$)	263
4.60 Horizontal Vibration Tests - Amplitude Reduction Factor versus 'n', ($L_r/L=B_r/B=1.0, 1.5, 1.875; \theta=4^\circ$)	263
4.61 Horizontal Vibration Tests - Amplitude Reduction Factor versus 'n', ($L_r/L=B_r/B=1.0, 1.5, 1.875; \theta=12^\circ$)	263
4.62 Horizontal Vibration Tests - Amplitude Reduction Factor versus 'n', ($L_r/L=B_r/B=1.0, 1.5, 1.875; \theta=20^\circ$)	264
4.63 Horizontal Vibration Tests - Amplitude Reduction Factor versus 'n', ($L_r/L=B_r/B=1.0, 1.5, 1.875; \theta=28^\circ$)	264
4.64 Horizontal Vibration Tests - Amplitude Reduction Factor versus 'n', ($L_r/L=1.25,1.5,1.875; B_r/B=2.5,3.0,3.75; \theta=4^\circ$)	264
4.65 Horizontal Vibration Tests - Amplitude Reduction Factor versus 'n', ($L_r/L=1.25,1.5,1.875; B_r/B=2.5,3.0,3.75; \theta=12^\circ$)	264
4.66 Horizontal Vibration Tests - Amplitude Reduction Factor versus 'n', ($L_r/L=1.25,1.5,1.875; B_r/B=2.5,3.0,3.75; \theta=20^\circ$)	265
4.67 Horizontal Vibration Tests - Amplitude Reduction Factor versus 'n', ($L_r/L=1.25,1.5,1.875; B_r/B=2.5,3.0,3.75; \theta=28^\circ$)	265
4.68 Horizontal Vibration Tests - $(C_{\tau 100})_{10R}/(C_{\tau 100})_{10U}$ versus 'n',	265

4.69 Horizontal Vibration Tests $-(C_{\tau 100})_{10R}/(C_{\tau 100})_{10U}$ versus Area Ratio of Reinforcement	265
4.70 Soil-Reinforcement Layered System	266
4.71 Experimental versus Predicted Values of C_u in Vertical Vibration Tests	266
4.72 Experimental versus Predicted Values of C_u in Cyclic Plate Load Tests	267
4.73 Experimental versus Predicted Values of C_{τ} in Horizontal Vibration Tests	267

LIST OF TABLES

Table No.	Description	Page No.
3.1	Physical and Mechanical Properties of Soil	46
3.2	Properties of Reinforcement Material, Geogrid Netlon CE-121	47
3.3	Details of Cyclic Plate Load Tests Conducted	53
3.4	Characteristics of the Foundation Block	56
3.5	Details of Block Vibration Tests Conducted	59
4.1	Cyclic Plate Load Tests - K_0 from Ultimate Bearing Pressure Values	213
4.2	Cyclic Plate Load Tests-Bearing Capacity Ratio (BCR), Settlement Ratio (SR), Coefficient of Elastic Uniform Compression C_u and C'_u and Damping Capacity Ratio	215
4.3	Coefficient of Elastic Uniform Compression, C_u at a Confining Pressure = 100 kN/m ² and Area of Foundation = 10 m ² at Factors of Safety 1, 2 and 3 and the Corresponding Strain Levels	217
4.4	Coefficient of Elastic Uniform Compression, C'_u at a Confining Pressure = 100 kN/m ² and Area of Foundation = 10 m ² at Factors of Safety 1, 0.67 and 0.5 and the Corresponding Strain Levels	219
4.5	Coefficient of Elastic Uniform Compression, $(C_{u100})_{10}$ and $(C'_{u100})_{10}$ Interpolated at Strain Levels - 2×10^{-3} , 4×10^{-3} & 6×10^{-3} and 10×10^{-3} and 15×10^{-3} respectively.	221
4.6	Analysis of vertical vibration test data of geogrid reinforced sand beds	223
4.7	Analysis of horizontal vibration test data of geogrid reinforced sand beds	226
4.8	Vertical vibration tests - C_u values interpolated at different strain levels and corresponding F/W ratios	229

4.9 Horizontal vibration tests - C_{τ} values interpolated at different strain levels and corresponding F_1/W ratios	230
4.10 Cyclic Plate Load Tests - Regression analysis for coefficient of Elastic uniform compression C_u	231
4.11 Regression analysis for damping capacity ratio	232
4.12 Cyclic Plate Load Tests - Regression analysis for ultimate bearing capacity ratio, BCR	233
4.13 Cyclic plate load tests-Regression analysis for settlement ratio, SR	234
4.14 Regression analysis for $(C_{u100})_{10}$ - vertical vibration tests	235
4.15 Regression analysis for $(C_{\tau100})_{10}$ - horizontal vibration tests	236
4.16 Regression analysis for damping ratio ξ - vertical vibration tests	237
4.17 Regression analysis for damping ratio ξ_1 - horizontal vibration tests	238
4.18 Regression analysis for amplitude reduction factor - vertical vibration tests	239
4.19 Regression analysis for amplitude reduction factor - horizontal vibration tests	240
4.20 Comparison of analytical and experimental values of coefficient of elastic uniform compression - vertical vibration tests	241
4.21 Comparison of analytical and experimental values of coefficient of elastic uniform compression - cyclic plate load tests	242
4.22 Comparison of analytical and experimental values of coefficient of elastic uniform shear - horizontal vibration tests	243

LIST OF NOTATIONS

Symbol	Description	Units
A	Area of the Foundation Base	m^2
A_r	Ratio of Area of Reinforcement to Footing/Block Area	
A'	Dimensionless Parameter	
A_{max}	Maximum Amplitude of Vibration of Footing	mm
A_0	Ratio of Area to Mass of Block Foundation	$kN^{-1}-m^3-sec^{-2}$
A_z	Amplitude of Motion of Footing in Vertical Vibration	mm
$(A_z)_d$	Damped Amplitude of Vertical Vibration of Footing	mm
A_2	Displacement Amplitude Factor	
$(A_{1,2})_{max}$	Maximum Displacement Amplitude Factors	
$(A_z)_{max}$	Maximum Amplitude of Vertical Vibration of Block	mm
$(A_z)_{maxu}, (A_z)_{maxr}$	Maximum Amplitudes of Vertical Vibration of Block on Unreinforced and Reinforced Sand Beds	mm
a	Dimensionless Frequency Factor	
a_{pr}	Proto-type Footing Radius	
a_r	Resonant Frequency Factor	
$(A_{x1})_{max}, (A_{x2})_{max}$	Maximum Amplitudes of Horizontal Vibration of Block in First and Second Modes	mm
$(A_{x1max})_r, (A_{x1max})_u$	Maximum Amplitudes of Horizontal Vibrations of Block in First Mode on Reinforced and Unreinforced Sand Beds	mm
$a_0, a_1, etc.$	Coefficients of Polynomial	
B	Width of Footing/Block Foundation	m,mm
B_r, B_{RN}	Width of Reinforcement along Width B	m,mm
B'_r	$\sqrt{A_r}$	m,mm
B_z	Modified Mass Ratio for Vertical Vibrations	
b	Dimensionless Mass Ratio	

BCR	Bearing Capacity Ratio	
C_{uSR} (observed), C_{uSR} (prediced)	Observed and Predicted Values of Coefficient of Elastic Uniform Compression of Reinforced Sand Bed	kN/m ³
$(C_{u100})_{10R}, (C_{u100})_{10U}$	Coefficients of Elastic Uniform Compression of Reinforced and Unreinforced Sand Beds at 100 kN/m ² Confining Pressure and 10m ² Area.	kN/m ³
$(C_{\tau 100})_{10R}, (C_{\tau 100})_{10U}$	Coefficients of Elastic Uniform Shear of Reinforced and Unreinforced Sand Beds at 100 kN/m ² Confining Pressure and 10m ² Area	kN/m ³
C	Damping Coefficient	
C_a	Adhesion Between the Soil and Sides of Embedded Footing	kN/m ²
C_c	Coefficient of Curvature	
C_r	Cohesion Intercept due to Reinforcement	kN/m ²
C_{τ}	Coefficient of Elastic Uniform Shear	kN/m ³
C_u	Coefficient of Elastic Uniform Compression	kN/m ³
C'_u	Coefficient of Elastic Uniform Compression Beyond Ultimate Bearing Pressure	kN/m ³
C_{u100}	Coefficient of Elastic Uniform Compression at 100 kN/m ² Confining Pressure	kN/m ³
$(C_{u100})_{10}$	Coefficient of Elastic Uniform Compression at 100 kN/m ² Confining Pressure and 10m ² Area	kN/m ³
C_{uSR}	Coefficient of Elastic Uniform Compression of Reinforcement Soil Mass	kN/m ³
$C_{\tau SR}$	Coefficient of Elastic Uniform Shear of Reinforcement Soil Mass	kN/m ³
$C_{\tau av}$	Average Coefficient of Elastic Uniform Shear of Soil Mass	kN/m ³
$C_{\tau R}$	Coefficient of Elastic Uniform Shear of Reinforced Sand Bed	kN/m ³

C_z	Frequency Dependent Damping Coefficient of Half-Space in z-Direction	
$C_{\tau 100}$	Coefficient of Elastic Uniform Shear at 100 kN/m ² Confining Pressure	kN/m ³
$(C_{\tau 100})_{10}$	Coefficient of Elastic Uniform Shear at 100 kN/m ² Confining Pressure and 10m ² Area	kN/m ³
C_1, C_2	Functions of Dimensionless Frequency Factor 'a' Related to Elastic Half Space	
$(C'_{u 100})_{10}$	Coefficient of Elastic Uniform Compression Beyond Ultimate Bearing Capacity at 100 kN/m ² Confining Pressure and 10m ² Area.	kN/m ³
C_{uR}, C_{uU}	Coefficients of Elastic Uniform Compression of Reinforced and Unreinforced Sand Beds	kN/m ³
D	Depth of Embedment of Footing	m
D_{cr}	Ratio of Damping Capacities of Reinforced and Unreinforced Sand Beds	
D_r	Relative Density of Sand	
D_{10}	Effective Size of Soil Particles	mm
D_x, D_z	Damping Factors for Sliding and Vertical Vibrations	
D^*	Hysteretic Damping of Soil	
D_{max}^*	Maximum Hysteretic Damping of Soil	
d	Diameter of Footing	m
E_0	Elastic Modulus of Sand	kN/m ²
E_1, E_i, E_N	Elastic Moduli of Sand Layers	kN/m ²
E_R, E_{Ri}, E_{Rn}	Elastic Moduli of Reinforcement Layers	kN/m ²
E_{SR}	Equivalent Elastic Modulus of Reinforced Sand	kN/m ²
e	Eccentricity	
e'	Void Ratio of Soil	mm
F	Dynamic Force	kN

$F(e')$	Function of Void Ratio of Sand	
F_0	Externally Applied Force Which Remains Constant with Frequency, ω	kN
F_1	Dynamic Force on Block for First Mode in Horizontal Vibrations	kN
F_s	Ratio of Confining Pressure Parallel to Direction of Reinforcement to Major Principal Stress	
F'	Coulomb Friction Force	kN
F'_1, F'_2	Dimensionless Functions of Poisson's Ratio (ν) & Frequency Factor 'a'	
f	Frequency	Hz
f_r	Resonant Frequency	Hz
f_1, f_2	Dimensionless Functions of Poisson's Ratio and Frequency Factor 'a'	
f_{nx}, f_{nz}	Horizontal and Vertical Resonant Frequencies of Block-Soil System	Hz
$(f_{nz})_d$	Vertical Damped Natural Frequency of Block Foundation-Soil System	Hz
f_{nx1}, f_{nx2}	Resonant Frequencies for First and Second Modes in Horizontal Vibrations	Hz
G, G_s	Shear Moduli of Elastic Half Space and Side Soil Layer	kN/m^2
G_{\max}, G^c	Maximum value of Shear Modulus of Soil at Low Strain (10^{-6})	kN/m^2
G_0, G_1, G_2	Shear Moduli of Soil at Confining Pressures $\sigma'_0, \sigma'_1, \sigma'_2$	kN/m^2
G_i	Shear Modulus of ith Soil Layer	kN/m^2
G_{Rj}, G_{Rn}	Shear Moduli of Reinforcement Layers	kN/m^2
G_{SR}	Equivalent Shear Modulus of Reinforced Soil Mass	kN/m^2
g	Acceleration due to Gravity	m/sec^2
H	Depth of Embedment of Footing	m
H_1, h	Stratum Thickness Below Footing Level	m

H_i, H_N	Thickness of i th and N th Sand Layer	m,mm
H_R, H_{Rj}, H_{Rn}	Thickness of Reinforcement Layers	mm
I	Moment of Inertia of Base Contact Area about Axis of Rotation, Y-Axis	m^4
I_0	Ratio $3.46 \times I / M_{m0}$	$kN^{-1}m^3/sec^2$
\bar{I}	Influence Factor for Determining Vertical Stress Below Corner of Loaded Rectangular Area	
K	Spring Constant	kN/m
K_a	Coefficient of Active Earth Pressure	
K_x, K_z	Frequency Dependent Spring Constants of Soil for Sliding and Vertical Vibrations	kN/m
K_2	Empirical Factor Depending Upon Relative Density of Sand	
k	A Factor Depending upon Plasticity Index of Clays	
L	Length of Footing/Block Foundation	m,mm
L_s, L_i	Length of Soil Layer over which Shear Stress is Acting	m,mm
L_p	Perimeter Length of Embedded Footing	m
L_r, L_{Rj}, L_{Rn}	Length of Reinforcement Layer along Length of Footing L	mm,m
M	Mass of Block and Vibrator	$kN \cdot sec^2/m$
M_m	Mass Moment of Inertia about Y-Axis, an Axis Passing Through the Combined Centre of Gravity of Block and Oscillator-Motor and Perpendicular to Plane of Vibration	
M_{m0}	Mass Moment of Inertia about Y-Axis Passing Through Centroid of Base	$kN \cdot m \cdot sec^2$
m	Total Mass of Vibrating Footing	$kN \cdot sec^2/m$
m_e	Total Eccentric Mass	$kN \cdot sec^2/m$
m'	Exponent Showing Dependence of Shear Modulus on Confining Pressure	
m_1	A Constant	
N	Number of Soil Layers	

\bar{N}	Number of Loading Cycles	
N_1	Number of Blows Recorded in Standard Penetration Test	
$(N_1)_{60}$	Corrected Value of N Measured in Standard Penetration Test Delivering 60% of Theoretical Free Fall Energy	
N_γ	Terzaghi's Bearing Capacity Factor	
n	Number of Reinforcement Layers	
n', n_1	Constants	
OCR	Over-Consolidation Ratio	
p	Loading Intensity on the Footing	kN/m^2
p_a	Atmospheric Pressure	kN/m^2
P_z	Vertical Unbalanced Force on Block Foundation	kN
p_{pr}	Static Foundation Bearing Pressure	kN/m^2
q	Uniform Vertical Loading Intensity Acting on the Footing	kN/m^2
q_u	Ultimate Bearing Capacity	kN/m^2
q_{uU}, q_{uR}	Ultimate Bearing Capacities of Unreinforced and Reinforced Sand Beds	kN/m^2
R	Dimensionless Measure of Mean Roundness	
R^2	Coefficient of Correlation	
R_d	Amplitude Reduction Factor	
r	Radius of Footing	m
r'	Ratio of Operating Frequency of Machine to Resonant Frequency of Soil-Foundation System	
r_1, r_2	Dimensionless Functions of Frequency Factor 'a' and Poisson's Ratio ' ν '.	
S_e, S_t	Elastic and Total Settlements of the Footing	mm
S_1, S_2	Functions of Dimensionless Frequency Factor 'a' Related to Side Soil	

S_{OU}, S_{RU}	Settlements of Footing on Unreinforced and Reinforced Sand Beds at a Pressure Equal to Ultimate Bearing Capacity of Unreinforced Sand Bed	mm
s_z	Vertical Distance Between Adjacent Reinforcement Layers	mm
SR	Settlement Ratio	
t	Time	sec.
U_C	Uniformity Coefficient	
u	Depth of Top Reinforcement Layer Below Footing/Block Base	mm
W	Weight of Vibrator and Block	kN
W_1	Weight of Block	kN
W_2	Weight of Motor and Oscillator	kN
Z	Depth under Consideration which is Equal to Half the Width of Footing	m
z	Vertical Displacement of Centre of Footing	mm
\dot{z}	Velocity of Vibration of Footing	mm/sec
\ddot{z}	Acceleration of Vibration of Footing	mm/sec ²
ϵ_z	Strain Level in z-Direction	
ϕ	Angle of Internal Friction of Soil	degrees
ϕ_r	Increased Internal Friction Angle due to Reinforcement	degrees
γ	Shear Strain	
γ_r	Reference Shear Strain	
γ_S	Unit Weight of Soil	kN/m ³
γ'	Ratio of Mass Moment of Inertia, M_m to Mass Moment of Inertia, M_{m0}	
μ_f	Coefficient of Kinematic Friction Between Soil and Sides of Embedded Footing	
ν	Poisson's Ratio of Soil Below Foundation	
ω	Circular Frequency	radians/sec
ω_1	Circular Resonant Frequency	radians/sec

ω_{nz}	Circular Natural Frequency in Vertical Vibrations	radians/sec
$(\omega_{nz})_d$	Damped Circular Natural Frequency in Vertical Vibrations	radians/sec
ρ, ρ_s	Mass Densities of Half Space Material and Side Soil	kN-sec ² /m ⁴
σ_r	Confining Pressure Parallel to Direction of Reinforcement	kN/m ²
σ_v	Vertical Stress Induced at the Centre of Pressure Bulb of Depth Equal to Footing Width due to Superimposed Static Load and Weight of Soil	kN/m ²
$\sigma'_m, \sigma'_0, \bar{\sigma}_1, \bar{\sigma}_2$	Mean Effective Confining Pressure	kPa, kN/m ²
σ_1, σ_3	Major and Minor Principal Stresses	kN/m ²
$\Delta\sigma_3$	Lateral Compression due to Reinforcement	kN/m ²
$\sigma_N, \text{etc.}$	Average Vertical Stress at the Centre of Nth Soil Layer	kN/m ²
$\sigma_{Rn}, \text{etc.}$	Average Vertical Stress at the Centre of nth Reinforcement Layer	kN/m ²
τ_r	Shear Stress Along the Soil-Reinforcement Interface	kN/m ²
τ_{max}	Shear Stress at Failure of Soil	kN/m ²
θ	Angle Between Eccentric Masses of Oscillator	degree
ξ	Damping Ratio in Vertical Vibrations	
ξ_1, ξ_2	Damping Ratios for First and Second Modes in Horizontal Vibration	
ξ_R, ξ_U	Damping Ratios of Reinforced and Unreinforced Sand Beds in Vertical Vibrations	
ξ_{1R}, ξ_{1U}	Damping Ratios of Reinforced and Unreinforced Sand Beds for First Mode in Horizontal Vibrations	
σ_i	Average Vertical Stress at the Centre of ith Soil Layer	kN/m ²
σ_{Rj}	Average Vertical Stress at the Centre of jth Reinforcement Layer	kN/m ²
τ_i	Average Shear Stress at the Centre of ith Soil Layer	kN/m ²
τ_{Rj}	Average Shear Stress at the Centre of jth Reinforcement Layer	kN/m ²

List of Papers

Published

1. Saran, S., Lavania, B.V.K., and Sharma, R.K., (1995), "*Cyclic Plate Load Tests on Reinforced Sand*", Third International Conference on Recent Advances in Geotechnical Earthquake Engineering and Soil Dynamics, St. Louis, Missouri (USA), April 2-7, 1995, Paper No. 2.19L.
2. Saran, S., Lavania, B.V.K., and Sharma, R.K., (1994), "*Horizontal Vibration Characteristics of Geogrid Reinforced Sand Beds*", 10th Symposium on Earthquake Engineering, Roorkee, India, Oct. 1994, Vol. 2.
3. Saran, S., Lavania, B.V.K., and Sharma, R.K., (1994), "*Vertical Vibration Response of Geogrid Reinforced Sand Beds*", Indian Geotechnical Conference, IGC-94, Warangal, India.
4. Saran, S., and Sharma, R.K., (1995), "*Dynamic Characteristics of Reinforced Earth*", Terzaghi-94, Seminar on Recent Advances in Geotechnical Engineering, IGS, Visakhapatnam, (A.P.), India.

INTRODUCTION

1.1 GENERAL

The understanding of dynamic behaviour of foundation-soil is essentially required in situations where human-caused dynamic loading or earthquakes occur. Modulus, damping, frequency and amplitude are important factors to be considered for this. During the past three decades, reinforcement of soil by high tensile strength materials has become a widespread technique for improvement of its properties. Metal strips, geogrids and fabrics have been used to increase the tensile strength, shear resistance and stiffness of soils. Generally, the analysis of reinforced soil has been limited to static loading conditions. The dynamic properties of the material are not available and so is the mechanics of material interaction under dynamic loads.

The present investigation is aimed at evaluation of dynamic properties and understanding of the material interaction mechanism in reinforced sand beds and thereby developing an analytical approach for use in design.

The methodology involves determining the dynamic properties of reinforced sand by conducting a series of cyclic plate load and block vibration tests in laboratory on unreinforced and reinforced sand beds. The results of the experiments are analysed and presented in the form of non-dimensional charts, and non-dimensional correlations are developed by regression analysis of the data. Also, an analytical approach is suggested to determine the coefficient of elastic uniform compression, C_u and the coefficient of elastic uniform shear, C_τ of reinforced sand treating it as a composite homogeneous elastic material.

1.2 BASIC MECHANISM OF REINFORCED EARTH

The basic mechanism of reinforced earth can be explained by using Rankine's state of stress theory. A two dimensional element of laterally unconfined cohesionless soil subjected to uniaxial stress will fail instantaneously as Mohr circle of stress will cut the strength envelope, which is inclined at an angle ϕ to the σ -axis and passes through the origin; ϕ being the angle of internal friction of soil and σ is the normal stress. If the same element is subjected to equal biaxial stresses, it will undergo uniform compression without failure. If, however, the stresses are unequal, it will behave like a triaxial sample in axial compression with failure occurring at large lateral strains. At failure, the lateral stress

$$\sigma_3 = K_a \sigma_1 \quad \dots(1.1)$$

where σ_1 is the major principal stress and K_a is the coefficient of active earth pressure. The Mohr circle is tangential to the strength envelope at this instant. To avoid the failure of the element, the lateral stress σ_3 must be increased. If reinforcement is provided in the soil element in the direction of σ_3 , the interaction between the soil and reinforcement will generate frictional forces along the interface. Tensile stresses are produced in the reinforcement and a corresponding lateral compression $\Delta\sigma_3$ in the soil element, as long as there is no slippage between the two. This additional lateral stress will shift the Mohr circle to the right and away from the strength envelope. Thus soil-reinforcement interface friction is the fundamental factor governing the design of reinforced earth.

Two theoretical models have been proposed for the strength of reinforced earth under static loads (Hausmann, 1976). The SIGMA-model assumes that reinforcement induces normal confining pressure σ_r in the specimen parallel to the direction of reinforcement. This additional confining pressure leads to enhanced strength of reinforced soil mass and appears as cohesion intercept C_r (rupture

failure) and increased internal friction angle ϕ_r (friction failure), with the following relationships :

$$C_r = \sigma_r / 2 \sqrt{K_a} \quad \dots(1.2)$$

and
$$\phi_r = (1 + F_s - K_a)/(1 - F_s + K_a) \quad \dots(1.3)$$

where

$$F_s = \sigma_r/\sigma_1$$

K_a = Coefficient of active earth pressure, and

σ_1 = major principal stress.

In the TAU-model, the reinforcement is assumed to introduce shear stresses τ_r , along the soil-reinforcement interface, resulting in an increase in the strength of the soil. The increase in strength in both the models is a function of the shear strength of soil and tensile strength, distribution, mode of placement and surface characteristics of the reinforcement.

The dynamic properties particularly the stiffness and damping of soil are likely to be affected by the introduction of reinforcement depending upon the modulus and surface characteristics of the reinforcing material. The stress-strain characteristics of soil are nonlinear upto very low strains, whereas those of the reinforcing materials are comparatively linear. It is expected that the dynamic properties of sand would change, if it is reinforced.

1.3 BRIEF REVIEW OF LITERATURE

The analysis and design of foundations subjected to dynamic loads require the estimation of dynamic soil properties at various mean stress and strain levels. Several approaches are available for obtaining the dynamic response of foundations on soils.

Barkan (1962) considers Winkler-Voigt model assuming the foundation to be supported on a weightless spring. Reissner (1936), Quinlan (1953) and Sung (1953) have considered the homogeneous, isotropic and elastic half-space model for

solving the dynamic problem. Hsieh (1962), Lysmer *et al.* (1966) and Richart *et al.* (1970) consider the mass-spring-dashpot system. The spring constants and damping are obtained from elastic half-space theory and their simplified analog. The above models are in vogue to obtain solutions for the foundations resting on soil-surface. Novak and Beredugo (1972) and Anandkrishnan & Krishnaswamy (1973) attempted to study the response of embedded block foundation analytically as well as experimentally. The dynamic response of block foundation has been studied experimentally by Barkan (1962), Novak (1970), Stokoe and Richart (1974), Petrovski (1975), Ranjan *et al.* (1978) and Saran & Vijayavargiya (1979). Further, studies in this field have been attempted by Gazetas & Roesset (1979), Sridharan *et al.* (1981), Nagendra & Sridharan (1981), Dobry and Gazetas (1986), Nayfeh & Serhan (1989), Sridharan *et al.* (1990a), Gazetas (1991), Navarro (1992), Gucunski and Peek (1993), Meek and Wolf (1994) and Pak and Guzina (1995).

The dynamic properties of unreinforced sands have been studied by Barkan (1962), Hardin (1965), Hardin and Black (1966), Hardin and Black (1969), Seed and Idriss (1970), Silver and Seed (1971), Ishihara (1971), Hardin and Drnevich (1972 a and b), Ohsaki and Iwasaki (1973), Prakash and Puri (1977), Woods (1978), Prakash and Puri (1981), Saha and Chattopadhyaya (1984), Seed *et al.* (1986), Ray and Woods (1988), Sridharan *et al.* (1990b), Khan *et al.* (1992), Hryciw and Thomann (1993), Pak and Guzina (1995) and Fahoum *et al.* (1996).

The static strength characteristics of reinforced earth slabs have been studied by a large number of investigators, since the introduction of the basic concept of reinforced earth by Vidal (1966). Binquet and Lee (1975a & b), have presented analysis for determining the ultimate bearing capacity of sand bed reinforced with metal strips and have verified the results experimentally. The effect of various parameters like soil-characteristics, type, geometry, surface texture, number, spacing and disposition of reinforcement on the ultimate bearing capacity of footings on reinforced sand beds have been investigated by Saran & Talwar (1978), Basset and Last (1978), Akinmusuru & Akinbolade (1981), Fragaszy

and Lawton (1984), Guido *et al.* (1986), Verma & Char (1986), Khing *et al.* (1994), Temel Yetimogulu *et al.* (1994), Sitharam *et al.* (1995) and Adams and Collin (1997). Srinivasa Murthy *et al.* (1993) attempted modifications in the analysis proposed by Binquet and Lee (1975b).

The dynamic loading characteristics of reinforced soil have been studied by a few investigators. Murray *et al.* (1979) studied the effect of vibration on interface friction. Patel and Paldas (1981), Kazuya Yasuhara *et al.* (1988) and Puri *et al.* (1991) conducted cyclic plate load tests on reinforced sand subgrades and reported an improvement in damping capacity, reduction in settlements and improvement in modulus respectively. Shewbridge and Sousa (1991) conducted dynamic shear tests on large hollow cylindrical reinforced and unreinforced sand specimens and reported that at low strains ($\leq 5\%$), the reinforcements have no effect on the complex shear modulus of the material whereas at large strains the reinforcements inhibited the formation of helical shear bands. Boominathan *et al.* (1991) conducted resonance tests on soil reinforced with steel and geotextile and reported that for steel reinforcement, the resonant frequency is increased and maximum amplitude is decreased whereas for geotextile reinforcement both the resonant frequency and maximum amplitude are decreased. Guido *et al.* (1994) performed dynamic plate loading tests on geogrid reinforced sand subgrade and reported an increase in the load carrying capacity of the subgrade. A detailed review of literature pertaining to various aspects covered in this thesis is presented in Chapter 2.

These investigations reveal that only a limited study has been conducted on the dynamic properties of reinforced sand beds and no detailed investigation has been performed regarding the effect of disposition, number and geometry of reinforcement layers on these properties. Further, no attempt has been made to study the behaviour of footings on geogrid reinforced sand beds under horizontal vibrations. Thus, there is a need to study the effect of various factors, as mentioned above, on the dynamic properties of reinforced sand.

1.4 SCOPE OF WORK

The dynamic response parameters e.g., stiffness, damping, amplitude and frequency are determined from laboratory model tests performed on reinforced and unreinforced sand beds. The results of the experiments are analysed and presented in the form of suitable non-dimensional charts. The experimental data are further analyzed to obtain non-dimensional correlations through regression analysis. An analysis is proposed for the determination of C_u and C_τ of reinforced sand from the individual stiffness of soil and reinforcement layers, at low strain levels, treating the reinforced sand as homogeneous composite material.

The experimental investigation consists of performing a series of cyclic plate load and vertical and horizontal vibration tests. In these tests the effect of density of sand, size of footing and size, shape & geometry of the reinforcement on the dynamic properties of reinforced sand have been studied.

1.4.1 Cyclic Plate Load Tests

The cyclic plate load tests were conducted on steel plate of size 150mm×150mm placed on unreinforced and reinforced sand bed prepared in a rigid steel tank of size 900mm×900mm×1000mm, at a relative density of 70%. The sand beds were reinforced with 2,3,4,6 and 8 geogrid Netlon CE-121 reinforcement layers of sizes one to five times the width of footing. The vertical spacing between the reinforcement layers and the depth of the first reinforcement layer below the footing base was kept 0.25 B each. Cyclic plate load tests were also performed on 150mm×150mm plate on unreinforced and reinforced sand beds in the above mentioned steel tank at 50% relative density keeping the number of reinforcement layers as 4 and varying the size of reinforcement from B to 5B. In order to study the effect of footing size on various dynamic response parameters, cyclic plate load tests were conducted on 300mm×300mm steel plate on unreinforced and reinforced sand beds prepared in a steel tank of size 1500mm×1500mm×1000mm, at 70% relative density. The sand beds were reinforced with four reinforcement layers of size B to 5B. The

experimental data of the cyclic plate load tests have been analyzed to incorporate the effect of mean effective confining pressure and the area of footing.

1.4.2 Block Vibration Tests

Vertical and horizontal vibration tests were performed on M-20 concrete block of size 800mm×400mm×400mm placed over unreinforced and reinforced sand beds deposited at 70% relative density in a steel tank of size 1500mm×1500mm×1000mm. The sizes of the reinforcement layers were kept 2.0B×B, 3.0B×1.5B, 3.75B×1.875B, 2.50B×2.50B, 3.0B×3.0B and 3.75B×3.75B; and the number of layers was kept 2,3,4 and 6. The block was excited at four force levels by keeping the angle between the eccentric masses of the oscillator as $\theta=4^\circ$, 12° , 20° and 28° , both in vertical as well as horizontal vibration tests. The details of the experimental investigations carried out on unreinforced and reinforced sand beds are described in Chapter 3.

1.4.3 Analysis of Experimental Data

The experimental data are analyzed and normalized for the effect of (i) average effective confining pressure, (ii) strain level and (iii) area of the footing. The normalized values are plotted and non-dimensional plots for the coefficient of elastic uniform compression C_u , damping, coefficient of elastic uniform shear C_τ , amplitude reduction factor, bearing capacity ratio and the settlement ratio are developed. Non-dimensional correlations for these variables have also been developed by the regression analysis of the experimental data.

1.4.4 Analytical Investigation

An analytical approach is proposed to determine the coefficient of elastic uniform compression, C_u and coefficient of elastic uniform shear, C_τ of the reinforced sand bed considering the C_u and C_τ respectively of sand and elastic modulus of reinforcement. The experimental values are compared with the results of this analytical approach.

1.5 CONCLUDING REMARKS

The static strength characteristics of reinforced sand have been studied in detail whereas only a limited account of the dynamic properties of reinforced soil is available in literature. The present investigation has been taken up with a view to study the dynamic response of foundations on reinforced sand beds experimentally and to interpret the dynamic stiffness properties of reinforced sand based on the experimental data and analytical analysis. It is expected that the results of study would lead to better understanding of the behaviour of foundations on reinforced sand beds under dynamic and cyclic loads and will help in realistic and safe design.

REVIEW OF LITERATURE

2.1 GENERAL

In this chapter, review of the work pertaining to the dynamic response analysis of foundations, reported in the available literature, has been presented still we do not pretend to be very exhaustive. First, the dynamic analysis of foundations on unreinforced soil has been reviewed. The experimental studies by various investigators, on large blocks in field and model scale tests in laboratory are then discussed. A critical review of the literature on the determination of dynamic stiffness properties of soils has also been described. Later, the work reported in literature, concerning the strength characteristics of reinforced earth slabs under static loads has been discussed. Lastly, the studies on the dynamic properties of reinforced soil have been presented and discussed. The inferences drawn on the basis of literature review and importance of present investigation have been brought out.

2.2 DYNAMIC RESPONSE OF BLOCK FOUNDATION ON UNREINFORCED SOIL

The dynamic response of foundation on unreinforced soil reported in literature has been reviewed in this section. The analytical approaches proposed by various investigations are reviewed first and the experimental studies conducted in the field and laboratory are presented and discussed subsequently.

2.2.1 Analytical Formulations

The analytical approaches proposed by various investigators can be classified

into four broad groups :

- (i) Dynamic Winkler model
- (ii) Elastic half space theory
- (iii) Lumped parameter system analog
- (iv) Computational techniques

These analytical formulations are described in the subsequent sections on the basis of the information available in literature.

2.2.1.1 Dynamic Winkler Model

This model was introduced as an extension of well known elastic subgrade reaction hypothesis. In this model, the stiffness characteristics of the actual system are simulated by replacing the soil by a bed of independent elastic springs resting on a rigid base. The spring constants are evaluated through plate bearing tests. Barkan (1962) has presented the formulae to evaluate the spring constants for various modes of vibration defining the dynamic coefficient as the ratio of the applied pressure increment to the resulting displacement during static repeated loading tests (also known as the coefficient of elastic uniform compression, C_u , etc.). In these tests, the static loads are applied first to simulate the dead and live loads, followed by the slow repeated loading tests. This model gives some reasonable information on the low frequency response of a foundation. But since no radiation damping is included, the amplitude of motion at frequencies near the resonance cannot be estimated realistically. Conservative estimates of the response and very good estimates of frequency are obtained by neglecting damping. But in translational modes of vibration, high damping values do affect the resonant frequencies, in addition to drastically reducing amplitudes.

An improved version of above model is Winkler-Voigt model in which foundation of mass m , is placed on a set of independent viscous dampers in parallel with the independent elastic springs. The spring and dashpot coefficients K and C are

determined from the dynamic plate-load tests conducted on the soil. The amplitude and frequency are used to determine the spring constant and damping coefficient C. Barkan *et al.* (1977) introduced the concept of in-phase soil mass, m_s , which is supposed to be vibrating alongwith the footing. The in-phase soil mass was found to depend on the size and embedment of foundation and on the nature and properties of soil for a given mode of vibration. Barkan (1962) has shown that the error involved in the determination of natural frequency of soil-foundation system by neglecting the in-phase soil mass is not more than 10 percent. Basavanna (1975) has shown, by finite element method, that this error is negligible if the stress-strain characteristics are nonlinear, which is the case of soil. This model essentially requires the determination of spring constant K and damping coefficient C from dynamic plate load tests.

2.2.1.2 Elastic Half Space Theory

The dynamic response of a vibrating circular footing on the surface of a soil mass was first studied by Reissner (1936). Representing soil mass by an elastic half space, he developed an expression for the vertical displacement z , of the centre of a circular footing of radius r , under uniform loading :

$$z = \frac{F_0}{Gr} (f_1 + if_2)e^{i\omega t} \quad \dots(2.1)$$

where

F_0 = externally applied force which remains constant with frequency, ω

G = shear modulus of the elastic half space,

f_1, f_2 = dimensionless functions of Poisson's ratio and frequency factor a ,

a = $\omega r(\rho/G)^{1/2}$, and

ρ = density of the half space material

Reissner developed the expression for the amplitude of motion (A_z) :

$$A_z = \frac{F_0}{Gr} \left[\frac{f_1^2 + f_2^2}{(1 + ba^2f_1)^2 + (ba^2f_2)^2} \right]^{1/2} \quad \dots(2.2)$$

where

$$b = \text{dimensionless mass ratio} = m/\rho r^3$$

m = total mass of vibrating footing

Reissner's theory revealed the existence of radiation damping. The work of Reissner was extended by Shekhter (1948), Sung (1953), Quinlan (1953) and Arnold, Bycroft and Warburton (1955); who developed expressions for centre and average footing displacements with three contact stress distributions as:

- (i) Uniform, as assumed by Reissner
- (ii) Parabolic, with zero stress at the circumference of footing, and
- (iii) Rigid base, as for purely static loading of a rigid footing.

The dynamic responses were different for the three stress distributions with maximum amplitude increasing and the resonant frequency decreasing as the load is concentrated near the centre of footing. Hsieh (1962) suggested that this effect can be accounted for by multiplying the footing radius by a factor : 0.78 for uniform stress distribution and 0.59 for parabolic stress distribution.

Using Reissner's equation, Sung expressed the amplitude of vibration at the centre of footing in the dimensionless form :

$$A_2 = \frac{GrA_z}{F_0} = \left[\frac{f_1^2 + f_2^2}{(1 + ba^2f_1)^2 + (ba^2f_2)^2} \right]^{1/2} \quad \dots(2.3)$$

Hsieh (1962), considering the vibration of a weightless circular disc on an elastic half space, developed the equation of motion for a footing of mass m . For vertical vibrations :

$$m\ddot{z} + (G\rho)^{1/2} r^2 F_2' \dot{z} + GrF_1' z = F_0 e^{i\omega t} \quad \dots(2.4)$$

which is identical to the equation of motion for a damped mass spring system, if

following substitutions are made :

$$C_z = (G\rho)^{1/2} r^2 F'_2 \quad \dots(2.5)$$

$$K_z = GrF'_1 \quad \dots(2.6)$$

where F'_1 and F'_2 are the dimensionless functions of Poisson's ratio (ν) and frequency factor (a).

For $0 < a < 1.5$

$$\begin{aligned} \nu = 0.0, \quad F'_1 &= 4.0 - 0.5a^2 \\ &F'_2 = 3.3 + 0.4a \\ \nu = 0.25, \quad F'_1 &= 5.3 - 1.0a^2 \\ &F'_2 = 4.4 + 0.8a \\ \nu = 0.50, \quad F'_1 &= 8.0 - 2.0a^2 \\ &F'_2 = 6.9 \end{aligned} \quad \dots(2.7)$$

Dynamic solutions by means of integral equations have been presented by Awojobi *et al.* (1965) and Robertson (1966). Awojobi *et al.* studied all possible modes of oscillation of rigid circular and strip footings on a half space and presented solution for zero value of Poisson's ratio. For other values of Poisson's ratio, they presented approximate solutions only. Robertson solution is in the form of a power series which is applicable for a frequency factor 'a' less than unity.

The solution to the horizontal translation of a rigid circular disc on an elastic half space was presented by Arnold *et al.* (1955) and Bycroft (1956). Based upon this solution, Hsieh (1962) developed a solution expressed in the form of equation (2.4), where F'_1 and F'_2 are given by :

$$\begin{aligned} \text{for } 0 < a < 2.0 \\ \nu = 0.0, \quad F'_1 &= 4.5 - 0.2a^2 \\ &F'_2 = 2.4 + 0.3a \\ \nu = 0.25, \quad F'_1 &= 4.8 - 0.2a^2 \\ &F'_2 = 2.5 + 0.3a \end{aligned}$$

$$\begin{aligned} \nu &= 0.50, \quad F'_1 = 5.3 - 0.1a^2 \\ F'_2 &= 2.8 + 0.4a \end{aligned} \quad \dots(2.8)$$

Baranov (1967) developed an analytical approach for embedded foundations, considering the soil underlying the foundation base as an elastic half space and side soil to be composed of a series of thin independent elastic layers.

Gladwell (1968) presented a dynamic solution to the equation of motion for a weightless rigid circular footing resting on an elastic solid in which the assumption of stress distribution beneath the footing did not have to be made. His solution was carried out by using integral equations and has been presented in the form :

$$A_2 = \frac{(2 - \nu)}{8 \left[\left(r_1 - \frac{b(2-\nu)a^2}{8} \right)^2 + r_2^2 \right]^{1/2}} \quad \dots(2.9)$$

where r_1 and r_2 are dimensionless functions of frequency factor a , and Poisson's ratio ν .

The effect of layering nonhomogeneity of soil was studied by many investigators using the half space solutions. Bycroft (1956) and Warburton (1957) have studied the vertical vibration response of a circular footing on an elastic layer underlain by a rigid base. Effect of layering on maximum vibration amplitude was evaluated by Warburton and calculated in terms of the magnification of static displacement of footing on elastic half space by Richart *et al.* (1970).

Novak *et al.* (1972) developed an approximate analytical solution for vertical vibrations of a footing embedded in elastic half space based upon the approach of Baranov (1967). They developed the expressions for frequency-dependent stiffness K_z and frequency-dependent damping coefficient C_z as :

$$K_z = Gr \left(C_1 + \frac{G_s}{G} \frac{H}{r} S_1 \right) \quad \dots(2.10)$$

$$C_z = \frac{Gr}{\omega} (C_2 + \frac{G_s}{G} \frac{H}{r} S_2) \quad \dots(2.11)$$

where

G = shear modulus of soil beneath the footing

G_s = shear modulus of side layer

ρ_s = mass density of side soil

r = radius of footing

H = depth of embedment of footing

C_1, C_2 are functions of dimensionless frequency, $a = \omega r(\rho/G)^{1/2}$

S_1, S_2 are functions of dimensional frequency, $a = \omega r(\rho_s/G_s)^{1/2}$

where C-terms relate to the elastic half space and S-terms to the side soil.

Awojobi (1972) developed an approximate solution for the vertical vibration response of a circular footing on the surface of an incompressible soil for which shear modulus increased linearly with depth, zero at surface. He found the footing response to be nearly the same as a footing on an elastic half space with a shear modulus, the same as that of the non-homogeneous soil at a depth equal to footing radius. Novak and Beredugo (1972) examined the vertical vibration response of footings embedded in an elastic layer. Their solution was in the form of equations (2.10) and (2.11) wherein C_1 and C_2 have different values for H_1/r ratios; H_1 is the stratum thickness below footing level.

Gazetas *et al.* (1979) developed a solution for the vertical vibration response of strip footing on the surface of a linearly hysteretic, elastic layer overlying rock. They found that response depends upon the mass ratio (b) and the relative rigidity of the soil and rock, and the presence of a thin layer tends to increase the resonant frequency and amplitude as compared to half space values.

Kagawa *et al.* (1981) carried out a parametric study in which the soil deposit was idealised by two layers, the bottom layer being treated as a half space. They concluded that a large amplitude magnification may be established due to layering effects as compared to half space solutions. Layering has a large effect on

resonant frequency for small mass ratios but a small effect at large mass ratios. As G_2/G_1 exceeds 20, the vibration response is similar to that for an infinitely stiff layer; G_1 and G_2 being the shear moduli of 1st and 2nd layers. The resonant frequency for a two layered system is generally less than that for an elastic half space contrary to the conclusions of Gazetas *et al.* (1979).

Nagendra *et al.* (1982) presented an analysis to evaluate the stiffness coefficients for vertical and horizontal modes, using theory of elasticity. The stiffness coefficients have been presented for rigid, uniform and parabolic pressure distributions considering central, average and weighted average displacements.

Gazetas *et al.* (1985) presented a simple method for estimating the dynamic stiffness and damping coefficients of arbitrarily shaped rigid foundation embedded in a homogeneous halfspace and with partial or complete sidewall-soil contact under vertical vibrations. The method provided an improvement over the existing 'equivalent circle' approximation for arbitrarily shaped foundations.

Wong *et al.* (1985) presented tables of horizontal, coupling, rocking, vertical and torsional impedance functions for a rigid massless square foundation resting on two types of layered visco-elastic soil models. The first model was corresponding to a uniform layer overlying a uniform half space while the second corresponds to a layer with linearly varying properties overlying a uniform half-space.

Dobry *et al.* (1986) presented analytical results for various vibration modes, frequency and foundation shapes, for effective dynamic stiffness and damping coefficients of rigid foundations on deep soil deposits. Both stiffness and damping are affected to various degrees by frequency and foundation shape; the effect being more for long foundations and saturated soils. The method provided an improvement of the 'equivalent circle' method which often caused errors in the calculations of stiffness and damping coefficients.

Gazetas (1991) presented simple algebraic formulas and charts for estimating

the dynamic impedances (springs and dashpots) of foundations for all the significant translational and rotational modes of vibration. The formulas and charts are valid only for a constant embedment depth and solid basemat of any shape and with any degree of contact with side soil.

Navarro (1992) carried out analysis to calculate the soil radiation damping for a rigid circular foundation subjected to the action of a vertical harmonic load of fixed amplitude. The foundation rested on an elastic layer of constant thickness overlying an elastic half-space. The radiation damping ratio is calculated as a function of layer thickness to foundation radius ratio, Poisson's ratio, and layer and half space mechanical impedances.

2.2.1.3 Lumped Parameter Approach

Hsieh (1962) and Lysmer *et al.* (1966) have shown that the elastic half space model behaves similarly to a damped mass-spring system. Lysmer *et al.* developed the following equation of motion for vertical vibration :

$$m\ddot{z} + \frac{3.4}{(1-\nu)} r^2(G\rho)^{1/2}\dot{z} + \frac{4Gr}{(1-\nu)} z = F_0 e^{i\omega t} \quad \dots(2.12)$$

where

$$\text{damping coefficient, } C_z = \frac{3.4}{1-\nu} r^2(G\rho)^{1/2} \quad \dots(2.13)$$

$$\text{and spring constant, } K_z = \frac{4Gr}{1-\nu} \quad \dots(2.14)$$

where m , ν , G , r and F_0 are as defined already in 2.2.1.2.

Displacement amplitude

$$A_z = \frac{(F_0/K_z)}{((1 - B_z a^2)^2 + (0.85a)^2)^{1/2}} \quad \dots(2.15)$$

and modified mass ratio for vertical vibrations,

$$B_z = \frac{(1-\nu)}{4} \frac{m}{\rho r^3} \quad \dots(2.16)$$

They found that resonance occurs only when $B_z > 0.36$.

The resonant frequency and maximum amplitude are:

$$\omega_r = (G/\rho)^{1/2} \frac{(B_z - 0.36)^{1/2}}{B_z r} \quad \dots(2.17)$$

$$A_{\max} = \frac{F_0}{K_z} \frac{B_z}{0.85(B_z - 0.18)^{1/2}} \quad \dots(2.18)$$

where resonant frequency factor

$$a_r = \frac{(B_z - 0.36)^{1/2}}{B_z} \quad \dots(2.19)$$

$$\text{and } A_{2\max} = \frac{GrA_{\max}}{F_0} = \frac{b(1-\nu)^2}{6.8(b(1-\nu) - 0.72)^{1/2}} \quad \dots(2.20)$$

$$D_z = \frac{0.85}{b^{1/2}(1-\nu)^{1/2}} \quad \dots(2.21)$$

Richart *et al.* (1967) extended the Lysmer analog by demonstrating that all modes of vibration can be studied by using lumped parameter model selecting the frequency independent parameters properly. They suggested the choice of stiffnesses appropriate for low frequencies, and of average damping values over the range of frequencies at which resonance usually occurs. They recommended that a fictitious mass be added to the actual foundation mass to obtain a good agreement between the resonant frequencies of the actual and lumped parameter system.

Richart *et al.* (1970) presented expressions for stiffness, mass ratio, damping ratio and fictitious added mass for all the four modes of vibration. For vertical vibrations, the frequency ratio and maximum amplitude can be expressed in the dimensionless form:

$$a_r = \frac{2}{(b(1-\nu) - 1.44)^{1/2}} \quad \dots(2.22)$$

$$\text{and } A_{1\max} = \frac{1 - \nu}{1.7(b(1 - \nu) - 0.72)^{1/2}} \quad \dots(2.23)$$

Bycroft (1956) has developed an expression for the spring constant for sliding motion to be used with lumped parameter model :

$$K_x = \frac{32(1-\nu)Gr}{(7-8\nu)} \quad \dots(2.24)$$

Richart *et al.* (1970) gave the expression for damping ratio D_x for sliding vibration

$$D_x = 1.63 \left[\frac{1-\nu}{b(7-8\nu)} \right]^{1/2} \quad \dots(2.25)$$

Anandakrishnan *et al.* (1973) used the lumped parameter model to develop an analytical solution for the effect of embedment on vertical vibration response of footings. They assumed that the force exerted on the vertical sides of the embedded footing could be represented by Coulomb friction damping. The Coulomb friction force F' , is given by

$$F' = (0.5 K_0 H_1^2 \rho g \mu_f + C_a H_1) L_p \quad \dots(2.26)$$

where

K_0 = Coefficient of earth pressure at rest

ρ = mass density of soil

g = gravitational acceleration

μ_f = coefficient of kinematic friction between the soil and sides of the embedded footing (typically, 0.15 - 0.20)

C_a = adhesion between the soil and the sides of the embedded footing (1% to 2% of undrained cohesive strength of soil).

L_p = perimeter length of embedded footing

A favourable comparison was reported, by authors, between the predictions and experimental observations.

Sridharan *et al.* (1981) described a theoretical procedure similar to that used by Anandakrishnan *et al.*; the two yielding similar results.

Nagendra *et al.* (1981) presented analog solutions for the response of a circular footing resting on an elastic half space with uniform and parabolic contact pressure distributions and subjected to frequency dependent and frequency independent excitations. They also presented analog solution to a rigid circular footing subjected to frequency dependent excitation. The results were compared with the rigorous solution of Sung (1953) and the agreement was found to be good.

Triantafyllidis *et al.* (1988) presented an analytical method to calculate the dynamic lumped parameter of a circular rigid foundation resting upon a homogeneous, isotropic, linear elastic half space subjected to harmonic excitation, using a system of integral equations. They presented the frequency dependent stiffness functions for all degrees of freedom, different Poisson's ratios and perfect as well as partial bonding between the foundation and half space.

Sridharan *et al.* (1990a) presented analog solutions in the form of equations (non-dimensional frequency factor vs. modified mass ratio, non-dimensional magnification factor vs. modified mass ratio) for all modes of vibration, viz., vertical, horizontal, rocking and torsional. The results obtained were found to have good agreement with those obtained from elastic half-space theory.

Baidya *et al.* (1996) presented a realistic method based on 'lumped parameter approach', to estimate the damping of machine foundation soil system on a stratum. It was reported that damping increases with the increase of stratum thickness and it attains the constant half space value when h/r becomes more than 6, where h is the thickness of stratum below the base of footing of radius r . A simple empirical equation is developed for damping which agrees very well with actual analysis for h/r greater than 1.5.

2.2.1.4 Approaches Based On Numerical Techniques

Luco *et al.* (1968) utilized mathematical techniques to solve mixed boundary-value elastodynamic problems.

Karasudhi *et al.* (1968) obtained the 'exact' numerical solutions for all modes of vibration of strip footings on a half space.

Lysmer *et al.* (1969) described a finite dynamic model for the infinite media using special viscous boundary to show the effects of embedment of a rigid circular footing on the response to vertical vibrations. They showed that the effect of embedment is to increase both stiffness as well as damping.

Kaldjian (1969), using elastic finite element method developed solution to show the effect of embedment on vertical vibrations of a circular footing. The sides of the footing were assumed to be adhered to the surrounding soil. He reported increased stiffness as compared to the case when soil is not in contact with the sides of footing.

Luco *et al.* (1971) extended the available halfspace solution for circular foundations to the high frequency range. Waas *et al.* (1972) used the finite element method to obtain the solution of dynamic problem for other modes of vibration. Veletsos *et al.* (1973) used the available solutions to a viscoelastic material with linear hysteretic damping.

Ulrich *et al.* (1973) compared the standard viscous boundary with Rayleigh wave boundary and recommended the use of Rayleigh wave boundary. A combination of these two boundaries was used by Brandow (1971),

Johnson *et al.* (1975), using finite element solution, examined the effect of layer thickness and embedment depth on the stiffness for various vibration modes. The stiffness is increased due to increasing depth of embedment and decreasing layer thickness.

Valliappan *et al.* (1977) preferred the use of consistent mass matrix over lumped mass matrix. They reported increase in stiffness and reduction in amplitude with increasing embedment of foundation.

DasGupta *et al.* (1978) analyzed the dynamic response of rectangular footings using three dimensional finite element model. They reported that embedment can reduce the amplitudes of vibration for small and high frequency ratios as does the

static surcharge as well.

Gazetas *et al.* (1979) presented a method based on direct solution of wave equations in term of displacements for vertical vibrations of massive, infinitely long foundations carrying constant force or rotating mass type of oscillators placed on the surface of a linearly hysteretic elastic layered half space.

Hadjian *et al.* (1985) presented a simple yet relatively accurate method for the calculation of equivalent elastic properties of layered media. In vertical motion, the nonuniform medium is modelled by a series of springs as influenced by stress level with depth. The spring system is then replaced by a single spring and hence a single uniform half-space. A set of equivalent uniform properties for each degree of freedom in stiffness as well as damping are obtained which provide good estimates of the correct analytical results for layered media.

Wong. *et al.* (1986) presented a boundary integral equation technique to calculate the dynamic response of a group of rigid foundation of arbitrary shape bonded to a layered viscoelastic half-space and subjected to external forces and seismic excitation. It was found that for small separations the calculated impedances are markedly affected by the choice of discretization of foundations.

Gazetas *et al.* (1987a), using a boundary element formulation developed simple algebraic formulas and dimensionless parametric charts for estimating the horizontal static and dynamic stiffness of a rigid foundation with arbitrary base-shape, embedded in a homogeneous halfspace. The results were applicable for a constant depth of embedment, but encompassed all types of sidewall-soil contact including perfect, partial symmetric, nonsymmetric and no contact at all. They also presented simple algebraic formulas and parametric charts for estimating radiation dashpot coefficients of horizontally oscillating rigid foundations that are embedded in a halfspace and have arbitrary base shapes and partial or complete sidewall-soil contact in a companion paper, Gazetas *et al.* (1987b).

Nayfeh *et al.* (1989) obtained an approximate analytical solution of the nonlinear dynamic response of foundation on soils under vertical vibrations. The

analysis accounted for the non-linearity of soil structure, radiation, hysteretic and viscous damping and the effect of embedment. They reported the presence of large responses at other subharmonics which implied that designing the foundation arbitrarily to have a natural frequency larger or smaller than the excitation frequency will not necessarily ensure safe design. The amplitude of vertical vibrations decreases with embedment.

Ahmad *et al.* (1991) studied the dynamic response of an embedded rigid strip footing in layered soil under horizontal excitation using a rigorous algorithm of the boundary element method incorporating isoparametric boundary elements. It was observed that the dynamic horizontal stiffness of strip footing is influenced by the depth of embedment, the height of side-wall-soil contact and the layering characteristics of soils. An additional damping is introduced in the system due to embedment of footing.

Gucunski *et al.* (1993) analysed the vertical oscillations of a flexible circular plate on the surface of an elastic half space and an elastic layered system to determine the displacement and soil reaction distributions at the soil-plate interface and the impedance functions. The response of a flexible plate is influenced by the stiffness ratio, mass and stiffness distribution of the plate, the loading distribution and the soil stratification.

Borja (1993) investigated the dynamic response of vertically excited rigid foundations on an elastic-viscoplastic half-space using nonlinear finite element. It was reported that the effect of repeated loading on machine foundation is to create a zone of intense yielding and inelastic deformation beneath the foundation, resulting in dynamic nonhomogeneity with respect to soil elasticities. The radiation damping is smaller for a half space problem containing a local yield zone than it is for the same half space problem without an yield zone.

Meek *et al.* (1994) presented the dynamic analysis of surface footings by idealising the soil as a truncated cone instead of an elastic half space. The embedded foundation is modelled by using a stack of disc pairs and making

subsequent calculations by conventional matrix methods and finite element method. The accuracy of both frequency-domain and time-domain formulations is just as good as for surface footings.

2.2.2 Experimental Investigations

Tests have been conducted by various researchers, to investigate the dynamic behaviour of foundations, on large sized blocks in the field and on small sized blocks in laboratory. Generally mechanical oscillators, capable of producing frequency dependent large dynamic loads, were used in field tests. Tests on small sized blocks have been performed in sand tank in the laboratory. Electromagnetic oscillator is normally used in these tests to apply dynamic loads of low magnitude which are independent of frequency.

2.2.2.1 Experimental Studies on Large Blocks

Savinov (1955) reported the experimental studies carried out by Kondin in the 1940's. Field tests were conducted considering all modes of vibration on surface and embedded foundations. The effect of side soil resistance was not significant in case of vertical vibrations. For horizontal translation and rocking, the effect of side fill can be neglected only if the embedment ratio D/B , (D =depth of embedment, B =width of foundation) is less than or equal to $1/2$. As compared to a surface foundation ($D/B=0$), Kondin reported an increase in resonant frequency between 1.5 to 2.0 and reduction of amplitude between 0.4 to 0.6 for $D/B=1/2$ to 1. Small change in vertical response was perhaps due to loose side fill.

Barkan (1962) compared the dynamic response of surface and embedded foundations on silty clay with interbedded sand layers. The ground water table was much below the foundation level. It was observed that amplitude of vibration reduced to $1/3.5$ and damping increased by 3.5 times upon embedment of the foundation. Barkan attributed this change in dynamic response to the development of elastic reactions between the foundation and sidefill. The increase in damping is due to dissipation of energy. In case of low tuned foundations, ignoring the

effect of embedment is likely to endanger dynamic stability. Novak (1970) conducted field tests on a concrete block of $1\text{m}\times 1\text{m}\times 1\text{m}$ placed on undisturbed loess loam which was also used as backfill material. He observed that embedment affected the dynamic response and the effect was maximum when the side soil was undisturbed.

Novak *et al.* (1972) performed field tests on two concrete blocks $68.6\text{cm}\times 68.6\text{cm}\times 122\text{cm}$ and $48.3\text{cm}\times 96.6\text{cm}\times 122\text{cm}$ cast directly into the foundation pit. The effect of embedment was studied by removing the undisturbed side soil around the blocks. The experimental results were compared with theoretical estimates based on Baranov's approach which showed overestimation of the resonant amplitudes.

Anandakrishnan *et al.* (1973) conducted vertical vibration tests on silty clay with river sand as backfill material. The sizes of the footings used in tests were $80\text{cm}\times 80\text{cm}\times 120\text{cm}$ (height), $105\text{cm}\times 105\text{cm}\times 75\text{cm}$ (height); and 90cm diameter $\times 120\text{cm}$ (height) and 120cm diameter $\times 67.5\text{cm}$ (height) respectively. It was observed that resonant frequency increased by 10% at embedment ratio < 0.4 and increased more for embedment ratio greater than 0.4. Stokoe *et al.* (1974) reported studies on two prototype foundations of size $221\text{cm}\times 140\text{cm}\times 122\text{cm}$ (height) in clayey silt deposit and $457\text{cm}\times 152\text{cm}\times 223\text{cm}$ (height) in silty fine sand deposit. The dynamic responses of the embedded and surface foundations were compared. They observed that the effect of embedment was not significant in case of foundation in clayey silt, which they attributed to the lack of confining pressure due to inadequate compaction of soil during backfilling or drying of the side soil or permanent deformation of backfill. For the foundation embedded in brown silty fine sand, they observed that the dynamic response was significantly affected by the embedment which they reported due to the confining pressure developed between the foundation block and adjacent soil.

Petrovski (1975) reported field tests on circular block of radius 1 m and rectangular block of size $1\text{m}\times 2\text{m}\times 2\text{m}$ with embedment ratios of 0, 1/3, 2/3 and 1.0.

The soil showed a non-linear behaviour with softening effect. The block was excited at four levels of excitation. The increase in excitation level resulted increase in resonant amplitude and decrease in resonant frequency. With the increase in embedment, it was observed that the resonant frequency increased, the resonant amplitude decreased and the damping coefficient increased twice or more.

Ranjan *et al.* (1978) conducted field tests on large concrete blocks of size 150cm×75cm×70 cm in field and small concrete blocks of size 15cm×15cm×15cm on silty sand in laboratory. The large block was subjected to frequency dependent dynamic loads while the small block was subjected to constant force dynamic load. The tests were conducted on block placed at surface and with embedment ratios of 0.25, 0.75 and 1.0. It was observed that the resonant amplitude decreased to about 1/3.3 when embedment ratio increased to 0.75. For large size block, the resonant frequency did not change appreciably. For small size block, the resonant amplitude decreased to about 1/4 and the resonant frequency increased to 2.4 times when the embedment ratio increased to 1.0.

Saran *et al.* (1979) conducted insite tests on existing embedded foundation of a sawing machine on poor silty sand. The size of the foundation was 1m×1m×0.75m with depth of embedment 0.65m. Both vertical and coupled horizontal and rocking tests were performed at four different excitation levels. It has been reported that at low exciting level, the effect of embedment in coupled vibration test was more pronounced than in vertical vibration test.

Vijayvargiya (1980) performed experiments in the field on concrete block of size 1.5m×0.75m×0.7m high on a uniform deposit of silty sand and on a clayey soil. The block was instrumented with specially designed cells to measure elastic side soil resistance and base pressures. The block was excited at four different excitation levels in vertical and coupled vibration modes. It was observed that as the excitation level increases, the amplitude of vibration increases and the resonant frequency decreases. For a constant excitation level, the increase in embedment ratio resulted in an increase in the resonant frequency and decrease in

resonant amplitude. For the same value of dynamic force to weight ratio, increase in embedment caused an increase in damping factor, stiffness coefficient and in-phase soil mass. The elastic average shear resistance developed at vertical side was found to vary exponentially with depth of embedment.

Prakash *et al.* (1981) have presented the data of a large number of forced vertical and horizontal vibration tests, free vibration tests, shear modulus (Rayleigh wave) tests and cyclic plate load tests conducted in the field on various Indian soils. They suggested an approach for determining the strain-dependent values of dynamic shear modulus from field tests particularly for the cohesionless soils below the water table. The approach was an attempt to account for the effect of significant parameters affecting the value of shear modulus G , while interpreting the field test data to determine a realistic value of G for use in dynamic soil structure interaction problems.

Lopes *et al.* (1985) presented the results of a set of in-situ vibration tests performed on a concrete block, resting on young residual soil, using a specially devised vibrator. It was suggested that a plot of stiffness versus dynamic force-block weight ratio should be produced and the appropriate design stiffness could be obtained from the plot for the actual machine's dynamic force-block weight ratio. The damping factor can be evaluated by using the bandwidth method.

Sridharan *et al.* (1990b) proposed a simple and approximate procedure called weighted average method to obtain the equivalent stiffness of a layered soil system knowing the individual values of the layers, their relative position with respect to the foundation base and their thicknesses. They conducted field vibration tests using a square footing over different two and three-layered systems and compared the experimental values with those obtained theoretically. The agreement was found to be good.

2.2.2.2 Model Tests in Laboratory

Large number of studies on small size blocks under controlled soil conditions

in laboratory have been reported in literature. Some of them are discussed below:

Chae (1971) conducted model tests on square and rectangular foundation blocks of sizes 30cm×30cm and 30cm×60cm and on circular blocks of diameter 20 cm, 30 cm and 40 cm having different weights. These foundations were made of 2.5 cm thick steel plates. The tests were performed in a sand bin of size 1.46m×1.46m×1.22m high and the depth of embedment was varied from 5 cm to 20 cm. The sand was compacted to a density of 1.76 g/cm³ in 6 layers of 20 cm thickness using a vibratory compactor. The range of frequency was 0.4 cps to 2000 cps in a constant force electromagnetic exciter. The test results indicated that the resonant amplitude of embedded foundation is greatly reduced by the additional shear resistance along the sides of the footing and a change in contact pressure distribution. For a given depth, the system with a higher mass produced greater amplitude. The amplitude reduction factor R_d , the ratio of maximum amplitude of embedded foundation to that of the surface foundation, was governed by the equation

$$R_d = 1 - 1.25(D/d) \quad \dots(2.27)$$

where D is depth of embedment and d is diameter of footing. The embedment does not change significantly the resonant frequency resulting from greater mass associated with the footing vibration.

Gupta (1972) reported model tests on eight wooden block-foundations. Four of these foundations had rectangular shape having same weight of 5.9 kg but different base areas, whereas the other four had same area 54.84 cm² and weight 2.04 kg but having different shapes i.e.; square, rectangular, triangular and circular. The areas of the footing varied from 9.4cm×5.8cm to 13.2cm×14.7cm and the depth of embedment upto 6 cm. The sand was uniformly graded and was compacted to a relative density of 55.4 percent. The coefficient of elastic uniform compression C_u of the soil was determined by the cyclic plate load test. It was observed that C_u increases directly with square root of embedment depth. The effective soil mass also increased with embedment ratio. The damping factor increased directly with an

increase in the embedment ratio as the square root of embedment ratio.

Stokoe and Richart (1974) reported model tests on dynamically loaded foundation resting on surface and embedded into ground. Cast-in-situ concrete model footings of sizes 20cm to 30cm diameter were tested varying the embedment ratio from 0 to 1.6. The soil was poorly graded sand with average void ratio of 0.52 and water content of 4 percent. The test results indicate that as the depth of embedment increases, good soil-foundation contact increases the damped natural frequency and damping ratio for this system. However, if the soil-foundation contact is not effective, no significant change in the dynamic response of the foundation is noted. As the depth of embedment increases, the coefficient of elastic uniform compression of soil C_u , also increases.

Yoshinori Nii (1987) performed experiments to determine the dynamic stiffness of circular and rectangular footings embedded in model half-space under vertical vibrations. The model half space was made of silicon rubber which has small hysteretic damping and a Poisson's ratio of 0.5. The measured static stiffness values coincide with the calculated value of the exact solution for circular footings and exact solution using equivalent circular footing for rectangular footings. The stiffness coefficient of the embedded footing was found to be similar to that for the surface footing.

Pak *et al.* (1995) conducted an experimental investigation to examine the vertical dynamic response of surface foundations on granular soils, using a geotechnical centrifuge. It was revealed that the foundation response has a significant nonlinear dependence on the soil bearing pressure and footing dimension. It was found that the equivalent homogeneous Poisson's ratio of the soil can be taken as 0.25 while the equivalent homogeneous shear modulus of soil can be related through a power law to the soil's void ratio, footing radius and the average foundation bearing pressure.

2.3 DETERMINATION OF DYNAMIC SOIL PROPERTIES

In this section, a brief description of the literature pertaining to the determination of the dynamic stiffness properties of soil has been brought out. The design of the foundations for cyclic and vibratory loads requires the determination of dynamic soil properties. Since the dynamic properties of soils are strain dependent, various laboratory and field techniques have been developed to measure these properties over a wide range of strain amplitudes. First, the use of cyclic plate load test for determining the dynamic properties of soil is described. Barkan (1962) first described the use of cyclic plate load test to evaluate the coefficient of elastic uniform compression C_u , for the design of a dynamically loaded foundation. The test consisted of a plate subjected to a few load repetitions of loading and unloading cycles. A graph of loading intensity p versus plate settlement S_t , was prepared, which permits the easy separation of elastic part of settlement S_e , from the total settlement S_t . A plot of p versus S_e was prepared, the slope of which gave the value of coefficient of elastic uniform compression C_u from which the spring constant K of the soil and the resonant frequency 'f' of the foundation soil system can be calculated as :

$$C_u = \frac{K}{A} = \frac{4\pi^2 f^2 M}{A} \quad \dots(2.28)$$

where M is the equivalent mass of the foundation-soil system and A is the base area of foundation.

Barkan (1962) also compared the natural frequency observed from free or forced vertical vibration tests with the one computed from ' C_u ' obtained from cyclic plate load tests and established that a good agreement existed between the two.

Richart *et al.* (1970) have suggested the cyclic plate load test for obtaining the shear modulus of soils. Hoadley (1985) recommends the use of cyclic plate load test on important projects to supplement the soil stiffness parameters obtained

from other methods. Moore (1985) illustrated the estimation of C_u and G from the cyclic plate load test and the use of the same in the design of foundation of a centrifugal pump. Puri *et al.* (1991) carried out cyclic plate load tests to study the effect of vertical reinforcements on C_u .

The cyclic plate load test is one of the field tests suggested in Indian Standard IS:5249-1977 for the determination of dynamic stiffness parameter C_u . The test is widely used in India to estimate C_u [Prakash *et al.* (1968, 1979), Prakash and Gupta (1971), Saha and Chattopadhyay (1984), Basavanna *et al.* (1984), Lavania and Mukherjee (1984), Ranjan and Kumar (1989), Saran (1990), Babushanker *et al.* (1991), Khan *et al.* (1992)].

The cyclic plate load test has been used to determine C_u for reinforced soils by Patel *et al.* (1983). The results of these tests on reinforced soils are described in the subsequent sections.

Hardin (1965) gave the following expression for the hysteretic damping D^* of sand in terms of the shear strain γ and the mean effective confining pressure σ'_0 (kPa) :

$$D^* = \frac{0.985\gamma^{0.2}}{(\sigma'_0)^{0.5}} \quad \dots(2.29)$$

Hardin and Black (1966) suggested the following relationship for G_{\max} for rounded and angular sands :

Rounded sand ($e' < 0.8$)

$$G_{\max} = \frac{6931(2.17 - e')^2 (\sigma'_0)^{1/2}}{(1 + e')} \quad \dots(2.30)$$

Angular sand

$$G_{\max} = \frac{3230(2.973 - e')^2 (\sigma'_0)^{1/2}}{(1 + e')} \quad \dots(2.31)$$

where e' is the void ratio of sand

G_{\max} is the maximum value of shear modulus.

σ'_0 is the mean effective confining pressure in kPa.

Hardin and Black (1969) gave the following expression for the maximum value of shear modulus G_{\max} (at low strain of 10^{-6}) :

$$G_{\max} = 1230 \text{ OCR}^k \frac{(2.973 - e')^2}{(1 + e')} (\sigma'_0)^{0.5} \quad \dots(2.32)$$

where

OCR is the over consolidation ratio

σ'_0 is the effective all-round stress in psi,

e' is the void ratio.

and k is a factor depending upon the plasticity index of clays.

Seed and Idriss (1970) gave the following equation for G_{\max} of sands :

$$G_{\max} = 1000 K_2 (\sigma'_m)^{0.5} \quad \dots(2.33)$$

where

σ'_m = mean effective confining stress in psf.

K_2 = an empirical factor depending upon the relative density of sand.

Ishihara (1971) discussed the strain levels associated with different phenomenon in the field and in corresponding field and laboratory tests. The shear strains associated with the in-situ vibratory tests are of the order of 10^{-3} to 10^{-5} whereas those associated with the repeated loading tests are 10^{-1} to 10^{-4} .

The effect of average effective confining pressure on shear modulus (or C_u) has been studied by Silver and Seed (1971).

$$G_1/G_2 = (\bar{\sigma}_1 / \bar{\sigma}_2)^{m'} \quad \dots(2.34)$$

where G_1 and G_2 are the shear moduli at effective confining pressures $\bar{\sigma}_1$ and $\bar{\sigma}_2$ and m' varies from 0.3 to 0.7. IS:5249-1977 recommends an average value of $m' = 0.5$.

Hardin and Drnevich (1972a) suggested an expression similar to (2.32) for G_{\max} of both sands and clays :

$$G_{\max} = 3230 \frac{(2.973 - e')^2}{(1 + e')} \text{OCR}^k (\sigma'_0)^{1/2} \quad \dots(2.35)$$

where σ'_0 is the mean effective confining stress in kPa .

Hardin and Drnevich (1972b) developed a unified stress-strain relationship for both sands and clays relating D^* to G . Initial loading stress-strain curve is approximated by a hyperbolic function defined in terms of initial shear modulus G_{\max} and a reference strain γ_r , where $\gamma_r = \tau_{\max}/G_{\max}$, τ_{\max} being the shear stress at failure in the soil.

D^* is related to D_{\max}^* as :

$$D^* = D_{\max}^* \left(1 - \frac{G}{G_{\max}} \right) \quad \dots(2.36)$$

The hyperbolic stress-strain curve defining the initial loading curve and also the end points of the complete stress-reversal loop is :

$$\frac{G}{G_{\max}} = \frac{1}{1 + \frac{\gamma}{\gamma_r}} \quad \dots(2.37)$$

where γ is the shear strain at which value of G is required to be determined.

The empirical relationship for D_{\max}^* is :

for clean dry sand,

$$D_{\max}^* (\%) = 33 - 1.5 \log_{10} \bar{N} \quad \dots(2.38)$$

and for clean saturated sands :

$$D_{\max}^* (\%) = 28 - 1.5 \log_{10} \bar{N} \quad \dots(2.39)$$

where \bar{N} is the number of cycles of loading.

Ohsaki and Iwasaki (1973) based upon seismic cross-hole survey gave the following expression for G_{\max} for sands and clays,

$$G_{\max} = 12000 N_1^{0.8} \text{ (kPa)} \quad \dots(2.40)$$

where

N_1 = N-value recorded in Standard Penetration test.

Richart (1977) gave the following expression for the shear modulus of clean sands :

For round-grained sands ($e' < 0.8$)

$$G_{\max} = \frac{700(2.17 - e')^2}{1 + e'} (\bar{\sigma}_0)^{0.5} \quad \dots(2.41)$$

and for angular sands :

$$G_{\max} = \frac{326(2.97 - e')^2}{(1 + e')} (\bar{\sigma}_0)^{0.5} \quad \dots(2.42)$$

where G and $\bar{\sigma}_0$ are expressed in Kg/cm^2 .

Iwasaki and Tatsuoka (1977) determined experimentally from tests on clean sands ($0.61 < e' < 0.86$ and $0.2 < \bar{\sigma}_0 < 5 \text{ Kg/cm}^2$) at shear strain amplitude of 10^{-6} that

$$G_{\max} = \frac{900(2.17 - e')^2}{(1 + e')} (\bar{\sigma}_0)^{0.38} \quad \dots(2.43)$$

Hardin (1978) refined and expressed equation (2.35) in non-dimensional form as :

$$G_{\max} = \frac{A' \text{OCR}^k (\sigma'_0)^{n'}}{F(e')} (p_a)^{1-n'} \quad \dots(2.44)$$

where

$$F(e') = 0.3 + 0.7 e'^2, \quad 0.4 \leq e' \leq 1.2$$

p_a is the atmospheric pressure.

A' is a dimensionless parameter.

for $n' = 0.5$, $A' = 625$.

Edil and Luh (1978) correlated G with grain characteristics of sands such as roundness and surface texture.

$$\text{For sands, } \frac{G}{G_0} = 1.004 - 345.4 \gamma \quad \dots(2.45)$$

where G and G₀ are in kP_a units.

In terms of void ratio (e')

$$G_0 = \left[0.769 + \ln \left(\frac{\sigma'_0}{98.07} + 1 \right) (2.793 - 2.195e') - 0.801R \right] \times 10^{-5} \quad \dots(2.46)$$

where R is a dimensionless measure of mean roundness assessed visually with the aid of standard chart.

Woods (1978) has presented an extensive overview of the available methods of measuring dynamic soil properties in the laboratory and field.

Prakash *et al.* (1981) suggested an approach for determining the strain dependent values of dynamic shear modulus from field tests; for use in dynamic soil structure interaction problems.

Seed *et al.* (1986) have related the standard penetration values with low strain shear modulus G_{max} in psf units :

$$G_{\max} = 1000 K_2 (\bar{\sigma}_0)^{0.5} \quad \dots(2.47)$$

where $K_2 = 20(N_1)_{60}^{1/3}$,

(N₁)₆₀ = corrected value of N measured in SPT delivering 60% of the theoretical free fall energy.

$\bar{\sigma}_0$ = mean effective confining pressure psf.

Ray and Woods (1988) conducted laboratory tests on five different cohesionless soils to determine their modulus and damping using torsional simple shear and resonant column tests. Modulus increases whereas damping decreases with the increase in number of cycles.

Sridharan *et al.* (1990b) proposed weighted average method to obtain the equivalent stiffness of layered soil system knowing the individual stiffnesses of the soil layers, their thicknesses and relative position with respect to the foundation base. Hryciw and Thomann (1993) gave an empirical, stress history based model for small strain shear modulus G^e of cohesionless soils. Various sands were tested in 18 cm diameter oedometer. It was found that G is approximately proportional to $1/2$ power of confining stress.

Pak and Guzina (1995) have given the following empirical relationship for shear modulus of sands:

$$G = 1.64 \frac{(2.97 - e')^2}{1 + e'} (a_{pr}/1m)^{0.1} (p_{pr}/1kPa)^{0.5} \quad \dots(2.48)$$

where

e' is void ratio of soil

a_{pr} is the proto-type footing radius (m), and

p_{pr} is the static foundation bearing pressure (kPa)

Fahoum *et al.* (1996) have studied the dynamic properties of compacted cohesive soils; kaolinite, sodium montmorillonite and calcium montmorillonite treated with time upto 8%. The cyclic shear modulus decreased for all types of soils and the equivalent viscous damping ratio increased with increase in strain levels.

2.4 STRENGTH CHARACTERISTICS OF REINFORCED EARTH SLABS UNDER STATIC LOAD

Since the introduction of basic concept of reinforced earth and visualization of the idea of improving bearing capacity of footings over inferior soil by Vidal (1966), the strength characteristics of reinforced earth slabs under static loads have been studied by a number of investigators experimentally as well as analytically.

Binquet and Lee (1975 a and b) conducted the bearing capacity analysis of a strip footing on granular soil containing horizontal layers of tensile reinforcement. They assumed the following three failure modes :

- (i) Shear failure above uppermost layer of reinforcement,
- (ii) Pull-out of reinforcement ties and,
- (iii) Breakage of reinforcement ties.

Based on the above failure modes, they developed a relationship for calculating the bearing capacity of the reinforced earth slab or alternatively designing a reinforced earth slab of certain bearing capacity based on the bearing capacity value of unreinforced earth slab. To verify the hypothesis expressed by the analytical method, they conducted laboratory tests on strip footing on sand reinforced by aluminium strips. The number of reinforcing layers and depth of first layer of reinforcement were varied. The optimal number of reinforcing layers to obtain maximum bearing capacity varied between six to eight. A reasonable agreement was obtained between the theoretical and experimental results.

Saran and Talwar (1978) studied the pressure settlement characteristics and bearing capacity of strip footing on sand beds reinforced with aluminium foil strip. The length and width of the strip were varied. It was observed that the bearing capacity of reinforced soil increases and settlement decreases with decrease in the spacing and increase in length of reinforcement strips.

Basset and Last (1978) assumed that the function of reinforcement is to restrict the dilatancy of soil leading to an increase in the mobilized shear strength. The reinforcement also causes a rotation of the principal strain directions relative to the unreinforced case. The most effective directions for the reinforcement can be estimated by the zero extension characteristics which are thought to represent potential slip surfaces. Based on this hypothesis, they investigated the possibility of using nonhorizontal reinforcements.

Akinmusuru *et al.* (1981) conducted laboratory scale bearing capacity model test on square footing on a homogeneous sand bed reinforced with strips of local

rope material. Results obtained showed that, depending upon the horizontal spacing between the ropes, vertical spacing between the layers, depth of first layer below the footing and number of reinforcement layers; the ultimate bearing capacity of reinforced sand bed improved upto three times that of the unreinforced sand. The optimum results were obtained with three layers of reinforcement and a horizontal and vertical spacing of half the width of footing between the fibres.

Fragaszy and Lawton (1984) conducted bearing capacity tests on reinforced sand subgrades to study the effect of optimum number of layers of reinforcement and the optimum depth to the first layer of reinforcement. The rectangular footing was used in the investigations and aluminium foil strips were used as reinforcements. The study was carried over a wide range of soil density and reinforcement length. It was observed that the percentage increase in bearing capacity was less for loose sands than for dense sands. As the strip length increased from 3 to 7 times the footing width, the bearing capacity increased rapidly.

Verma *et al.* (1986) conducted bearing capacity tests on model footings on sand subgrades reinforced with galvanized rods placed vertically. The improvement in bearing capacity was observed to be a function of spacing, diameter, roughness and extent of reinforcing elements. It was observed that flexible reinforcements with a height of one-and-a-half times the footing width for a length of twice the footing width on either side and with a spacing of six diameters can be used to derive substantial improvement in the bearing capacity.

Guido *et al.* (1986) conducted laboratory model tests on reinforced soil foundations and compared the performance of geotextile and geogrid as soil reinforcement. It was observed that the geogrid reinforcement was more effective than the geotextile in improving the bearing capacity of footing.

Dimbicki (1986) investigated the bearing capacity of strip foundation on two layers of soil (sand over mud) reinforced by non-woven geotextile inserted at the interface between the sand and mud. They observed that the influence of the

geotextile on ultimate bearing capacity was discernible at relatively large displacement which started to mobilize tensile stress in the fabric.

Sridharan *et al.* (1988) performed tests to study the effect of shape and size of foundation on bearing capacity of reinforced soil beds. It was brought out that the shape of the foundation does not affect the behaviour of reinforced as well as unreinforced sand beds, while the size of footing has the similar effect on the behaviour of reinforced sand bed as in the unreinforced case.

Huang *et al.* (1990) carried out experimental investigation on a series of strip model footings resting on sandy soil reinforced with tensile reinforcing layers of four types made of a combination of phosphor bronze coated with sand, phosphor bronze with mild steel bars and aluminium with mild steel bar placed beneath footing. The effect of length, arrangement, rigidity and rupture strength of reinforcement were examined. It was concluded that the bearing capacity in sand increased remarkably even by means of reinforcement layers of length equal to width of footing. A method of analysis by limit equilibrium predicted the values well in accordance with the measured ones.

Haroon *et al.* (1990) conducted small scale model tests on geotextile reinforced sand bed using rectangular footing to study the improvement in bearing capacity. The tests results compared well with the analytical approach suggested by them.

Shankaran (1991) conducted bearing capacity tests on square footing resting on sand bed reinforced with three types of geogrid CE-121, CE-131 and CE-153 with three different aperture sizes. It was observed that the geogrid having maximum aperture size i.e. CE-153, was most effective in improving the bearing capacity.

Srinivasa Murthy *et al.* (1993) attempted modifications in the method of analysis proposed by Binquet and Lee (1975b) for reinforced soil bed below strip footing by considering the mobilized frictional strength. From this approach, it is possible to design the reinforced soil bed for an allowable soil pressure

corresponding to a permissible settlement. The validity of the approach was brought out in relation to the experimental data.

Omar *et al.* (1994) conducted laboratory model tests to determine the ultimate bearing capacity of shallow rectangular foundations supported by geogrid reinforced sand varying the length to width ratio of foundation as 0 (strip) 0.333, 0.5 and 1.0. It was observed that the critical depth of reinforcement for mobilization of maximum possible ultimate bearing capacity ratio decreases with width to length ratio of the foundation. It is about $2B$ for strip foundations and about $1.2B$ for square foundation. Also the optimum size of reinforcing layers varied based on the B/L ratio of the foundation.

Khing *et al.* (1994) performed model tests for the ultimate bearing capacity of a surface strip foundation supported by a strong sand layer of limited thickness underlain by weak clay with a layer of geogrid at the sand clay interface. It was observed that maximum benefit from geogrid reinforcement in increasing the ultimate bearing capacity occurs when the thickness of strong sand layer is about two-thirds the width of foundation and the width of geogrid layer is six times the width of foundation.

Temel Yetimoglu (1994) investigated the effects of the depth to the first reinforcement layer, vertical spacing of reinforcement layers, number of reinforcement layers and the size of the reinforcement sheet on the bearing capacity of rectangular footing on geogrid-reinforced sand. Both the experimental and analytical studies indicated that the optimum depth of first reinforcement layer be $0.25B$, the optimum vertical spacing be between $0.2B$ and $0.4B$, and the extent of effective reinforcing zone be within $1.5B$ from the base and edge of footing for obtaining maximum increase in the bearing capacity.

Sitharam *et al.* (1995) attempted the nonlinear finite element analysis of reinforced soil beds. The load-settlement curves obtained in the analysis compared well with the experimental data available in literature. They also observed that the bearing capacity increases with the increase in number of reinforcement layers

and the reinforcement position has significant effect on the bearing capacity.

Youssef (1995) conducted model scale tests on strip footing placed over geogrid Netlon CE-121 reinforced sand beds. It was observed that the bearing capacity of the reinforced sand bed increased with the increase in number of reinforcement layers and width of reinforcement.

Ramaswamy *et al.* (1996) conducted the viscoelastic analysis of strip footing on geogrid reinforced soil bed using finite element analysis. It was observed that the moduli and time dependent behaviour of geogrid did not have a significant influence on the settlement. Geogrid CE-131 exhibited a linear visco-elastic behaviour while SR55 and CE301 exhibited nonlinear behaviour. The increase in moduli of reinforcement reduced the magnitude of settlement.

Adams *et al.* (1997) investigated the benefits of geosynthetic reinforced soil foundation using large scale model footing load tests. Geogrid and geocell reinforcements were placed under the shallow spread footings. The effects of the parameters like, number of reinforcement layers, spacing between reinforcement layers, depth of first reinforcement layer, plan area of reinforcement, type of reinforcement and soil density were studied. They reported that the ultimate bearing capacity of shallow spread footing increases by a factor of 2.5 by using geosynthetic reinforcements.

2.5 DYNAMIC CHARACTERISTICS OF REINFORCED EARTH

The dynamic characteristics of reinforced earth including the behaviour of reinforced earth under cyclic loads have been studied by a few investigators.

Murray *et al.* (1979) carried out pull-out tests on metal and fibre reinforced plastic reinforcements in an experimental earth wall constructed with uniformly graded sand. A significant reduction in the interface friction was observed when the surface of the fill above the reinforcement was vibrated. The vibrations resulted in a temporary reduction of overburden stress acting on the reinforcements. Due to this, a reduction in the pull out resistance was observed.

Patel *et al.* (1983) conducted cyclic plate load tests on a strip footing on sand beds reinforced with fibre glass woven rovings. They reported that the elastic settlements of the footing for both optimally reinforced and unreinforced sand beds are linearly varying with load and have nearly the same slope but the range of load for the former is higher than that for the latter. The non-recoverable component of the settlement of the footing is also a linear function of load for optimally reinforced sand bed but the same is non-linear for the unreinforced sand bed. Also, at a particular load level, the optimally reinforced sand bed has a higher damping capacity than that of the unreinforced one.

Kazuya Yasuhara *et al.* (1988) performed small-scaled model tests on geomesh and geogrid reinforced subgrade under repeated loading (traffic-induced cyclic). They observed that the cellular layout of geogrid takes more advantage in reducing the settlement of soft clay under cyclic loading than the planar layout. The bag-type geo-mattress by polymer grid containing the gravels inside is most desirable for reducing the settlements of soft grounds under repeated loading.

Saxena *et al.* (1990) carried out the seismic analysis of geotextile reinforced embankment for a plane strain two dimensional case incorporating the interface elements between the soil and geotextile with experimentally determined value of friction between soil and geotextile. They concluded that the reinforcement of the softer foundation layer by geotextile will enhance the stability and decrease the deformation.

Puri *et al.* (1991) performed laboratory scale model strip footing tests to determine the cyclic load resistance of sand subgrades reinforced with semi-flexible rough and smooth steel bars placed vertically. The test results indicated that the coefficient of elastic uniform compression C_u , of vertically reinforced sand subgrades is increased to more than twice the C_u value for unreinforced sand bed. The rough reinforcements cause more improvement in C_u value. The improvement in C_u value was found to depend upon the length, extent, spacing and surface roughness of the reinforcement and the initial relative density of sand, and tends

to become constant at 70% relative density.

Shewbridge *et al.* (1991) conducted a series of dynamic shear tests on large hollow cylindrical reinforced and unreinforced sand samples. The sand samples were reinforced with steel rods placed longitudinally and both longitudinally and in the form of hoops. Test results indicated that confining pressure and strain level affect the dynamic shear modulus and damping of reinforced and unreinforced sand beds, whereas frequency (upto 10 Hz.) has no effect on both the parameters. The complex shear modulus was not affected, by the provision of reinforcements, upto strain amplitude of 5%. At strains greater than 7%, the formation of the rupture surface was inhibited, thus increasing the ductility of the material. They indicated that the effect of reinforcements on dynamic properties of reinforced soil composite can be ignored when analyzing the dynamic response at small strains, but should be considered when evaluating the dynamic response at larger strains.

Boominathen *et al.* (1991) studied the dynamic properties of reinforced earth by performing a few forced block resonance tests over a base of silty sand in natural state and in the reinforced state with (i) high modulus materials such as steel (ii) low modulus material such as geotextiles (iii) a combination of both type of reinforcing materials within the significant depth of stress bulb. The test results indicated that with steel reinforcement, the shear modulus G (or the coefficient of elastic uniform compression C_u) is increased by 60% and the maximum amplitude is reduced by about 50%. With two geotextile layers as reinforcement, the coefficient of elastic uniform compression C_u (or shear modulus) is reduced by about 20% and the maximum amplitude is reduced to about 45%.

Guido *et al.* (1994), conducted dynamic plate load tests to determine the effect of various parameters on the load capacity and settlement of geogrid-reinforced earth slabs. The parameters studied were the number of reinforcement layers, the width of reinforcement, the amplitude and frequency of dynamic loading. They observed that the dynamic load capacity of the reinforced sand

increased to 1.5 to 3 times that of the unreinforced sand, when the number of reinforcement layers was increased from 2 to 4, and the settlement decreased. For an increase in the amplitude and frequency of loading, the dynamic load capacity of soil increased with the insertion of geogrid layers.

2.6 CONCLUDING REMARKS

The literature review reveals that a number of analytical techniques based on elastic half space theory, lumped parameter approach and numerical methods exist to determine the dynamic response of unreinforced soil. Also sufficient experimental data is available on the effect of various parameters e.g. embedment of footing, soil layering and nonhomogeneity of soils etc., on the dynamic response parameters of footings on soil. Again, a number of analytical techniques and experimental procedures exist in literature to work out the static strength characteristics of reinforced soil.

It is established, from the work reported in literature, that the inclusion of reinforcements in the soil affects its dynamic properties. Most of the tests conducted, however, are small scale laboratory cyclic plate load tests and detailed investigation of the influence of various factors on dynamic properties of reinforced soil has not been performed. The effect of size and type of reinforcement, number of reinforcement layers, soil density etc., on frequency, amplitude, damping and stiffness of the reinforced soil need be studied in detail using full scale model tests such as block resonance tests and cyclic plate load tests; which are commonly used in India to determine the dynamic properties of soils. There exists a need to develop an analysis in which the influence of reinforcements on the important dynamic properties e.g., stiffness and damping of soil is accounted for. The experimental data available in literature is meagre and hence there is a need to evolve sufficient data on the effect of reinforcement on dynamic properties of reinforced soil by conducting sufficient number of large scale tests on foundation blocks and plates.

EXPERIMENTAL INVESTIGATIONS

3.1 GENERAL

Model tests are useful for studying the behaviour and performance of new materials like reinforced earth under varied loading conditions. Carefully conducted model tests help in identifying various parameters influencing the behaviour and thereby help in improving the design procedures.

In this investigation, the dynamic response of block foundation on reinforced sand beds has been investigated by conducting a series of large scale model tests. A number of cyclic plate load tests have been performed to study the behaviour of geogrid Netlon CE-121 reinforced sand beds at 50% and 70% relative densities. The vertical and horizontal forced vibration tests have been conducted on M-20 concrete block of size 800mm×400mm×400mm high following the procedure specified in IS:5249-1977.

The soil used in the preparation of reinforced sand beds has been deposited in steel test tanks by rainfall technique. Two rigid steel test tanks of size 900mm×900mm×1000mm and 1500mm×1500mm×1000mm assembled under a loading frame of 100 kN capacity, have been used for conducting cyclic plate load tests. Two steel plates of size 150mm×150mm and 300mm×300mm and thickness 20 mm each have been used as test footings. The sand bed was reinforced with geogrid layers varying in size from one to five times the width of footing and in number from 2 to 8. In forced vibration tests, the size of the test tank used was 1500mm×1500mm×1000mm and the sand bed was reinforced with two to six geogrid layers of size one to 1.875 times the length and one to 3.75 times the width of block. The details of soil and reinforcing material used, the test tank and

equipments, preparation of reinforced sand bed, the test procedure, the tests performed and test results are elucidated in this chapter.

3.2 SOIL USED

The soil used in the experimental investigations was dry Amanantgarh sand. The particle size distribution curve is shown in Fig.3.1. According to Indian standard on soil classification for general engineering purposes (IS : 1498-1970), the test soil is classified as poorly graded sand (SP). The maximum and minimum void ratios were determined in accordance with procedure laid down in Indian standard IS : 2720 (Part XIV-1983). Fig.3.2 shows the direct shear tests conducted on sand at 50% and 70% relative densities. The relevant physical and mechanical properties of the soil are listed in Table 3.1

Table 3.1 Physical and Mechanical Properties of Soil

S.No.	Property	Value
1.	Soil type	SP (as per IS:1498-1970)
2.	Effective size (D_{10})	0.188 mm
3.	Uniformity coefficient (U_c)	1.51
4.	Coefficient of curvature (C_c)	1.10
5.	Mean specific gravity	2.65
6.	Minimum voids ratio	0.533
7.	Maximum voids ratio	0.928
8.	Angle of Internal friction (ϕ) at relative density	
		70% 40°
		50% 37°

3.3 REINFORCING MATERIAL

The reinforcing material used in the model tests was geogrid Netlon CE-121. The physical, chemical and mechanical properties of the reinforcement are listed in Table 3.2

Table 3.2 *Properties of Reinforcement Material, Geogrid Netlon CE-121

S.No.	Property	Description
1.	Physical	Colour - Black Roll width - 2 m Roll length - 15 m Mesh aperture - 8 mm x 6 mm Mesh thickness - 3.3 mm Structural weight - 720 g/m ²
2.	Chemical	100% High density polyethylene Excellent resistance to chemical and microbiological agents. Poor resistance to oxidising agents and ultraviolet light.
3.	Mechanical	Maximum load - 7.68 kN/m

* Properties given by manufacturer.

The stress-strain characteristics of geogrid Netlon CE-121 have been studied by conducting tensile strength test in the universal testing machine. Fig.3.3 shows the stress-strain curve of the reinforcing material. A specimen of size 50mm×200mm of geogrid has been tested in the universal testing machine. The strain rate was kept 0.45 mm/minute. The stress is calculated by dividing the force per unit width by the thickness of the specimen.

3.4 CYCLIC PLATE LOAD TESTS

The cyclic plate load tests provide a simple approach for the evaluation of coefficient of elastic uniform compression, C_u , of soils. The cyclic plate load

tests have been conducted as per the procedure specified in IS : 1888-1982 and IS:5249-1977. The tests have been performed with square footings of size 150mm×150mm and 300mm×300mm. The details of various components of test set-up are described below.

3.4.1 Test Tanks

Two rigid steel tanks of sizes, 900mm×900mm×1000 mm made of 6 mm thick plates and 1500mm×1500mm×1000mm made of 8 mm thick plates have been used for preparation of sand beds in the testing programme. The smaller tank has been fabricated by modifying a tank of size 2200mm×900mm×1000mm high into two portions of size 900mm×900mm×1000mm each. The partition provided is made of 20 mm thick board mounted on rigid frame made of steel angles of size 40mm×40mm×3mm. The bottom of the tank is made of 9 mm thick steel sheet welded to the base frame of channels 100mm×50mm×4mm size. The arrangement of smaller tank is illustrated in Fig. 3.4.

The larger tank is made of four box sections welded double channels face to face (1750 mm long), four channels (1750 mm long) and 8 channel sections with plates welded at ends (1500 mm long), to give internal dimensions of 1500mm×1500mm×1000mm. All the channel sections are of size 250mm×125mm×8mm thick. The tank was fabricated by nuts and bolts and the floor was used as the bottom of the tank.

In order to avoid outflow of sand particles through the bottom and sides, lime putty was used to seal the gaps between the plates. Fig.3.5 gives a general view of the larger tank.

3.4.2 Loading Arrangement

The tanks were fabricated under a loading frame of 100 kN capacity for applying load either by a hydraulic jack or through reaction loading by lever arm mechanism. The load was applied through a hydraulic jack on 150 mm square footing tested in the smaller tank, whereas lever arm mechanism alongwith a hydraulic jack was used to apply load on 300 mm square footing in the larger tank. The details of

the loading frame, test tanks and the loading mechanism are shown in Fig. 3.4, Fig.3.5 and Fig.3.6.

The loading frame consists of four vertical steel columns of single channel section 150mm×75mm×6mm. The columns about 3000 mm high above the floor level are rigidly embedded to the floor through steel plates and are braced at the top by 25 mm diameter mild steel rods so as to provide adequate rigidity to the system. Four main beams made of 150mm×75mm×6mm single I-sections are fixed to the column at heights of 2000 mm and 2300 mm respectively. These beams can be adjusted at any desired elevation by nuts and bolts.

The cross beams of box section (double channel sections 100mm×50mm×5mm welded face to face) are fitted one each at the top and bottom of the main beams at a suitable distance to provide reaction to the lever arm mechanism as shown in Fig.3.5 and Fig.3.6. One of the cross beams is positioned along the centre line of the tank while conducting tests. A 3000 mm long beam 150mm×75mm×6mm mild steel I-section with two holes provided one at the end and the other at 1/6 of the length from the other end acts as a lever arm for applying the load through lever arm mechanism. The complete arrangement of the loading mechanism through dead weights, hydraulic jack, positioning of square footing, dial gauges, proving ring, loading plunger and the double channel beam (100mm×100mm×5mm box section) with holes to ensure vertical position of loading plunger can be seen in Fig.3.5 and Fig.3.6. The fixing of dial gauges on box beam, proving ring, loading plunger placed on ball, roller plate, lever arm fulcrum and the reaction hydraulic jack is shown in Fig.3.7.

The loading arrangement for 150 mm square footing is shown in Fig.3.4. Since the settlements were large in case of smaller footing, it was not possible to measure settlements by placing the dial gauge tips directly on the plate. To ensure accurate measurements of settlements, four 12 mm diameter, 120 mm long steel bars were rigidly fixed to the corners of the plate. On the top of these bars, 40 mm square and 3 mm thick steel strips were tightly screwed as shown in

Fig.3.8. The tips of dial gauges were centrally mounted on these strips.

3.4.3 Load Measuring Device

The load on the 150 mm square footing was applied through a hydraulic jack of 100 kN capacity. The reaction to jack was provided by the reaction loading frame. The load was measured through a calibrated proving ring of capacity 100 kN, which was placed over a steel block resting centrally on the footing as shown in Fig.3.4.

On 300 mm square footing, the load was applied through the lever arm mechanism. The load was transferred by lever arm mechanism through the fulcrum to the plunger. A 300 kN capacity proving ring mounted onto the plunger placed on the footing through ball and socket arrangement was used to measure the load.

3.4.4 Settlement Measuring Arrangement

The settlements of the test plates were measured by four dial gauges of least count 0.01 mm and 50 mm travel, arranged at the corners of the footing. In order to ensure accurate measurements of settlements, the tips of the dial gauges were made to rest on four smoothed aluminium strips rigidly secured to the corners of the footing. The dial gauges were supported on datum bar using magnetic bases. The whole arrangement is shown in Fig.3.4 and Fig.3.9.

3.4.5 Preparation of Sand Bed

The sand was filled in the tanks using rainfall technique, at 50% and 70% relative densities. The height of fall versus relative density curve for Amanantgarh sand is shown in Fig.3.10. The sand was poured through G.I. sheet stainers of sizes 860mm×860mm and 1460mm×1460mm for smaller and larger tanks respectively. Mild steel chains were attached at the corners of the stainers and they were hung above the tank by securing the other ends of the chains to the vertical angle sections fixed to the tanks (Fig.3.11).

To start the sand filling, the stainer was kept at a predetermined height



above the bottom of the tank and sand was poured by spreading uniformly over the stainer. When a layer of 100 mm thickness was deposited, the stainer was lifted by another 100 mm and pouring of sand was resumed. In this way, the sand was filled in the tank upto the test-level i.e. 1000 mm (Fig.3.11). In order to check the density of the sand bed continuously, a set of containers of known volume were placed at different locations in the tank during filling. A density variation of about $\pm 1.5\%$ was observed during filling.

While placing the geogrid layers, the sand was deposited upto the required level carefully. The reinforcement layer was then placed centrally below the footing (Fig.3.12) and sand was poured very slowly and carefully in small quantities above the reinforcement layer to avoid segregation of sand particles which may result in variation of density (Fig.3.11). Finally the sand surface was given a finished level and the test footing was placed centrally over it.

3.4.6 Arrangement of Reinforcement Layers

The reinforcement layers were placed at respective locations centrally below the footing as shown in Fig.3.12. The size of the reinforcement layers was varied from one to five times the width of footing and 2,3,4,6 and 8 number layers were used. The details of the arrangement of reinforcement layers used in cyclic plate load tests are given in Table 3.3.

3.4.7 Test Procedure

The cyclic plate load tests were conducted as per the procedure specified in IS:1888-1982 and IS:5249-1977. The procedure is briefly described below :

The test footing of requisite size was placed at the centre of the smooth and levelled sand bed. Hydraulic jack, proving ring, dial gauges and the lever arm loading arrangement (as the case may be) were arranged as shown in Fig.3.6 and Fig.3.7. A seating pressure of 7 kN/m^2 was applied on the plate to eliminate bedding errors, if any. The seating pressure was then released and the actual test was started.

The initial readings of the dial gauges were noted and the first load increment was applied on the footing. This load was maintained constant till no further settlement occurred. The final readings of the dial gauges were then recorded. The entire load was then released gradually and the footing was allowed to rebound. When no further rebound occurred or the rate of rebound became negligible, the dial gauge readings were again noted. The load was then increased gradually till its magnitude reached a value equal to the next higher stage of loading. The load was maintained constant and the final readings of the dial gauges were noted as described earlier. The total load was then removed and the dial gauge readings were recorded when no further rebound occurred. The cycles of loading, unloading and reloading were continued till sufficient number of observations were obtained to plot pressure intensity versus elastic settlement curve for the evaluation of coefficient of elastic uniform compression, C_u .

The load increments were decided such that the footing was loaded to about 50% of the estimated ultimate load capacity of the sand bed in about five to six load increments. In case of sand bed containing large size reinforcements, the load increment was kept the same, in general, as that for the sand bed containing small size reinforcements in order to have a comparative idea of the elastic settlements. In case of tests on reinforced sand bed, larger increments of load were applied as compared to the load increments on unreinforced sand bed.

3.4.8 Tests Performed

A series of cyclic plate load tests were carried out on 150 mm square footing at the two relative densities of 50% and 70% and on 300 mm square footing at 70% relative density. The size of the reinforcement layers was varied from B to 5B and their number was kept 2,3,4,6 and 8. The distance of the top reinforcement layer below the footing base and the distance between the layers was kept as 0.25 B each, B being the width of the footing.

Table 3.3 : Details of Cyclic Plate Load Tests Conducted

Sl. No.	Name of test	Relative density D_r (%)	LxB (mm)	Size of tank (mm)	u/B	s_z / B	L_r / L	B_r / B	No. of reinforcement layers (n)	No. of tests performed
1.	Cyclic plate load tests	70	150x150	900x900x1000	0.25	0.25	1.0	1.0	2,3,4,6,8	5
							2.0	2.0	2,3,4,6,8	5
							3.0	3.0	2,3,4,6,8	5
							4.0	4.0	2,3,4,6,8	5
							5.0	5.0	2,3,4,6,8	5
							Unreinforced sand bed			
2.	Cyclic plate load tests	50	150x150	900x900x1000	0.25	0.25	1,2,3,4,5	1,2,3,4,5	4	5
										Unreinforced sand bed
3.	Cyclic plate load tests	70	300x300	1500x1500x1000	0.25	0.25	1,2,3,4,5	1,2,3,4,5	4	5
										Unreinforced sand bed
Total no. of tests										38

L = Length of footing

B = Width of footing

L_r = length of reinforcement along length L

B_r = width of reinforcement along width B

u = distance of top reinforcement layer below footing base

s_z = vertical distance between adjacent reinforcement layers

The details of the tests conducted are given in Table 3.3. The following parameters were varied to study their effect on the value of coefficient of elastic uniform compression, C_u :

- i) Relative density of sand - 50% and 70%.
- ii) Size of footing - 150 mm square and 300 mm square.
- iii) Size of reinforcement layers - B to 5B at intervals of B.
- iv) No. of reinforcement layers - 2,3,4,6 and 8.

A total of 38 cyclic plate load tests were conducted by varying the parameters considered.

3.5 BLOCK VIBRATION TESTS

The block vibration tests provide a rational and direct method of obtaining the resonant frequency and amplitude of the foundation - soil system. The stiffness and damping of soils at strain levels closer to those occurring in machine foundations can be obtained by conducting vertical and horizontal vibration tests on a block of size 1500mm×750mm×700mm as per IS:5249-1977. However, since the size of tank fabricated for the laboratory model tests was 1500mm×1500mm, the tests were conducted on a modified M-20 block of size 800mm×400mm×400mm high. The details of various components of the test set up are described below :

3.5.1 Test Tank

The experimental set up consisted of a rigid steel tank of size 1500mm×1500mm×1000mm made of four box sections double channels welded face to face (1750 mm long), four channels (1750 mm long) and 8 channel sections with plates welded at ends (1500 mm long). All the channel sections were of size 250mm×125mm×8mm thick. The tank was fabricated as described earlier in 3.4.1 (Fig.3.13 and Fig.3.14).

A chain pulley system rolling over a channel section was fabricated to place the concrete block gently over the finished surface of sand bed (Fig.3.13 and Fig.3.14).

3.5.2 Foundation Block

A rectangular block of size 800mm×400mm×400mm high was planned for the block vibration tests. The block was provided with four 360 mm long embedded bolts to fix the oscillator and motor assembly through a base plate placed over it. The bolts were tied together at the bottom by 6 mm diameter bars and nominal reinforcement was provided in the block allowing an around cover of 40 mm. M-20 concrete mix was used for casting the block. The block was cast without disturbing the reinforcement and was cured for 28 days. Four hooks were provided at the corners to lift the block as shown in Fig.3.15.

3.5.3 Characteristics of Foundation Block

The size of the block was planned on the basis of the size of test tank, the size of oscillator and proportioning as per IS:5249-1977. Motor and oscillator were mounted on the block for excitation. Their positions and other details are shown in Fig.3.13 and Fig.3.14. The main characteristics of the block are given in Table 3.4.

3.5.4 Frequency Measuring Device

A microprocessor controlled instrument, soil-data 4201 was used to measure the frequency as shown in Fig.3.16. The tacho input connector is connected to the 3 pin coaxial connector provided on signal conditioner DA-464 module. The mechanical oscillator and a variable speed motor were mounted on the block. The frequency values are displayed on the panel of soil data logger through tacho input. The frequency values were also recorded from the vibrationmeter connected to the other side of the tacho input on the oscillator for cross checking and were found to match with the values displayed by soil data logger.

Table 3.4 Characteristics of the Foundation Block

S.No.	Description	Quantity	Unit
1.	Base Area, A	0.32	m ²
2.	Weight of block, W ₁	3.07	kN
3.	Weight of motor and oscillator, W ₂	1.23	kN
4.	Weight of Vibrator+Block, W	4.30	kN
5.	Mass of block & vibrator, M	0.4383	kN-sec ² /m
6.	Moment of Inertia of base contact area about axis of rotation, Y-axis, I	0.01707	m ⁴
7.	Mass moment of Inertia about Y-axis, an axis passing through combined centre of gravity and perpendicular to plane of vibration, M _m	0.0447	kN-m-sec ²
8.	Mass moment of inertia about Y-axis passing through centroid of base, M _{m0}	0.09682	kN-m-sec ²
9.	Ratio $\gamma' = \frac{M_m}{M_{m0}}$	0.4616	
10.	Ratio of area to mass, A/M	0.7300	
11.	Ratio $I_0 = 3.46 I/M_{m0}$	0.6100	

The dynamic force produced by the oscillator is given by equation 3.1.

$$F = m_e e \omega^2 \quad \dots(3.1)$$

$$= 0.000126 \frac{\omega^2}{g} \sin \theta/2$$

where,

F = dynamic force, kN

m_e = total eccentric mass, kN-sec²/m

e = eccentricity,

ω = circular frequency, rad/sec

$$= 2\pi f$$

f = frequency in cycles per second

g = acceleration due to gravity, 9.81 m/sec²

θ = angle between the eccentric masses in degrees

Substituting values of ω and g in equation 3.1, we obtain

$$F = 0.00507 f^2 \sin \theta/2 \quad \dots(3.2)$$

The variation of dynamic force F with frequency f is given in Fig.3.17. The values of eccentric moment ($m_e e$) for $\theta = 4^\circ, 12^\circ, 20^\circ$ and 28° are 4.4825×10^{-6} , 1.3426×10^{-5} , 2.2303×10^{-5} and 3.1073×10^{-5} kN-sec² respectively.

3.5.5 Amplitude Measuring Device

The amplitudes were measured by mounting the accelerometers (sensors) on the block as shown in Fig.3.13 and Fig.3.15 for vertical and horizontal vibration tests respectively. The signals of the sensors were fed into channels of soil data logger, CH-0 of signal conditioner module DA-464 for vertical vibration tests and into CH-0 and CH-1 of signal conditioner modules DA-464 and DA-465 respectively for horizontal vibration tests. The amplitude values can be read directly from LCD display unit and can be stored in the memory of the unit. A printout of the values were obtained by connecting a compatible printer.

3.5.6 Preparation of Sand bed

The sand bed was prepared at 70% relative density by depositing the sand in 100 mm layers in the tank through a stainer of size 1460mm×1460mm as already explained in 3.4.5. A regular check on the density values was exercised and the reinforcement in layers were placed as described earlier. After the preparation of sand bed, the test block alongwith the motor and oscillator assembly mounted on it was gently placed over the smooth finished bed using chain pulley block system as shown in Fig.3.18.

3.5.7 Arrangement of Reinforcement Layers

The reinforcement layers were placed centrally below the footing block as shown in Fig.3.12. The number of geogrid layers was kept 2,3,4 and 6 and their size varied as shown in Table 3.4. Block vibration tests were conducted by exciting the block at four force levels keeping the eccentricity values 4°, 12°, 20° and 28°. The details of the number and arrangement of reinforcement layers used in the block vibration tests are given in Table 3.5.

3.5.8 Testing Equipment

The mechanical oscillator and dc motor were fixed on the concrete block and suitable connections between the power supply, speed control unit, dc motor, vibration meter, soil data logger and the printer were made as shown in Fig.3.13, Fig.3.14 and block diagram 3.19. The three pin coaxial connector from tacho input of speed control unit was connected to the tacho input of signal conditioner DA-464 module. Connection of 5 pin coaxial male connector of first acceleration sensor was made to the mating connector CH-0 in signal conditioner DA-464 module for both vertical as well as horizontal vibrations. Similarly, 5 pin coaxial male connector of second acceleration sensor is connected to the mating connector CH-1 in signal conditioner DA-465 module in case of horizontal vibration tests.

The sensors were calibrated by pressing the <RESET> key, the <CAL> key, entering type of test - '0' for vertical and '1' for horizontal putting the switch

Table 3.5 : Details of Block Vibration Tests Conducted

Sl. No.	Name of test	Relative density D_r (%)	$L \times B \times H_t$ (mm)	Size of tank (mm)	u/B	s_z/B	L_r/L	B_r/B	No. of reinforcement layers (n)	No. of tests performed
Block vibration tests										
1.	Vertical vibration tests Eccentricity (4°, 12°, 20°, 28°)	70	800x400x400 M-20 concrete block	1500x1500x1000	0.25	0.25	1.0	1.0	2,3,4,6	4
							1.5	1.5	2,3,4,6	4
							1.875	1.875	2,3,4,6	4
							1.25	2.50	2,3,4,6	4
							1.50	3.00	2,3,4,6	4
							1.875	3.75	2,3,4,6	4
									Unreinforced sand bed	1
2.	Horizontal vibration tests Eccentricity (4°, 12°, 20°, 28°)	70	800x400x400 M-20 concrete block	1500x1500x1000	0.25	0.25	1.0	1.0	2,3,4,6	4
							1.5	1.5	2,3,4,6	4
							1.875	1.875	2,3,4,6	4
							1.25	2.50	2,3,4,6	4
							1.50	3.00	2,3,4,6	4
							1.875	3.75	2,3,4,6	4
									Unreinforced sand bed	1
Total no. of tests									50x4 = 200	

L = Length of block

B = Width of block

H_t = Height of block

L_r = Length of reinforcement along length L

B_r = Width of reinforcement along width B

u = Distance of top reinforcement layer below footing base

s_z = Vertical distance between adjacent reinforcement layers

provided on DA-464 (or DA-465) module at <CAL> position and pressing <ENTER> key. The sensor connected in DA-464 (or DA-465) module is placed horizontal and <ENTER> key is pressed. Then the sensor is turned by 180° and again <ENTER> key is pressed. A message "SUCCESSFULLY CALIBRATED" is displayed.

The details of testing equipments used in block vibration tests are described below :

Mechanical Oscillator (SEA-350A) : It is used for producing sinusoidally varying dynamic force. Eccentricity θ of the oscillator varies from 0° to 140°. The range of operating frequency is from 0 to 60 Hz. Dynamic load at 45 Hz is ± 1200 kg.

Variable Speed dc Motor (SEA-351A) : It is used to drive the mechanical oscillator and its speed ranges from 0 to 3600 rpm. The capacity of the motor is 3.0 H.P.

Speed Control Unit (SEA-352A) : It is used to control the speed of the motor from its rated minimum to maximum rpm values. The capacity of the unit is 3.0 H.P. and input is 220 V ac, output being variable dc voltage with maximum voltage drop of 2 percent at full load.

Vibrationmeter : It can measure the frequency from 0 to 60 Hz of steady-state vibrations.

Datalogger Soil Data

The needed specifications of soil data logger are given below :

(a) **Accelerometer - Model A02 :** Maximum range shall be commensurate with the oscillator. Natural frequency should 220 Hz undamped and 140 Hz damped. The response should be linear, deviation from linearity being 1 percent or less with amplitude changes. It is strain gauge based type acceleration sensor.

(b) **Geophone :** It shall be highly sensitive with natural frequency 20 Hz and damping less than 1 percent of the critical damping.

Soil data 4201 : It is a microprocessor controlled instrument which can acquire data from the accelerometer and tacho. The data is displayed specially on the LCD display (2 line \times 16 column alphanumeric dot matrix display) and can be stored in memory; a printout of which can be obtained from a compatible printer. Memory size is 32K which can store the programmed parameters, data and calculated test coefficients during operation. It consists of the following mainframes and modules:

(a) Mainframe MF-4201

(b) Modules :

Power supply module POW 4100

CPU module

Signal conditioner module DA-464

Signal conditioner module DA-465.

3.5.9 Test Procedure

The vibration tests were conducted as per the procedure laid down in IS:5249-1977. The procedure is briefly described below :

The sand bed was prepared afresh for each test and the motor oscillator block assembly was gently placed over the smooth finished sand bed. The usual connections were made between different components as per the requirements of test laid down earlier. The angle of eccentricity of the oscillator was arranged to the desired level of excitation. The acceleration sensors were calibrated as already explained. The speed of the motor was gradually increased using the speed control unit and the corresponding frequency and amplitude values displayed on the data logger were recorded. The frequency values were also recorded from vibrationmeter in order to cross-check the frequency values. Then angle of eccentricity of the oscillator was changed to the next excitation level and the above procedure was repeated to obtain another record of frequency and amplitude values. The above procedure was repeated at all excitation levels.

3.5.10 Tests Performed

A series of vertical and horizontal vibration tests were conducted on M-20 block at four excitation levels. The sand bed was prepared at 70% relative density keeping the number of reinforcement layers 2,3,4 and 6 and their size varied as given in Table 3.5. The following parameters were studied in the experimental programme :

- i) Number of reinforcement layers
- ii) Size of reinforcement layers
- iii) Four excitation levels in terms of the eccentricity settings of the eccentric mass of the oscillator.
- iv) Different modes of vibration, i.e. vertical and horizontal.

A total of 50 tests each at four eccentricity values were conducted by varying various parameters.

3.6 TEST RESULTS

The data obtained from various tests are plotted and representative curves are drawn for the parameters considered. The test result-plots for different tests are as under:

3.6.1 Cyclic Plate Load Tests

Figures 3.20 to 3.51 show the pressure versus total settlement curves obtained from the cyclic plate load tests conducted on 150 mm square footing at 70% and 50% relative densities. The pressure versus total settlement curves for 300 mm square footing at 70% relative density are shown in Figures 3.52 to 3.57. In these figures, the curves of best fit have been drawn and the ultimate bearing pressure has been determined by double tangent method. The loading and unloading cycles have been depicted smoothly and approximately. The ultimate bearing pressure values were also determined from the pressure versus total settlement data plotted on log-log scale and the values nearly match with those obtained from double tangent method. A typical pressure-settlement plot on log-log scale is

shown in Figure 3.20(b) for the footing on unreinforced sand bed.

The pressure versus elastic settlement curves for 150 mm square and 300 mm square footings have been shown in Figures 3.58 to 3.88 and are bilinear; the two lines meeting at a pressure value close to the ultimate bearing capacity of the sand bed. The slope of initial line gives coefficient of elastic uniform compression C_u and that of the other has been represented by the symbol C'_u . The C'_u values are determined to have an idea about the coefficient of elastic uniform compression beyond the ultimate bearing pressure.

3.6.2 Vertical Vibration Tests

Figures 3.89 to 3.113 represent the response curves drawn from the frequency and amplitude values obtained from the vertical vibration tests on block placed over unreinforced and reinforced sand beds. The force levels (eccentricity values), corresponding values of resonant frequency and maximum amplitude are shown along. Representative curves have been drawn through the average data points obtained by repeating the tests.

3.6.3 Horizontal Vibration Tests

The amplitude versus frequency curves for horizontal vibration tests are shown in Figures 3.114 to 3.138. The configuration of sand bed is depicted alongwith. The resonant frequency and maximum amplitude values for both first and second modes of vibration at various levels of excitation can be seen from the above mentioned figures.

3.7 CONCLUDING REMARKS

A total of 38 cyclic plate load tests were conducted on unreinforced and reinforced sand beds. This data have been further analysed and interpreted to give the ultimate bearing capacity, settlement, damping capacity and coefficient of elastic uniform compression. The details of these are given in next chapter with further interpretation of these quantities in non-dimensional form.

Also a total of 200 vertical and horizontal vibration tests on unreinforced and reinforced sand beds were conducted. The frequency-amplitude curves have been plotted for various excitation levels from which the resonant frequency and the maximum amplitude values are determined. The damping ratio has been calculated by bandwidth method from the response curves of vertical vibration tests. The coefficient of elastic uniform compression C_u has been determined from vertical vibration tests and the coefficient of elastic uniform shear, C_τ has been evaluated from the horizontal vibration test data. The details of their determination with appropriate interpretation are given in next chapter.

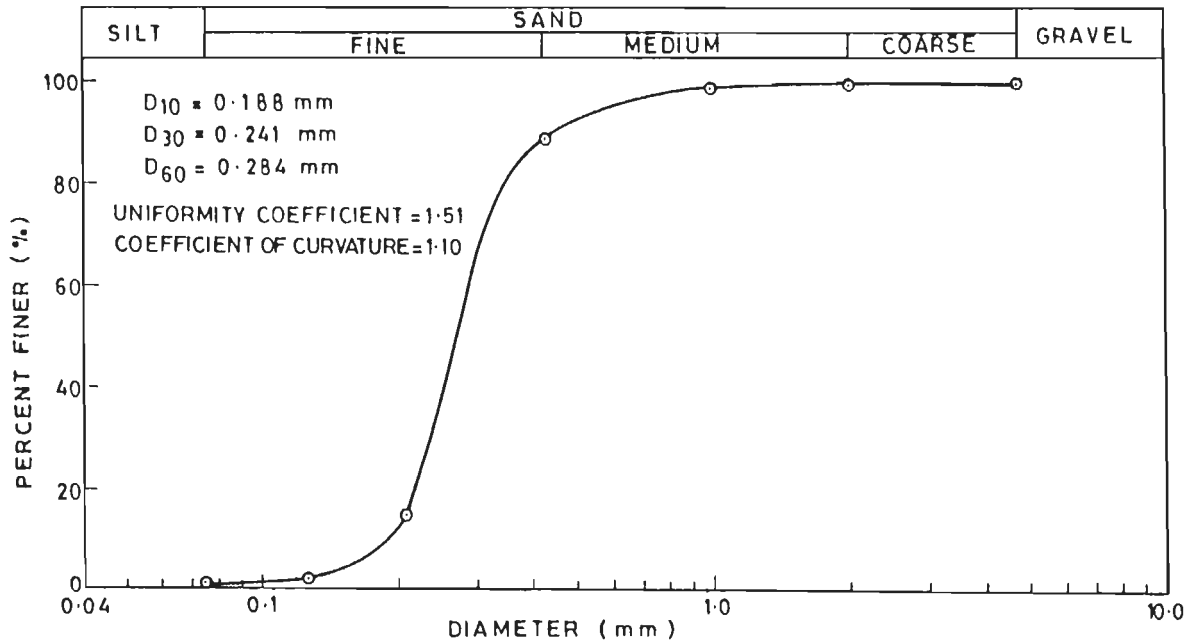


FIG. 3.1 GRAIN SIZE DISTRIBUTION CURVE OF AMANANTGARH SAND

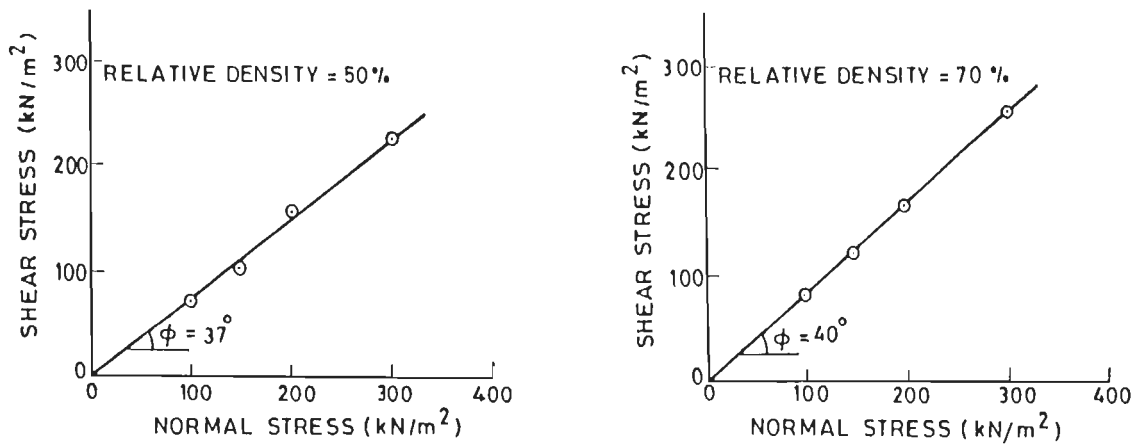


FIG. 3.2 DIRECT SHEAR TESTS ON AMANANTGARH SAND

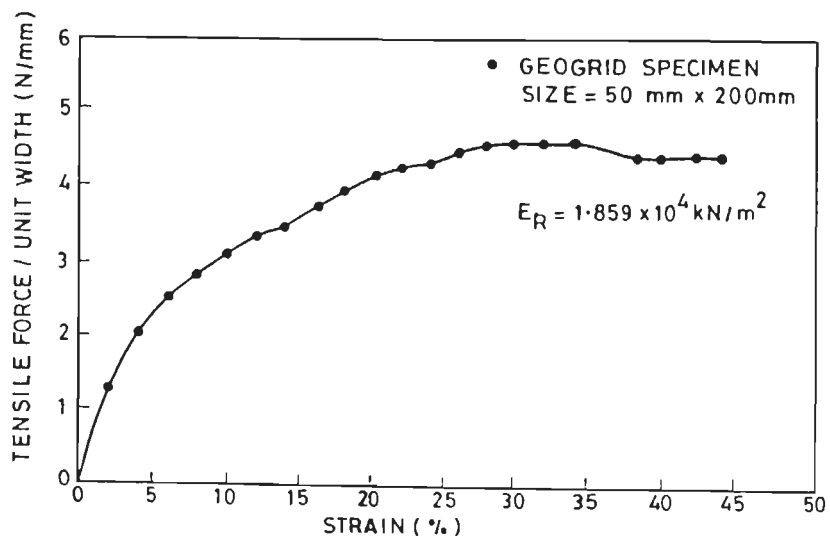


FIG. 3.3 STRESS-STRAIN CURVE OF GEOGRID NETLON CE-121

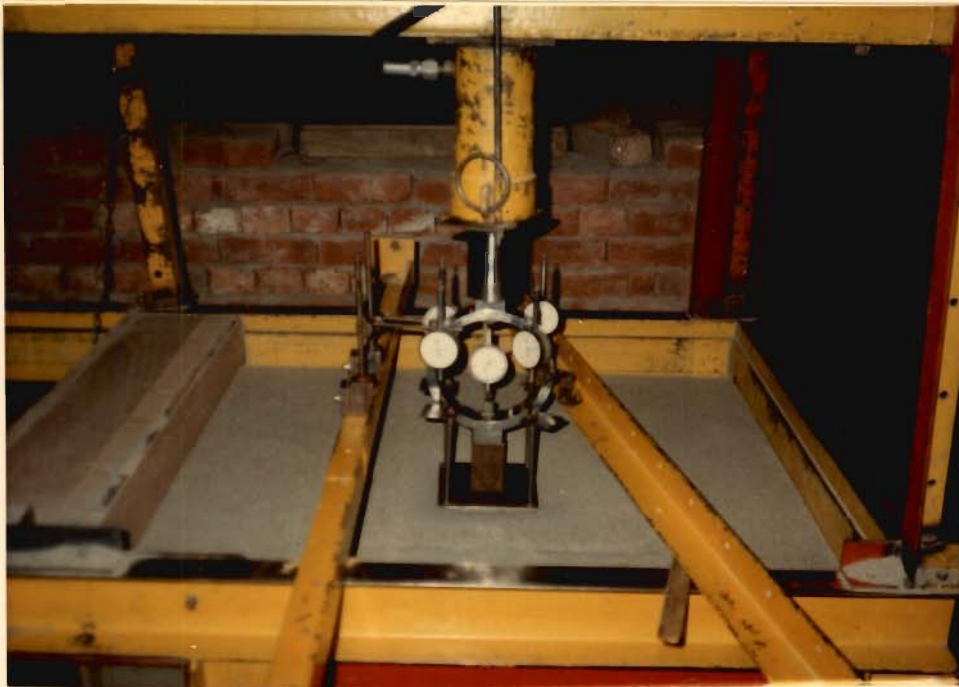
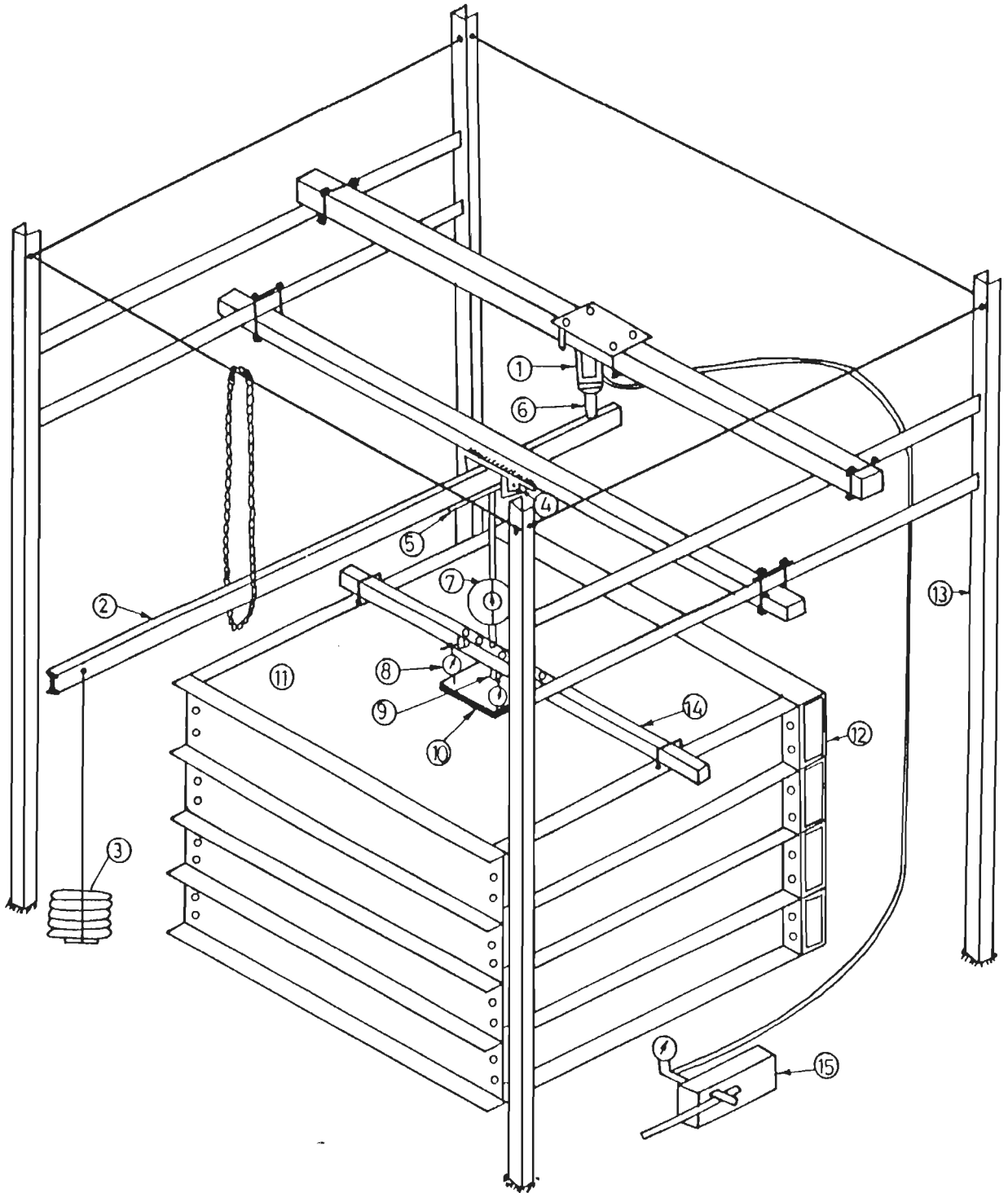


FIG 3.4 EXPERIMENTAL SET-UP OF CYCLIC PLATE
LOAD TEST ON 150 mm SQUARE FOOTING



- | | | |
|-------------------|----------------------|---|
| 1. HYDRAULIC JACK | 6. LOAD SHAFT | 11. SAND BED |
| 2. LEVER ARM | 7. PROVING RING | 12. STEEL TANK |
| 3. WEIGHTS | 8. DIAL GAUGE | 13. LOADING FRAME |
| 4. SLOT | 9. PLUNGER | 14. BOX BEAM TO ENSURE VERTICAL POSITION OF PLUNGER |
| 5. ROLLERS | 10. FOOTING OR PLATE | 15. PUMP |

FIG.3.5 EXPERIMENTAL SET-UP FOR CYCLIC PLATE LOAD TEST



FIG. 3·6 LEVER ARM LOADING ARRANGEMENT FOR CYCLIC PLATE LOAD TEST

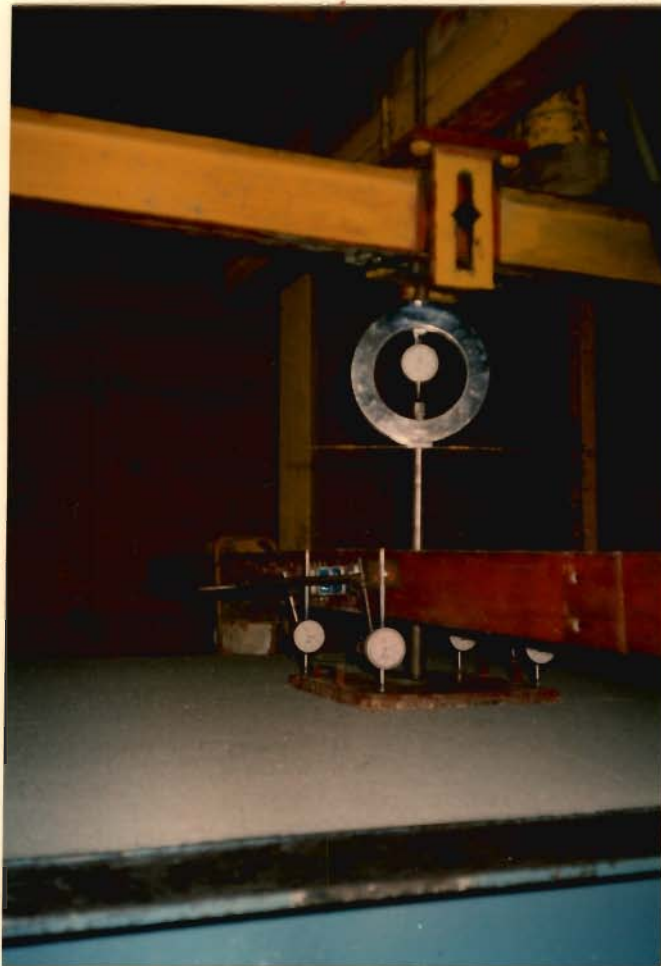


FIG. 3·7 EXPERIMENTAL SET-UP FOR CYCLIC PLATE LOAD TEST ON 300mm SQUARE FOOTING



FIG. 3.8 SETTLEMENT PATTERN IN CYCLIC
PLATE LOAD TEST ON GEOGRID
REINFORCED SAND BED



FIG. 3.9 CYCLIC PLATE LOAD
TEST IN PROGRESS

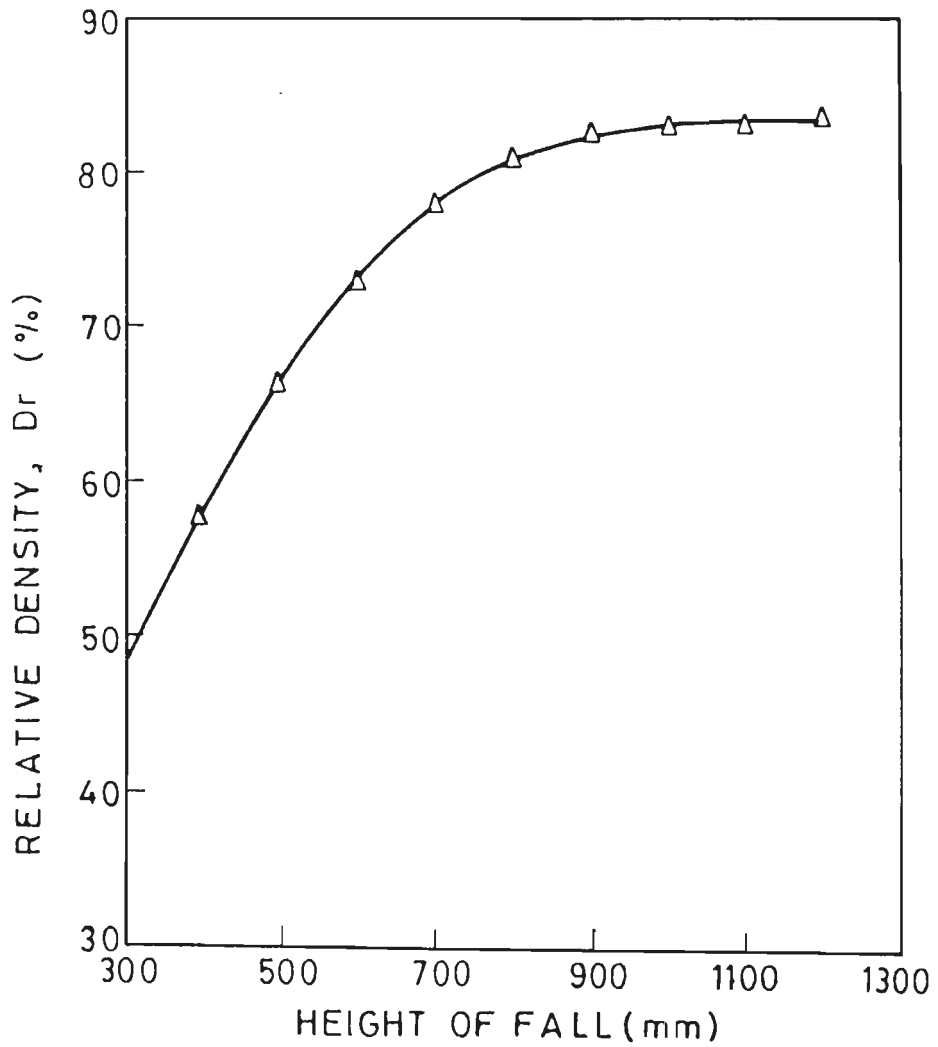


FIG. 3-10 HEIGHT OF FALL VERSUS RELATIVE DENSITY FOR AMANANTGARH SAND

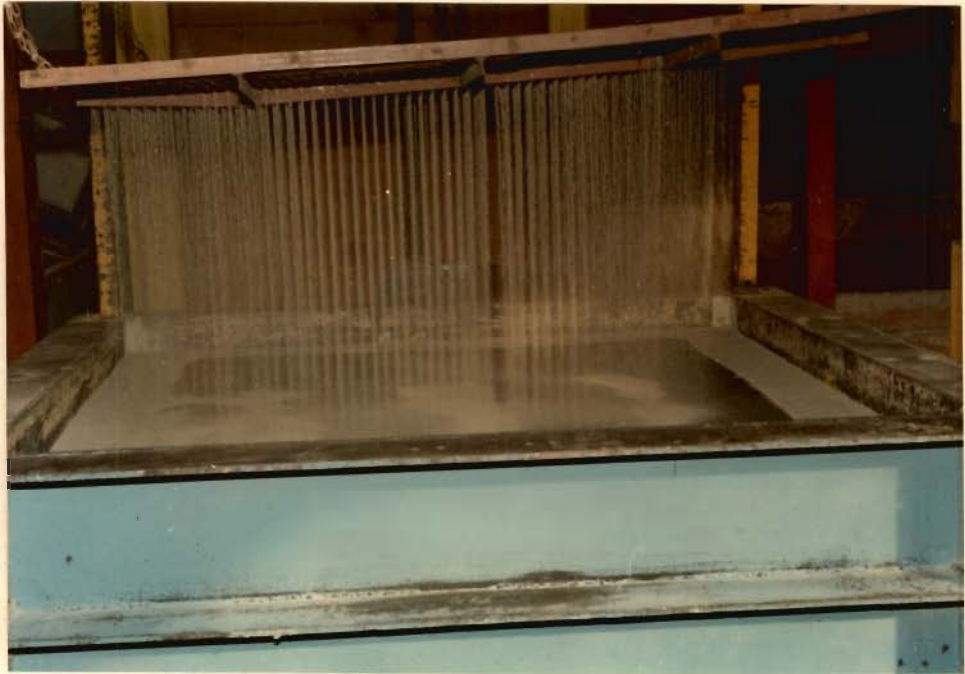


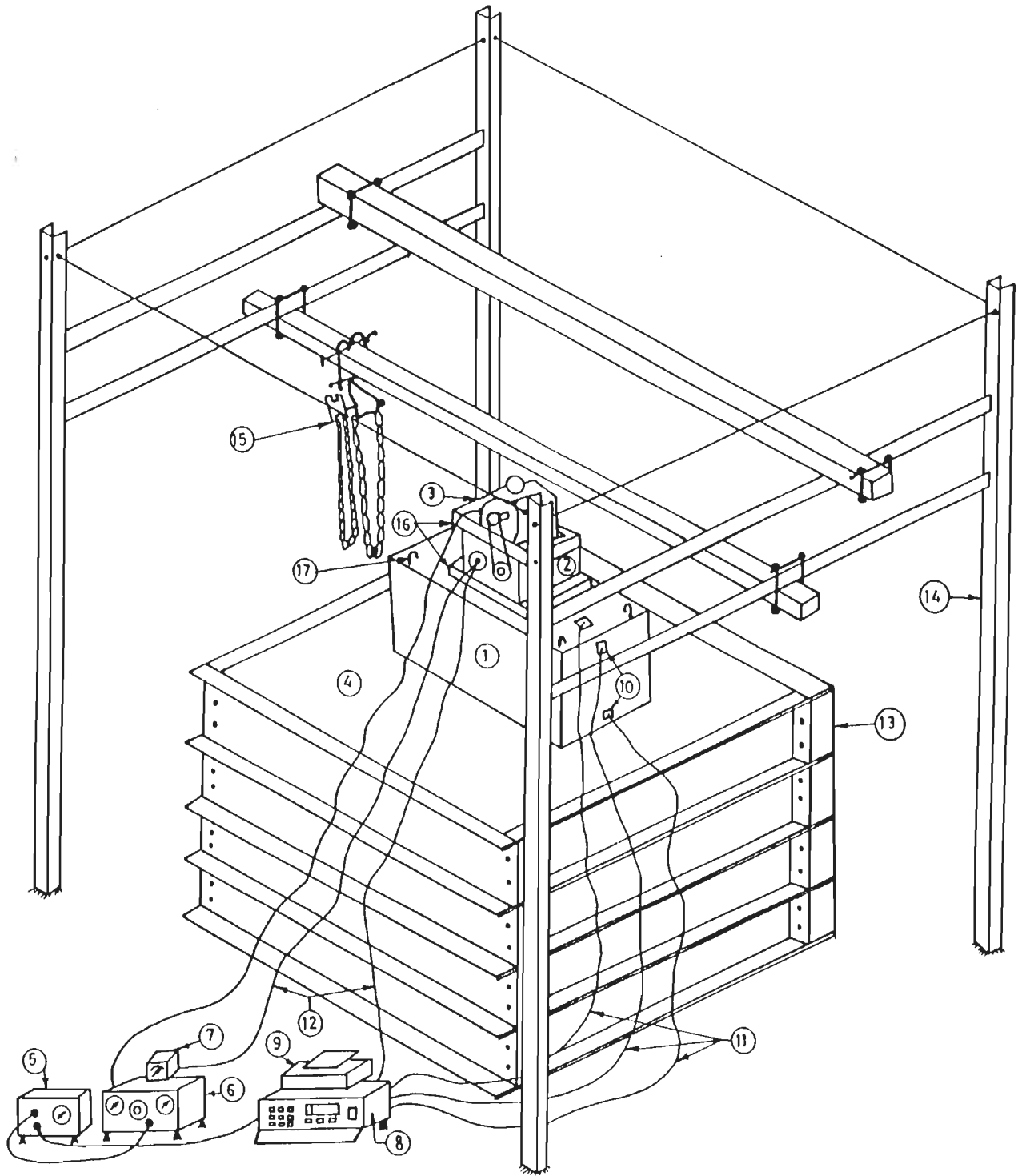
FIG.3.11 SAND FILLING BY RAINFALL TECHNIQUE



FIG. 3.12 LAYING OF REINFORCEMENT
LAYER IN SAND BED



FIG. 3.13 EXPERIMENTAL SET-UP FOR
VERTICAL BLOCK VIBRATION TEST



- | | | |
|-----------------------|--|--|
| 1. BLOCK | 7. FREQUENCY METER | 13. STEEL TANK |
| 2. OSCILLATOR | 8. DATA LOGGER | 14. LOAD FRAME FOR LIFTING AND PLACING BLOCK |
| 3. D/C MOTOR | 9. PRINTER | 15. CHAIN PULLEY BLOCK |
| 4. SAND BED | 10. ACCELERATION SENSORS | 16. BASE AND TOP PLATES FOR OSCILLATOR |
| 5. POWER SUPPLY | 11. WIRES CONNECTING ACCELEROMETERS TO DA-465 MODULES OF DATA LOGGER | 17. HOOKS FOR LIFTING THE BLOCK |
| 6. SPEED CONTROL UNIT | 12. WIRES CONNECTING TACHO INPUT TO DATA LOGGER AND FREQUENCY METER | |

FIG. 3-14 EXPERIMENTAL SET-UP FOR BLOCK VIBRATION TESTS



FIG. 3-15 EXPERIMENTAL SET-UP
FOR HORIZONTAL BLOCK
VIBRATION TESTS



FIG. 3-16 SOIL DATA LOGGER-4201

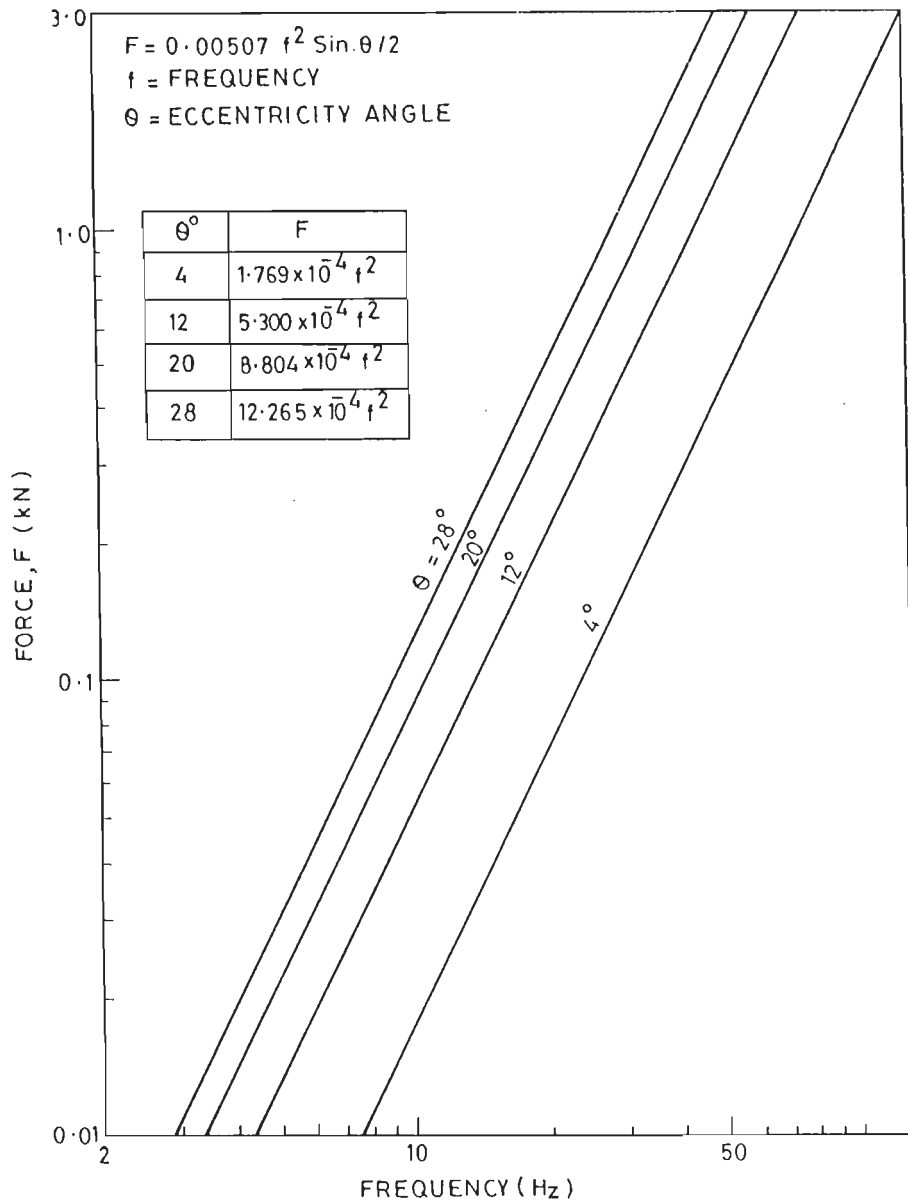


FIG. 3-17 DYNAMIC FORCE VERSUS FREQUENCY OF OSCILLATOR

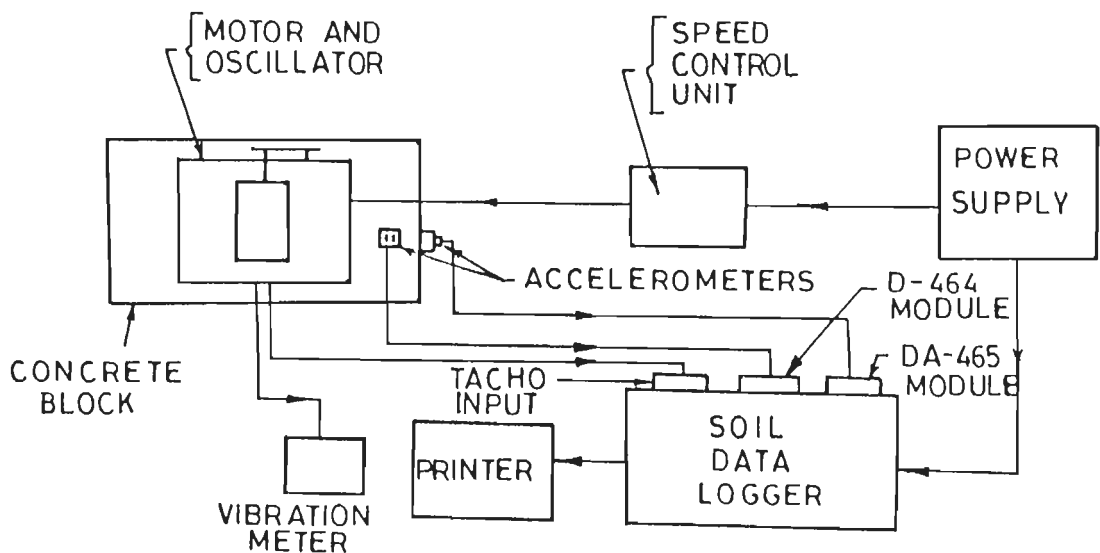


FIG. 3-19 BLOCK DIAGRAM OF TESTING EQUIPMENT FOR BLOCK VIBRATION TESTS

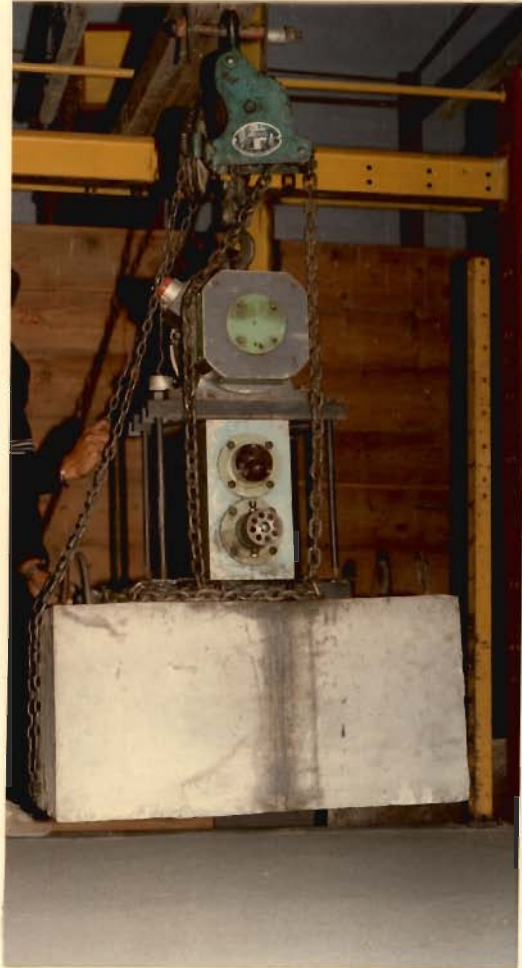


FIG.3.18 PLACING THE BLOCK OVER SAND BED

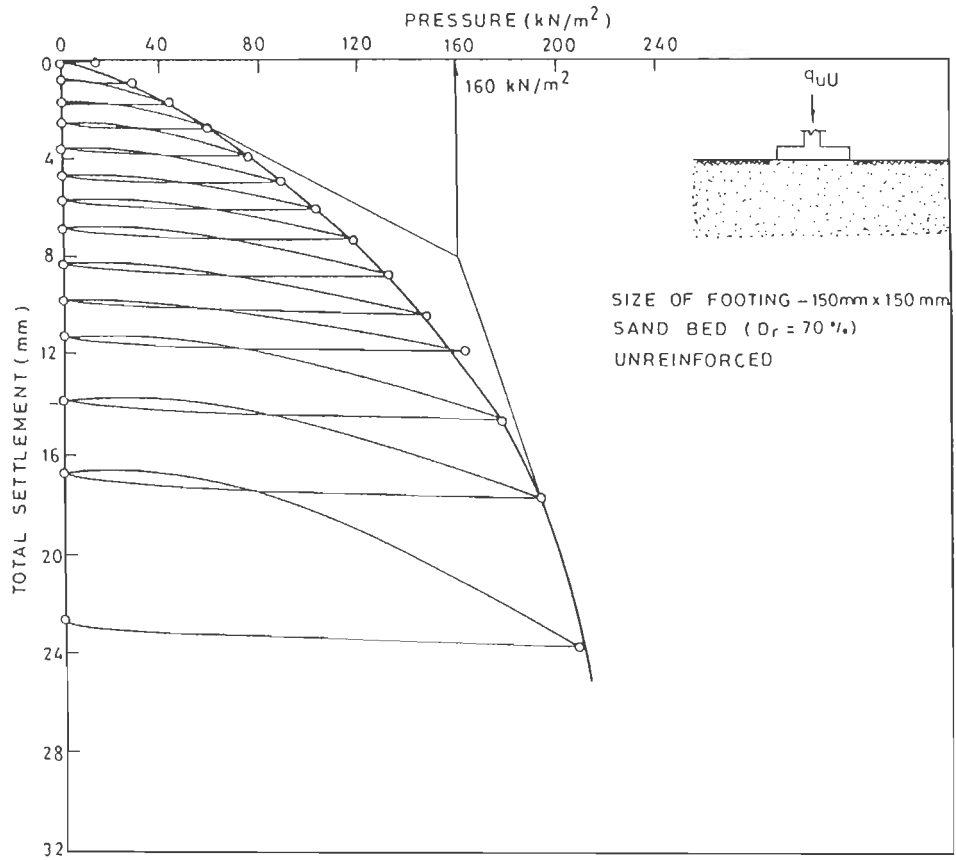


FIG. 3.20(a) CYCLIC PLATE LOAD TEST — PRESSURE VERSUS TOTAL SETTLEMENT

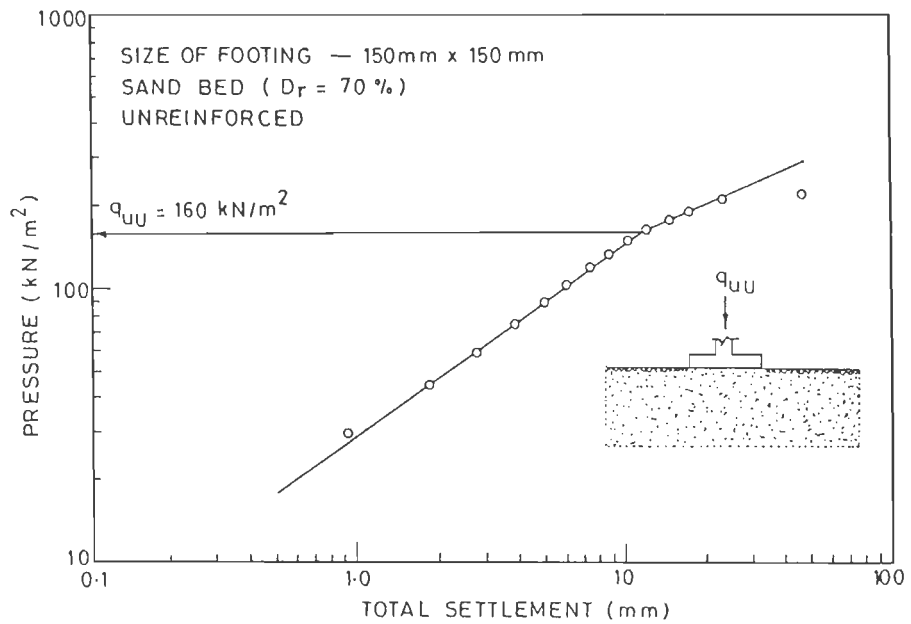


FIG. 3.20(b) CYCLIC PLATE LOAD TEST — PRESSURE VERSUS TOTAL SETTLEMENT — LOG-LOG PLOT

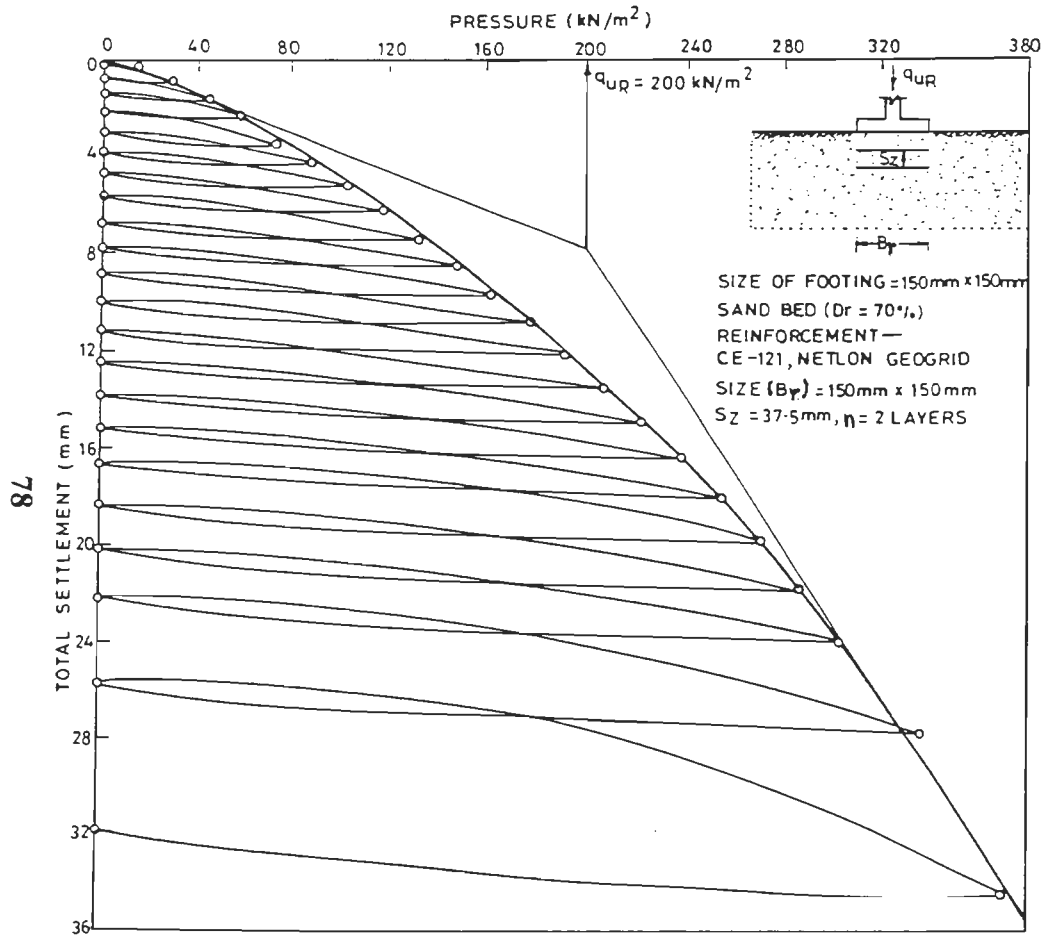


FIG. 3:21 CYCLIC PLATE LOAD TEST PRESSURE VERSUS TOTAL SETTLEMENT

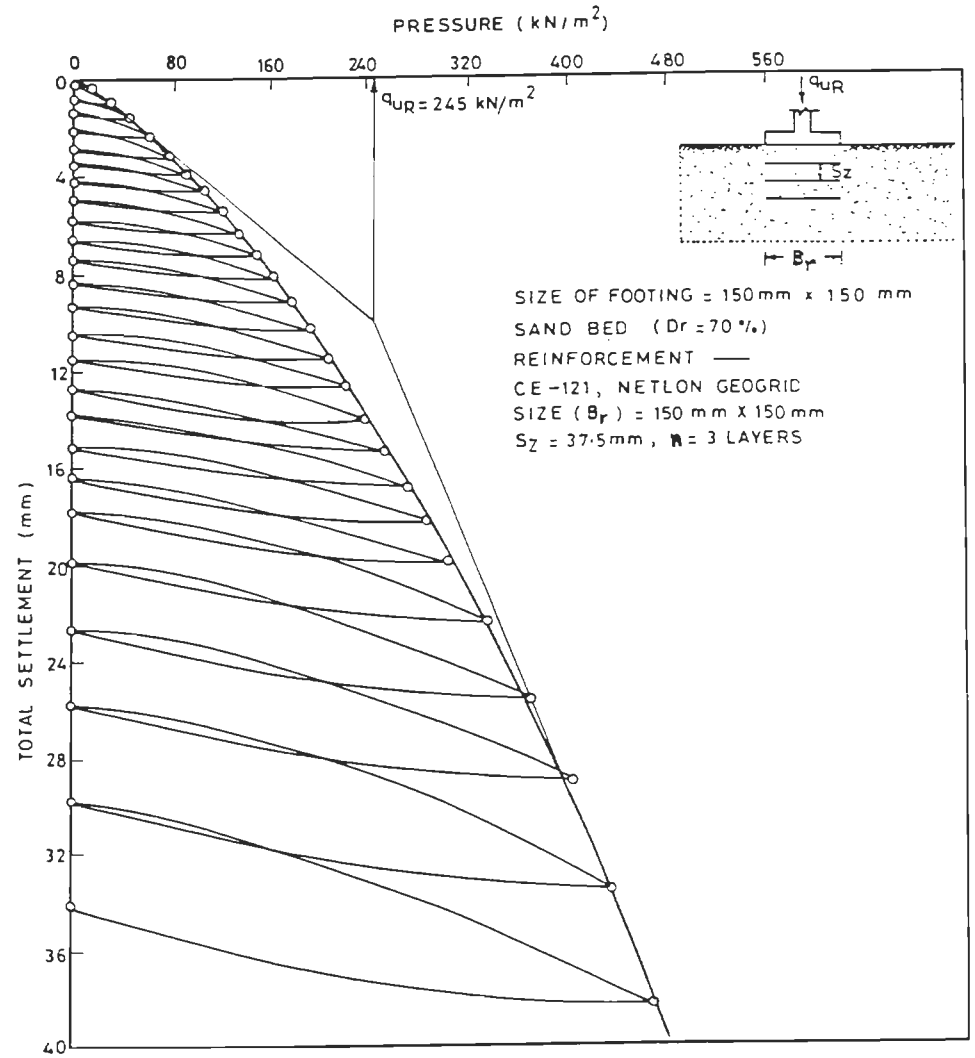


FIG. 3:22 CYCLIC PLATE LOAD TEST—PRESSURE VERSUS TOTAL SETTLEMENT

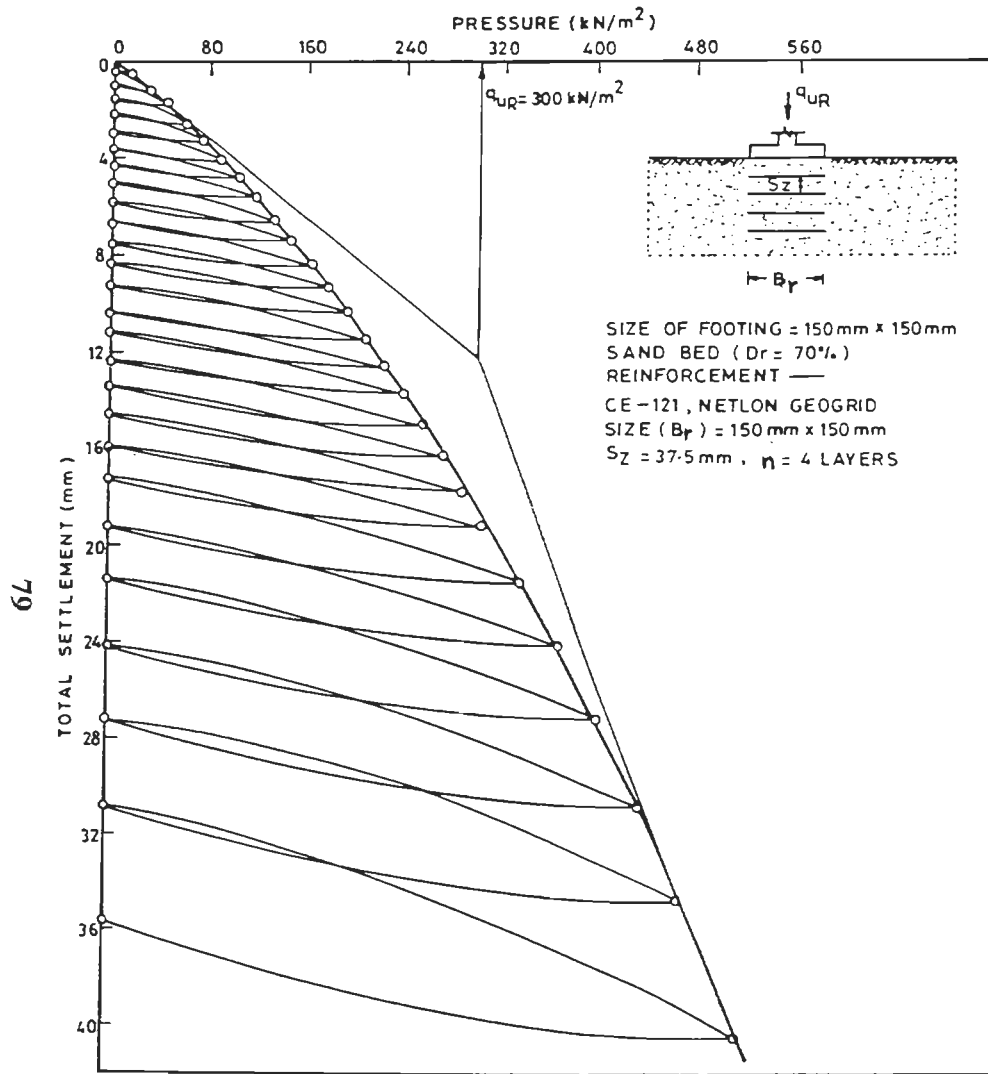


FIG.3-23 CYCLIC PLATE LOAD TEST—PRESSURE VERSUS TOTAL SETTLEMENT

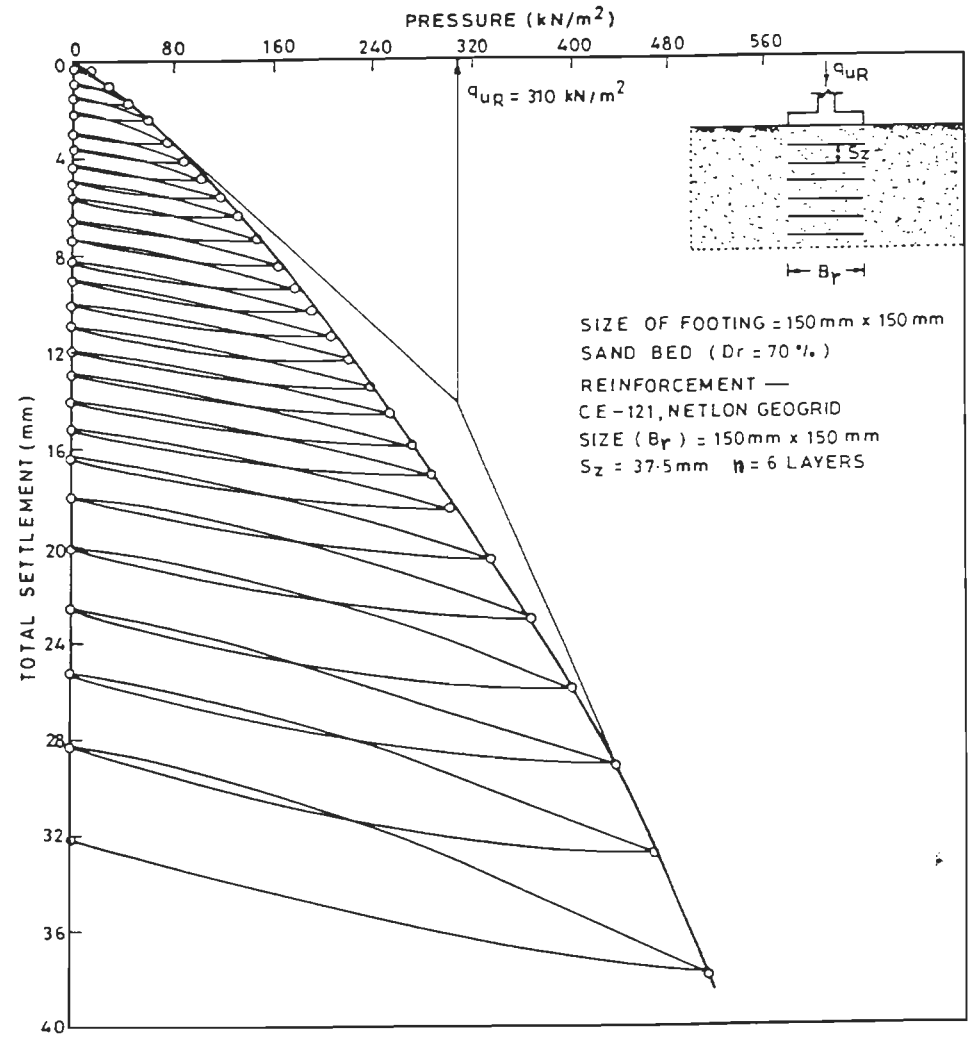


FIG.3-24 CYCLIC PLATE LOAD TEST—PRESSURE VERSUS TOTAL SETTLEMENT

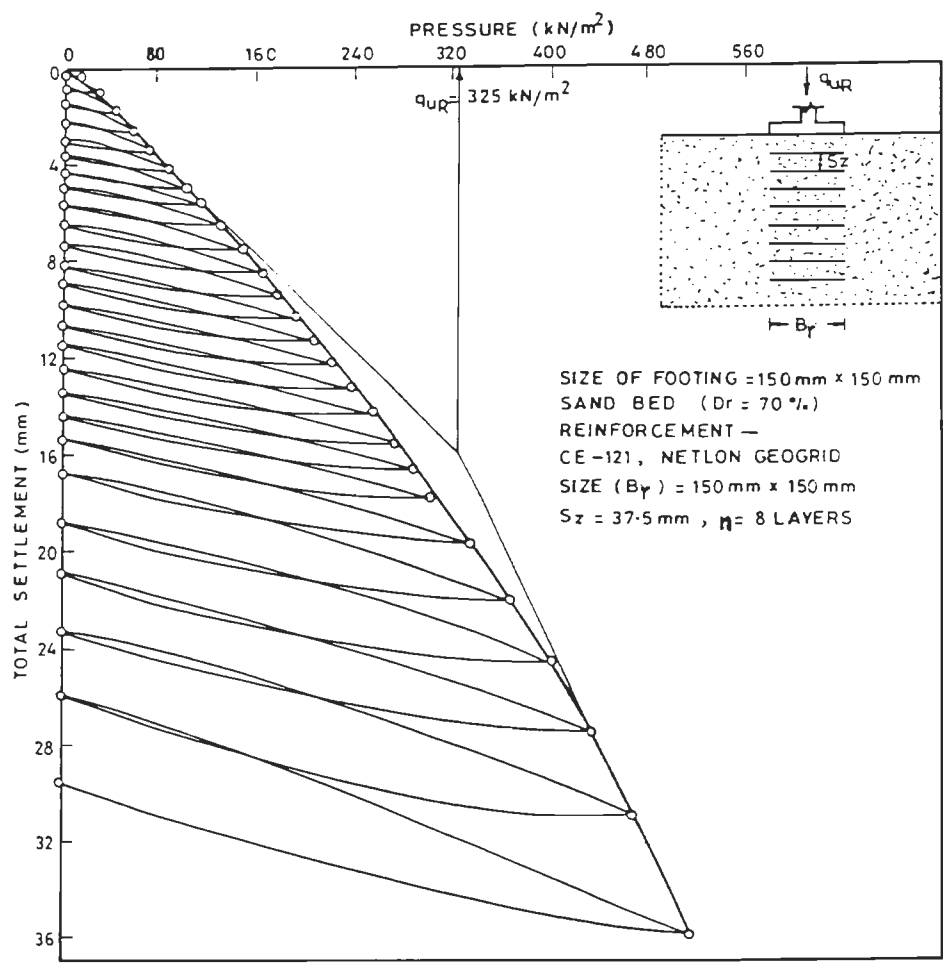


FIG.3-25 CYCLIC PLATE LOAD TEST—PRESSURE VERSUS TOTAL SETTLEMENT

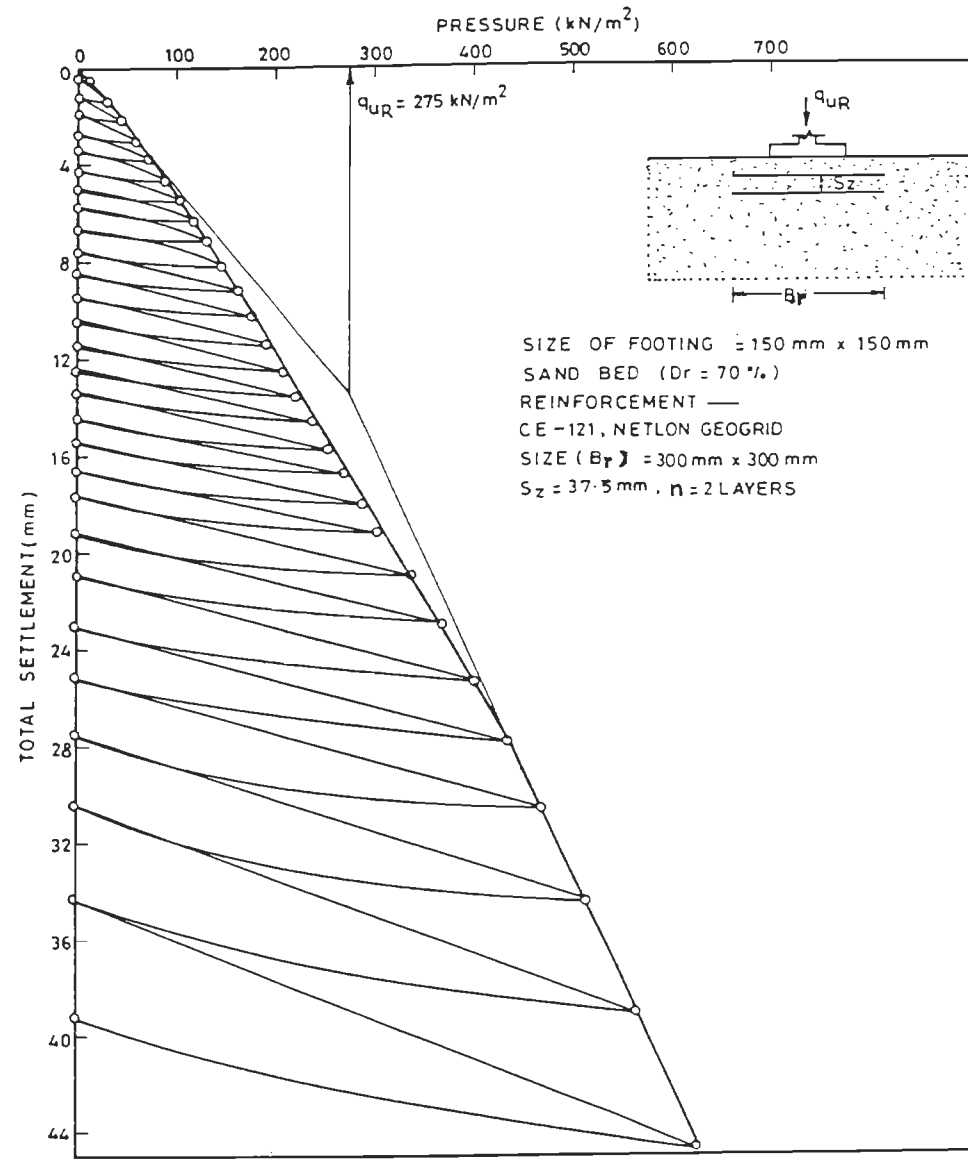


FIG.3-26 CYCLIC PLATE LOAD TEST—PRESSURE VERSUS TOTAL SETTLEMENT

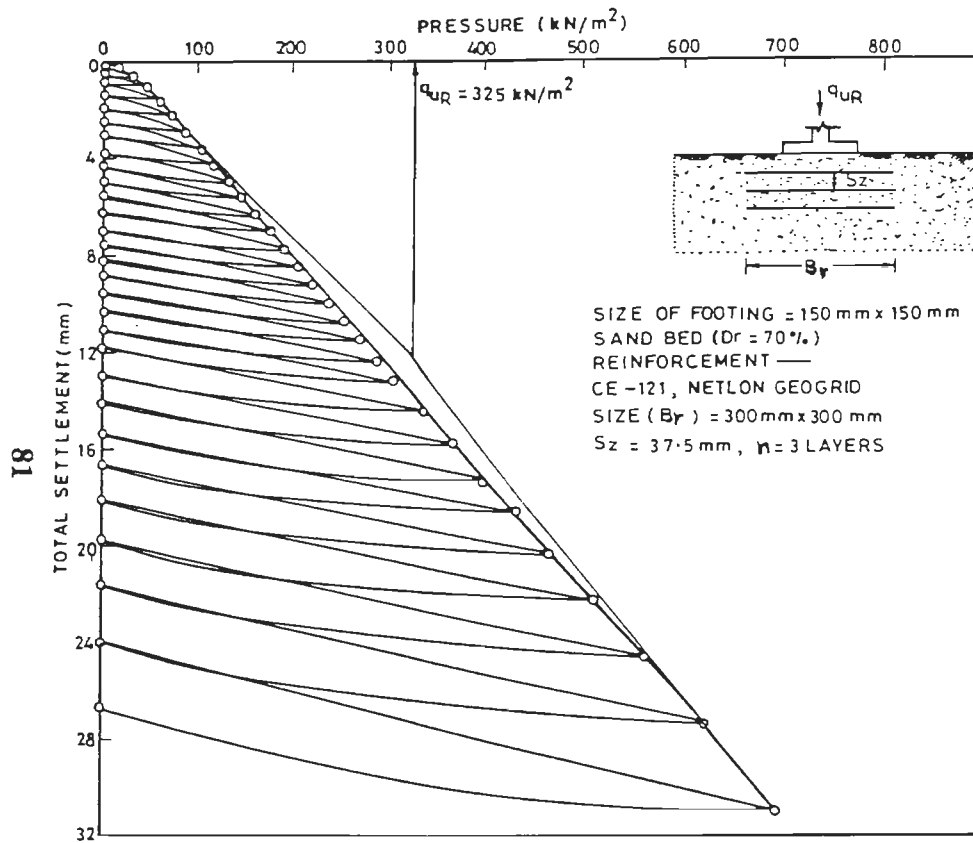


FIG. 3-27 CYCLIC PLATE LOAD TEST - PRESSURE VERSUS TOTAL SETTLEMENT

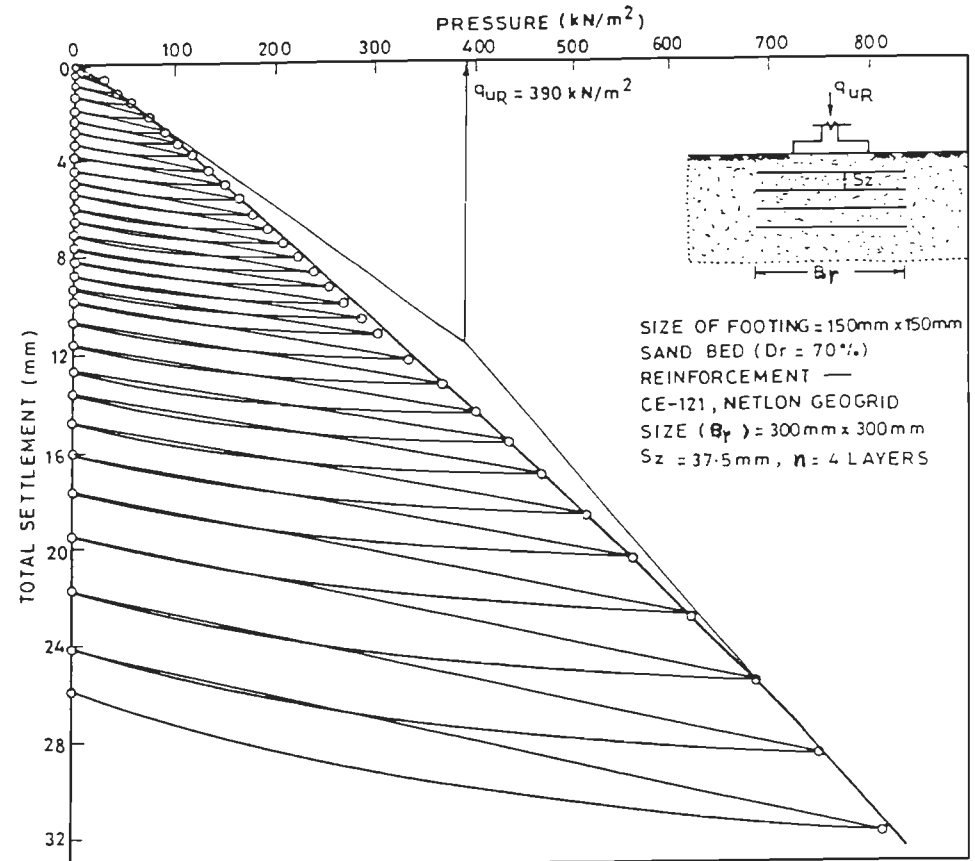


FIG. 3-28 CYCLIC PLATE LOAD TEST - PRESSURE VERSUS TOTAL SETTLEMENT

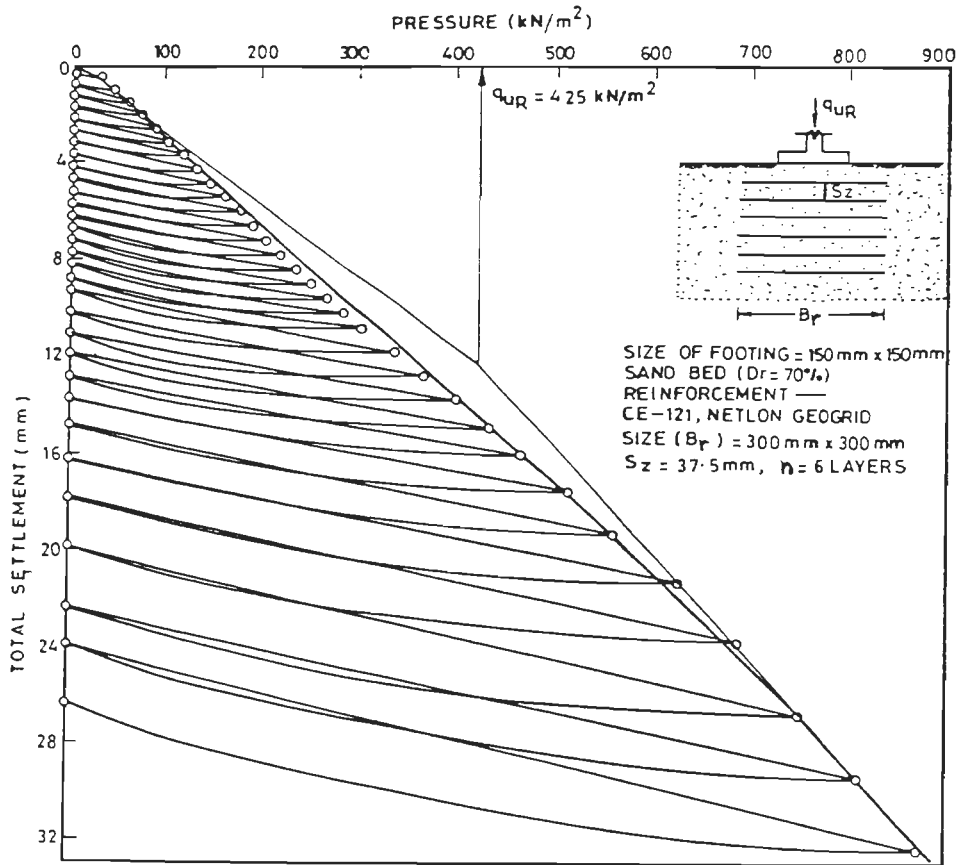


FIG. 3-29 CYCLIC PLATE LOAD TEST—PRESSURE VERSUS TOTAL SETTLEMENT

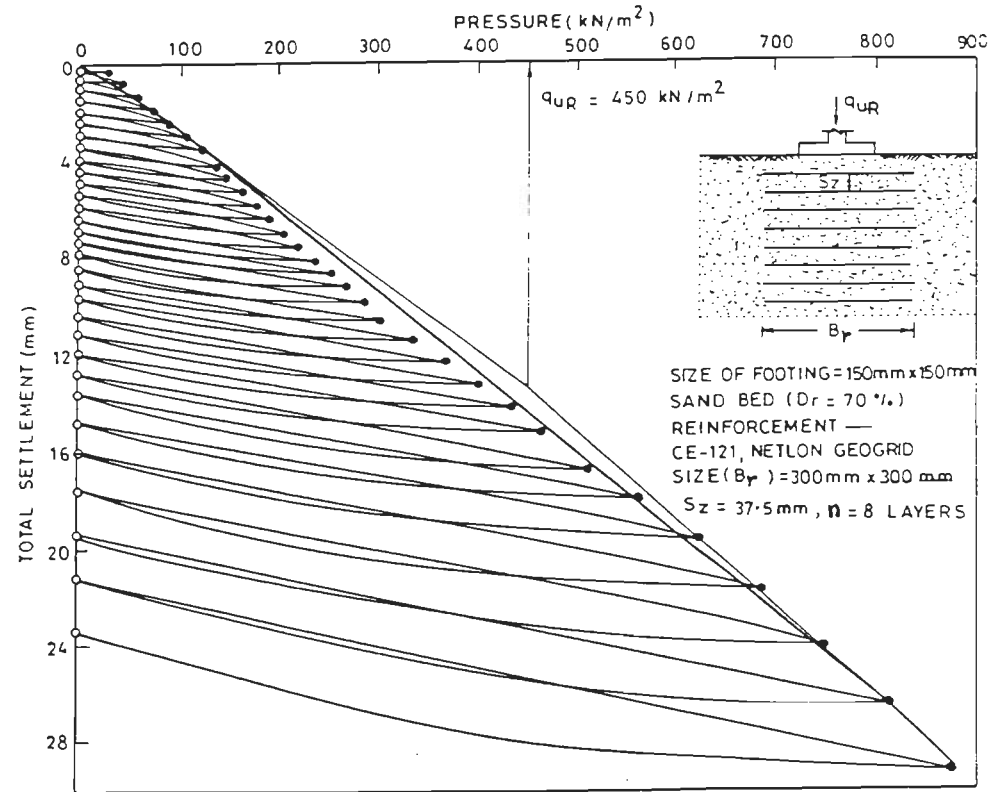


FIG. 3-30 CYCLIC PLATE LOAD TEST—PRESSURE VERSUS TOTAL SETTLEMENT

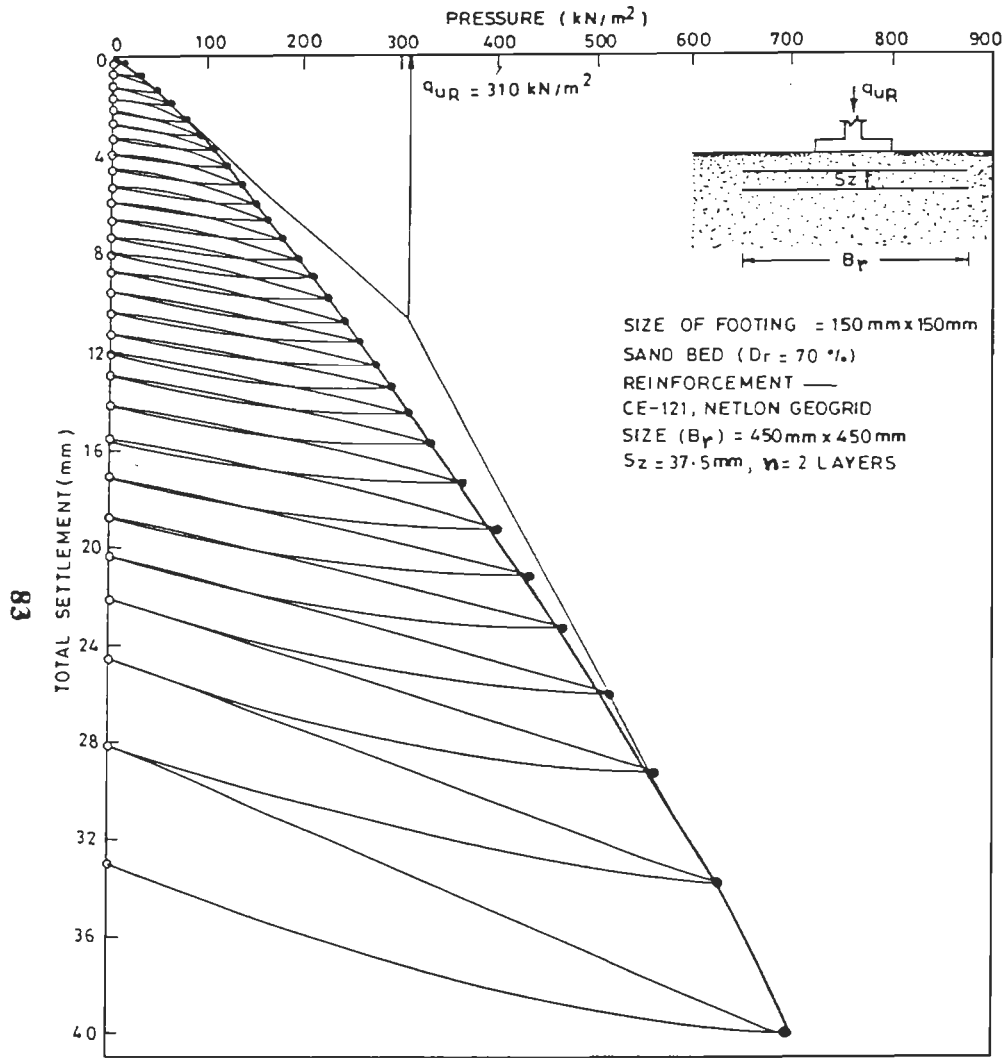


FIG. 3-31 CYCLIC PLATE LOAD TEST — PRESSURE VERSUS TOTAL SETTLEMENT

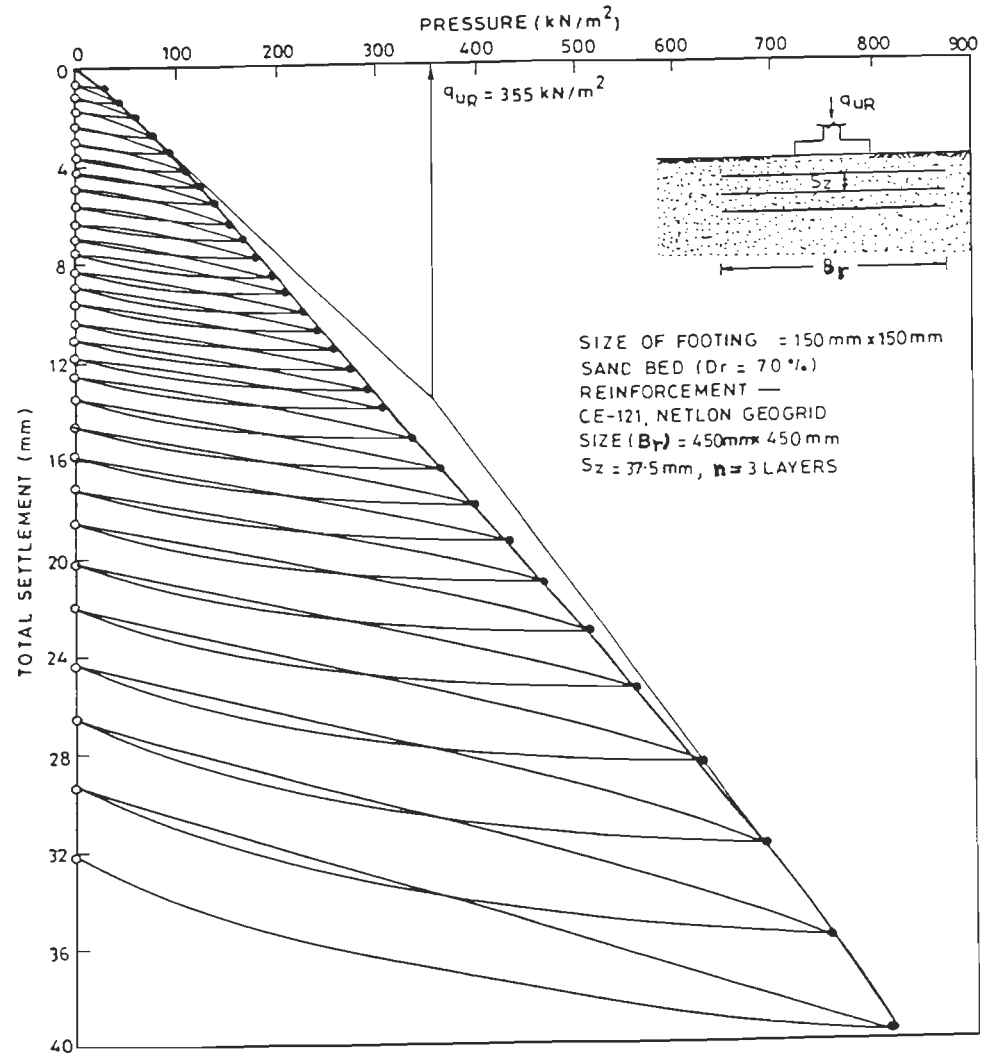


FIG. 3-32 CYCLIC PLATE LOAD TEST — PRESSURE VERSUS TOTAL SETTLEMENT

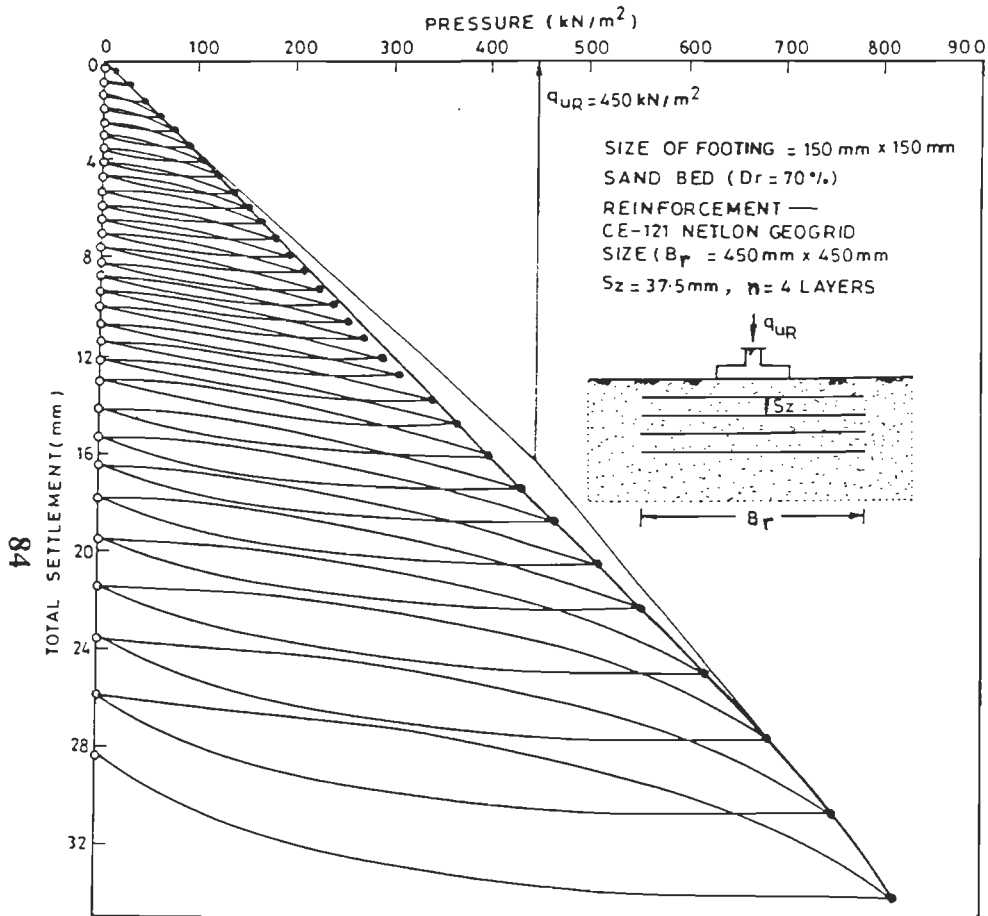


FIG. 3.33 CYCLIC PLATE LOAD TEST- PRESSURE VERSUS TOTAL SETTLEMENT

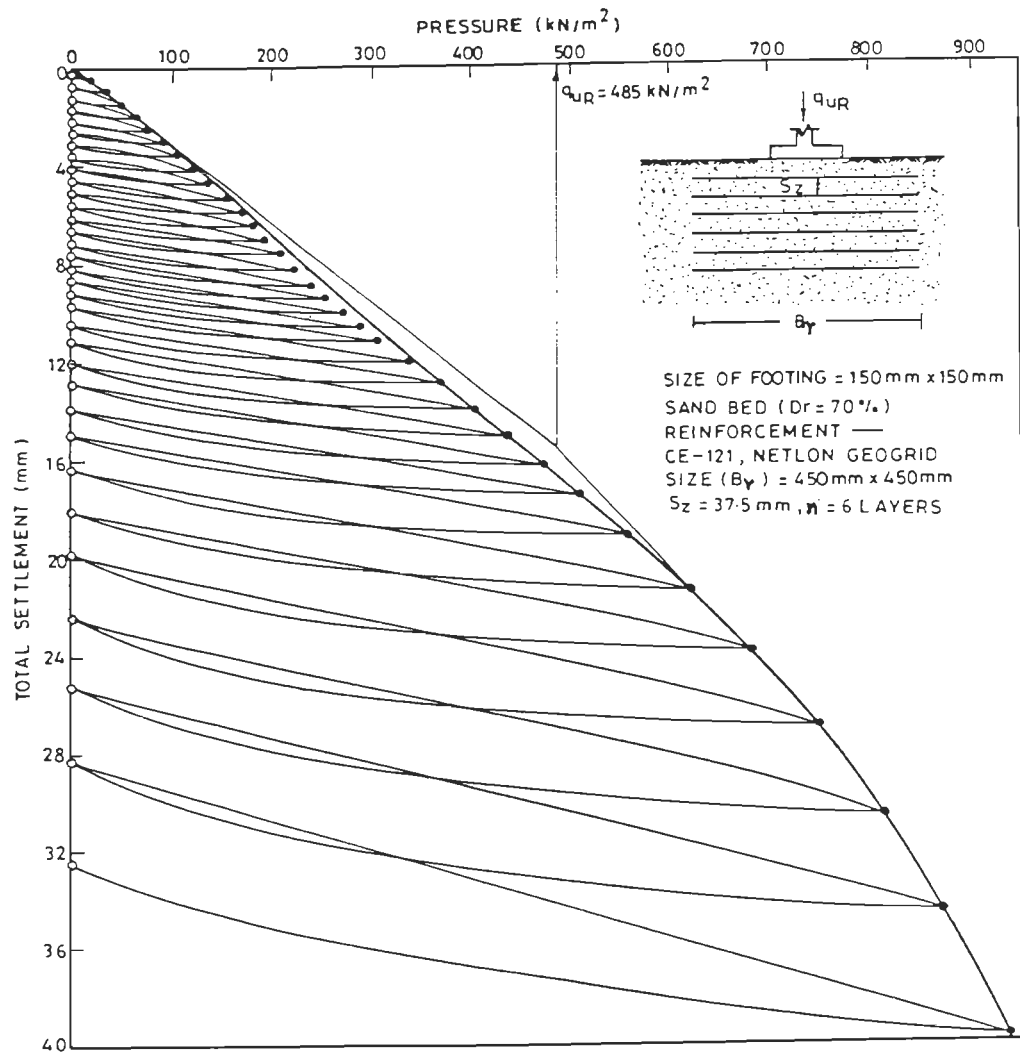


FIG. 3.34 CYCLIC PLATE LOAD TEST — PRESSURE VERSUS TOTAL SETTLEMENT

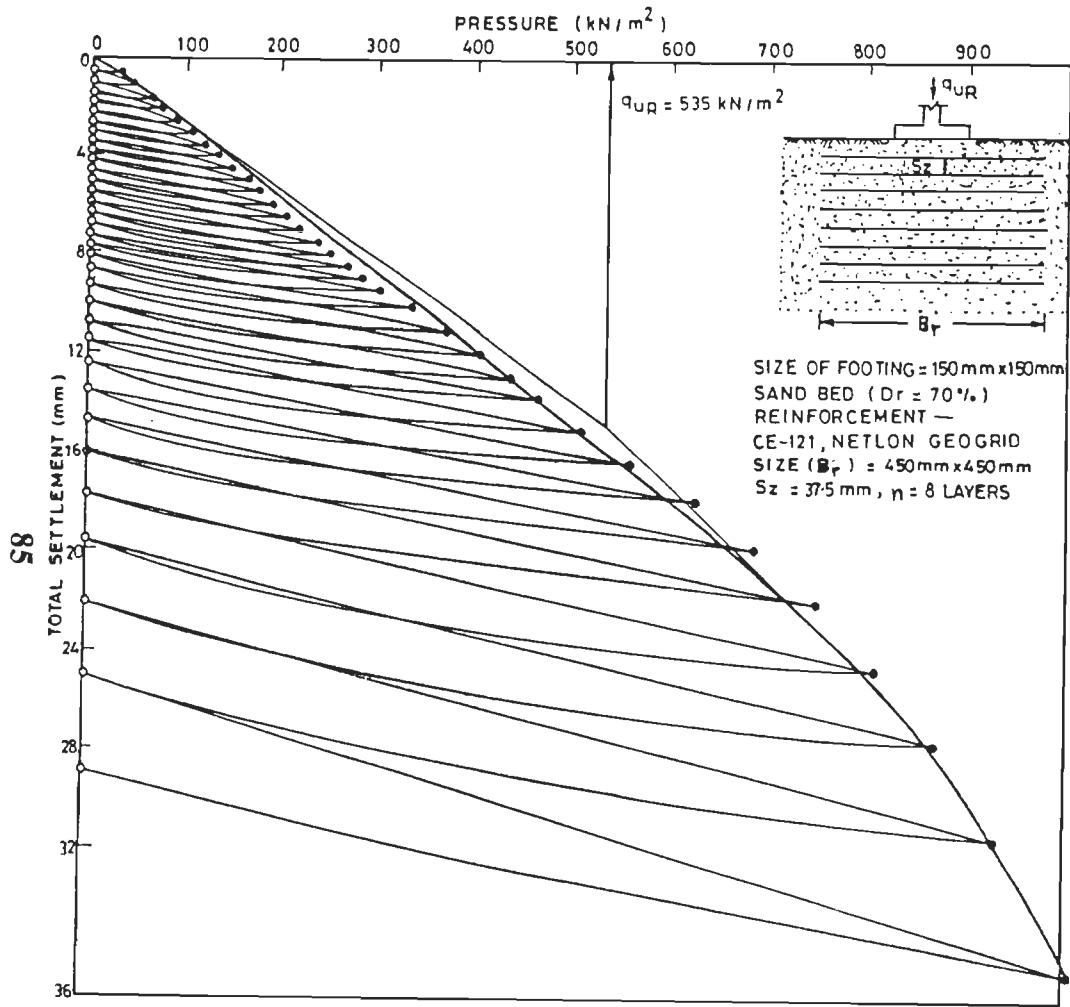


FIG. 3-35 CYCLIC PLATE LOAD TEST — PRESSURE VERSUS TOTAL SETTLEMENT

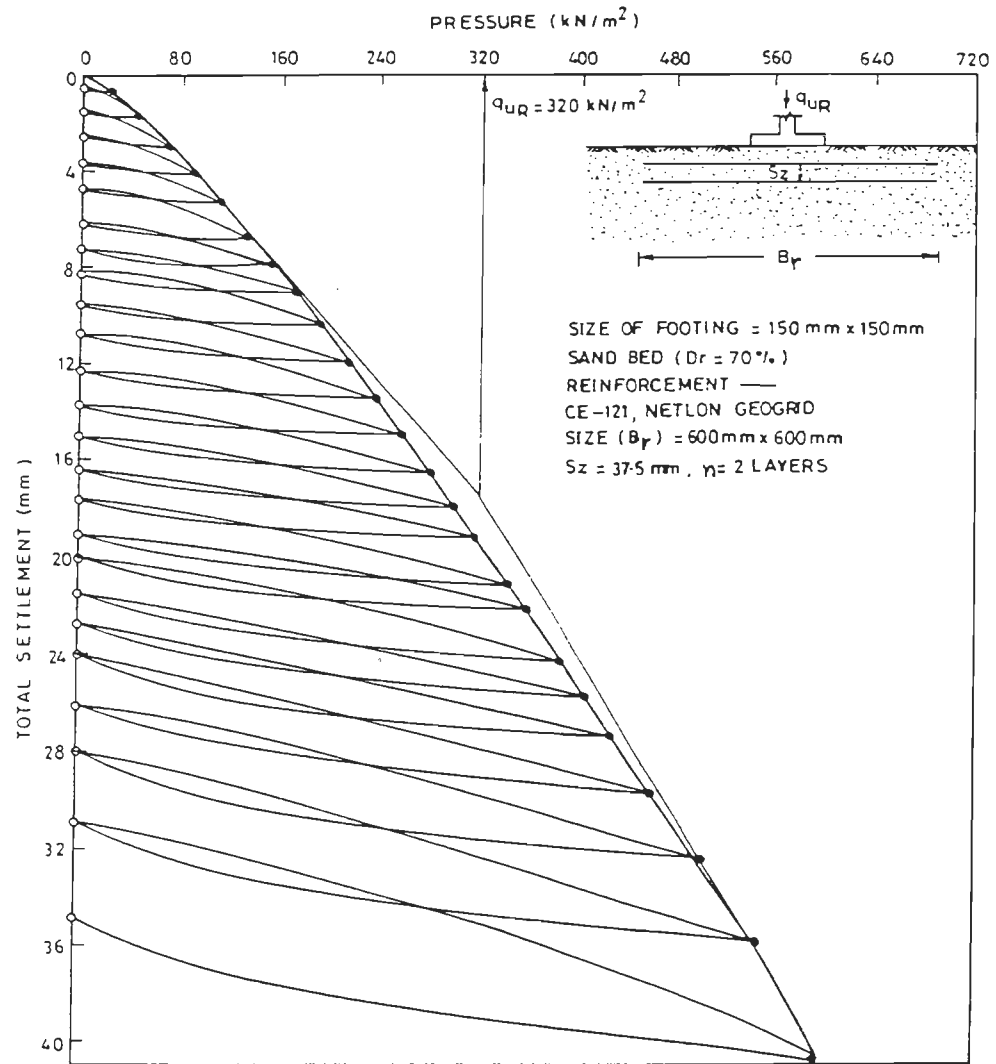


FIG. 3-36 CYCLIC PLATE LOAD TEST — PRESSURE VERSUS TOTAL SETTLEMENT

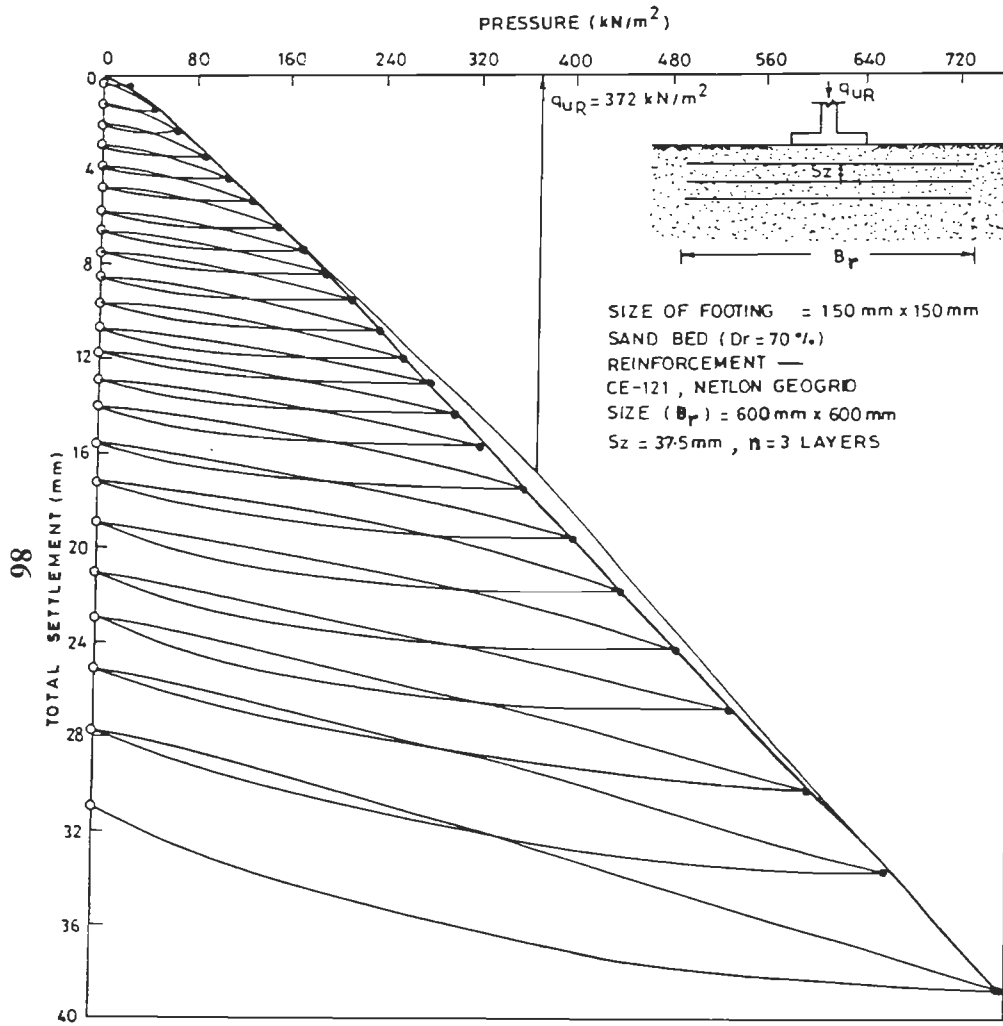


FIG. 3-37 CYCLIC PLATE LOAD TEST — PRESSURE VERSUS TOTAL SETTLEMENT

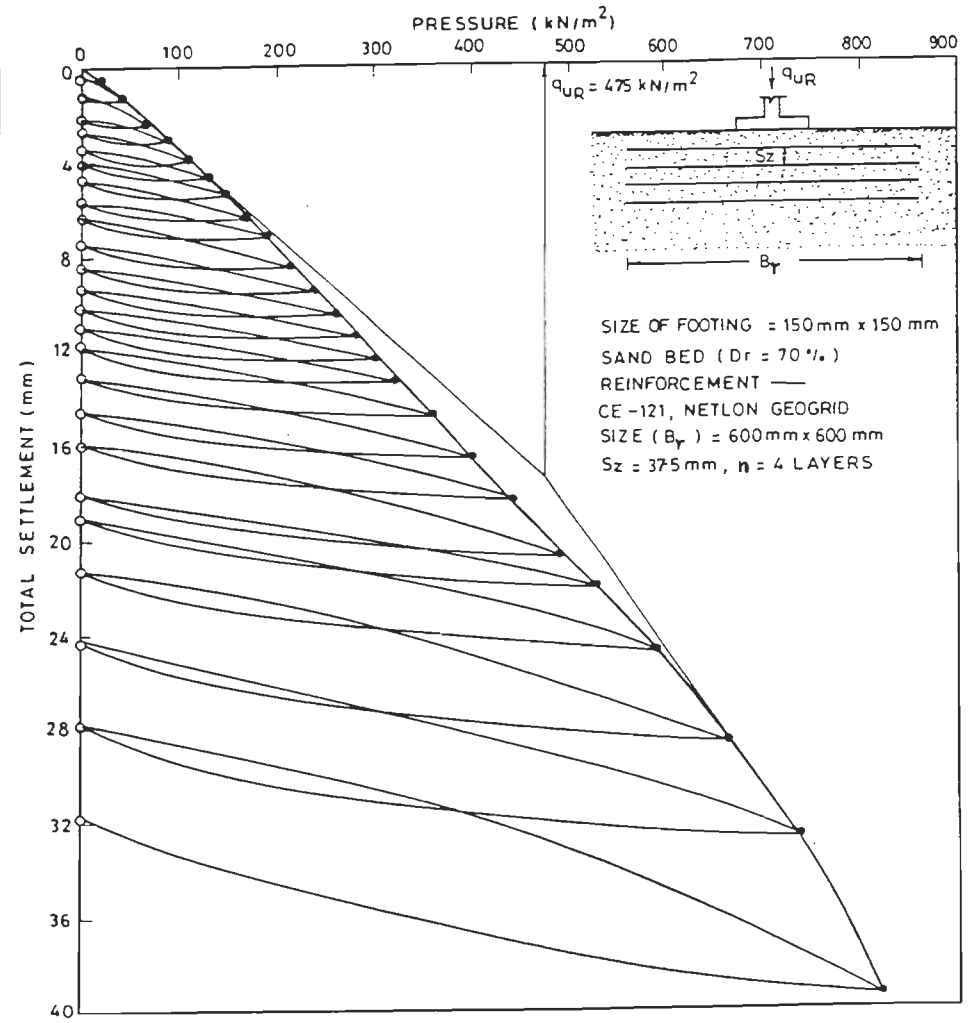


FIG. 3-38 CYCLIC PLATE LOAD TEST — PRESSURE VERSUS TOTAL SETTLEMENT

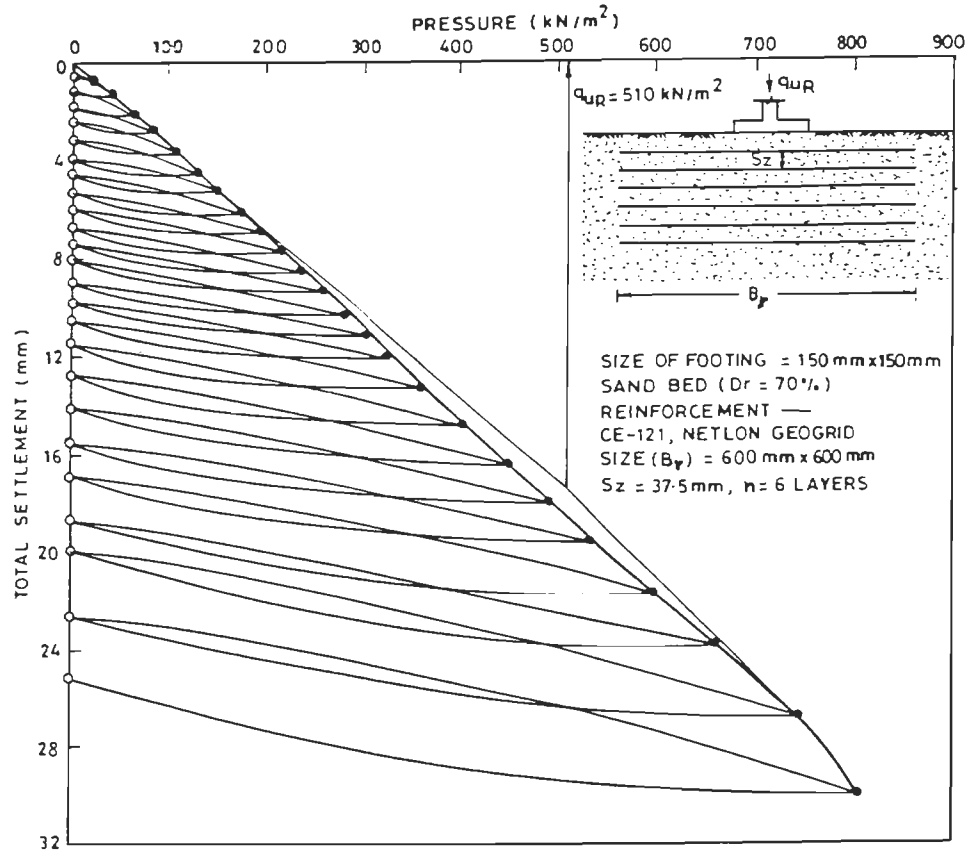


FIG. 3-39 CYCLIC PLATE LOAD TEST — PRESSURE VERSUS TOTAL SETTLEMENT

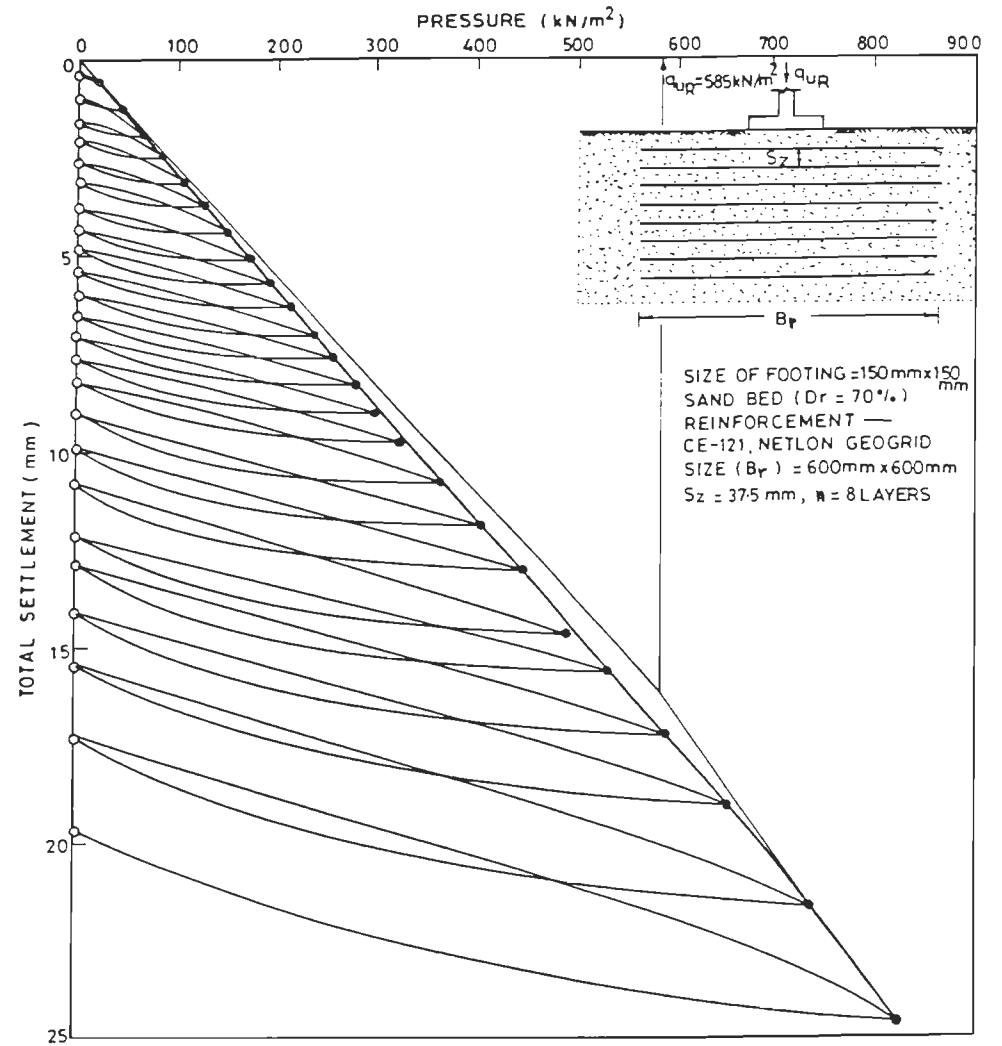


FIG. 3-40 CYCLIC PLATE LOAD TEST — PRESSURE VERSUS TOTAL SETTLEMENT

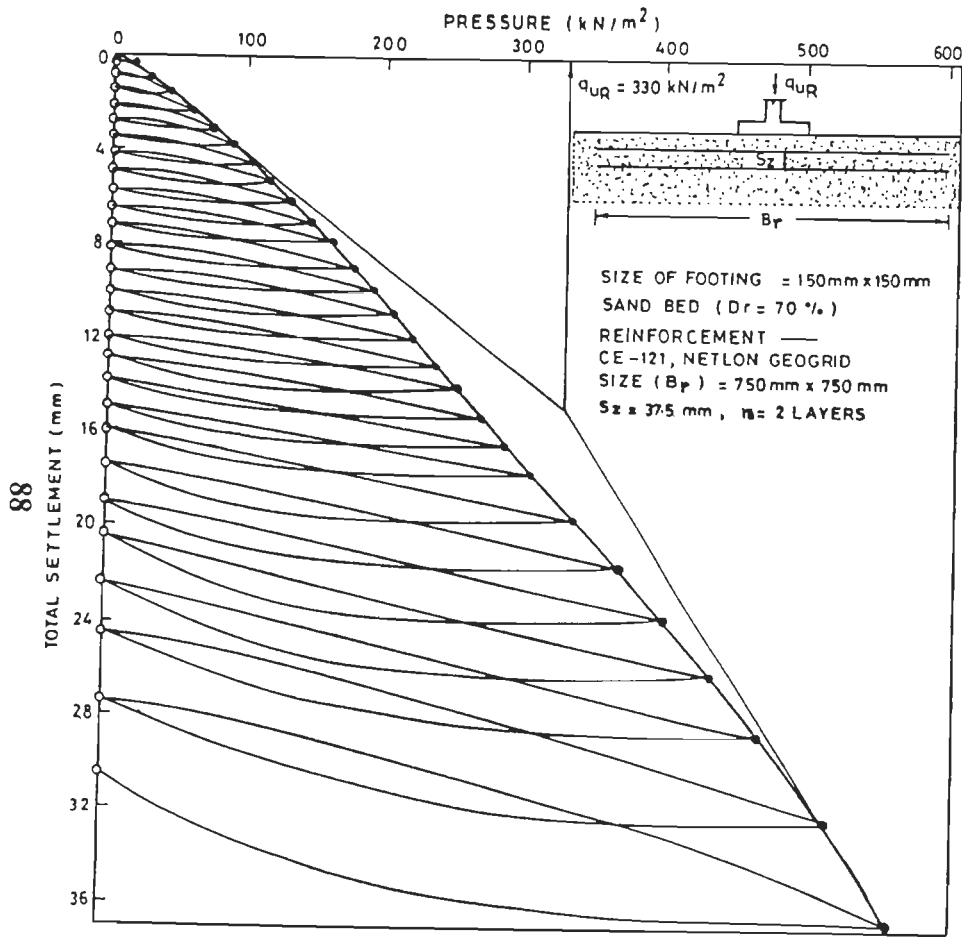


FIG. 3-41 CYCLIC PLATE LOAD TEST — PRESSURE VERSUS TOTAL SETTLEMENT

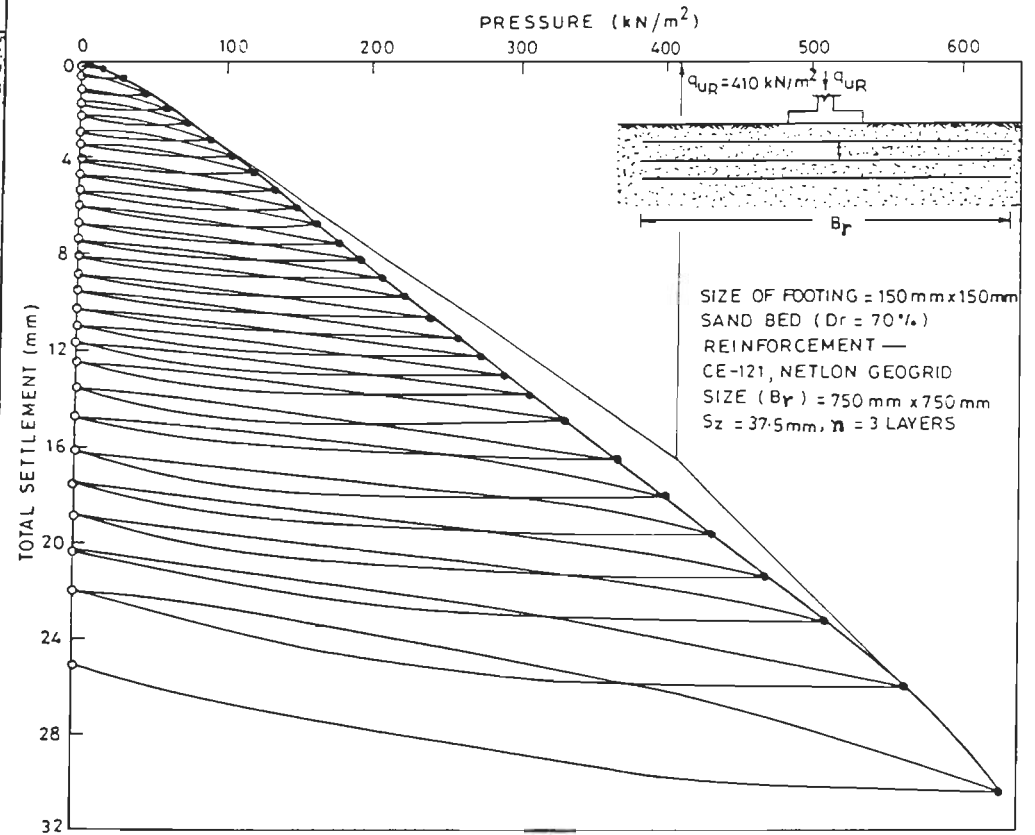


FIG. 3-42 CYCLIC PLATE LOAD TEST — PRESSURE VERSUS TOTAL SETTLEMENT

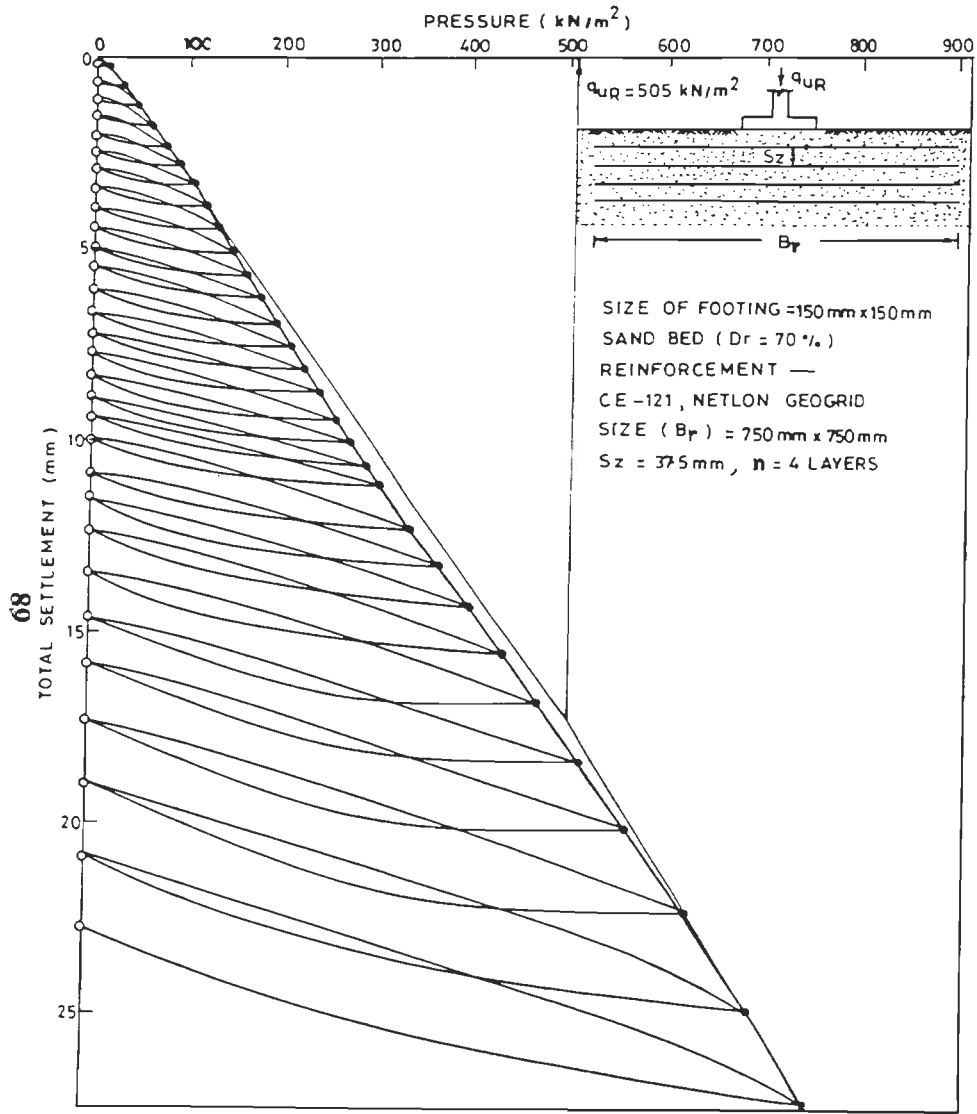


FIG. 3-43 CYCLIC PLATE LOAD TEST — PRESSURE VERSUS TOTAL SETTLEMENT

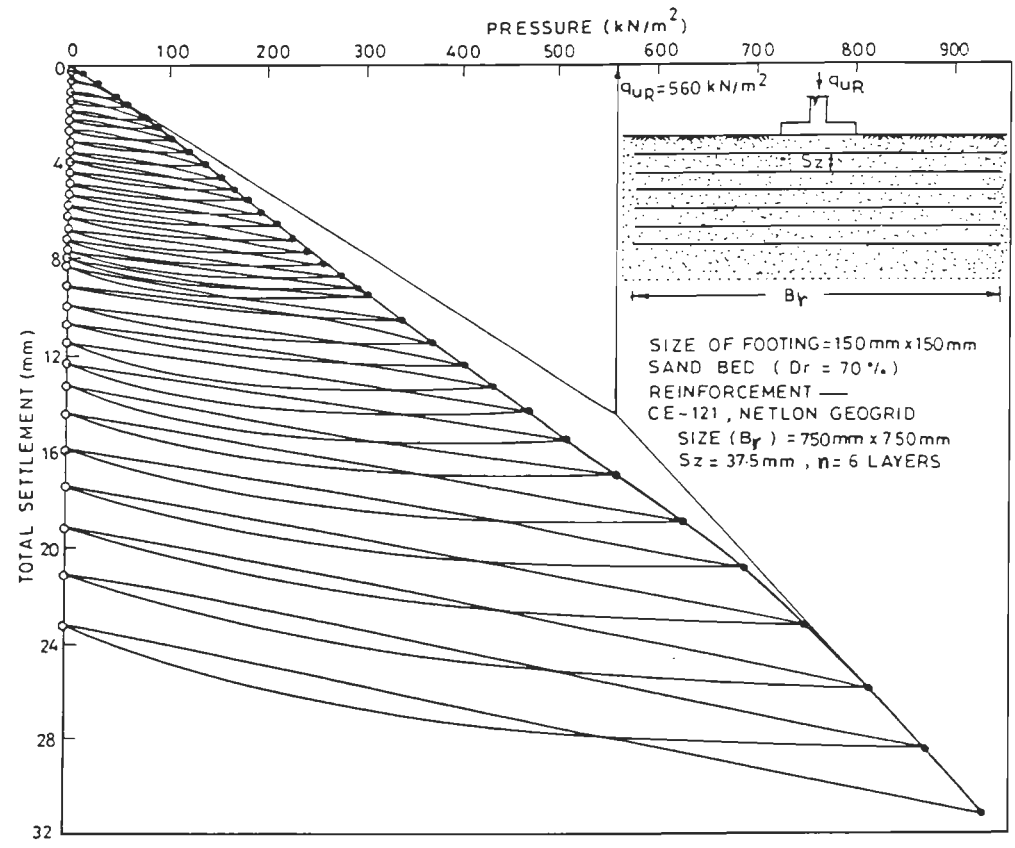


FIG. 3-44 CYCLIC PLATE LOAD TEST — PRESSURE VERSUS TOTAL SETTLEMENT

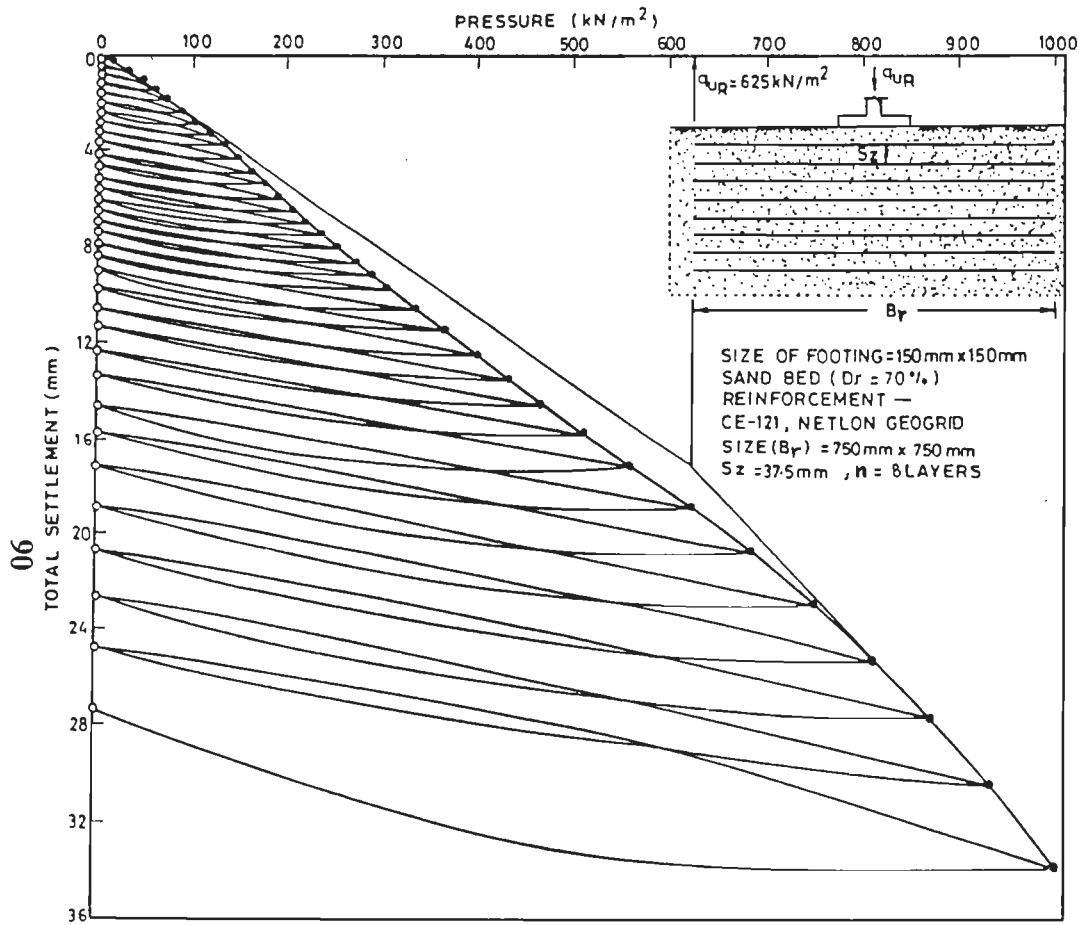


FIG. 3-45 CYCLIC PLATE LOAD TEST — PRESSURE VERSUS TOTAL SETTLEMENT

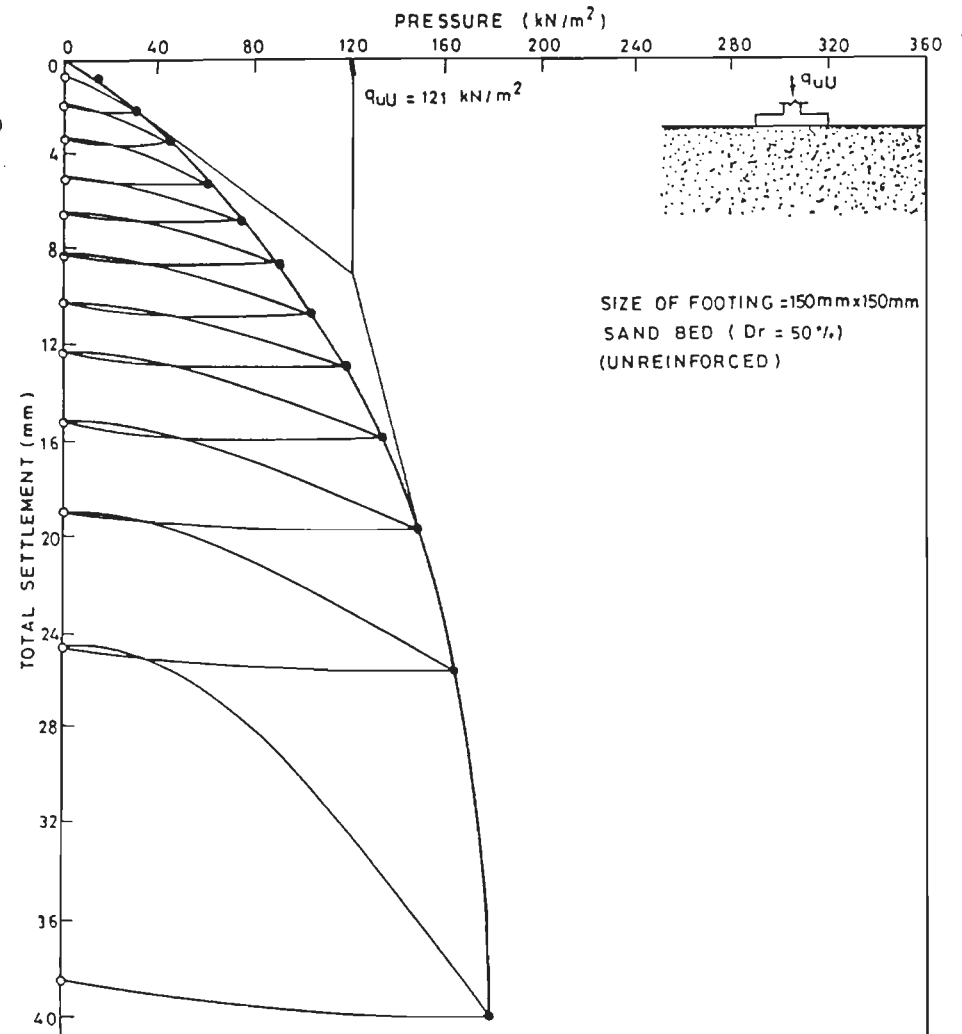


FIG. 3-46 CYCLIC PLATE LOAD TEST — PRESSURE VERSUS TOTAL SETTLEMENT

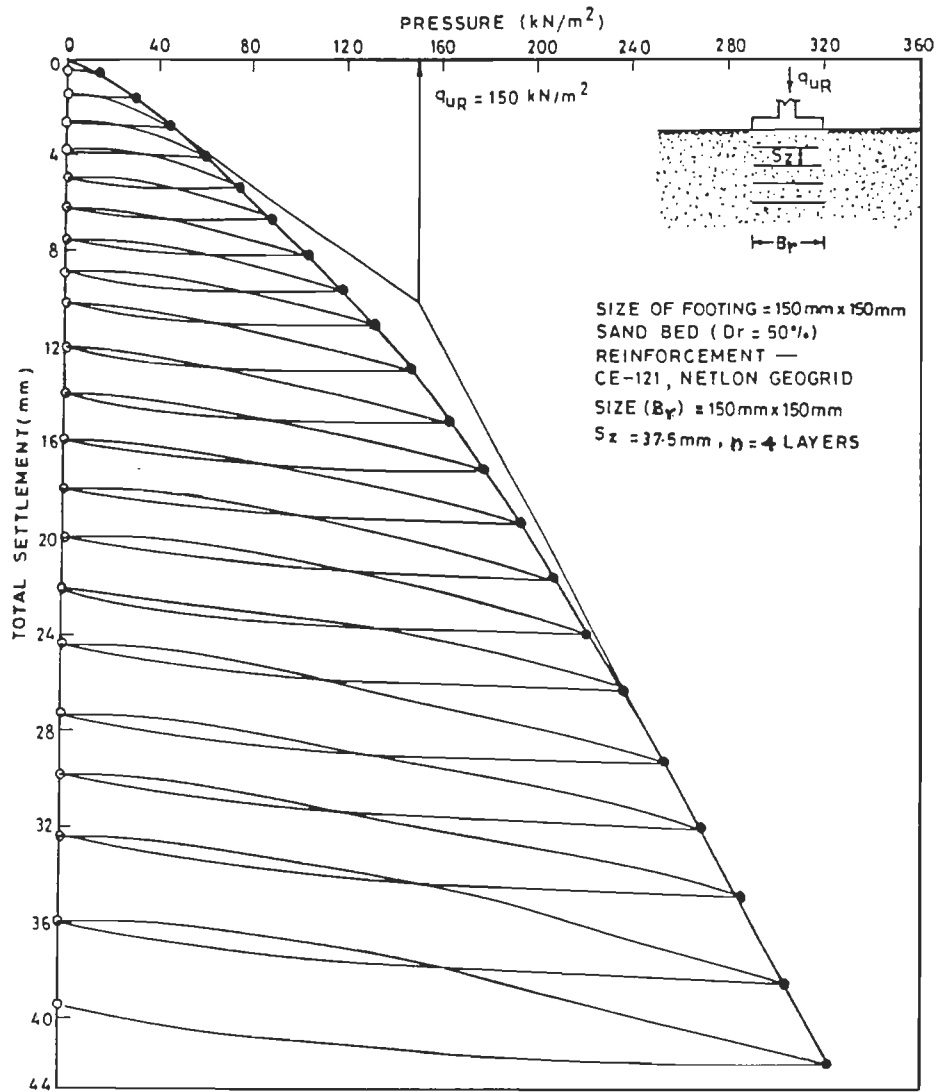


FIG. 3-47 CYCLIC PLATE LOAD TEST — PRESSURE VERSUS TOTAL SETTLEMENT

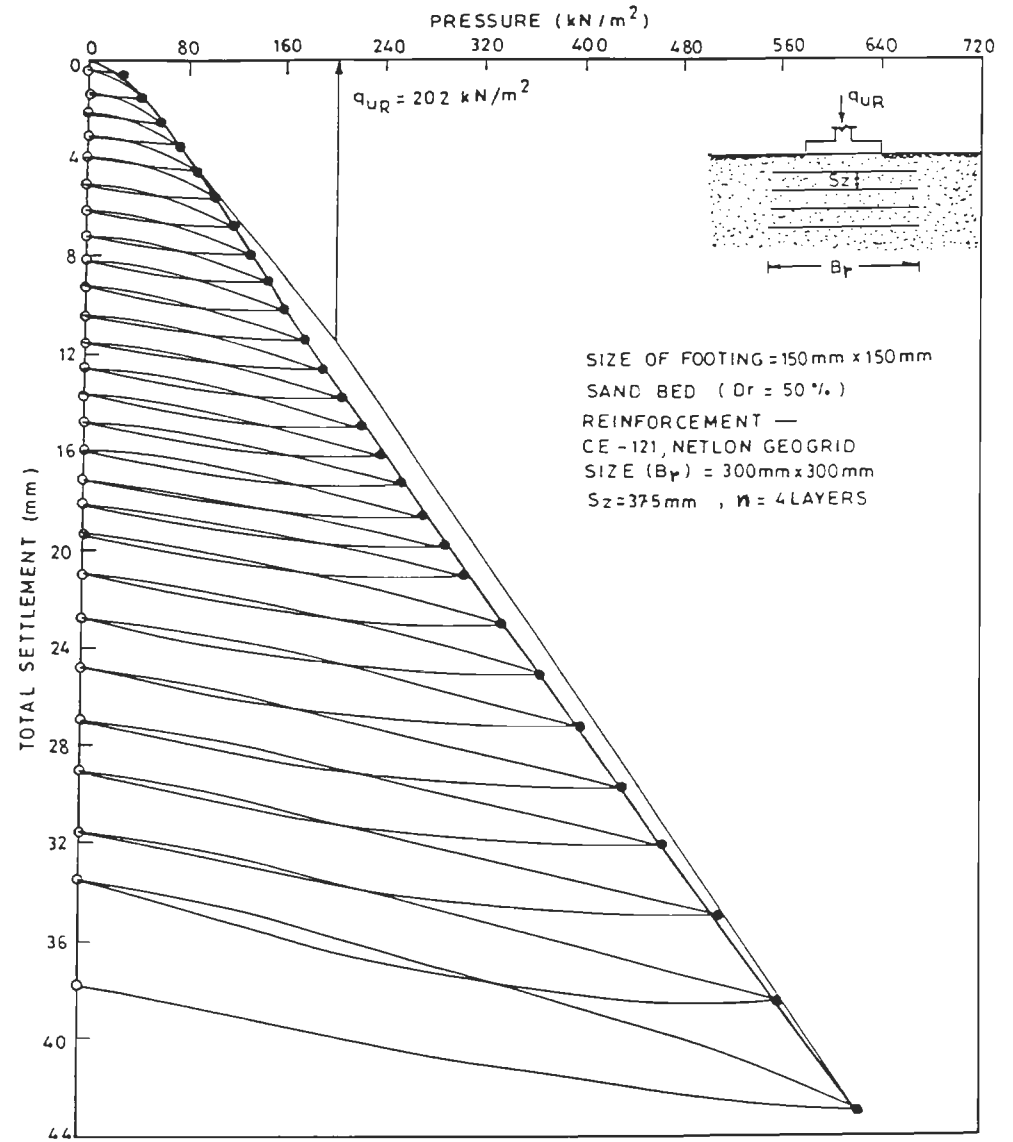


FIG. 3-48 CYCLIC PLATE LOAD TEST — PRESSURE VERSUS TOTAL SETTLEMENT

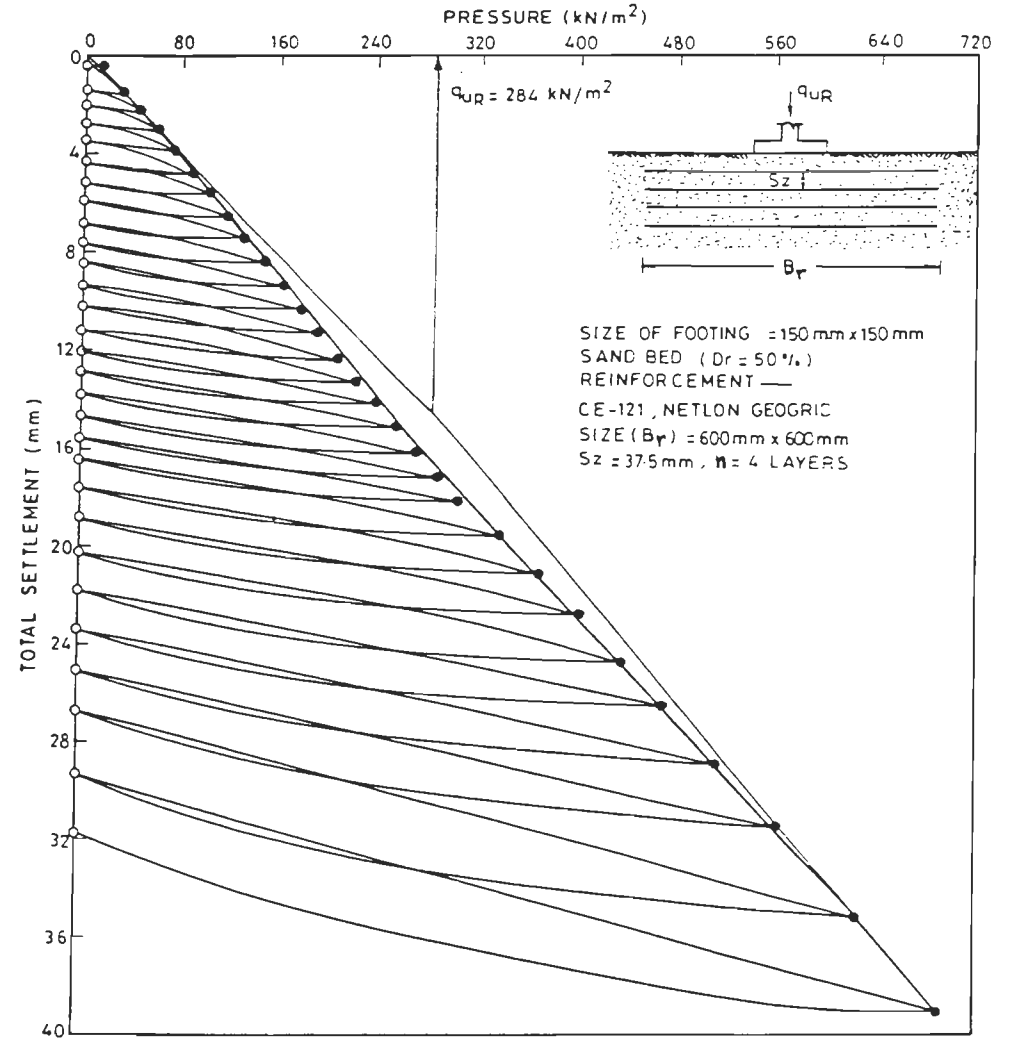
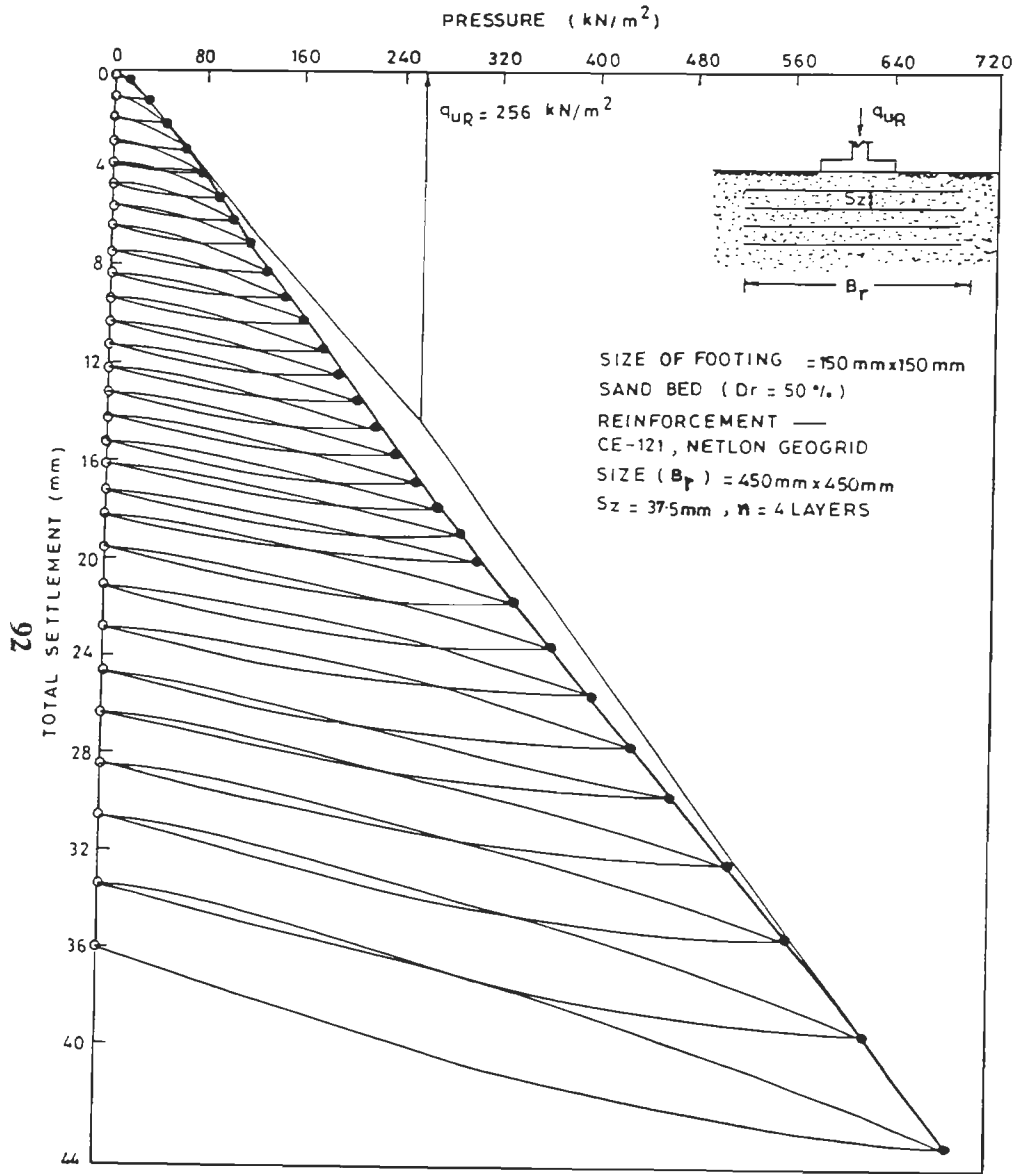


FIG. 3-49 CYCLIC PLATE LOAD TEST — PRESSURE VERSUS TOTAL SETTLEMENT FIG. 3-50 CYCLIC PLATE LOAD TEST — PRESSURE VERSUS TOTAL SETTLEMENT

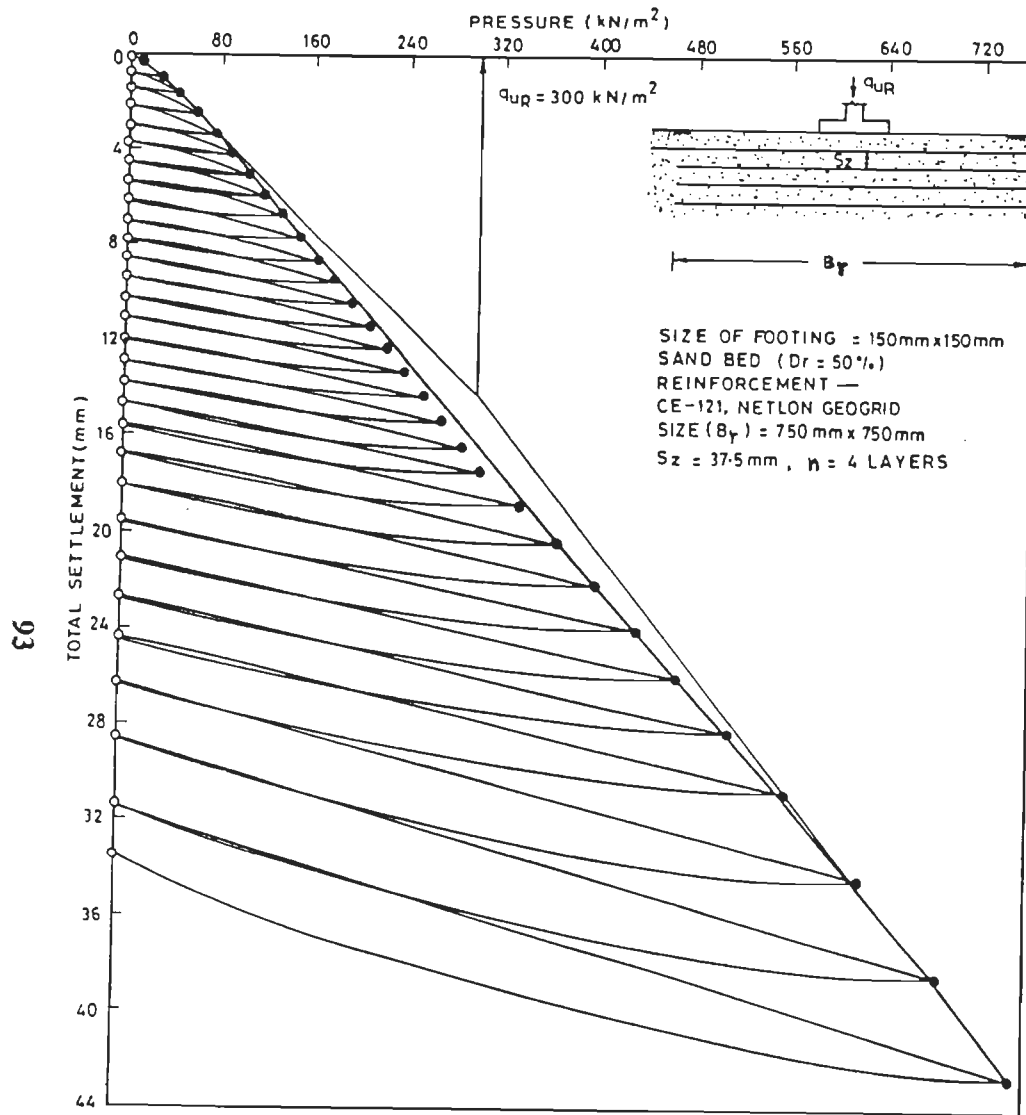


FIG. 3-51 CYCLIC PLATE LOAD TEST — PRESSURE VERSUS TOTAL SETTLEMENT

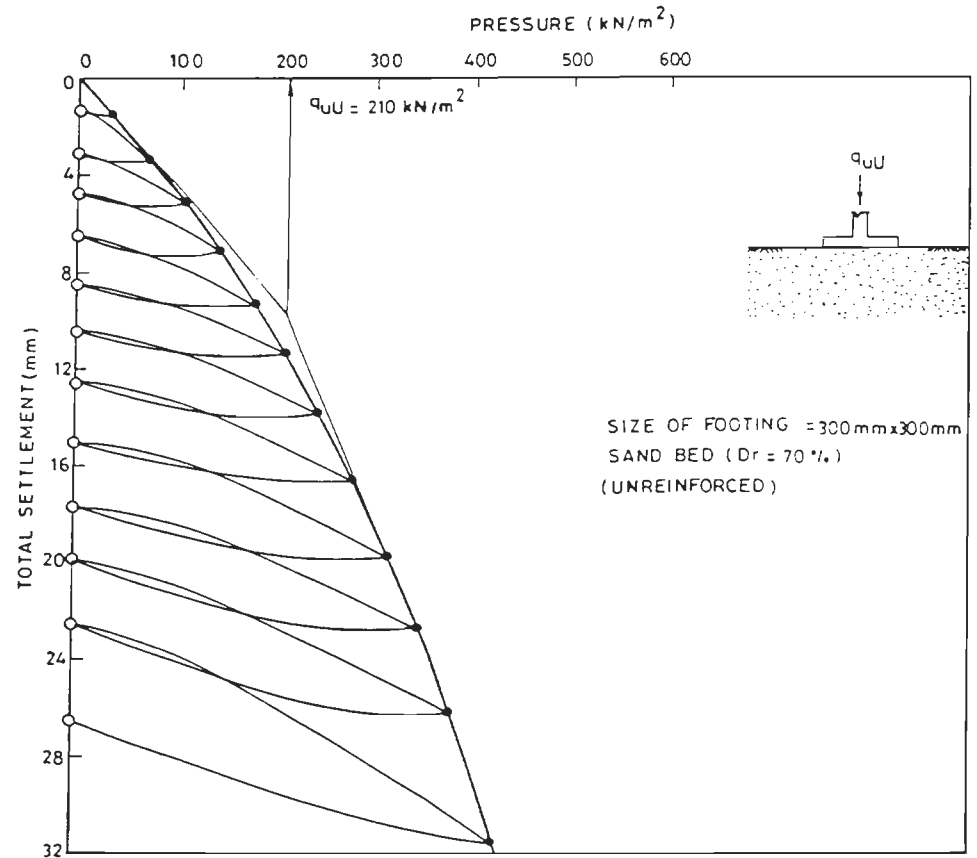


FIG. 3-52 CYCLIC PLATE LOAD TEST — PRESSURE VERSUS TOTAL SETTLEMENT

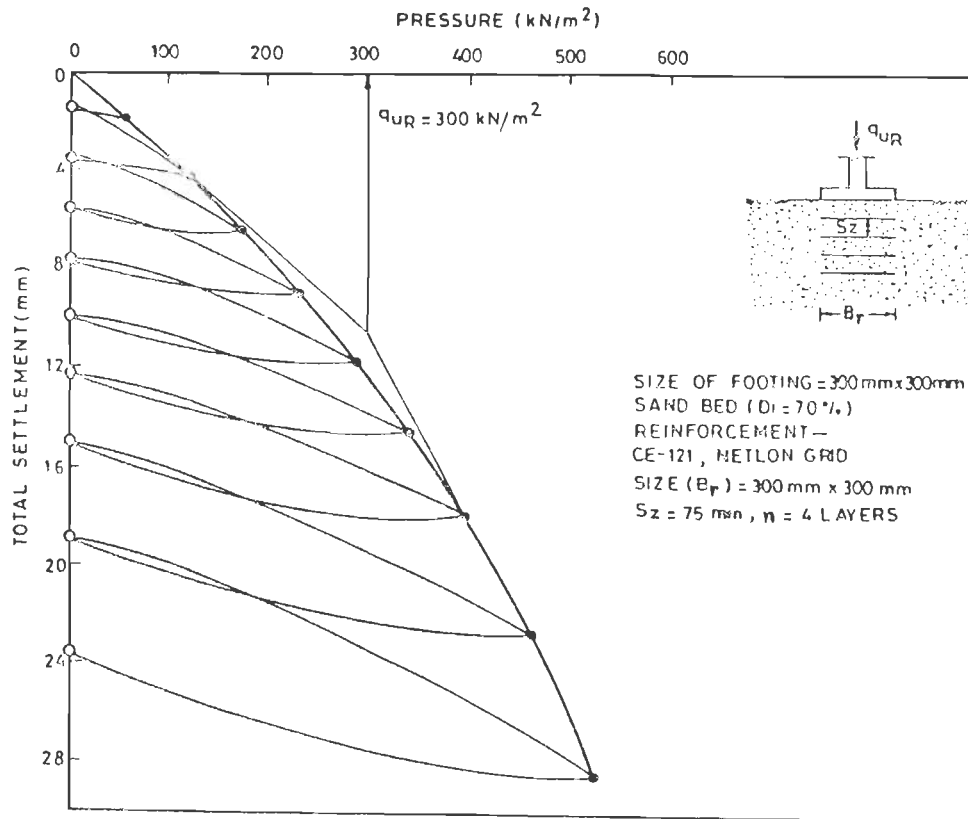


FIG. 3-53 CYCLIC PLATE LOAD TEST—PRESSURE VERSUS TOTAL SETTLEMENT

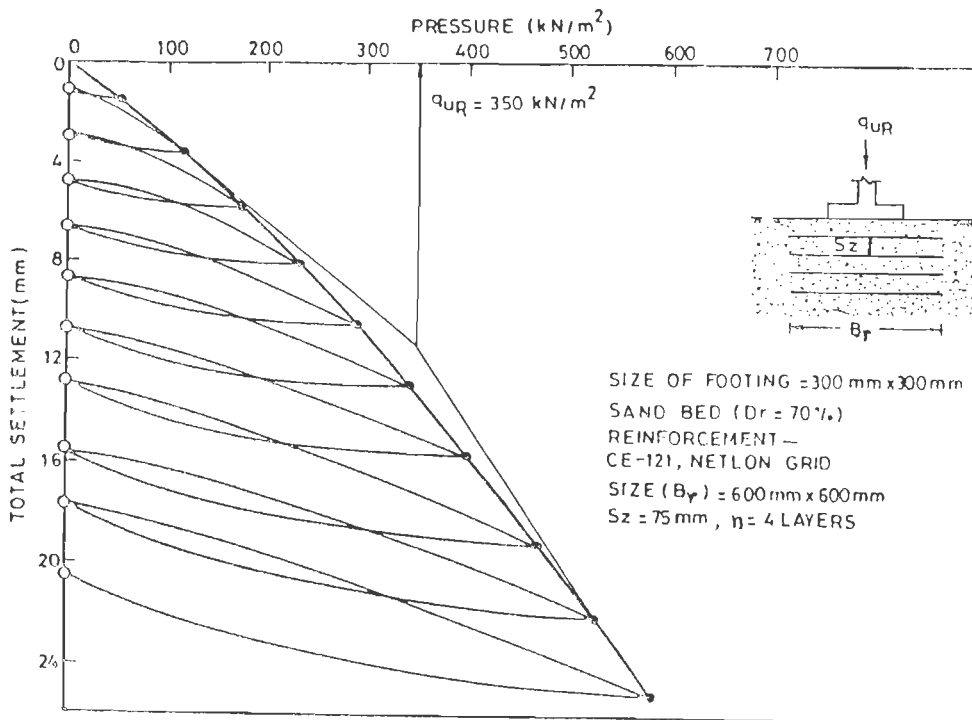


FIG. 3-54 CYCLIC PLATE LOAD TEST — PRESSURE VERSUS TOTAL SETTLEMENT

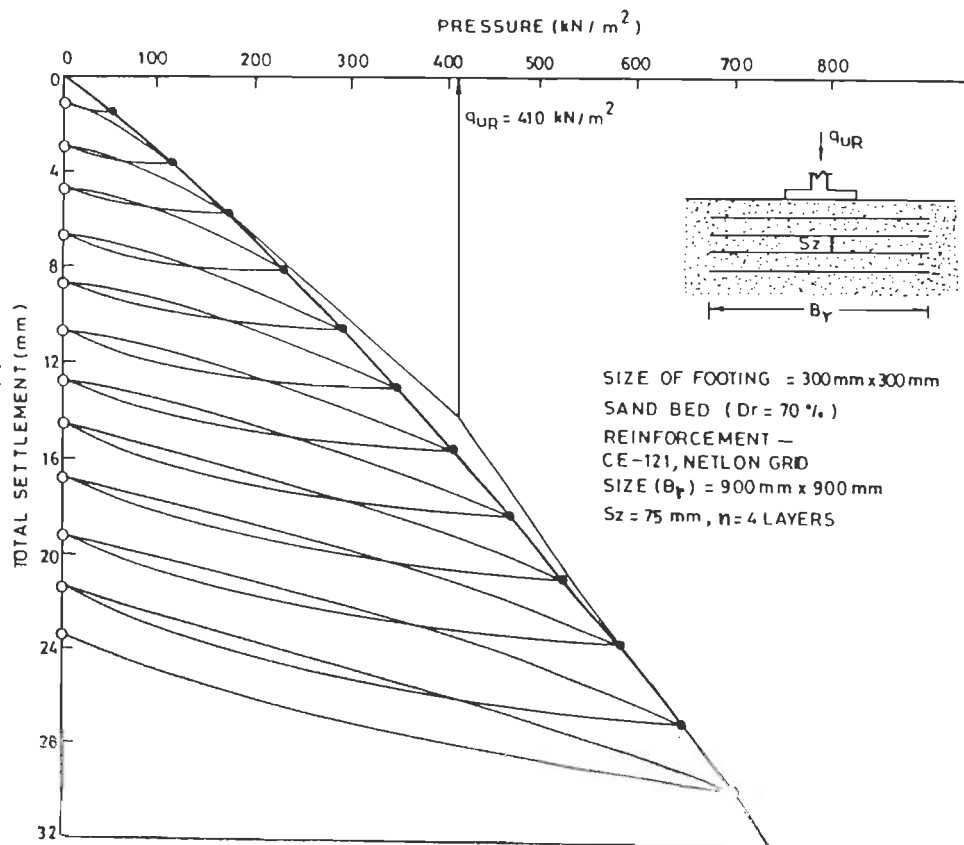


FIG. 3-55 CYCLIC PLATE LOAD TEST - PRESSURE VERSUS TOTAL SETTLEMENT

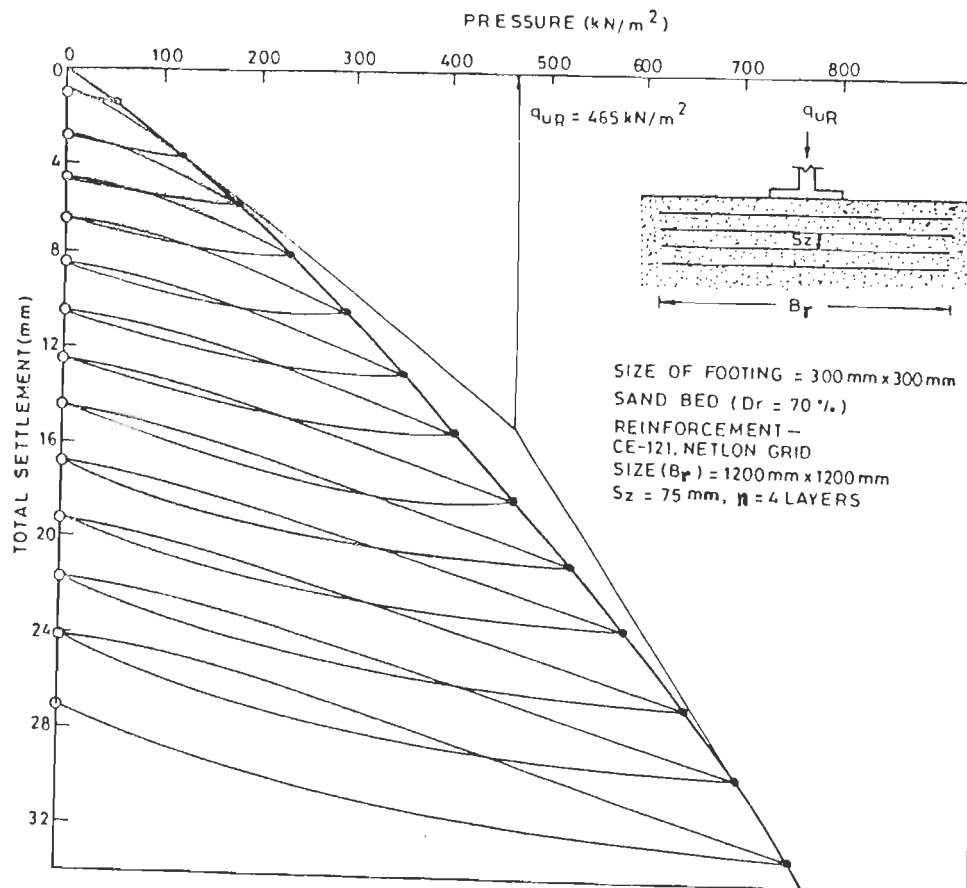


FIG. 3-56 CYCLIC PLATE LOAD TEST - PRESSURE VERSUS TOTAL SETTLEMENT

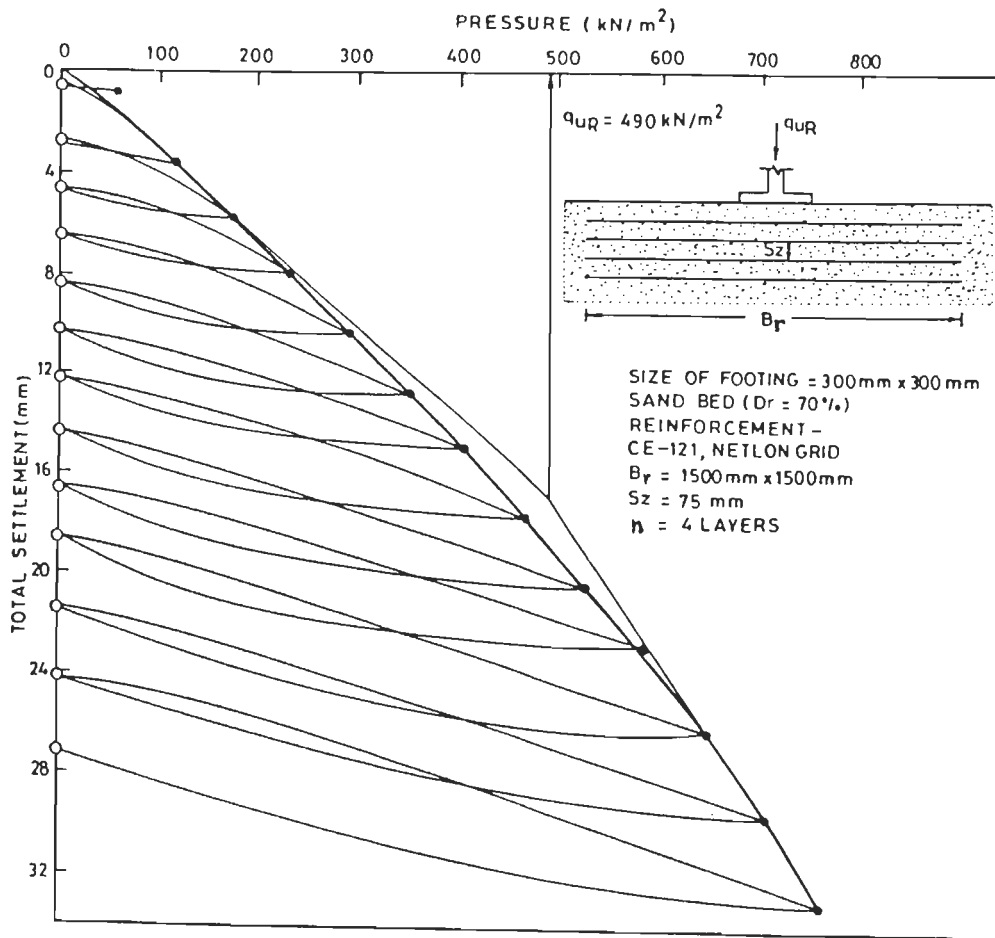


FIG. 3-57 CYCLIC PLATE LOAD TEST - PRESSURE VERSUS TOTAL SETTLEMENT

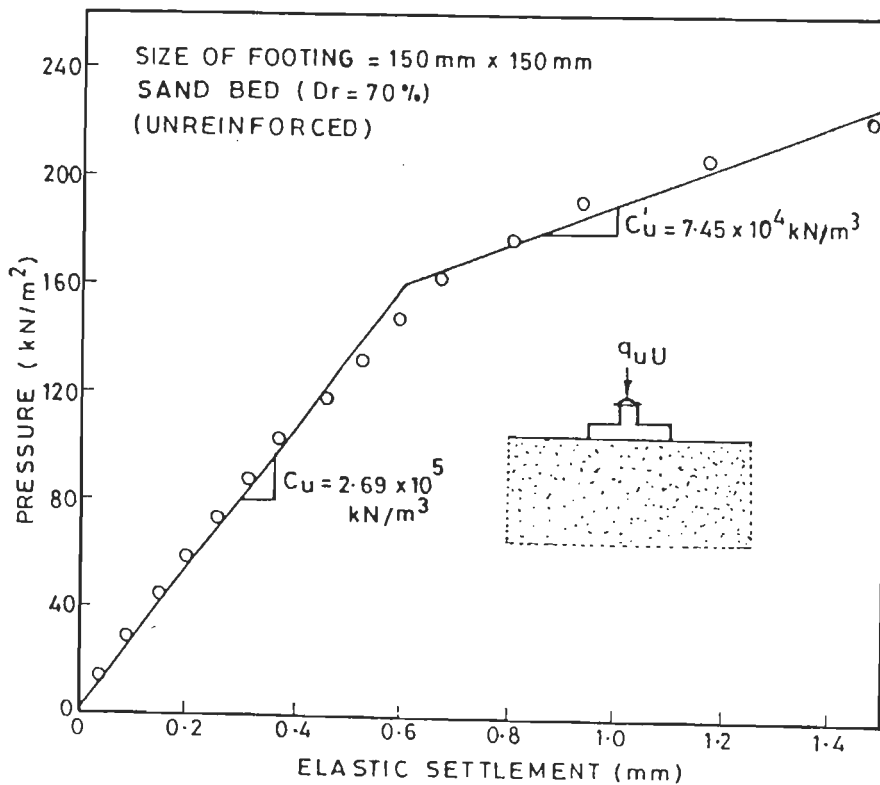


FIG. 3-58 CYCLIC PLATE LOAD TEST - PRESSURE VERSUS ELASTIC SETTLEMENT

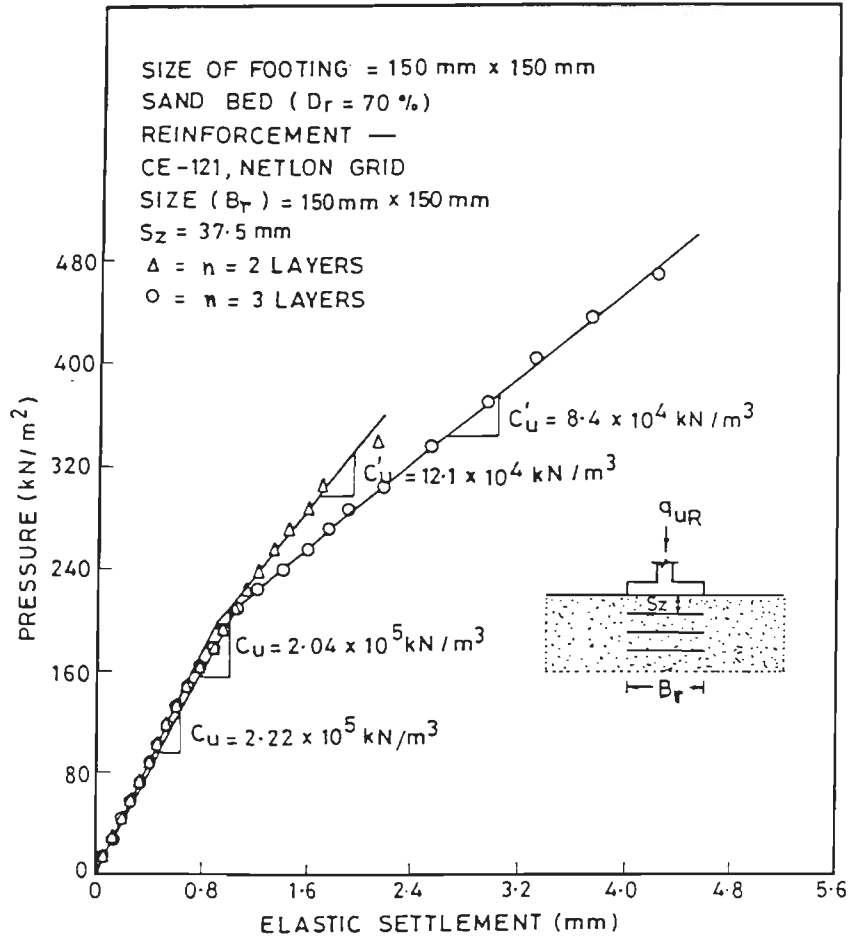


FIG. 3-59 CYCLIC PLATE LOAD TEST — PRESSURE VERSUS ELASTIC SETTLEMENT

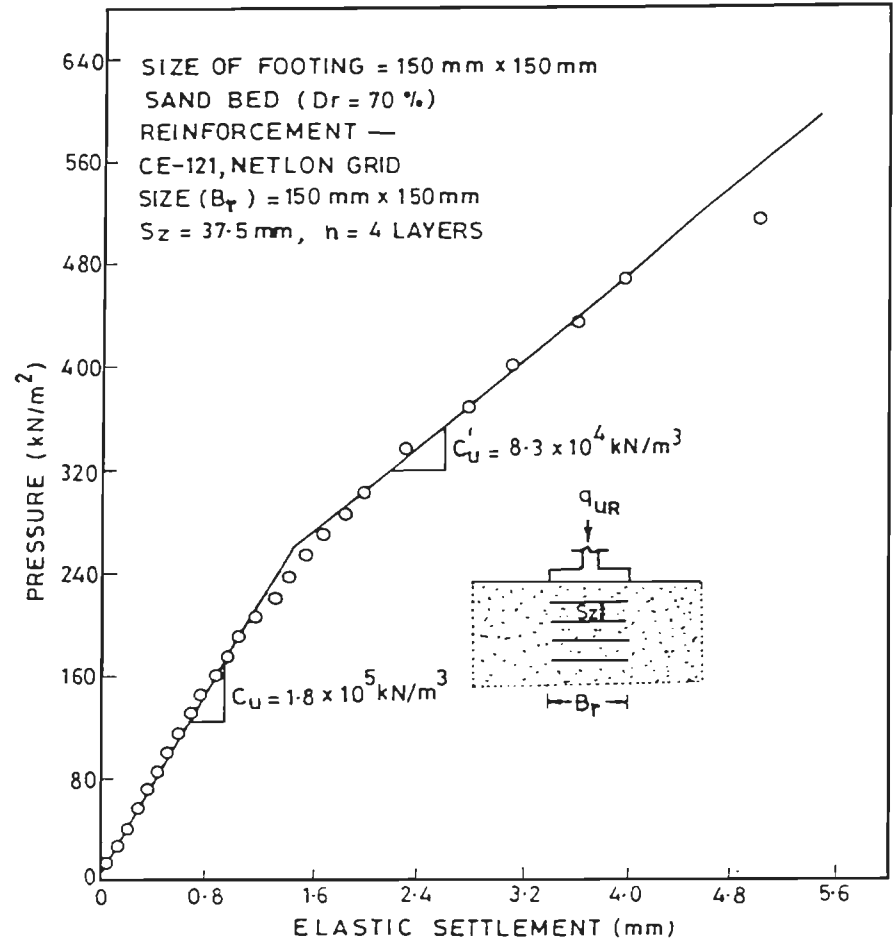


FIG. 3-60 CYCLIC PLATE LOAD TEST — PRESSURE VERSUS ELASTIC SETTLEMENT

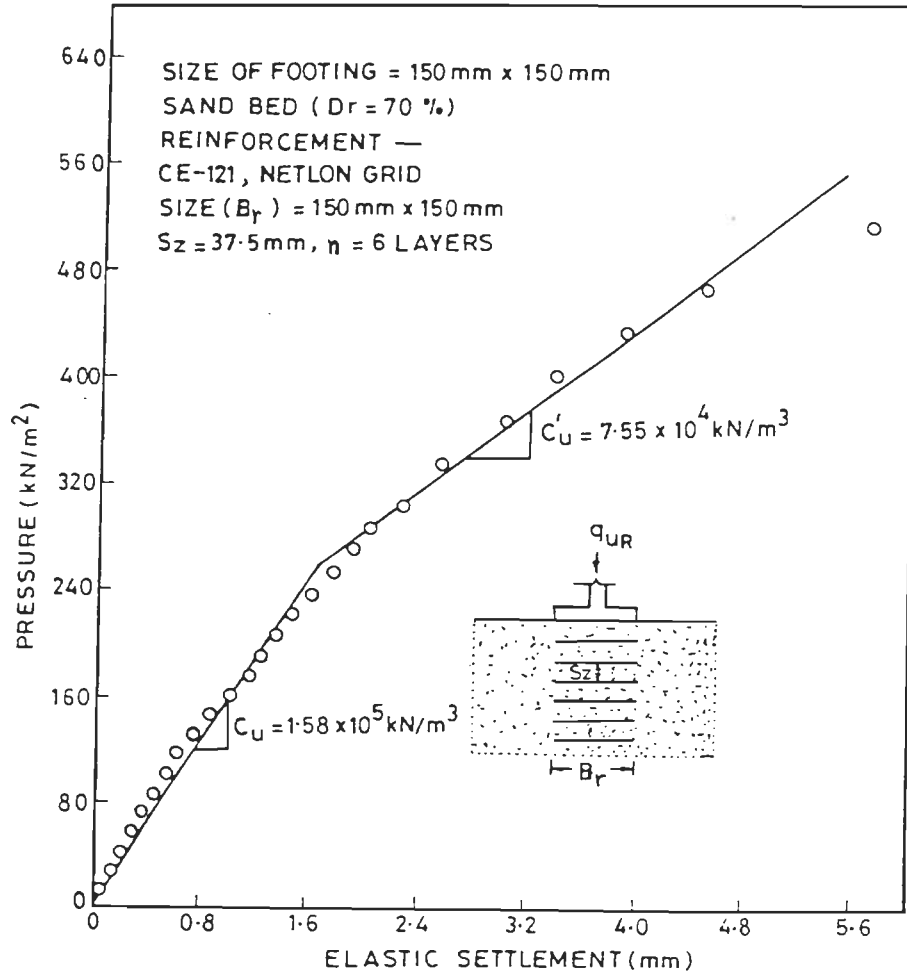


FIG. 3-61 CYCLIC PLATE LOAD TEST — PRESSURE VERSUS ELASTIC SETTLEMENT

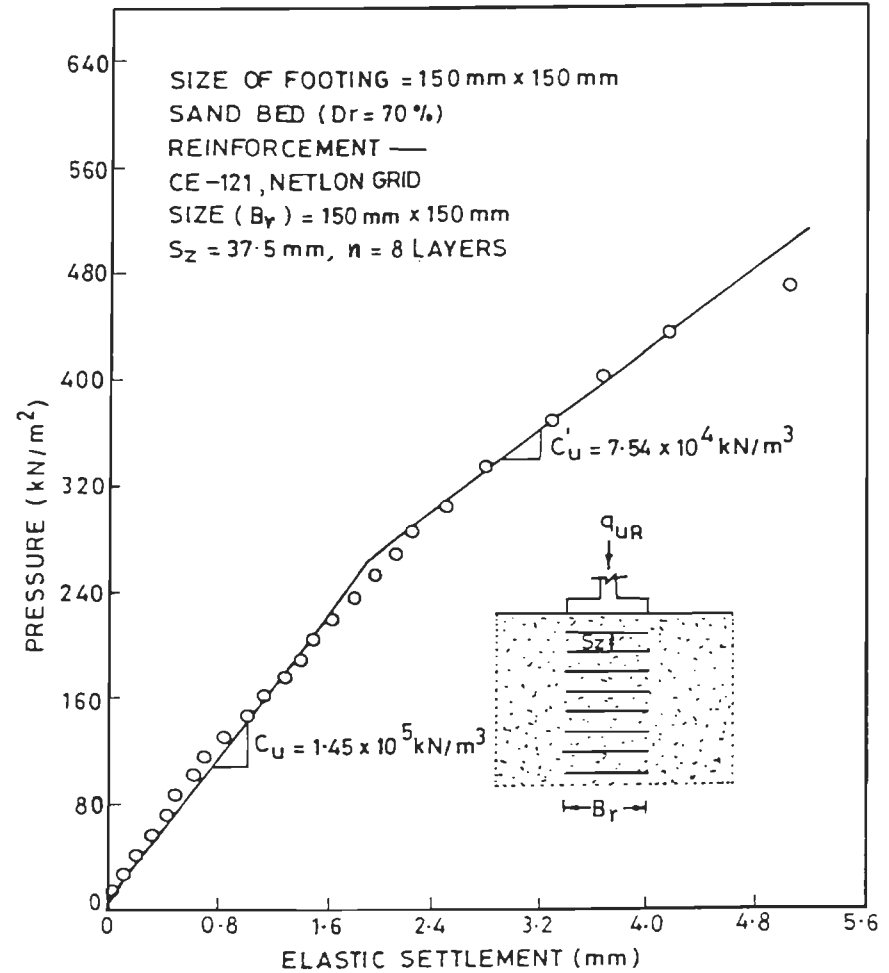


FIG. 3-62 CYCLIC PLATE LOAD TEST — PRESSURE VERSUS ELASTIC SETTLEMENT

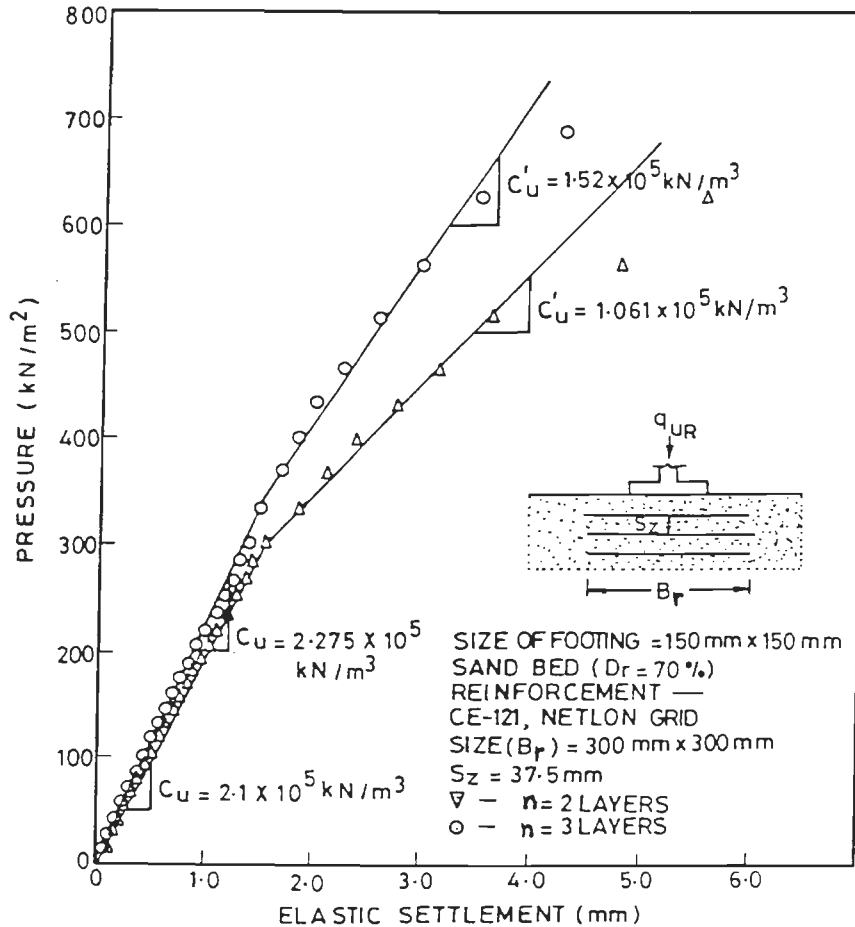


FIG. 3-63 CYCLIC PLATE LOAD TEST — PRESSURE VERSUS ELASTIC SETTLEMENT

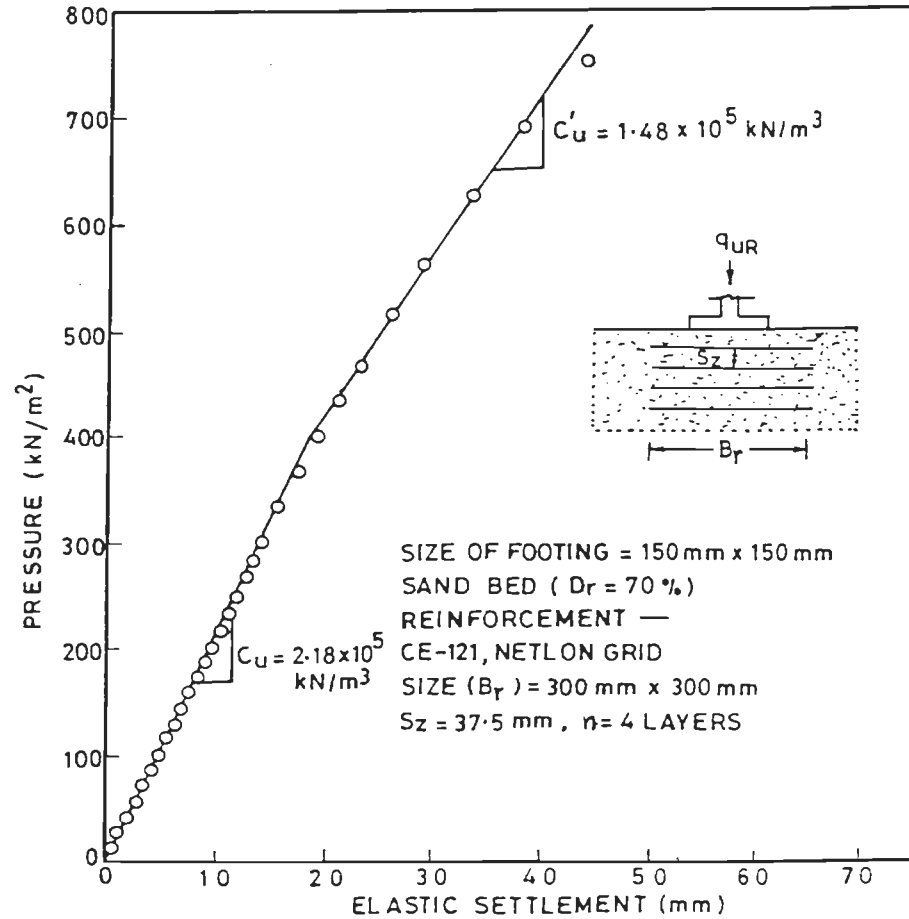


FIG. 3-64 CYCLIC PLATE LOAD TEST — PRESSURE VERSUS ELASTIC SETTLEMENT

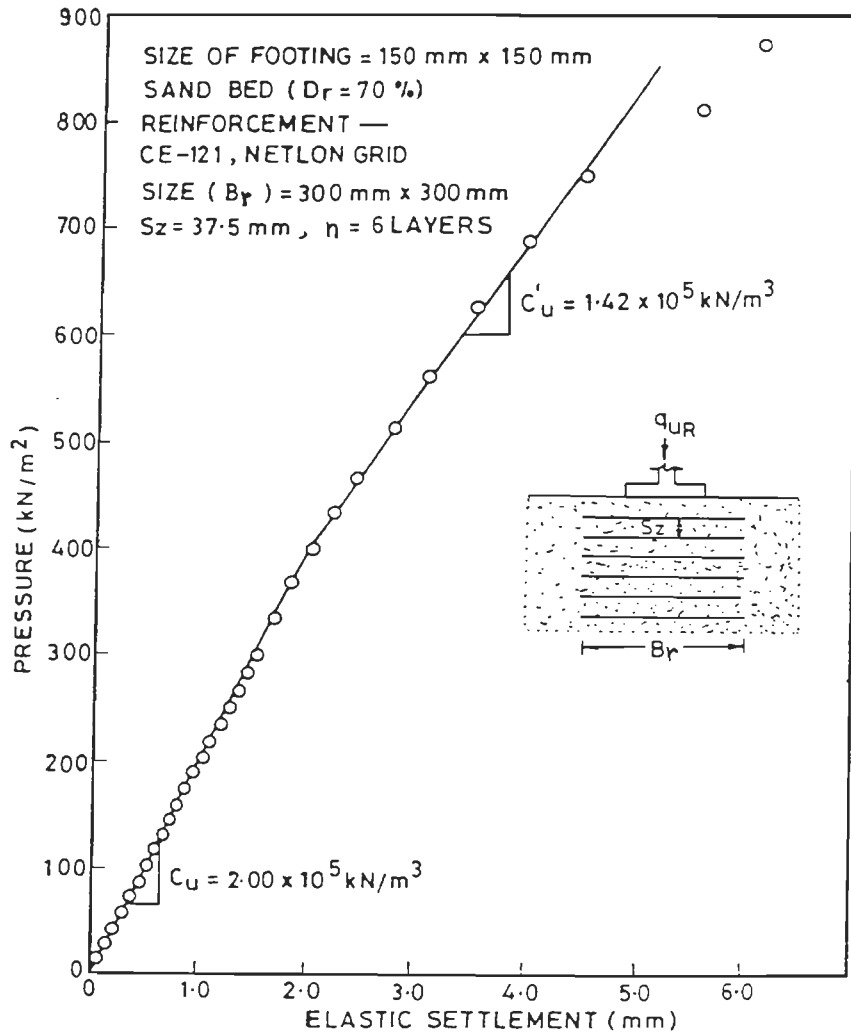


FIG. 3-65 CYCLIC PLATE LOAD TEST — PRESSURE VERSUS ELASTIC SETTLEMENT

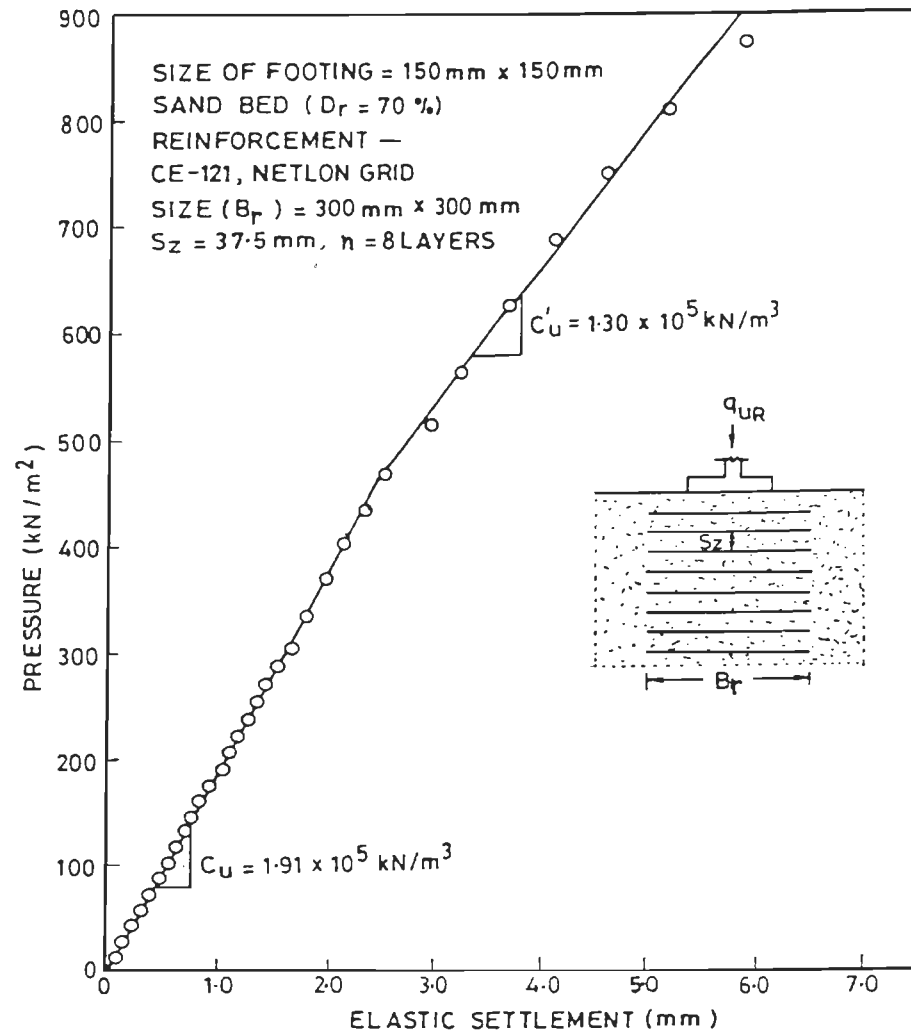


FIG. 3-66 CYCLIC PLATE LOAD TEST — PRESSURE VERSUS ELASTIC SETTLEMENT

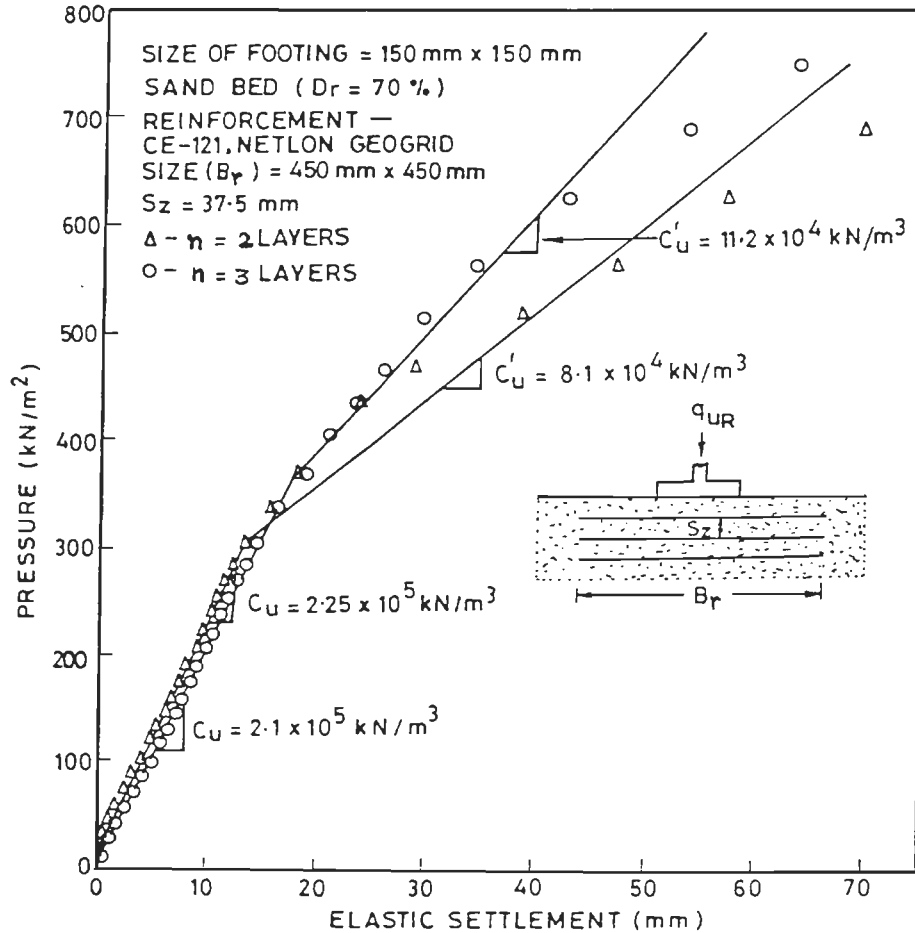


FIG. 3-67 CYCLIC PLATE LOAD TEST—PRESSURE VERSUS ELASTIC SETTLEMENT

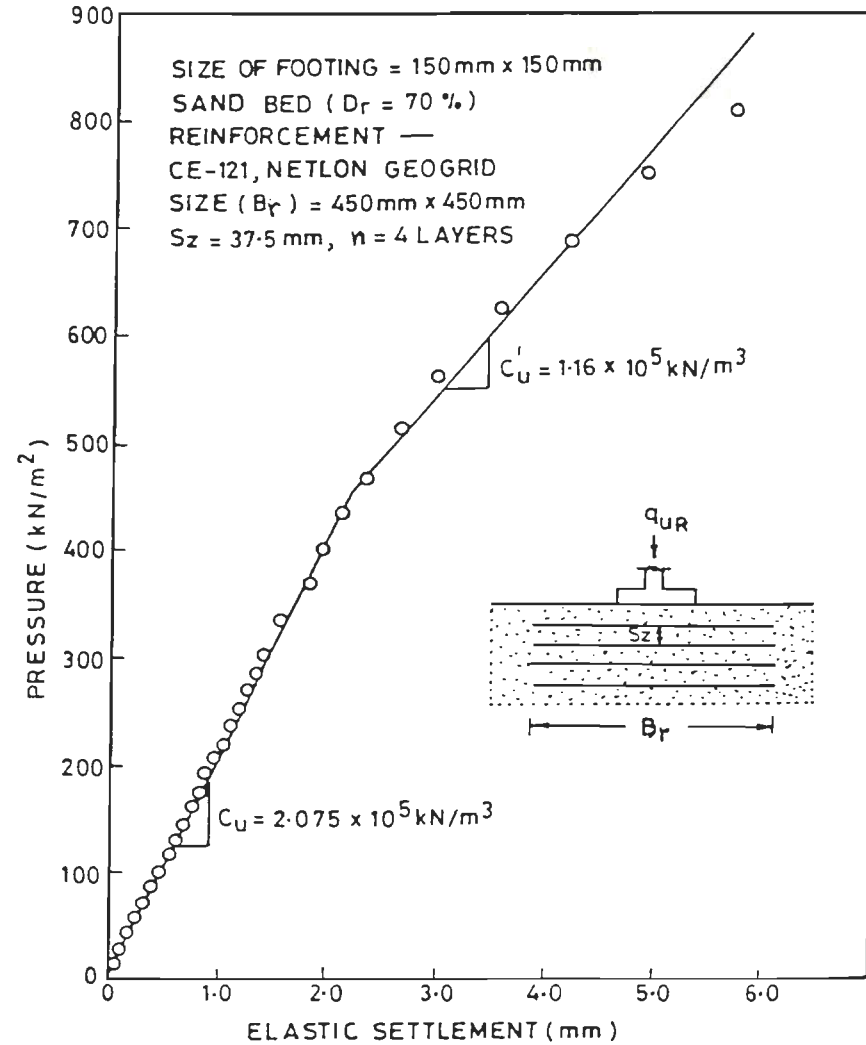


FIG. 3-68 CYCLIC PLATE LOAD TEST—PRESSURE VERSUS ELASTIC SETTLEMENT

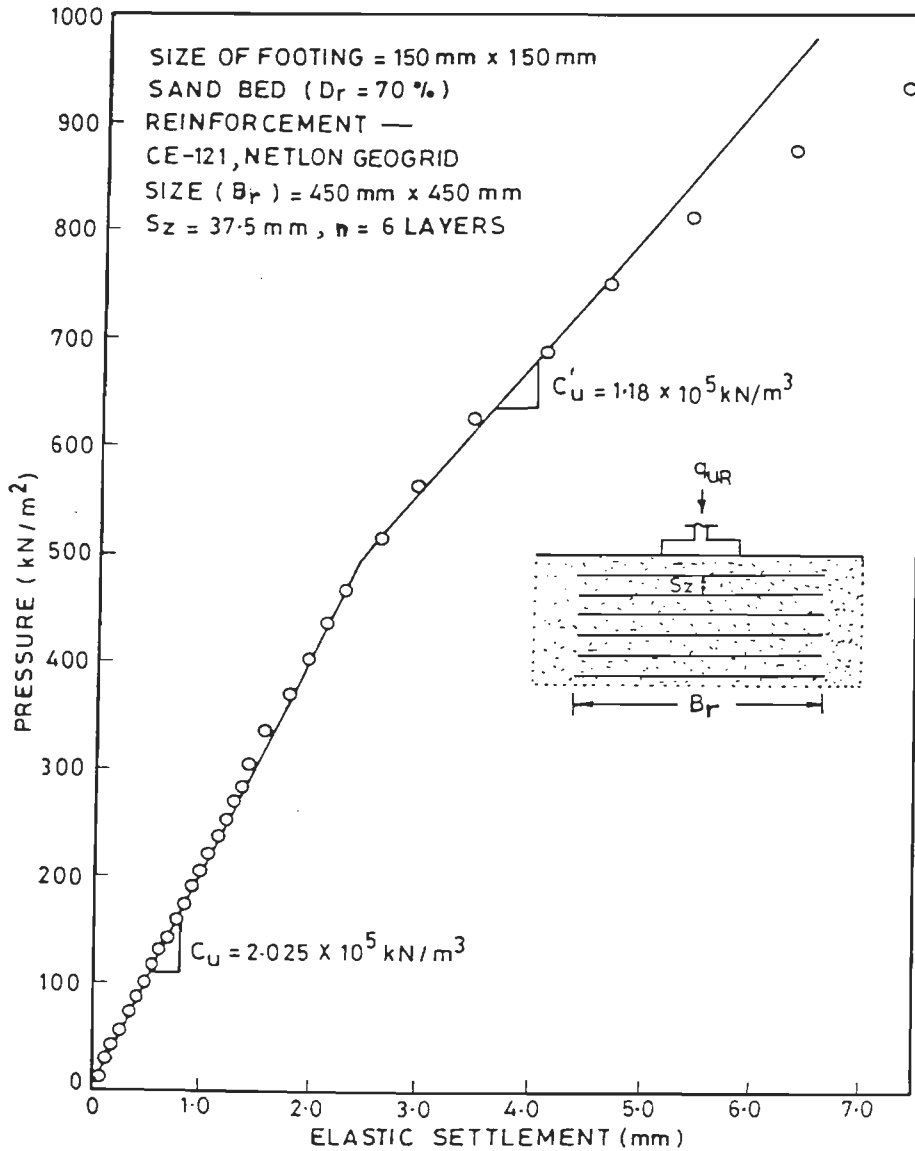


FIG. 3-69 CYCLIC PLATE LOAD TEST — PRESSURE VERSUS ELASTIC SETTLEMENT

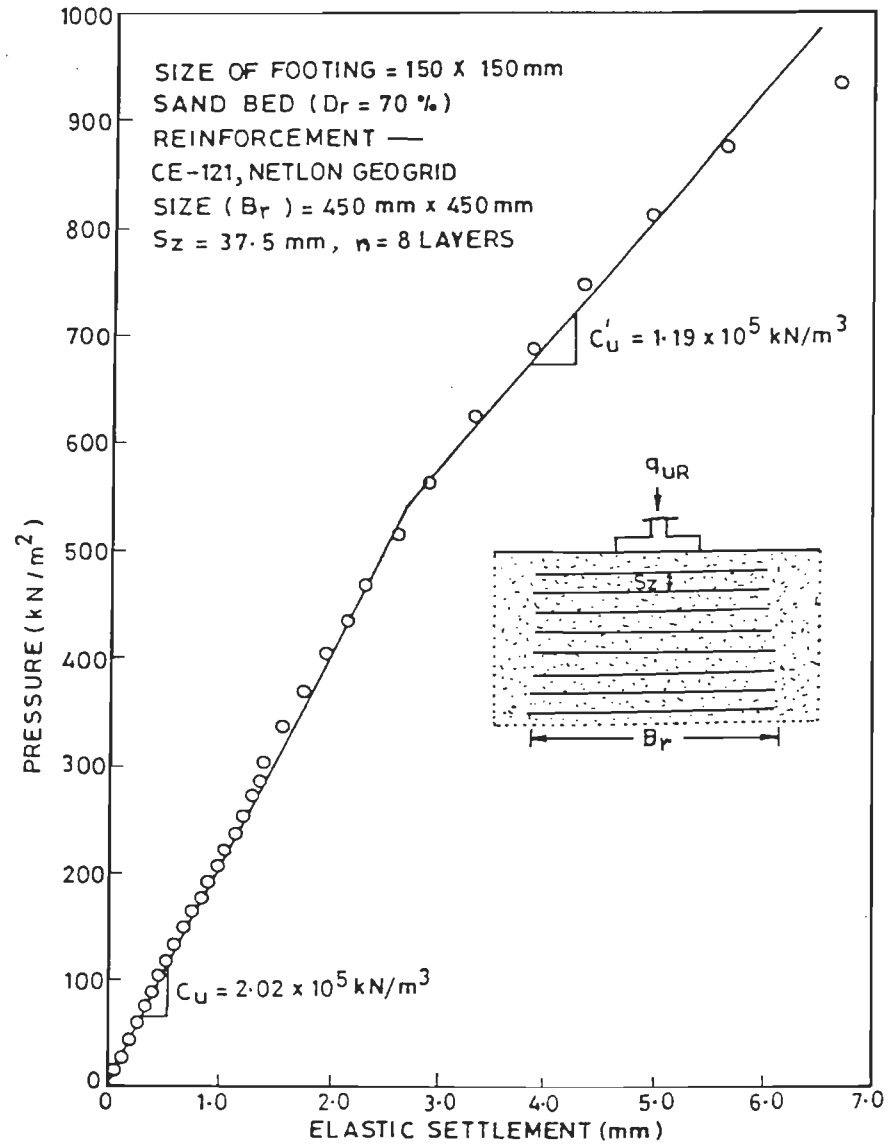


FIG. 3-70 CYCLIC PLATE LOAD TEST — PRESSURE VERSUS ELASTIC SETTLEMENT

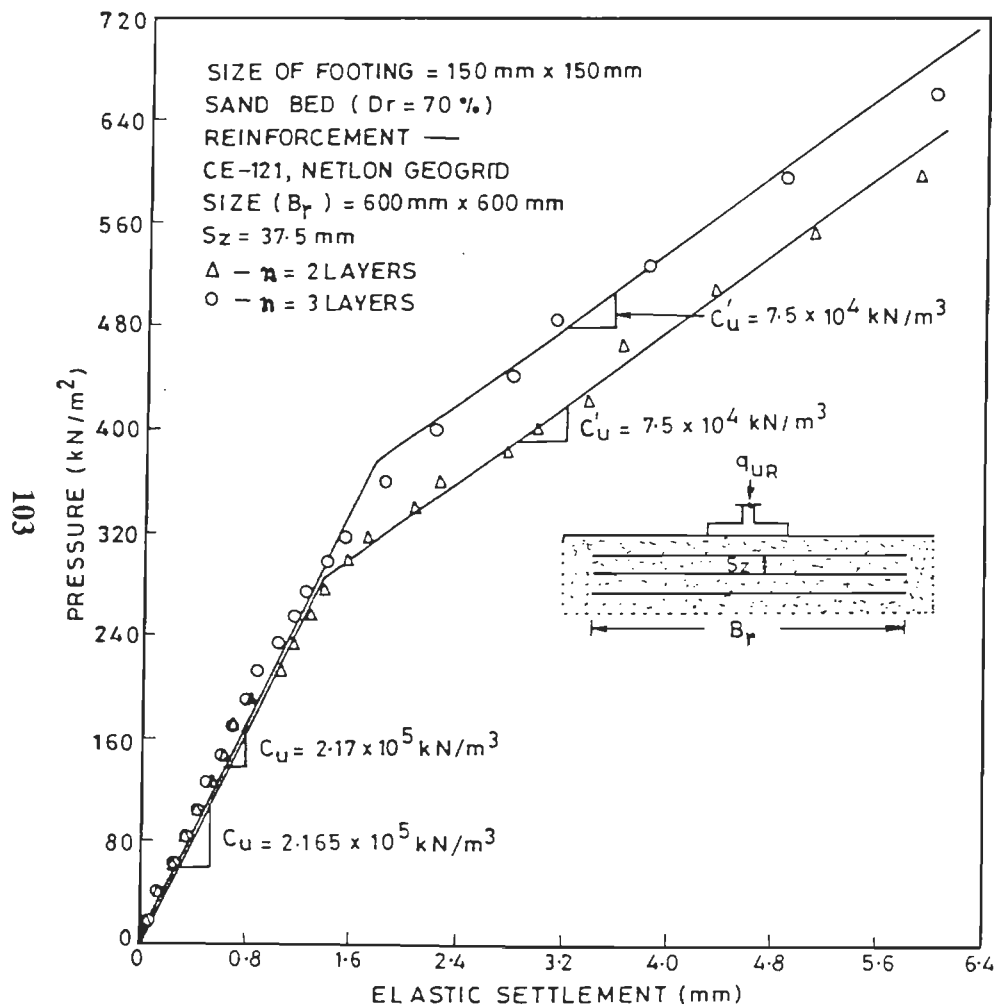


FIG. 3-71 CYCLIC PLATE LOAD TEST — PRESSURE VERSUS ELASTIC SETTLEMENT

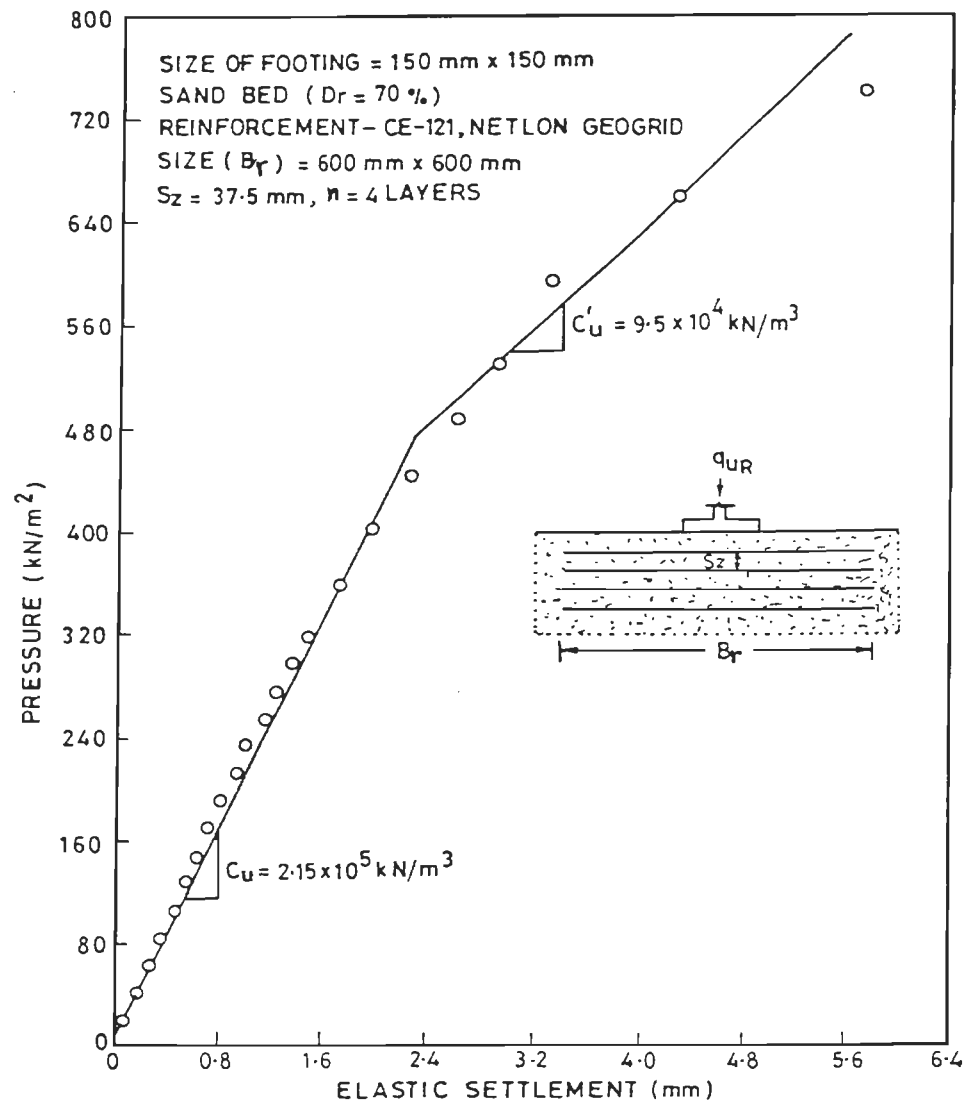


FIG. 3-72 CYCLIC PLATE LOAD TEST — PRESSURE VERSUS ELASTIC SETTLEMENT

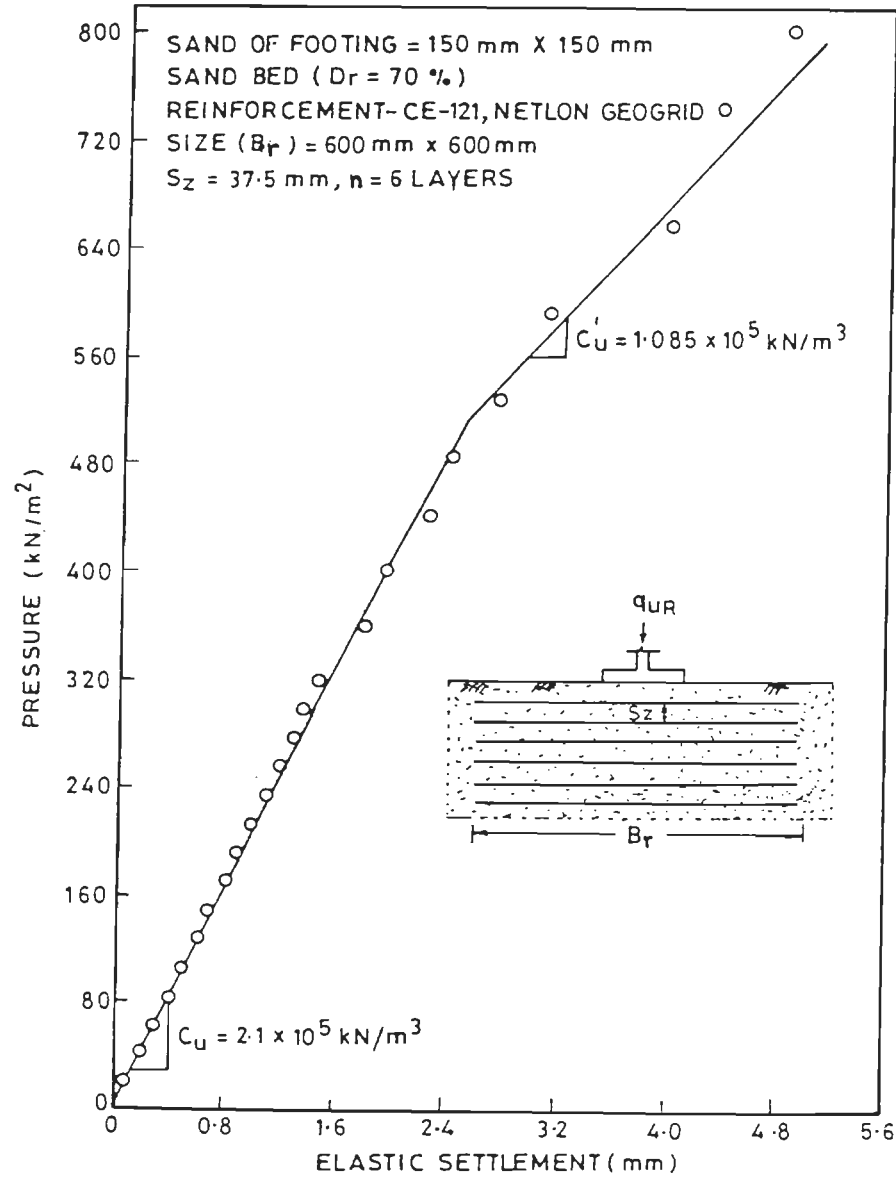


FIG. 3.73 CYCLIC PLATE LOAD TEST—PRESSURE VERSUS ELASTIC SETTLEMENT

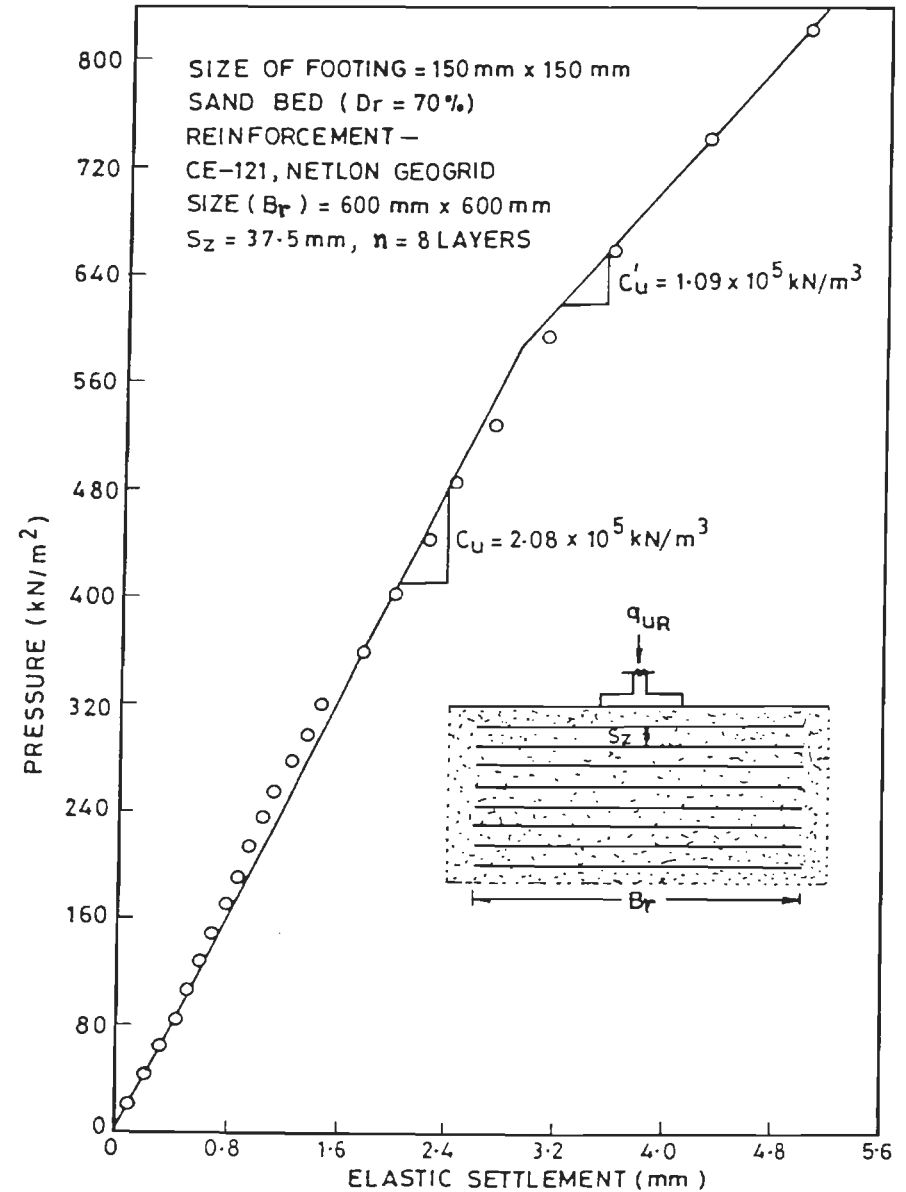


FIG. 3.74 CYCLIC PLATE LOAD TEST—PRESSURE VERSUS ELASTIC SETTLEMENT

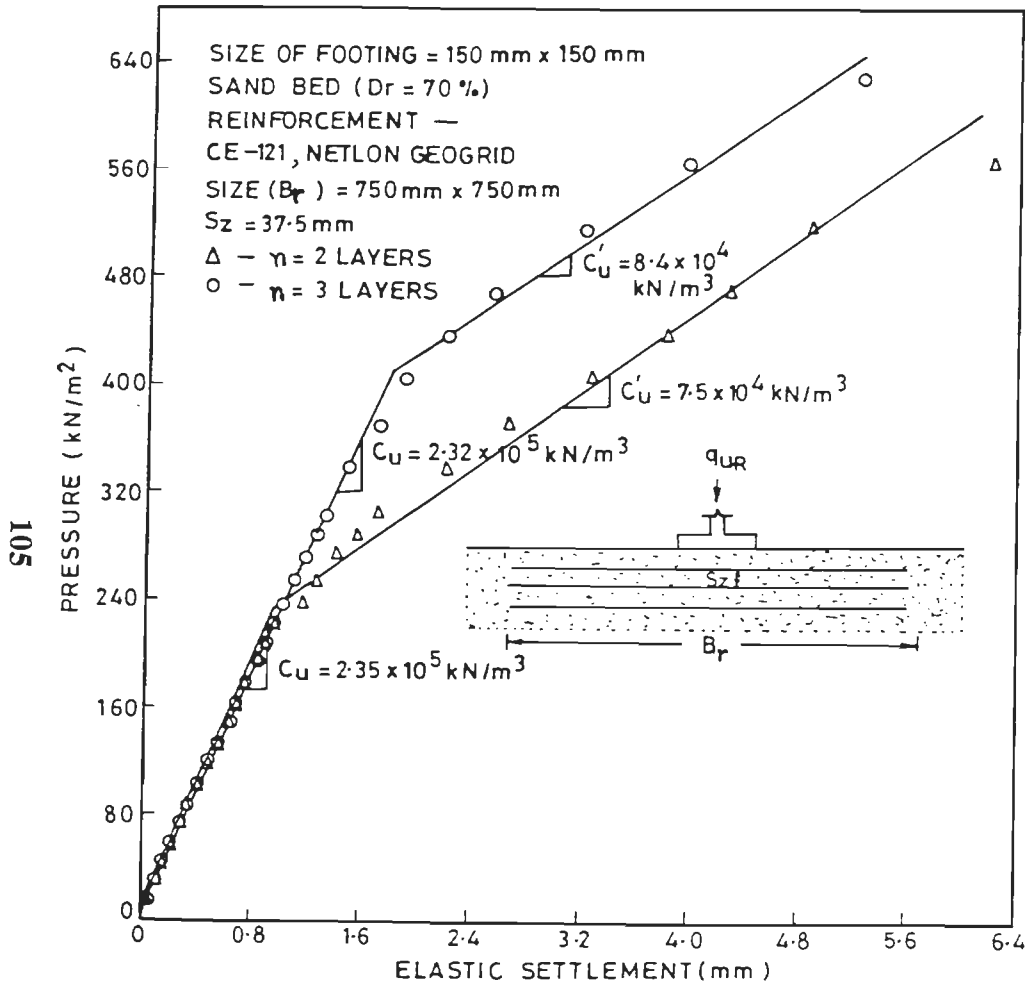


FIG. 3.75 CYCLIC PLATE LOAD TEST — PRESSURE VERSUS ELASTIC SETTLEMENT

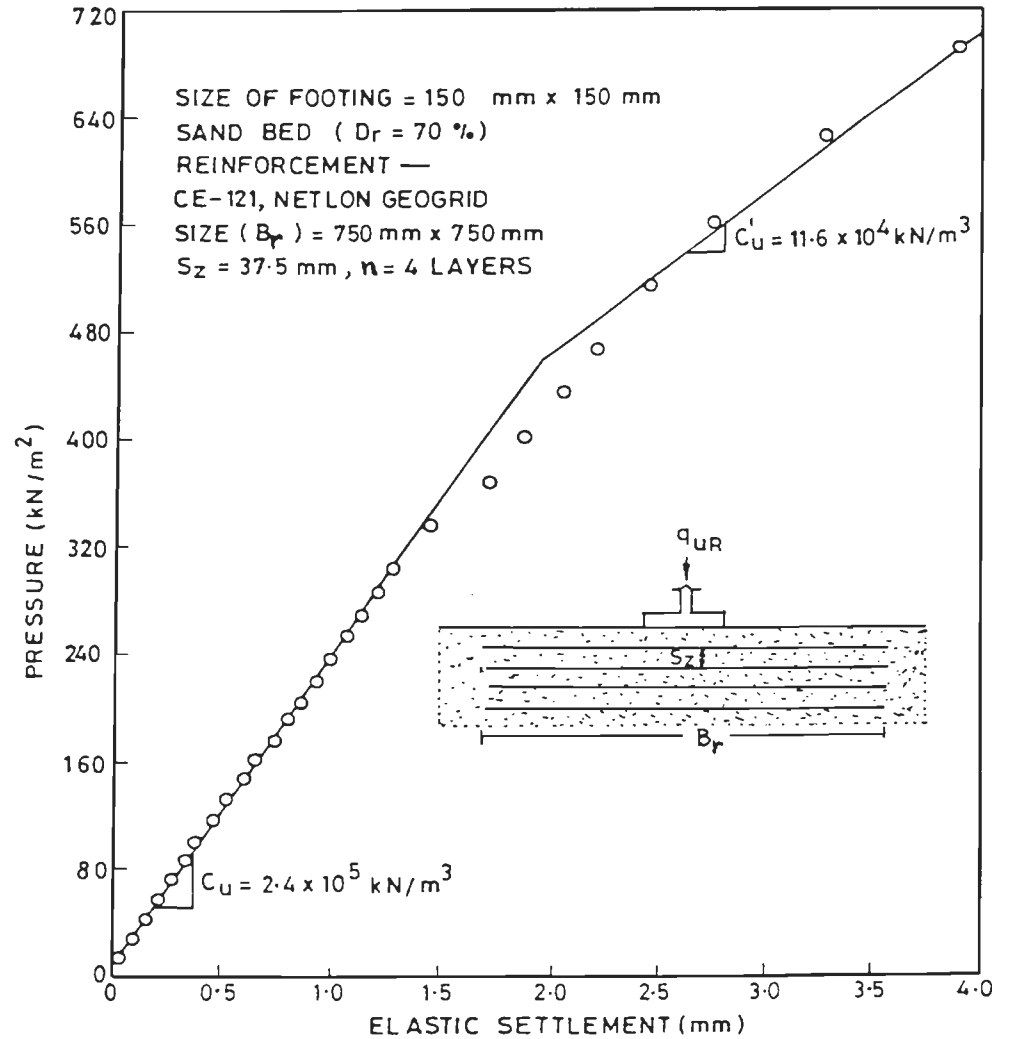


FIG. 3.76 CYCLIC PLATE LOAD TEST — PRESSURE VERSUS ELASTIC SETTLEMENT

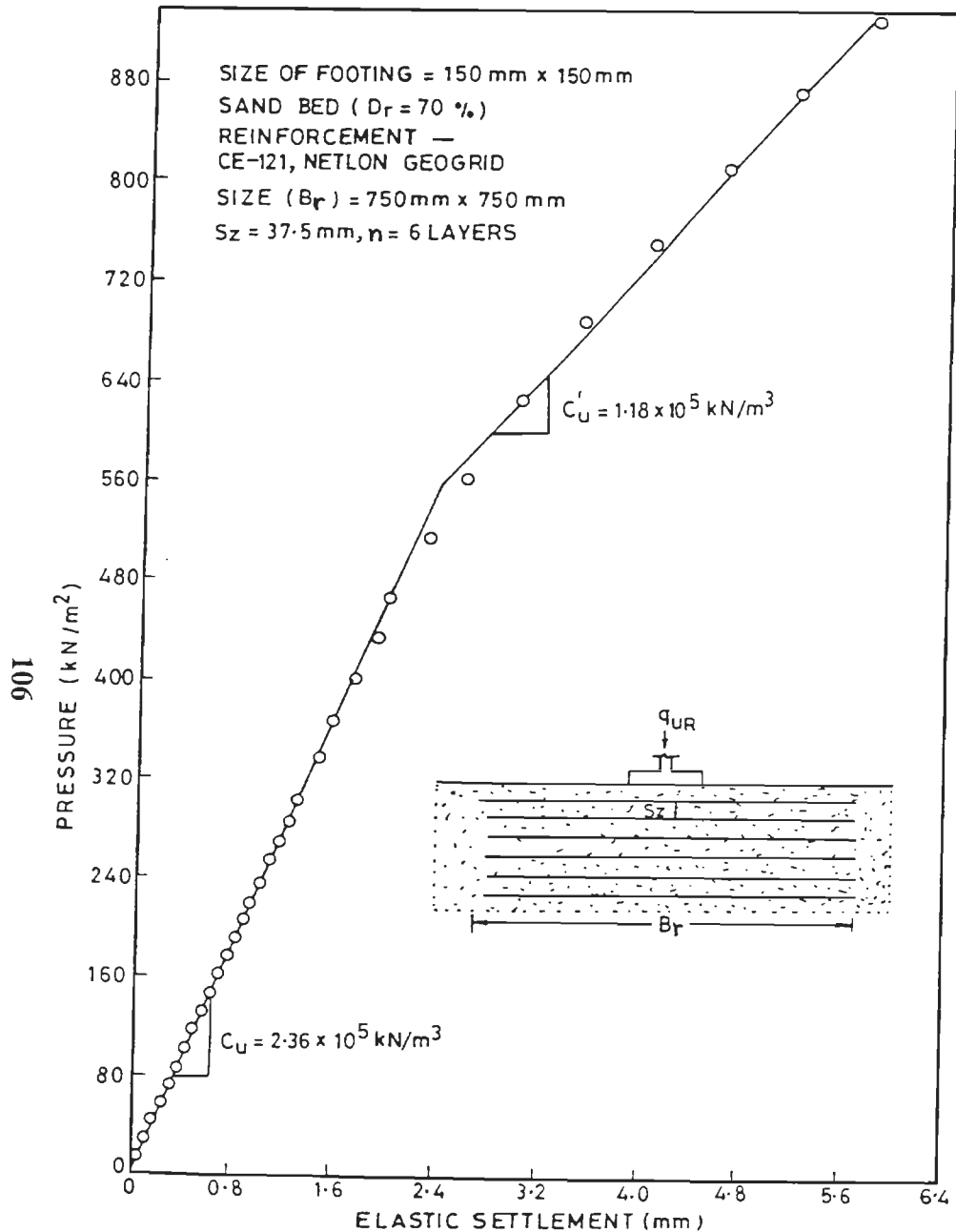


FIG. 3-77 CYCLIC PLATE LOAD TEST—PRESSURE VERSUS ELASTIC SETTLEMENT

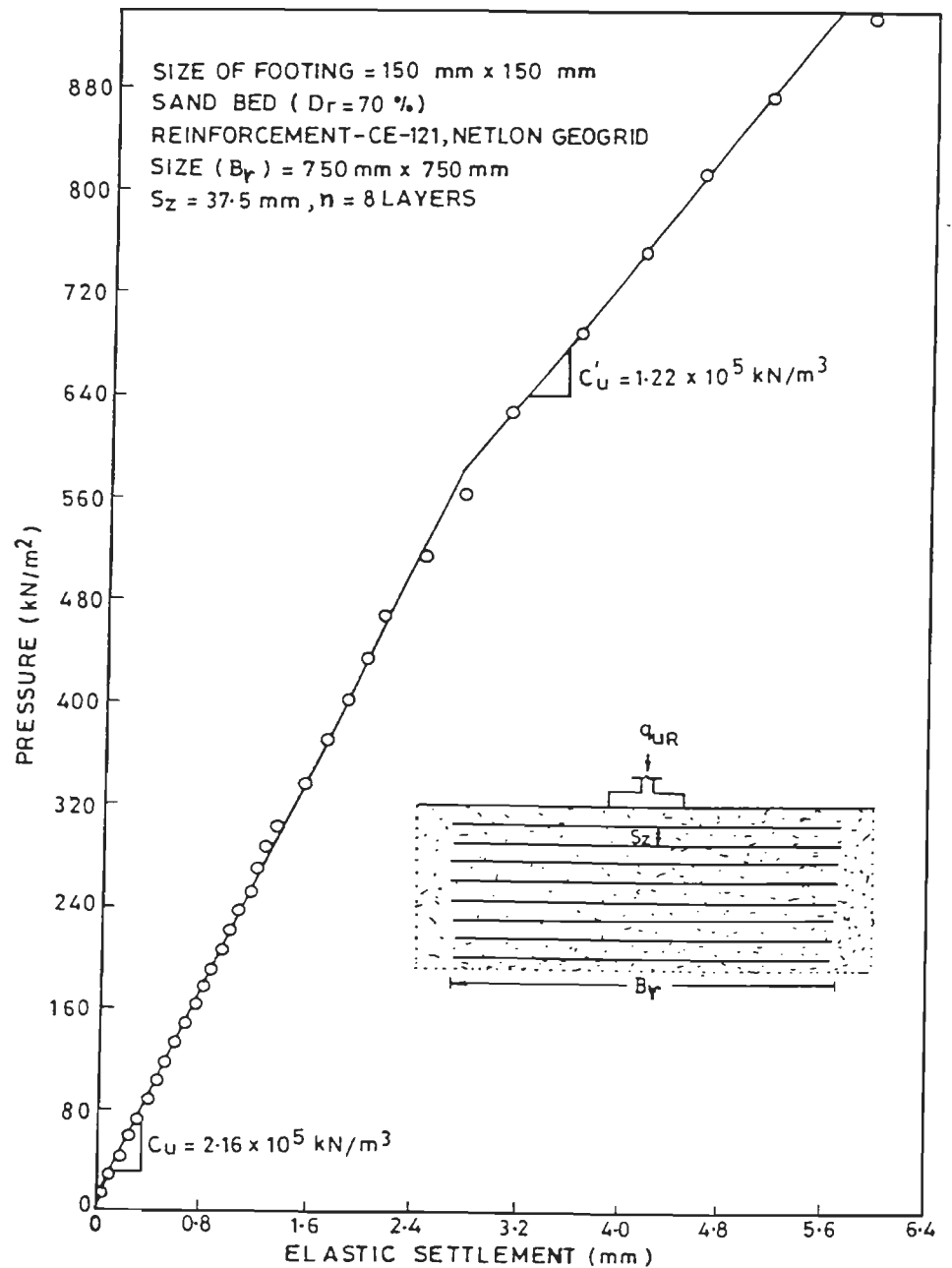


FIG. 3-78 CYCLIC PLATE LOAD TEST—PRESSURE VERSUS ELASTIC SETTLEMENT

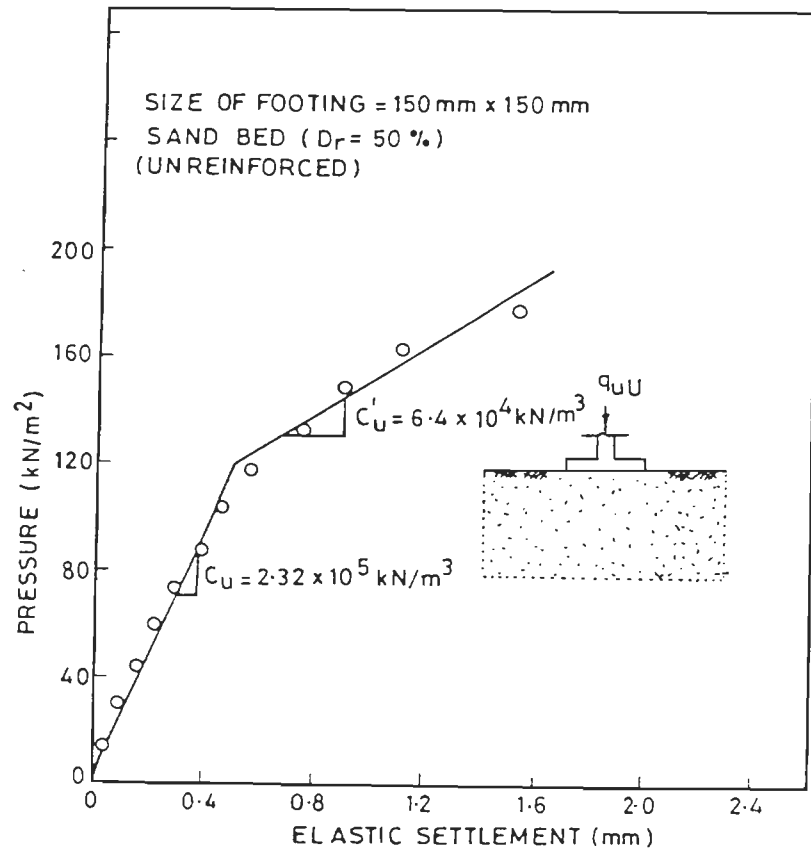


FIG. 3.79 CYCLIC PLATE LOAD TEST — PRESSURE VERSUS ELASTIC SETTLEMENT

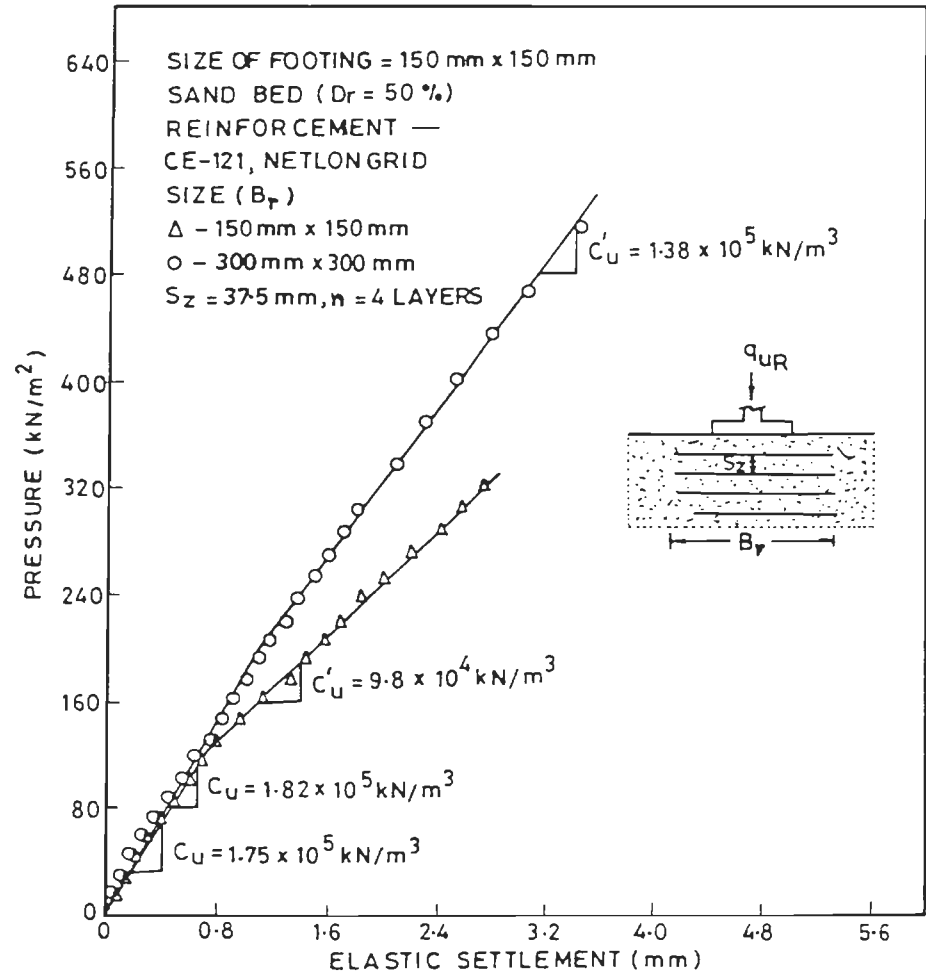


FIG. 3.80 CYCLIC PLATE LOAD TEST — PRESSURE VERSUS ELASTIC SETTLEMENT

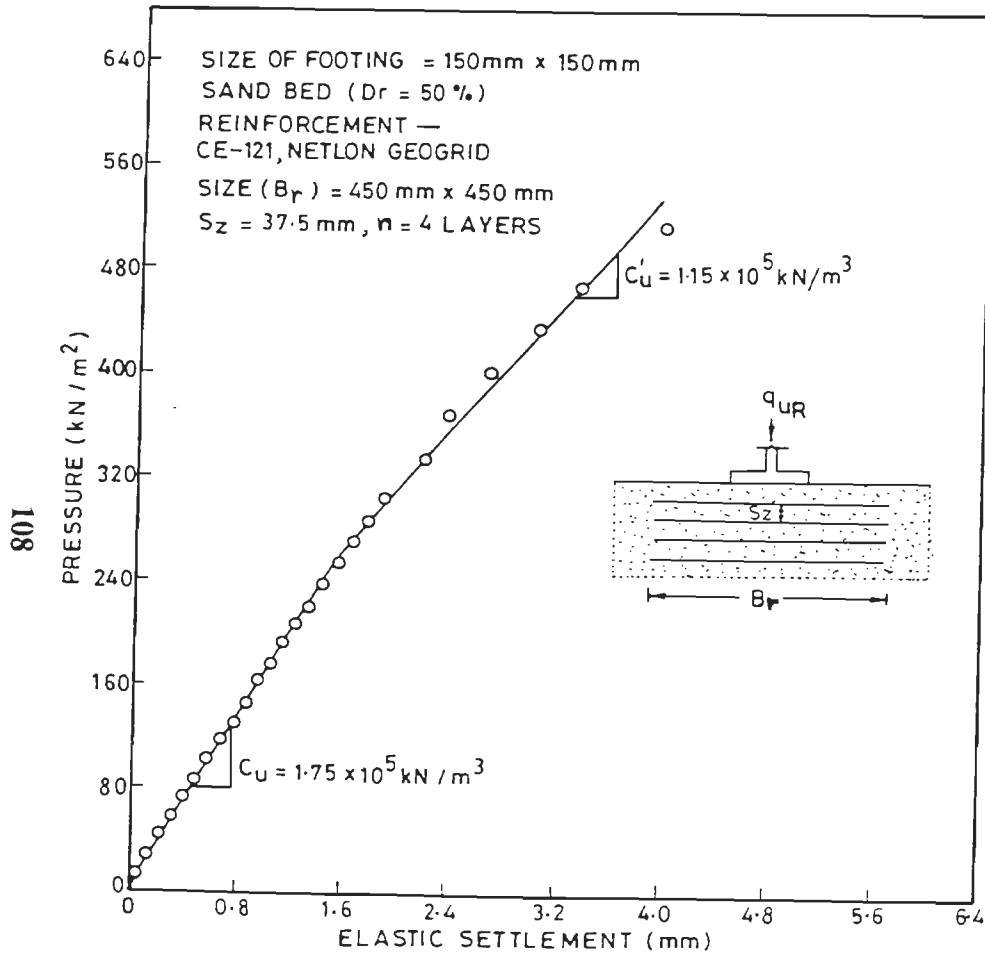


FIG. 3-81 CYCLIC PLATE LOAD TEST — PRESSURE VERSUS ELASTIC SETTLEMENT

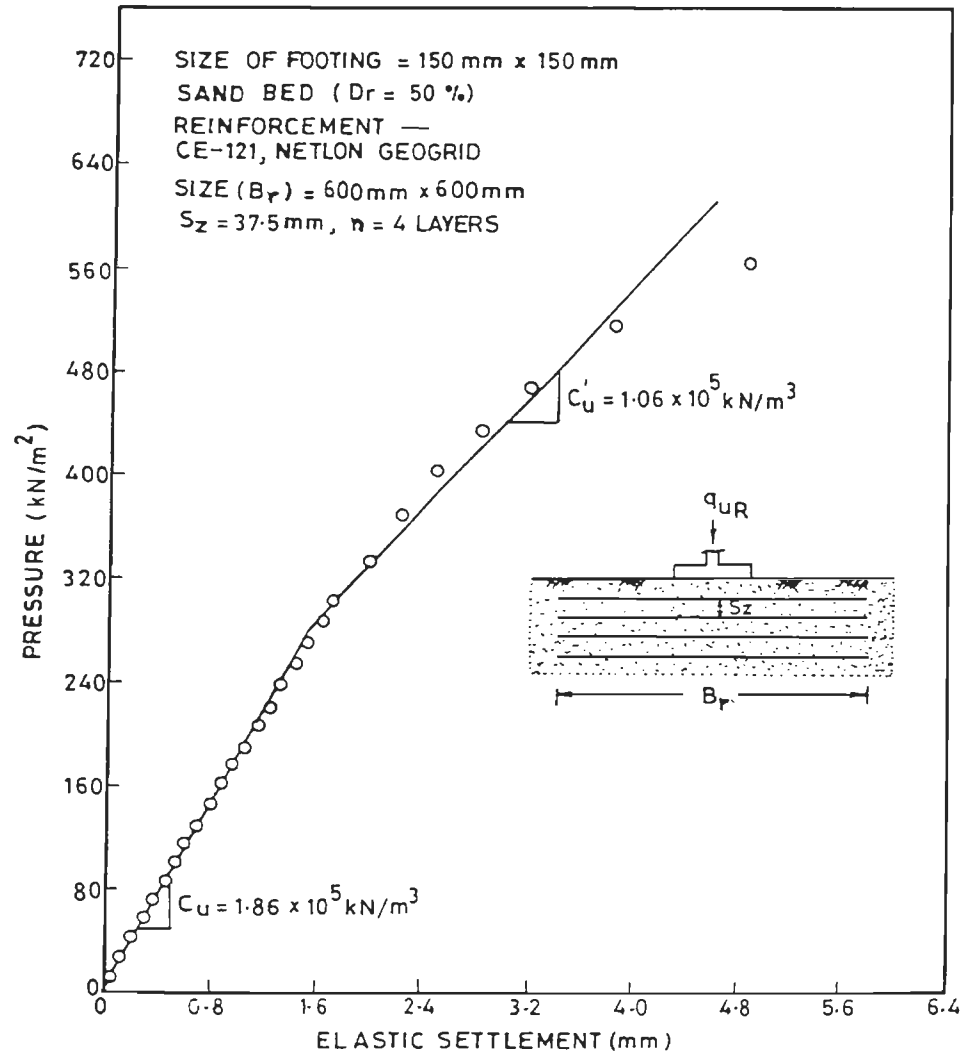


FIG. 3-82 CYCLIC PLATE LOAD TEST — PRESSURE VERSUS ELASTIC SETTLEMENT

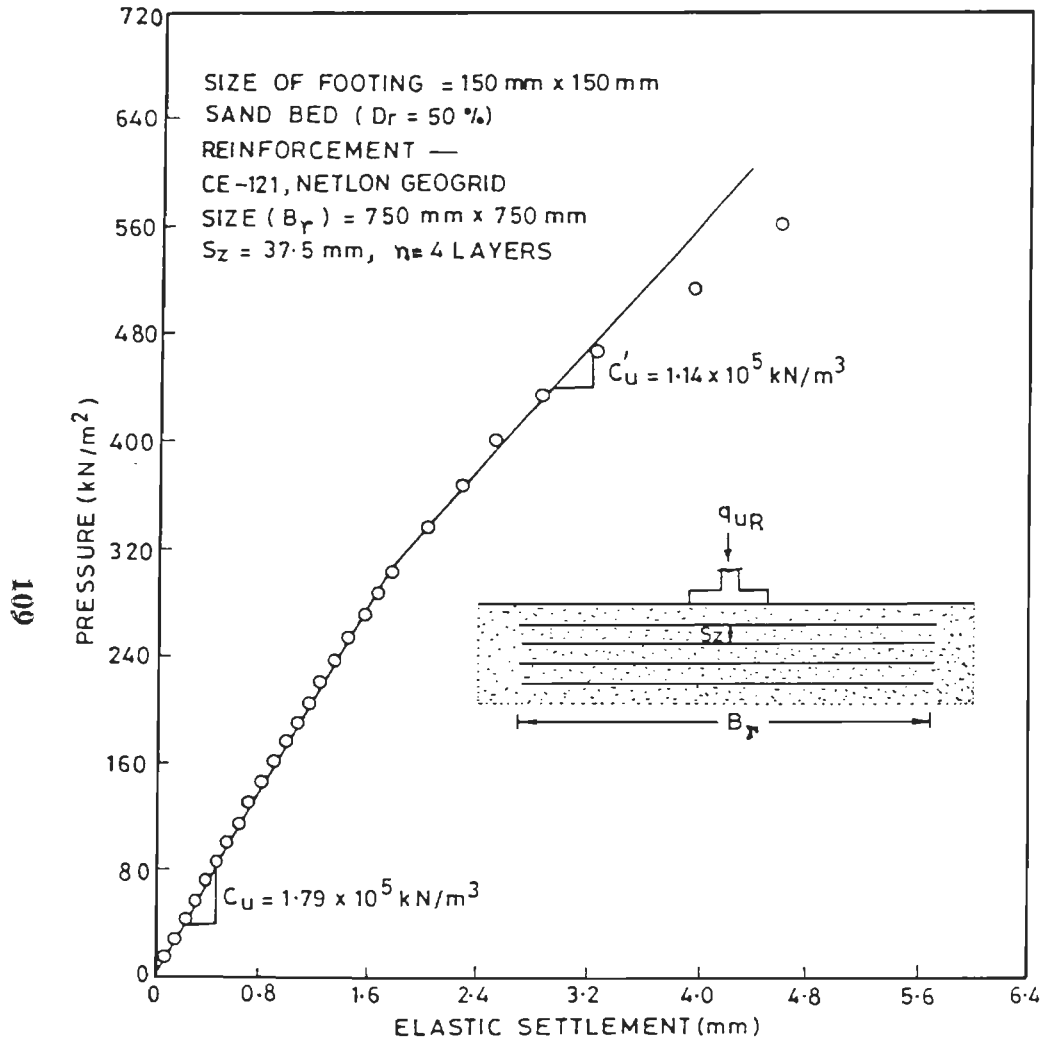


FIG. 3-83 CYCLIC PLATE LOAD TEST — PRESSURE VERSUS ELASTIC SETTLEMENT

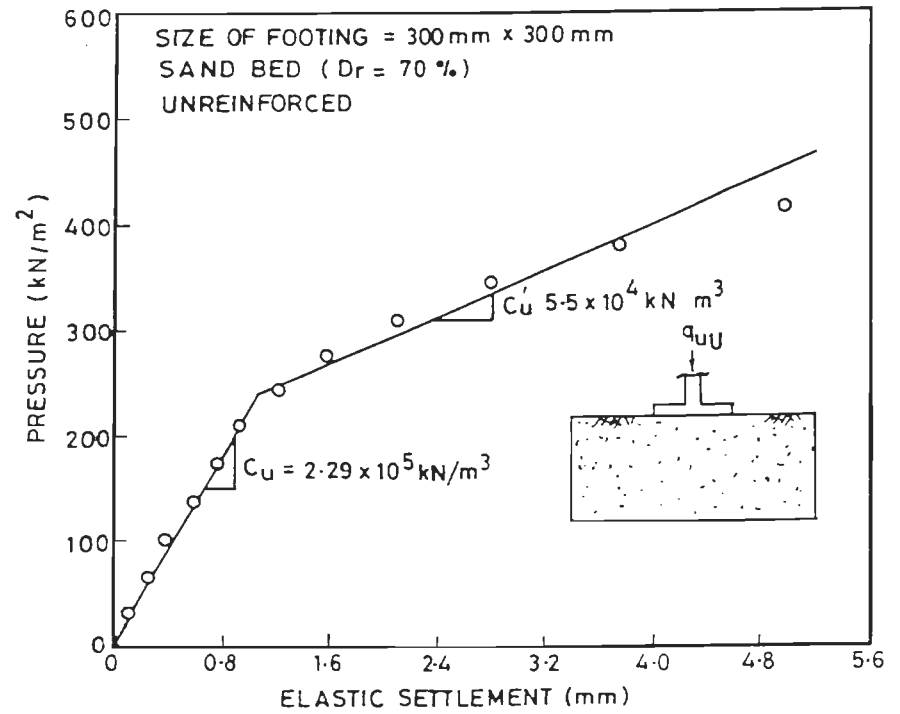


FIG. 3-84 CYCLIC PLATE LOAD TEST — PRESSURE VERSUS ELASTIC SETTLEMENT

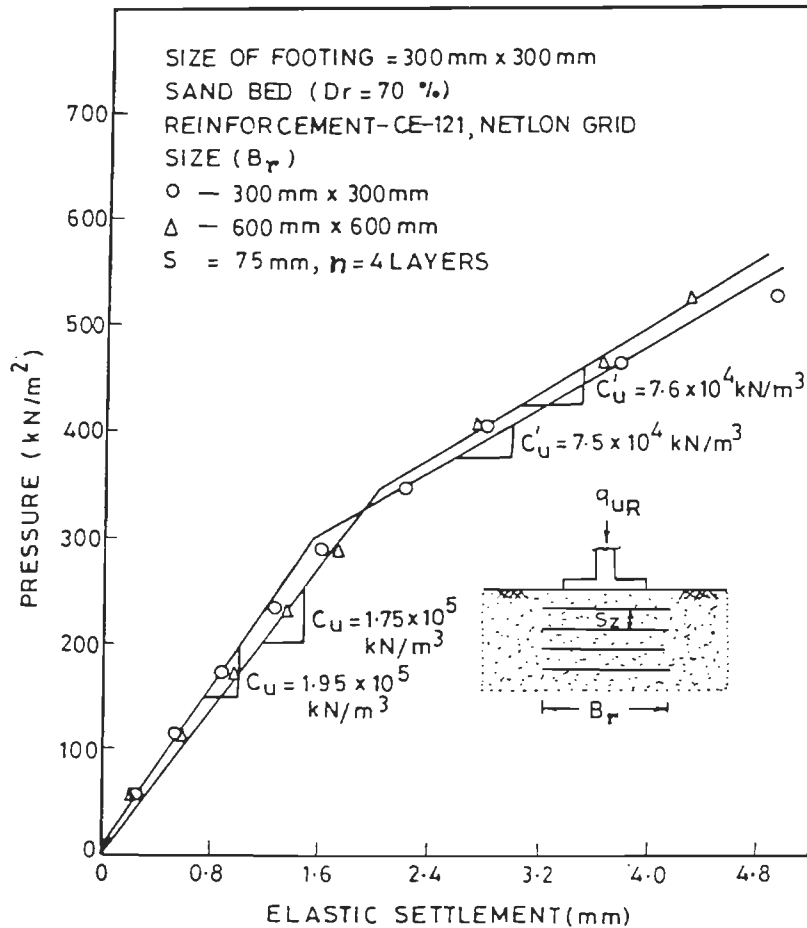


FIG.3-85 CYCLIC PLATE LOAD TEST - PRESSURE VERSUS ELASTIC SETTLEMENT

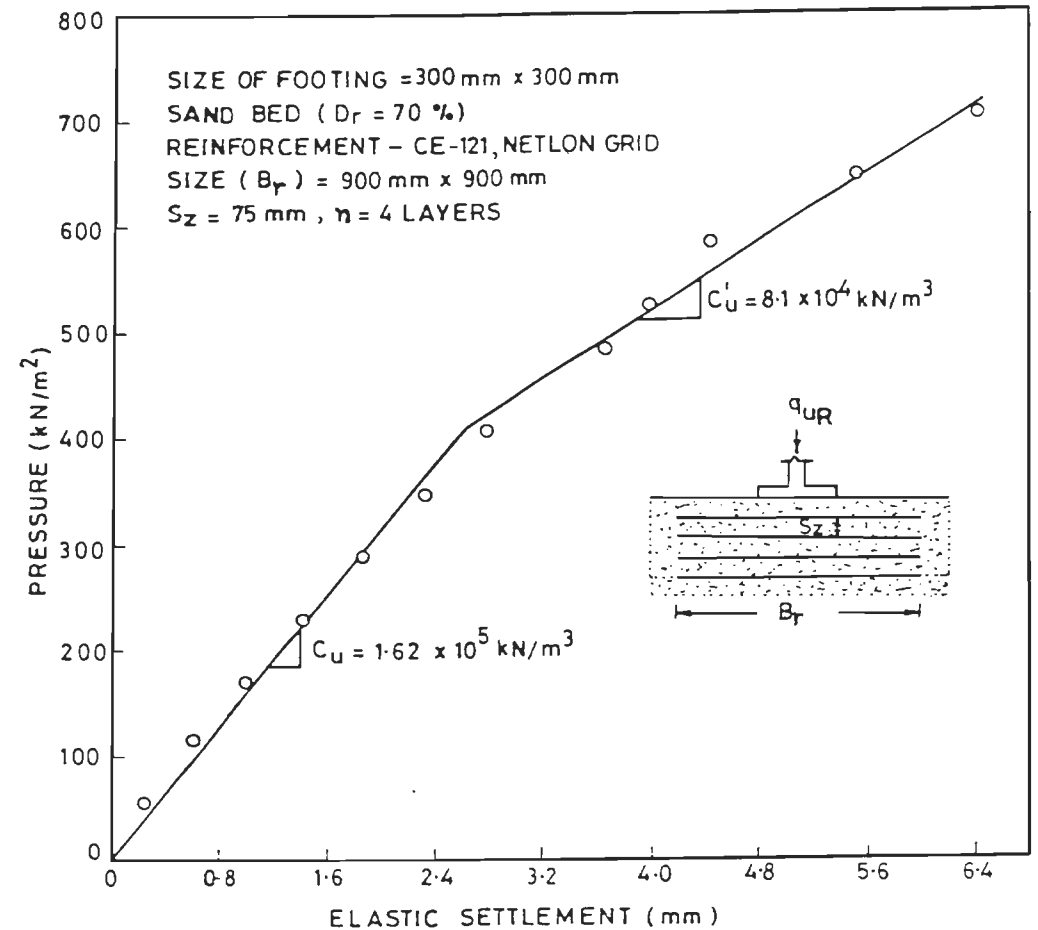


FIG.3-86 CYCLIC PLATE LOAD TEST - PRESSURE VERSUS ELASTIC SETTLEMENT

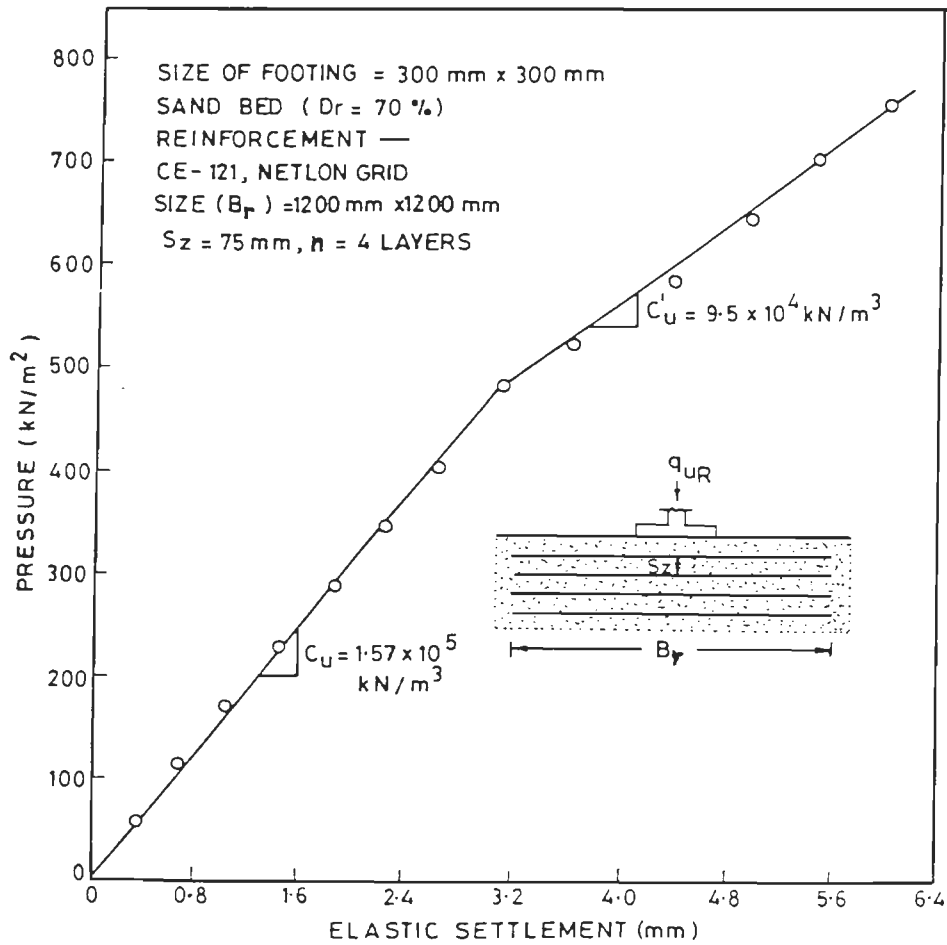


FIG.3-87 CYCLIC PLATE LOAD TEST — PRESSURE VERSUS ELASTIC SETTLEMENT

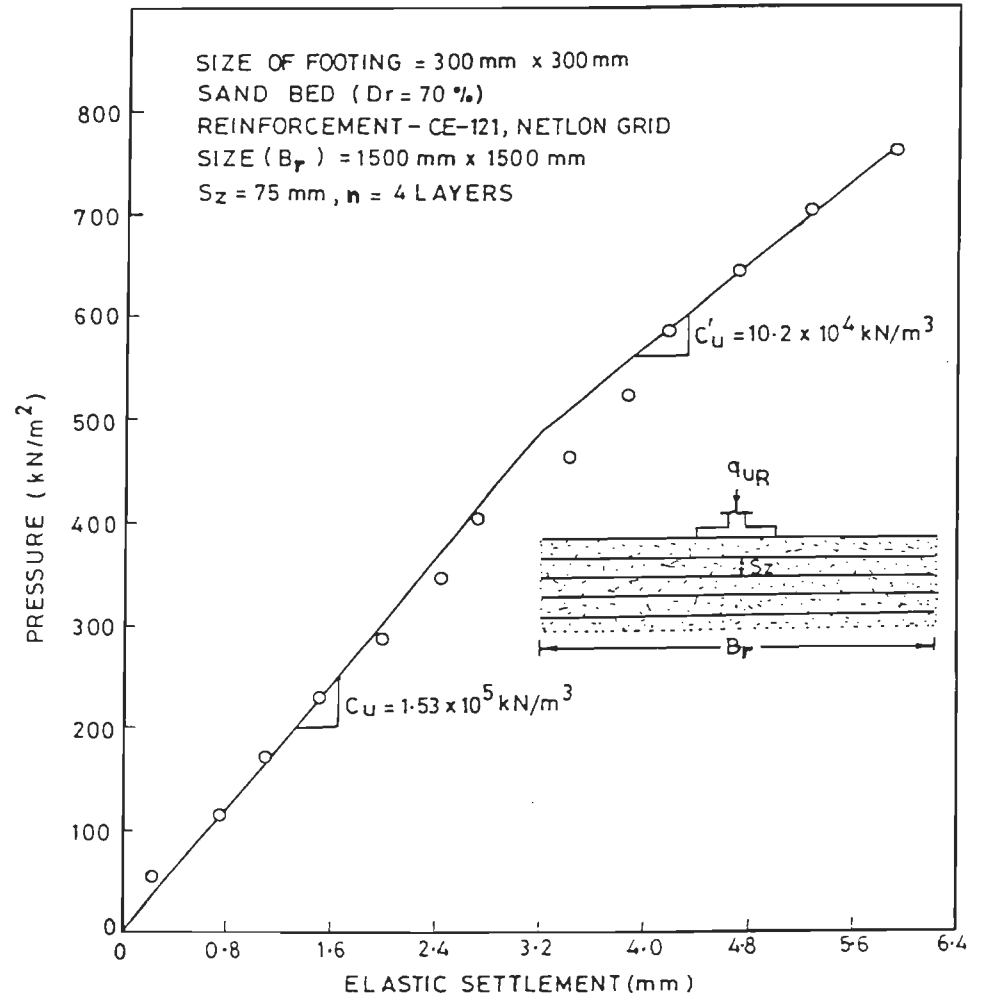


FIG.3-88 CYCLIC PLATE LOAD TEST — PRESSURE VERSUS ELASTIC SETTLEMENT

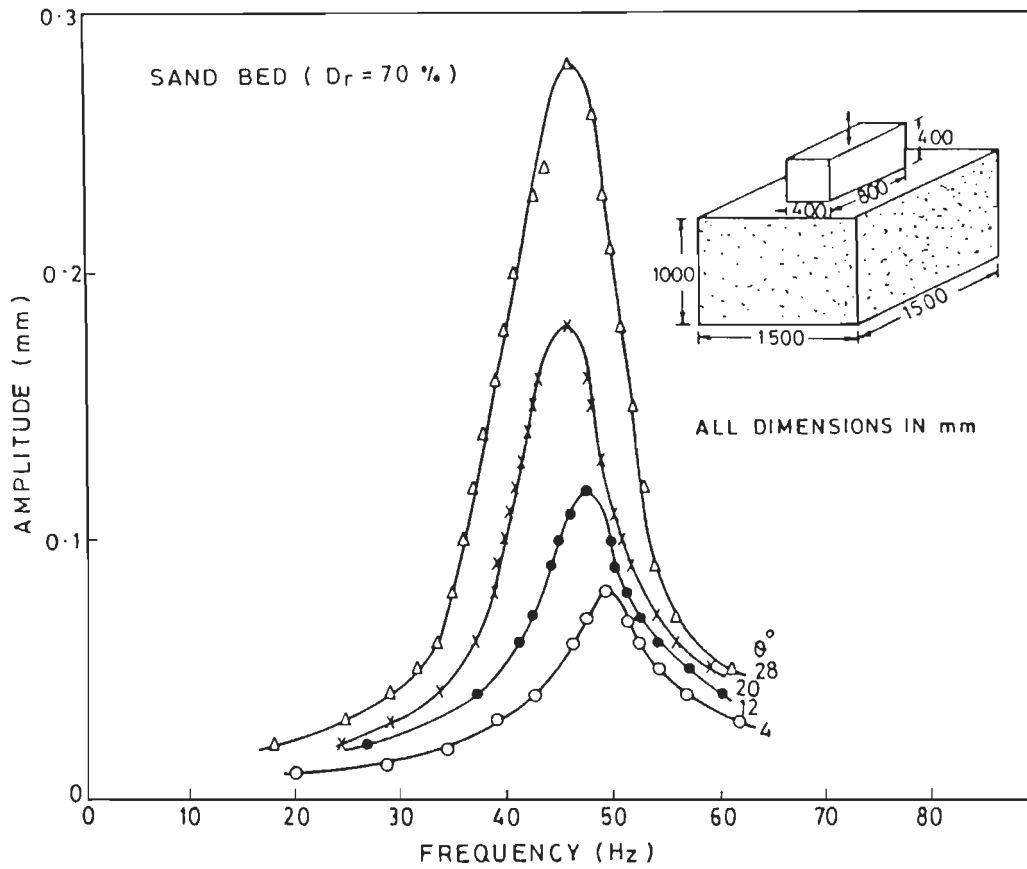


FIG.3-89 VERTICAL VIBRATION TEST ON UNREINFORCED SAND

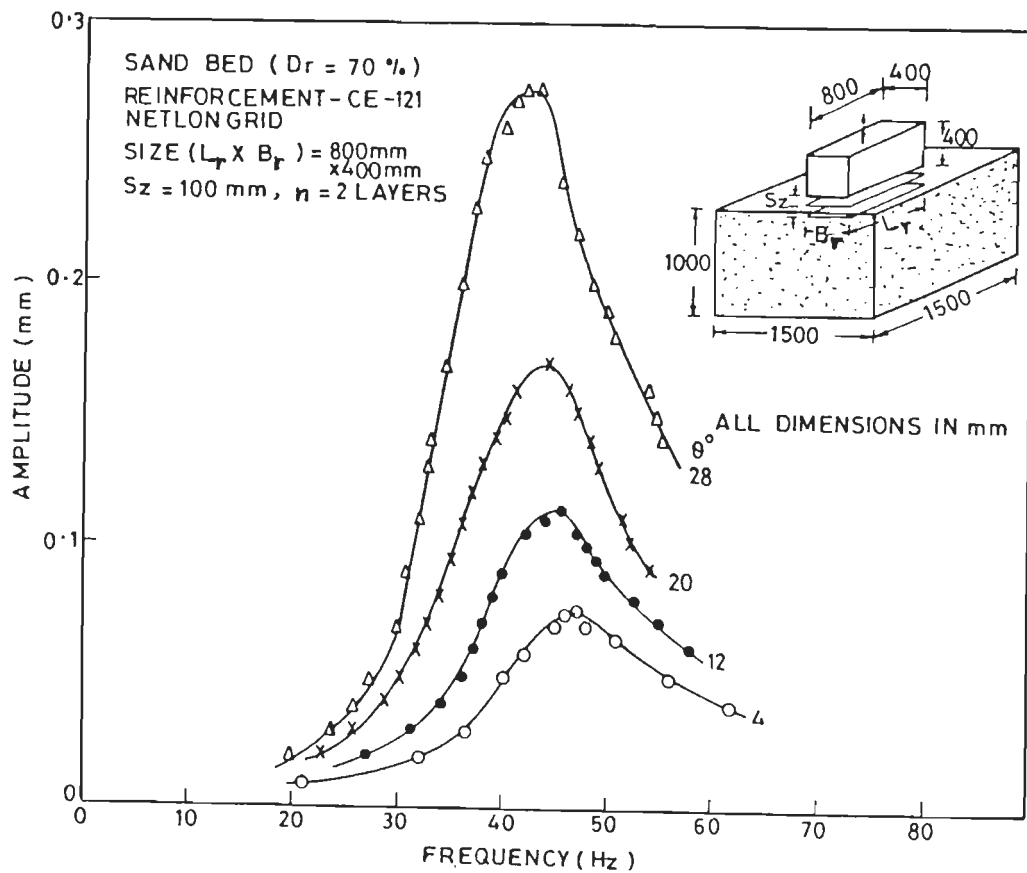


FIG. 3-90 VERTICAL VIBRATION TEST ON REINFORCED SAND

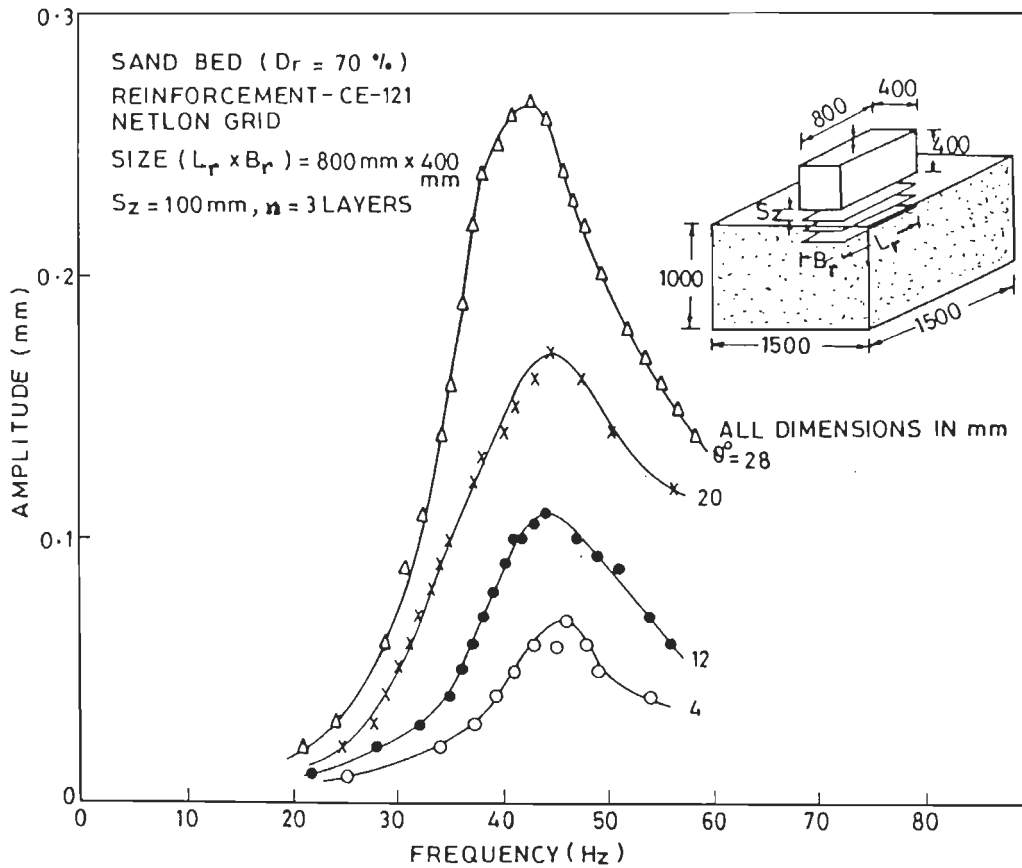


FIG. 3.91 VERTICAL VIBRATION TEST ON REINFORCED SAND

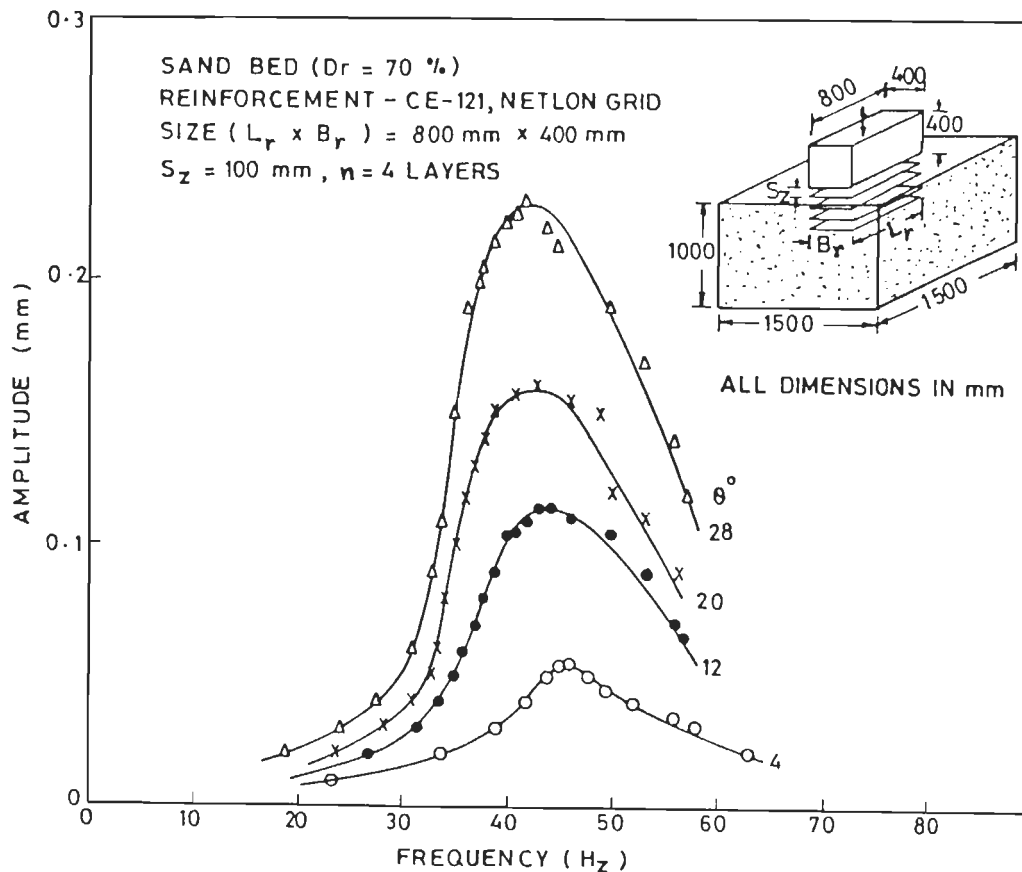


FIG. 3.92 VERTICAL VIBRATION TEST ON REINFORCED SAND

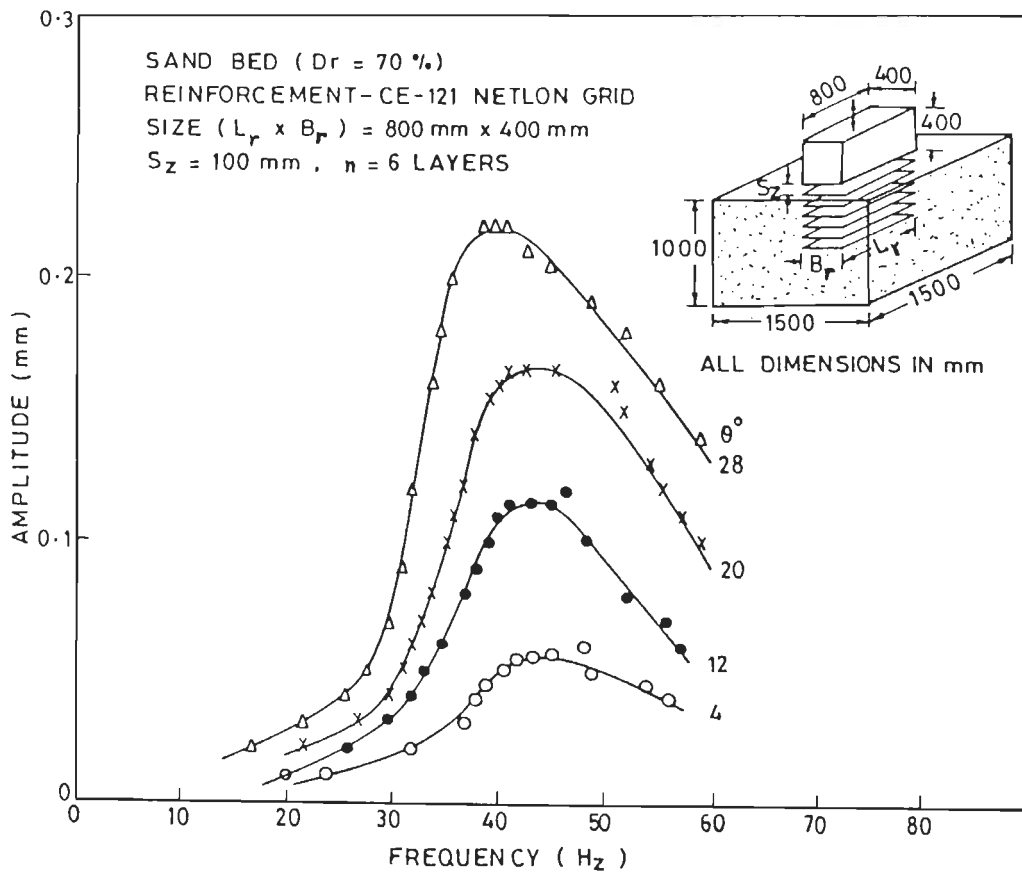


FIG. 3-93 VERTICAL VIBRATION TEST ON REINFORCED SAND

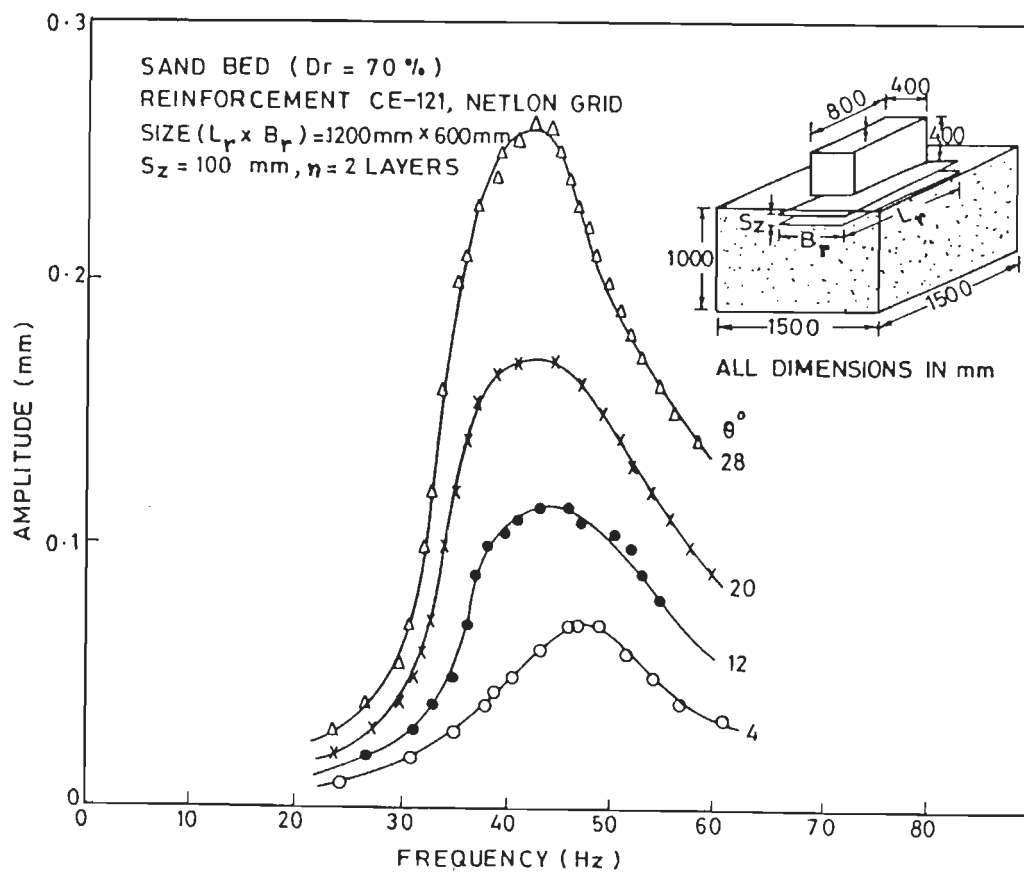


FIG. 3-94 VERTICAL VIBRATION TEST ON REINFORCED SAND

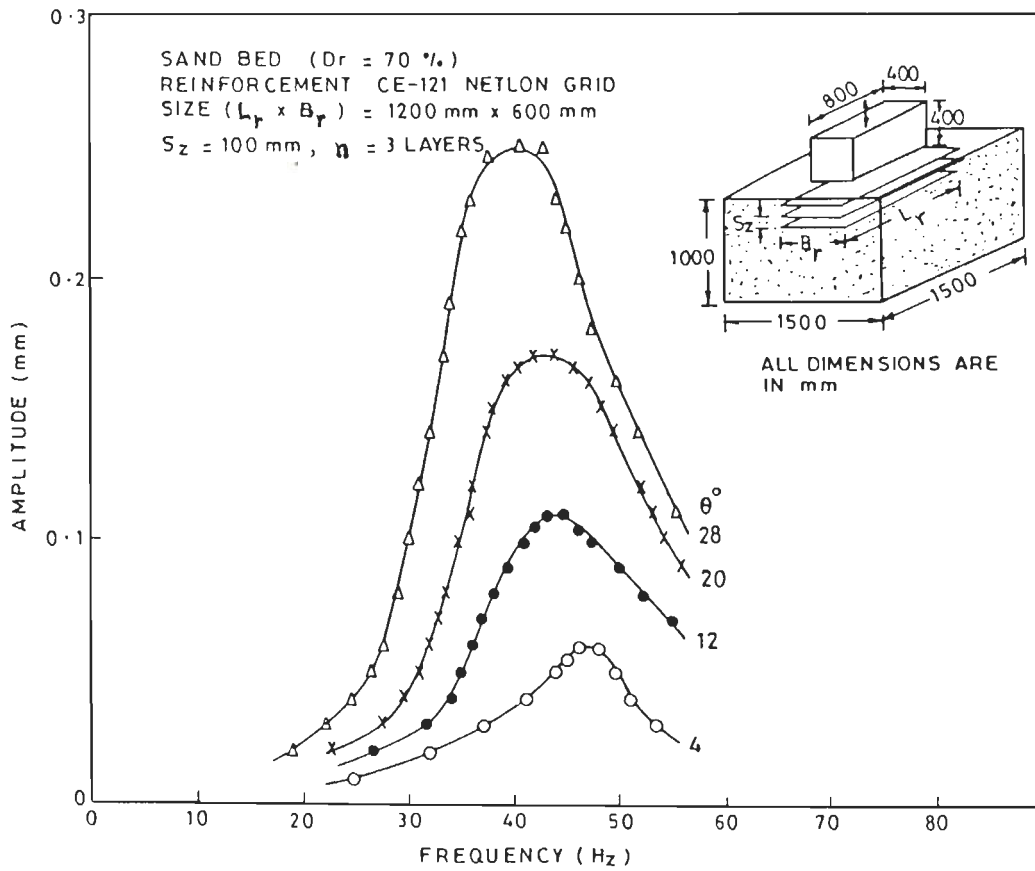


FIG.3-95 VERTICAL VIBRATION TEST ON REINFORCED SAND

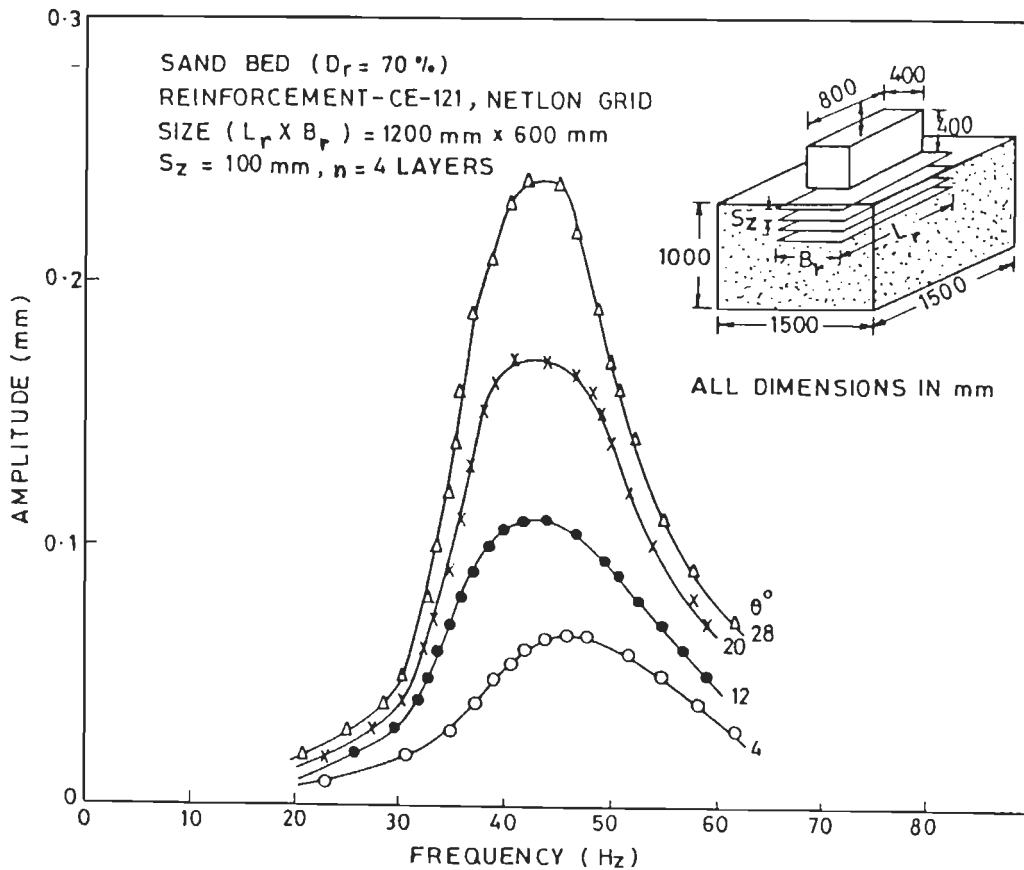


FIG.3-96 VERTICAL VIBRATION TEST ON REINFORCED SAND

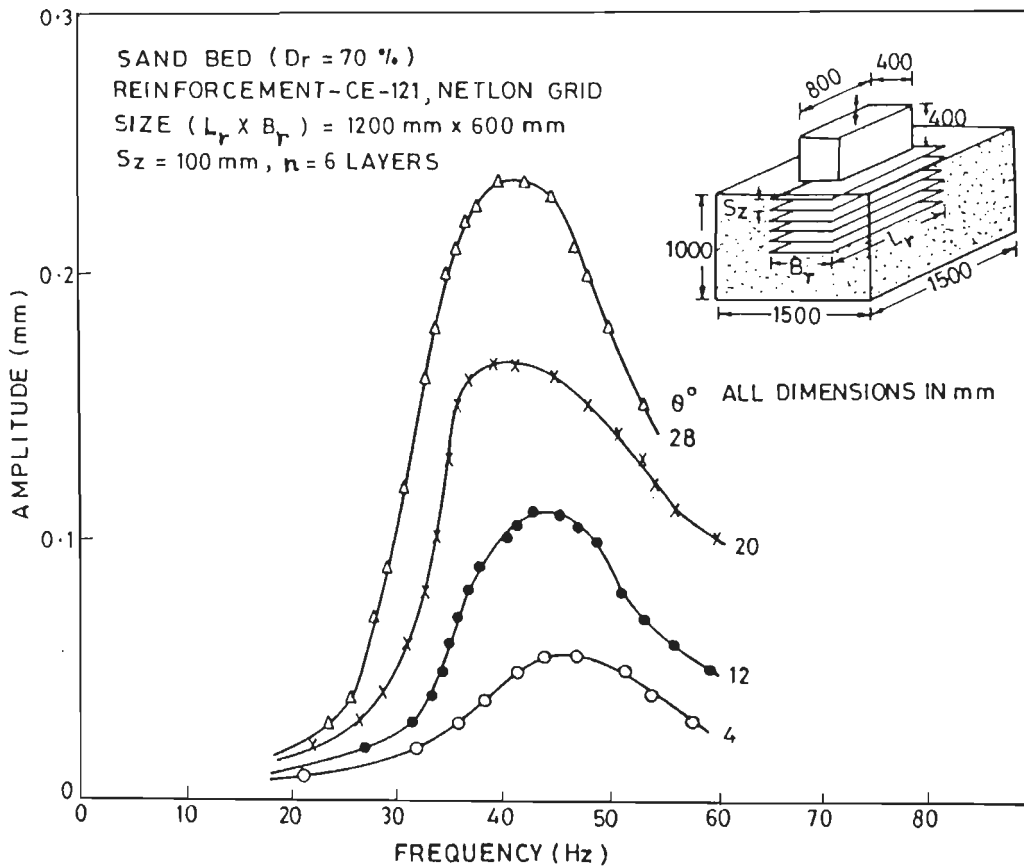


FIG.3-97 VERTICAL VIBRATION TEST ON REINFORCED SAND

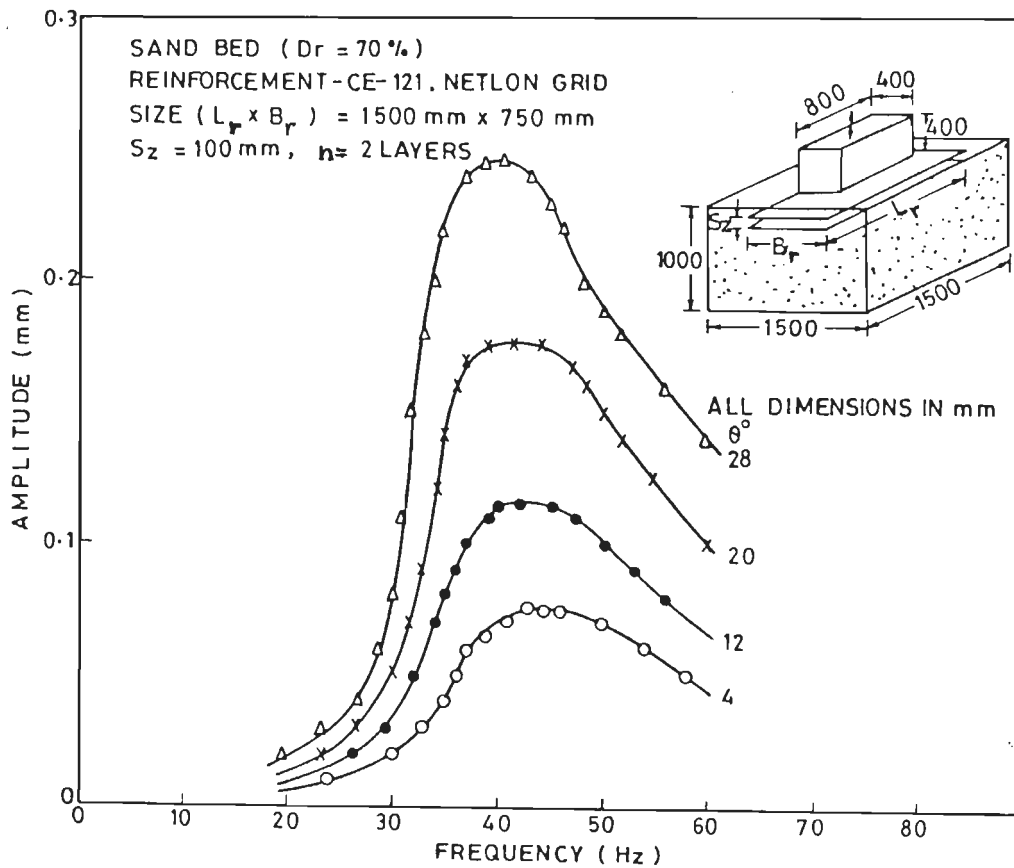


FIG.3-98 VERTICAL VIBRATION TEST ON REINFORCED SAND

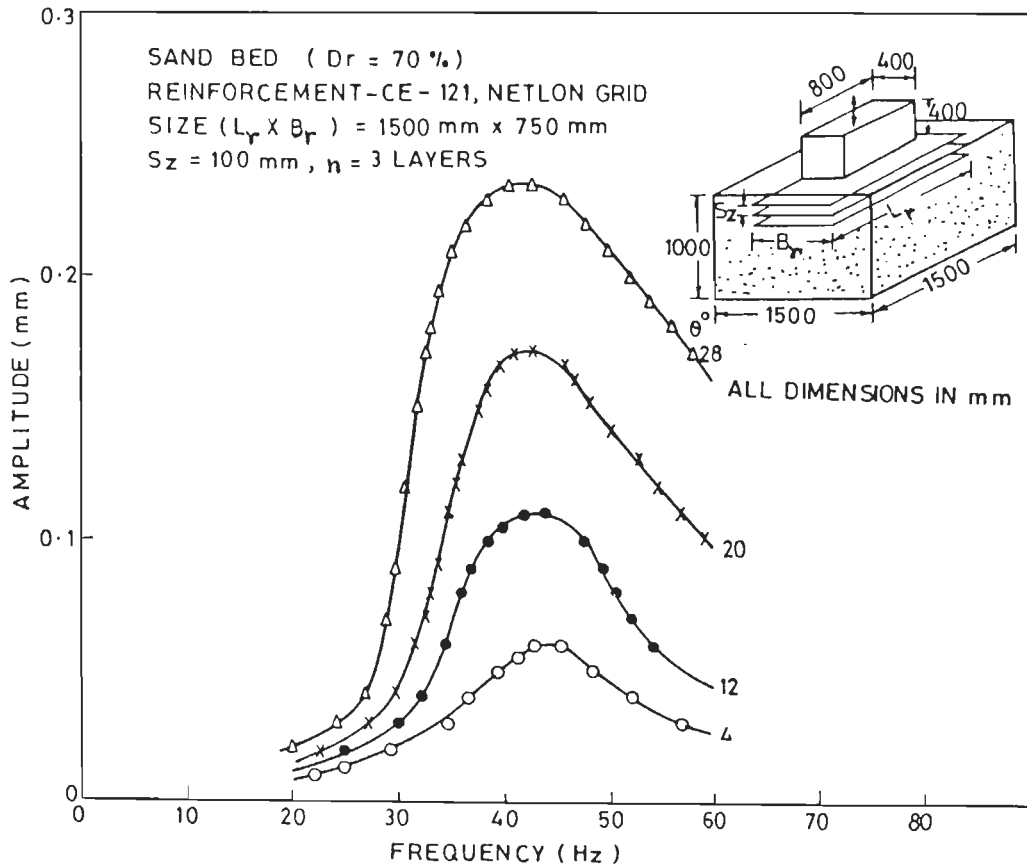


FIG. 3-99 VERTICAL VIBRATION TEST ON REINFORCED SAND

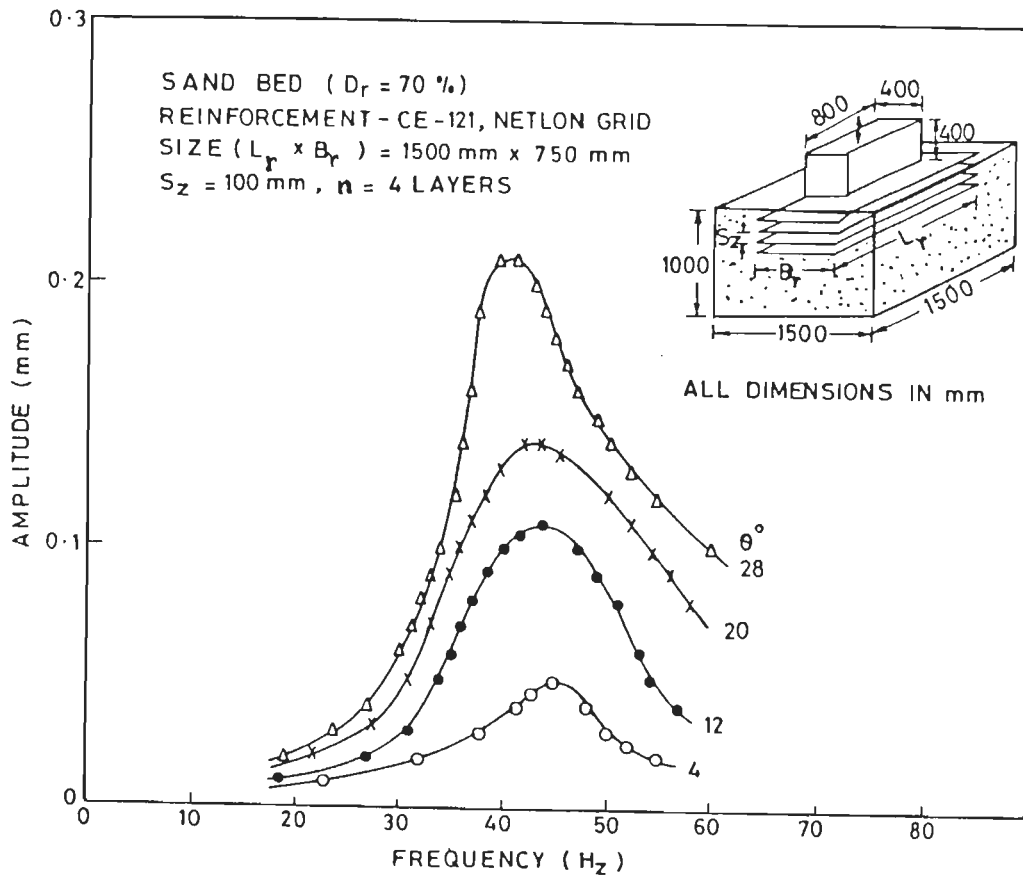


FIG. 3-100 VERTICAL VIBRATION TEST ON REINFORCED SAND

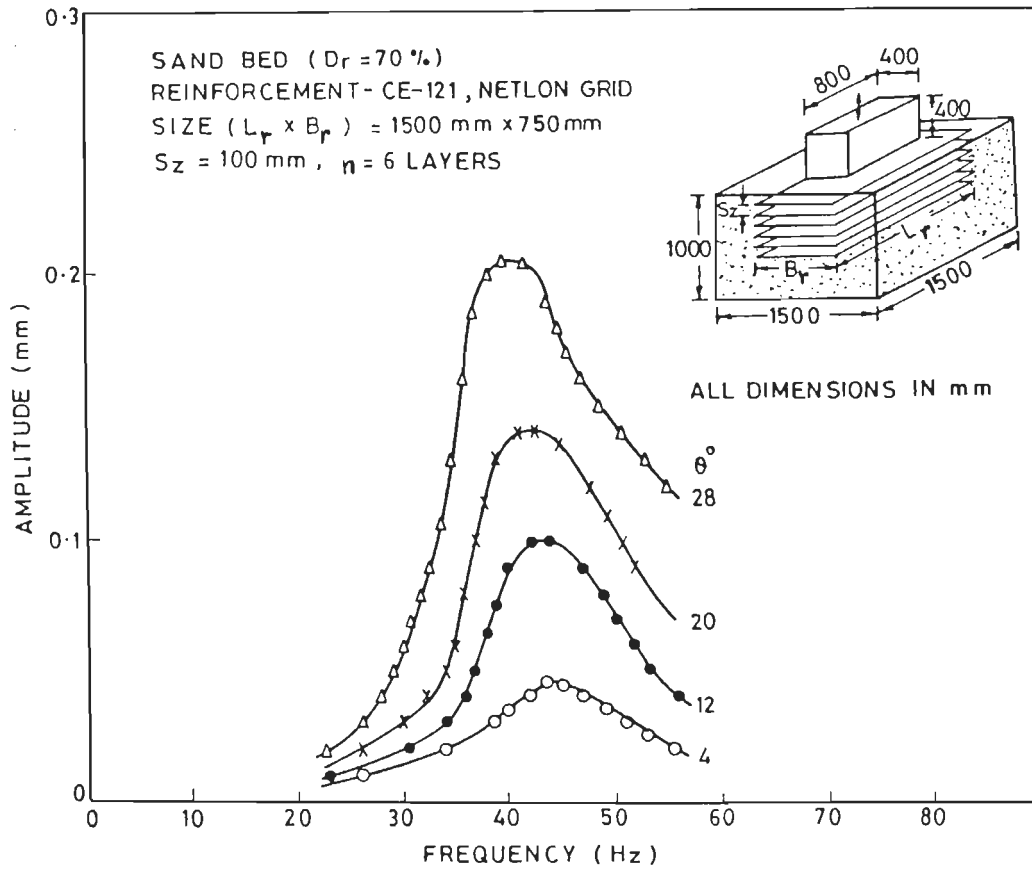


FIG. 3.101 VERTICAL VIBRATION TEST ON REINFORCED SAND

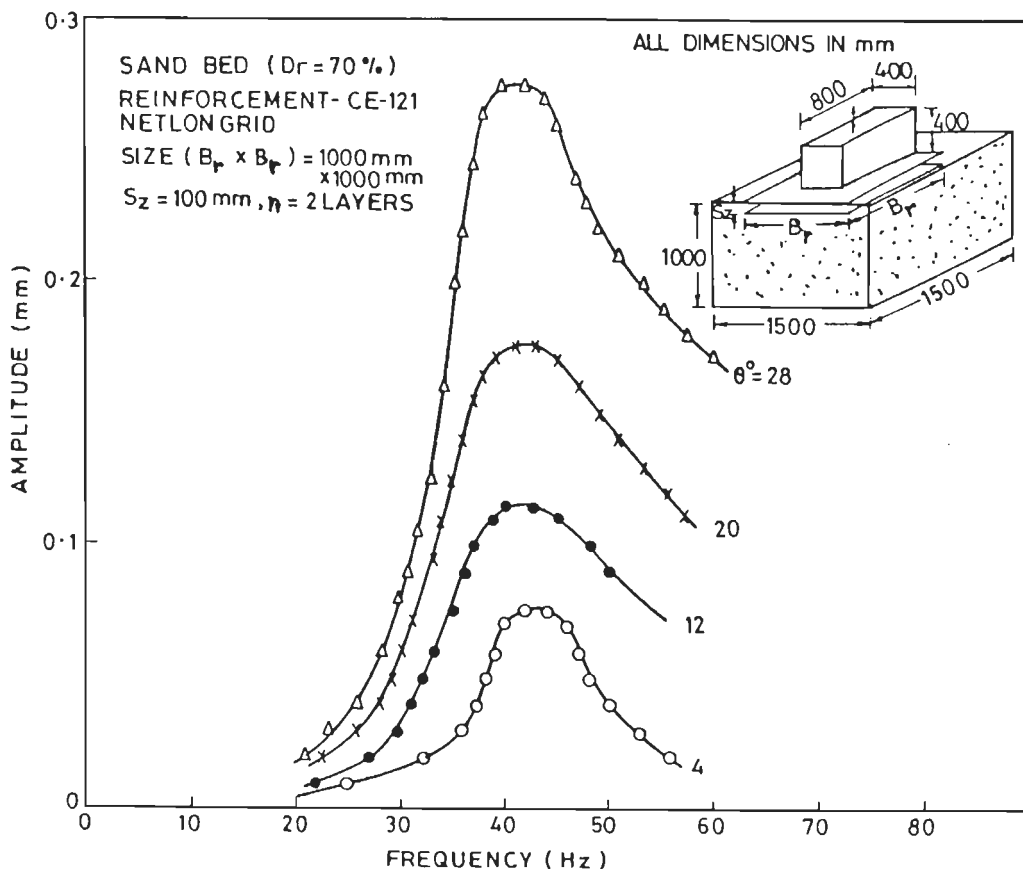


FIG. 3.102 VERTICAL VIBRATION TEST ON REINFORCED SAND

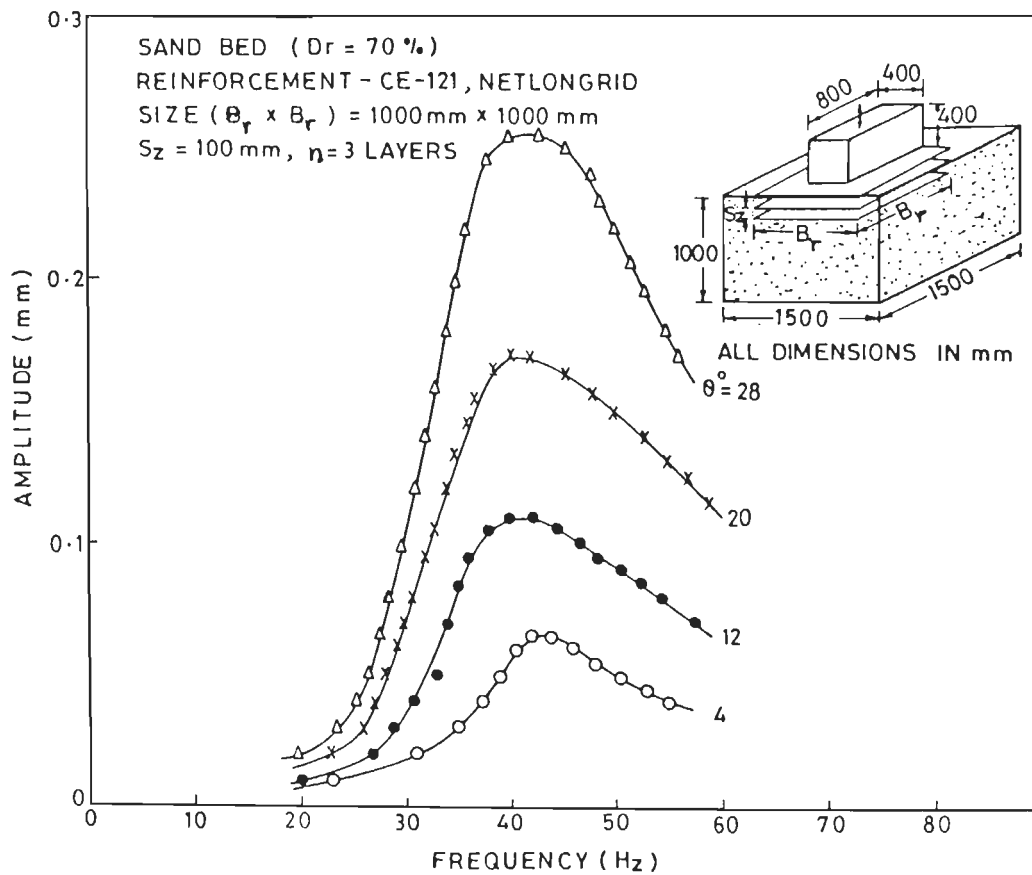


FIG.3-103 VERTICAL VIBRATION TEST ON REINFORCED SAND

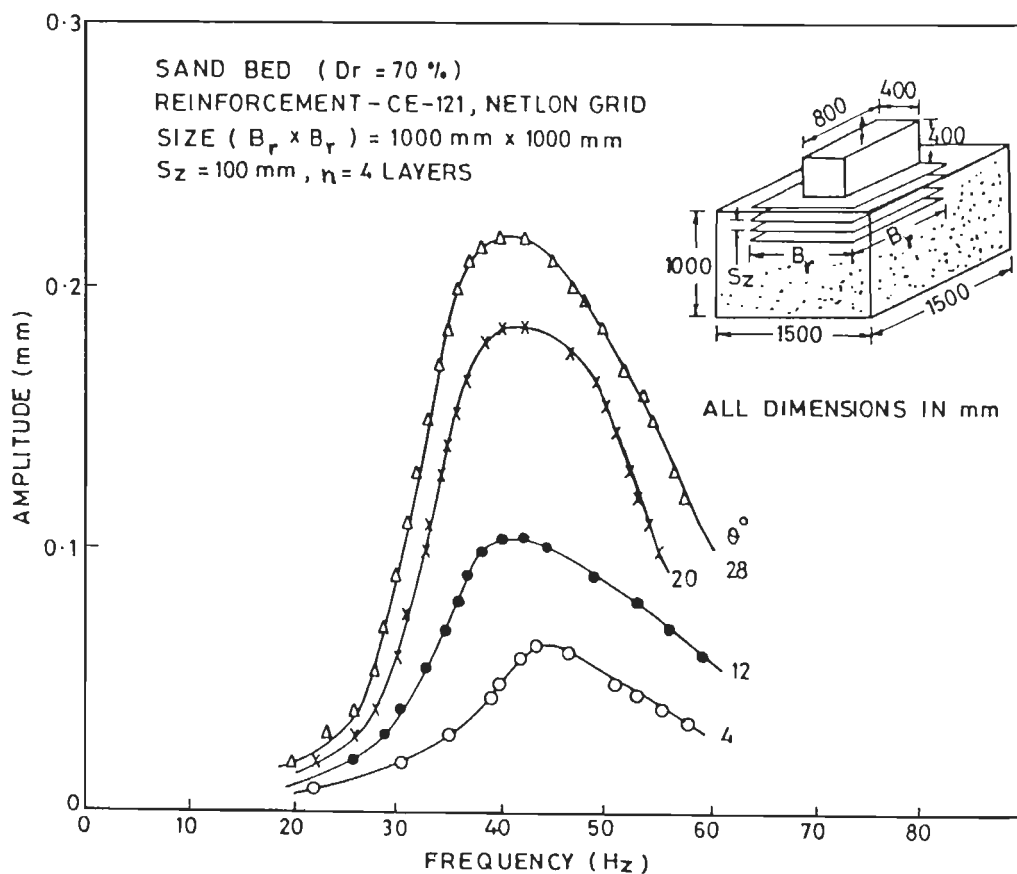


FIG.3-104 VERTICAL VIBRATION TEST ON REINFORCED SAND

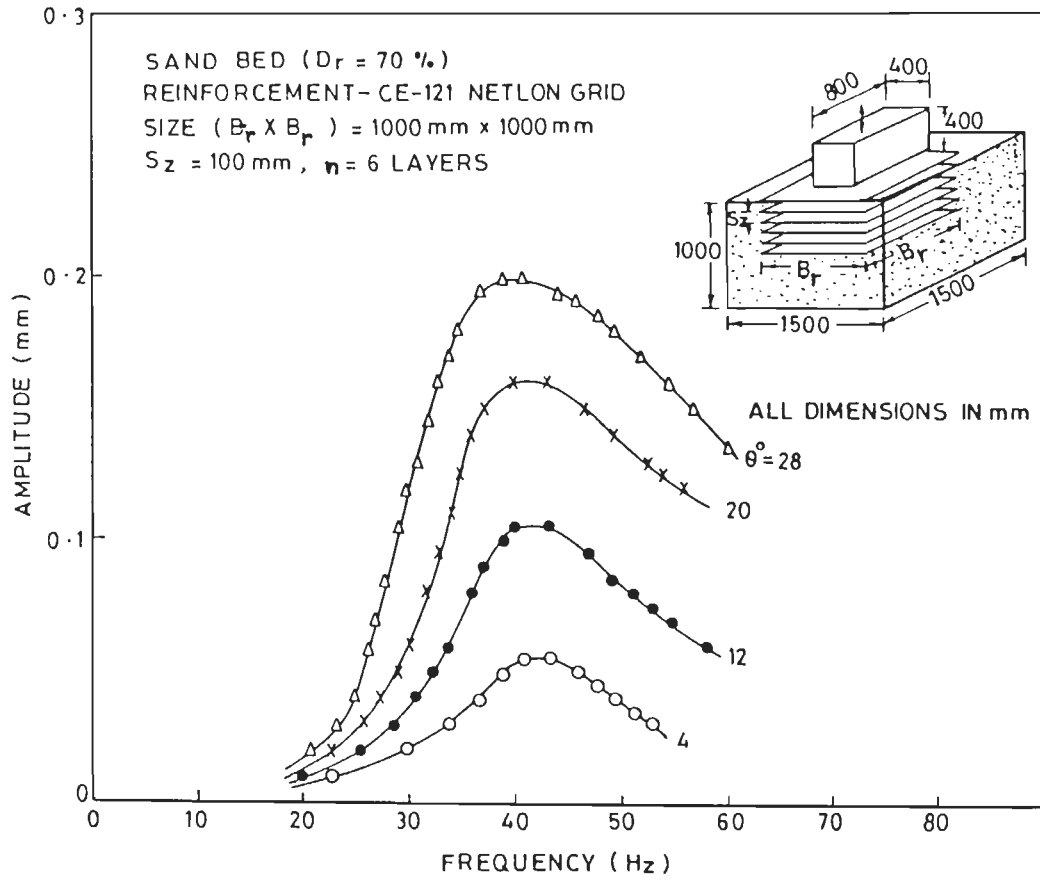


FIG.3.105 VERTICAL VIBRATION TEST ON REINFORCED SAND

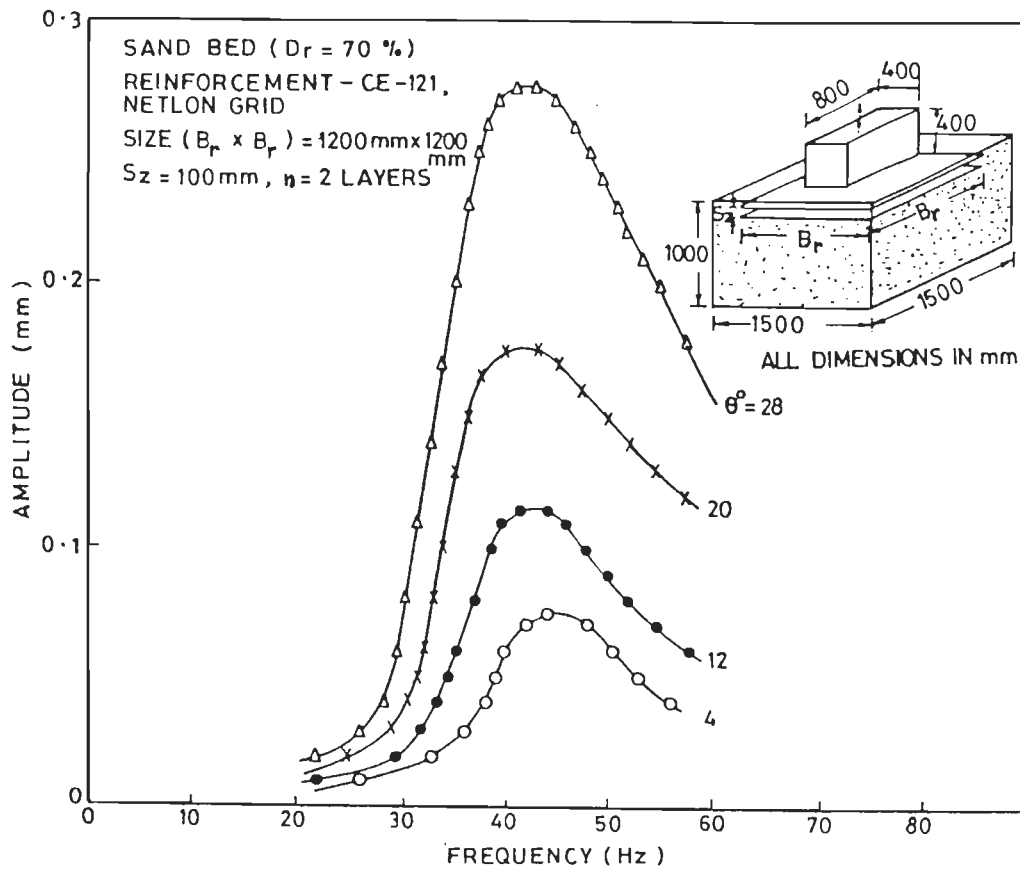


FIG.3.106 VERTICAL VIBRATION TEST ON REINFORCED SAND

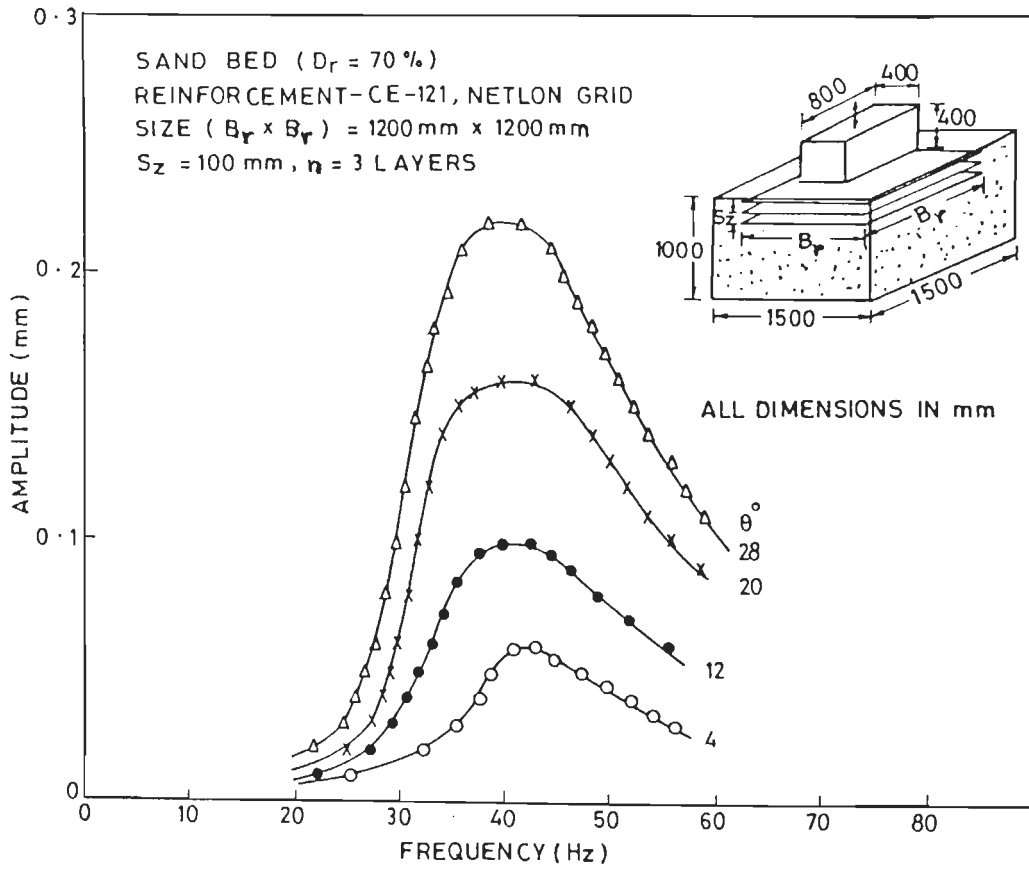


FIG. 3-107 VERTICAL VIBRATION TEST ON REINFORCED SAND

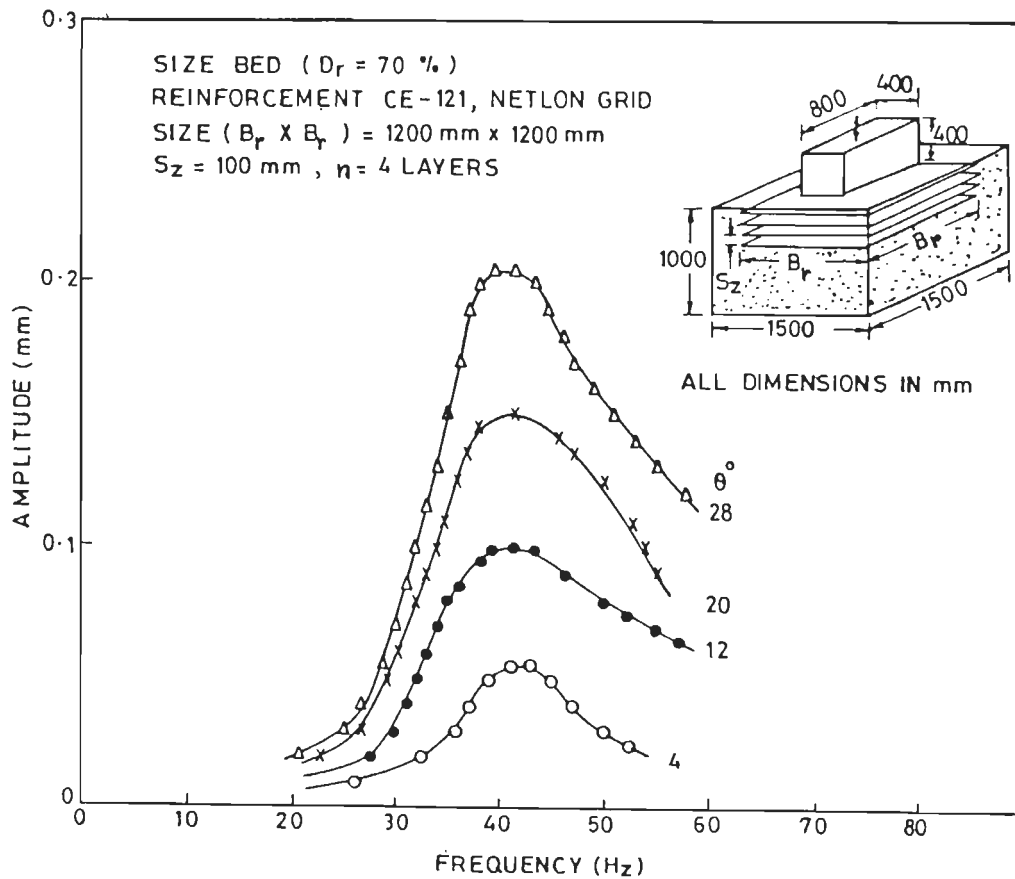


FIG. 3-108 VERTICAL VIBRATION TEST ON REINFORCED SAND

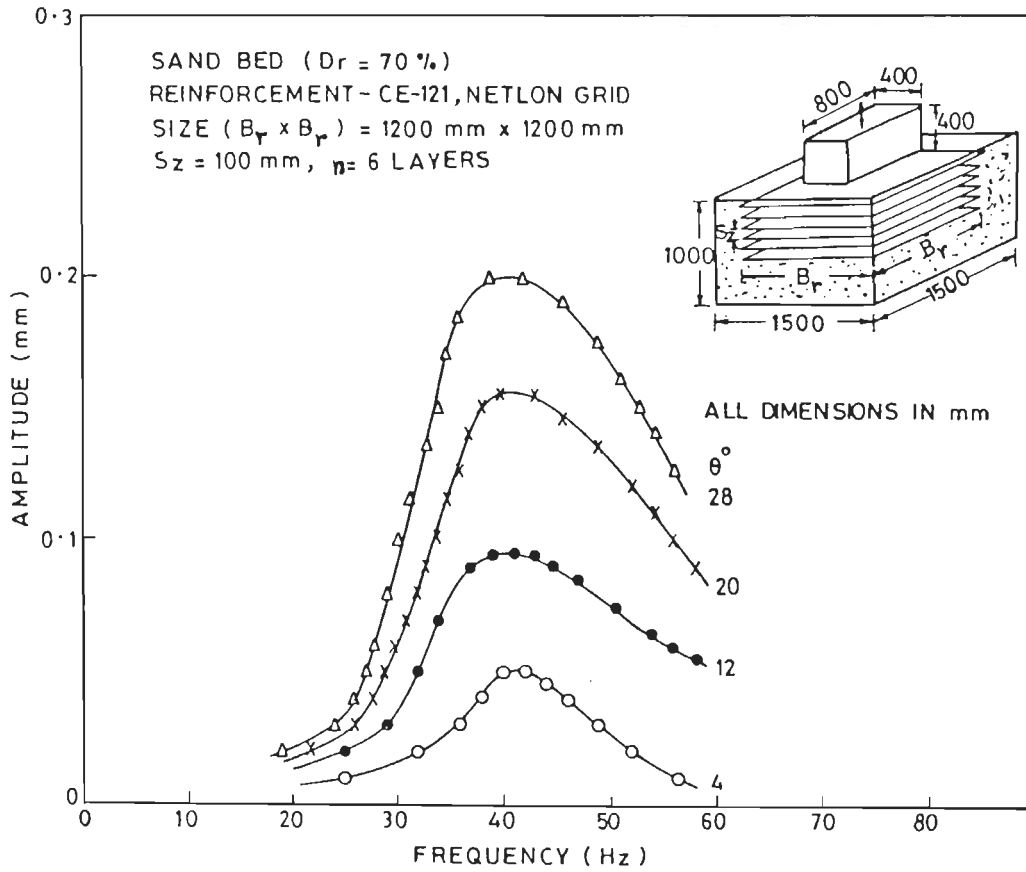


FIG.3.109 VERTICAL VIBRATION TEST ON REINFORCED SAND

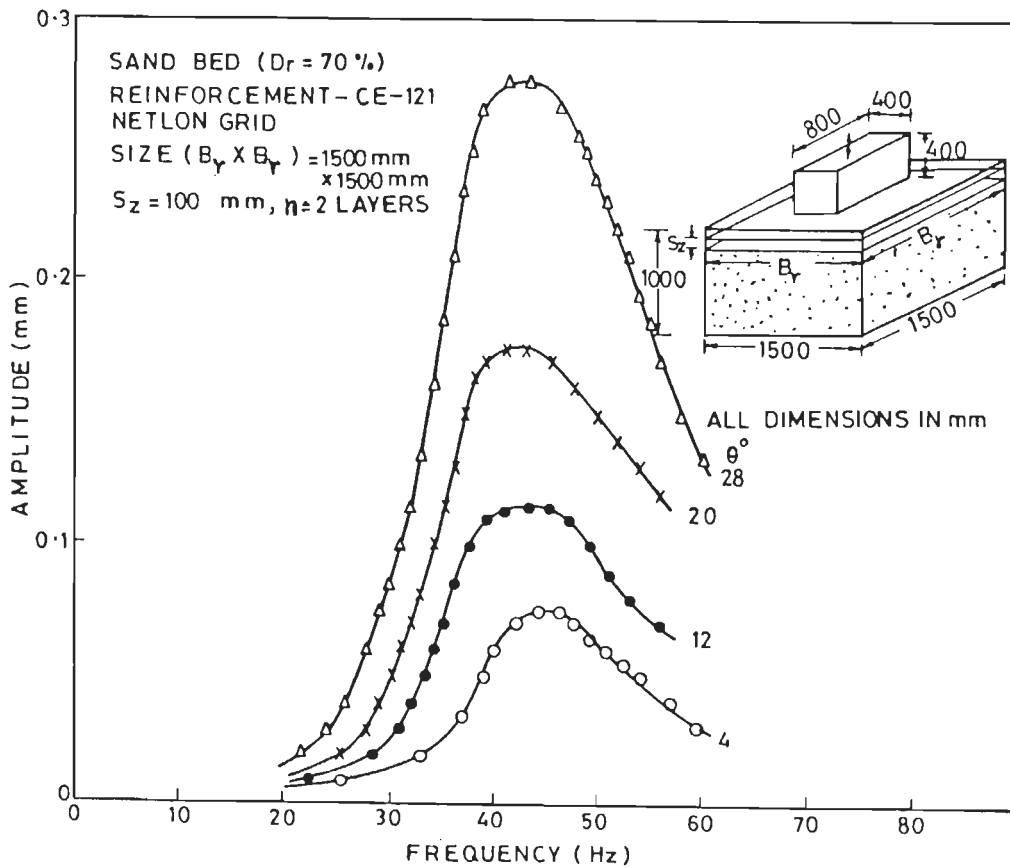


FIG.3.110 VERTICAL VIBRATION TEST ON REINFORCED SAND

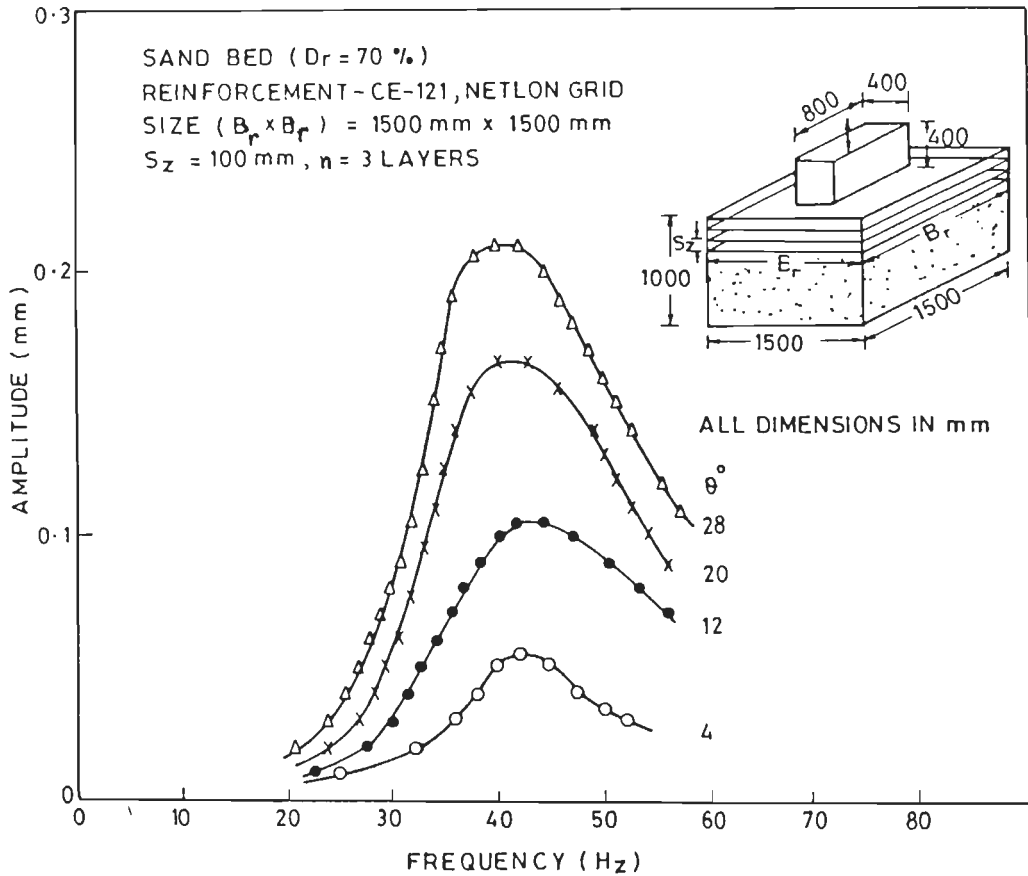


FIG.3:111 VERTICAL VIBRATION TEST ON REINFORCED SAND

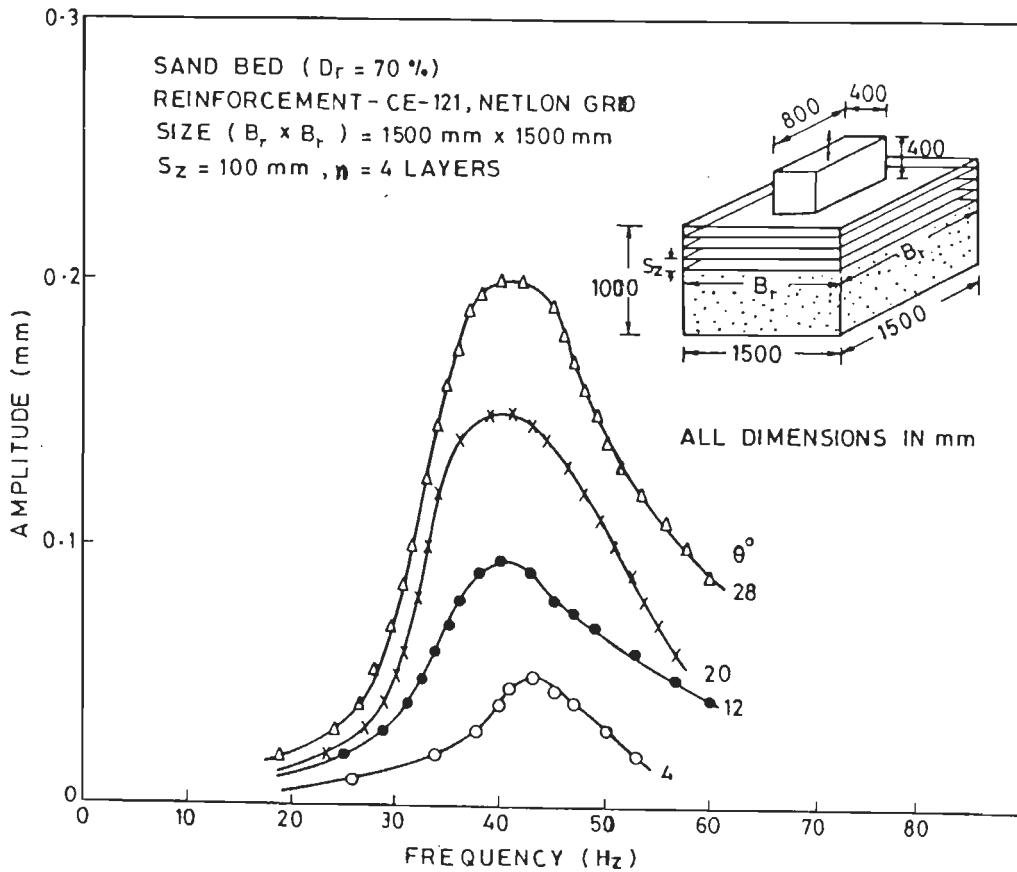


FIG.3:112 VERTICAL VIBRATION TEST ON REINFORCED SAND

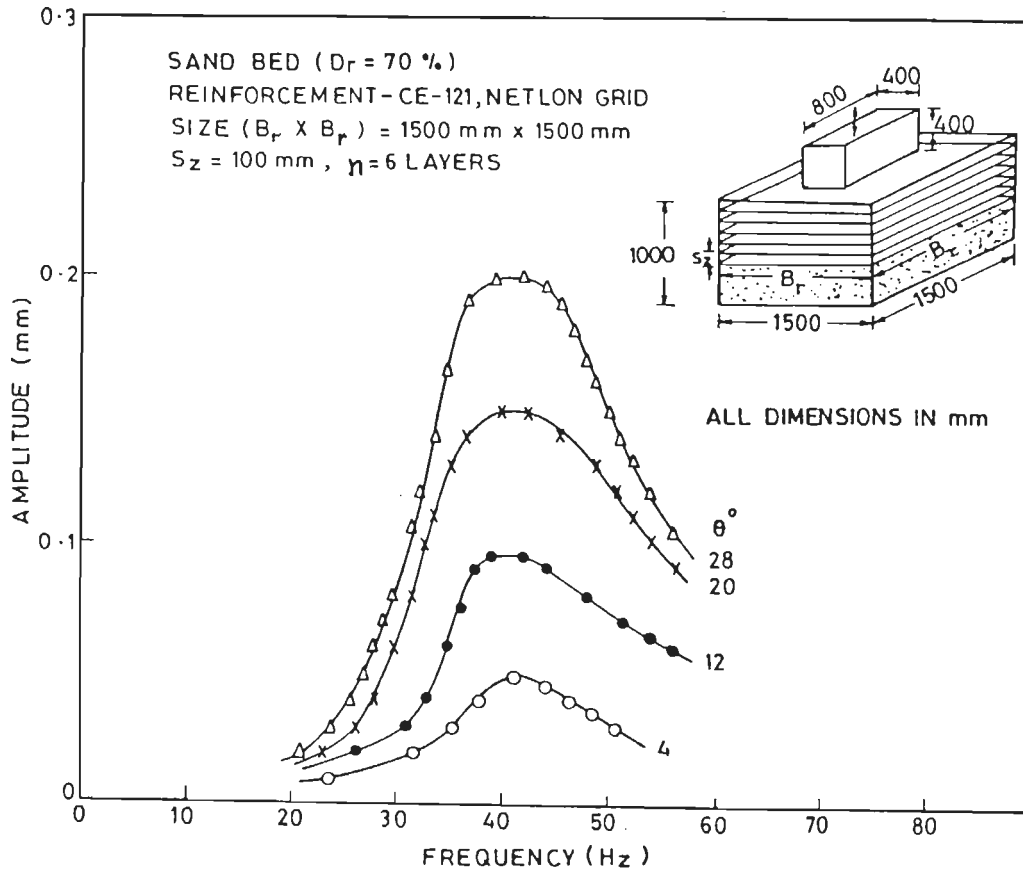


FIG. 3-113 VERTICAL VIBRATION TEST ON REINFORCED SAND

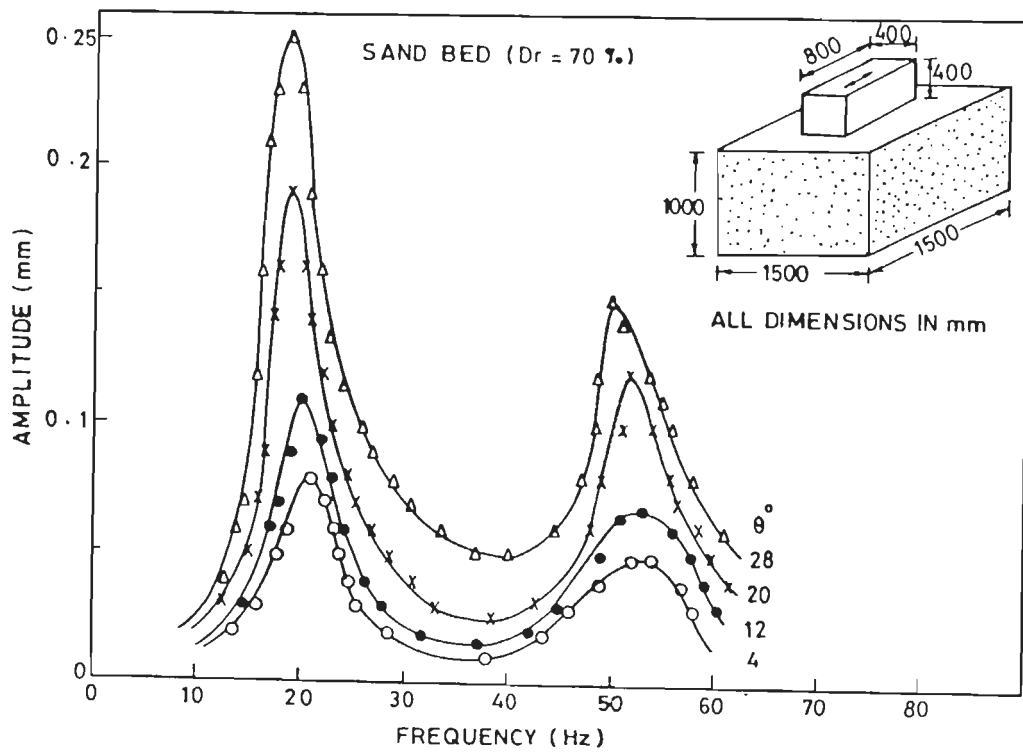


FIG. 3-114 HORIZONTAL VIBRATION TEST ON UNREINFORCED SAND

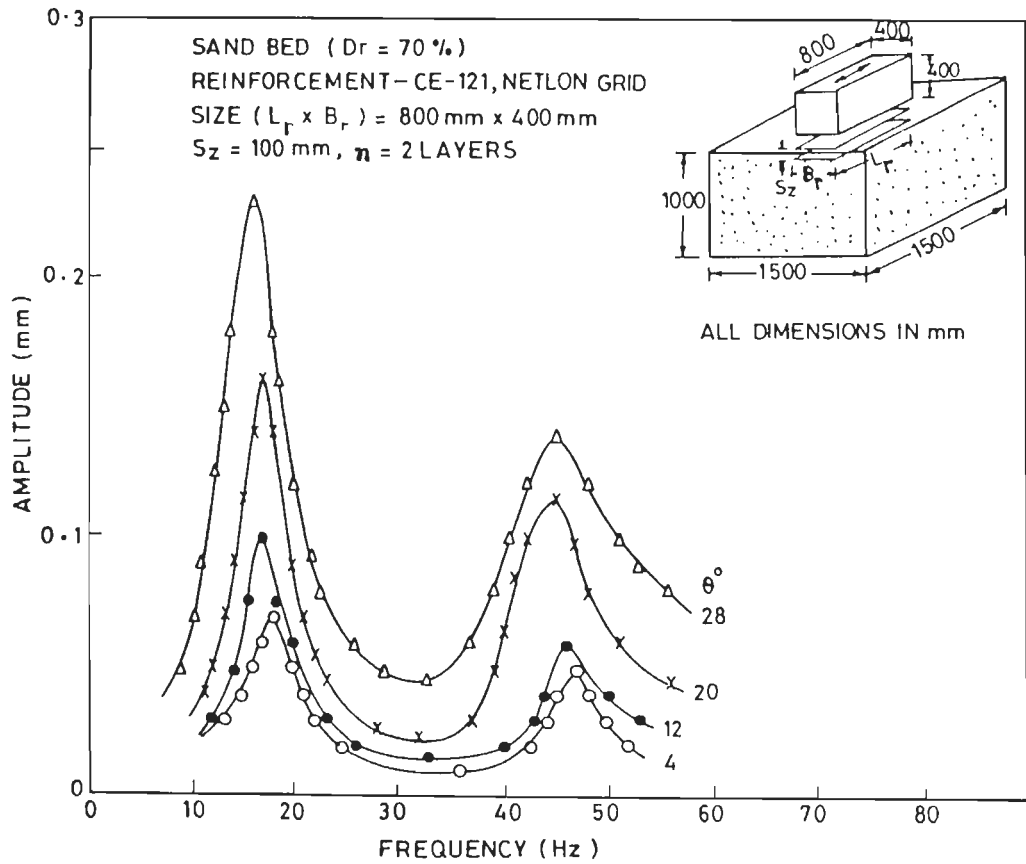


FIG. 3-115 HORIZONTAL VIBRATION TEST ON REINFORCED SAND

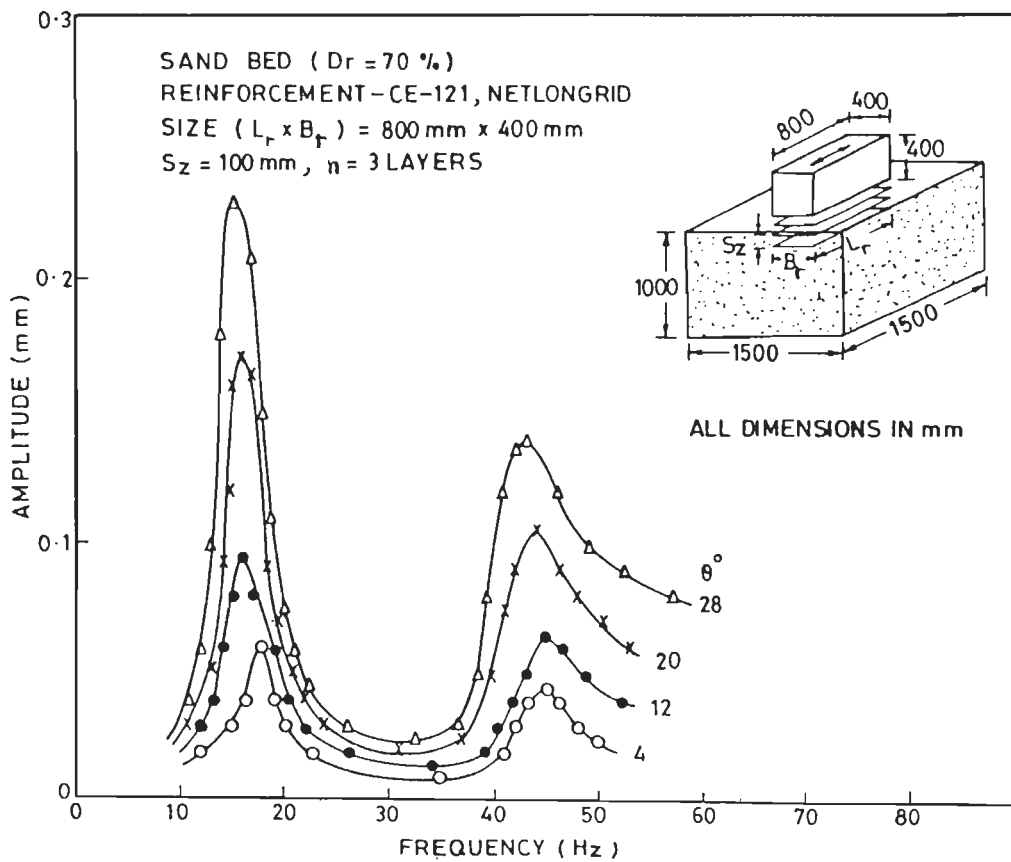


FIG. 3-116 HORIZONTAL VIBRATION TEST ON REINFORCED SAND

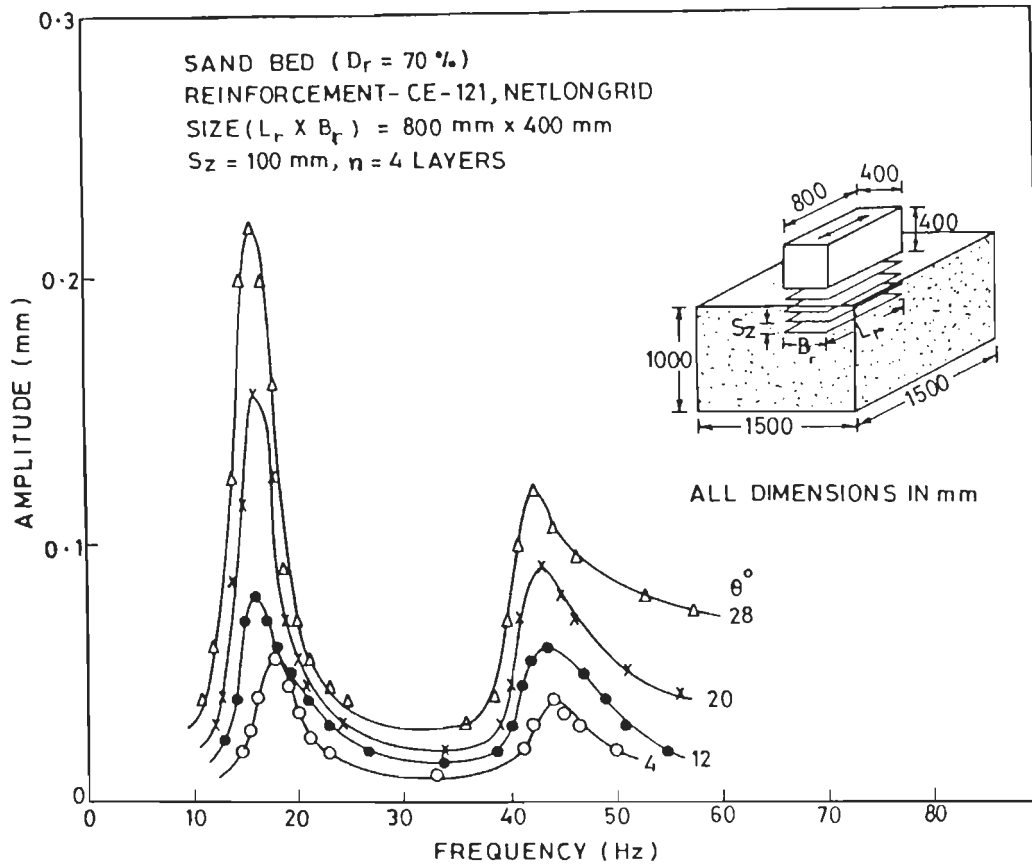


FIG. 3-117 HORIZONTAL VIBRATION TEST ON REINFORCED SAND

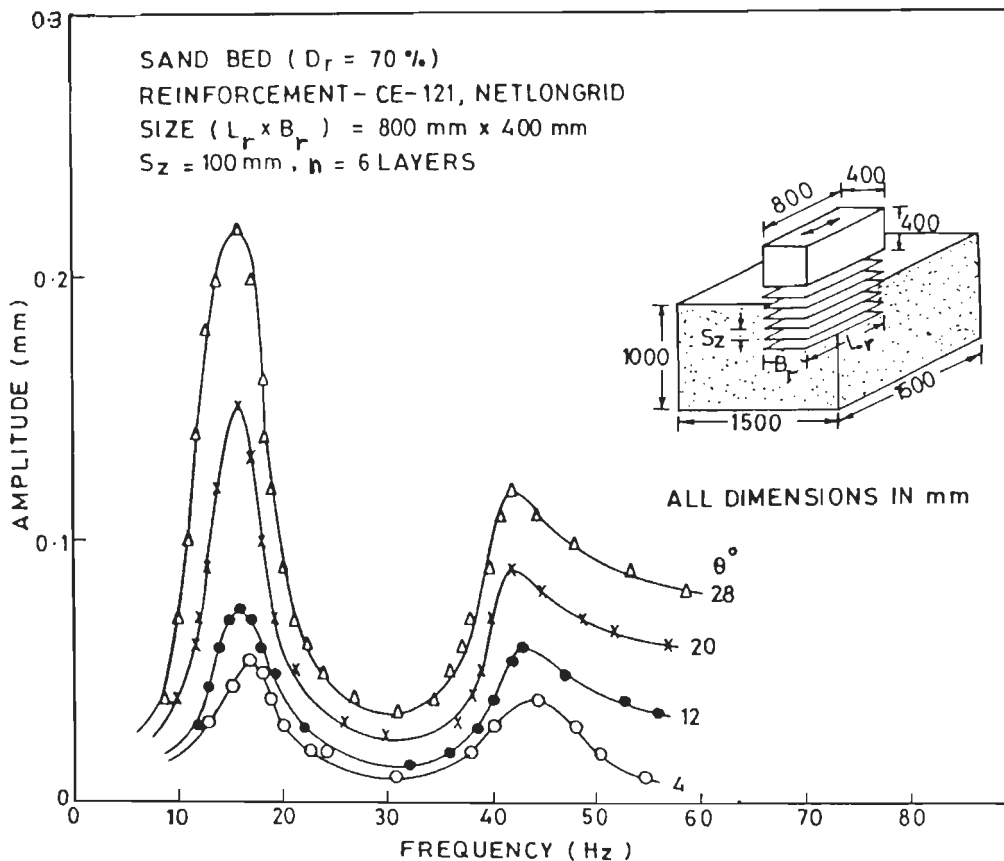


FIG. 3-118 HORIZONTAL VIBRATION TEST ON REINFORCED SAND

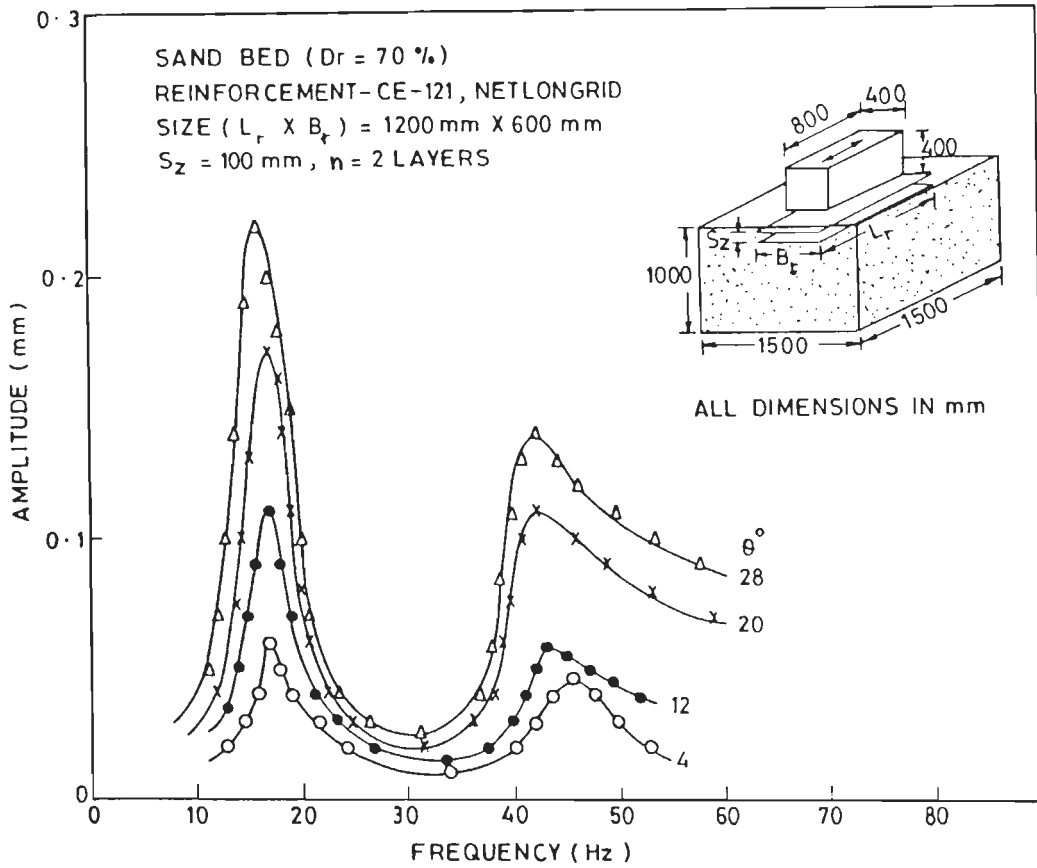


FIG.3-119 HORIZONTAL VIBRATION TEST ON REINFORCED SAND

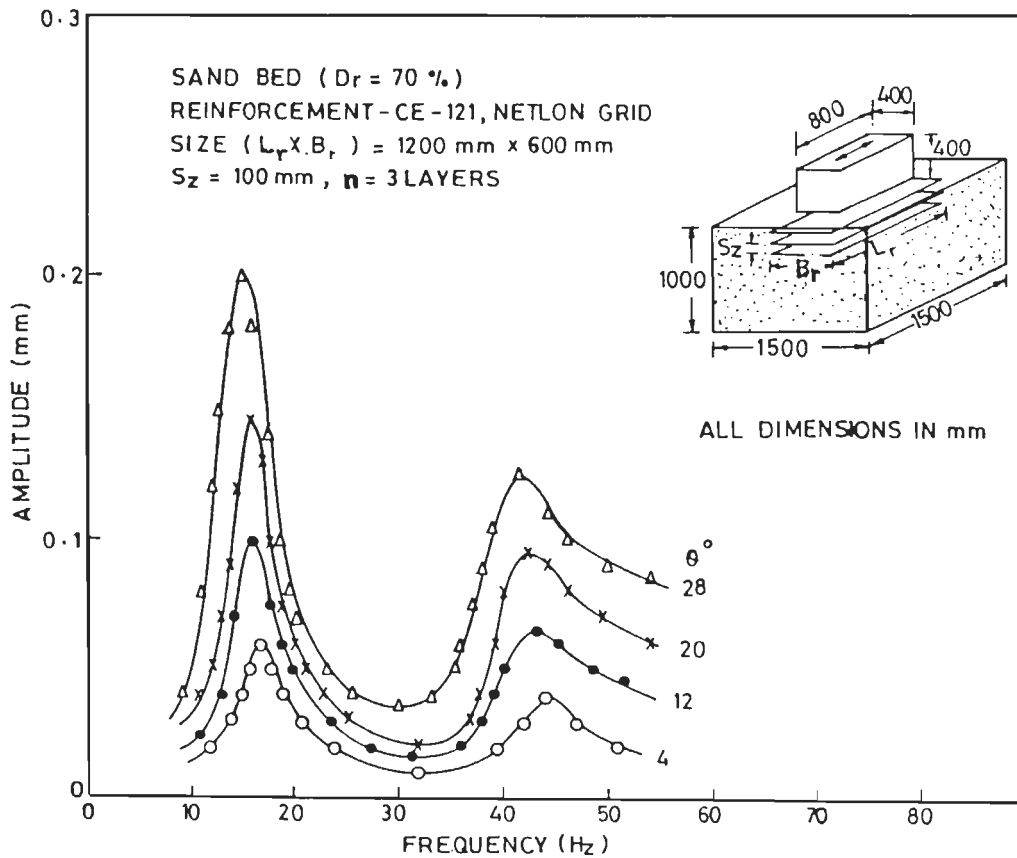


FIG.3-120 HORIZONTAL VIBRATION TEST ON REINFORCED SAND

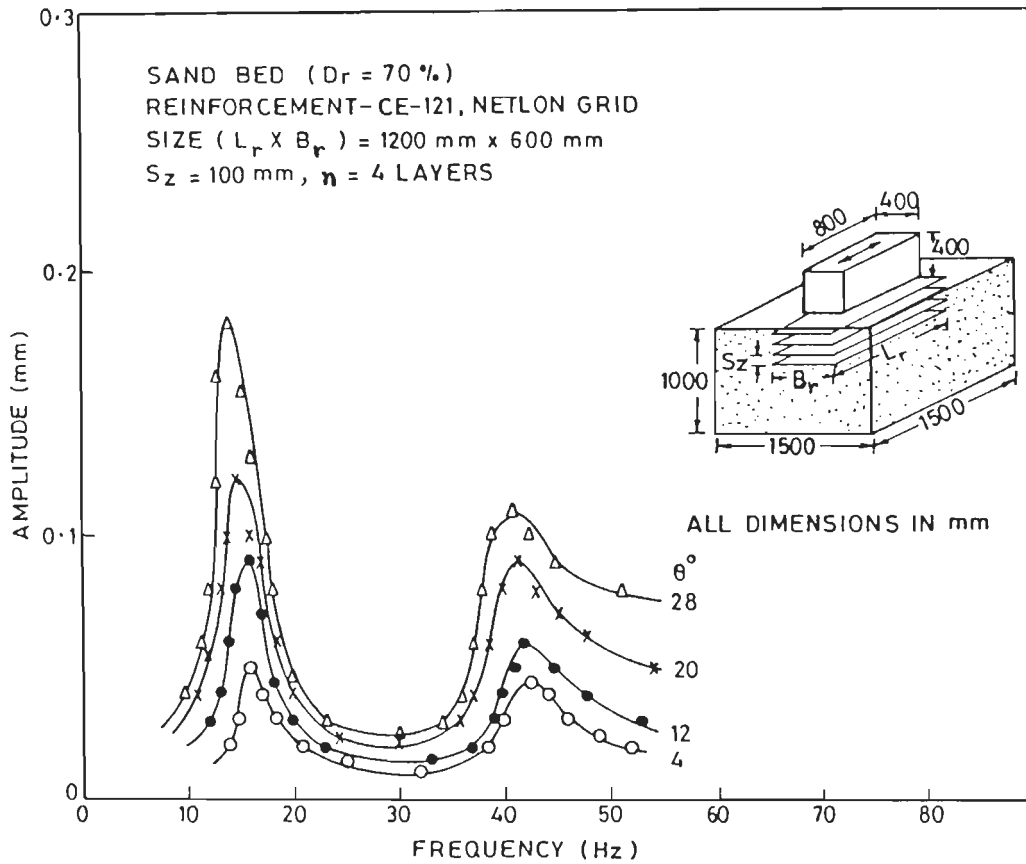


FIG.3-121 HORIZONTAL VIBRATION TEST ON REINFORCED SAND

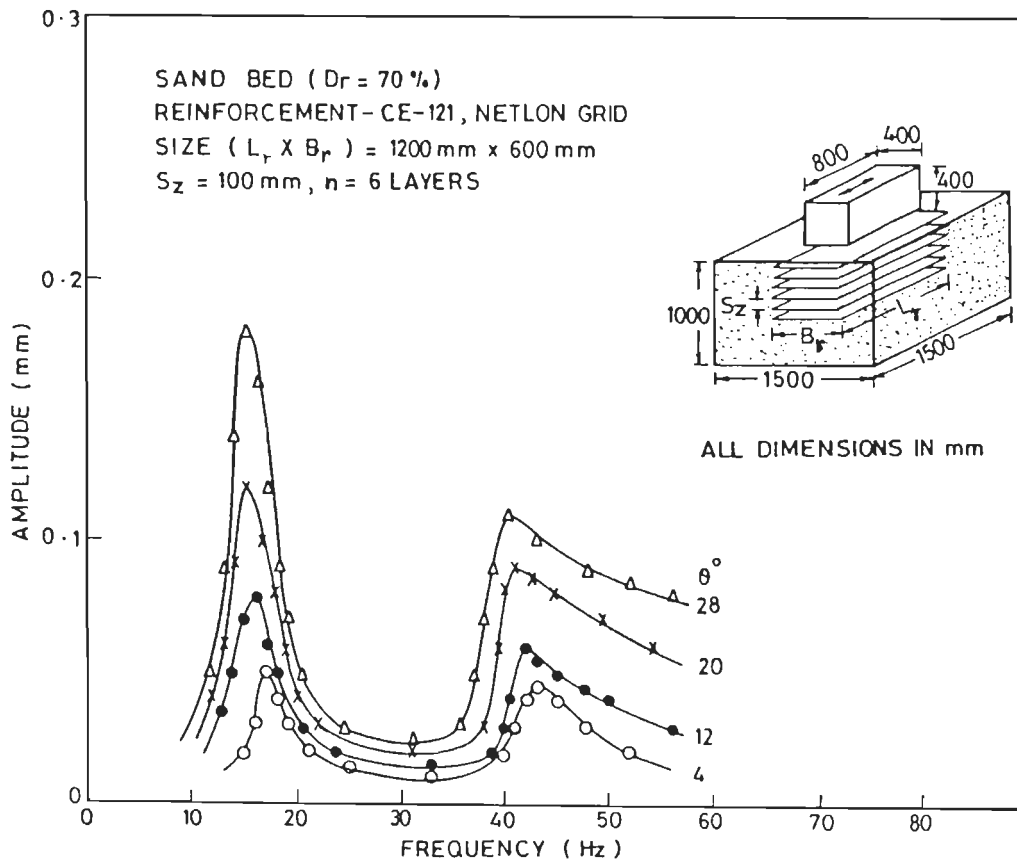


FIG.3-122 HORIZONTAL VIBRATION TEST ON REINFORCED SAND

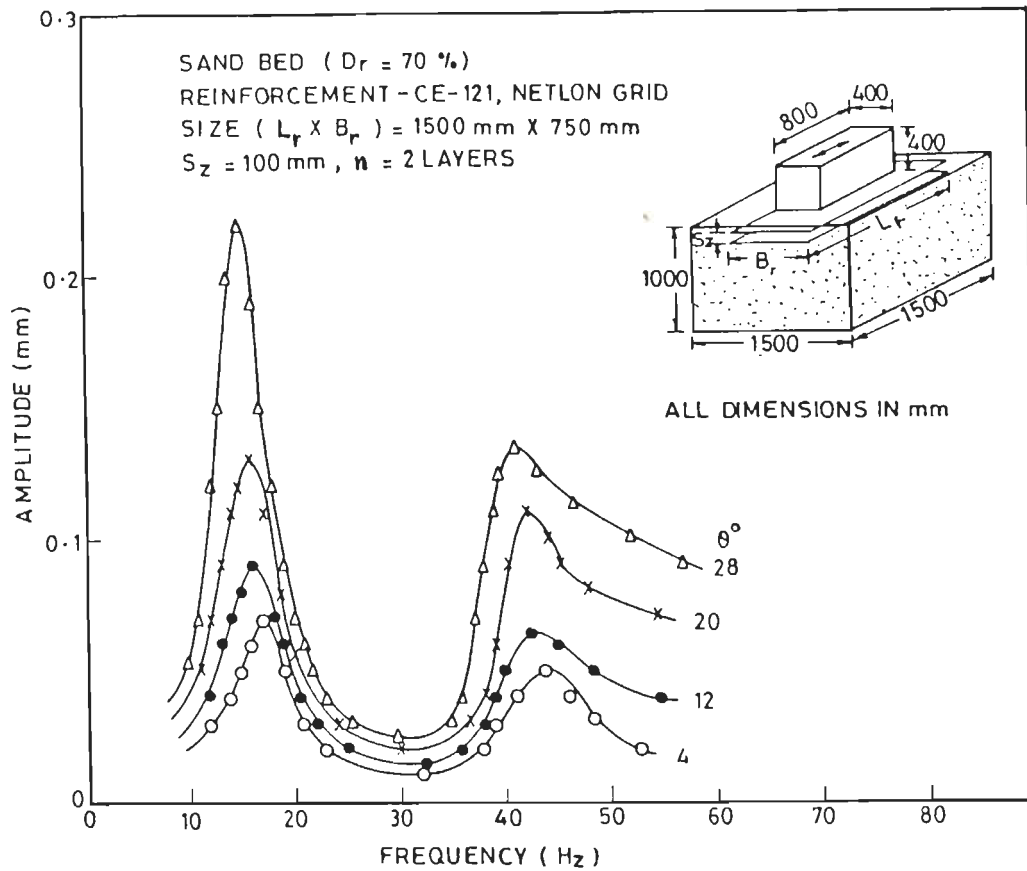


FIG.3:123 HORIZONTAL VIBRATION TEST ON REINFORCED SAND

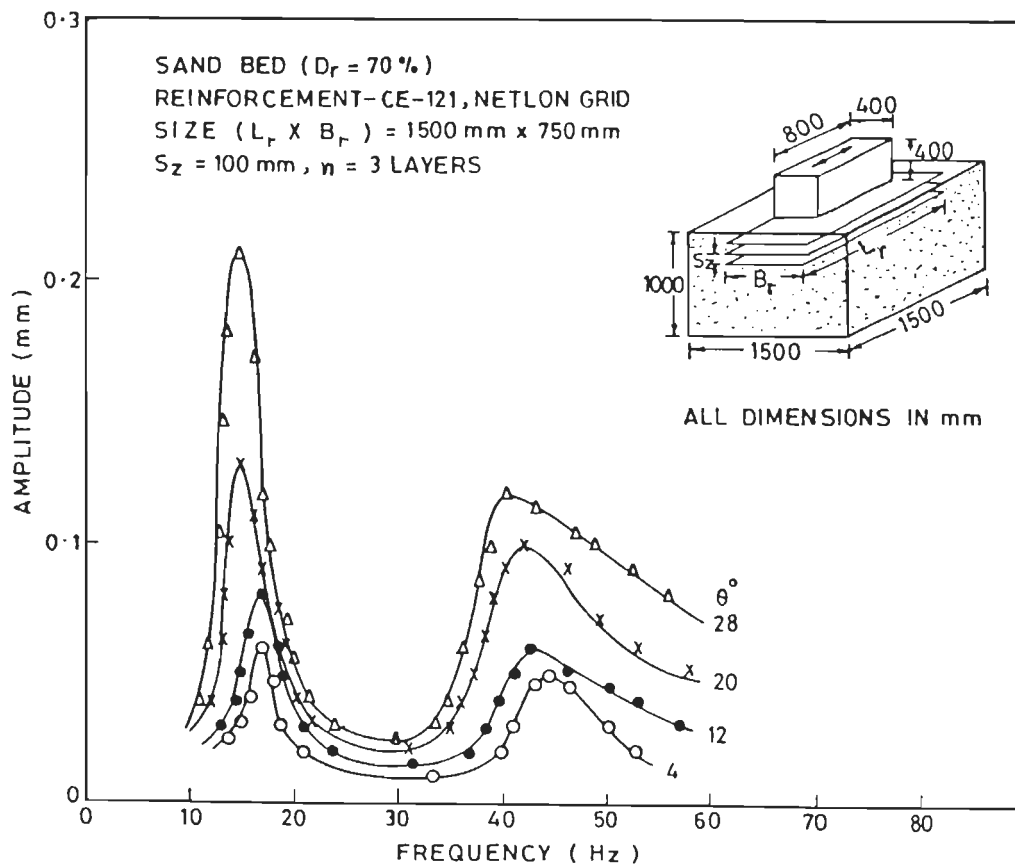


FIG.3:124 HORIZONTAL VIBRATION TEST ON REINFORCED SAND

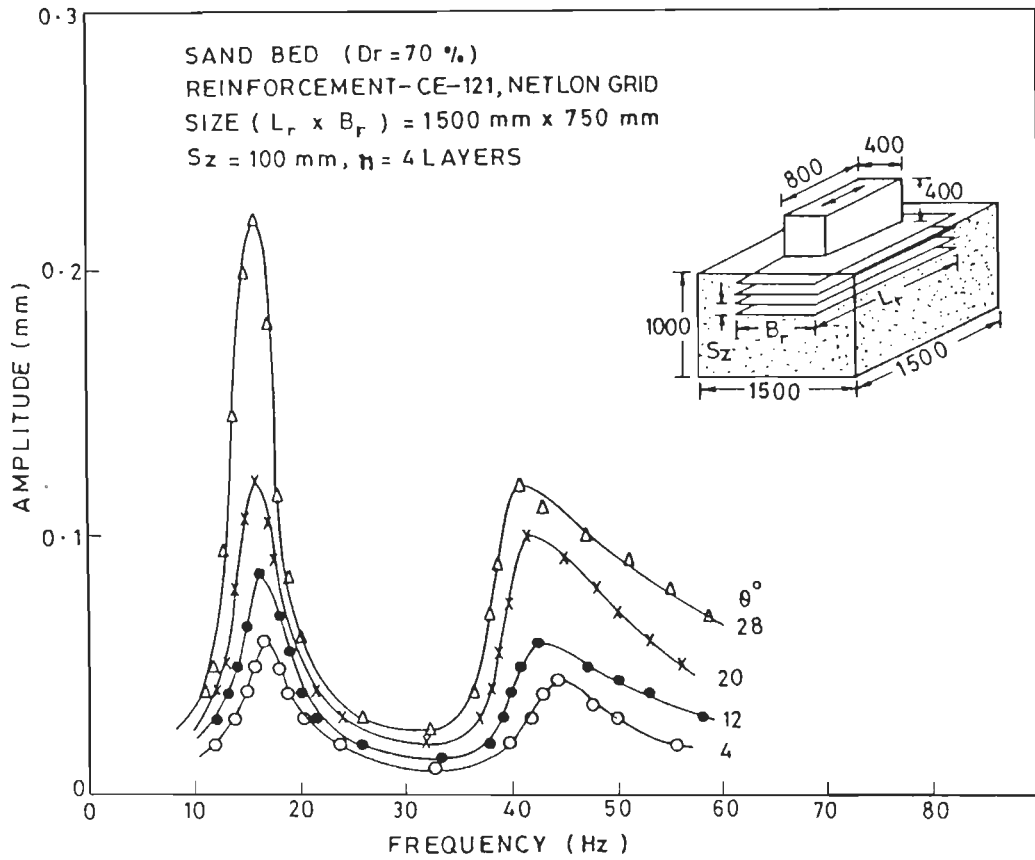


FIG.3:125 HORIZONTAL VIBRATION TEST ON REINFORCED SAND

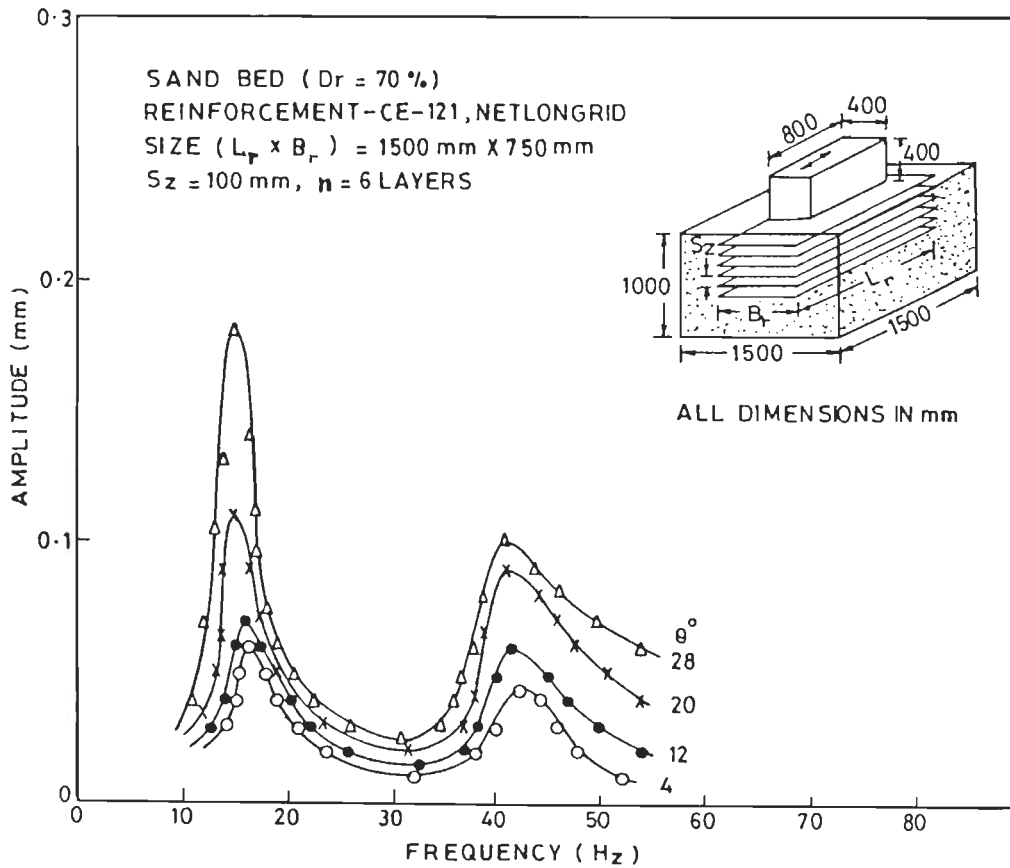


FIG.3:126 HORIZONTAL VIBRATION TEST ON REINFORCED SAND

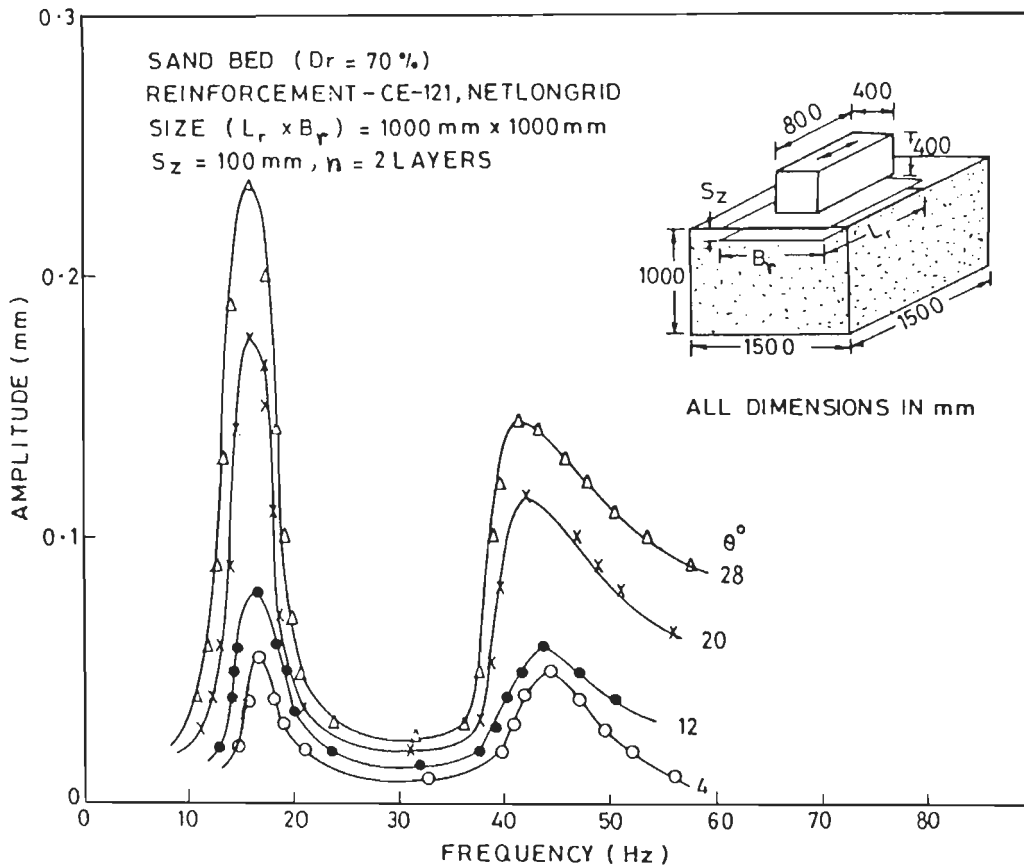


FIG.3.127 HORIZONTAL VIBRATION TEST ON REINFORCED SAND

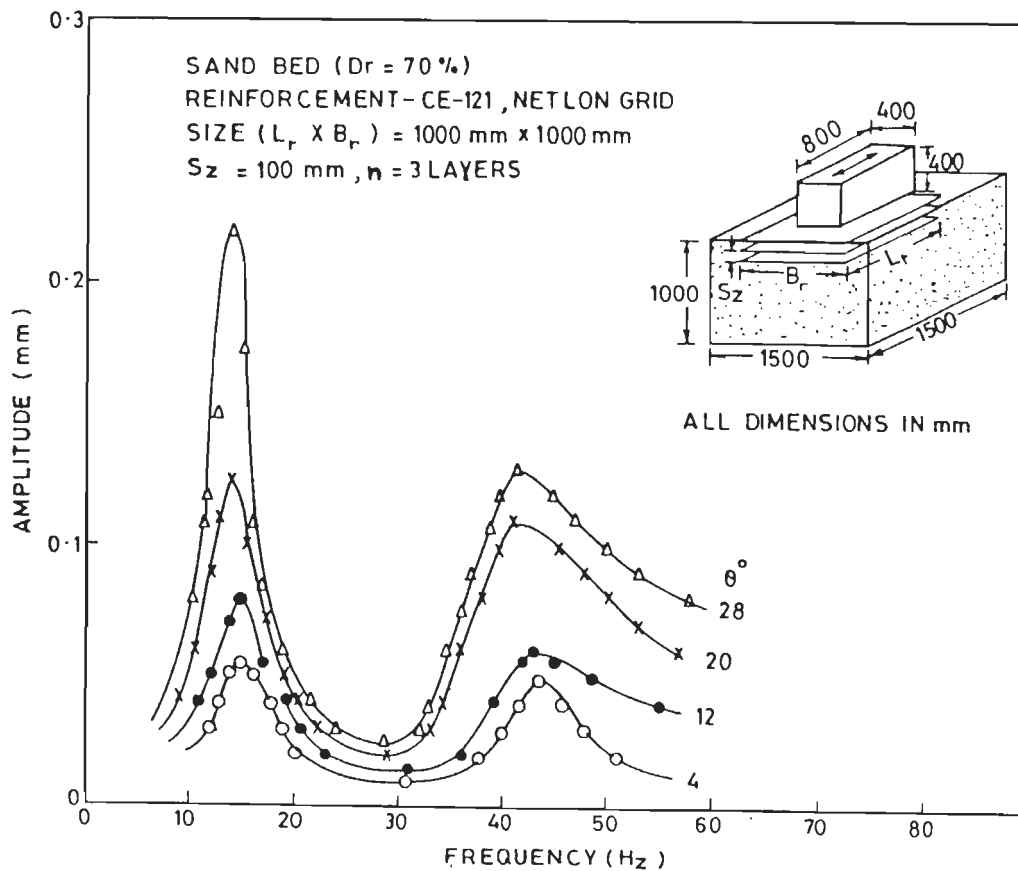


FIG.3.128 HORIZONTAL VIBRATION TEST ON REINFORCED SAND

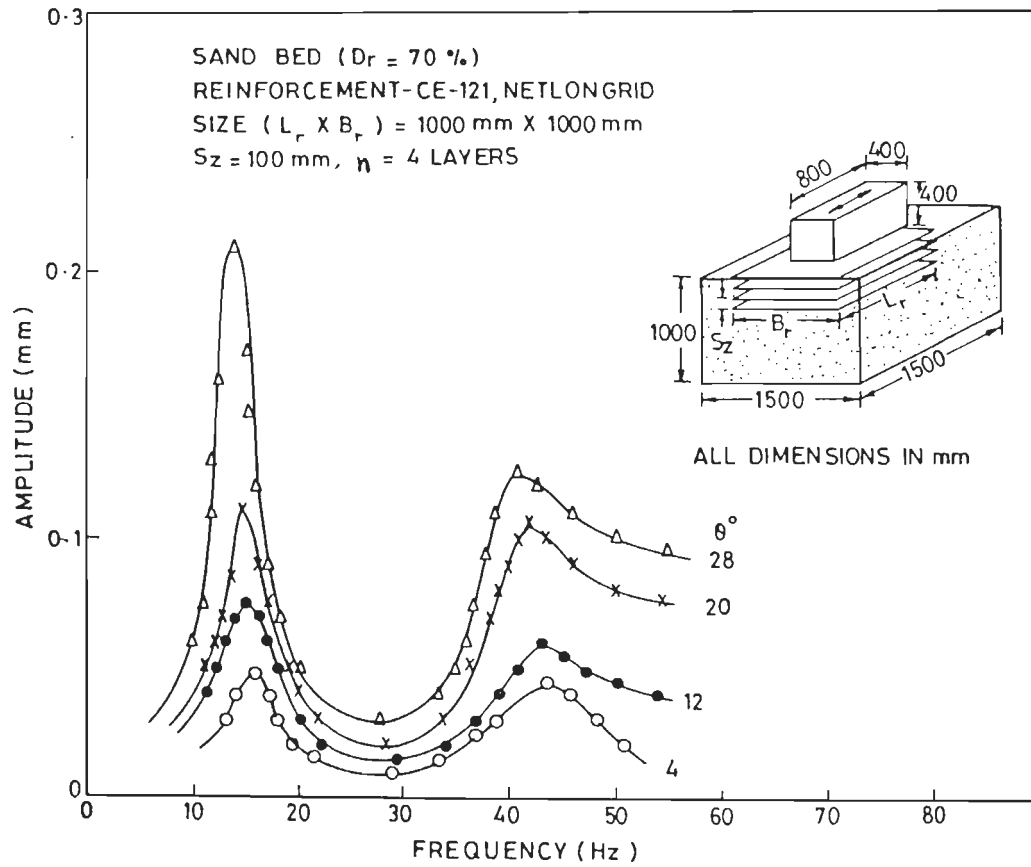


FIG.3.129 HORIZONTAL VIBRATION TEST ON REINFORCED SAND

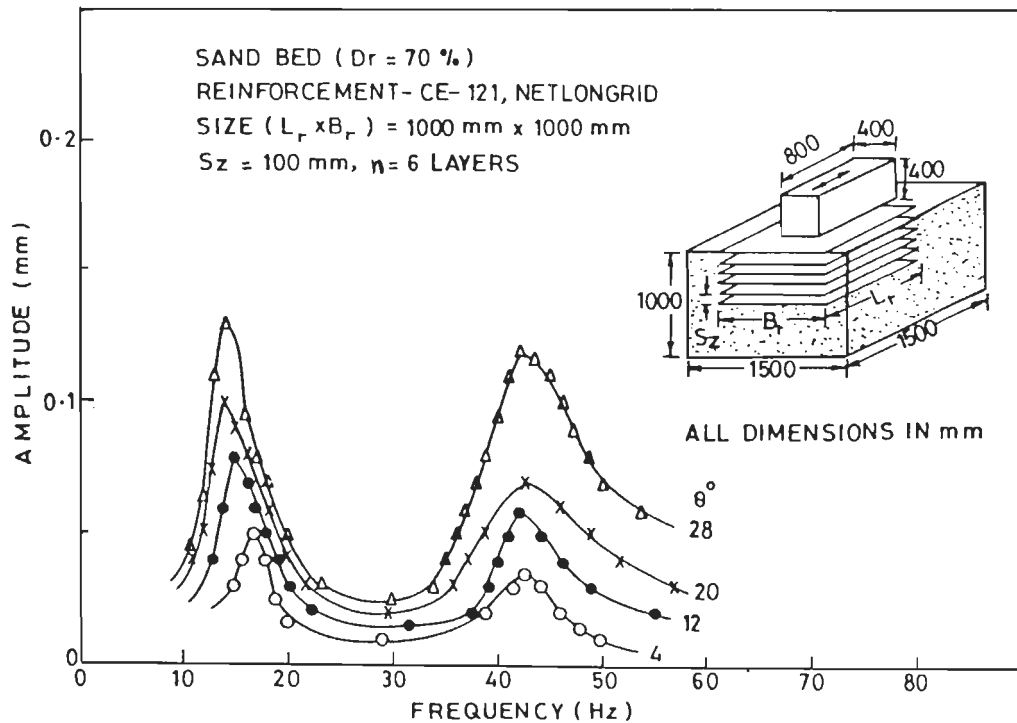


FIG.3.130 HORIZONTAL VIBRATION TEST ON REINFORCED SAND

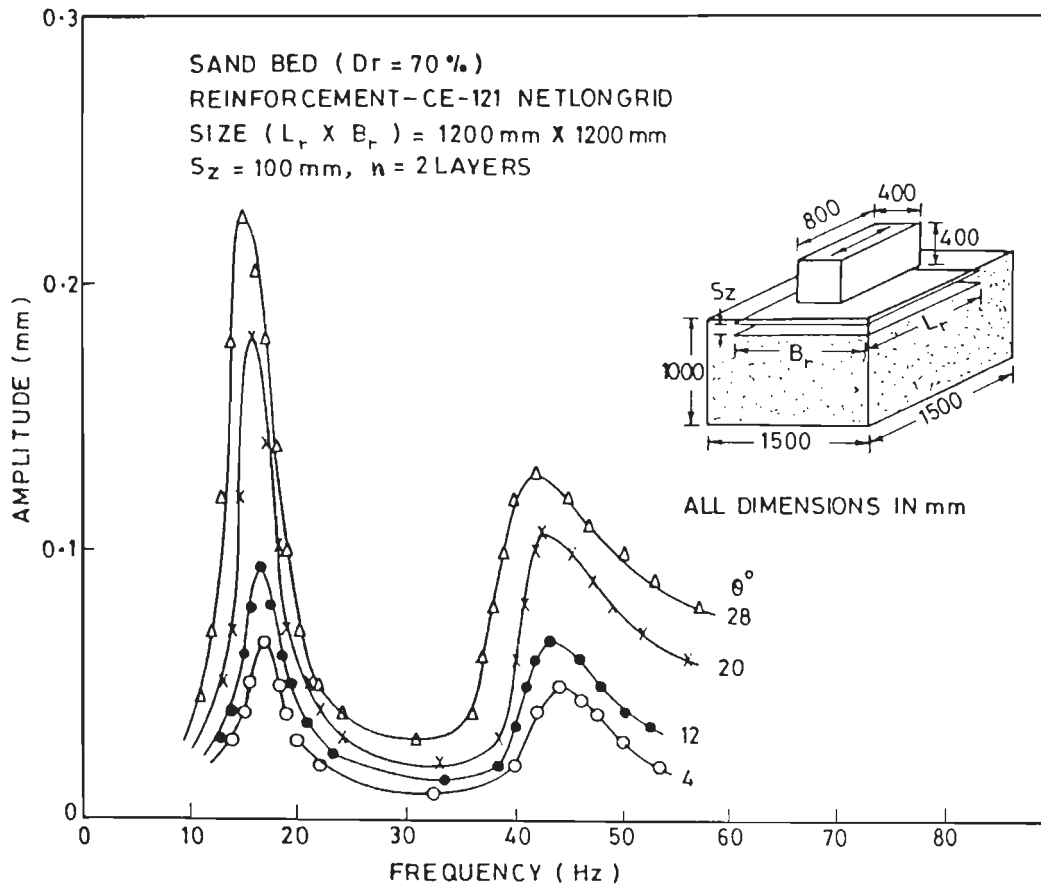


FIG.3-131 HORIZONTAL VIBRATION TEST ON REINFORCED SAND

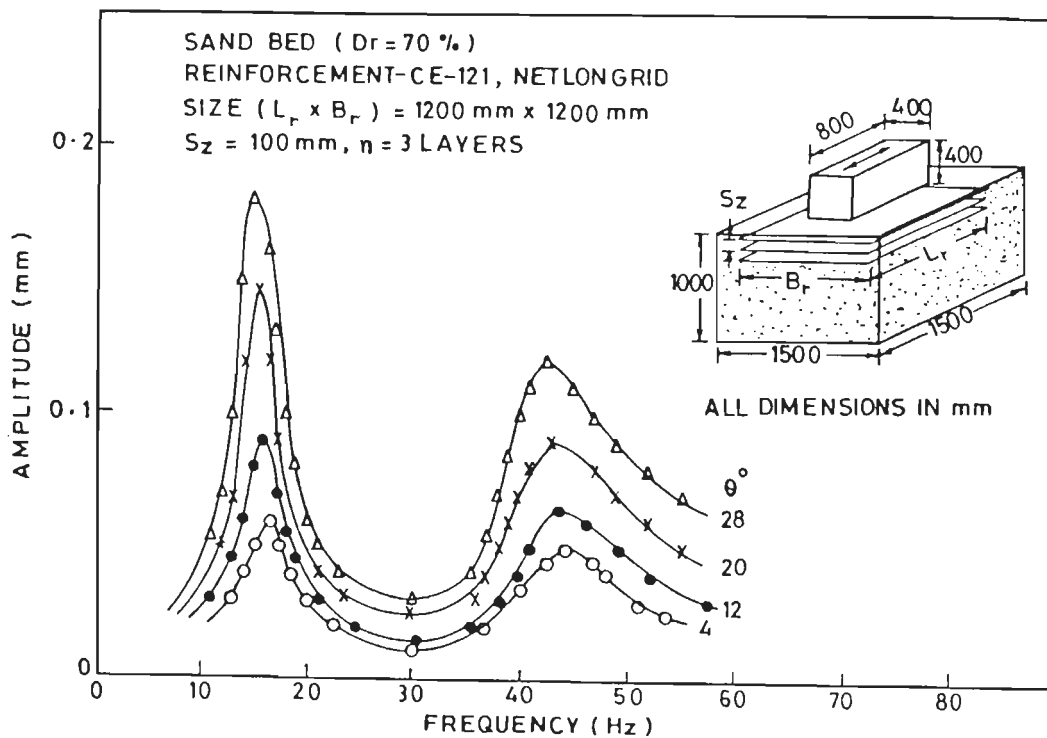


FIG.3-132 HORIZONTAL VIBRATION TEST ON REINFORCED SAND

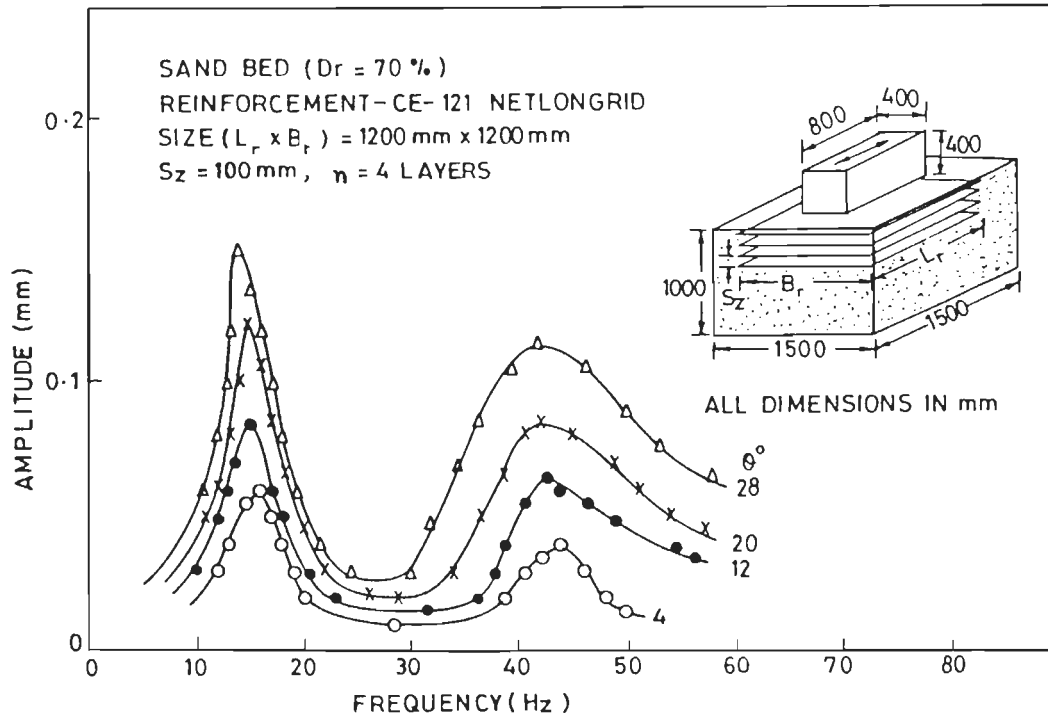


FIG. 3.133 HORIZONTAL VIBRATION TEST ON REINFORCED SAND

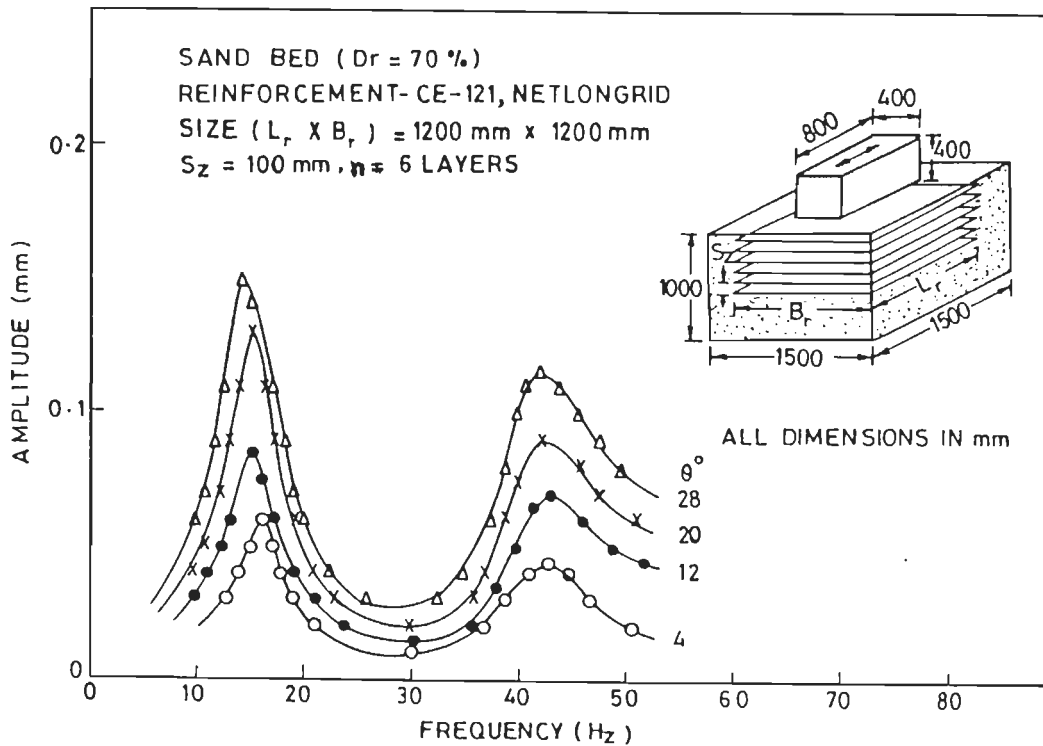


FIG. 3.134 HORIZONTAL VIBRATION TEST ON REINFORCED SAND

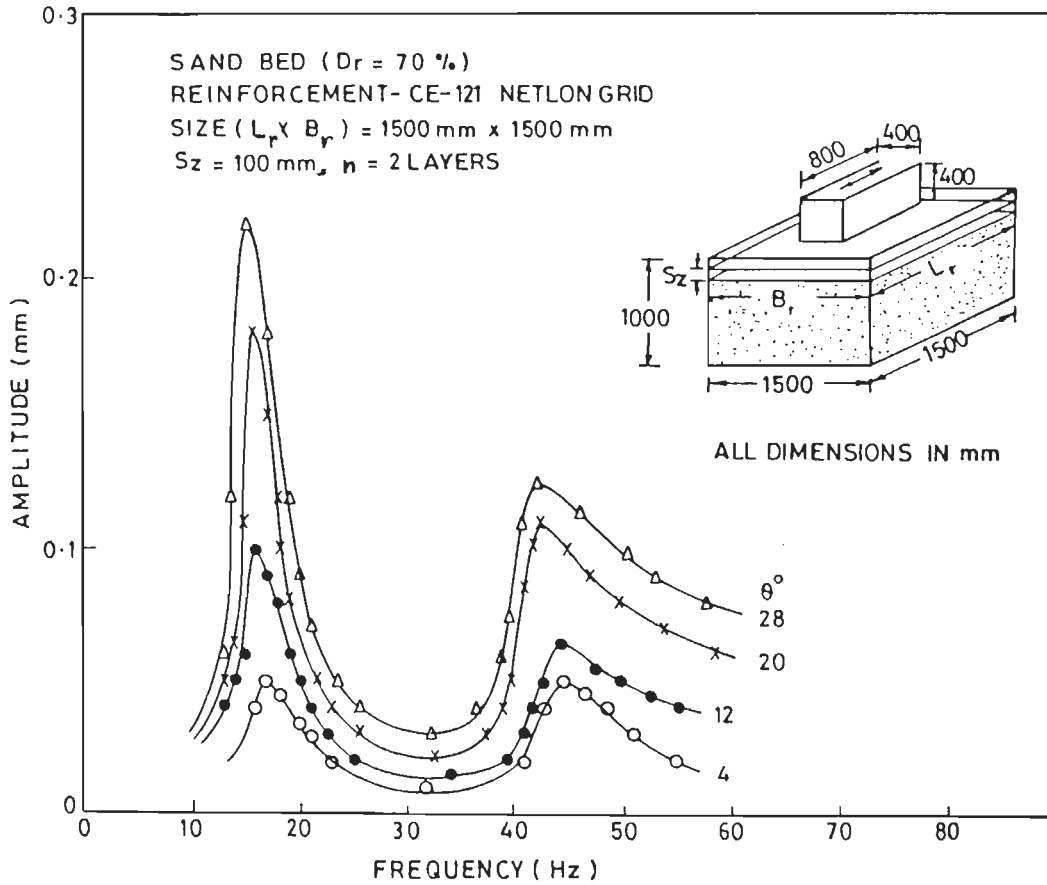


FIG. 3.135 HORIZONTAL VIBRATION TEST ON REINFORCED SAND

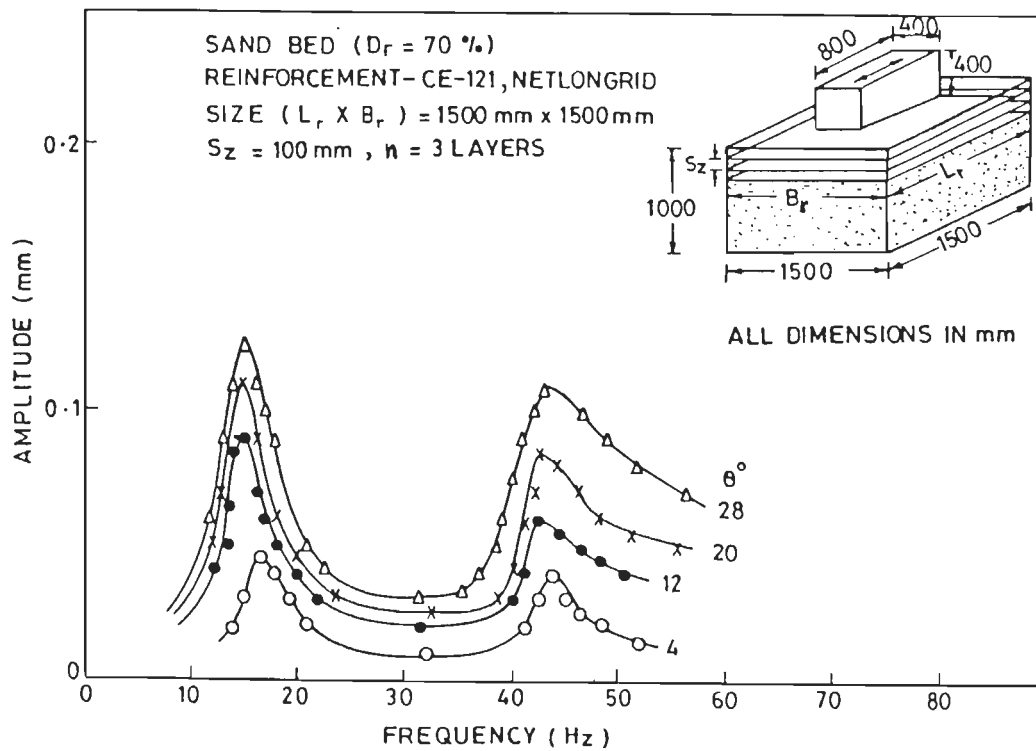


FIG. 3.136 HORIZONTAL VIBRATION TEST ON REINFORCED SAND

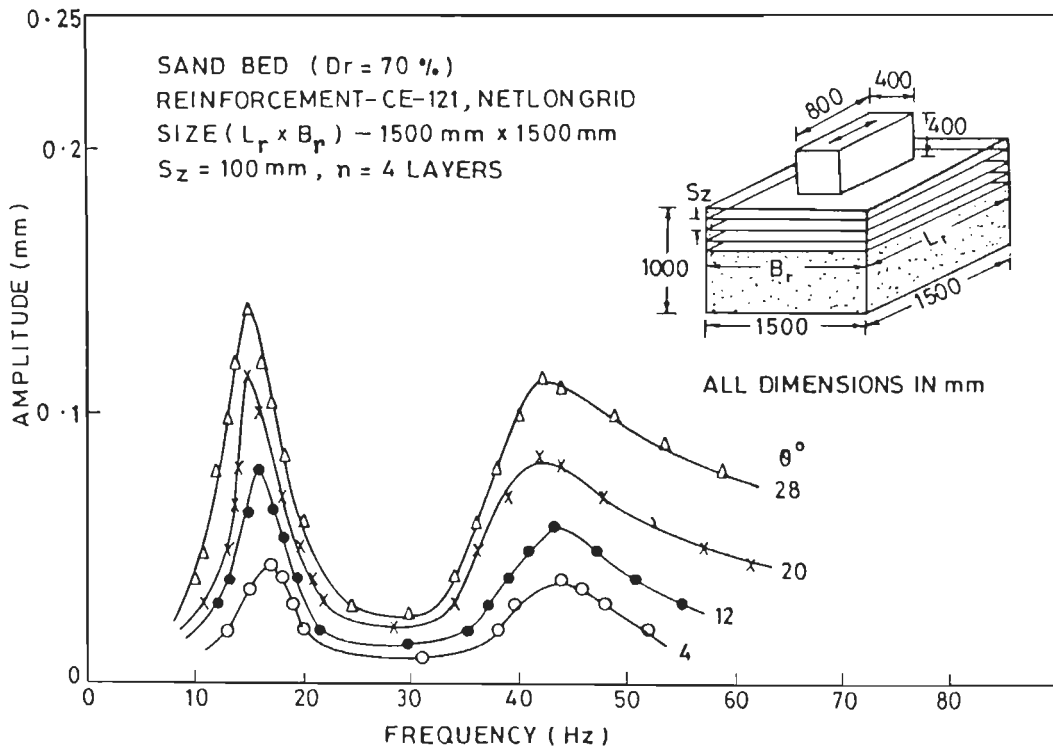


FIG. 3-137 HORIZONTAL VIBRATION TEST ON REINFORCED SAND

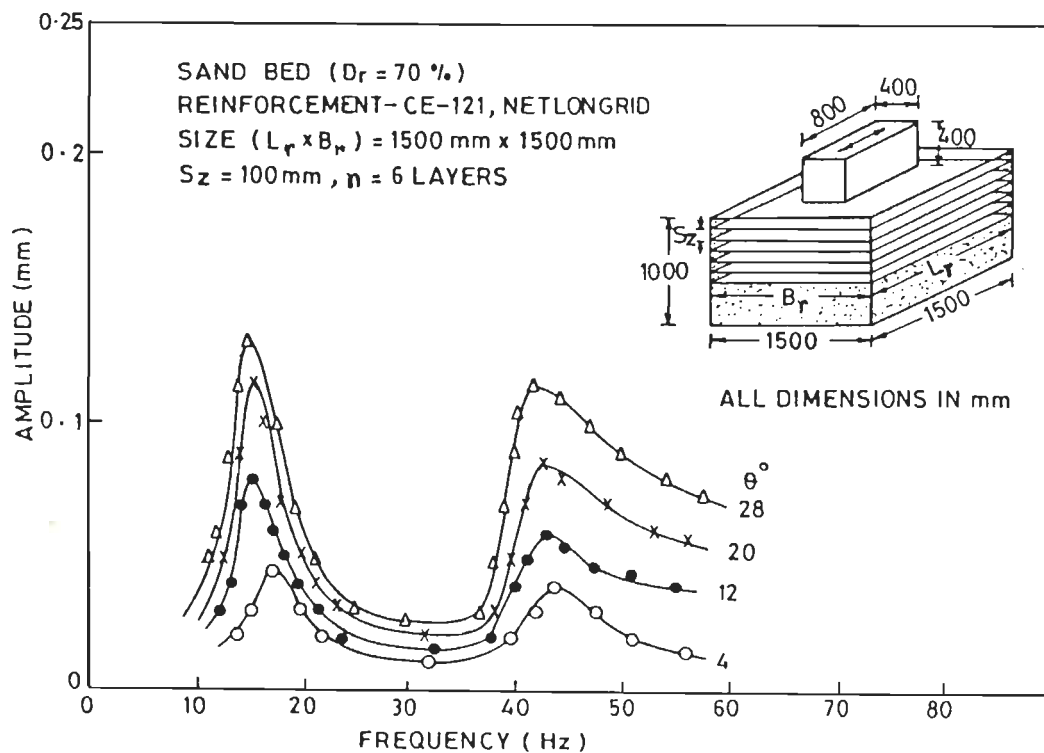


FIG. 3-138 HORIZONTAL VIBRATION TEST ON REINFORCED SAND

INTERPRETATION AND ANALYSIS

4.1 GENERAL

In this chapter, the experimental results data are analysed to identify the factors influencing dynamic properties of reinforced sand. The data obtained from cyclic plate load tests are first analyzed to determine the coefficient of elastic uniform compression and the damping capacity of reinforced sand beds. Then, data obtained from vertical and horizontal vibration tests are analyzed for determining coefficient of elastic uniform compression, coefficient of elastic uniform shear and damping ratio. Procedures for analysing the experimental data obtained from cyclic plate load, vertical and horizontal vibration tests have been described and the results are discussed in detail.

Non-dimensional plots have been prepared for the ratios of the values of (i) coefficient of elastic uniform compression C_u , damping capacity, ultimate bearing capacity and settlements in cyclic plate load tests, (ii) coefficient of elastic uniform compression C_u , damping ratio ξ and amplitude reduction factor in vertical vibration tests, and (iii) coefficient of elastic uniform shear C_τ , damping ratio ξ_1 , and amplitude reduction factor in horizontal vibration tests; for the reinforced and unreinforced sand beds. Non-dimensional correlations have also been developed for the above ratios through regression analysis of experimental data.

An equivalent parameter approach has been presented to determine the coefficient of elastic uniform compression, C_u and coefficient of elastic uniform shear, C_τ of reinforced sand, treating the composite material macro-homogeneous, based upon the coefficient of elastic uniform compression and coefficient of

elastic uniform shear respectively of unreinforced sand and elastic modulus of geogrid reinforcements. The results of this proposed approach have been compared with the experimental data results.

The use of reinforced sand for block foundation of a compressor has been illustrated by presenting and comparing the solution of a design problem for unreinforced and reinforced sand beds.

4.2 CYCLIC PLATE LOAD TESTS

4.2.1 General

A total of 38 cyclic plate load tests were performed on unreinforced and reinforced sand beds as mentioned earlier. The pressure versus total settlement plots, as shown in Figures 3.20 to 3.57, have been obtained from cyclic plate load tests. The pressure versus elastic settlement plots are shown in Figure 3.58 to 3.88. From pressure versus total settlement plots, ultimate bearing capacity and the corresponding settlements are noted. The damping capacity ratios are interpreted from the pressure versus settlement plots (Figures 3.20 to 3.57). It is observed that pressure versus elastic settlement plots are bilinear, the two lines meeting at a pressure value close to ultimate bearing capacity of the sand bed. The slope of initial line gives the coefficient of elastic uniform compression C_u . The slope of the other line, showing the post-failure behaviour, has been represented by a symbol C'_u .

The ratios with regard to (i) ultimate bearing capacity (ii) settlement and (iii) damping capacity, of reinforced and unreinforced sand beds are obtained (Table 4.2). These ratios are plotted with respect to the number of geogrid layers of different sizes to bring out the influence of reinforcement (Figures 4.1 to 4.3).

The values of C_u and C'_u have been corrected for confining pressure and base area of footing and are interpreted over a range of factors of safety (Tables 4.3 and 4.4). The associated strain levels have been calculated and the values of C_u

and C'_u are interpreted at the corresponding strain levels (Table 4.5). Thereafter, the values of C_u and C'_u have been plotted with respect to normal strain, the number of reinforcement layers and size of reinforcement (Figures 4.4 to 4.10). The influence of reinforcement size, size of footing and density of sand on coefficient of elastic uniform compression C_u has also been studied (Figure 4.11).

4.2.2 Pressure-Settlement Characteristics

Pressure-settlement characteristics obtained from various cyclic plate load tests listed in Table 3.3 are shown in Figures 3.20 to 3.57. The ultimate bearing capacity values determined from pressure versus total settlement plots by joining the boundary points and using double tangent method as per IS:1888-1982 are listed in Table 4.1. A typical pressure-settlement plot on log-log scale is shown in Figure 3.20(b) for the footing over unreinforced sand bed which gives the same value of ultimate bearing capacity as obtained from double tangent method. It can be seen from Table 4.1 that the value of ultimate bearing capacity increases with the increase in amount of reinforcement i.e. number of reinforcement layers (n) and size of reinforcement ($L_r \times B_r$). For more clear understanding non-dimensional plots have been prepared between bearing capacity ratio (BCR) and number of layers for different reinforcement sizes. The BCR is defined as

$$\text{BCR} = \frac{\text{ultimate bearing capacity of footing on reinforced sand bed}}{\text{ultimate bearing capacity of footing on unreinforced sand bed}}$$

The pressure values at the point of contraflexure of slopes C_u and C'_u on pressure versus elastic rebound plots (Figures 3.58 to 3.88) are also listed alongwith in Table 4.1. The settlement values at a pressure equal to the ultimate bearing pressure of unreinforced sand bed have been used to calculate settlement ratio. The settlement ratio is the ratio of the total settlements of the footing on reinforced and unreinforced sand beds; observed at a pressure equal to the ultimate bearing capacity of the latter. The settlement ratios are listed in Table 4.2. The ratio of ultimate bearing capacities and settlements listed in Table 4.2

are plotted in Figures 4.1 and 4.2 respectively, for different configurations of reinforced sand beds. Figure 4.1 indicates that BCR increases with the increase in n and B_r/B ratio. However, the increase in BCR is more significant upto $n=6$ and $B_r/B=4$. Beyond these values of n and B_r/B ratio, the increase in BCR is marginal.

The pressure versus total settlement plot for a footing of size $150\text{mm}\times 150\text{mm}$ placed over unreinforced sand bed at 70% relative density is shown in Figure 3.20. The ultimate bearing pressure of unreinforced sand bed is 160 kN/m^2 and the corresponding settlement is 12.5 mm. When the sand bed is reinforced with 2 layers of $150\text{mm}\times 150\text{mm}$ geogrid, the ultimate bearing capacity increases by 25% and the settlement reduces by 26% as seen in Figure 3.21. For the sand bed reinforced with 3 layers having same size, the ultimate bearing capacity increases by 53% and the settlement decreases by 34% as observed from Figure 3.22.

Upon increasing the number of reinforcement layers to 4, the ultimate bearing capacity increases by 88% and total settlement reduces by 34% as illustrated in Figure 3.23. For 6 and 8 reinforcement layers, the ultimate bearing capacity and settlement values are 194% & 203% and 65% (for both) of the corresponding values for unreinforced sand bed (Figures 3.24 and 3.25). It is observed that increasing the number of reinforcement layers from 6 to 8, does not result in an appreciable increase in ultimate bearing capacity or decrease in settlement.

When the sand bed is reinforced with two layers of size $300\text{mm}\times 300\text{mm}$, the ultimate bearing capacity is increased to 172% and the settlement is reduced to 70% (Figure 3.26). Increasing the geogrid layers to three, increases ultimate bearing capacity to 203% and decreases the settlement to 52% as seen in Figure 3.27. Four reinforcement layers of size $300\text{mm}\times 300\text{mm}$, increase the ultimate bearing capacity to 2.44 times and decreases the settlement to 46% as shown in Figure 3.28. Similarly, the ultimate bearing capacity values increase by 166% and 181% and total settlements decrease by 56% and 58% for the sand bed reinforced with 6 and 8 geogrid layers of the same size over the corresponding values for the unreinforced sand bed.

Figures 3.31 to 3.35 show the pressure versus total settlement plots for sand beds reinforced with 2,3,4,6 and 8 geogrid layers of size 450mm×450mm. The ultimate bearing capacity values are increased from 1.9 to 3.3 times and the settlement is reduced upto 0.38 times the corresponding values for the unreinforced sand bed. There is increase in bearing capacity and decrease in settlement as reinforcement size increases from 300mm square to 450mm square.

The pressure versus settlement plots for the footing over sand beds reinforced with 2,3,4,6 and 8 geogrid layers of size 4B; (B being the width of footing), are shown in Figures 3.36 to 3.40. The ultimate bearing capacity increases from 2.0 to 3.6 times and settlements reduce upto 0.38 times the corresponding values of unreinforced sand bed. It is observed that increase in bearing capacity and decrease in settlements is not much higher as compared to that for reinforcements of size 3B.

For the footing over sand beds reinforced with 2,3,4,6 and 8 reinforcement layers of size 5B; the pressure-settlement plots are shown in Figures 3.41 to 3.45. The ultimate bearing capacity increases from 2 to 3.9 times and settlement reduces upto 0.38 times the corresponding values for the unreinforced sand bed. The increase in ultimate bearing capacity and the decrease in settlement are not substantial in this case as compared to the corresponding values for sand beds reinforced with geogrid layers of size 4B.

It is clearly observed that for optimal increase in bearing capacity and decrease in total settlement; the sand bed may be reinforced with 6 reinforcement layers of size 4B. Further, increase in number and size of reinforcement layers, does not result in significant improvement in bearing capacity or reduction in total settlement.

The effect of density of sand on pressure-settlement characteristics of footing over reinforced sand beds subjected to cyclic loading can be observed by comparing the pressure-settlement plots shown in Figures 3.46 to 3.51 at 50% relative density to the corresponding plots at $D_r=70\%$, shown in Figures 3.23,

3.28, 3.33, 3.38 and 3.43 for 4 layers of reinforcement of size varying from B to 5B.

The increase in bearing capacity and decrease in total settlement at 50% relative density are not as much as for corresponding reinforced sand beds at 70% relative density. For 4 geogrid layers of size 150mm×150mm provided in the sand beds at 70% and 50% relative densities, the bearing capacities increase by 88% and 25% and total settlements decrease by 35% and 27% over the corresponding values for unreinforced sand beds as can be seen from Figures 3.20 and 3.23 & 3.45 and 3.47, and Table 4.2.

The density of sand has, therefore, significant effect on pressure settlement characteristics of footing on reinforced sand beds. This may be attributed to the greater mobilization of interface friction between the soil and reinforcement at high density.

The effect of size of footing on ultimate bearing capacity and total settlement has been studied by performing cyclic plate load tests on 150mm square and 300mm square footings over unreinforced and reinforced sand beds, at 70% relative density. From the pressure-settlement plots shown in Figures 3.23, 3.28, 3.33, 3.38 and 3.43 for 150mm square footing and Figures 3.52 to 3.57 for 300mm square footing, it is observed that for larger footing the improvement in ultimate bearing capacity and reduction in total settlement over the corresponding values for unreinforced sand beds is less than that for smaller footing placed over a similar reinforced sand bed. For footings of sizes 150mm square and 300mm square over sand beds reinforced with 4 geogrid layers of size equal to size of footing, the ultimate bearing capacities increase by 88% and 43% and the total settlements decrease by 35% and 29% respectively over the corresponding values for unreinforced sand beds as is observed from Figures 3.23 and 3.53 and Table 4.2. A similar trend is observed for the sand beds reinforced with geogrid layers of larger sizes. This may be due to lesser mobilization of reinforcing effect with increase in size of footing.

The above mentioned results are similar to those obtained by earlier investigators for the footings on reinforced sand beds subjected to static loads (Binquet and Lee, 1975a).

4.2.3 Bearing Capacity Ratio

The bearing capacity ratio (BCR) for a given reinforced sand bed is the ratio of the ultimate bearing pressures of footings on reinforced (q_{uR}) to unreinforced (q_{uU}) sand beds, as defined earlier.

As an illustration, for 150mm square footing over sand bed reinforced with two layers of 150mm×150mm geogrid, from Table 4.1

$$\text{BCR} = q_{uR}/q_{uU} = 1.25$$

The bearing capacity ratios have been calculated for other reinforced sand beds and are listed in Table 4.2. Figure 4.1 shows a plot of bearing capacity ratio with respect to number of reinforcement layers of sizes varying from B to 5B for 150mm square footing over reinforced sand bed at 70% relative density. This plot shows that the bearing capacity increases with increase in number of geogrid layers for all reinforcement sizes. For example, BCR increases from 1.25 to 2.06, for 150mm square reinforcement size, when the number of reinforcement layers increases from 2 to 8. Similar trend is observed for other reinforcement sizes at 70% relative density, at 50% relative density and for the footing of size 300mm square as seen from the values listed in Table 4.2. However, increase in BCR is not significant when the number of reinforcement layers increases beyond 6 as observed from Figure 4.1 and Table 4.2. Thus, for any reinforcement size, six geogrid layers give significant increase in bearing capacity, beyond which the increase in BCR is not appreciable.

The bearing capacity ratio increases with increase in size of reinforcement as shown in Figure 4.1 and Table 4.2. For example, for 150mm square footing placed over sand bed (70% relative density) reinforced with 4 reinforcement layers of size varying from B to 5B, the BCR values vary from 1.88 to 3.16. The increase in

BCR is not significant when the reinforcement size increases beyond 4B. Thus, it can be concluded that increase in BCR is not significant when the number of reinforcement layers increases beyond six and the size of reinforcement increases beyond 4B.

Binquet and Lee (1975, a & b), Temel Yetimoglu et al. (1994) have reported a similar trend of increase in BCR with respect to the number of reinforcement layers for static plate load tests on reinforced sand beds.

4.2.4 Settlement Ratio

As explained earlier, the settlement ratio (SR) for a reinforced sand bed is the ratio of settlements of footing on reinforced and unreinforced sand beds; observed at a pressure equal to ultimate bearing capacity of the latter.

For 150mm square footing placed over unreinforced sand bed, and on the sand bed reinforced with two geogrid layers of size 150mm×150mm (Figures 3.20 and 3.21).

$$SR = S_{RU}/S_{OU} = 0.736$$

The settlement ratios have been calculated for different reinforced sand beds and are listed in Table 4.2. Figure 4.2 shows a plot of settlement ratio with respect to number of reinforcement layers of size varying from B to 5B for 150mm square footing over reinforced sand beds at 70% relative density.

This plot shows that settlement ratio decreases with an increase in the number of reinforcement layers for all sizes of reinforcement which seems to be due to greater mobilisation of interface friction between the soil and reinforcements. Thus, SR decreases from 0.74 to 0.64 for 150mm square reinforcement size, when the number of reinforcement layers increases from 2 to 8. Similar trend is observed for other reinforcement sizes at 70% relative density, at 50% relative density and for the footing of size 300mm square as seen from the values listed in Table 4.2. But the rate of decrease in SR is not significant when the number of reinforcement layers increases beyond 6. Thus, for any reinforcement

size, six reinforcement layers provide optimum decrease in settlement after which the rate of decrease in SR is not significant.

The settlement ratio decreases with increase in size of reinforcement as shown in Figure 4.2 and Table 4.2. For 150mm square footing placed over sand bed (70% relative density) reinforced with 6 reinforcement layers of size B to 5B, SR values decrease from 0.64 to 0.40. The decrease in SR is not significant when reinforcement size increases beyond 4B. Thus, it can be concluded that the rate of decrease in SR is not significant when the number of reinforcement layers increases beyond six and reinforcement size increases beyond 4B.

Similar behaviour of geogrid reinforced sand beds under static loads has been reported by Youssef (1995).

4.2.5 Damping Capacity

The damping capacity of sand bed is the ratio of the area of first ten hysteresis loops (upto the pressure at failure of unreinforced sand bed) to the total area under the pressure-settlement curve upto the same pressure. The areas, in this study, were measured by an electronic digital planimeter. The damping capacity ratio is the ratio of the damping capacities of the reinforced and unreinforced sand beds. For example, the damping capacity ratio of sand bed reinforced with two layers of size 150mm square at 70% relative density is 1.17 (Table 4.2).

The damping capacity ratios have been calculated for other reinforced sand beds and are listed in Table 4.2. Figure 4.3 shows a plot of damping capacity ratio with respect to the number of reinforcement layers of sizes varying from B to 5B for 150mm square footing over reinforced sand bed at 70% relative density.

It is observed from this plot that damping capacity ratio increases with an increase in number of reinforcement layers for all sizes of reinforcement. For example, damping capacity ratio increases from 1.17 to 1.28 for 150mm square reinforcement, when the number of reinforcement layers increases from 2 to 8.

Similar behaviour is observed for other reinforcement sizes at 70% relative density, at 50% relative density and for 300mm square footing as seen from the values listed in Table 4.2. However, the rate of increase in damping capacity ratio is not significant when number of reinforcement layers increases beyond 6.

With the increase in size of reinforcement, damping capacity ratio generally increases as shown in Figure 4.3 and Table 4.2. For 150mm square footing placed over sand bed at 70% relative density reinforced with 6 reinforcement layers of sizes varying from B to 5B, the damping capacity ratio varies from 1.27 to 2.06. The increase in damping capacity ratio is not appreciable when size of reinforcement increases beyond 4B. It can be concluded that the rate of improvement in damping capacity is not significant when the number of reinforcement layers increases beyond six and size of reinforcement increases beyond 4B.

Patel and Paldas (1983) have reported improvement in damping capacity of sand bed reinforced with fibre-glass woven rovings under cyclic loading conditions.

4.2.6 Coefficient of Elastic Uniform Compression

From Figures 3.58 to 3.88, it is observed that pressure versus elastic settlement plots are bilinear, the two lines meeting at a pressure values close to the ultimate bearing capacity of the sand bed. The slope of the initial line gives the coefficient of elastic uniform compression C_u . The slope of the other line has been represented by a symbol C'_u . The coefficient C'_u has been introduced to study the variation of coefficient of elastic uniform compression beyond the ultimate bearing capacity of unreinforced and reinforced sand beds. The values of C_u and C'_u determined from Figures 3.58 to 3.88, for various configurations of sand bed are given in Table 4.2.

The pressure versus elastic settlement plot for 150mm square footing placed over unreinforced sand bed at 70% relative density is shown in Figure 3.58. The values of C_u and C'_u for this sand bed are 2.69×10^5 kN/m³ and 7.45×10^4 kN/m³

respectively. When this sand bed is reinforced with two 150mm square geogrid layers, the value of C_u decreases to 83% whereas C'_u becomes 1.62 times as seen in Figure 3.59. For the sand bed reinforced with 3 layers having same size, C_u and C'_u values are 76% and 113% respectively as observed in Figure 3.59. The values of C_u and C'_u for the sand bed reinforced with 4, 6 and 8 reinforcement layers of 150mm square size are 67%, 59% & 54% and 111%, 102% & 101% of respective values for unreinforced sand bed as shown in Figures 3.60 to 3.62 and Table 4.2. The values of C_u decreases while that of C'_u generally increases upon reinforcing the sand bed. This shows an extension of the linear elastic range of the reinforced sand bed.

When the sand bed is reinforced with two 300mm square layers, the values of C_u and C'_u are 0.78 and 1.42 times the respective values for unreinforced sand bed (Figure 3.63). Increasing the reinforcement layers to three gives the values of C_u and C'_u as 0.85 and 2.04 times as seen from Figure 3.63. The values of C_u and C'_u for sand bed reinforced with 4,6 and 8 geogrid layer of 300mm square size are 0.81, 0.74 and 0.71 and 1.99, 1.91 and 1.74 times the corresponding values for unreinforced sand bed respectively as shown in Figures 3.64 to 3.66 and Table 4.2. It is observed that C_u decreases and C'_u generally increases when the sand bed is reinforced. But the decrease in C_u value as compared to that for 150mm square reinforcements, is less.

The pressure versus elastic settlement plots for footing over sand beds reinforced with 2,3,4,6 and 8 number 450mm square geogrid layers are shown in Figures 3.67 to 3.70. The C_u values decrease to 84%, 78%, 77%, 76% and 76% for 2,3,4,6 and 8 reinforcement layers respectively. The values of C'_u increase to 109%, 150%, 156%, 158% and 160% for 2,3,4,6 and 8 layers respectively. It is observed that the rate of decrease in C_u values is less and regular, in this case, as compared to that for reinforcement layers of smaller size. Figures 3.71 to 3.74 show pressure versus elastic settlement plots for the footing over sand beds reinforced with 2,3,4,6 and 8 number 600mm square geogrid layers. The C_u values

decrease to 81%, 81%, 80%, 78% and 77% for 2,3,4,6 and 8 reinforcement layers respectively. The corresponding values of C'_u are 1.01, 1.01, 1.28, 1.46 and 1.46 times of C'_u value for unreinforced sand bed for 2,3,4,6 and 8 layers respectively. Again, in this case, the decrease in C_u values is further less as compared to that for the reinforcements of smaller sizes.

For the footing over sand bed reinforced with 2,3,4,6 and 8 number 750mm square geogrid layers, pressure versus elastic settlement plots are shown in Figures 3.75 to 3.78. The values of C_u decrease to 87%, 86%, 89%, 88% and 80% for 2,3,4,6 and 8 reinforcement layers respectively. The values of C'_u for 2,3,4,6 and 8 layers are 1.01, 1.13, 1.56, 1.58 and 1.64 times the C'_u value for unreinforced sand bed. The decrease in C_u values, in this case, is the least as compared to that of the reinforcements having smaller sizes. Thus, larger the reinforcement size, lesser is the decrease in C_u as compared to that of unreinforced sand bed. However, C'_u generally increases upon reinforcing the sand bed with geogrid reinforcements; increase being more with increasing number of reinforcement layers. This is due to an extended linear elastic range of the geogrid reinforced sand beds. It should be noted that the pressure range for C'_u values of reinforced sand beds is much higher than the pressure range of C'_u values of unreinforced sand bed.

The effect of density of sand on pressure versus elastic settlement characteristics of footing over reinforced sand beds subjected to cyclic loading can be observed by comparing pressure-elastic settlement plots shown in Figures 3.79 to 3.83 at 50% relative density to corresponding plots at 70% relative density shown in Figures 3.60, 3.64, 3.68, 3.72 and 3.76, for 4 layers of reinforcement of size varying from B to 5B. The decrease in C_u value at 50% relative density is somewhat more than that for the corresponding reinforced sand beds at 70% relative density. For 4 geogrid layers of size 450mm square provided in sand beds at 70% and 50% relative densities, the reductions in C_u values are 23% and 25%; but the C'_u values increase by 55% and 80% over the values for the

corresponding unreinforced sand beds as seen from Figures 3.60 and 3.80 and Table 4.2.

The effect of size of footing on C_u and C'_u has been studied by conducting cyclic plate load tests on 150mm square and 300mm square footings over unreinforced and reinforced sand beds at 70% relative density. From pressure elastic settlement plots shown in Figures 3.60, 3.64, 3.68, 3.72 and 3.76 for 150mm square footing and Figures 3.84 to 3.88 for 300mm square footing; it is observed that for a footing of larger size placed over a similar reinforced sand bed, the decrease in C_u values is somewhat more for larger size reinforcements. For footings of 150mm square and 300mm square sizes placed over sand beds reinforced with 4 geogrid layers of size 3B, the reductions in C_u values are 23% and 29% and the increase in C'_u values are 55% and 47% respectively over the values for the corresponding unreinforced sand bed as can be seen in Figures 3.68 and 3.86 and Table 4.2. Similar trend, in general, is observed for the sand beds reinforced with geogrid layers of other sizes.

Owing to the above discussions, it can be concluded that the reinforced sand beds have a lesser value of the coefficient of elastic uniform compression C_u as compared with the unreinforced sand bed. The reinforcements, however, provide a longer linear elastic range to the reinforced sand bed, that is the values of C_u for reinforced sand beds are applicable upto much higher loading intensities as compared to that of unreinforced sand bed. The values of coefficient of elastic uniform compression beyond the ultimate bearing pressure of reinforced sand beds i.e. C'_u , are much higher for the reinforced sand bed than the unreinforced one.

4.2.6.1 Corrections for Confining Pressure and Area of Footing

The mean effective confining pressure below the footing $\bar{\sigma}_0$ has been calculated using the expression (Prakash & Puri, 1977);

$$\bar{\sigma}_0 = \sigma_v (2K_0 + 1)/3 \quad \dots(4.1)$$

where

σ_v = vertical stress induced at the centre of the pressure bulb having its depth equal to the width of the test area, because of the superimposed static loads and weight of soil mass above that point.

K_0 = coefficient of earth pressure at rest,

$K_0 = 1 - \sin\phi$. (After Jaky, 1948),

ϕ = angle of shearing resistance of soil.

$$\sigma_v = \gamma_s Z + 4\bar{I}q \quad \dots(4.2)$$

where

γ_s = unit weight of soil

Z = depth under consideration which is equal to half the width of footing.

$$\bar{I} = \frac{1}{4\pi} \left[\frac{2m_1 n_1 \sqrt{m_1^2 + n_1^2 + 1}}{m_1^2 + n_1^2 + 1 + m_1^2 n_1^2} \cdot \frac{m_1^2 + n_1^2 + 2}{m_1^2 + n_1^2 + 1} + \sin^{-1} \frac{2 m_1 n_1 \sqrt{m_1^2 + n_1^2 + 1}}{m_1^2 + n_1^2 + 1 + m_1^2 n_1^2} \right] \dots(4.3)$$

[After Taylor, 1948]

$$m_1 = 0.5L/Z \quad \text{and} \quad n_1 = 0.5 B/Z$$

where L and B are the length and width of footing respectively.

\bar{I} = influence factor for determining vertical stress below the corners of loaded rectangular surface area based on Westergaard (no lateral strain) classic case.

q = uniform vertical loading intensity acting on the surface footing, which is taken as the pressure intensity at the point of intersection of C_u and C'_u lines.

The coefficient of elastic uniform compression C_u is corrected to a confining pressure of 100 kN/m^2 to obtain C_{u100} as

$$(C_{u100}/C_u) = (100/\sigma_0)^{0.5} \quad \dots(4.4)$$

The variation of coefficient of elastic uniform compression C_u with confining pressure is considered to be similar to the variation of shear modulus G with the confining pressure and the exponent value m' is taken as 0.5 in expression (4.4) (Silver and Seed, 1971 and IS:5249 - 1977).

Applying area correction, the corrected value of coefficient of elastic uniform compression $(C_{u100})_{10}$ for 10 m² area is obtained [Barkan, 1962] :

$$(C_{u100})_{10}/C_{u100} = (A/10)^{0.5} \quad \dots(4.5)$$

where A is the area of test plate in m²

The coefficient of earth pressure at rest K_0 is calculated as :

1. The ultimate bearing pressure q_u , is obtained from the pressure-settlement plots [Figure 3.20 to 3.57].
2. Terzaghi's bearing capacity factor N_γ for the square footing is calculated from the expression :

$$N_\gamma = q_u/(0.4\gamma_s B) \quad \dots(4.6)$$

3. From the tables of ϕ versus N_γ [IS:6403-1981], the value of ϕ is determined.
4. K_0 is determined using the expression

$$K_0 = 1 - \sin\phi \quad \dots(4.7)$$

The values of K_0 for different cyclic plate load tests are shown in Table 4.1.

As an example, for 2 reinforcement layers of 150mm square size placed in sand bed below the footing of the same size and at unit weight of sand, $\gamma_s = 16.3 \text{ kN/m}^3$ (Figure 3.21).

$$q_u = 200 \text{ kN/m}^2,$$

$$N_\gamma = 200/(0.4 \times 16.3 \times 0.15) = 204.5$$

From tables, $\phi = 42.9^\circ$

$$K_0 = 0.32$$

$$\begin{aligned} \text{The vertical stress } \sigma_v &= \gamma_s Z + 4\bar{I}q \\ &= 16.3 \times 0.075 + 4 \times 0.17522q, \end{aligned}$$

For square footing, $m_1 = n_1 = 0.5L/Z = 0.075/0.075 = 1$

$$\bar{I} = 0.17522 \text{ [Taylor, 1948].}$$

$$\text{or } \sigma_v = 1.2225 + 0.70088q$$

At factor of safety = 1.0, $q = 200 \text{ kN/m}^2$

$$\sigma_v = 141.40 \text{ kN/m}^2$$

$$\bar{\sigma}_0 = 77.30 \text{ kN/m}^2$$

$$\begin{aligned} C_{u100} &= 2.22 \times 10^5 \left(\frac{100}{77.30} \right)^{0.5} \\ &= 2.52 \times 10^5 \text{ kN/m}^3 \end{aligned}$$

$$\begin{aligned} \text{and } (C_{u100})_{10} &= 2.52 \times 10^5 \sqrt{\frac{(0.15)^2}{10}} \\ &= 1.2 \times 10^4 \text{ kN/m}^3 \end{aligned}$$

The corrected values of coefficient of elastic uniform compression have been calculated at factors of safety of 1, 2 and 3 and are listed in Table 4.3. The corrected values of C'_u are calculated at factors of safety of 1, 0.67 and 0.5 and have been listed in Table 4.4. The factor of safety is defined with respect to the ultimate bearing pressure of the reinforced sand bed; this is the reason that C_u and C'_u values appear alternatively in Tables 4.3 and 4.4, at factor of safety of 1.0; depending upon whether the pressure at the point of intersection of C_u and C'_u is higher or lower than the ultimate bearing pressure.

For reinforced sand bed containing two 150mm square geogrid layers below a footing of the same size, at a relative density of 70%;

q value for a factor of safety of 2 is given by

$$q = \frac{q_u}{2} = 100 \text{ kN/m}^2$$

4.2.6.2 Strain Level

The strain level ϵ_z associated with the cyclic plate load tests is calculated as the ratio of settlement to the width of the test plate [Prakash and Puri, 1981].

$$\epsilon_z = S_e/B \quad \dots(4.8)$$

where

S_e = elastic settlement of plate corresponding to the load intensity q .

B = width of footing

For example, at $D_r=70\%$ for reinforced sand bed containing two 150mm square geogrid layers below a footing of the same size, at a factor of safety of 2 :

$$q = 200/2 = 100 \text{ kN/m}^2$$

and $S_e = 0.45 \text{ mm}$; from pressure versus elastic settlement curve [Figure 3.59].

$$\epsilon_z = S_e/B = 0.45/150 = 3 \times 10^{-3}$$

The strain levels at different values of C_u and C'_u have been calculated and are tabulated in Table 4.3 and Table 4.4 respectively.

The strain levels associated with the C_u values of reinforced sand beds are upto 18×10^{-3} whereas those for C_u value of the unreinforced sand bed are upto about 4×10^{-3} only. Thus the strain levels associated with the C_u value of reinforced sand beds are much higher. Hence the reduction in C_u values for reinforced sand beds is also due to the higher strain levels. However, the reduced C_u values are valid upto very high strain levels (more than four times), at which C'_u values of unreinforced sand bed are very small.

4.2.6.3 Coefficient of Elastic Uniform Compression versus Strain level

The values of $(C_{u100})_{10}$ given in Tables 4.3 and 4.4 respectively for the sand beds correspond to different strain levels and so direct comparison of these values for different reinforced sand beds with the values for unreinforced sand bed at a particular strain level is not possible. Therefore, for comparison, the values of C_u are interpreted from pressure versus elastic settlement plots shown

in Figures 3.58 to 3.88 at strain levels of 2×10^{-3} , 4×10^{-3} and 6×10^{-3} . The values of C'_u are also interpreted from pressure versus elastic settlement plots at strain levels of 10×10^{-3} and 15×10^{-3} . The procedure given in 4.2.6.1 has been used for the purpose. The interpreted values of $(C_{u100})_{10}$ and $(C'_{u100})_{10}$ are listed in Table 4.5. The value of $(C'_{u100})_{10}$ for unreinforced sand beds (Figures 3.58 and 3.79) at strain levels of 15×10^{-3} are determined by linearly extrapolating the plots.

The coefficient of elastic uniform compression C_u decreases with the increase in strain level for unreinforced and reinforced sand beds as is seen from the value listed in Tables 4.3 and 4.5. For example, for 150mm square footing over a sand bed (at 70% relative density) reinforced with two geogrid layers having size B, the C_u values at strain levels of 2×10^{-3} , 3×10^{-3} and 6×10^{-3} are 2.06×10^4 , 1.69×10^4 and 1.2×10^4 kN/m³ respectively. The values of C'_u also decrease with the increase in strain for unreinforced and reinforced sand beds as observed from Table 4.4 and 4.5. As an illustration, for 150mm square footing over the sand bed (at 70% relative density) reinforced with three 150mm square geogrid layers the C'_u values at strain levels of 9.55×10^{-3} , 19.27×10^{-3} and 28.99×10^{-3} are 4.15×10^3 , 3.39×10^3 and 2.94×10^3 kN/m³ respectively. Similar trend is observed for other configurations of reinforced sand beds. The decrease in the coefficient of elastic uniform compression of sand beds with increasing strain levels is due to the softening behaviour of sand.

The values of coefficient of elastic uniform compression determined at different factors of safety, as defined earlier, (given in Tables 4.3 and 4.4) are plotted with respect to strain level on a semilog plot in Figure 4.4. It is observed that variation of C_u with strain level is similar to the variation of shear modulus G , with strain level, as reported for sands, by Seed and Idriss (1970). The curves for the unreinforced sand bed and the reinforced sand beds containing 2 layers of 150mm square size and 8 layers of 750mm square size (minimum and maximum area of geogrid reinforcements in this investigation) are close to each other.

This indicates that C_u values are marginally reduced with the inclusion of geogrid reinforcements in sand bed at the same strain level.

The curves for the other reinforcement configurations of sand bed lie in between the curves for the reinforced sand beds containing the minimum and maximum area of geogrid reinforcements and therefore, are not shown in Figure 4.4. Also, it is observed from Figure 4.4 that the curve for sand bed reinforced with 8 number 750mm square geogrid layers, has higher range of strain level as compared with that of the unreinforced sand bed. This indicates that C'_u for the reinforced sand bed is higher than C'_u of unreinforced sand bed at larger strain levels. This seems to be due to significant mobilization of the interface friction between the sand and geogrid reinforcements at higher strain levels.

4.2.6.4 Coefficient of Elastic Uniform Compression versus Number of Geogrid Layers

As mentioned earlier in 4.2.6, the coefficient of elastic uniform compression C_u decreases with increasing number of reinforcement layers, in general. The values of C'_u , however, generally increase slightly with the increase in number of reinforcement layers, which seems to be due to the mobilisation of interface friction at higher strain levels.

The interpreted values of coefficient of elastic uniform compression $(C_{u100})_{10}$ given in Table 4.5, are plotted with respect to number of reinforcement layers of different sizes at strain levels of 2×10^{-3} , 4×10^{-3} and 6×10^{-3} in Figures 4.5, 4.6 and 4.7 respectively. From these plots and the values listed in Table 4.5, it is observed that there is a reduction in coefficient of elastic uniform compression with the increase in the number of geogrid layers. However, the pressure range of C_u values in reinforced sand beds is much higher than that for C_u values of unreinforced sand bed. As the number of geogrid layers in sand bed increase, the rate of decrease in C_u values reduces.

Figure 4.8 shows the variation of $(C'_{u100})_{10}$, (some results are in C_u range) with number of reinforcement layers for different sizes of reinforcement. It is

observed that values of C'_u are higher for the reinforced sand beds than for the unreinforced sand bed. C'_u generally increases with increase in number of reinforcement layers. This seems to be due to a longer elastic range of the reinforced sand beds than the unreinforced sand beds. At higher strain levels, the coefficient of elastic uniform compression, C'_u is more for reinforced sand beds due to the mobilization of interface friction between sand and reinforcements.

4.2.6.5 Coefficient of Elastic Uniform Compression versus Size of Reinforcement

As mentioned earlier in 4.2.6, coefficient of elastic uniform compression, C_u of reinforced sand bed is less as compared to that of unreinforced one. This difference goes on reducing with increase in reinforcement size.

Figures 4.9 and 4.10 show the plots of interpreted values of coefficient of elastic uniform compression, $(C_{u100})_{10}$ given in Table 4.5, with respect to reinforcement size at strain levels of 4×10^{-3} and 6×10^{-3} respectively. These plots and the values listed in Table 4.5 indicate that as the size of reinforcement increases, the decrease in C_u with respect to that of unreinforced sand bed is lesser and becomes almost negligible for the reinforcements of size 5B.

As an illustration, at strain level of 2×10^{-3} , values of $(C_{u100})_{10}$ for 150mm square footing over sand beds (70% relative density) reinforced with 4 geogrid layers having size B to 5B are 1.88×10^4 , 2.09×10^4 , 2.05×10^4 , 2.09×10^4 and 2.22×10^4 kN/m³ respectively as compared to the value of $(C_{u100})_{10}$ of 2.22×10^4 kN/m³ for the unreinforced sand bed (see Table 4.5).

Further, as the strain level increases, the curves shown in Figures 4.9 and 4.10 tend to converge indicating that the decrease in C_u values is further less at higher strain levels.

From Table 4.5, it is observed that values of $(C'_{u100})_{10}$ generally increase with increase in size of geogrid reinforcements.

4.2.6.6 C_u versus Relative Density of Sand and Size of Footing

As mentioned earlier in 4.2.6, the coefficient of elastic uniform compression increases with increase in relative density for both reinforced as well as unreinforced sand beds. Figure 4.11 shows the effect of relative density of sand on the coefficient of elastic uniform compression. It is observed that decrease in C_u value is slightly more for sand bed of lower relative density.

The effect of size of footing on the coefficient of elastic uniform compression has been discussed in 4.2.6. The value of coefficient of elastic uniform compression for larger footing is less than that of small footing as can be seen from Table 4.2, but the strain levels for the two cases are different. Table 4.5 shows the values of $(C_{u100})_{10}$ interpreted at the same strain levels both for small as well as large footing. It is observed that interpreted values of C_u for larger footing, at a particular strain level, are more. The variation of coefficient of elastic uniform compression $(C_{u100})_{10}$ with reinforcement size is shown in Figure 4.11 at a strain level of 4×10^{-3} .

4.2.7 Discussion Summary

The results of the cyclic plate load tests show that by reinforcing the sand bed with geogrid layers, there is significant improvement in the ultimate bearing capacity and the total settlements are significantly reduced. With the increase in size and number of reinforcement layers, larger increase in ultimate bearing capacity and more reduction in total settlements is achieved. The damping capacity of the sand bed is improved upon reinforcing it with geogrid layers, the improvement being more with larger number and size of reinforcement layers. The coefficient of elastic uniform compression decreases with the inclusion of geogrid layers in the sand bed, the decrease being dependent upon the number and size of geogrid layers. However, the pressure range to which the C_u value for reinforced sand corresponds is higher as compared to that for the unreinforced sand. For larger size of footing, the decrease in C_u value is observed to be more with the

inclusion of geogrid layers in the sand bed. Further, the decrease in C_u values of reinforced sand bed is less with increase relative density. The decrease in C_u value may be attributed to low modulus of geogrid material. The value of the coefficient of elastic uniform compression beyond the ultimate bearing capacity i.e. C'_u is higher for reinforced sand bed than for the unreinforced sand bed; and increases, in general, with the increase in size and number of reinforcement layers. This may be because of greater mobilisation of interface friction between sand and geogrid reinforcements.

4.3 VERTICAL VIBRATION TESTS

4.3.1 General

The experimental data obtained from vertical vibration tests have been utilized to plot amplitude versus frequency curves shown in Figures 3.89 to 3.113. The resonant frequencies and the maximum amplitudes of vibration have been determined at different force levels from these plots and are listed in Table 4.6. The damping ratio ξ , coefficient of elastic uniform compression C_u , strain levels and the ratio of dynamic force to weight of block F/W have been calculated and listed in Table 4.6. The confining pressure and area corrections have been applied to determine the corrected values of coefficient of elastic uniform compression $(C_{u100})_{10}$, which are listed in Table 4.6. The values of $(C_{u100})_{10}$ and the corresponding F/W ratios have been interpolated at strain levels of 2×10^{-4} , 4×10^{-4} and 6×10^{-4} and are given in Table 4.8. The values of $(C_{u100})_{10}$ and the damping ratio ξ are plotted to bring out the influence of different parameters affecting the behaviour of block foundation on reinforced sand beds under vertical vibrations. The amplitude reduction factor which is the ratio of the amplitude of vibration of block foundation over reinforced sand bed to the corresponding value for block foundation over unreinforced sand bed has also been plotted with respect to the number of reinforcement layers.

4.3.2 Amplitude-Frequency Plots

The amplitude versus frequency plots for block foundation placed over unreinforced sand bed subjected to vertical vibrations are shown in Figure 3.89 at four force levels with eccentricity $\theta=4^\circ, 12^\circ, 20^\circ$ and 28° . These curves show that as the force level increases, the amplitude of vibration increases whereas the resonant frequency decreases slightly. Further, with increase in force level, the response curves become steeper.

The amplitude versus frequency plots for block foundation over reinforced sand beds subjected to vertical vibrations are shown in Figures 3.90 to 3.113. With the increase in excitation level, the amplitude of vibration increases whereas the resonant frequency decreases slightly, similar to those for the unreinforced sand bed. Again, with the increase in force level, the response curves becomes steeper, generally, but the steepness is not as much as for the curves of unreinforced case. The decrease in resonant frequency with increase in force level, may be due to softening behaviour of soil, which is observed both for reinforced and unreinforced sand beds. Table 4.6 gives the values of the maximum amplitudes and resonant frequencies for different vertical vibration tests.

When the block foundation is placed over sand bed reinforced with 2 geogrid layers having same size as that of the block and is subjected to vertical vibrations, the resonant frequency decreases by about 5% as compared to the resonant frequency of block foundation over unreinforced sand bed. The maximum amplitudes are, however, reduced by about 6% as compared to the values of maximum amplitudes for foundation on unreinforced sand bed (Figures 3.89 and 3.90 and Table 4.6). The reductions in resonant frequency and amplitude values are represented as an average of the values for the four force levels. When the sand bed is reinforced with 3 geogrid layers of the same size, the decrease in resonant frequency is about 7.5% and the decrease in maximum amplitude is about upto 12% (Figures 3.89 and 3.91) as compared to the corresponding values for the unreinforced sand bed. Reinforcing the sand bed with 4 and 6 geogrid layers of

800mm×400mm size results in reductions of about upto 9% and 10% in resonant frequency and 20% and 25% in the maximum amplitude compared to the corresponding values for unreinforced sand bed as can be seen from Figures 3.89, 3.92 and 3.93, and Table 4.6.

The reductions in the resonant frequency and maximum amplitudes for the foundation over sand bed reinforced with 2 layers of 1200mm×600mm geogrid are upto 7.5% and 12% respectively as compared to the corresponding values for the unreinforced sand bed as can be seen from Figures 3.89 and 3.94. Similarly, for the sand beds reinforced with 3,4 and 6 geogrid layers of the same size, the reductions in resonant frequency and maximum amplitude values are upto about 9%, 10% & 12%; and 20%, 24% & 30% respectively as compared to the corresponding values for the unreinforced sand bed as observed from Figures 3.89 and 3.95 to 3.97 respectively. The decrease in resonant frequency and maximum amplitudes is more for reinforcements of this size as compared to that for reinforcements of smaller size (800mm×400mm) and is more for more number of layers.

For the block foundation placed over sand bed reinforced with 2,3,4 and 6 layers of 1500mm×750mm geogrid, the resonant frequency and maximum amplitude values decrease upto about 10%, 11%, 12% & 12%; and 12%, 25%, 37% & 43% respectively as compared to the corresponding values for the block over unreinforced sand bed as seen by comparing Figure 3.89 with Figures 3.98 to 3.101 (see Table 4.6). With the increase in number and size of geogrid layers, the decrease in resonant frequency and maximum amplitude is more.

Figures 3.102 to 3.105 show the amplitude versus frequency plots for vertical vibrations of block foundation on sand bed reinforced with 2, 3, 4 and 6 layers of 1000mm square geogrid. It is observed by comparing these plots with Figure 3.89, that the resonant frequency and maximum amplitude values decrease by about 11%, 12%, 13% & 13%; and 6%, 18%, 21% and 31% respectively as compared to the corresponding values for the block over unreinforced sand bed (Table 4.6).

The frequency-amplitude curves for the vertical vibrations of block over sand bed reinforced with 2,3,4 and 6 layers of 1200mm square geogrid are shown in Figures 3.106 to 3.109 respectively. These plots show that the resonant frequency and maximum amplitude values decrease by about 9%, 11%, 12% & 13%; and 6%, 21%, 31% and 37% respectively as compared to the corresponding values for the block over unreinforced sand bed (Fig. 3.89 and Table 4.6). Figures 3.110 to 3.113 show the frequency-amplitude plots for vertical vibrations of block foundation on sand bed reinforced with 2,3,4 and 6 layers of 1500mm×1500mm geogrid. It is observed from these plots that the resonant frequency and maximum amplitude values decrease by maximum of about 10%, 12%, 13% & 14%; and 6%, 25%, 37% and 37% respectively. as compared to the corresponding values for the unreinforced sand bed (Fig.3.89 and Table 4.6).

The response curves for vertical vibrations of block over reinforced sand beds indicate that both resonant frequency and maximum amplitude values decrease as compared to the corresponding values for the vertical vibrations of block over unreinforced sand bed. From the above discussions, it can be seen that the decrease in both resonant frequency and maximum amplitude values is more with increase in the number and size of the geogrid layers, in general. Also the frequency-amplitude curves become somewhat flatter as the number and size of geogrid layers in reinforced sand bed increase. The decrease in maximum amplitude values is generally more as compared to the decrease in resonant frequency and both vary with force level. The maximum decrease in the maximum amplitude values is upto 43% whereas the maximum decrease in resonant frequency values is 14%.

This reduction in natural frequency may be due to low modulus of the geogrid material and practically negligible mobilization of interface friction between sand and reinforcement at low strain levels associated with vertical vibration tests.

A similar decrease in maximum amplitude and resonant frequency has been reported by Boominathan et al. (1991) for vertical vibration of block over sand

bed reinforced with two geotextiles layers. They reported a decrease of 11% in resonant frequency and 55% in maximum amplitude for a base reinforced with 2 layers of sand coated geotextile. However, they conducted only two tests with limited number of variables and therefore, their results cannot be generalized.

4.3.3 Analysis of the Amplitude-Frequency Data

The data obtained from the vertical block vibration tests have been analysed to obtain the damping ratio ξ , coefficient of elastic uniform compression C_u , strain levels and the rate of the dynamic force to weight of block F/W . From the amplitude-frequency response curves, the maximum amplitude of forced vertical vibrations $(A_z)_{\max}$ and the resonant frequency f_{nz} are obtained. The damping ratio ξ is obtained from the response curves by bandwidth method [Richart et al., 1970; IS:5249-1977]. The frequencies f_1 and f_2 corresponding to the amplitude $(A_z)_{\max}/\sqrt{2}$ are found and the damping ratio ξ is given by the equation

$$\xi = \frac{f_2 - f_1}{2f_{nz}} \quad \dots(4.9)$$

The coefficient of elastic uniform compression C_u is calculated using the expression [IS:5249-1977] :

$$C_u = 4\pi^2 f_{nz}^2 (M/A) \quad \dots(4.10)$$

where

M = mass of block, oscillator and motor, and

A = area of the block

For the test block in this investigation,

$$C_u = 54.1 f_{nz}^2 \text{ kN/m}^3$$

The confining pressure correction is applied to obtain the value of coefficient of elastic uniform compression C_{u100} at 100 kN/m² as [Equation 4.4]

$$C_{u100} = C_u \sqrt{\frac{100}{\bar{\sigma}_0}}$$

where $\bar{\sigma}_0 = \sigma_v(2K_0+1)/3$

$\bar{\sigma}_0$ = mean effective confining pressure at a depth of one half the width of block.

$$\sigma_v = \gamma_s Z + 4\bar{I}q$$

where

γ_s = unit weight of soil

z = depth under consideration equal to one half the width of block.

q = uniform vertical loading intensity acting on the soil under the block.

\bar{I} = influence factor as defined in 4.2.6.1.

$K_0 = 0.5$

K_0 and σ_v = as already defined in 4.2.6.1.

Further, the area correction is applied for an area of 10 m² to obtain the corrected value of coefficient of elastic uniform compression $(C_{u100})_{10}$ using the expression [4.5].

$$(C_{u100})_{10} = C_{u100} \left(\frac{A}{10} \right)^{0.5}$$

where A = area of the block in m²

For the test block,

$$(C_{u100})_{10} = 0.6636 C_u$$

The corrected values of coefficient of elastic uniform compression $(C_{u100})_{10}$ are listed in Table 4.6.

The strain levels are calculated using the expression [Prakash & Puri, 1981]:

$$\varepsilon_v = (A_z)_{\max} / B \quad \dots(4.11)$$

where $(A_z)_{\max}$ = maximum amplitude of vertical vibration of block.

and B = depth upto which the vibrations are effective taken equal to the width of block.

The ratio of the dynamic force F to the weight of the block W is calculated using the expression

$$F/W = \frac{m_e e \omega^2}{W} = \frac{0.00507 f_{nz}^2 \sin \theta / 2}{W} \quad \dots(4.12)$$

where m_e, e, ω and θ are already defined in 3.5.4.

The values of strain levels and ratio F/W are listed in Table 4.6 for vertical block vibration tests on unreinforced and reinforced sand beds.

4.3.4 Effect of F/W on Resonant Frequency and Damping Ratio ξ

The resonant frequency decreases slightly with the increase in dynamic force level for unreinforced as well as reinforced sand beds as mentioned earlier in 4.3.2. As an illustration, when F/W ratio increases from 0.0988 to 0.2781, the resonant frequency decreases from 49Hz to 47.5Hz for the unreinforced sand bed. Similarly, for the sand bed reinforced with 2 layers of 800mm×400mm geogrid, the resonant frequency decreases from 46.5 Hz to 45 Hz when F/W increases from 0.089 to 0.2496 as given in Table 4.6. It indicates softening behaviour of soil with the increase in dynamic force.

The damping ratio ξ , for unreinforced sand bed increases from 0.076 to 0.103 as the F/W ratio increases from 0.0988 to 0.6037. Similar, increase in damping ratio with increase in F/W is observed for reinforced sand beds, in general, as can be noted from the values given in Table 4.6. The variation of damping ratio with F/W for different configurations of reinforced sand beds is illustrated in Figures 4.12 to 4.17. These figures indicate that damping ratio increases with the

increase in F/W , the rate of increase being more for the reinforced sand beds than for the unreinforced sand bed.

4.3.5 Effect of Reinforcement on Damping Ratio ξ

The damping ratio ξ is plotted with respect to F/W ratio for different reinforcement sizes and reinforcement layers as shown in Figures 4.12 to 4.17. At the same values of F/W ratio, the damping ratio ξ , is found to increase with the increase in number of reinforcement layers, in general, as can be seen from the values listed in Table 4.6. The effect of size of reinforcement on damping ratio ξ is not distinct from these plots, however, it is observed that as the reinforcement size increases, the damping ratio versus F/W curves tend to converge. The increase in damping ratio is possibly due to dissipation of energy at the surfaces of geogrid layers.

4.3.6 Strain Level versus F/W Ratio

The maximum amplitudes increase with increase in force level as discussed earlier in 4.3.2. The strain level ϵ_v increases with increase in F/W ratio both for unreinforced and reinforced sand beds. Figures 4.18 to 4.23 show the variation of strain level with F/W ratio for the unreinforced and reinforced sand beds. The curves for different layers of reinforcement of size $L_r/R = B_r/B = 1$, lie quite to each other (Figure 4.18) and therefore, it was considered appropriate to represent ϵ_v versus F/W plot for other reinforcement sizes by single curve [Figures 4.19 to 4.23]. It is observed that for the same F/W ratio less than 0.2 nearly, the strain level is less for reinforced sand beds than that for unreinforced sand bed. For F/W greater than 0.2, the trend is reversed. The variation of strain level ϵ_v with F/W ratio for reinforced sand beds tends to be linear as compared to that for unreinforced sand bed.

4.3.7 Amplitude Reduction Factor versus Number of Reinforcement Layers

The decrease in amplitude is more with increase in number of geogrid layers for all sizes of reinforcement, as discussed in detail in 4.3.2. The effect of number of geogrid layers of different sizes on maximum amplitude is expressed in terms of the ratio of the maximum amplitudes of vibration of foundation on reinforced and the unreinforced sand beds which is designated as amplitude reduction factor. As pointed out earlier in 4.3.2, the maximum amplitudes are reduced by a maximum of 43% with the increase in size and number of geogrid layers in the reinforced sand bed.

Figures 4.24 to 4.31 show the variation of amplitude reduction factor $(A_z)_{\max r}/(A_z)_{\max u}$ with the number of reinforcement layers n for different reinforcement sizes at eccentricity levels $\theta=4^\circ$, 12° , 20° and 28° . The curves for rectangular and square shaped reinforcements are drawn separately to study the effect of shape of reinforcement on amplitude reduction factor. The rectangular shaped reinforcements seem to have, generally, more effect on the amplitude reduction factor.

4.3.8 Coefficient of Elastic Uniform Compression $(C_{u100})_{10}$ versus Number of Reinforcement Layers

The values of coefficient of elastic uniform compression C_u for unreinforced and reinforced sand beds, determined by using expression (4.10) are given in Table 4.6. The coefficient of elastic uniform compression for the sand bed reinforced with two geogrid layers of size 800mm×400mm is less by 10% to 12% from the C_u values of the unreinforced sand bed, at different force levels. For the sand bed reinforced with 3 layers of same size geogrid, the values of C_u decrease by 13% to 15% as compared to the corresponding values for the unreinforced sand bed. Similarly for 4 and 6 layers of the same size geogrid reinforcement, the values of C_u decrease by 15% to 17% and 18% to 20% respectively as compared to the values of C_u at the corresponding force levels for the unreinforced sand bed. The values of

C_u , therefore, decrease with the inclusion of geogrid layers in sand bed and the decrease is more with increasing number of reinforcement layers.

When the sand bed is reinforced with 2,3,4 and 6 layers of size 1200mm×600mm, the decrease in C_u values is in the range of 12% to 14%, 12% to 18%, 15% to 18% and 17% to 20% respectively; as compared to the values of C_u for unreinforced sand bed at the corresponding force levels. It is observed that the decrease in C_u values is more for larger size of reinforcement layers.

For the sand bed reinforced with 2,3,4 and 6 layers of 1500mm×750mm geogrid, the reductions in C_u values are in the range of 14% to 20%, 16% to 20%, 16% to 22% and 17% to 22% respectively; compared with the C_u values for the unreinforced sand bed at the corresponding force levels. The decrease in C_u values is observed to be more with the increase in number and size of geogrid layers.

The decrease in C_u values for the sand bed reinforced with 2,3,4 and 6 layers of 1000mm×1000mm geogrid is in the range of 19% to 22%, 21% to 22%, 21% to 24% and 22% to 24% respectively; compared with the corresponding values for the unreinforced sand bed. The decrease in C_u values is observed to be more, in this case, as compared to the reinforcement of size 1500mm×750mm.

The values of coefficient of elastic uniform compression decrease in the range of 15% to 19%, 19% to 23%, 24% to 26% and 24% to 26% for the sand bed reinforced with 2,3,4 and 6 layers of 1200mm×1200mm geogrid as compared to the corresponding values for the unreinforced sand bed. The C_u values decrease upto a maximum of 26% and the decrease is more for larger number of geogrid layers.

When the sand bed is reinforced with 2,3,4 and 6 layers of 1500mm×1500mm, the decrease in C_u values is in the range of 19% to 20%, 20% to 23%, 23% to 25% and 24% to 26% respectively; as compared to the values of C_u for reinforced sand bed at the corresponding force levels. The decrease in C_u values is upto a maximum of 26% for the maximum size and number of reinforcement layers used in this investigation.

From the above discussions, it can be seen that the coefficient of elastic

uniform compression decreases with the increase in force level both for unreinforced and reinforced sand beds; indicating the softening of soil at higher force levels. The coefficient of elastic uniform compression decreases upon reinforcing the sand bed with geogrid layers, compared to its value for the unreinforced sand bed at the corresponding force levels. The decrease in C_u values is more with increase in number of geogrid layers for all sizes of reinforcement.

The values of coefficient of elastic uniform compression are corrected for confining pressure and area of footing and are listed in Table 4.6. These values of $(C_{u100})_{10}$ are interpreted at strain levels of 2×10^{-4} , 4×10^{-4} and 6×10^{-4} and are given in Table 4.8. The corresponding F/W ratios are also interpolated and are presented in Table 4.8 at the three strain levels. Figures 4.38 and 4.40 show the variation of coefficient of elastic uniform compression with number of reinforcement layers n of different sizes at a strain level of 2×10^{-4} . It is observed that there is a decrease of 10% to 26% in C_u values which increases with the increase in number of reinforcement layers and size of reinforcement, in general. The coefficient of elastic uniform compression reduces asymptotically to a nearly constant value as the size and number of reinforcement layers increase. The decrease in C_u values seems to be somewhat less at higher strain levels of 4×10^{-4} and 6×10^{-4} as can be seen from the values given in Table 4.8. The decrease in coefficient of elastic uniform compression may be due to low modulus of geogrid material. Also, at small strain levels associated with vertical vibration tests, the mobilization of interface friction between sand and reinforcements is negligible.

Boominathan et al. (1991) have reported a decrease of about 20% in the coefficient of elastic uniform compression of sand reinforced with two layers of sand-coated geotextile under vertical vibrations. Shewbridge and Sousa (1991) have shown that dynamic shear modulus G decreases slightly with the inclusion of steel reinforcements in sand specimen tested in torsional shear in dynamic loading system.

4.3.9 Coefficient of Elastic Uniform Compression $(C_{u100})_{10}$ versus F/W Ratio

The coefficient of elastic uniform compression decreases with increase in force level for unreinforced and reinforced sand beds as discussed in 4.3.8. The values of coefficient of elastic uniform compression $(C_{u100})_{10}$ at different F/W ratios are given in Table 4.6 and are interpolated at the same strain levels as shown in Table 4.8. As an illustration, the coefficient of elastic uniform compression decreases from 8.62×10^4 kN/m³ to 7.6×10^4 kN/m³ as F/W increases from 0.0988 to 0.6037, for the unreinforced sand bed. Similarly, for the sand bed reinforced with 2 layers of 800mm×400mm geogrid, $(C_{u100})_{10}$ decreases from 7.76×10^4 kN/m³ to 6.64×10^4 kN/m³ as F/W increases from 0.089 to 0.5275.

Figures 4.32 to 4.37 show the variation of $(C_{u100})_{10}$ with F/W ratio for different number and sizes of reinforcement layers. The rate of decrease in coefficient of elastic uniform compression with increase in F/W seems to be nearly constant with increase in number of reinforcement layers. With increase in size of reinforcement, decrease in C_u values with increasing number of layers, is not significant as can be seen from Figures 4.32 and 4.34. This appears to be due to the softening behaviour of soil with the increase in dynamic force level.

4.3.10 Coefficient of Elastic Uniform Compression versus Reinforcement Area

The coefficient of elastic uniform compression generally decreases with the increase in size of reinforcement as mentioned in 4.3.8. From Table 4.8, it is observed that as the area ratio of reinforcement A_r (which is ratio of area of reinforcement layer to the base area of block) increases from 1.0 to 2.25; $(C_{u100})_{10}$ decreases from 7.7×10^4 kN/m³ to 7.49×10^4 kN/m³ for two reinforcement layers at a strain levels of 2×10^{-4} . Similar, behaviour is observed for other area ratios also but the rate of decrease in C_u is very small at larger area ratios.

Figure 4.39 shows the variation of ratio of $(C_{u100})_{10R}/(C_{u100})_{10U}$ with area of reinforcement for different reinforcement layers at a strain level of 2×10^{-4} , where $(C_{u100})_{10R}$ and $(C_{u100})_{10U}$ are the values of coefficient of elastic uniform

compression for reinforced and unreinforced sand beds. It is observed that at smaller area ratios, the rate of decrease in C_u value is significant, but it diminishes with the increase in area ratio.

4.3.11 Coefficient of Elastic Uniform Compression – Vertical Vibration Tests vis-a-vis Cyclic Plate Tests

Since the coefficient of elastic uniform compression is strain-dependent, the C_u values obtained from vertical vibration tests and cyclic plate load tests are different and fall in different ranges of strain level. The ranges of strain level for the cyclic plate load and vertical block vibration tests in the experimental investigations reported in this work are 5×10^{-2} to 1×10^{-3} and 6×10^{-3} to 1×10^{-4} respectively. Figure 4.41 shows a plot of corrected values of coefficient of elastic uniform compression $(C_{u100})_{10}$ versus strain level for the vertical block vibration and cyclic plate load tests for unreinforced sand bed and sand bed reinforced with 2 geogrid layers having size equal to size of block/footing. The curves obtained are similar to those reported by Seed and Idriss (1970). It is interesting to note that curve for reinforced sand bed is below the curve for unreinforced sand bed upto strain level of 3×10^{-2} , whereas for higher strain levels, the curve for reinforced sand bed lies above. This shows that for strain levels less than nearly 3%, the mobilisation of interface friction between geogrid reinforcement and sand is not significant to contribute to the C_u -value of the reinforced sand bed. This is in agreement with the results reported by Shewbridge and Sousa (1991) for steel rod-reinforced sand, that the reinforcing effect of reinforcements on dynamic properties of reinforced sand should be neglected for strain levels less than 5%.

4.3.12 Discussion Summary

In vertical block vibration tests, the resonant frequency decreases upto about 14% upon reinforcing the sand bed with geogrid layers and the maximum amplitudes decrease maximum upto 43%. The decrease in the resonant frequency and

maximum amplitudes is more with the increase in number and size of the geogrid layers. The damping ratio ξ of the reinforced sand bed increases with increase in size and number of geogrid layers. The increase in damping ratio seems to be due to the dissipation of energy along the surfaces of the geogrid layers. The coefficient of elastic uniform compression is decreased by a maximum of about 26% depending upon the size and number of the geogrid layers below the base of block. Thus, geogrid reinforced sand beds provide reduced amplitudes and increased damping capacity but with a marginal reduction in the coefficient of elastic uniform compression at low strain levels. The decrease in the resonant frequency and the coefficient of elastic uniform compression seems to be due to the low modulus of the geogrid material and negligible mobilization of the interface friction between the sand and reinforcement at strain levels associated with vertical vibration tests. For strain levels less than 3×10^{-2} , the C_u for unreinforced sand bed is higher than C_u for the reinforced sand beds and at higher strain levels C_u for reinforced sand bed is more, indicating that mobilisation of interface friction contributes to C_u -values of reinforced sand beds at strain levels higher than 3%.

4.4 HORIZONTAL VIBRATION TESTS

4.4.1 General

The amplitude versus frequency curves have been plotted in Figures 3.114 to 3.138 using the data obtained from forced horizontal vibration tests. The resonant frequencies f_{nx1} and f_{nx2} for the first and second modes of vibration have been determined from these curves and are listed in Table 4.7. The maximum amplitudes $(A_{x1})_{max}$ and $(A_{x2})_{max}$ corresponding to the first and second modes of vibration have also been determined from the frequency-amplitude curves and are presented in Table 4.7. Since the amplitude-frequency curves are nearly symmetrical, the damping ratios, ξ_1 and ξ_2 for the first and second modes of vibration have been determined by the bandwidth method. The values of coefficient of elastic uniform

shear C_τ for the two modes of vibration have been calculated. The amplitude to width ratios have been calculated and the ratio of the dynamic force to weight of block F_1/W for the first mode of vibration has been determined. The values of all these parameters are listed in Table 4.7 for different reinforced sand beds. The confining pressure and area corrections have been applied to determine the corrected values of coefficient of elastic uniform shear $(C_{\tau 100})_{10}$ which are given in Table 4.7. The values of $(C_{\tau 100})_{10}$ and the corresponding F_1/W ratios have been interpolated at strain levels of 2×10^{-4} , 4×10^{-4} and 6×10^{-4} , and are listed in Table 4.9. The values of $(C_{\tau 100})_{10}$ and the damping ratio ξ_1 have been plotted to bring out the influence of various parameters affecting the behaviour of the reinforced sand beds under horizontal vibrations. The amplitude reduction factor (ratio of the maximum amplitudes of vibration of block on reinforced sand bed to that on the unreinforced sand bed) has been plotted with respect to the number of reinforcement layers.

4.4.2 Amplitude-Frequency Curves

The amplitude versus frequency plots for block foundation placed over unreinforced sand bed and subjected to horizontal vibrations are shown in Figure 3.114, at four force levels with eccentricity values $\theta = 4^\circ$, 12° , 20° and 28° . It is observed from these curves that as the force level increases, the amplitudes of vibration increase whereas the resonant frequencies for both modes of vibration decrease slightly. The response curves become steeper with the increase in force level. The amplitudes corresponding to the second mode of vibration are less than those for the first mode of vibration.

The frequency-amplitude plots for block foundation over reinforced sand beds subjected to horizontal vibrations are shown in Figures 3.115 to 3.138. With the increase in excitation level, the amplitudes of vibration increase whereas the resonant frequencies corresponding to both the mode of vibration decrease slightly, similar to those for the unreinforced sand bed. With the increase in

excitation level, the response curves become steeper. This decrease in the resonant frequencies, may be due to the softening behaviour of soil, which is observed both for the unreinforced and reinforced sand beds. Table 4.7 gives the values of the maximum amplitudes and resonant frequencies for both vibration modes for different tests.

When the block foundation is placed over sand bed reinforced with 2 geogrid layers of size 800mm×400mm and subjected to horizontal vibrations, the resonant frequencies for the first and second modes of vibration decrease by an average of 15% and 11% respectively as compared to the resonant frequencies of block foundation over the unreinforced sand bed. The maximum amplitudes are however, reduced by an average of 12% and 9% for the first and second modes of vibration as compared to the corresponding values for the block foundation over unreinforced sand bed (Figures 3.114 and 3.115 and Table 4.7). For the sand bed reinforced with 3 geogrid layers of the same size, the resonant frequencies decrease by maximum of 18% and 15% and the maximum amplitudes decrease by 8% to 25% and 6% to 10% for the first and second modes of vibration as compared with the corresponding values for the unreinforced sand bed (Figure 3.116). Similarly, for 4 reinforcement layers of the same size, the resonant frequencies decrease by maximum of 16.5% and 16% whereas the maximum amplitudes decrease by 12% to 30% and 14% to 25% for the first and second modes of vibration (Figure 3.117). For 6 reinforcement layers of the same size, the resonant frequencies decrease by maximum of 17% and 16% and the maximum amplitudes decrease by 12% to 30% and 14% to 25% for the first and second modes of vibration [Figure 3.118]. It is, therefore, observed from the above discussion that the decrease in the resonant frequencies for both modes of vibration is generally more with increasing number of reinforcement layers. Similarly, the decrease in maximum amplitudes of vibration is also more with the increasing number of reinforcement layers.

For the sand bed reinforced with 2 layers of 1200mm×600mm geogrid, the resonant frequencies, decrease by maximum of 16% for both the modes of vibration,

whereas the maximum amplitudes decrease upto 25% and upto 14% for the first and second modes of vibration (Figure 3.119). Similarly, for 3 geogrid layers of the same size, the reductions in the resonant frequencies are upto 18% and 17% and the reductions in the maximum amplitudes are upto 25% and upto 20% for the first and second modes of vibration respectively (Figure 3.120). For 4 geogrid layers of the same size, the resonant frequencies decrease upto 26% and 21% and the maximum amplitudes decrease upto 37% and 26% for the first and second modes of vibration respectively (Figure 3.121). Similarly for the sand bed reinforced with 6 geogrid layers of the same size, the decrease in resonant frequencies is upto 21% and 21.5% and the decrease in maximum amplitudes is upto 37% and 26% for the first and second modes of vibration respectively (Figure 3.122). It is, thus, observed that the decrease in the resonant frequencies and maximum amplitudes is more for larger sized reinforcements.

When the sand bed is reinforced with 2,3,4 and 6 geogrid layers of size 1500mm×750mm, the resonant frequencies decrease upto 21%, 23%, 20% and 24% for the first vibration mode and upto 19%, 20%, 20% and 21% for the second vibration mode respectively. While the corresponding maximum amplitudes are reduced by maximum of 31%, 31%, 37% and 42% for the first vibration mode and 10%, 20%, 20% and 33% for the second vibration mode respectively (Figures 3.123 to 3.126). The reductions in resonant frequencies and maximum amplitudes are more with increase in the number of reinforcement layers, in general.

For the sand bed reinforced with 2,3,4 and 6 layers of size 1000mm square, the resonant frequencies decrease maximum by 19%, 28%, 26% and 28% for first mode of vibration and maximum by 18%, 19%, 19% and 20% for second mode of vibration respectively. The corresponding maximum amplitudes are reduced by the maximum of 31%, 34%, 42% and 48% for first mode of vibration and 14%, 14%, 17% and 41% for second mode of vibration respectively. [Figures 3.127 to 3.130]. The decrease in the resonant frequencies for first mode of vibration is more than that for the second mode.

Again, when the sand bed is reinforced with 2,3,4 and 6 geogrid layers of size 1200mm×1200mm, the resonant frequencies decrease upto 21%, 21%, 25% and 25% for first vibration mode and upto 18%, 18%, 19% and 19% for second vibration mode respectively. The corresponding maximum amplitudes are reduced by the maximum of 19%, 28%, 40% and 40% for first vibration mode and 13%, 25%, 29% and 25% for second vibration mode respectively (Figures 3.131 to 3.134). The maximum amplitudes for the first mode of vibration are reduced more than those for the second mode.

If the sand bed is reinforced with 2,3,4 and 6 geogrid layers of size 1500mm square, the resonant frequencies decrease maximum by 21%, 25%, 23% and 25% for the first mode of vibration and 18%, 19%, 19% and 19% for the second mode of vibration respectively. The corresponding maximum amplitude are reduced by a maximum of 37%, 44%, 44% and 48% for first mode of vibration and 17%, 29%, 29% and 29% for the second mode of vibration respectively (Figures 3.135 to 3.138).

The response curves for horizontal vibrations of block foundation over reinforced sand beds indicate that the resonant frequencies and maximum amplitudes for both the modes of vibration decrease as compared with the corresponding values for horizontal vibrations of block over unreinforced sand bed. In view of the above, it can be said that the decrease in the resonant frequencies and maximum amplitudes is more with increase in number and size of reinforcement layers, in general. The decrease in maximum amplitude values is more as compared to that in resonant frequencies and depends upon the force level. The reductions in resonant frequencies, for a given reinforced sand bed, also depend upon the force level. The maximum amplitudes decrease by a maximum of 48% whereas the maximum decrease in the resonant frequencies is 28%. Also, the reductions in resonant frequency and maximum amplitude values for first mode of vibration are more than those for the second mode.

The reduction in natural frequencies is possibly due to the low modulus of geogrid material and practically negligible mobilization of interface friction

between sand and reinforcement at low strain levels associated with horizontal vibrations tests.

4.4.3 Analysis of Amplitude-Frequency Data

The amplitude-frequency data of horizontal vibration tests is analysed to obtain the damping ratios ξ_1 and ξ_2 , amplitude/width ratios and the values of coefficient of elastic uniform shear for the first and second modes of vibration. The ratio of the dynamic force for first mode of vibration to weight of block F_1/W , has also been calculated. From the amplitude frequency curves, the maximum amplitudes $(A_{x1})_{\max}$ and $(A_{x2})_{\max}$ and the resonant frequencies f_{nx1} and f_{nx2} for the first and second modes of vibration are noted down. The damping ratios ξ_1 and ξ_2 are obtained from the response curves using the bandwidth method, because the response curves are nearly symmetrical :

$$\xi_1 = \frac{f_2 - f_1}{2f_{nx1}} \quad \dots(4.13)$$

where f_1 and f_2 are the frequency values corresponding to the amplitude $(A_{x1})_{\max}/\sqrt{2}$ on the first peak.

The values of damping ratios ξ_2 for the second mode of vibration have been calculated similarly.

The coefficient of elastic uniform shear C_τ is calculated by using the expression : [IS:5249-1977].

$$C_\tau = \frac{8\pi^2 \gamma' f_{nx1,2}^2}{(A_0 + I_0) \pm \sqrt{(A_0 + I_0)^2 - 4\gamma' A_0 I_0}} \quad \dots(4.14)$$

where $\gamma' = \frac{M_m}{M_{m0}}$

M_m = mass moment of inertia of block, oscillator, motor etc., about the horizontal axis passing through the centre of gravity of the block and perpendicular to the direction of vibration.

M_{m0} = mass moment of inertia of block, oscillator, motor etc. about the horizontal axis passing through the centre of contact area of block and soil and perpendicular to the direction of vibration.

$f_{nx1,2}$ = horizontal resonant frequencies of the block soil system in first and second modes of vibration

$A_0 = A/M$, A = area of block foundation

M = mass of the block

$$I_0 = 3.46 \frac{I}{M_{m0}} \quad [\text{Table 3.4}]$$

I = moment of inertia of the foundation contact area about the horizontal axis passing through the centre of gravity of area and perpendicular to the direction of vibrations.

Using plus sign in expression (4.14) when f_{nx} corresponds to higher (second) natural frequency and minus sign when f_{nx} corresponds to lower (first) natural frequency;

for the test block in this investigation :

$$C_\tau = 103 f_{nx1}^2 \text{ kN/m}^3 \quad (\text{for first vibration mode})$$

$$\text{and } C_\tau = 15.6 f_{nx2}^2 \text{ kN/m}^3 \quad (\text{for second vibration mode})$$

The C_τ values are corrected to confining pressure of 100 kN/m² and footing area of 10m² [Prakash & Puri, 1981].

$$C_{\tau 100} = C_\tau \sqrt{\frac{100}{\bar{\sigma}_0}} \quad \dots(4.15)$$

where $\bar{\sigma}_0$ is the mean effective confining pressure at a depth equal to one half the width of block and is calculated as explained in 4.3.3. The corrected value of coefficient of elastic uniform shear $(C_{\tau 100})_{10}$ is calculated as

$$(C_{\tau 100})_{10} = C_{\tau 100} (A/10)^{1/2} \quad \dots(4.16)$$

where A is the area of block foundation in m².

The corrected values of coefficient of elastic uniform shear $(C_{\tau 100})_{10}$ are listed in Table 4.7. It is observed that the values of coefficient of elastic uniform shear obtained from both the modes of vibration are nearly the same.

The amplitude to width of block ratio for the first and second modes of vibration have been determined and are also presented in Table 4.7.

The ratio of the dynamic force for the first mode of vibration to the weight of block, F_1/W is calculated as :

$$F_1/W = \frac{0.00507f_{nx1}^2 \sin\theta/2}{W} \quad \dots(4.17)$$

where θ is the setting of angle of the eccentric mass of the oscillator.

The analysed data for horizontal vibration tests are presented in Table 4.7.

4.4.4 Effect of F_1/W on Resonant Frequencies and Damping Ratios

The resonant frequencies for both the modes of vibration in horizontal vibration tests decrease slightly for unreinforced and reinforced sand beds with the increase in dynamic force levels as discussed earlier in 4.4.2. As an illustration, as F_1/W ratio increases from 0.0181 to 0.1030, the resonant frequency for first mode of vibration decreases from 21 Hz to 19 Hz for the unreinforced sand bed. Similarly, for the sand bed reinforced with 2 layers of 800mm×400mm geogrid, the resonant frequency for the first mode of vibration decreases from 18 Hz to 16 Hz with increase in F_1/W from 0.0133 to 0.0730 as given in Table 4.7. This decrease in resonant frequencies is possibly due to softening behaviour of soil with the increase in dynamic force level.

The damping ratios ξ_1 and ξ_2 for the unreinforced sand bed slightly decrease with increase in dynamic force level. The damping ratios ξ_1 and ξ_2 for the first and second modes of vibration, follow a mixed trend with dynamic force levels, for the reinforced sand beds as is observed from the values given in Table 4.7. The variation of damping ratio ξ_1 with F_1/W for unreinforced and reinforced sand beds is illustrated in the Figures 4.54 to 4.59.

4.4.5 Effect of Reinforcement on Damping Ratios ξ_1 and ξ_2

The damping ratios ξ_1 and ξ_2 for the first and second modes of vibration are given in Table 4.7. The variation of damping ratio ξ_1 with the ratio of dynamic force to weight of block F_1/W for the sand beds reinforced with different sizes and number of reinforcement layers, and the unreinforced sand bed is shown in Figures 4.54 to 4.59. For the unreinforced sand, ξ_1 slightly decreases with increase in F_1/W . For the reinforced sand beds, ξ_1 is found to increase slightly with increase in number of reinforcement layers, in general, but a definite trend of variation of damping ratio ξ_1 can not be established with the increase in size of reinforcement layers. The damping ratio ξ_1 , however, increases upon reinforcing the sand bed with geogrid layers. A similar trend is observed for the damping ratio ξ_2 for the reinforced sand beds. The increase in damping ratio in reinforced sand beds may be because of the dissipation of energy at the surfaces of the reinforcements, but the increase is not as much as for vertical vibration tests on the reinforced sand beds.

4.4.6 Amplitude/Width Ratio versus F_1/W

The maximum amplitudes for both the modes of vibration increase with increase in force level as discussed in 4.4.2. The amplitude to width ratio increases with increase in force level F_1/W both for unreinforced and reinforced sand beds as shown in Table 4.7.

Figures 4.42 to 4.47 show the variation of the amplitude/width ratio with the ratio of dynamic force to weight of block F_1/W , for first mode of vibration for the unreinforced and reinforced sand beds. It is observed that the amplitude/width ratio increases with the increase in F_1/W for the unreinforced and the reinforced sand beds. For a given value of F_1/W less than 0.03 nearly, the amplitude/width ratio for the reinforced sand beds is less than that for the unreinforced sand bed. For F_1/W greater than 0.03, it is more for the reinforced sand beds than for the unreinforced sand bed.

4.4.7 Amplitude Reduction Factor versus Number of Reinforcement Layers

The decrease in amplitudes for both modes of vibration is generally more with increase in number of geogrid layers of all the sizes as discussed in 4.4.2.

The amplitude reduction factor, which is the ratio of the maximum amplitude of the horizontal vibration of block on reinforced sand bed to the corresponding value of maximum amplitude of horizontal vibrations of block on unreinforced sand bed, is plotted with respect to the number of reinforcement layers of various sizes in Figures 4.60 to 4.67 for the first mode of vibration. The maximum amplitude is reduced upto 48% with the increase in number and size of geogrid layers in the reinforced sand bed. After the number of geogrid layers increases to four, the reduction in amplitude is very less and the amplitude is observed to attain a nearly constant value. A similar trend is observed for the maximum amplitude in second mode of vibration.

4.4.8 Coefficient of Elastic Uniform Shear $(C_{\tau 100})_{10}$ versus Number of Reinforcement Layers

The values of coefficient of elastic uniform shear $(C_{\tau 100})_{10}$ for the unreinforced and reinforced sand beds determined by using expression (4.14) and corrected for confining pressure and footing area are given in Table 4.7. The coefficient of elastic uniform shear for the sand bed reinforced with two geogrid layers of size 800mm×400mm is less by 26% to 29% from the $(C_{\tau 100})_{10}$ values for the unreinforced sand bed depending upon the dynamic force level. For the sand bed reinforced with 3 geogrid layers of the same size, the values of $(C_{\tau 100})_{10}$ decrease by 30% to 33% as compared to the corresponding values for the unreinforced sand bed. Similarly, for 4 and 6 layers of geogrid of same size, the $(C_{\tau 100})_{10}$ values decrease by 26% to 33% and 29% to 35% respectively compared with the values of $(C_{\tau 100})_{10}$ for the unreinforced sand bed at the corresponding force levels. The values of $(C_{\tau 100})_{10}$, therefore, decrease with the introduction of geogrid layers in sand bed and the decrease is more with increase in number of

reinforcement layers.

When the sand bed is reinforced with 2,3,4 and 6 layers of size 1200mm×600mm, the reductions in $(C_{\tau 100})_{10}$ values are in the range of 24% to 30%, 32% to 34%, 35% to 45% and 35% to 37% respectively; compared with the corresponding values of $(C_{\tau 100})_{10}$ for unreinforced sand bed. It is observed that the decrease in $(C_{\tau 100})_{10}$ values is somewhat more for larger size of reinforcement. For the sand bed reinforced with 2,3,4 and 6 layers of size 1500mm×750mm, the decrease in $(C_{\tau 100})_{10}$ values is in the range of 33% to 37%, 28% to 41%, 29% to 36% and 37% to 42% respectively; as compared to the corresponding values for the unreinforced sand bed. The decrease in $(C_{\tau 100})_{10}$ values is further more for this case as compared to reinforcements of smaller size.

The decrease in $(C_{\tau 100})_{10}$ values for the sand bed reinforced with 2,3,4 and 6 layers of 1000mm×1000mm geogrid is in the range of 29% to 34%, 43% to 48%, 40% to 45% and 34% to 48% respectively; compared with the corresponding values for the unreinforced sand bed. The $(C_{\tau 100})_{10}$ values decrease upto a maximum of 48% for this case.

The coefficient of elastic uniform shear decreases in the range of 32% to 38%, 35% to 38%, 40% to 42% and 40% to 42% for the sand bed reinforced with 2,3,4 and 6 layers of 1200mm×1200mm geogrid as compared to the corresponding values for the unreinforced sand bed. Thus the maximum decrease in $(C_{\tau 100})_{10}$ values is 42% for this case.

When the sand bed is reinforced with 2,3,4 and 6 layers of 1500mm×1500mm geogrid, the decrease in $(C_{\tau 100})_{10}$ values is in the range of 33% to 38%, 37% to 43%, 34% to 41% and 34% to 44% respectively; compared with the corresponding values of $(C_{\tau 100})_{10}$ for the unreinforced sand bed. Thus, the decrease in $(C_{\tau 100})_{10}$ values is 44% for the maximum size and number of reinforcement layers used in this test programme.

From the above discussions, it can be seen that the coefficient of elastic uniform shear decreases with the increase in force level both for the unreinforced

and reinforced sand beds; indicating the softening behaviour of soil at higher force levels. The coefficient of elastic uniform shear decreases upon reinforcing the sand bed with geogrid, compared to its values for the unreinforced sand bed at the corresponding force levels. The decrease in $(C_{\tau 100})_{10}$ values is observed to be more with the increase in number of reinforcement layers for all reinforcement sizes.

The values of coefficient of elastic uniform shear calculated by using the expression (4.14) and corrected for confining pressure and area of footing, $(C_{\tau 100})_{10}$ are interpreted at strain levels of 2×10^{-4} , 4×10^{-4} and 6×10^{-4} . The corresponding values of dynamic force level to weight of block, F_1/W ratio are also interpreted. All these interpreted values are listed in Table 4.9. The variation of $(C_{\tau 100})_{10}$ with number of geogrid layers of different sizes is shown in Figure 4.68 at a strain level of 2×10^{-4} . A decrease of upto 44% is observed in values of $(C_{\tau 100})_{10}$, however, C_{τ} approaches a nearly constant value asymptotically for number of layers, $n=6$.

The decrease in the coefficient of elastic uniform shear of reinforced sand beds is possibly due to the low modulus of the geogrid material. Also, the interface friction between the geogrid layers and sand is not mobilised at low strain levels associated with horizontal vibration tests. Further, it is observed that the decrease in $(C_{\tau 100})_{10}$ values for the reinforced sand beds becomes somewhat less at higher strain levels as can be seen by comparing the values given in Table 4.9.

4.4.9 Coefficient of Elastic Uniform Shear $(C_{\tau 100})_{10}$ versus F_1/W

The coefficient of elastic uniform shear decreases with increase in force level for unreinforced as well as reinforced sand beds as discussed in 4.3.8. The values of coefficient of elastic uniform shear $(C_{\tau 100})_{10}$ at different F_1/W ratios are given in Table 4.7 and are interpolated at the same strain levels as shown in Table 4.9. As an illustration, the coefficient of elastic uniform shear decreases

from 3.01×10^4 kN/m³ to 2.46×10^4 kN/m³ as F_1/W increases from 0.0181 to 0.1030, for the unreinforced sand bed. Similarly, for the sand bed reinforced with 2 layers of 800mm×400mm geogrid, $(C_{\tau 100})_{10}$ decreases from 2.21×10^4 kN/m³ to 1.75×10^4 kN/m³ as F_1/W increases from 0.0133 to 0.0730.

The variation of coefficient of elastic uniform shear $(C_{\tau 100})_{10}$ with dynamic force to weight of block ratio, F_1/W for different reinforced sand beds is shown in Figures 4.48 to 4.53. $(C_{\tau 100})_{10}$ decreases with the increase in dynamic force level for the unreinforced as well as reinforced sand beds. It is observed that $(C_{\tau 100})_{10}$ for the reinforced sand beds decreases at nearly the same rate as $(C_{\tau 100})_{10}$ for the unreinforced sand bed. Also, at a given value of F_1/W , $(C_{\tau 100})_{10}$ decreases with increase in number of reinforcement layers, in general. The curves of $(C_{\tau 100})_{10}$ versus F_1/W for the reinforced sand beds lie in a close spectrum under the curve for the unreinforced sand bed.

4.4.10 Coefficient of Elastic Uniform Shear versus Size of Reinforcement

The coefficient of elastic uniform shear generally decreases with the increase in size of reinforcement as discussed in 4.4.8. From Table 4.9, it is observed that as the area ratio of reinforcement A_r (which is the ratio of the area of reinforcement layer to the base area of block) increases from 1.0 to 2.25; $(C_{\tau 100})_{10}$ decreases from 2.17×10^4 kN/m³ to 2.00×10^4 kN/m³ for two reinforcement layers at amplitude/width ratio of 2×10^{-4} . Similar behaviour is observed for other area ratios also but the rate of decrease in $(C_{\tau 100})_{10}$ is small at larger area ratios.

Figures 4.69 shows the variation of the ratio $(C_{\tau 100})_{10R}/(C_{\tau 100})_{10U}$ with the area ratio of reinforcement A_r for different numbers of reinforcement layers at amplitude/width ratio of 2×10^{-4} ; where $(C_{\tau 100})_{10R}$ and $(C_{\tau 100})_{10U}$ are the coefficients of elastic uniform shear for the reinforced and unreinforced sand beds respectively. It is observed that $(C_{\tau 100})_{10}$ is reduced upto 60% upon reinforcing the sand bed with geogrid layers. For area ratio $A_r=7$, $(C_{\tau 100})_{10}$

reaches asymptotically constant value. Similar trend is observed for the variation of coefficient of elastic uniform shear with area of reinforcement at higher strain levels also.

4.4.11 Comparison of $(C_{u100})_{10}$ and $(C_{\tau100})_{10}$

Upon comparing the values of coefficient of elastic uniform compression $(C_{u100})_{10}$ listed in Table 4.6 with the corresponding values of coefficient of elastic uniform shear $(C_{\tau100})_{10}$ listed in Table 4.7, for the unreinforced and reinforced sand beds, it is observed that $(C_{u100})_{10}/(C_{\tau100})_{10}$ ratio varies from 2.80 to 2.95 for the unreinforced sand bed and it varies from 3.2 to 3.9 for the reinforced sand beds. Barkan (1962) has mentioned that for fine gray sand, C_u/C_τ ratio varies from 2.20 to 2.40.

4.4.12 Discussion Summary

The resonant frequencies for the first and second modes of vibration are reduced by the maximum of 28% and 20% respectively whereas the maximum amplitudes are reduced by the maximum of 48% and 41% respectively depending upon the size and number of geogrid layers. The damping ratios ξ_1 and ξ_2 increase depending upon the configuration and number of the reinforcement layers in the reinforced sand bed. The coefficient of elastic uniform shear is reduced by the maximum of 48%, the decrease being dependent upon the size and number of the reinforcement layers in the sand bed. The reinforced sand bed, therefore, gives reduced amplitudes and improved damping capacity but the coefficient of elastic uniform shear is reduced. The decrease in the resonant frequencies and coefficient of elastic uniform shear seems to be due to low modulus of geogrid material and negligible mobilization of interface friction between the sand and reinforcements at low strain levels associated with horizontal vibration tests.

4.5 NON-DIMENSIONAL CORRELATIONS

4.5.1 General

Non dimensional correlations have been developed through the regression analysis of the data obtained from cyclic plate load and vertical and horizontal block vibration tests. The computer software SIGMAPLOT has been used for the regression analysis of the experimental data. Non-dimensional correlations have been obtained from cyclic plate load test data for the ultimate bearing capacity ratio, settlement ratio, coefficient of elastic uniform compression and the damping capacity ratio. Also, non-dimensional correlations have been obtained from vertical and horizontal vibration test data for coefficient of elastic uniform compression, coefficient of elastic uniform shear, damping ratios and the amplitude reduction factors.

4.5.2 Cyclic Plate Load Tests

4.5.2.1 Coefficient of Elastic Uniform Compression

The regression analysis of the test data listed in Table 4.2 for the coefficient of elastic uniform compression has been carried out. Various polynomials of single to higher degrees have been tested bringing out the following expressions as the best fit of the data :

For cyclic plate load tests on 150mm square footing, at relative density, $D_r=70\%$:

$$C_{uR}/C_{uU} = a_0 + a_1n + a_1n^2 + a_3n^3 + a_4n^4 \quad \dots(4.18)$$

where n is the number of reinforcement layers. The values of the polynomial coefficients for different area ratios A_r , of the reinforcement area to the footing area are listed in Table 4.10.a. The coefficient of correlation ranges from 0.97 to 0.99. For cyclic plate load tests on 150mm square footing at $D_r=50\%$ and 300 mm square footing at $D_r=70\%$, for four reinforcement layers:

$$C_{uR}/C_{uU} = a_0 + a_1B'_r + a_2B'^2_r + a_3B'^3_r + a_4B'^4_r \quad \dots(4.19)$$

where

$$B'_r = \sqrt{A_r} \quad \text{and}$$

C_{uR} and C_{uU} are the coefficients of elastic uniform compression for the reinforced and unreinforced sand beds respectively.

The polynomial coefficients a_0 , a_1 , etc., and coefficients of correlation are given in Table 4.10b.

4.5.2.2 Damping Capacity Ratio

The regression analysis of the data for the damping capacity ratio D_{cr} listed in Table 4.2 has been carried out and a polynomial of fourth degree is found to give the best fit of the data.

For 150mm square footing at $D_r=70\%$:

$$D_{cr} = a_0 + a_1n + a_2n^2 + a_3n^3 + a_4n^4 \quad \dots(4.20)$$

The coefficients of polynomial and coefficients of correlation are given in Table 4.11a.

For 150mm square footing at $D_r=50\%$ and 300mm square footing at $D_r=70\%$, for four reinforcement layers:

$$D_{cr} = a_0 + a_1B'_r + a_2B'^2_r + a_3B'^3_r + a_4B'^4_r \quad \dots(4.21)$$

The coefficients of the polynomial and the coefficients of correlation are given in Table 4.11b.

4.5.2.3 Ultimate Bearing Capacity Ratio, BCR

The values of ultimate bearing capacity ratio (BCR), q_{uR}/q_{uU} given in Table 4.2 have been analysed.

A polynomial of fifth degree gives the best fit of the data.

For 150mm square footing at $D_r=70\%$:

$$BCR = a_0 + a_1n + a_2n^2 + a_3n^3 + a_4n^4 + a_5n^5 \quad \dots(4.22)$$

The polynomial coefficients and coefficient of correlation are given in Table 4.12a. Similarly for 150mm square footing at $D_r=50\%$ and 300mm square footing at $D_r=70\%$ and number of layers $n=4$:

$$BCR = a_0 + a_1B'_r + a_2B'^2_r + a_3B'^3_r + a_4B'^4_r + a_5B'^5_r \quad \dots(4.23)$$

The polynomial coefficients and coefficients of correlation are given in Table 4.12b.

4.5.2.4 Settlement Ratio (SR)

The regression analysis of the data for the settlement ratio (SR), given in the Table 4.2, shows that a polynomial of third degree provides the best fit.

For the footing of size 150mm square at $D_r=70\%$:

$$SR = a_0 + a_1n + a_2n^2 + a_3n^3 \quad \dots(4.24)$$

Similarly, for 150mm square footing at $D_r=50\%$ and 300mm square footing at $D_r=70\%$ and for four geogrid layers:

$$SR = a_0 + a_1B'_r + a_2B'^2_r + a_3B'^3_r \quad \dots(4.25)$$

The results of the regression analysis are given in Tables 4.13 a and b.

4.5.3 Vertical Vibration Tests

4.5.3.1 Coefficient of Elastic Uniform Compression $(C_{u100})_{10}$

The data for the regression analysis has been interpolated from Table 4.8 and Figures 4.32 to 4.37 at various values of F/W ranging from 0.1 to 0.5. Regression analysis has been carried out and the following expression in terms of the natural logarithm provides the best fit of the test data :

$$(C_{u100})_{10R}/(C_{u100})_{10U} = \exp (a_0 + a_1n + a_2n^2) \quad \dots(4.26)$$

where \exp stands for the exponential. $(C_{u100})_{10R}$ and $(C_{u100})_{10U}$ are the coefficients of elastic uniform compression for the reinforced and unreinforced sand beds respectively, and n is number of geogrid layers.

The coefficients of the polynomial for different values of area ratio of reinforcement, A_r and F/W are listed in Table 4.14. The coefficient of correlation ranges from 0.96 to 0.99.

A generalised expression has been developed to determine the coefficient of elastic uniform compression of the reinforced sand bed in terms of the area ratio A_r , number of layers of reinforcement n and F/W as :

$$(C_{u100})_{10R}/(C_{u100})_{10U} = 1 - 0.11(1.01 - 0.1 F/W)\sqrt{A_r} e^{-0.5A_r^{0.5}/n^{2.19}} \quad \dots(4.27)$$

which gives the coefficient of correlation, as 0.99.

4.5.3.2 Damping Ratio ξ

The data for the regression analysis of the damping ratio ξ has been interpolated from the Figures 4.12 to 4.17 at F/W ratios of 0.1 to 0.5. It is observed that a polynomial of second degree gives the best fit to the data as:

$$\xi_R/\xi_U = a_0 + a_1n + a_2n^2 \quad \dots(4.28)$$

where ξ_R and ξ_U are the damping ratios for the reinforced and unreinforced sand beds respectively. The coefficients of the polynomial for different values of A_r and F/W are listed in Table 4.16. The coefficient of correlation varies from 0.95 to 0.99.

4.5.3.3 Amplitude Reduction Factor

The data for the regression analysis of the amplitude reduction factor $(A_{zmax})_r/(A_{zmax})_u$ has been worked out from Table 4.6. The following polynomial gives the best fit to the data:

$$(A_{zmax})_r/(A_{zmax})_u = a_0 + a_1n + a_2n^2 + a_3n^3 + a_4n^4 \quad \dots(4.29)$$

where $(A_{zmax})_r$ and $(A_{zmax})_u$ are the maximum amplitudes of vertical vibration of block over the reinforced and unreinforced sand beds respectively. The coefficients of the polynomial for various area ratios A_r and eccentricity values e are given in Table 4.18. The coefficient of correlation is found to be 1.

4.5.4 Horizontal Vibration Tests

4.5.4.1 Coefficient of Elastic Uniform Shear $(C_{\tau 100})_{10}$

The regression analysis has been carried out using the data interpolated from Table 4.9 and Figures 4.48 to 4.53 for different values of F_1/W ranging from 0.02 to 0.08. The best fit is provided by the following polynomial in terms of the natural logarithm:

$$(C_{\tau 100})_{10R}/(C_{\tau 100})_{10U} = \exp (a_0 + a_1 n + a_2 n^2) \quad \dots(4.30)$$

where $(C_{\tau 100})_{10R}$ and $(C_{\tau 100})_{10U}$ are the coefficients of elastic uniform shear for the reinforced and unreinforced sand beds and n is the number of reinforcement layers of geogrid. The coefficients of the polynomial for different values of A_r and F_1/W (for the first mode of vibration) are listed in Table 4.15. The coefficient of correlation varies from 0.93 to 0.99.

4.5.4.2 Damping Ratio ξ_1

The data for the regression analysis of the damping ratio ξ_1 for the first mode of vibration has been interpolated from the Figures 4.54 to 4.59 at different F_1/W ratios varying from 0.02 to 0.08. A polynomial of second degree gives the best fit to the data.

$$\xi_{1R}/\xi_{1U} = a_0 + a_1 n + a_2 n^2 \quad \dots(4.31)$$

where ξ_{1R} and ξ_{1U} are the damping ratios for the reinforced and unreinforced sand beds respectively. The coefficients of the polynomial are listed in Table 4.17 for different values of area ratio A_r and F_1/W . The coefficient of correlation varies from 0.92 to 0.99, except for two cases.

4.5.4.3 Amplitude Reduction Factor

The regression analysis has been carried out using the data worked out from Table 4.6. The following polynomial gives the best fit to the data :

$$(A_{x1max})_r/(A_{x1max})_u = a_0 + a_1 n + a_2 n^2 + a_3 n^3 + a_4 n^4 \quad \dots(4.32)$$

where $(A_{x1max})_r$ and $(A_{x1max})_u$ are the maximum amplitudes of vibration in the first mode for reinforced and unreinforced sand beds respectively and n is the number of reinforcement layers. The coefficients of the polynomial for different eccentricity values θ and area ratios A_r are given in Table 4.19. The coefficient of correlation is found to be 1.

4.5.5 Discussion Summary

The non-dimensional correlations add to the understanding of the variation of the different parameters with the number and size of reinforcement layers. These correlations reveal that the effect of the ratio of dynamic force, to weight of block F/W is not significant on the damping ratio ξ , and coefficient of elastic uniform compression C_u , in the vertical vibration tests. Also in the horizontal vibration tests, the effect of F_1/W is not much more pronounced on C_τ and ξ_1 , whereas it is significant on the amplitude reduction factors. The non-dimensional correlations can be used to determine the values of different parameters of a sand bed reinforced with given number and size of reinforcement layers. The parameters determined thus, can be used for the design purposes.

4.6 EQUIVALENT PARAMETER ANALYSIS

4.6.1 General

The stiffness or spring constant of the supporting soil is the most important property required in the design of foundations subjected to dynamic loads. For a soil mass containing layers, the idealisation of the soil layers as springs in series gives the same value of stiffness regardless of their thickness, extent and location with respect to the foundation base. Reinforced soil consists of a combination of layers of reinforcement embedded in the soil mass at different locations below the foundation base. The size and thickness of the layers may be different as can be their moduli and surface characteristics.

In reinforced earth mass, under static loading conditions, the transfer of

load is dependent upon the mobilised angle of interface friction at the particular reinforcement level. The mobilisation of the interfacial friction depends upon the relative displacement between the soil and the reinforcement layer. The relative displacements between soil and reinforcement or the strain levels in block vibration tests are too small to mobilise the interface friction of appreciable magnitude. The reinforcing effect of the reinforcements through the mobilisation of interface friction may not contribute appreciably to the stiffness of the reinforced soil mass at low strain levels. The contribution to the stiffness of reinforced soil comes through the stiffness or modulus of the reinforcing material. As the strain level increases, the interface friction between the soil and reinforcement is also mobilised and therefore, it contributes to the stiffness of the reinforced soil mass. In general, it can be concluded that the reinforcements in the reinforced soil can contribute to the overall stiffness of the soil mass in two ways namely, the contribution from the modulus of the reinforcing material and the contribution due to the mobilisation of interface friction between the soil and the reinforcing material. At low strain levels such as those occurring in block vibration tests, the contribution from the second factor is almost non-existent and only the first factor contributes to the overall stiffness of the composite reinforced soil. As the strain levels increase and approach appreciable magnitudes such as those occurring in cyclic plate load tests, the mobilisation of the interface friction starts and therefore, it also contributes towards the overall stiffness of the reinforced soil mass. Further, the modulus degradation in soil with increase in strain level is faster than in the reinforcement. The overall stiffness of the reinforced soil should depend upon (i) modulus of the soil, (ii) the modulus of the reinforcement and (iii) size, thickness, surface texture, location and displacement of reinforcement relative to soil, which governs the contribution due to the mobilisation of the interface friction. This concept forms the basis for the equivalent parameter analysis proposed for determining equivalent stiffness of reinforced soil mass.

4.6.2 Analysis

In the design of foundations such as for the machines, the soil is idealised as an elastic half space or mass-spring-dashpot system. The dynamic response of the reinforced soil can be analyzed by replacing the layered soil mass by an equivalent homogeneous soil with equivalent parameters. The analysis is based upon the equivalence of the displacements of the layered reinforced soil mass with that of an equivalent homogeneous soil. It utilizes a numerical procedure to determine the equivalent coefficient of elastic uniform compression of the reinforced soil from the coefficient of elastic uniform compression of the unreinforced soil and the modulus of the reinforcements, depending upon their number, size, extent and location below the footing base.

4.6.2.1 Assumptions

The following simplifying assumptions have been made in the analysis :

- (i) The reinforced soil mass is homogeneous, elastic and cohesionless.
- (ii) The stress distribution in the reinforced soil mass is governed by Boussinesq theory irrespective of the fact whether the soil is reinforced or not.
- (iii) The effective depth of influence is taken to be three times the width of footing.
- (iv) The soil mass is supported over a hard stratum.
- (v) The layers of soil and reinforcement are perfectly horizontal and their individual properties do not vary with thickness.
- (vi) The mobilisation of interface friction between the soil and reinforcement is negligibly small at low strain levels.
- (vii) The foundation is rigid and there is no relative displacement between it and the soil.

- (vii) There exists a linear relationship between the displacement of the foundation and the reactions offered by the soil which is expressed in terms of elastic constants.

4.6.2.2 Justification of Assumptions

The assumptions made in the analysis are justified as discussed below:

- (i) The soil is assumed to be homogeneous, elastic and cohesionless. In reinforced earth, the soil used is normally cohesionless. The soil is assumed to be elastic at low strain levels. In vertical vibration tests, the strain levels are small and this assumption is justified [Richart et al., 1970]. Since the quantity of reinforcement is small in the reinforced soil, it can be taken as homogeneous at macro-level [Binquet and Lee, 1975b].
- (ii) The stress distribution in the reinforced soil mass is governed by Boussinesq equation. Akai et al. (1971) have verified that Boussinesq theory is applicable to layered soil without significant loss of accuracy. Binquet & Lee (1975b) have assumed the stress distribution in the reinforced soil to be governed by Boussinesq theory.
- (iii) The effective depth of influence is taken to be 3 times the width of footing. Based upon the observations of Eastwood (1953) and Arnold et al. (1955), the effective depth is assumed to be three times the width of footing. Sridharan et al. (1990b) have also considered the same effective depth in analysis.
- (iv) The soil mass is supported over hard stratum. The sand is deposited in rigid test tanks and therefore, this assumption is valid.
- (v) The layers of soil and reinforcement are perfectly horizontal and their individual properties do not vary with thickness. Sridharan et al. (1990b) have taken this assumption to be valid in the analysis of the stiffness of

layered soils. At low strain levels, such as those occurring in block vibration tests, the soil and reinforcement layers normally remain horizontal and their individual properties normally remain the same.

- (vi) The mobilisation of the interface friction between the soil and reinforcement is negligible at low strains. This assumption is justified since the interface friction is mobilised when the displacement between the soil and reinforcement is appreciable [Binquet & Lee, 1975b, Srinivasa-Murthy et al., 1993]. Shewbridge and Sousa (1991) have brought out that the effect of reinforcement on dynamic properties of reinforced sand can be neglected at strain levels $< 5\%$. Murray et al. (1979) have shown that the angle of shearing resistance between soil and reinforcement is reduced under vibrations.
- (vii) The foundation is rigid and there is no relative displacement between it and soil. The assumption is justified as the foundation is rigid and soil is compressible, the relative displacement between the foundation and soil at low strains is almost non-existent.
- (viii) The linear relationship between the displacement of the foundation and reactions offered by the soil has been expressed in terms of the elastic constants by Barkan (1962).

4.6.2.3 Analytical Formulation

The analysis is based upon the equivalence of the displacements of individual soil and reinforcement layers with those of an equivalent homogeneous soil mass. Consider a reinforced soil mass consisting of N soil layers and n reinforcement layers placed in between. The analysis is based upon Boussinesq theory and can be used for any number of layers. A soil mass of depth $3B$ and of lateral extent $5B$ is considered for the purpose of analysis as shown in Figure 4.70; B being the width of the footing.

For unreinforced soil :

Let, E_0 = overall elastic modulus of unreinforced soil.

$E_1, E_2, \dots, E_i, \dots, E_N$ be the elastic moduli of N soil layers

Let $H_1, H_2, \dots, H_i, \dots, H_N$ be the thicknesses of N soil layers.

Based upon the equivalence of the displacement of the soil mass to the sum of the displacements of individual soil layers, the following expression is obtained.

$$\frac{\sigma_1 H_1}{E_0} + \frac{\sigma_2 H_2}{E_0} + \dots + \frac{\sigma_N H_N}{E_0} = \frac{\sigma_1 H_1}{E_1} + \frac{\sigma_2 H_2}{E_2} + \dots + \frac{\sigma_N H_N}{E_N} \quad \dots(4.33)$$

$$\text{or } \sum (\sigma_i H_i) / E_0 = \sum (\sigma_i H_i / E_i) \quad \dots(4.34)$$

where $\sigma_1, \sigma_2, \dots, \sigma_i, \dots, \sigma_N$ are the average vertical stress values at the centres of the respective soil layers. The average vertical stress value at the centre of the soil layer is determined by calculating the vertical stresses at different points at the centre of the layer of lateral extent $5B$ (say) at certain intervals (say, $0.25 B$ or less depending upon the accuracy desired), summing up all the stress values and dividing the sum by the number of stress ordinates. The vertical stress values have been calculated using a computer program based upon the solution for the indefinite integral in Boussinesq equation provided by Damy and Casales (1985).

If soil is reinforced with 'n' layers of reinforcement of size $L_{Rn} \times B_{Rn}$ and thicknesses $H_{R1}, H_{R2}, \dots, H_{Ri}, \dots, H_{Rn}$ the equivalent elastic modulus of the reinforced soil mass, considered to be homogeneous, can be calculated from the expression :

$$E_{SR} = \frac{(\sigma_1 H_1 + \sigma_2 H_2 + \dots + \sigma_N H_N) + (\sigma_{R1} H_{R1} + \sigma_{R2} H_{R2} + \dots + \sigma_{Rn} H_{Rn})}{\left[\frac{\sigma_1 H_1}{E_1} + \frac{\sigma_2 H_2}{E_2} + \dots + \frac{\sigma_N H_N}{E_N} \right] + \left[\frac{\sigma_{R1} H_{R1}}{E_{R1}} + \frac{\sigma_{R2} H_{R2}}{E_{R2}} + \dots + \frac{\sigma_{Rn} H_{Rn}}{E_{Rn}} \right]} \quad \dots(4.35)$$

Simplifying and substituting the value of $\sum(\sigma_i H_i / E_i)$ from Eqn.(4.34)

$$E_{SR} = \frac{\sum \sigma_i H_i + \sum \sigma_{Rj} H_{Rj}}{(\sum \sigma_i H_i) / E_0 + \sum (\sigma_{Rj} H_{Rj} / E_{Rj})} \quad \dots(4.36)$$

where

$$i = 1 \text{ to } N, \quad j = 1 \text{ to } n$$

E_{SR} = equivalent modulus of the composite reinforced soil mass.

$\sigma_{R1}, \sigma_{R2}, \dots, \sigma_{Rj}, \dots, \sigma_{Rn}$ are the average vertical stress values at the centres of the reinforcement layers of size $L_{Rn} \times B_{Rn}$ calculated as for the soil layers.

$E_{R1}, E_{R2}, \dots, E_{Rj}, \dots, E_{Rn}$ are the elastic moduli of the reinforcement layers 1, 2, ..., j, ..., N.

and

From E_{SR} , the coefficient of elastic uniform compression of the reinforced soil, C_{uSR} can be obtained as (Barkan, 1962 and IS:5249-1977).

$$C_{uSR} = \frac{1.13 E_{SR}}{(1-\nu^2) \sqrt{A}} \quad \dots(4.37)$$

where ν is the Poisson's ratio and A is the base area of the footing.

4.6.3 Application of the Analysis to Vertical Vibration Tests

The strain levels in the vertical vibration tests are very small to mobilise the interface friction between the soil and geogrid reinforcements. The stiffness of reinforced soil will depend upon the individual stiffnesses of the soil and geogrid material and the contribution from the interface friction is assumed to be negligible. The equivalent parameter analysis has been used to estimate the equivalent coefficient of elastic uniform compression of reinforced sand bed under vertical vibrations.

A soil mass of lateral extent $3.75B$ and depth $2.5B$ has been considered in the analysis (equal to the dimensions of the test tank); where B is the width of the block. The soil mass is divided into ten layers of thickness $0.25B$ each. The average vertical stresses $\sigma_1, \sigma_2, \dots, \sigma_{10}$ at the centres of the layers are calculated by adding up the vertical stresses determined at lateral intervals of $0.25B$ and dividing the sum by the number of stress ordinates.

From the elastic modulus E_0 of sand, it is obtained :

$$\sum(\sigma_i/E_i) = \sum\sigma_i/E_0 \quad \dots(4.38)$$

by substituting $H_1 = H_2 = \dots = H_{10} = 0.25B$ in equation (4.34). The elastic modulus E_0 of sand has been determined from the coefficient of elastic uniform compression as :

$$E_0 = \frac{(1 - \nu^2)\sqrt{A}}{1.13} C_u \quad \dots(4.39)$$

As an illustration :

Width of block $B=0.4\text{m}$

$H_1 = H_2 = \dots = H_{10} = 0.1\text{m}$

From Table 4.6, at $\theta = 4^\circ$

$C_u = 1.3 \times 10^5 \text{ kN/m}^3$

From Table 4.1, $\nu = 0.2631$ (at $D_r = 70\%$)

$E_0 = 6.06 \times 10^4 \text{ kN/m}^3$

Let the soil be reinforced with two geogrid layers of size equal to size of block, provided at depths $0.25 B$ and $0.5 B$ below the base of block.

For Netlon CE - 121, from Figure 3.3,

$E_R = 1.859 \times 10^4 \text{ kN/m}^2$ and,

$H_R = 0.0033 \text{ m}$

The average vertical stress values over the reinforcement layers are determined as already mentioned in 4.6.2.3.

Substituting the values of the average vertical stresses over the soil and reinforcement layers, their elastic moduli and the thickness values in expression (4.36) :

$$E_{SR} = 5.68 \times 10^4 \text{ kN/m}^2$$

Substituting the value of E_{SR} in equation (4.37)

$$C_{uSR} = 1.22 \times 10^5 \text{ kN/m}^3$$

$$\text{Observed value of } C_{uSR} = 1.17 \times 10^5 \text{ kN/m}^3$$

$$\text{Difference} = 4.1\% \text{ (Table 4.20).}$$

The values of C_{uSR} for different reinforced sand beds at different force levels are calculated and are compared with the experimental values in Table 4.20. The predicted values are on the higher side of the observed values. These results show that the equivalent parameter analysis, overestimate the values of the coefficient of elastic uniform compression by 5% to 20% of the experimentally observed values. This is because of the simplifying assumptions in the analysis. Further, the geogrid layers are assumed to be continuous whereas they actually contain holes of size 8mm×6mm. The predicted and the observed values are plotted in Figure 4.71 which shows that the analysis overestimates the values of the coefficient of elastic uniform compression of the reinforced soil under vertical vibrations.

4.6.4 Application of the Analysis to Cyclic Plate Load Tests

The analysis has been applied to calculate the coefficient of elastic uniform compression of reinforced sand under cyclic loads ignoring the direct consideration of the mobilisation of interface friction at the strain levels involved.

A soil mass of depth 3B and lateral extent 5B has been considered, where B is the width of the footing. The soil is divided into 12 layers of thickness 0.25 B

each. The average vertical stresses at the centres of the layers have been calculated as already explained in 4.6.2.3.

From the elastic modulus E_0 of sand, $\sum(\sigma_i/E_i)$ has been determined using the equation (4.38) by substituting $H_1=H_2=\dots=H_{12}=0.25B$.

where E_0 has been calculated using the expression (4.39).

As an illustration, width of footing = 0.15m

H_1 etc. = 0.0375 m.

From the cyclic plate load tests on unreinforced sand, Table 4.2, at $D_r=70\%$.

$$C_u = 2.69 \times 10^5 \text{ kN/m}^3$$

and $\nu = 0.2631$

$$E_0 = \frac{(1-\nu^2)\sqrt{A}}{1.13} C_u = 3.32 \times 10^4 \text{ kN/m}^2$$

For geogrid Netlon CE-121,

$$E_R = 1.859 \times 10^4 \text{ kN/m}^2 \text{ [Figure 3.3]}$$

$$H_R = 0.0033\text{m}$$

Let the soil be reinforced with two layers of geogrid of size equal to the size of footing, provided at depths 0.25B and 0.5B, below the base of the footing. The average vertical stress values over the reinforcement layers are determined as mentioned in 4.6.2.3. Substituting the values of various parameters in equation (4.36).

$$E_{SR} = 3.15 \times 10^4 \text{ kN/m}^2$$

Substituting the value of E_{SR} in equation (4.37)

$$C_{uSR} = 2.55 \times 10^5 \text{ kN/m}^3$$

From Table 4.21, observed value of $C_{uSR}=2.22 \times 10^5 \text{ kN/m}^3$, Difference=12.9%.

Similarly the values of coefficient of elastic uniform compression for different reinforced sand beds have been calculated and are compared with the experimental values in Table 4.21. The predicted and the observed values of the coefficient of elastic uniform compression are plotted in Figure 4.72. It is observed that the analytical approach overestimates the values of the coefficient

of elastic uniform compression by 10% to 25%. This can be attributed to a number of simplified assumptions in the analysis.

4.6.5 Application of Analysis to Horizontal Vibration Tests

The analytical analysis has been extended to determine the coefficient of elastic uniform shear of the geogrid reinforced sand using the coefficient of elastic uniform shear of unreinforced sand and the shear modulus of geogrid. The strain levels associated with horizontal vibration tests are very small to mobilise the interface friction between sand and geogrid reinforcements. The horizontal stiffness of reinforced sand will depend upon the individual stiffness of sand and geogrid material and the contribution from the interface friction is assumed to be negligible.

The assumptions given in 4.6.2.1 are valid for the analysis. Further, the shear stresses have been calculated by using Cerutti's problem for the horizontal shear acting along the surface of a semi-infinite mass given by Poulos and Davis (1974).

The analysis is based upon the equivalence of the shear displacements of individual soil layer with that of an equivalent homogeneous soil mass. A soil mass of lateral extent $3.75 B$ and depth $2.5 B$ has been considered in the analysis (equal to the dimensions of test tank). The soil mass is divided into ten layers of thickness $0.25 B$ each. The average shear stresses $\tau_1, \tau_2, \dots, \tau_{10}$ at the centres of the layers are calculated by adding up the shear stress values determined at lateral intervals of $0.25 B$ over the area of the layers and dividing the sum by the number of stress ordinates.

Let, G_0 = overall shear modulus of unreinforced soil,

$G_1, G_2, \dots, G_i, \dots, G_N$ be the shear moduli of N layers of soil,

$\tau_1, \tau_2, \dots, \tau_i, \dots, \tau_N$ be the average shear stresses at the centres of the respective soil layers, and

$L_1, L_2, \dots, L_i, \dots, L_N$ be the lengths of the soil layers over which the

average shear stresses are determined. Based upon the equivalence of the displacement of unreinforced soil mass to the sum of the displacement of individual soil layers, the following expression is obtained :

$$\frac{\tau_1 L_1}{G_0} + \frac{\tau_2 L_2}{G_0} + \dots + \frac{\tau_i L_i}{G_i} + \dots + \frac{\tau_N L_N}{G_N} = \frac{\tau_1 L_1}{G_1} + \frac{\tau_2 L_2}{G_2} + \dots + \frac{\tau_i L_i}{G_i} + \dots + \frac{\tau_N L_N}{G_N} \quad \dots(4.40)$$

$$\text{or } \frac{\sum \tau_i L_i}{G_0} = \sum \left(\frac{\tau_i L_i}{G_i} \right), \quad i = 1 \text{ to } N \quad \dots(4.41)$$

$$\text{or } \sum \left(\frac{\tau_i L_i}{G_i} \right) = \frac{1}{G_0} \sum (\tau_i L_i) \quad \dots(4.42)$$

If the soil is reinforced with 'n' layers of reinforcement of lengths L_{Rn} , and shear moduli G_{Rn} the equivalent shear modulus of the reinforced soil mass, considered to be homogeneous, can be determined from the expression.

$$G_{SR} = \frac{(\tau_1 L_1 + \dots + \tau_i L_i + \dots + \tau_N L_N) + \tau_{R1} L_{R1} + \dots + \tau_{Rj} L_{Rj} + \dots + \tau_{Rn} L_{Rn}}{\left(\frac{\tau_1 L_1}{G_1} + \dots + \frac{\tau_i L_i}{G_i} + \dots + \frac{\tau_N L_N}{G_N} \right) + \left(\frac{\tau_{R1} L_{R1}}{G_{R1}} + \dots + \frac{\tau_{Rj} L_{Rj}}{G_{Rj}} + \dots + \frac{\tau_{Rn} L_{Rn}}{G_{Rn}} \right)} \quad \dots(4.43)$$

where

τ_{Rj} is the average shear stress at the level of jth reinforcement layer of size $L_{Rj} \times B_{Rj}$ determined as for the soil layers ($j = 1$ to n).

$$\text{or } G_{SR} = \frac{\sum \tau_i L_i + \sum \tau_{Rj} L_{Rj}}{\sum \left(\frac{\tau_i L_i}{G_i} \right) + \sum \left(\frac{\tau_{Rj} L_{Rj}}{G_{Rj}} \right)} \quad \dots(4.44)$$

Substituting the value of $\sum \left(\frac{\tau_i L_i}{G_i} \right)$ from (4.42)

$$G_{SR} = \frac{\sum \tau_i L_i + \sum \tau_{Rj} L_{Rj}}{\frac{1}{G_0} \sum \tau_i L_i + \sum \left(\frac{\tau_{Rj} L_{Rj}}{G_{Rj}} \right)} \quad \dots(4.45)$$

For the soil layers of equal length $L_i=L_s$ and reinforcement layers of equal length $L_{Rj}=L_R$ and of same material $G_{Rj}=G_R$ the above expression reduces to :

$$G_{SR} = \frac{L_s \left(\sum \tau_i \right) + L_R \left(\sum \tau_{Rj} \right)}{\frac{L_s}{G_0} \left(\sum \tau_i \right) + \frac{L_R}{G_R} \left(\sum \tau_{Rj} \right)} \quad \dots(4.46)$$

The shear modulus G_0 of unreinforced soil has been determined using the expression:

$$G_0 = \frac{(1 - \nu) \sqrt{A} C_u}{2.26} \quad \dots(4.47)$$

where

$$C_u = 2.8 C_\tau \quad \dots(4.48)$$

Ratio of C_u/C_τ is taken 2.8 from the experimental data.

As an illustration :

Width of block B = 0.4 m

Length of soil layers = 3.75 B

From Table 4.7, at $\theta = 4^\circ$

Average value of coefficient of elastic uniform shear

$$C_{\tau_{av}} = 3.01 \times 10^4 \text{ kN/m}^3$$

$$C_u = 2.8 C_{\tau_{av}} = 8.43 \times 10^4 \text{ kN/m}^3$$

From Table 4.1, $\nu = 0.2631$ (at $D_r=70\%$)

$$G_0 = 1.56 \times 10^4 \text{ kN/m}^2$$

Let the soil be reinforced with two geogrid layers of size equal to size of block, provided at depth $0.25 B$ and 0.5 below the base of block.

For Netlon CE - 121,

$$\text{From Figure 3.3, } E_R = 1.859 \times 10^4 \text{ kN/m}^2$$

Assuming Poisson ratio ν of reinforcement to be 0.18,

$$G_R = \frac{E_R}{2(1 + \nu)} = 0.7877 \times 10^4 \text{ kN/m}^2$$

The average shear stresses are calculated as mentioned earlier. Substituting the various values in expression (4.46):

$$G_{SR} = 1.09 \times 10^4 \text{ kN/m}^2$$

$$\text{and } C_{uSR} = \frac{2.26 G_{SR}}{(1 - \nu)\sqrt{A}} \quad \dots(4.49)$$

$$C_{uSR} = 5.9 \times 10^4 \text{ kN/m}^3$$

$$C_{\tau SR} = 2.11 \times 10^4 \text{ kN/m}^3$$

Experimental value of $C_{\tau SR} = 2.21 \times 10^4 \text{ kN/m}^3$

$$\text{Difference} = 4.5\% \quad (\text{See Table 4.22})$$

The values of $C_{\tau SR}$ are calculated for different reinforced sand beds at different force levels and are compared with the experimental values in Table 4.22. Most of the predicted values are on the higher side of the observed values. These results show that the equivalent parameter analysis predicts the values of the coefficient of elastic uniform shear with a difference of -6% to 31% from the experimentally observed values. This difference is due to a number of simplifying assumptions in the analysis. The predicted and the observed values are plotted in

Figure 4.73 which indicates that the analysis overestimates the values of coefficient of elastic uniform shear.

4.6.6 Concluding Remarks

The analysis is based upon a number of simplifying assumptions and therefore, the predicted values of the coefficient of elastic uniform compression would not be matching exactly with the observed ones. The C_u values are overestimated by about 5% to 20% in vertical vibration tests and about 10% to 25% in the cyclic plate load tests, and the variation in C_τ values obtained from horizontal vibration tests is -6% to 31%; which is expected due to a number of simplifying assumptions and the mobilisation of interface friction and nonlinearity of soil at large strain levels in the cyclic plate load tests have been neglected. It can be concluded that with the reinforcement of sand by geogrid layers, the coefficient of elastic uniform compression and the coefficient of elastic uniform shear are reduced as is clear from the predicted and the observed values, the reduction is more with the increase in number and size of geogrid layers, in general. Further, the top reinforcement layers cause a greater reduction in the coefficient of elastic uniform compression than the bottom ones, which is expected from the elastic theory of stress distribution in the soil mass. It can be concluded that the proposed analysis predicts the trend of decrease in the coefficient of elastic uniform compression and coefficient of elastic uniform shear of geogrid reinforced sand beds and the agreement obtained between the predicted and the observed values may be considered to be reasonable within practical limits.

4.7 DESIGN PROBLEM

A compressor is proposed to be supported over a concrete foundation block of size 3m×3m×1.25m; located over a medium sand deposit. The total weight of the compressor is 104 kN and operating frequency is 15 Hz. The vertical unbalanced force at operating frequency is estimated to be 48 kN. The steady-state vertical

vibration tests conducted at the level of foundation on 1.5m×0.75m×0.7m high concrete block gave the following data (after Prakash and Puri, 1977 - Diesel power house site, Nakodar, Punjab) :

Eccentricity (θ°)	Observed Natural frequency f_{nz} (Hz)	Maximum Amplitude (mm)	Damping Ratio ξ_z
35	26.3	0.0825	-
70	24.5	0.1650	0.093
105	23.7	0.2100	0.078
140	22.9	0.2250	0.075

The unit weight of sand is 17 kN/m^3 . The design requirements are that the resonant and operating frequencies be separated by a factor of at least 1.6 and the maximum amplitude should not exceed 0.20 mm. Determine whether the proposal would satisfy the design requirements, if not, examine the possibility of providing geogrid reinforcements below foundation base. The strain level below the foundation should not exceed 3×10^{-4} .

Solution:

1. Machine Data :

Weight of compressor = 104 kN

Operating frequency of compressor = 15 Hz

Vertical unbalanced force, $P_z = 48 \text{ kN}$

2. Foundation Data:

Taking unit weight of concrete to be 24 kN/m^3

Weight of foundation = $(3 \times 3 \times 1.25)24 = 270 \text{ kN}$

Total weight of compressor and foundation = 374 kN

Area of base of foundation = $3 \times 3 = 9 \text{ m}^2$

3. Soil Data

Unit weight of soil, $\gamma_s = 17 \text{ kN/m}^3$

Take $K_0 = 0.5$

C_u for Foundation

Size of block = $1.5\text{m} \times 0.75\text{m} \times 0.7\text{m}$

Area of block, $A = 1.5 \times 0.75 = 1.125 \text{ m}^2$

Weight of block = $(1.5 \times 0.75 \times 0.7) \times 24 = 18.9 \text{ kN}$

Weight of vibrator = 1.1 kN

Weight of block + vibrator = $18.9 + 1.1 = 20 \text{ kN}$

$$C_u = 4\pi^2 f_{nz}^2 (M/A) \quad [\text{Equation 4.10}]$$

$$= \frac{4\pi^2 \times 20}{1.125 \times 9.81} f_{nz}^2 = 71.54 f_{nz}^2 \text{ kN/m}^3$$

$$\text{for } f_{nz} = 26.3 \text{ Hz, } C_u = 4.95 \times 10^4 \text{ kN/m}^3$$

Correction for confining pressure

Mean effective confining pressure $\bar{\sigma}_{01}$ at a depth equal to half of width below centre of block is

$$\begin{aligned} \bar{\sigma}_{01} &= \sigma_v(2K_0 + 1)/3 \quad [\text{Equation 4.1}] \\ &= (\gamma_s z + 4\bar{I}q)(2K_0 + 1)/3 \\ &= (17 \times 0.375 + 4 \times 0.199 \times 24 \times 0.7) \left(\frac{2 \times 0.5 + 1}{3} \right) \\ &= 13.17 \text{ kN/m}^2 \end{aligned}$$

At 100 kN/m^2 confining pressure :

$$\begin{aligned} C_{u100} &= C_u \sqrt{\frac{100}{13.17}} = 4.95 \times 10^4 \sqrt{\frac{100}{13.17}} \\ &= 13.65 \times 10^4 \text{ kN/m}^3 \end{aligned}$$

The values of C_{u100} and associated strain levels are :

Eccentricity (θ°)	C_{u100} (kN/m ³) ($\times 10^4$)	Strain levels $\times (10^{-4})$	Damping Ratio
35	13.65	1.1	-
70	11.85	2.2	0.093
105	11.11	2.8	0.078
140	10.30	3.0	0.075

Since the strain level below the foundation should not exceed 3×10^{-4} , therefore,

$$C_{u100} = 10.3 \times 10^4 \text{ kN/m}^3$$

Confining pressure below actual foundation

$$\bar{\sigma}_{02} = \bar{\sigma}_v (2K_0 + 1)/3 \quad [\text{equation 4.1}]$$

$$= (\gamma_s z + 4\bar{I}q) (2K_0 + 1)/3$$

$$= (17 \times 0.625 + 4 \times 0.17522 \times 24 \times 1.25) \left(\frac{2 \times 0.5 + 1}{3} \right)$$

$$= 21.10 \text{ kN/m}^2$$

$$C_u = C_{u100} \sqrt{\frac{21.10}{100}} = 10.3 \times 10^4 \sqrt{\frac{21.10}{100}}$$

$$= 4.73 \times 10^4 \text{ kN/m}^3$$

Applying area correction

$$C_u \text{ foundation} = 4.73 \times 10^4 \sqrt{\frac{1.125}{9}}$$

$$C_u \text{ foundation} = 1.67 \times 10^4 \text{ kN/m}^3$$

5. Spring Constant

$$\begin{aligned}K_z &= C_u A && \dots(4.50) \\&= 1.67 \times 10^4 \times 9 \\&= 15.03 \times 10^4 \text{ kN/m}\end{aligned}$$

Damping ratio, $\xi = 0.075$

6. Natural Frequency

$$\begin{aligned}\omega_{nz} &= \sqrt{\frac{K_z}{m}} = \sqrt{\frac{15.03 \times 10^4 \times 9.81}{374}} && \dots(4.51) \\&= 62.8 \text{ rad./sec}\end{aligned}$$

$$f_{nz} = 10 \text{ Hz}$$

Damped natural frequency

$$\begin{aligned}(\omega_{nz})_d &= \omega_{nz} \sqrt{1 - \xi^2} && \dots(4.52) \\&= 62.8 \sqrt{1 - (0.075)^2} \\&= 62.6 \text{ rad/sec.}\end{aligned}$$

$$(f_{nz})_d = 9.96 \text{ Hz}$$

$$\text{Frequency ratio, } r' = \frac{15}{10} = 1.5 < 1.6$$

Amplitude of vibration

$$(A_z)_d = \frac{P_z}{K_z [(1 - (\omega/\omega_{nz})^2)^2 + (2\xi \omega/\omega_{nz})^2]^{1/2}} \quad \dots(4.53)$$

$$= \frac{48}{15.03 \times 10^4 \left[(1 - (94.25/62.8)^2)^2 + \left(2 \times 0.075 \times \frac{94.25}{62.8} \right)^2 \right]^{1/2}}$$

$$= 0.251 \text{ mm} > 0.2 \text{ mm}$$

Reinforced Sand

Since the design requirements are not satisfied, let the sand be reinforced with 6 geogrid layers of size $2.65B \times 2.65B$, $A_f=7$; placed at intervals of $0.25 B$ each below the foundation with first layer at depth $0.25 B$, where B is the width of foundation.

7. For Foundation

$$\text{Dynamic force/weight of block, } F/W = 48/374 = 0.128$$

C_{uR} : Using non-dimensional correlation, equation (4.27)

$$\begin{aligned} C_{uR} &= 0.718 C_{uU} \\ &= 1.198 \times 10^4 \text{ kN/m}^3 \end{aligned}$$

From analytical analysis :

$$\begin{aligned} C_{uR} &= 0.88 C_{uU} \\ &= 1.47 \times 10^4 \text{ kN/m}^3 \end{aligned}$$

ξ_R : From non-dimensional correlation, equation (4.28)

$$\begin{aligned} \xi_R &= 2.36 \xi_U \quad [\text{Table 4.16}] \\ &= 0.075 \times 2.36 \\ &= 0.177 \end{aligned}$$

Amplitude reduction factor, equation (4.29)

$$= 0.665 \quad [\text{Table 4.18}]$$

8. Natural Frequency

Using equation (4.51)

$$\omega_{nz} = \sqrt{\frac{K_z}{m}} = \sqrt{\frac{C_{uR} \times A}{m}} = \sqrt{\frac{1.198 \times 10^4 \times 9 \times 9.81}{374}}$$

$$= 53.18 \text{ rad/sec.}$$

$$f_{nz} = 8.46 \text{ Hz}$$

$$\text{Frequency ratio } r' = \frac{15}{8.46} = 1.77 > 1.6 \text{ O.K.}$$

Damped natural frequency [equation 4.52]

$$\begin{aligned}(\omega_{nz})_d &= \omega_{nz} \sqrt{1 - \xi_R^2} \\ &= 53.18 \sqrt{1 - (0.177)^2} \\ &= 52.34 \text{ rad./sec.}\end{aligned}$$

$$(f_{nz})_d = 8.33 \text{ Hz}$$

Amplitude of vibration [equation 4.53]

$$\begin{aligned}(A_z)_d &= \frac{P_z}{K_z [(1 - (\omega/\omega_{nz})^2)^2 + (2\xi \omega/\omega_{nz})^2]^{1/2}} \\ &= \frac{48}{10.78 \times 10^4 [(1 - (15/8.46)^2)^2 + (2 \times 0.177 \times 15/8.46)^2]^{1/2}}\end{aligned}$$

$$= 0.199 \text{ mm} < 0.2 \text{ mm O.K.}$$

Alternatively, from amplitude reduction factor

$$(A_z)_d = 0.665 \times 0.251 = 0.167 \text{ mm}$$

From analytical approach

$$C_{uR} = 1.47 \times 10^4 \text{ kN/m}^3$$

Substituting in equation (4.51),

$$\omega_{nz} = 58.9 \text{ rad./sec. and,}$$

$$f_{nz} = 9.37 \text{ Hz}$$

$$r' = 1.6 \quad \text{O.K.}$$

Substituting the values in equation (4.53),

$$(A_z)_d = 0.219 \text{ mm}$$

A comparison of the results is shown below :

	f_{nz} (Hz)	Amplitude (mm)	frequency ratio r'
Unreinforced Sand	10	0.251	1.5
Reinforced Sand			
Non-dimensional correlations	8.46	0.199	1.77
Analysis	9.37	0.219	1.60

A block foundation has been designed for compressor on the sand bed reinforced with six layers of geogrid of reinforcement having area ratio, $A_r=7.0$. The values of the coefficient of elastic uniform compression, damping ratio and the amplitude reduction factor have been determined from the non-dimensional correlations. The C_u -value for the reinforced sand bed has been determined from analytical analysis also. It is observed that the resonant frequency is reduced and the amplitudes are also reduced upon reinforcing the sand bed.

From the results of the design problem, it can be concluded that the reinforced sand beds can be used for the design of foundations of machines, where the natural frequency of the soil-foundation system may lie close to the operating frequency of the machine otherwise. The maximum amplitude can be brought within the permissible limits thereby reducing the disturbance during the starting and stopping of the machine.

Table 4.1 Cyclic Plate Load Tests - K_0 from Ultimate Bearing Pressure Values

Configuration of Sand Bed	Ultimate Bearing Pressure, q_u kN/m^2	Pressure at Point of Intersection of C_u and C'_u kN/m^2	$N_\gamma = \frac{q_u}{0.4\gamma B}$	ϕ°	$K_0 = 1 - \sin\phi$
Footing Size=150mm × 150mm $\gamma_s = 16.3 \text{ kN/m}^3, D_r = 70\%$					
Unreinforced	160	160	-	40.0	0.36
Reinforcement Size =150mm × 150mm					
Number of Layers, n = 2	200	200	205	42.9	0.32
3	245	212	251	44.4	0.30
4	300	260	307	45.4	0.29
6	310	260	317	45.5	0.29
8	325	264	332	45.6	0.28
Reinforcement Size =300mm × 300mm					
Number of Layers, n = 2	275	285	281	45.1	0.29
3	325	335	332	45.6	0.28
4	390	390	399	46.3	0.28
6	425	405	435	46.6	0.27
8	450	450	460	46.9	0.27
Reinforcement Size =450mm × 450mm					
Number of Layers, n = 2	310	310	317	45.5	0.29
3	355	360	363	45.9	0.28
4	450	450	460	46.9	0.27
6	485	490	496	47.3	0.26
8	535	535	547	47.8	0.26
Reinforcement Size =600mm × 600mm					
Number of Layers, n = 2	320	288	327	45.6	0.29
3	372	376	380	46.1	0.28
4	475	475	486	47.2	0.27
6	510	510	522	47.5	0.26
8	585	585	598	48.3	0.25
Reinforcement Size =750mm × 750mm					
Number of Layers, n = 2	330	232	337	45.7	0.28
3	410	410	419	46.5	0.27
4	505	460	516	47.5	0.26
6	560	560	573	48.1	0.26
8	625	588	639	48.7	0.25

Contd...

Configuration of Sand Bed	Ultimate Bearing Pressure, q_u kN/m^2	Pressure at Point of Intersection of C_u and C'_u kN/m^2	$N_\gamma = \frac{q_u}{0.4\gamma B}$	ϕ°	$K_0 = 1 - \sin\phi$
Footing Size=150mm × 150mm $\gamma_s = 15.7 \text{ kN/m}^3, D_r = 50\%$					
Unreinforced	121	120	-	37.0	0.40
Number of Layers, n=4 Size of Reinforcement					
150mm × 150mm	150	124	159	41.5	0.34
300mm × 300mm	202	202	214	42.8	0.32
450mm × 450mm	256	256	272	45.0	0.29
600mm × 600mm	284	280	301	45.3	0.29
750mm × 750mm	300	300	318	45.5	0.29
Footing Size=300mm × 300mm $\gamma_s = 16.3 \text{ kN/m}^3, D_r = 70\%$					
Unreinforced	210	240	-	40.0	0.36
Number of Layers, n=4 Size of Reinforcement					
300mm × 300mm	300	300	153	41.4	0.34
600mm × 600mm	350	350	179	42.1	0.33
900mm × 900mm	410	410	210	43.1	0.32
1200mm × 1200mm	465	465	238	44.0	0.31
1500mm × 1500mm	490	490	250	44.4	0.30

Table 4.2 Cyclic Plate Load Tests-Bearing Capacity Ratio (BCR), Settlement Ratio (SR), Coefficient of Elastic Uniform Compression C_u and C'_u and Damping Capacity Ratio

Configuration of Sand Bed	Bearing Capacity Ratio	Settlement Ratio	Coefficient of Elastic Uniform Compression		Damping Capacity Ratio
	$\frac{q_{uR}}{q_{qU}}$	$\frac{S_{Ru}}{S_{Ou}}$	C_u	C'_u	
Footing Size=150mm × 150mm $\gamma_s = 16.3 \text{ kN/m}^3, D_r = 70\%$					
Unreinforced	-	-	2.69	0.75	-
Reinforcement Size =150mm × 150mm					
Number of Layers, n = 2	1.25	0.74	2.22	1.21	1.17
3	1.53	0.66	2.04	0.84	1.24
4	1.88	0.65	1.80	0.83	1.25
6	2.00	0.64	1.58	0.76	1.27
8	2.06	0.64	1.45	0.75	1.28
Reinforcement Size =300mm × 300mm					
Number of Layers, n = 2	1.72	0.71	2.10	1.06	1.19
3	2.03	0.52	2.28	1.52	1.62
4	2.44	0.46	2.18	1.48	1.80
6	2.66	0.44	2.00	1.42	1.82
8	2.81	0.42	1.91	1.30	1.91
Reinforcement Size =450mm × 450mm					
Number of Layers, n = 2	1.94	0.53	2.25	0.81	1.55
3	2.22	0.52	2.10	1.12	1.56
4	2.81	0.50	2.08	1.16	1.63
6	3.03	0.43	2.03	1.18	1.88
8	3.34	0.38	2.02	1.19	2.11
Reinforcement Size =600mm × 600mm					
Number of Layers, n = 2	2.00	0.66	2.17	0.75	1.55
3	2.33	0.52	2.17	0.75	1.64
4	2.97	0.45	2.15	0.95	1.82
6	3.19	0.43	2.10	1.09	1.79
8	3.66	0.38	2.08	1.09	2.16
Reinforcement Size =750mm × 750mm					
Number of Layers, n = 2	2.06	0.62	2.35	0.75	1.31
3	2.56	0.51	2.32	0.84	1.55
4	3.16	0.44	2.40	1.16	1.80
6	3.50	0.40	2.36	1.18	2.06
8	3.91	0.38	2.16	1.22	2.12

contd...

Configuration of Sand Bed	Bearing Capacity Ratio $\frac{Q_{uR}}{Q_{qU}}$	Settlement Ratio $\frac{S_{Ru}}{S_{Ou}}$	Coefficient of Elastic Uniform Compression ($\text{kN/m}^3 \times 10^5$)		Damping Capacity Ratio
			C_u	C'_u	
Footing Size=150mm × 150mm $\gamma_s = 15.7 \text{ kN/m}^3, D_r = 50\%$					
Unreinforced	-	-	2.32	0.64	-
Number of Layers, n=4 Size of Reinforcement					
150mm × 150mm	1.25	0.73	1.75	0.98	1.22
300mm × 300mm	1.67	0.54	1.82	1.38	1.61
450mm × 450mm	2.13	0.52	1.75	1.15	1.62
600mm × 600mm	2.37	0.49	1.86	1.06	1.73
750mm × 750mm	2.50	0.44	1.79	1.14	1.90
Footing Size=300mm × 300mm $\gamma_s = 16.3 \text{ kN/m}^3, D_r = 70\%$					
Unreinforced	-	-	2.29	0.55	-
Number of Layers, n=4 Size of Reinforcement					
300mm × 300mm	1.43	0.71	1.95	0.75	1.36
600mm × 600mm	1.67	0.64	1.75	0.76	1.48
900mm × 900mm	1.95	0.62	1.63	0.81	1.50
1200mm × 1200mm	2.21	0.61	1.57	0.95	1.51
1500mm × 1500mm	2.33	0.60	1.54	1.02	1.52

Table 4.3 Coefficient of Elastic Uniform Compression, C_u at a Confining Pressure =100 kN/m² and Area of Foundation = 10 m² at Factors of Safety 1, 2 and 3 and the Corresponding Strain Levels

Configuration of Sand Bed	Coefficient of Elastic Uniform Compression (C_{u100}) ₁₀ (kN/m ³ × 10 ⁴) at Factor of Safety			Corresponding Strain Levels (×10 ⁻³) at Factor of Safety		
	1	2	3	1	2	3
Footing Size=150mm × 150mm $\gamma_s = 16.3 \text{ kN/m}^3, D_r = 70\%$						
Unreinforced	1.59	2.23	2.70	3.96	1.98	1.33
Reinforcement Size =150mm × 150mm						
Number of Layers, n = 2	1.20	1.69	2.06	6.00	3.00	2.00
3	-	1.42	1.73	-	4.00	2.67
4	-	1.14	1.39	-	5.55	3.70
6	-	0.99	1.21	-	6.54	4.36
8	-	0.89	1.08	-	7.47	4.98
Reinforcement Size =300mm × 300mm						
Number of Layers, n = 2	0.98	1.39	1.69	8.73	4.37	2.91
3	0.99	1.39	1.70	9.50	4.75	3.17
4	0.87	1.22	1.50	11.93	5.96	3.98
6	-	1.08	1.32	-	7.08	4.72
8	0.71	1.00	1.23	15.70	7.85	5.23
Reinforcement Size =450mm × 450mm						
Number of Layers, n = 2	1.00	1.41	1.72	9.18	4.59	3.06
3	0.87	1.23	1.50	11.27	5.63	3.76
4	0.77	1.09	1.33	14.42	7.21	4.81
6	0.73	1.03	1.26	16.16	8.08	5.39
8	0.69	0.98	1.20	17.66	8.83	5.89
Reinforcement Size =600mm × 600mm						
Number of Layers, n = 2	-	1.33	1.63	-	4.93	3.28
3	0.88	1.24	1.52	11.43	5.71	3.81
4	0.78	1.10	1.35	14.73	7.36	4.91
6	0.74	1.04	1.27	16.19	8.09	5.40
8	0.69	0.97	1.19	18.75	9.38	6.25
Reinforcement Size =750mm × 750mm						
Number of Layers, n = 2	-	1.43	1.74	-	4.68	3.12
3	0.90	1.27	1.55	11.78	5.89	3.93
4	-	1.20	1.46	-	7.01	4.68
6	0.79	1.12	1.37	15.82	7.91	5.27
8	-	0.98	1.20	-	9.64	6.43

contd...

Configuration of Sand Bed	Coefficient of Elastic Uniform Compression (C_{u100}) ₁₀ (kN/m ³ × 10 ⁴) at Factor of Safety			Corresponding Strain Levels (×10 ⁻³) at Factor of Safety		
	1	2	3	1	2	3
Footing Size=150mm × 150mm $\gamma_s = 15.7 \text{ kN/m}^3, D_r = 50\%$						
Unreinforced	-	2.15	2.62	-	1.74	1.16
Number of Layers, n=4 Size of Reinforcement						
150mm × 150mm	-	1.52	1.85	-	2.86	1.90
300mm × 300mm	0.98	1.38	1.68	7.40	3.70	2.47
450mm × 450mm	0.85	1.20	1.46	9.75	4.88	3.25
600mm × 600mm	-	1.21	1.48	-	5.09	3.39
750mm × 750mm	0.81	1.14	1.39	11.17	5.59	3.72
Footing Size=300mm × 300mm $\gamma_s = 16.3 \text{ kN/m}^3, D_r = 70\%$						
Unreinforced	2.35	3.30	4.00	3.06	1.53	1.02
Number of Layers, n=4 Size of Reinforcement						
300mm × 300mm	1.70	2.38	2.90	5.13	2.57	1.71
600mm × 600mm	1.42	2.00	2.43	6.67	3.33	2.22
900mm × 900mm	1.22	1.72	2.10	8.44	4.22	2.81
1200mm × 1200mm	1.12	1.58	1.93	9.87	4.94	3.29
1500mm × 1500mm	1.07	1.51	1.84	10.68	5.34	3.56

Table 4.4 Coefficient of Elastic Uniform Compression, C_u at a Confining Pressure =100 kN/m² and Area of Foundation = 10 m² at Factors of Safety 1, 0.67 and 0.5 and the Corresponding Strain Levels

Configuration of Sand Bed	Coefficient of Elastic Uniform Compression (C_{u100}) ₁₀ (kN/m ³ × 10 ³) at Factor of Safety			Corresponding Strain Levels (×10 ⁻³) at Factor of Safety		
	1	0.67	0.5	1	0.67	0.5
Footing Size=150mm × 150mm $\gamma_s = 16.3 \text{ kN/m}^3, D_r = 70\%$						
Unreinforced	-	3.59	3.11	-	11.12	18.28
Reinforcement Size =150mm × 150mm						
Number of Layers, n = 2	-	5.34	4.63	-	11.51	17.03
3	4.15	3.39	2.94	9.55	19.27	28.99
4	3.73	3.05	2.64	12.84	24.89	36.94
6	3.34	2.73	2.37	15.38	29.07	42.76
8	3.27	2.67	2.31	17.53	31.90	46.27
Reinforcement Size =300mm × 300mm						
Number of Layers, n = 2	-	4.06	3.52	-	17.06	25.70
3	-	5.38	4.66	-	16.51	23.63
4	-	4.81	4.17	-	20.71	29.49
6	5.43	4.43	3.84	14.44	24.42	34.39
8	-	3.95	3.42	-	27.25	38.78
Reinforcement Size =450mm × 450mm						
Number of Layers, n = 2	-	2.93	2.54	-	21.94	34.70
3	-	3.80	3.30	-	21.70	32.26
4	-	3.53	3.06	-	27.39	40.32
6	-	3.47	3.00	-	29.55	43.25
8	-	3.34	2.90	-	32.64	47.63
Reinforcement Size =600mm × 600mm						
Number of Layers, n = 2	3.27	2.67	2.32	11.71	25.94	40.16
3	-	2.49	2.16	-	27.73	44.26
4	-	2.82	2.44	-	31.40	48.06
6	-	3.11	2.70	-	31.86	47.53
8	-	2.94	2.55	-	36.64	54.53
Reinforcement Size =750mm × 750mm						
Number of Layers, n = 2	2.92	2.64	2.28	15.29	29.96	44.63
3	-	2.67	2.31	-	28.05	44.32
4	4.09	3.34	2.90	15.36	29.87	44.39
6	-	3.25	2.81	-	31.64	47.46
8	3.91	3.19	2.77	20.17	37.25	54.32

contd...

Configuration of Sand Bed	Coefficient of Elastic Uniform Compression (C'_{u100}) ₁₀ (kN/m ³ × 10 ³) at Factor of Safety			Corresponding Strain Levels (×10 ⁻³) at Factor of Safety		
	1	0.67	0.5	1	0.67	0.5
Footing Size=150mm × 150mm $\gamma_s = 15.7 \text{ kN/m}^3, D_r = 50\%$						
Unreinforced	4.23	3.46	3.00	3.55	9.85	16.16
Number of Layers, n=4 Size of Reinforcement						
150mm × 150mm	6.04	4.94	4.28	6.49	11.59	16.70
300mm × 300mm	-	6.06	5.25	-	12.28	17.16
450mm × 450mm	-	4.56	3.95	-	17.17	24.59
600mm × 600mm	4.90	4.00	3.47	10.29	19.22	28.15
750mm × 750mm	-	4.20	3.64	-	19.95	28.72
Footing Size=300mm × 300mm $\gamma_s = 16.3 \text{ kN/m}^3, D_r = 70\%$						
Unreinforced	-	4.62	4.01	-	8.04	14.40
Number of Layers, n=4 Size of Reinforcement						
300mm × 300mm	-	5.34	4.63	-	11.79	18.46
600mm × 600mm	-	5.04	4.37	-	14.34	22.02
900mm × 900mm	-	5.00	4.33	-	16.87	25.31
1200mm × 1200mm	-	5.55	4.81	-	18.03	26.19
1500mm × 1500mm	-	5.82	5.04	-	18.68	26.69

Table 4.5 Coefficient of Elastic Uniform Compression, $(C_{u100})_{10}$ and $(C'_{u100})_{10}$ Interpolated at Strain Levels - 2×10^{-3} , 4×10^{-3} & 6×10^{-3} and 10×10^{-3} and 15×10^{-3} respectively

Configuration of Sand Bed	Coefficient of Elastic Uniform Compression				
	$(C_{u100})_{10}$ ($\text{kN/m}^3 \times 10^4$)			$(C'_{u100})_{10}$ ($\text{kN/m}^3 \times 10^3$)	
	At Strain Levels ($\times 10^{-3}$)				
Footing Size= $150\text{mm} \times 150\text{mm}$ $\gamma_s = 16.3 \text{ kN/m}^3, D_r = 70\%$	2.0	4.0	6.0	10.0	15.0
UNREINFORCED	2.22	1.58	0.411*	3.69	3.31
Reinforcement Size = $150\text{mm} \times 150\text{mm}$					
Number of Layers, n = 2	2.06	1.47	1.20	5.61	4.86
3	1.99	1.42	1.16	4.10	3.67
4	1.88	1.34	1.10	3.97	3.58
6	1.76	1.26	1.03	8.00**	3.37
8	1.69	1.21	0.99	7.67**	3.42
Reinforcement Size = $300\text{mm} \times 300\text{mm}$					
Number of Layers, n = 2	2.04	1.45	1.19	4.76	4.24
3	2.13	1.52	1.24	6.45	5.58
4	2.09	1.49	1.22	9.46**	5.43
6	2.01	1.43	1.17	9.09**	5.35
8	1.97	1.40	1.15	8.90**	7.27**
Reinforcement Size = $450\text{mm} \times 450\text{mm}$					
Number of Layers, n = 2	2.11	1.50	1.23	3.53	3.24
3	2.05	1.46	1.19	9.26**	4.28
4	2.05	1.46	1.19	9.28**	4.27
6	2.03	1.45	1.18	9.19**	7.51**
8	2.04	1.45	1.19	9.22**	7.53**
Reinforcement Size = $600\text{mm} \times 600\text{mm}$					
Number of Layers, n = 2	2.07	1.48	1.21	3.38	3.10
3	2.09	1.48	1.22	9.43**	2.89
4	2.09	1.49	1.22	9.46**	3.43
6	2.07	1.48	1.21	9.38**	7.66**
8	2.08	1.48	1.21	9.39**	7.67**
Reinforcement Size = $750\text{mm} \times 750\text{mm}$					
Number of Layers, n = 2	2.17	1.54	1.26	3.56	3.24
3	2.17	1.54	1.26	9.78**	3.11
4	2.22	1.58	1.29	10.02**	4.12
6	2.21	1.57	1.29	9.99**	8.16**
8	2.12	1.51	1.24	9.60**	7.85**

contd...

Configuration of Sand Bed	Coefficient of Elastic Uniform Compression				
	$(C_{u100})_{10}$ ($\text{kN/m}^3 \times 10^4$)			$(C'_{u100})_{10}$ ($\text{kN/m}^3 \times 10^3$)	
	At Strain Levels ($\times 10^{-3}$)				
Footing Size=150mm \times 150mm $\gamma_s = 15.7 \text{ kN/m}^3$, $D_r = 50\%$	2.0	4.0	6.0	10.0	15.0
Unreinforced	2.01	0.42*	0.39*	3.45	3.07
Number of Layers, n=4 Size of Reinforcement					
150mm \times 150mm	1.80	1.29	0.62*	5.21	4.47
300mm \times 300mm	1.86	1.32	1.08	6.59	5.56
450mm \times 450mm	1.85	1.32	1.08	5.54	4.80
600mm \times 600mm	1.92	1.36	1.12	8.67**	4.36
750mm \times 750mm	1.88	1.34	1.10	8.52**	4.65
Footing Size=300mm \times 300mm $\gamma_s = 16.3 \text{ kN/m}^3$, $D_r = 70\%$					
Unreinforced	2.89	0.52*	0.49*	4.40	3.96
Number of Layers, n=4 Size of Reinforcement					
300mm \times 300mm	2.69	1.92	0.63*	5.59	4.96
600mm \times 600mm	2.56	1.83	1.49	5.59	4.97
900mm \times 900mm	2.48	1.77	1.45	5.85	5.20
1200mm \times 1200mm	2.46	1.75	1.44	6.76	5.92
1500mm \times 1500mm	2.43	1.74	1.42	11.03**	6.32

* C'_u range

** C_u range

**Table 4.6 : Analysis of vertical vibration test data of geogrid reinforced sand beds
size of block-800mmx400mmx400mm**

Configuration of sand bed, $D_r = 70\%$		Eccentricity θ°	$(A_z)_{max}$ (mm)	f_{nz} Hz	Damping ratio ξ	C_u ($kN/m^3 \times 10^5$)	$(C_{u100})_{10}$ ($kN/m^3 \times 10^4$)	Strain level ($\epsilon_z \times 10^{-4}$)	F/W
Unreinforced		4	0.080	49.0	0.0760	1.300	8.62	2.000	0.0988
		12	0.120	47.5	0.0763	1.220	8.10	3.000	0.2781
		20	0.180	46.5	0.0810	1.170	7.76	4.500	0.4428
		28	0.280	46.0	0.1030	1.145	7.60	7.000	0.6037
Reinforcement size-800mmx400mm $L_r / L = B_r / B = 1.0$	n=2	4	0.075	46.5	0.1505	1.170	7.76	1.875	0.0890
		12	0.115	45.0	0.1528	1.095	7.27	2.875	0.2496
		20	0.170	44.0	0.1563	1.047	6.95	4.250	0.3964
		28	0.275	43.0	0.1599	1.000	6.64	6.875	0.5275
	3	4	0.070	45.0	0.1055	1.095	7.27	1.750	0.0833
		12	0.110	44.0	0.1477	1.047	6.95	2.750	0.2386
		20	0.170	43.5	0.2098	1.024	6.79	4.250	0.3875
		28	0.265	42.5	0.1735	0.977	6.49	6.625	0.5153
	4	4	0.055	45.0	0.1222	1.095	7.27	1.375	0.0833
		12	0.115	43.0	0.1860	1.000	6.64	2.875	0.2279
		20	0.160	42.5	0.1912	0.977	6.49	4.000	0.3699
		28	0.230	42.0	0.2083	0.954	6.33	5.750	0.5032
	6	4	0.055	44.0	0.1853	1.047	6.95	1.375	0.0797
		12	0.115	42.5	0.2074	0.977	6.49	2.875	0.2226
		20	0.165	42.0	0.2352	0.954	6.33	4.125	0.3612
		28	0.220	41.0	0.2683	0.909	6.04	5.500	0.4796
Reinforcement size-800mmx400mm $L_r / L = B_r / B = 1.5$	2	4	0.070	46.0	0.1576	1.145	7.60	1.750	0.0871
		12	0.115	44.5	0.2050	1.071	7.11	2.875	0.2441
		20	0.170	43.5	0.2184	1.024	6.79	4.250	0.3875
		28	0.260	42.5	0.2000	0.977	6.49	6.500	0.5153
	3	4	0.060	46.0	0.1033	1.145	7.60	1.500	0.0871
		12	0.110	44.0	0.1705	1.047	6.95	2.750	0.2386
		20	0.170	43.0	0.1860	1.000	6.64	4.250	0.3786
		28	0.250	41.5	0.1777	0.932	6.18	6.250	0.4913
	4	4	0.065	45.0	0.2000	1.095	7.27	1.625	0.0833
		12	0.110	43.0	0.2064	1.000	6.64	2.750	0.2279
		20	0.170	42.5	0.1824	0.977	6.49	4.250	0.3699
		28	0.240	42.0	0.1667	0.954	6.33	6.000	0.5032
	6	4	0.055	44.5	0.1854	1.071	7.11	1.375	0.0815
		12	0.110	43.0	0.1744	1.000	6.64	2.750	0.2279
		20	0.165	42.0	0.2440	0.954	6.33	4.125	0.3612
		28	0.235	41.0	0.2256	0.909	6.04	5.875	0.4796

contd...

Configuration of sand bed, $D_r = 70\%$		Eccentricity θ^0	$(A_z)_{\max}$ (mm)	f_{nz} Hz	Damping ratio ξ	C_u ($\text{kN}/\text{m}^3 \times 10^5$)	$(C_{u100})_{10}$ ($\text{kN}/\text{m}^3 \times 10^4$)	Strain level ($\epsilon_z \times 10^{-4}$)	F/W
Reinforcement size- 1500mmx750mm $L_r / L = B_r / B = 1.875$	n=2	4	0.075	45.5	0.2253	1.120	7.43	1.875	0.0852
		12	0.115	43.5	0.2328	1.024	6.79	2.875	0.2332
		20	0.170	42.5	0.2441	0.977	6.49	4.375	0.3699
		28	0.245	41.0	0.2500	0.909	6.04	6.125	0.4796
	3	4	0.060	45.0	0.1528	1.095	7.27	1.500	0.0833
		12	0.110	43.0	0.1744	1.000	6.64	2.750	0.2279
		20	0.170	42.0	0.2321	0.954	6.33	4.250	0.3612
		28	0.235	41.0	0.3171	0.909	6.04	5.875	0.4796
	4	4	0.050	45.0	0.1056	1.095	7.27	1.250	0.0833
		12	0.110	43.0	0.1657	1.000	6.64	2.750	0.2279
		20	0.140	42.0	0.2232	0.954	6.33	3.500	0.3612
		28	0.210	40.5	0.1698	0.887	5.89	5.250	0.4679
	6	4	0.045	44.5	0.1292	1.071	7.11	1.125	0.0815
		12	0.100	43.0	0.1395	1.000	6.64	2.500	0.2279
		20	0.140	41.5	0.1687	0.932	6.18	3.500	0.3527
		28	0.205	40.5	0.1728	0.887	5.89	5.125	0.4679
Reinforcement size- 1000mmx1000mm $L_r / L = 1.25,$ $B_r / B = 2.50$	2	4	0.075	44.0	0.1080	1.047	6.95	1.875	0.0797
		12	0.115	42.5	0.2059	0.977	6.49	2.875	0.2226
		20	0.175	41.5	0.2380	0.932	6.18	4.375	0.3527
		28	0.275	40.5	0.2377	0.887	5.89	6.875	0.4679
	3	4	0.065	43.5	0.1523	1.024	6.79	1.625	0.0779
		12	0.110	42.0	0.2380	0.954	6.33	2.750	0.2174
		20	0.170	41.0	0.2927	0.909	6.04	4.250	0.3442
		28	0.255	40.5	0.2562	0.887	5.89	6.375	0.4679
	4	4	0.065	43.5	0.1552	1.024	6.79	1.625	0.0779
		12	0.105	42.0	0.2380	0.954	6.33	2.625	0.2174
		20	0.175	40.5	0.2315	0.887	5.89	4.375	0.3359
		28	0.220	40.0	0.2531	0.866	5.74	5.500	0.4565
	6	4	0.055	43.0	0.1541	1.000	6.64	1.375	0.0761
		12	0.105	41.5	0.2108	0.932	6.18	2.625	0.2123
		20	0.160	40.5	0.2901	0.887	5.89	4.000	0.3359
		28	0.200	40.0	0.3406	0.866	5.74	5.000	0.4565

contd...

Configuration of sand bed, $D_r = 70\%$		Eccentricity θ^0	$(A_z)_{max}$	f_{nz} Hz	Damping ratio ξ	C_u ($kN/m^3 \times 10^5$)	$(C_{u100})_{10}$ ($kN/m^3 \times 10^4$)	Strain level ($\epsilon_z \times 10^{-4}$)	F/W
Reinforcement size- 1200mmx1200mm $L_r / L = 1.5,$ $B_r / B = 3.0$	n=2	4	0.075	44.5	0.1433	1.071	7.11	1.875	0.0815
		12	0.115	42.5	0.1706	0.977	6.49	2.875	0.2226
		20	0.175	42.0	0.2500	0.954	6.33	4.375	0.3612
		28	0.275	41.5	0.2470	0.932	6.18	6.875	0.4913
	3	4	0.060	43.0	0.1395	1.000	6.64	1.500	0.0761
		12	0.100	42.5	0.2029	0.977	6.49	2.500	0.2226
		20	0.160	41.5	0.2470	0.932	6.18	4.000	0.3527
		28	0.220	41.0	0.2378	0.909	6.04	5.500	0.4796
	4	4	0.055	42.0	0.1220	0.954	6.33	1.375	0.0726
		12	0.100	41.0	0.2349	0.932	6.18	2.500	0.2123
		20	0.150	40.5	0.2284	0.887	5.89	3.750	0.3359
		28	0.205	40.0	0.2188	0.866	5.74	5.125	0.4565
	6	4	0.050	42.0	0.1250	0.954	6.33	1.250	0.0726
		12	0.095	41.0	0.2378	0.909	6.04	2.375	0.2072
		20	0.155	40.5	0.2407	0.887	5.89	3.875	0.3359
		28	0.200	40.0	0.2594	0.866	5.74	5.000	0.4565
Reinforcement size- 1500mmx1500mm $L_r / L = 1.875,$ $B_r / B = 3.75$	2	4	0.075	44.0	0.1543	1.047	6.95	1.875	0.0797
		12	0.115	42.5	0.2000	0.977	6.49	2.875	0.2226
		20	0.175	41.5	0.2349	0.932	6.18	4.375	0.3527
		28	0.275	41.0	0.2256	0.909	6.04	6.875	0.4796
	3	4	0.055	43.0	0.1221	1.000	6.64	1.375	0.0761
		12	0.105	42.5	0.2176	0.977	6.49	2.625	0.2226
		20	0.165	41.0	0.2104	0.909	6.04	4.125	0.3442
		28	0.210	40.5	0.2191	0.887	5.89	5.250	0.4679
	4	4	0.050	42.5	0.1147	0.977	6.49	1.250	0.0743
		12	0.095	41.0	0.1829	0.909	6.04	2.375	0.2072
		20	0.150	40.5	0.2068	0.887	5.89	3.750	0.3359
		28	0.200	40.0	0.2063	0.866	5.74	5.000	0.4565
	6	4	0.050	42.0	0.1429	0.954	6.33	1.250	0.0726
		12	0.095	41.0	0.2134	0.909	6.04	2.375	0.2072
		20	0.150	40.5	0.2469	0.887	5.89	3.750	0.3359
		28	0.200	40.0	0.2188	0.866	5.74	5.000	0.4565

Table 4.7 Analysis of horizontal vibration test data of geogrid reinforced sand beds
Size of block - 0.8mx0.4mx0.4m

Configuration of sand bed, $D_r = 70\%$	θ°	Amplitude (mm)		Frequency (Hz)		$(C_{\tau 100})_{10}$ ($\text{kN}/\text{m}^3 \times 10^4$)		Damping ratio		Amplitude/Width		F_1 / W	
		$(A_{x1})_{\max}$	$(A_{x2})_{\max}$	f_{nx1}	f_{nx2}	1	2	ξ_1	ξ_2	$(\times 10^{-4})_1$	$(\times 10^{-4})_2$		
Unreinforced	4	0.080	0.050	21.0	54.0	3.01	3.01	0.1071	0.0926	2.000	1.250	0.0181	
	12	0.110	0.070	20.0	53.0	2.73	2.90	0.1063	0.0920	2.750	1.750	0.0493	
	20	0.190	0.120	19.5	52.0	2.60	2.78	0.0994	0.0553	4.750	3.000	0.0779	
	28	0.250	0.150	19.0	50.0	2.46	2.57	0.1085	0.0650	6.250	3.750	0.1030	
Reinforcement Size=0.8mx0.4m	n=2	4	0.070	0.050	18.0	47.0	2.21	2.28	0.1111	0.0426	1.750	1.250	0.0133
	12	0.100	0.060	17.5	46.0	2.10	2.18	0.1071	0.0543	2.500	1.500	0.0377	
	20	0.160	0.115	17.0	45.5	1.97	2.13	0.1176	0.0742	4.000	2.875	0.0592	
	28	0.230	0.140	16.0	45.0	1.75	2.09	0.1562	0.1111	5.750	3.500	0.0730	
3	4	0.060	0.045	17.5	45.5	2.10	2.13	0.0893	0.0577	1.500	1.125	0.0126	
	12	0.095	0.065	16.0	44.5	1.75	2.04	0.1250	0.0787	2.375	1.625	0.0316	
	20	0.170	0.105	16.0	43.5	1.75	1.94	0.1016	0.0977	4.250	2.625	0.0524	
	28	0.230	0.140	15.5	43.0	1.64	1.90	0.1290	0.1105	5.750	3.500	0.0685	
4	4	0.055	0.40	18.0	44.0	2.21	1.99	0.1007	0.0568	1.375	1.000	0.0133	
	12	0.080	0.060	16.5	43.5	1.86	1.94	0.1288	0.0848	2.000	1.500	0.0336	
	20	0.155	0.090	16.0	43.0	1.75	1.90	0.1016	0.0814	3.875	2.250	0.0524	
	28	0.220	0.120	16.0	42.5	1.75	1.86	0.1133	0.1118	5.500	3.000	0.0730	
6	4	0.055	0.040	17.0	44.0	1.97	1.99	0.1324	0.0966	1.375	1.000	0.0119	
	12	0.075	0.060	16.0	43.0	1.75	1.90	0.1523	0.1192	1.875	1.500	0.0316	
	20	0.150	0.090	16.0	42.0	1.75	1.81	0.1406	0.1503	3.750	2.250	0.0524	
	28	0.220	0.120	16.0	42.0	1.75	1.81	0.1797	0.1845	5.500	3.000	0.0730	
Reinforcement Size=1.2mx0.6m	n=2	4	0.060	0.045	17.5	45.5	2.10	2.13	0.0928	0.0810	1.500	1.125	0.0126
	12	0.110	0.060	17.0	43.0	1.97	1.90	0.1029	0.1105	2.750	1.500	0.0356	
	20	0.170	0.110	17.0	42.5	1.97	1.86	0.1176	0.1588	4.250	2.750	0.0592	
	28	0.220	0.140	16.0	42.0	1.75	1.81	0.1484	0.1637	5.500	3.500	0.0730	
3	4	0.060	0.040	17.0	44.0	1.97	1.99	0.1103	0.0710	1.500	1.000	0.0119	
	12	0.100	0.065	16.0	43.0	1.75	1.90	0.1133	0.1221	2.500	1.625	0.0316	
	20	0.145	0.095	16.0	42.0	1.75	1.81	0.1172	0.1310	3.625	2.375	0.0524	
	28	0.200	0.125	15.5	41.5	1.64	1.77	0.1532	0.1566	5.000	3.125	0.0685	
4	4	0.050	0.045	16.0	43.0	1.75	1.90	0.1016	0.0640	1.250	1.125	0.0105	
	12	0.090	0.060	16.0	42.0	1.75	1.81	0.1055	0.0878	2.250	1.500	0.0316	
	20	0.120	0.090	15.0	41.5	1.54	1.77	0.1250	0.0964	3.000	2.500	0.0461	
	28	0.180	0.110	14.0	41.0	1.34	1.73	0.1250	0.1707	4.500	2.750	0.0559	
6	4	0.050	0.045	17.0	43.0	1.97	1.90	0.0846	0.0727	1.250	1.125	0.0119	
	12	0.080	0.060	16.0	42.0	1.75	1.81	0.1133	0.0982	2.000	1.500	0.0316	
	20	0.120	0.090	15.5	41.0	1.64	1.73	0.1210	0.1494	3.000	2.250	0.0492	
	28	0.180	0.110	15.0	40.5	1.54	1.68	0.1250	0.2253	4.500	2.750	0.0642	

contd...

Configuration of sand bed, $D_r = 70\%$	θ°	Amplitude (mm)		Frequency (Hz)		$(C_{\tau 100})_{10}$ ($\text{kN/m}^3 \times 10^4$)		Damping ratio		Amplitude/Width		F_1 / W
		$(A_{x1})_{\max}$	$(A_{x2})_{\max}$	f_{nx1}	f_{nx2}	1	2	ξ_1	ξ_2	$(\times 10^{-4})_1$	$(\times 10^{-4})_2$	
Reinforcement Size=1.5m x 0.75m n=2	4	0.070	0.050	17.0	44.0	1.97	1.99	0.1066	0.0824	1.750	1.250	0.0119
	12	0.090	0.065	16.0	43.0	1.75	1.90	0.1484	0.1192	2.250	1.625	0.0316
	20	0.130	0.110	16.0	42.0	1.75	1.81	0.1563	0.1190	3.250	2.750	0.0524
	28	0.220	0.135	15.0	41.0	1.54	1.73	0.1333	0.1951	5.500	3.375	0.0642
3	4	0.060	0.050	17.0	44.0	1.97	1.99	0.0993	0.0881	1.500	1.250	0.0119
	12	0.080	0.060	17.0	42.5	1.97	1.86	0.1066	0.1353	2.000	1.500	0.0356
	20	0.130	0.100	15.0	42.0	1.54	1.81	0.1250	0.1235	3.250	2.500	0.0461
	28	0.210	0.120	15.0	40.5	1.54	1.68	0.1208	0.2068	5.250	3.000	0.0642
4	4	0.060	0.045	17.0	44.0	1.97	1.99	0.1066	0.0767	1.500	1.125	0.0119
	12	0.085	0.060	16.0	42.5	1.75	1.86	0.1133	0.1294	2.125	1.500	0.0316
	20	0.120	0.100	16.0	41.5	1.75	1.77	0.1250	0.1310	3.000	2.500	0.0524
	28	0.220	0.120	16.0	41.0	1.75	1.73	0.1250	0.1784	5.500	3.000	0.0730
6	4	0.060	0.045	16.0	42.5	1.75	1.86	0.1094	0.0706	1.500	1.125	0.0105
	12	0.070	0.060	15.5	41.5	1.64	1.77	0.1290	0.0889	1.750	1.500	0.0296
	20	0.110	0.090	15.0	41.0	1.54	1.73	0.1167	0.1006	2.750	2.250	0.0461
	28	0.180	0.100	15.0	40.5	1.54	1.68	0.1208	0.1373	4.500	2.500	0.0642
Reinforcement Size=1.0m x 1.0m n=2	4	0.055	0.050	17.0	44.5	1.97	2.04	0.0919	0.0786	1.375	1.250	0.0119
	12	0.080	0.060	16.5	44.0	1.86	1.99	0.1250	0.0980	2.000	1.500	0.0336
	20	0.175	0.115	16.0	42.5	1.75	1.86	0.1211	0.1265	4.375	2.875	0.0524
	28	0.235	0.145	16.0	41.5	1.75	1.77	0.1367	0.1686	5.875	3.625	0.0730
3	4	0.055	0.050	15.0	44.0	1.54	1.99	0.1583	0.0682	1.375	1.250	0.0093
	12	0.080	0.060	15.0	43.5	1.54	1.94	0.1458	0.1494	2.000	1.500	0.0277
	20	0.125	0.110	14.0	42.0	1.34	1.81	0.1518	0.1607	3.125	2.750	0.0401
	28	0.220	0.130	14.0	41.5	1.34	1.77	0.1339	0.1777	5.500	3.250	0.0559
4	4	0.050	0.045	16.0	43.5	1.75	1.94	0.1250	0.1006	1.250	1.125	0.0105
	12	0.075	0.060	15.0	43.0	1.54	1.90	0.1667	0.1395	1.875	1.500	0.0277
	20	0.110	0.105	15.0	42.0	1.54	1.81	0.1333	0.1830	2.750	2.625	0.0461
	28	0.210	0.125	14.0	41.0	1.34	1.73	0.1295	0.2561	5.250	3.125	0.0559
6	4	0.050	0.035	17.0	43.0	1.97	1.90	0.1029	0.0581	1.250	0.875	0.0119
	12	0.080	0.060	15.0	42.5	1.54	1.86	0.1250	0.0647	2.000	1.500	0.0277
	20	0.100	0.070	14.0	42.0	1.34	1.81	0.1473	0.1250	2.500	1.750	0.0401
	28	0.130	0.120	14.0	42.0	1.34	1.81	0.1339	0.1042	3.250	3.000	0.0559

contd...

Configuration of sand bed, $D_r = 70\%$	θ°	Amplitude (mm)		Frequency (Hz)		$(C_{\tau 100})_{10}$ ($\text{kN/m}^3 \times 10^4$)		Damping ratio		Amplitude/Width		F_1 / W	
		$(A_{x1})_{\max}$	$(A_{x2})_{\max}$	f_{nx1}	f_{nx2}	1	2	ξ_1	ξ_2	$(\times 10^{-4})_1$	$(\times 10^{-4})_2$		
Reinforcement Size=1.2mx1.2m	n=2	4	0.065	0.050	17.0	44.5	1.97	2.04	0.1029	0.0785	1.625	1.250	0.0117
		12	0.095	0.065	16.5	43.5	1.86	1.94	0.1042	0.0891	2.375	1.625	0.0336
		20	0.180	0.105	16.0	42.5	1.75	1.86	0.1094	0.1176	4.500	2.625	0.0524
		28	0.225	0.130	15.0	42.0	1.54	1.81	0.1292	0.1607	5.625	3.250	0.0642
	3	4	0.060	0.050	16.5	44.0	1.86	1.99	0.1136	0.1023	1.500	1.250	0.0112
		12	0.090	0.065	16.0	43.5	1.75	1.94	0.1094	0.1092	2.250	1.625	0.0316
		20	0.145	0.090	15.5	43.0	1.64	1.90	0.1048	0.1279	3.625	2.250	0.0492
		28	0.180	0.120	15.0	42.5	1.54	1.86	0.1375	0.1294	4.500	3.000	0.0642
	4	4	0.060	0.040	16.0	44.0	1.75	1.99	0.1445	0.0710	1.500	1.000	0.0105
		12	0.085	0.065	15.0	43.0	1.54	1.90	0.1375	0.1221	2.125	1.625	0.0277
		20	0.120	0.085	15.0	42.5	1.54	1.86	0.1292	0.1559	3.000	2.125	0.0461
		28	0.150	0.115	14.5	42.0	1.44	1.81	0.1336	0.1905	3.750	2.875	0.0600
	6	4	0.060	0.045	16.0	43.5	1.75	1.94	0.1016	0.0876	1.500	1.125	0.0105
		12	0.085	0.070	15.0	43.0	1.54	1.90	0.1292	0.1061	2.125	1.750	0.0277
		20	0.130	0.090	15.0	42.5	1.54	1.86	0.1333	0.1206	3.250	2.250	0.0461
		28	0.150	0.115	14.5	42.0	1.44	1.81	0.1638	0.1250	3.750	2.875	0.0600
Reinforcement Size=1.5mx1.5m	n=2	4	0.050	0.050	17.0	44.5	1.97	2.04	0.1103	0.0785	1.250	1.250	0.0119
		12	0.100	0.065	16.0	44.0	1.75	1.99	0.1133	0.1051	2.500	1.625	0.0316
		20	0.180	0.110	16.0	43.0	1.75	1.90	0.1016	0.1134	4.500	2.750	0.0524
		28	0.220	0.125	15.0	42.5	1.54	1.86	0.1292	0.1588	5.500	3.125	0.0642
	3	4	0.045	0.040	16.5	44.0	1.86	1.99	0.1136	0.0483	1.125	1.000	0.0112
		12	0.090	0.060	15.0	43.5	1.54	1.94	0.1167	0.1035	2.250	1.500	0.0277
		20	0.110	0.085	15.0	43.0	1.54	1.90	0.1250	0.0872	2.750	2.125	0.0461
		28	0.125	0.110	15.0	43.0	1.54	1.90	0.1542	0.1453	3.125	2.750	0.0642
	4	4	0.045	0.040	17.0	44.0	1.97	1.99	0.1250	0.0994	1.125	1.000	0.0119
		12	0.080	0.060	16.0	43.5	1.75	1.94	0.1250	0.1207	2.000	1.500	0.0316
		20	0.115	0.085	15.0	42.5	1.54	1.86	0.1292	0.1765	2.875	2.125	0.0461
		28	0.140	0.115	15.0	42.0	1.54	1.81	0.1500	0.2321	3.500	2.875	0.0642
	6	4	0.045	0.040	17.0	43.5	1.97	1.94	0.1176	0.0746	1.125	1.000	0.0119
		12	0.080	0.060	15.0	43.0	1.54	1.90	0.1292	0.1279	2.000	1.500	0.0277
		20	0.115	0.085	15.0	42.5	1.54	1.86	0.1333	0.1500	2.875	2.125	0.0461
		28	0.130	0.115	14.5	42.0	1.44	1.81	0.1572	0.1667	3.250	2.875	0.0600

Table 4.8 : Vertical vibration tests - C_u values interpolated at different strain levels and corresponding F/W ratios

Size of block = 0.8m x 0.4m x 0.4m

Configuration of sand bed $D_r = 70\%$		$(C_{u100})_{10}$ $\text{kN/m}^3 (\times 10^4)$ at strain level			F/W ratio at strain level		
Reinforcement size	No. of layers (n)	2×10^{-4}	4×10^{-4}	6×10^{-4}	2×10^{-4}	4×10^{-4}	6×10^{-4}
Unreinforced		8.62	7.88	7.66	0.0988	0.3879	0.5393
0.8m x 0.4m, $A_r = 1.0$	2	7.70	7.01	6.74	0.1091	0.3697	0.4838
	3	7.19	6.82	6.57	0.1221	0.3627	0.4817
	4	7.01	6.49	6.31	0.1436	0.3699	0.5222
	6	6.76	6.35	5.93	0.1392	0.3473	0.5227
1.2m x 0.6m, $A_r = 2.25$	2	7.49	6.85	6.55	0.1220	0.3625	0.4869
	3	7.34	6.69	6.24	0.1477	0.3553	0.4772
	4	7.06	6.51	6.33	0.1315	0.3462	0.5032
	6	6.90	6.36	6.01	0.1480	0.3491	0.4881
1.5m x 0.75m, $A_r = 3.516$	2	7.35	6.56	6.07	0.1037	0.3357	0.4718
	3	7.02	6.38	6.01	0.1411	0.3390	0.4887
	4	6.95	6.21	5.70	0.1556	0.3917	0.5136
	6	6.81	6.09	5.73	0.1747	0.3881	0.5299
1.0m x 1.0m, $A_r = 3.125$	2	6.89	6.26	5.99	0.0976	0.3202	0.4276
	3	6.64	6.09	5.91	0.1244	0.3231	0.4461
	4	6.62	5.98	5.68	0.1302	0.3105	0.5101
	6	6.41	5.89	5.60	0.1442	0.3359	0.5771
1.2m x 1.2m, $A_r = 4.5$	2	7.03	6.37	6.24	0.0991	0.3266	0.4458
	3	6.56	6.18	5.99	0.1494	0.3527	0.5219
	4	6.25	5.86	5.65	0.1502	0.3578	0.5332
	6	6.13	5.87	5.62	0.1623	0.3493	0.5637
1.5m x 1.5m $A_r = 7.031$	2	6.89	6.26	6.09	0.0976	0.3202	0.4352
	3	6.56	6.07	5.79	0.1494	0.3341	0.5504
	4	6.18	5.86	5.63	0.1629	0.3600	0.5530
	6	6.13	5.86	5.63	0.1623	0.3600	0.5530

Table 4.9 : Horizontal vibration tests - C_r values interpolated at different strain levels and corresponding F_1 / W ratios

Size of block = 0.8mx0.4mx0.4m

Configuration of sand bed $D_r = 70\%$		C_r value $\text{kN/m}^3 (\times 10^4)$ at amplitude/width ratio			F_1 / W ratio at amplitude/width ratio		
Reinforcement size	No. of layers (n)	2×10^{-4}	4×10^{-4}	6×10^{-4}	2×10^{-4}	4×10^{-4}	6×10^{-4}
Unreinforced		2.95	2.69	2.51	0.0181	0.0672	0.0988
0.8mx0.4m, $A_r=1.0$	2	2.17	2.02	1.86	0.0214	0.0592	0.0750
	3	1.95	1.82	1.72	0.0235	0.0496	0.0712
	4	1.88	1.79	1.76	0.0336	0.0556	0.0793
	6	1.79	1.75	1.75	0.0330	0.0553	0.0789
1.2mx0.6m, $A_r=2.25$	2	2.00	1.89	1.69	0.0218	0.0553	0.0923
	3	1.88	1.74	1.62	0.0218	0.0568	0.0802
	4	1.76	1.54	1.39	0.0263	0.0526	0.0657
	6	1.75	1.61	1.51	0.0316	0.0592	0.0792
1.5mx0.75m, $A_r=3.516$	2	1.88	1.71	1.57	0.0218	0.0563	0.0668
	3	1.89	1.62	1.57	0.0356	0.0529	0.0710
	4	1.81	1.72	1.71	0.0277	0.0606	0.0771
	6	1.67	1.60	1.57	0.0337	0.0590	0.0797
1.0mx1.0m, $A_r=3.125$	2	1.89	1.79	1.72	0.0336	0.0494	0.0747
	3	1.71	1.54	1.53	0.0277	0.0459	0.0592
	4	1.68	1.58	1.47	0.0303	0.0510	0.0588
	6	1.67	1.55	1.55	0.0277	0.0717	0.1138*
1.2mx1.2m, $A_r=4.5$	2	1.92	1.79	1.61	0.0228	0.0480	0.0681
	3	1.83	1.71	1.54	0.0248	0.0556	0.0899
	4	1.72	1.57	1.39	0.0243	0.0646	0.1017*
	6	1.71	1.57	1.29	0.0243	0.0670	0.1225*
1.5mx1.5m $A_r=7.031$	2	1.89	1.81	1.61	0.0237	0.0472	0.0701
	3	1.75	1.69	1.69	0.0240	0.1064*	0.2030*
	4	1.81	1.62	1.61	0.0316	0.0787	0.1366*
	6	1.69	1.46	1.43	0.0277	0.0878	0.1619*

* Extrapolated

Table 4.10(a) - Cyclic Plate Load Tests - Regression analysis for coefficient of

Elastic uniform compression C_u

$$\frac{C_{uR}}{C_{uU}} = a_0 + a_1 n + a_2 n^2 + a_3 n^3 + a_4 n^4. \quad n = \text{No. of reinforcement layers}$$

Footing size = 150mm square		Coefficients of polynomial					coefficient of correlation R^2
$D_r = 70\%$,	A_r	a_0	a_1	a_2	a_3	a_4	
	1	0.999	-0.073	-0.011	2.92×10^{-3}	-1.63×10^{-4}	0.99
	4	0.999	-0.294	0.140	-0.025	1.46×10^{-3}	0.97
	9	1.000	-0.118	0.019	-1.01×10^{-3}	-9.97×10^{-7}	0.99
	16	0.999	-0.203	0.074	-0.011	6.04×10^{-4}	0.99
	25	1.000	-0.146	0.053	-7.30×10^{-3}	3.15×10^{-4}	0.99

$$(b) \quad \frac{C_{uR}}{C_{uU}} = a_0 + a_1 B_r' + a_2 B_r'^2 + a_3 B_r'^3 + a_4 B_r'^4, \quad A_r = \frac{\text{Area of reinforcement}}{\text{area of footing}}$$

$$\text{No. of layers, } n = 4, \quad B_r' = \sqrt{A_r}$$

Footing Size	a_0	a_1	a_2	a_3	a_4	R^2
150 mm square ($D_r = 50\%$)	0.997	-0.411	0.230	-0.050	3.75×10^{-3}	0.95
300 mm square ($D_r = 70\%$)	0.999	-0.185	0.042	-4.58×10^{-3}	2.08×10^{-4}	0.99

Table 4.11 - Regression analysis for damping capacity ratio

(a) $(D)_{cr} = a_0 + a_1n + a_2n^2 + a_3n^3 + a_4n^4$. n=No. of reinforcement layers

Footing size = 150mm square		Coefficients of Polynomial					Coefficient of Correlation
$D_r=70\%$,	A_r	a_0	a_1	a_2	a_3	a_4	R^2
	1	0.999	0.108	-8×10^{-3}	-1.27×10^{-3}	1.411	0.99
	4	0.998	-0.395	0.388	-0.0780	4.68×10^{-3}	0.99
	9	1.000	0.606	-0.241	0.411	-2.29×10^{-3}	0.99
	16	1.002	0.262	0.027	-0.0168	1.44×10^{-3}	0.99
	25	1.000	-0.011	0.120	-0.0211	1.06×10^{-3}	0.99

(b) $(D)_{cr} = a_0 + a_1B_r' + a_2B_r'^2 + a_3B_r'^3 + a_4B_r'^4$, $A_r = \frac{\text{Area of reinforcement}}{\text{area of footing}}$

No. of layers, $n = 4$, $B_r' = \sqrt{A_r}$

Footing Size	a_0	a_1	a_2	a_3	a_4	R^2
150 mm square ($D_r = 50\%$)	0.994	0.104	0.240	-0.098	0.0106	0.98
300 mm square ($D_r = 70\%$)	0.999	0.547	-0.224	0.0407	2.71×10^{-3}	0.99

Table 4.12(a) -Cyclic Plate Load Tests - Regression analysis for ultimate bearing capacity ratio, BCR

$$\text{BCR} = a_0 + a_1n + a_2n^2 + a_3n^3 + a_4n^4 + a_5n^5. \quad n=\text{No. of reinforcement layers}$$

Footing size = 150mm square	Coefficients of Polynomial						Coefficient of Correlation R^2
	a_0	a_1	a_2	a_3	a_4	a_5	
$D_r=70\%$, A_r							
1	1	0.350	-0.350	0.171	-0.030	1.66×10^{-3}	1
4	1	1.040	-0.747	0.281	-0.043	2.29×10^{-3}	1
9	1	2.197	-1.838	0.665	-0.099	5.13×10^{-4}	1
16	1	2.255	-1.886	0.691	-0.104	5.42×10^{-3}	1
25	1	1.320	-0.892	0.347	-0.055	2.96×10^{-3}	1

(b) $\text{BCR} = a_0 + a_1B_r' + a_2B_r'^2 + a_3B_r'^3 + a_4B_r'^4 + a_5B_r'^5,$

$$A_r = \frac{\text{Area of reinforcement}}{\text{area of footing}}$$

No. of layers, $n = 4$, $B_r' = \sqrt{A_r}$

Footing Size	Coefficients of Polynomial						Coefficient of Correlation R^2
	a_0	a_1	a_2	a_3	a_4	a_5	
150 mm square ($D_r = 50\%$)	1	0.254	-0.118	0.157	-0.047	4.17×10^{-3}	1
300 mm square ($D_r = 70\%$)	1	0.720	-0.439	0.178	-0.031	1.92×10^{-3}	1

Table 4.13(a)-Cyclic plate load tests - Regression analysis for settlement ratio, SR

$$SR = a_0 + a_1n + a_2n^2 + a_3n^3. \quad n = \text{No. of reinforcement layers}$$

Footing size 150 mm square		Coefficients of Polynomial				Coefficient of Correlation
$D_r=70\%$,	A_r	a_0	a_1	a_2	a_3	R^2
	1	1.001	-0.196	0.034	-1.92×10^{-3}	0.99
	4	1.009	-0.218	0.025	-8.53×10^{-4}	0.98
	9	0.990	-0.316	0.062	-4.08×10^{-3}	0.98
	16	1.005	-0.253	0.037	-1.93×10^{-3}	0.99
	25	1.001	-0.280	0.037	-1.84×10^{-3}	0.99

$$(b) \quad SR = a_0 + a_1B_r' + a_2B_r'^2 + a_3B_r'^3, \quad A_r = \frac{\text{Area of reinforcement}}{\text{area of footing}}$$

$$\text{No. of layers, } n = 4, \quad B_r' = \sqrt{A_r}$$

Footing Size	Coefficients of Polynomial				Coefficient of Correlation R^2
	a_0	a_1	a_2	a_3	
150 mm square ($D_r = 50\%$)	1.005	-0.396	0.106	-9.82×10^{-3}	0.99
300 mm square ($D_r = 70\%$)	0.994	-0.369	0.115	-11.43×10^{-3}	0.99

Table 4.14 : Regression analysis for $(C_{u100})_{10}$ - vertical vibration tests

$$(C_{u100})_{10R} / (C_{u100})_{10U} = \exp(a_0 + a_1 n + a_2 n^2),$$

n = No. of reinforcement layers

A_r	F/W	Coefficients of Polynomial			Coefficient of Correlation R^2
		a_0	a_1	a_2	
1.0	0.1	1.36×10^{-3}	-0.066	4.62×10^{-3}	0.99
	0.2	3.12×10^{-4}	-0.068	5.07×10^{-3}	0.99
	0.3	-3.88×10^{-4}	-0.071	5.20×10^{-3}	0.99
	0.4	-1.75×10^{-3}	-0.073	5.30×10^{-3}	0.99
	0.5	-1.95×10^{-3}	-0.078	5.92×10^{-3}	0.99
2.25	0.1	-3.66×10^{-3}	-0.066	5.71×10^{-3}	0.98
	0.2	-2.74×10^{-3}	-0.073	6.35×10^{-3}	0.99
	0.3	-2.82×10^{-3}	-0.081	7.31×10^{-3}	0.99
	0.4	-3.30×10^{-3}	-0.092	8.75×10^{-3}	0.99
	0.5	-2.99×10^{-3}	-0.103	10.02×10^{-3}	0.99
3.516	0.1	-5.72×10^{-3}	-0.084	8.87×10^{-3}	0.98
	0.2	-6.71×10^{-3}	-0.094	10.01×10^{-3}	0.97
	0.3	-7.90×10^{-3}	-0.103	10.90×10^{-3}	0.97
	0.4	-8.99×10^{-3}	-0.118	12.84×10^{-3}	0.97
	0.5	-10.39×10^{-3}	-0.128	13.67×10^{-3}	0.97
3.125	0.1	-8.15×10^{-3}	-0.119	0.0128	0.97
	0.2	-9.54×10^{-3}	-0.124	0.0134	0.97
	0.3	-9.95×10^{-3}	-0.132	0.0142	0.97
	0.4	-11.06×10^{-3}	-0.141	0.0151	0.97
	0.5	-12.88×10^{-3}	-0.148	0.0159	0.96
4.5	0.1	-1.46×10^{-3}	-0.122	0.0116	0.99
	0.2	-2.38×10^{-3}	-0.121	0.0116	0.99
	0.3	-3.26×10^{-3}	-0.124	0.0121	0.99
	0.4	-4.42×10^{-3}	-0.127	0.0125	0.99
	0.5	-5.91×10^{-3}	-0.130	0.0130	0.98
7.031	0.1	-5.51×10^{-3}	-0.122	0.0119	0.99
	0.2	-5.85×10^{-3}	-0.126	0.0126	0.99
	0.3	-7.49×10^{-3}	-0.130	0.0133	0.98
	0.4	-8.45×10^{-3}	-0.138	0.0145	0.98
	0.5	-9.18×10^{-3}	-0.145	0.0156	0.98

Table 4.15 : Regression analysis for $(C_{\tau 100})_{10}$ - horizontal vibration tests

$$(C_{\tau 100})_{10R} / (C_{\tau 100})_{10U} = \exp(a_0 + a_1 n + a_2 n^2),$$

n = No. of reinforcement layers

A_r	F_1 / W	Coefficients of Polynomial			Coefficient of Correlation R^2
		a_0	a_1	a_2	
1.0	0.02	-9.08×10^{-3}	-0.164	0.0164	0.99
	0.04	-8.01×10^{-3}	-0.177	0.0169	0.99
	0.06	-6.95×10^{-3}	-0.194	0.0184	0.99
	0.08	-6.11×10^{-3}	-0.214	0.0204	0.99
2.25	0.02	-8.15×10^{-3}	-0.200	0.0191	0.99
	0.04	-6.34×10^{-3}	-0.207	0.0194	0.99
	0.06	-3.97×10^{-3}	-0.215	0.0198	0.99
	0.08	-1.62×10^{-3}	-0.224	0.0201	0.99
3.516	0.02	-0.026	-0.208	0.0202	0.93
	0.04	-0.025	-0.227	0.0233	0.94
	0.06	-0.024	-0.248	0.0266	0.95
	0.08	-0.021	-0.273	0.0305	0.96
3.125	0.02	9.65×10^{-4}	-0.285	0.0288	0.99
	0.04	4.62×10^{-3}	-0.293	0.0292	0.99
	0.06	8.58×10^{-3}	-0.302	0.0296	0.99
	0.08	13.42×10^{-3}	-0.313	0.0301	0.98
4.5	0.02	-0.013	-0.241	0.0250	0.99
	0.04	-0.014	-0.252	0.0260	0.99
	0.06	-0.014	-0.265	0.0272	0.99
	0.08	-0.014	-0.279	0.0286	0.99
7.031	0.02	-0.018	-0.226	0.0235	0.97
	0.04	-0.019	-0.243	0.0254	0.97
	0.06	-0.020	-0.262	0.0274	0.97
	0.08	-0.021	-0.284	0.0298	0.97

Table 4.16 : Regression analysis for damping ratio ξ - vertical vibration tests

$$\frac{\xi_R}{\xi_U} = a_0 + a_1 n + a_2 n^2, \quad n = \text{No. of reinforcement layers}$$

A_r	F/W	Coefficients of Polynomial			Coefficient of Correlation R^2
		a_0	a_1	a_2	
1.0	0.1	1.035	0.568	-0.0529	0.98
	0.2	1.032	0.485	-0.0362	0.99
	0.3	1.031	0.416	-0.0223	0.99
	0.4	1.028	0.335	-0.0070	0.99
	0.5	1.026	0.265	0.0063	0.99
2.25	0.1	1.010	0.590	-0.0532	0.99
	0.2	1.013	0.574	-0.0517	0.99
	0.3	1.016	0.584	-0.0546	0.99
	0.4	1.024	0.538	-0.0489	0.99
	0.5	1.026	0.513	-0.0462	0.99
3.516	0.1	1.004	0.419	-0.0107	0.99
	0.2	1.008	0.451	-0.0198	0.99
	0.3	1.009	0.477	-0.0273	0.99
	0.4	1.008	0.492	-0.0333	0.99
	0.5	1.006	0.506	-0.0390	0.99
3.125	0.1	1.017	0.620	-0.0589	0.99
	0.2	1.031	0.772	-0.0687	0.99
	0.3	1.042	0.816	-0.0781	0.99
	0.4	1.053	0.878	-0.0839	0.98
	0.5	1.063	0.930	-0.0882	0.99
4.5	0.1	1.045	0.552	-0.0569	0.97
	0.2	1.056	0.655	-0.0696	0.96
	0.3	1.066	0.754	-0.0820	0.96
	0.4	1.075	0.822	-0.0908	0.95
	0.5	1.082	0.883	-0.0984	0.95
7.031	0.1	1.018	0.532	-0.0518	0.99
	0.2	1.034	0.606	-0.0610	0.98
	0.3	1.048	0.671	-0.0690	0.97
	0.4	1.060	0.711	-0.0740	0.96
	0.5	1.066	0.760	-0.0807	0.96

Table 4.17 : Regression analysis for damping ratio ξ_1 - horizontal vibration tests

$$\frac{\xi_{1R}}{\xi_{1U}} = a_0 + a_1 n + a_2 n^2,$$

n = No. of reinforcement layers

A_r	F_1 / W	Coefficients of Polynomial			Coefficient of Correlation R^2
		a_0	a_1	a_2	
1.0	0.02	1.007	-0.0209	0.0128	0.98
	0.04	1.008	-0.0155	0.0125	0.98
	0.06	1.008	-0.0100	0.0121	0.98
	0.08	1.009	-0.0042	0.0117	0.98
2.25	0.02	1.000	0.0231	-1.02×10^{-3}	0.99
	0.04	0.999	0.0260	-7.74×10^{-4}	0.99
	0.06	0.998	0.0302	-9.76×10^{-4}	0.99
	0.08	0.997	0.0328	-5.95×10^{-4}	0.99
3.516	0.02	1.000	0.0268	1.48×10^{-3}	0.99
	0.04	1.001	0.0299	1.42×10^{-3}	0.99
	0.06	1.002	0.0361	1.28×10^{-3}	0.99
	0.08	1.001	0.0410	1.79×10^{-3}	0.99
3.125	0.02	0.996	0.0888	-3.93×10^{-3}	0.99
	0.04	1.001	0.0826	-3.23×10^{-3}	0.99
	0.06	1.008	0.0726	-1.98×10^{-3}	0.98
	0.08	1.015	0.0620	-6.79×10^{-4}	0.99
4.5	0.02	1.105	-0.300	0.0214	0.69
	0.04	0.983	0.0284	5.46×10^{-3}	0.85
	0.06	0.989	0.0320	5.12×10^{-3}	0.92
	0.08	0.997	0.0306	5.37×10^{-3}	0.96
7.031	0.02	0.988	0.0417	-3.45×10^{-3}	0.92
	0.04	0.987	0.0537	-8.33×10^{-4}	0.93
	0.06	0.985	0.0633	-8.33×10^{-4}	0.94
	0.08	0.983	0.0772	-1.48×10^{-4}	0.94

Table 4.18 :Regression analysis for amplitude reduction factor - vertical vibration tests

$$\frac{(A_{zmax})_r}{(A_{zmax})_u} = a_0 + a_1n + a_2n^2 + a_3n^3 + a_4n^4, \quad n = \text{No. of reinforcement layers}$$

A _r	Eccentricity θ°	Coefficients of Polynomial					Coefficient of Correlation R ²
		a ₀	a ₁	a ₂	a ₃	a ₄	
1	4	0	-0.359	0.340	-0.109	0.01	1
	12	0	0.183	-0.193	0.055	-4.64 × 10 ⁻³	1
	20	0	-0.203	0.163	-0.046	3.98 × 10 ⁻³	1
	28	0	-0.190	0.191	-0.061	5.63 × 10 ⁻³	1
2.25	4	1	0.176	-0.210	0.054	-4.17 × 10 ⁻³	1
	12	1	0.083	-0.094	0.025	-2.02 × 10 ⁻³	1
	20	1	-0.065	0.026	-4.06 × 10 ⁻³	1.94 × 10 ⁻⁴	1
	28	1	-0.045	0.010	-3.41 × 10 ⁻³	3.78 × 10 ⁻⁴	1
3.516	4	1	0.281	-0.247	0.0521	-3.47 × 10 ⁻³	1
	12	1	0.097	-0.109	0.0302	-2.60 × 10 ⁻³	1
	20	1	-0.292	0.282	-0.0873	-7.90 × 10 ⁻³	1
	28	1	-0.223	0.150	-0.0424	3.72 × 10 ⁻³	1
3.125	4	1	0.349	-0.340	0.0898	-7.37 × 10 ⁻³	1
	12	1	-3.8 × 10 ⁻³	-7.83 × 10 ⁻³	-9.39 × 10 ⁻⁴	2.95 × 10 ⁻⁴	1
	20	1	0.127	-0.136	0.0394	-3.47 × 10 ⁻³	1
	28	1	-0.039	0.054	-0.0250	2.60 × 10 ⁻³	1
4.5	4	1	0.411	-0.376	0.0911	-6.94 × 10 ⁻³	1
	12	1	0.361	-0.337	0.0868	-6.94 × 10 ⁻³	1
	20	1	0.115	-0.099	0.0196	-1.15 × 10 ⁻³	1
	28	1	0.507	-0.436	0.1048	-7.93 × 10 ⁻³	1
7.031	4	1	0.604	-0.541	0.1315	-9.98 × 10 ⁻³	1
	12	1	0.045	-0.039	2.60 × 10 ⁻³	2.90 × 10 ⁻⁴	1
	20	1	-0.028	0.032	-0.0157	1.74 × 10 ⁻³	1
	28	1	0.657	-0.571	0.1402	-0.0108	1

Table 4.19 :Regression analysis for amplitude reduction factor - horizontal vibration tests

$$\frac{(A_{x1max})_r}{(A_{x1max})_u} = a_0 + a_1n + a_2n^2 + a_3n^3 + a_4n^4, \quad n = \text{No. of reinforcement layers}$$

A _r	Eccentricity θ°	Coefficients of Polynomial					Coefficient of Correlation R ²
		a ₀	a ₁	a ₂	a ₃	a ₄	
1	4	1	0.120	-0.154	0.0365	-2.60 × 10 ⁻³	1
	12	1	-0.245	0.199	-0.0603	5.42 × 10 ⁻³	1
	20	1	-0.530	0.396	-0.1017	8.24 × 10 ⁻³	1
	28	1	-0.183	0.127	-0.0333	2.78 × 10 ⁻³	1
2.25	4	1	-0.573	0.398	-0.1042	8.68 × 10 ⁻³	1
	12	1	0.121	-0.085	0.0133	-6.33 × 10 ⁻⁴	1
	20	1	0.025	-0.043	6.88 × 10 ⁻⁴	6.74 × 10 ⁻⁴	1
	28	1	-0.057	6.67 × 10 ⁻³	-5.83 × 10 ⁻³	8.33 × 10 ⁻⁴	1
3.516	4	1	0.250	-0.283	0.0755	-6.08 × 10 ⁻³	1
	12	1	0.188	-0.276	0.0830	-7.31 × 10 ⁻³	1
	20	1	-0.495	0.274	-0.0621	4.72 × 10 ⁻³	1
	28	1	0.090	-0.158	0.0508	-4.72 × 10 ⁻³	1
3.125	4	1	-0.521	0.303	-0.0716	5.64 × 10 ⁻³	1
	12	1	-0.443	0.253	-0.0594	4.71 × 10 ⁻³	1
	20	1	0.600	-0.544	0.1320	-0.0100	1
	28	1	0.09	-0.111	0.0312	-2.92 × 10 ⁻³	1
4.5	4	1	-0.031	-0.072	0.0247	-2.17 × 10 ⁻³	1
	12	1	-0.168	0.088	-0.0230	2 × 10 ⁻³	1
	20	1	0.250	-0.209	0.0397	-2.22 × 10 ⁻³	1
	28	1	0.210	-0.203	0.0421	-2.64 × 10 ⁻³	1
7.031	4	1	-0.266	0.032	5.21 × 10 ⁻³	-8.68 × 10 ⁻⁴	1
	12	1	-0.061	0.031	-0.0152	1.74 × 10 ⁻³	1
	20	1	1.184	-1.062	0.2714	-0.0215	1
	28	1	1.217	-1.136	0.2967	-0.0239	1

Table 4.20 : Comparison of analytical and experimental values of coefficient of elastic uniform compression - vertical vibration tests

Size of block - 0.8mx0.4mx0.4m, $D_r = 70\%$, $n = \text{No. of reinforcement layers}$

Reinforcement Size	$\theta^0 \rightarrow$	Predicted value of C_u ($\text{kN/m}^3 \times 10^5$)				Observed value of C_u ($\text{kN/m}^3 \times 10^5$)				Difference (%)			
		4	12	20	28	4	12	20	28	4	12	20	28
0.8mx0.4m	n=2	1.22	1.15	1.11	1.08	1.17	1.095	1.047	1.000	4.1	4.8	5.6	7.4
	3	1.19	1.12	1.08	1.06	1.095	1.047	1.024	0.977	8.0	6.5	5.2	7.8
	4	1.16	1.10	1.06	1.04	1.095	1.000	0.977	0.954	5.6	9.1	7.8	8.3
	6	1.13	1.08	1.04	1.02	1.047	0.977	0.954	0.909	7.3	9.5	8.3	10.9
1.2mx0.6m	n=2	1.24	1.17	1.12	1.10	1.145	1.071	1.024	0.977	7.7	8.5	8.6	11.2
	3	1.22	1.15	1.105	1.08	1.145	1.047	1.000	0.932	6.1	8.9	9.5	13.7
	4	1.20	1.13	1.09	1.07	1.095	1.000	0.977	0.954	8.7	11.5	10.4	10.8
	6	1.17	1.107	1.067	1.047	1.071	1.000	0.954	0.909	8.5	9.7	10.6	13.2
1.5mx0.75m	n=2	1.25	1.18	1.13	1.11	1.120	1.024	0.977	0.909	10.4	13.2	13.5	18.1
	3	1.23	1.16	1.12	1.096	1.095	1.000	0.954	0.909	11.9	13.8	14.8	17.1
	4	1.22	1.15	1.106	1.085	1.095	1.000	0.954	0.887	10.2	13.0	13.7	18.2
	6	1.19	1.13	1.087	1.067	1.071	1.000	0.932	0.887	10.0	11.5	14.3	16.9
1.0mx1.0m	n=2	1.26	1.187	1.14	1.117	1.047	0.977	0.932	0.887	16.9	17.7	18.2	20.6
	3	1.245	1.17	1.128	1.105	1.024	0.954	0.909	0.887	17.7	18.5	19.4	19.7
	4	1.23	1.16	1.117	1.095	1.024	0.954	0.887	0.866	16.7	17.8	20.6	20.9
	6	1.21	1.144	1.10	1.08	1.000	0.932	0.887	0.866	17.4	18.5	19.4	19.8
1.2mx1.2m	n=2	1.267	1.192	1.144	1.12	1.071	0.977	0.954	0.932	15.5	18.0	16.6	16.8
	3	1.25	1.18	1.134	1.11	1.000	0.977	0.932	0.909	20.0	17.2	17.8	18.1
	4	1.24	1.17	1.125	1.10	0.954	0.932	0.887	0.866	23.1	20.3	21.2	21.3
	6	1.224	1.155	1.11	1.09	0.954	0.909	0.887	0.866	22.1	21.3	20.1	20.6
1.5mx1.5m	n=2	1.27	1.195	1.148	1.124	1.047	0.977	0.932	0.909	17.6	18.2	18.8	19.1
	3	1.26	1.185	1.139	1.115	1.000	0.977	0.909	0.887	20.6	17.6	20.2	20.4
	4	1.25	1.176	1.13	1.108	0.977	0.909	0.887	0.866	21.8	22.7	21.5	21.8
	6	1.233	1.163	1.118	1.096	0.954	0.909	0.887	0.866	22.6	21.8	20.7	21.0

Table 4.21 : Comparison of analytical and experimental values of coefficient of elastic uniform compression - cyclic plate load tests, n = No. of reinforcement layers

Footing Size - 150mm x 150mm $D_r = 70\%$	n=	Predicted value of C_u ($\text{kN/m}^3 \times 10^5$)					Observed value of C_u ($\text{kN/m}^3 \times 10^5$)					Difference (%)				
		2	3	4	6	8	2	3	4	6	8	2	3	4	6	8
Reinforcement Size																
150mm x 150mm		2.55	2.51	2.49	2.46	2.44	2.22	2.04	1.80	1.58	1.45	12.9	18.7	27.7	35.8	40.5
300mm x 300mm		2.59	2.56	2.53	2.50	2.48	2.10	2.28	2.18	2.00	1.91	18.9	10.9	13.8	20.0	23.0
450mm x 450mm		2.61	2.58	2.56	2.53	2.51	2.25	2.10	2.08	2.03	2.02	13.8	18.6	18.8	19.8	19.5
600mm x 600mm		2.62	2.60	2.58	2.55	2.54	2.17	2.17	2.15	2.10	2.08	17.2	16.5	16.7	17.6	18.1
750mm x 750mm		2.63	2.61	2.59	2.57	2.55	2.35	2.32	2.40	2.36	2.16	10.6	11.1	7.3	8.2	15.3
Footing Size = 150mm x 150mm $D_r = 50\%$		n = 4					n = 4									
Reinforcement Size																
150mm x 150mm		2.20					1.75					18.2				
300mm x 300mm		2.23					1.82					18.4				
450mm x 450mm		2.24					1.75					21.9				
600mm x 600mm		2.25					1.86					17.3				
750mm x 750mm		2.26					1.79					20.8				
Footing Size = 300mm x 300mm $D_r = 70\%$		n = 4					n = 4									
Reinforcement Size																
300mm x 300mm		2.06					1.95					5.3				
600mm x 600mm		2.11					1.75					17.1				
900mm x 900mm		2.15					1.63					24.2				
1200mm x 1200mm		2.17					1.57					27.6				
1500mm x 1500mm		2.19					1.54					29.7				

**Table 4.22 : Comparison of analytical and experimental values of coefficient of elastic uniform shear -
horizontal vibration tests**
Size of block - 0.8mx0.4mx0.4m, $D_r = 70\%$, n = No. of reinforcement layers

Reinforcement Size	$\theta^0 \rightarrow$	Predicted value of C_r ($\text{kN/m}^3 \times 10^4$)				Observed value of C_r ($\text{kN/m}^3 \times 10^4$)				Difference (%)			
		4	12	20	28	4	12	20	28	4	12	20	28
0.8mx0.4m	n=2	2.11	2.05	2.02	1.96	2.25	2.14	2.05	1.92	-6.6	-4.4	-1.5	2.0
	3	2.05	1.99	1.97	1.91	2.12	1.90	1.85	1.77	-3.4	4.5	6.1	7.3
	4	2.01	1.96	1.93	1.89	2.10	1.90	1.83	1.80	-4.5	3.1	5.2	4.8
	6	1.98	1.94	1.91	1.87	1.98	1.83	1.78	1.78	-	5.7	6.8	4.8
1.2mx0.6m	n=2	2.15	2.08	2.05	1.98	2.12	1.94	1.92	1.78	1.4	6.7	6.3	10.1
	3	2.10	2.04	2.00	1.95	1.98	1.83	1.78	1.71	5.7	10.3	11.0	12.3
	4	2.07	2.01	1.98	1.93	1.83	1.78	1.66	1.54	11.6	11.4	16.2	20.2
	6	2.04	1.99	1.96	1.91	1.94	1.78	1.69	1.61	4.9	10.6	13.8	15.7
1.5mx0.75m	n=2	2.44	2.33	2.27	2.17	1.98	1.83	1.78	1.64	18.9	21.5	21.6	24.4
	3	2.34	2.25	2.19	2.11	1.98	1.92	1.68	1.61	18.2	14.7	23.3	23.7
	4	2.28	2.19	2.14	2.07	1.98	1.81	1.76	1.74	13.2	17.4	17.8	15.9
	6	2.21	2.14	2.09	2.02	1.81	1.71	1.64	1.61	18.1	20.1	21.5	20.3
1.0mx1.0m	n=2	2.56	2.44	2.36	2.25	2.01	1.93	1.81	1.76	21.5	20.1	23.3	21.8
	3	2.48	2.36	2.30	2.20	1.77	1.74	1.58	1.56	28.6	26.3	31.3	29.1
	4	2.42	2.32	2.26	2.16	1.85	1.72	1.68	1.54	23.6	25.9	25.7	28.7
	6	2.37	2.27	2.22	2.13	1.94	1.70	1.58	1.58	18.1	25.1	28.8	25.8
1.2mx1.2m	n=2	2.59	2.45	2.38	2.26	2.01	1.90	1.81	1.68	22.4	22.4	23.9	25.7
	3	2.50	2.38	2.31	2.21	1.93	1.85	1.77	1.70	22.8	22.3	23.4	23.1
	4	2.44	2.33	2.27	2.17	1.87	1.72	1.70	1.63	23.4	26.2	25.1	24.9
	6	2.37	2.28	2.22	2.13	1.85	1.72	1.70	1.63	21.9	24.6	23.4	23.5
1.5mx1.5m	n=2	2.59	2.46	2.38	2.27	2.01	1.87	1.83	1.70	22.4	24.0	23.1	25.1
	3	2.50	2.38	2.31	2.21	1.93	1.74	1.72	1.72	22.8	26.9	25.5	22.2
	4	2.43	2.33	2.27	2.17	1.98	1.85	1.70	1.68	18.5	20.6	25.1	22.6
	6	2.36	2.27	2.21	2.12	1.96	1.72	1.70	1.63	16.9	24.2	23.1	23.1

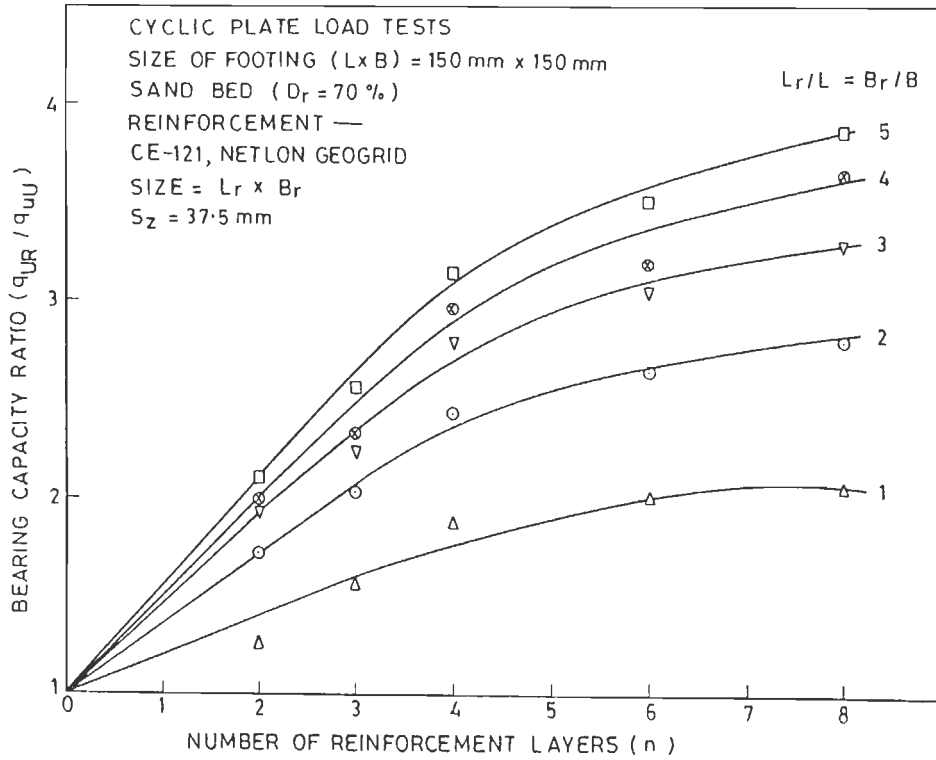


FIG. 4.1 BEARING CAPACITY RATIO VERSUS NUMBER OF REINFORCEMENT LAYERS (FACTOR OF SAFETY = 1)

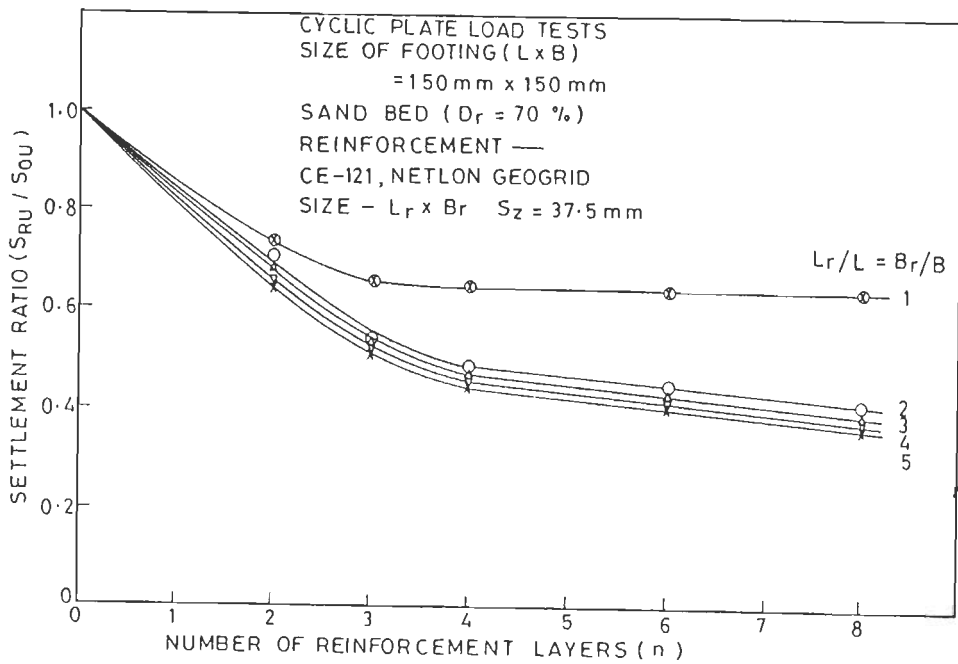


FIG. 4.2 SETTLEMENT RATIO VERSUS NUMBER OF REINFORCEMENT LAYERS (FACTOR OF SAFETY = 1)

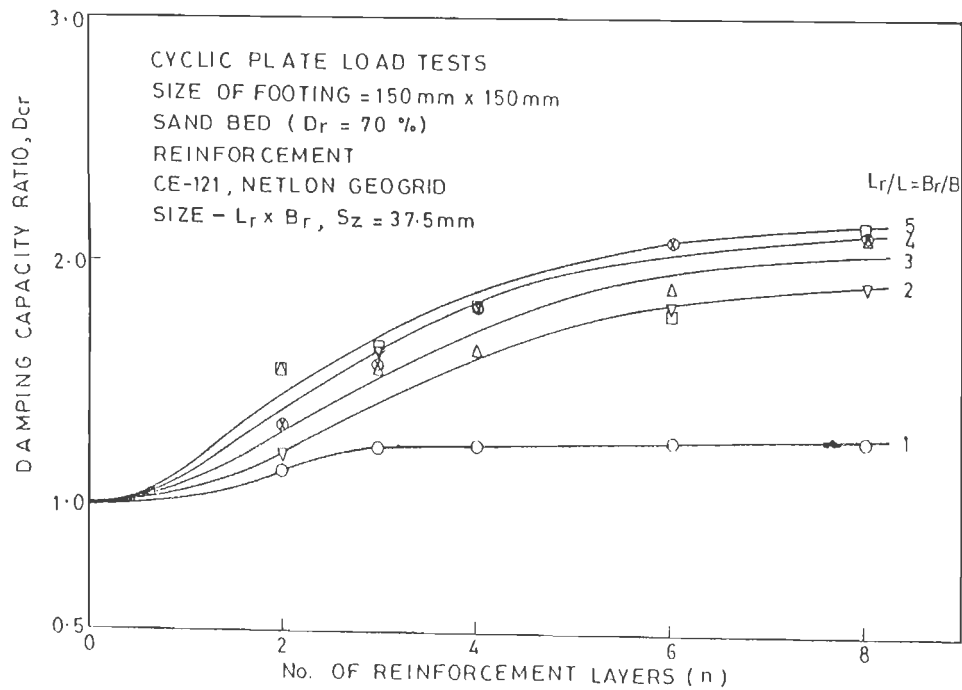


FIG. 4.3 DAMPING CAPACITY RATIO VERSUS NUMBER OF REINFORCEMENT LAYERS

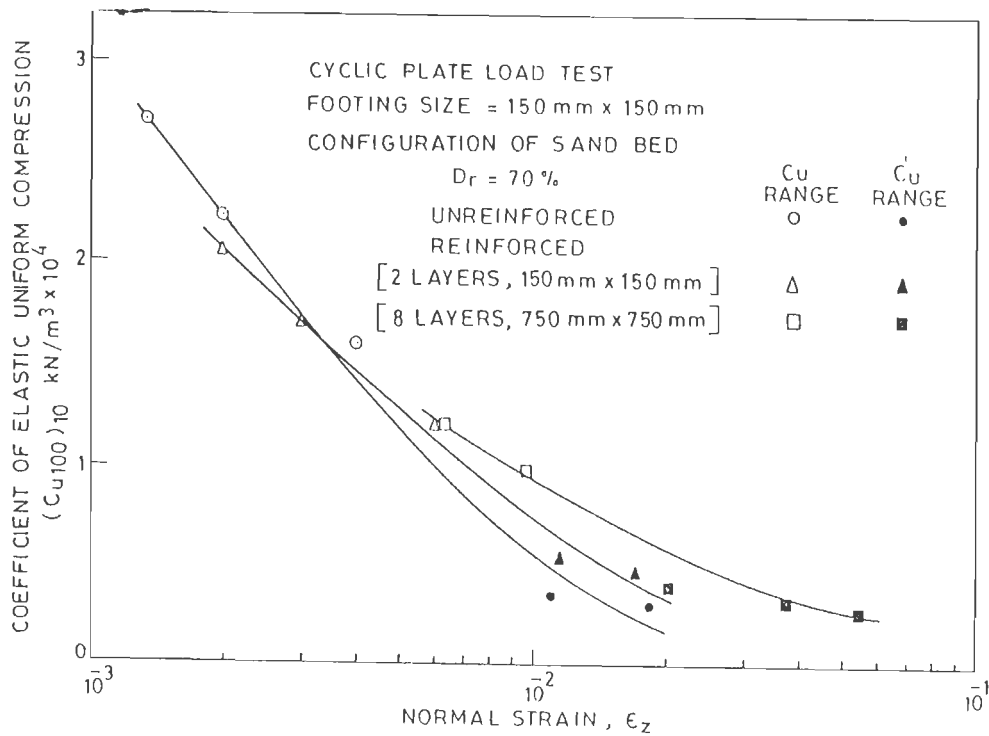


FIG. 4.4 COEFFICIENT OF ELASTIC UNIFORM COMPRESSION $(C_{u100})_{10}$ VERSUS NORMAL STRAIN [EFFECT OF GEOGRID NETLON CE-121 REINFORCEMENT]

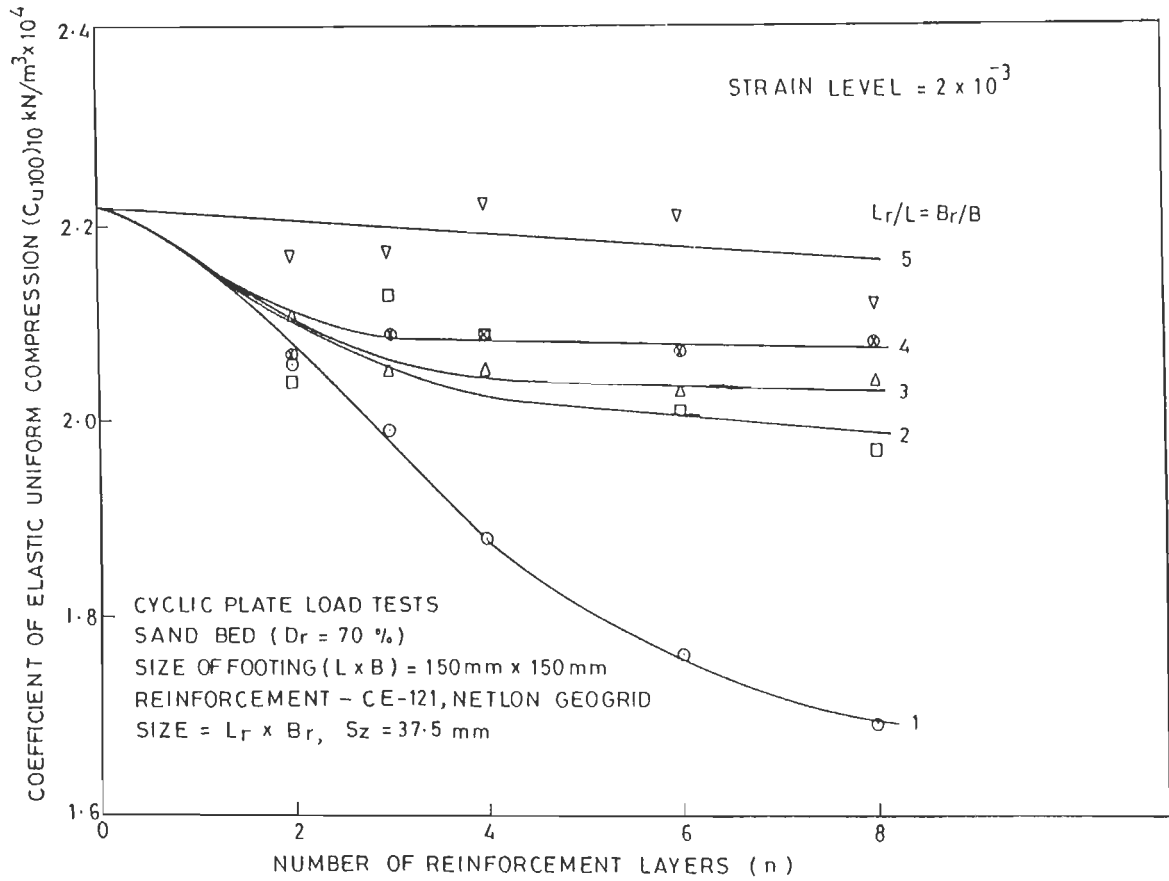


FIG. 4.5 COEFFICIENT OF ELASTIC UNIFORM COMPRESSION VERSUS NUMBER OF REINFORCEMENT LAYERS

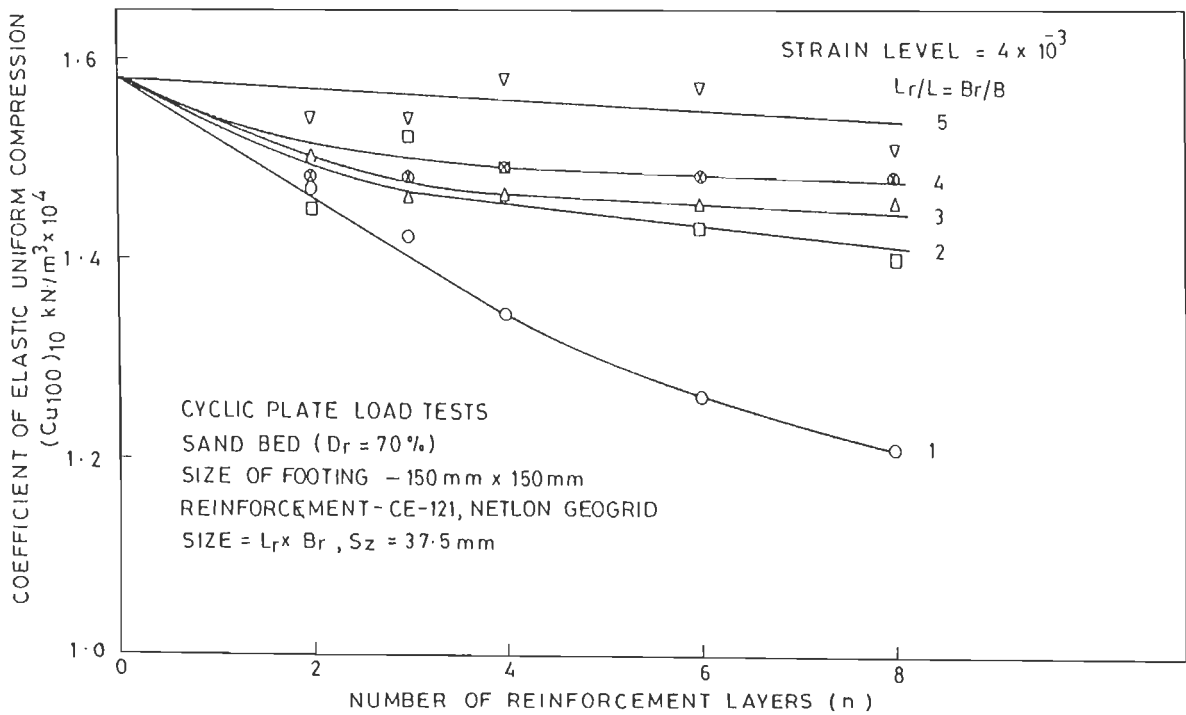


FIG. 4.6 COEFFICIENT OF ELASTIC UNIFORM COMPRESSION VERSUS NUMBER OF REINFORCEMENT LAYERS

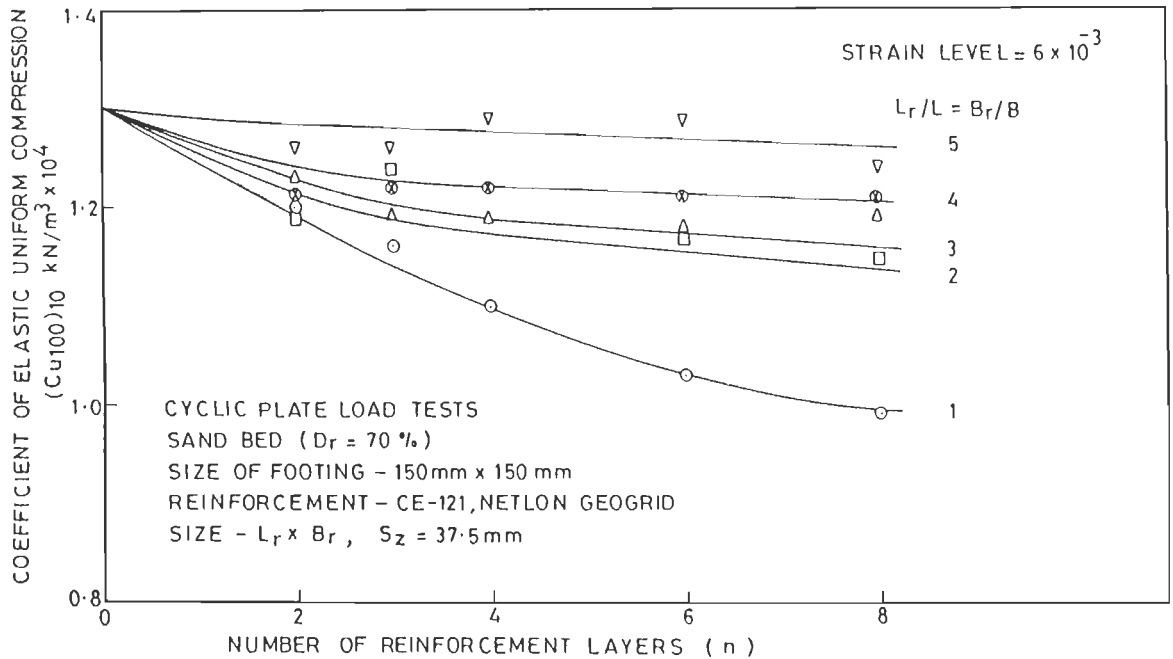


FIG. 4.7 COEFFICIENT OF ELASTIC UNIFORM COMPRESSION VERSUS NUMBER OF REINFORCEMENT LAYERS

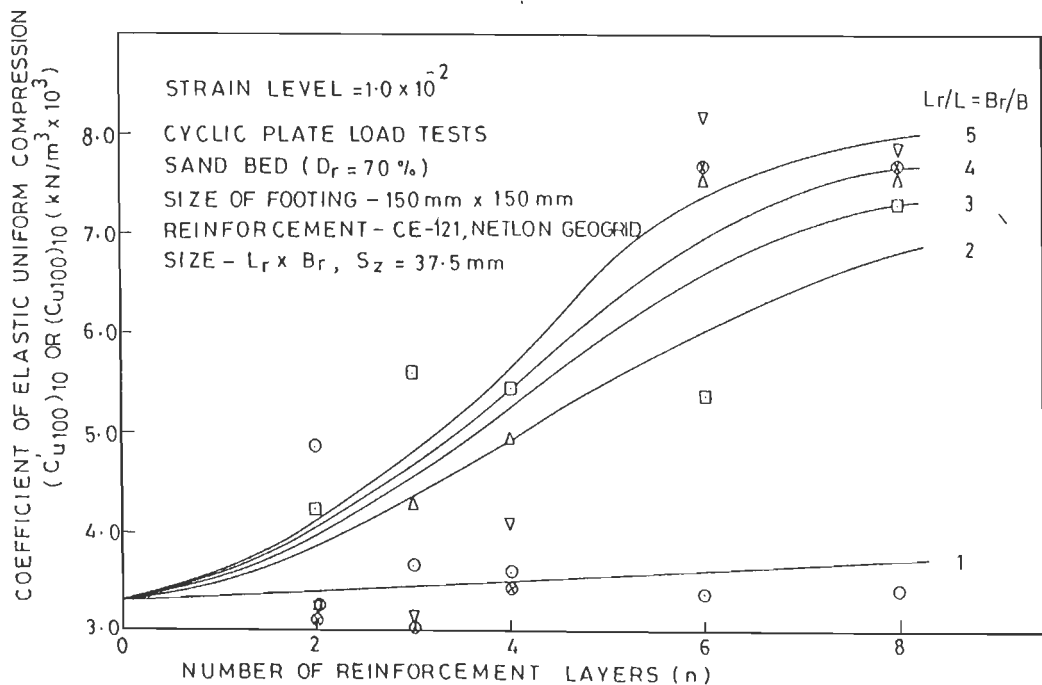


FIG. 4.8 COEFFICIENT OF ELASTIC UNIFORM COMPRESSION VERSUS NUMBER OF REINFORCEMENT LAYERS

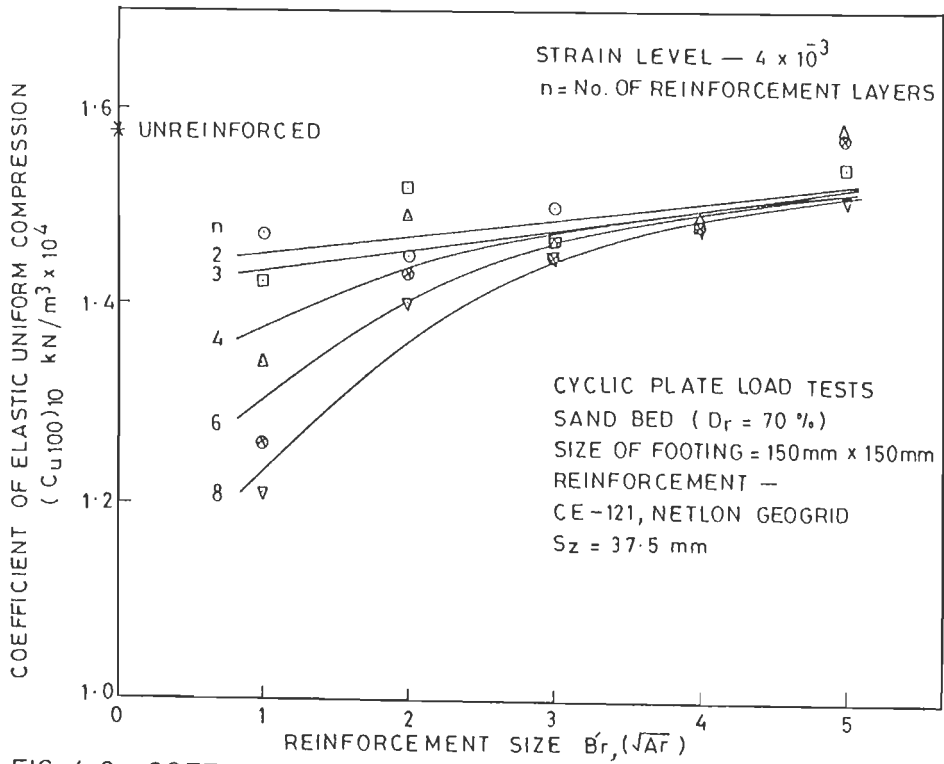


FIG. 4.9 COEFFICIENT OF ELASTIC UNIFORM COMPRESSION VERSUS REINFORCEMENT SIZE

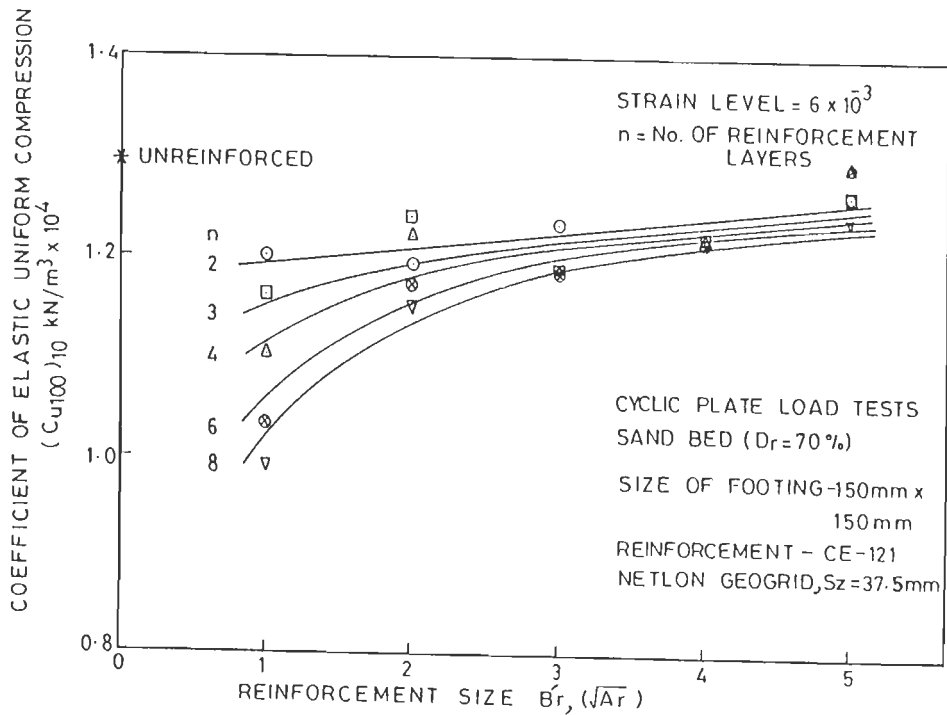


FIG. 4.10 COEFFICIENT OF ELASTIC UNIFORM COMPRESSION VERSUS REINFORCEMENT SIZE

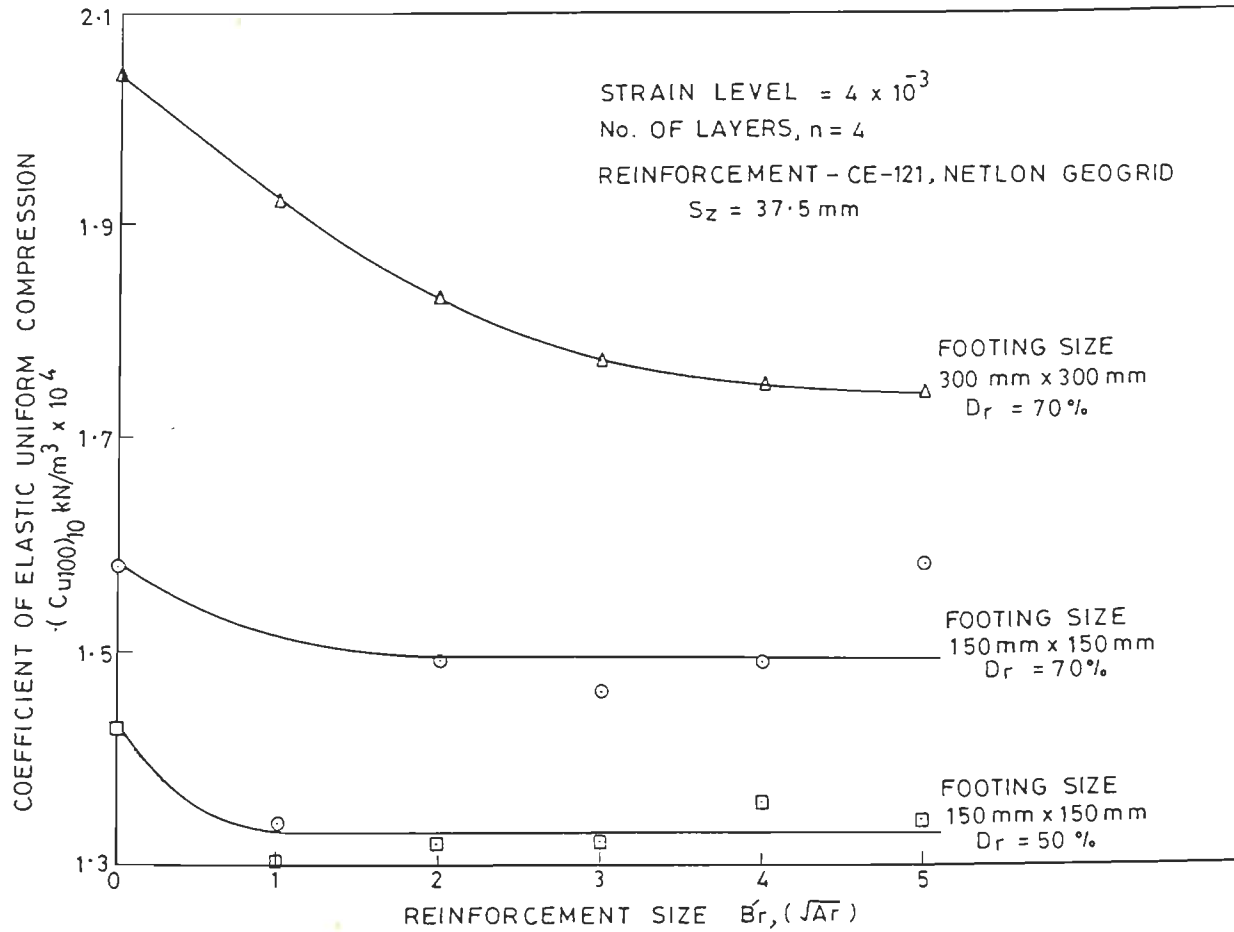


FIG. 4.11 INTERPRETATION OF CYCLIC PLATE LOAD TEST DATA — EFFECT OF SOIL DENSITY AND FOOTING SIZE ON C_u

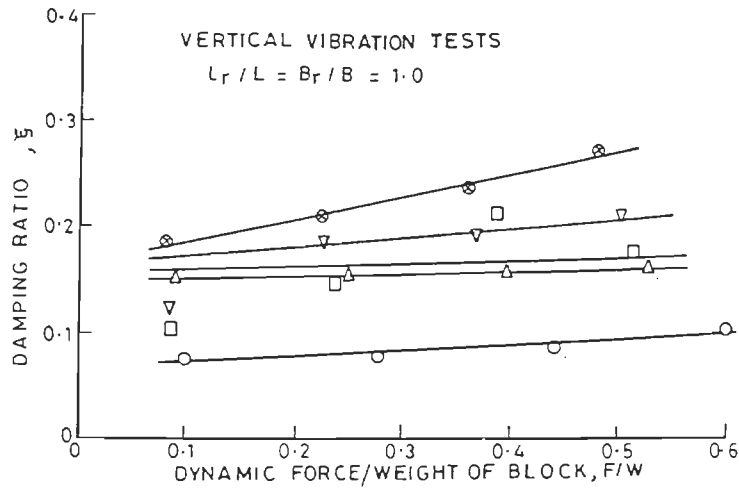


FIG. 4.12 DAMPING RATIO VERSUS F/W

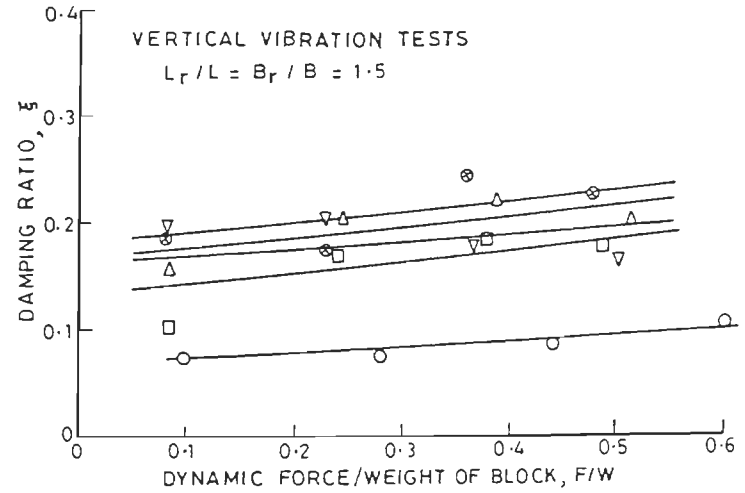


FIG. 4.13 DAMPING RATIO VERSUS F/W

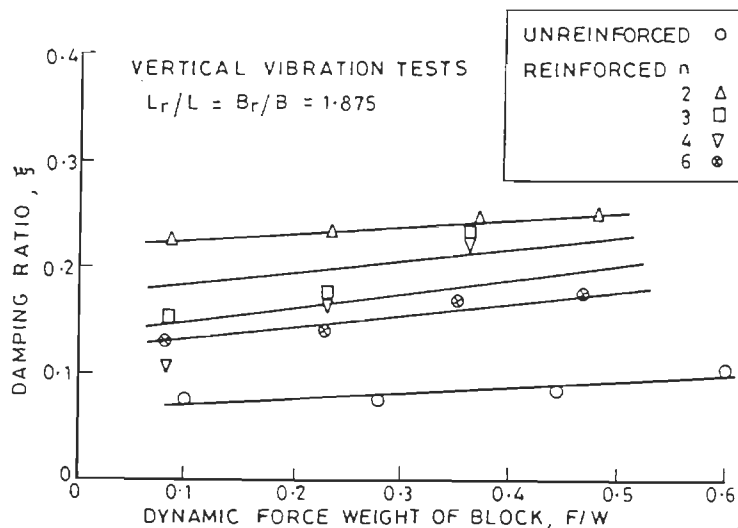


FIG. 4.14 DAMPING RATIO VERSUS F/W

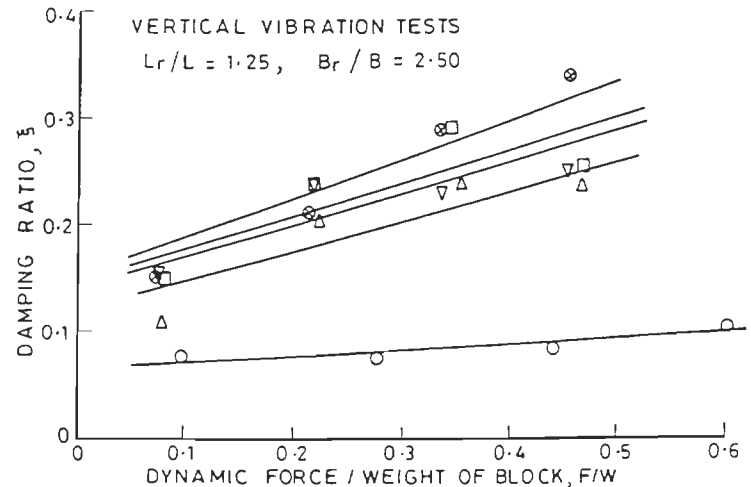


FIG. 4.15 DAMPING RATIO VERSUS F/W

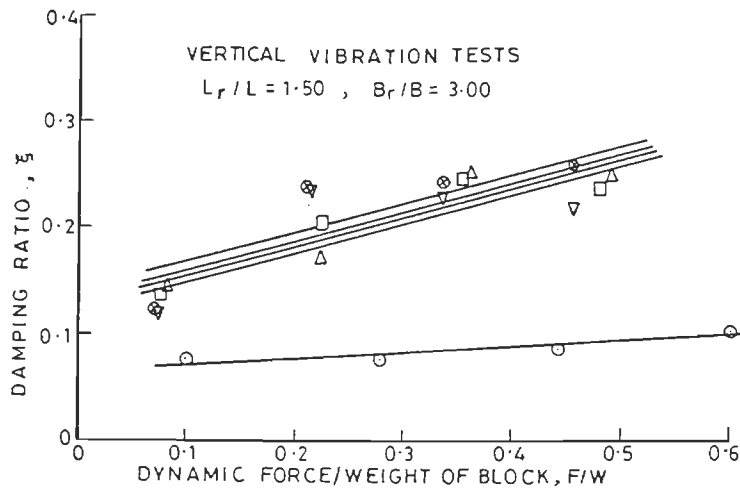


FIG. 4.16 DAMPING RATIO VERSUS F/W

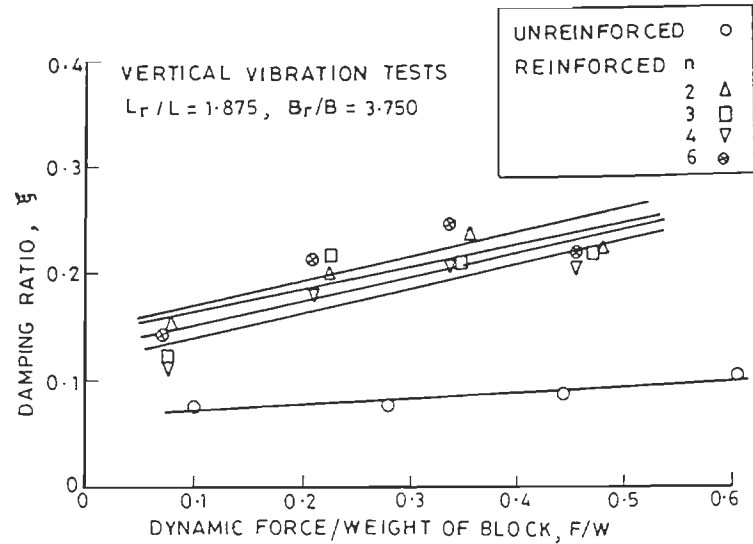


FIG. 4.17 DAMPING RATIO VERSUS F/W

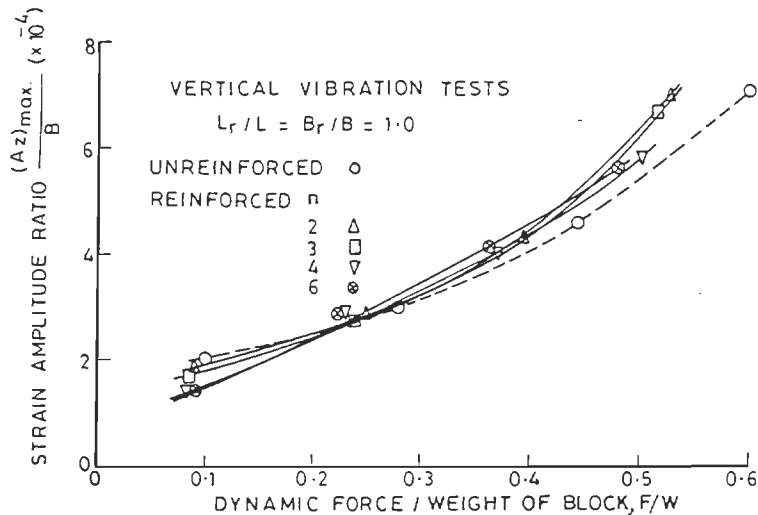


FIG. 4.18 STRAIN AMPLITUDE RATIO VERSUS F/W

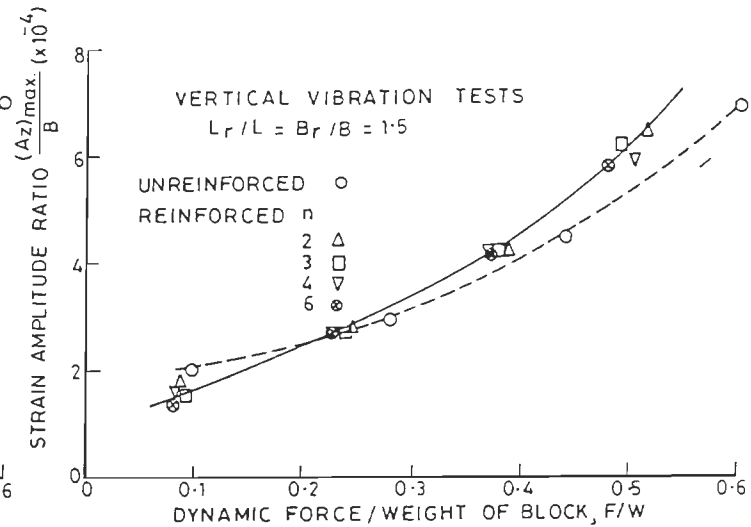


FIG. 4.19 STRAIN AMPLITUDE RATIO VERSUS F/W

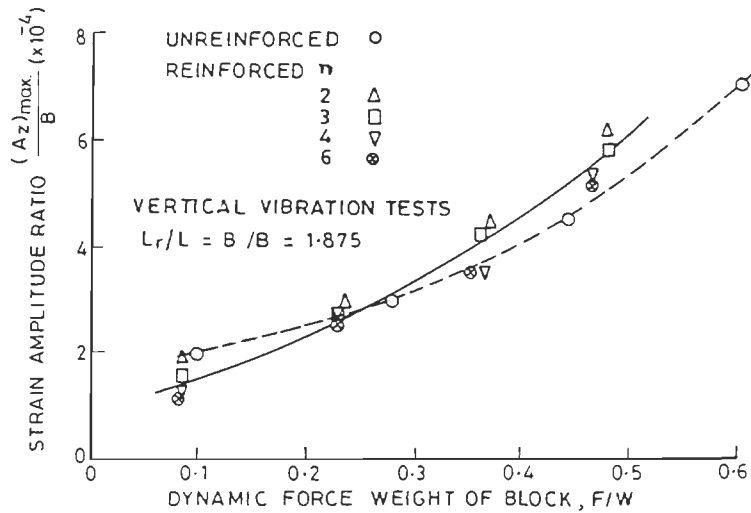


FIG. 4.20 STRAIN AMPLITUDE RATIO VERSUS F/W

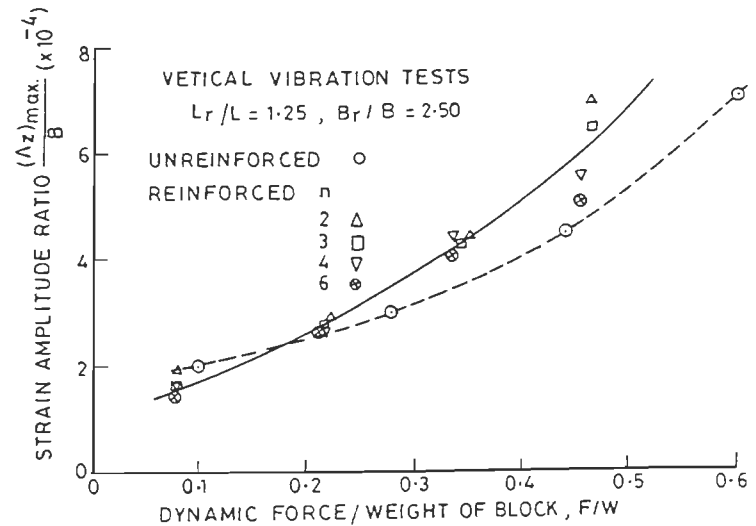


FIG. 4.21 STRAIN AMPLITUDE RATIO VERSUS F/W

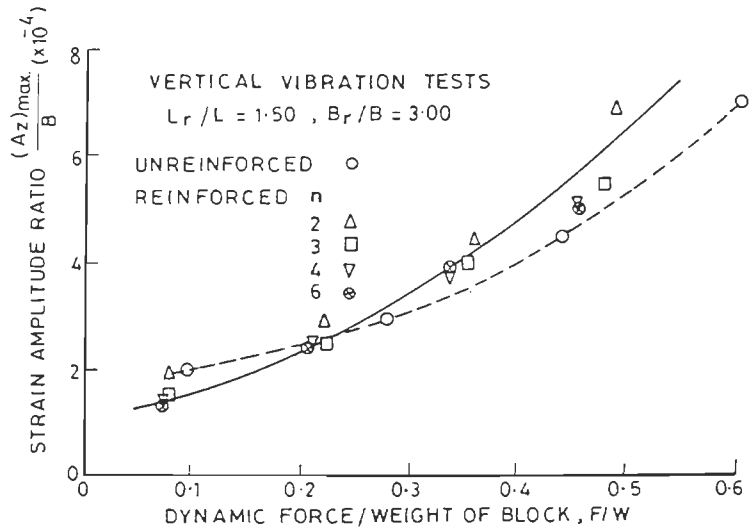


FIG. 4.22 STRAIN AMPLITUDE RATIO VERSUS F/W

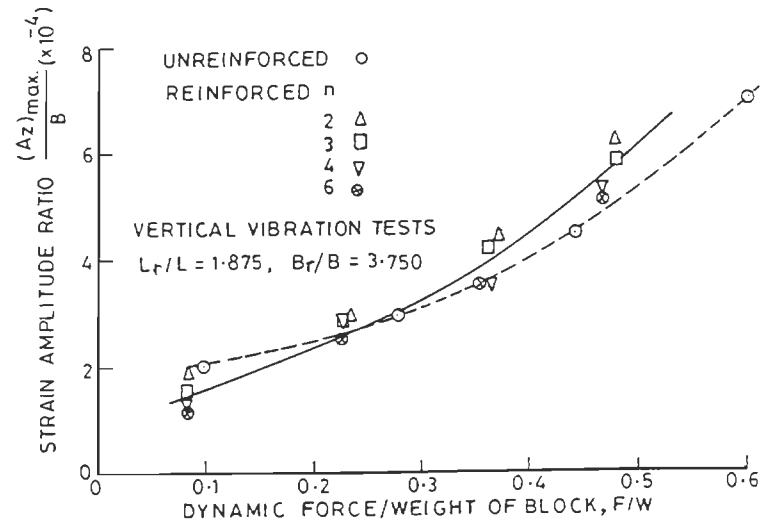


FIG. 4.23 STRAIN AMPLITUDE RATIO VERSUS F/W

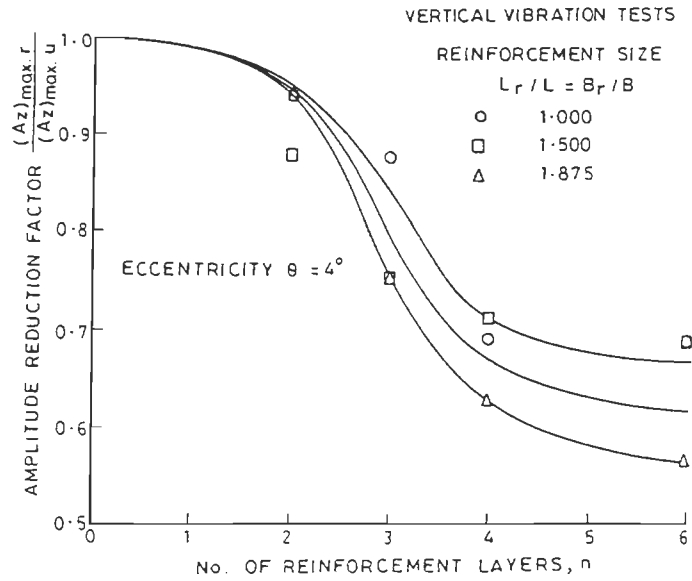


FIG. 4.24 AMPLITUDE REDUCTION FACTOR VERSUS n

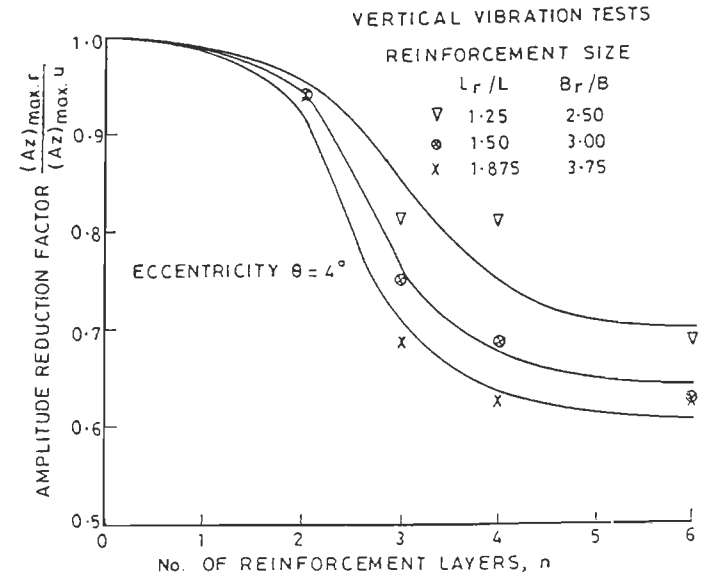


FIG. 4.25 AMPLITUDE REDUCTION FACTOR VERSUS n

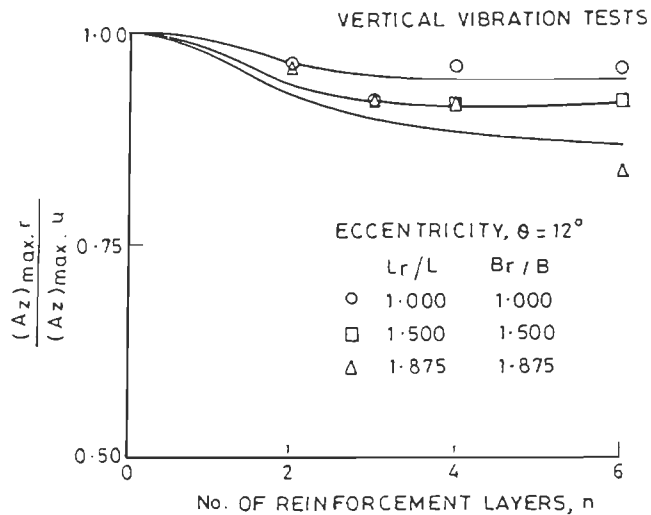


FIG. 4.26 AMPLITUDE REDUCTION FACTOR VERSUS n

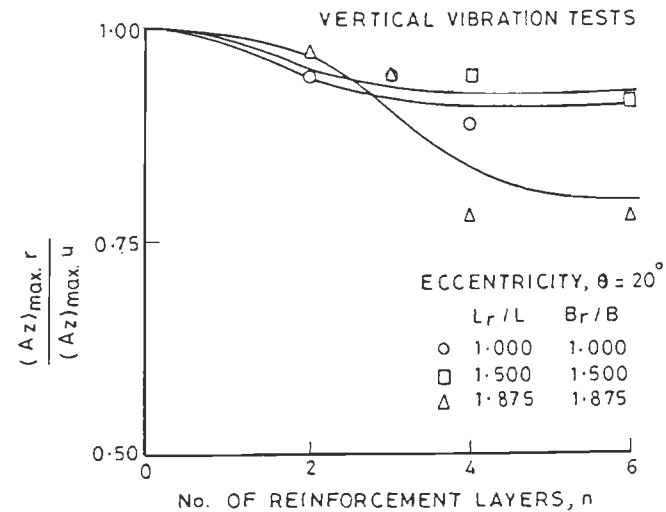


FIG. 4.27 AMPLITUDE REDUCTION FACTOR VERSUS n

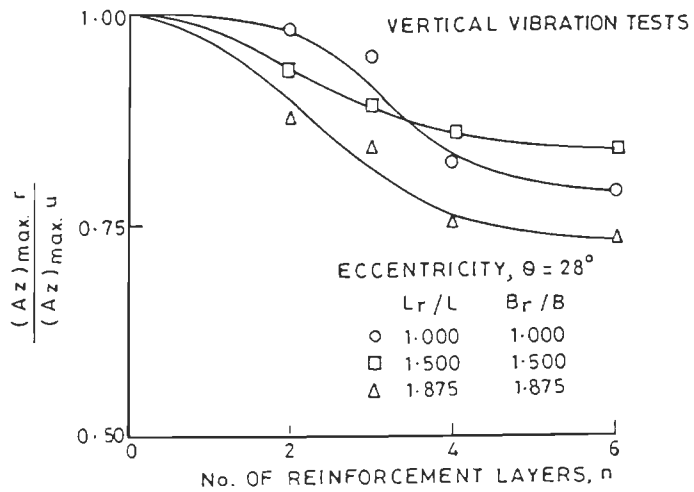


FIG. 4-28 AMPLITUDE REDUCTION FACTOR VERSUS n

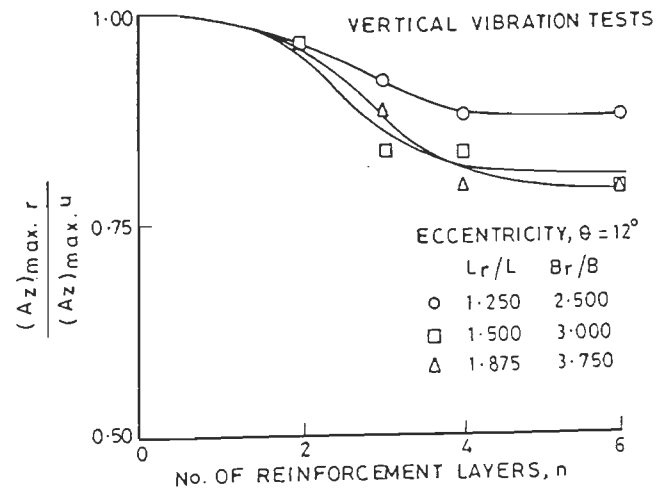


FIG. 4-29 AMPLITUDE REDUCTION FACTOR VERSUS n

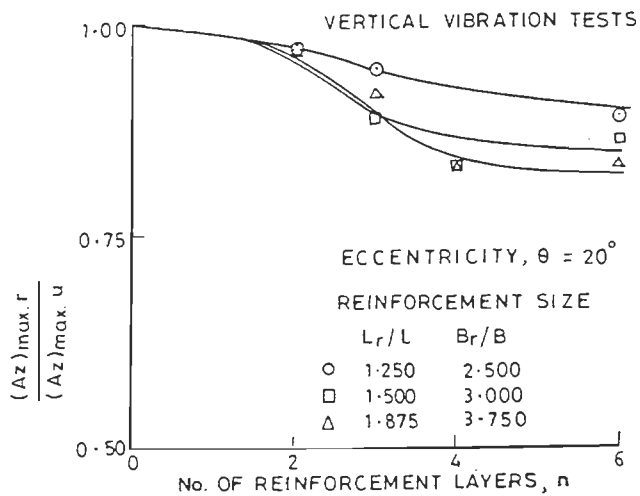


FIG. 4-30 AMPLITUDE REDUCTION FACTOR VERSUS n

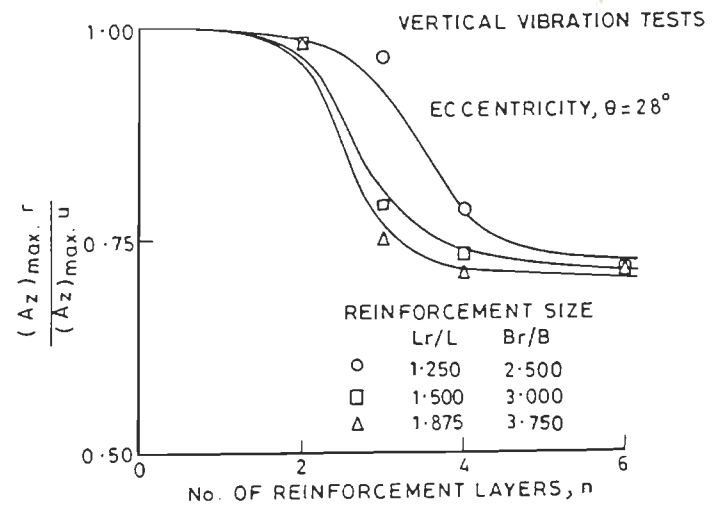


FIG. 4-31 AMPLITUDE REDUCTION FACTOR VERSUS n

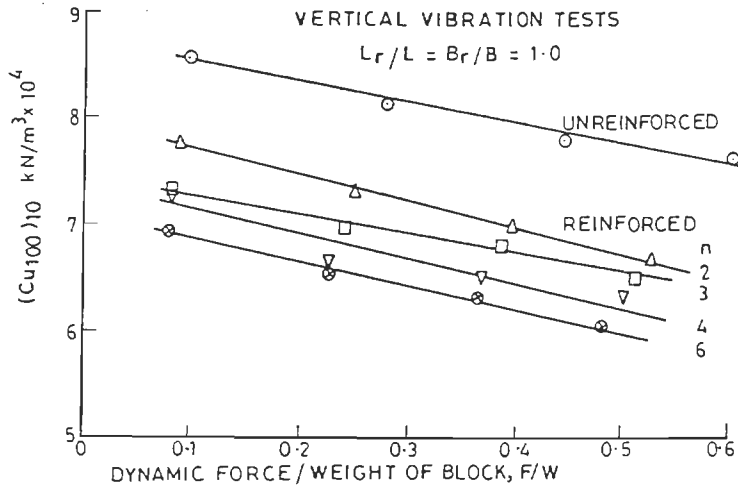


FIG. 4.32 $(C_{u100})_{10}$ VERSUS F/W

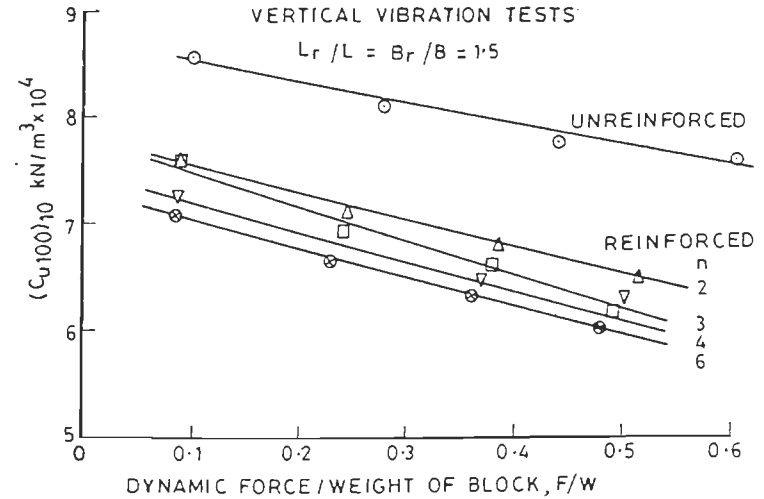


FIG. 4.33 $(C_{u100})_{10}$ VERSUS F/W

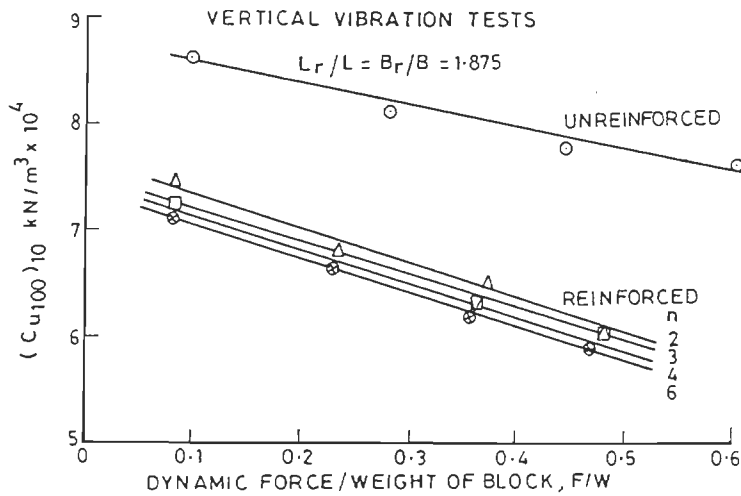


FIG. 4.34 $(C_{u100})_{10}$ VERSUS F/W

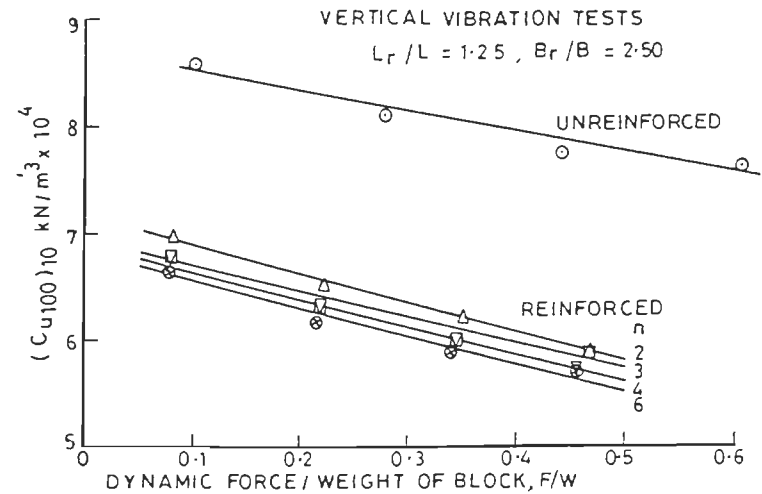


FIG. 4.35 $(C_{u100})_{10}$ VERSUS F/W

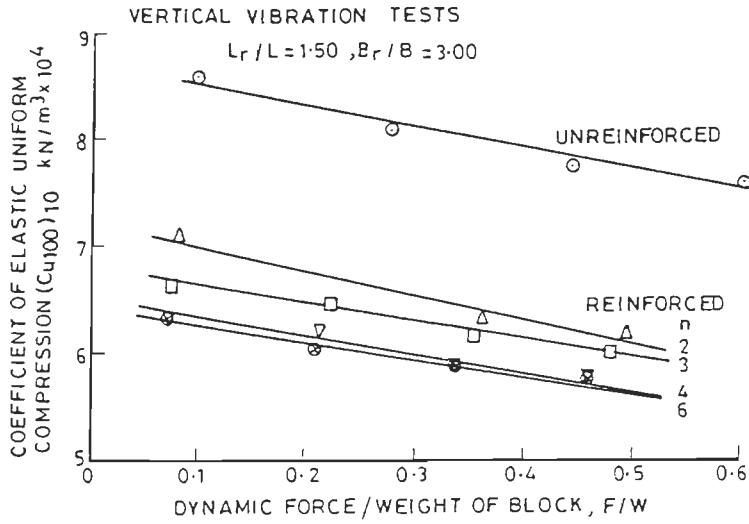


FIG. 4.36 $(C_{u100})_{10}$ VERSUS F/W

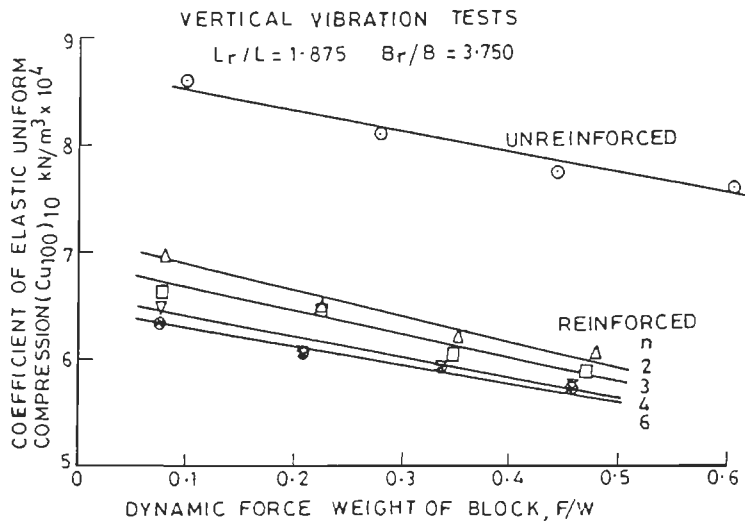


FIG. 4.37 $(C_{u100})_{10}$ VERSUS F/W

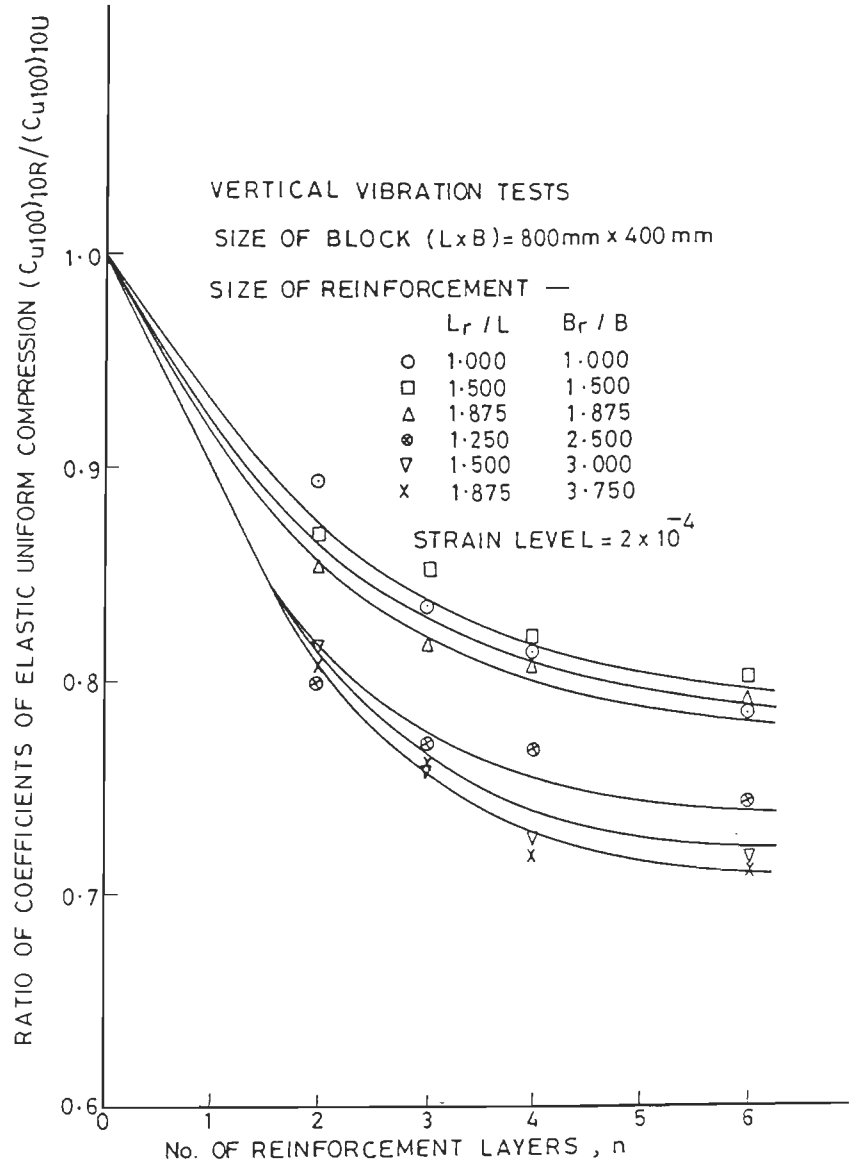


FIG. 4.38 $(C_{u100})_{10R} / (C_{u100})_{10U}$ RATIO VERSUS No. OF REINFORCEMENT LAYERS 'n'

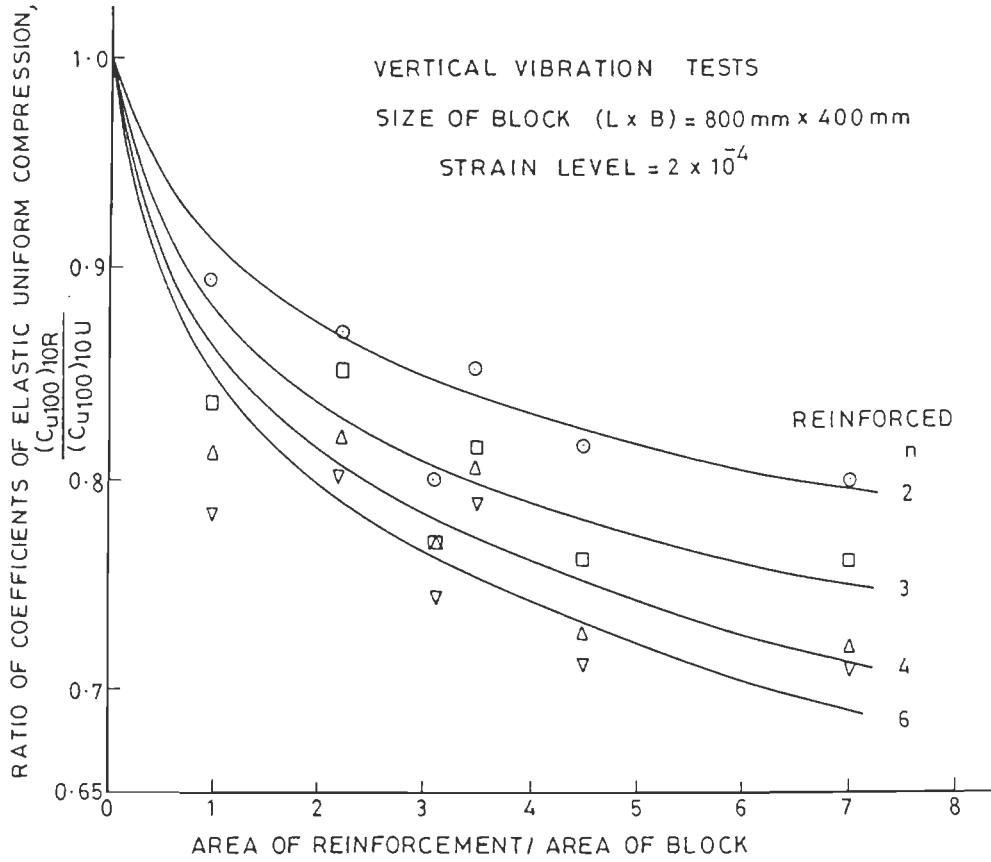


FIG. 4.39 C_u -RATIO VERSUS RATIO OF REINFORCEMENT AREA/ AREA OF BLOCK

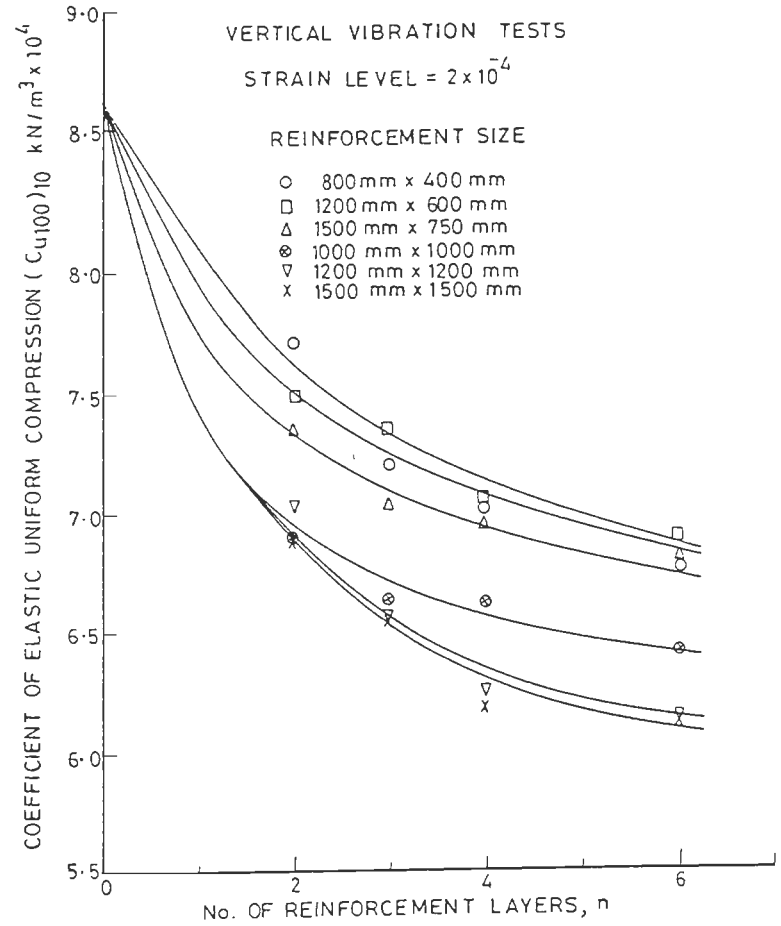


FIG. 4.40 $(C_{u100})_{10}$ VERSUS No. OF REINFORCEMENT LAYERS

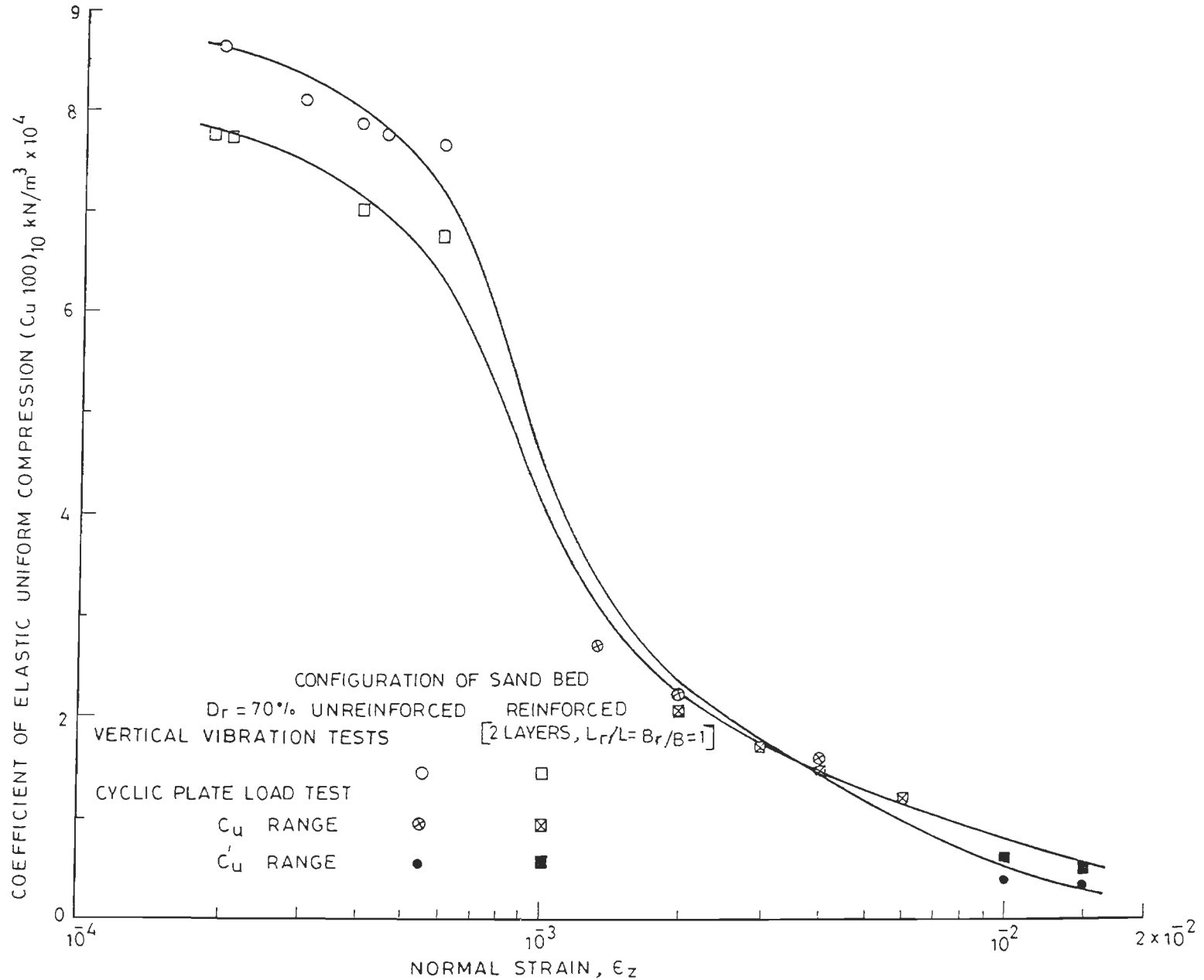


FIG. 4.41 COEFFICIENT OF ELASTIC UNIFORM COMPRESSION C_u (OR C'_u) VERSUS NORMAL STRAIN (EFFECT OF GEOGRID REINFORCEMENT ON C_u)

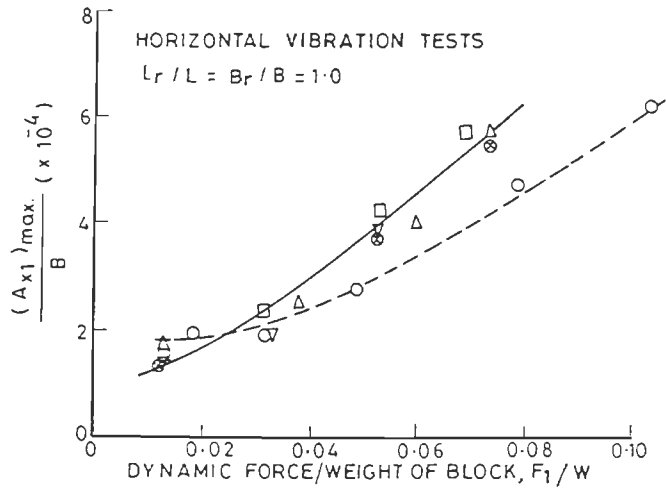


FIG. 4.42 STRAIN AMPLITUDE RATIO VERSUS F_1/W

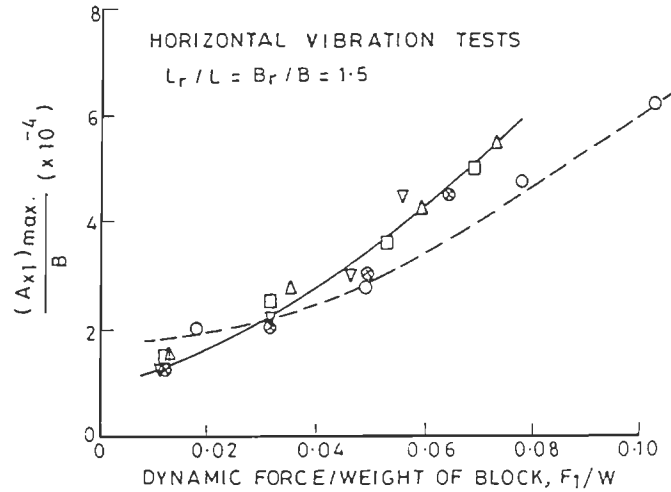


FIG. 4.43 STRAIN AMPLITUDE RATIO VERSUS F_1/W

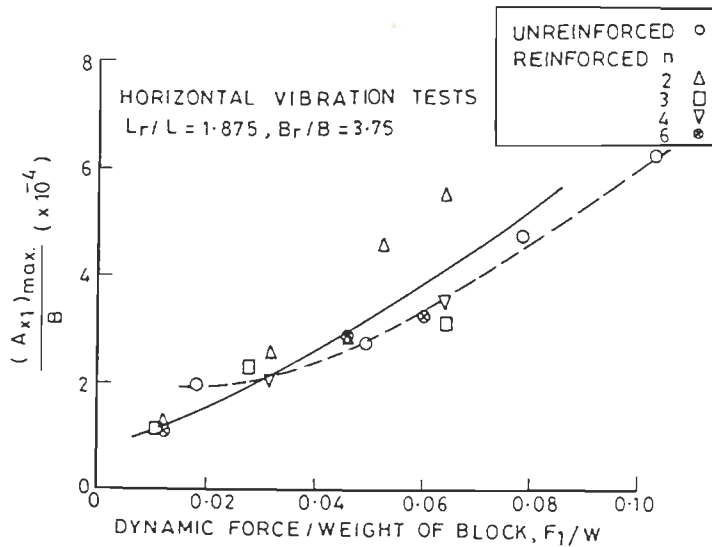


FIG. 4.45 STRAIN AMPLITUDE RATIO VERSUS F_1/W

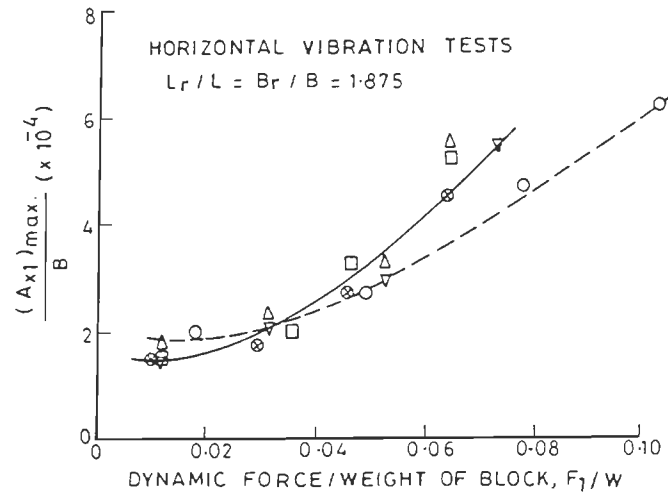


FIG. 4.44 STRAIN AMPLITUDE RATIO VERSUS F_1/W

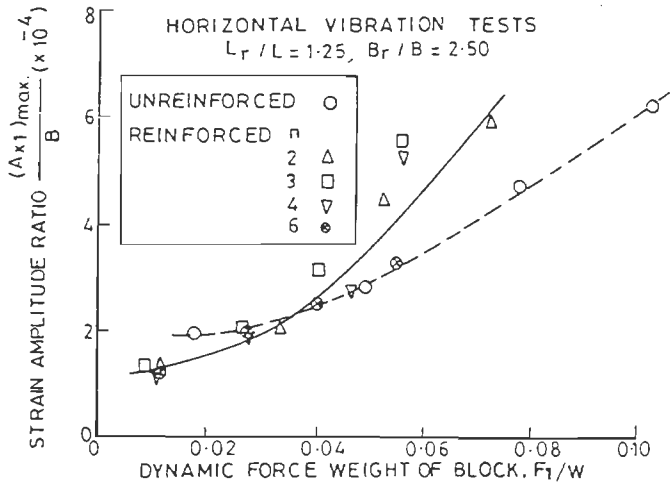


FIG. 4.46 STRAIN AMPLITUDE RATIO VERSUS F_1/W

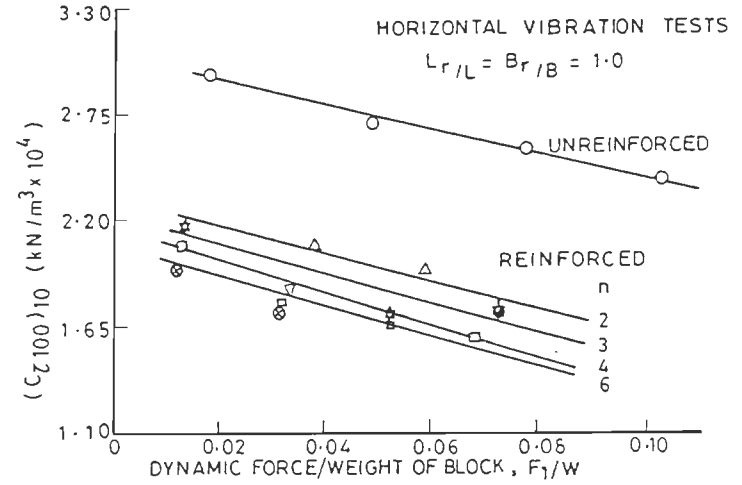


FIG. 4.48 $(C_{z100})_{10}$ VERSUS F_1/W

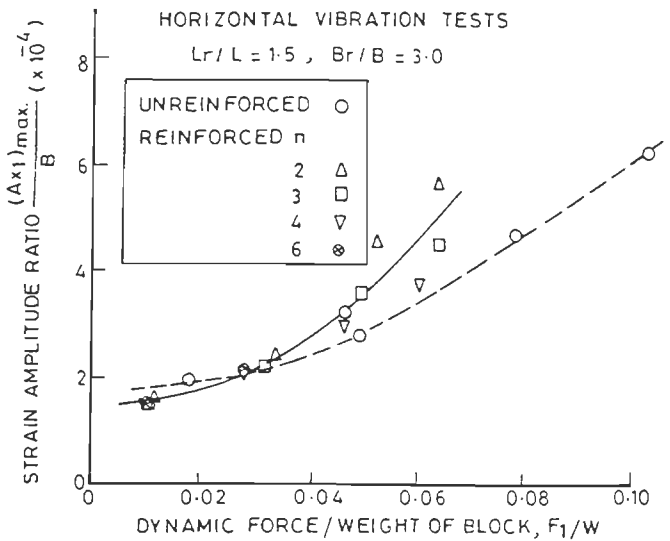


FIG. 4.47 STRAIN AMPLITUDE RATIO VERSUS F_1/W

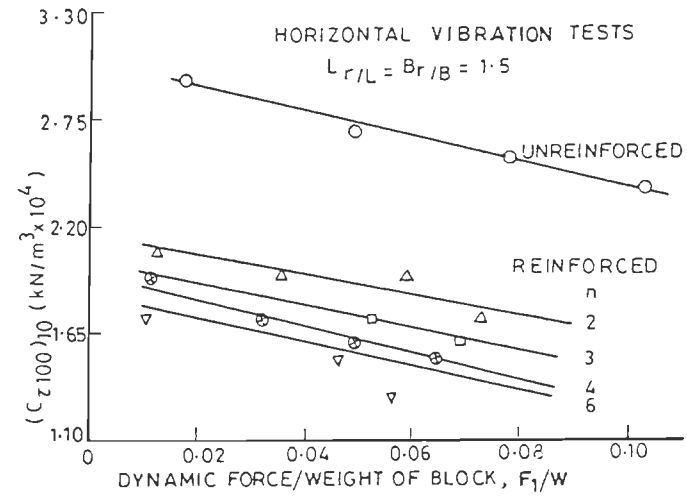


FIG. 4.49 $(C_{z100})_{10}$ VERSUS F_1/W

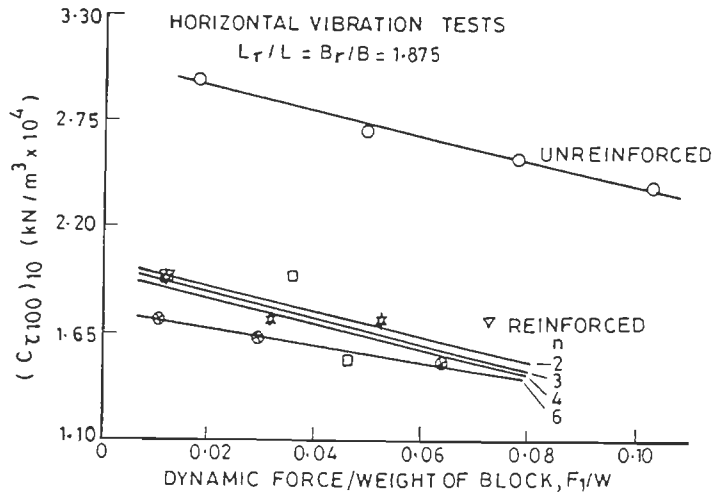


FIG. 4-50 $(C_{Z100})_{10}$ VERSUS F_1/W

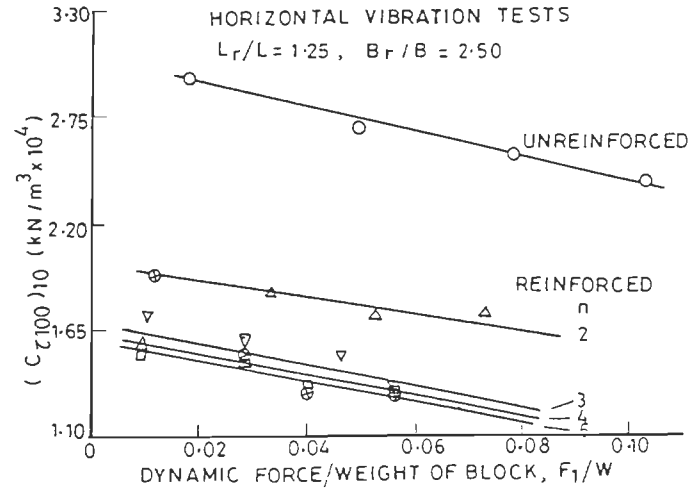


FIG. 4-51 $(C_{Z100})_{10}$ VERSUS F_1/W

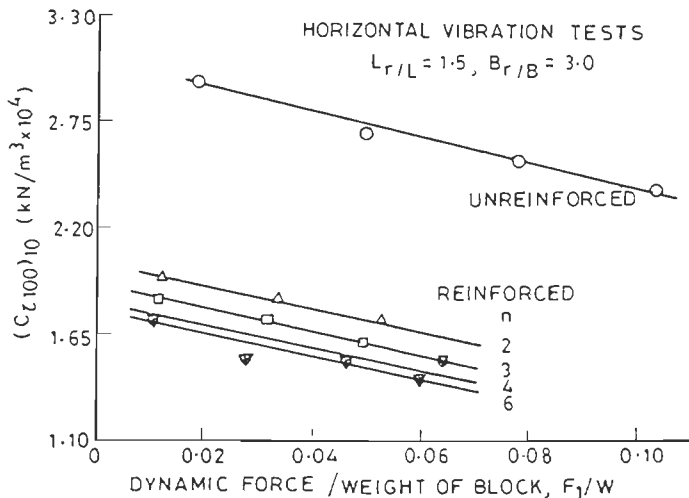


FIG. 4-52 COEFFICIENT OF ELASTIC UNIFORM SHEAR VERSUS F_1/W

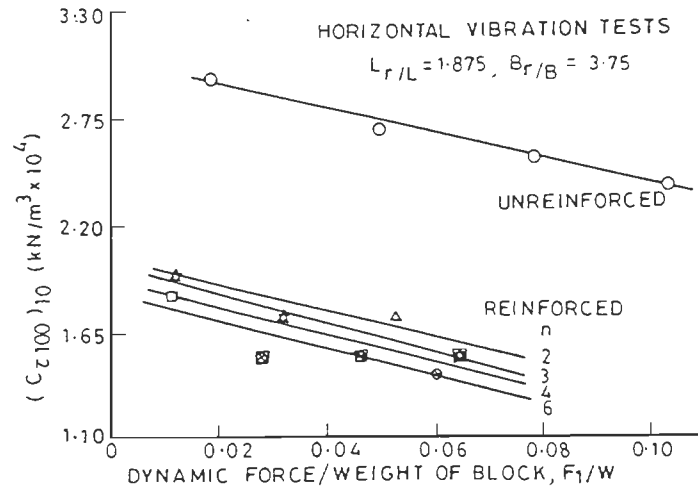


FIG. 4-53 COEFFICIENT OF ELASTIC UNIFORM SHEAR VERSUS F_1/W

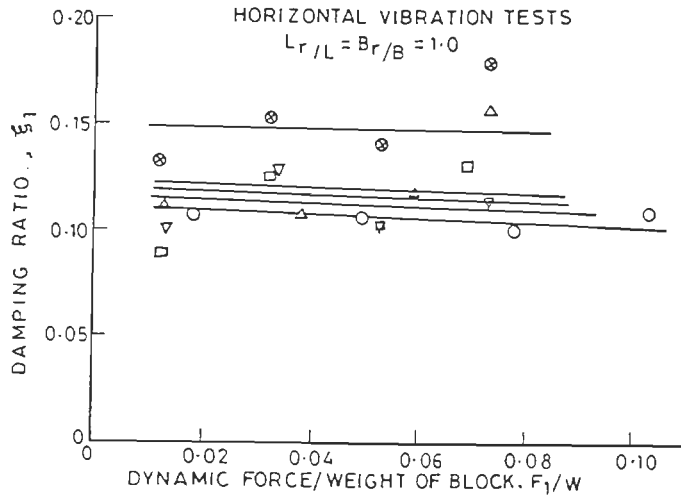


FIG. 4-54 DAMPING RATIO VERSUS F_1/W

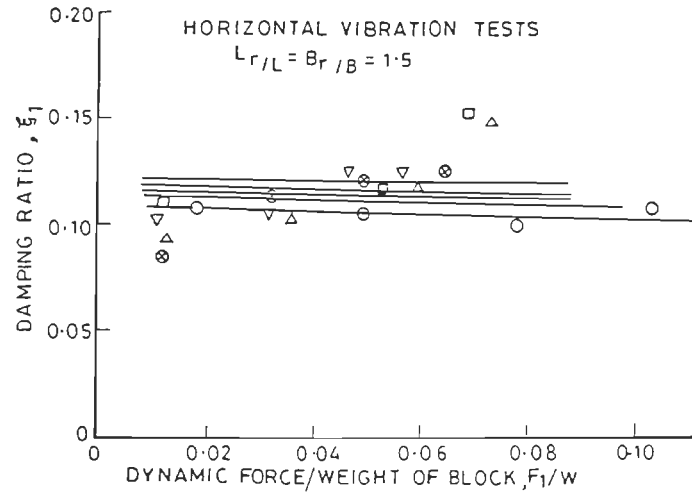


FIG. 4-55 DAMPING RATIO VERSUS F_1/W

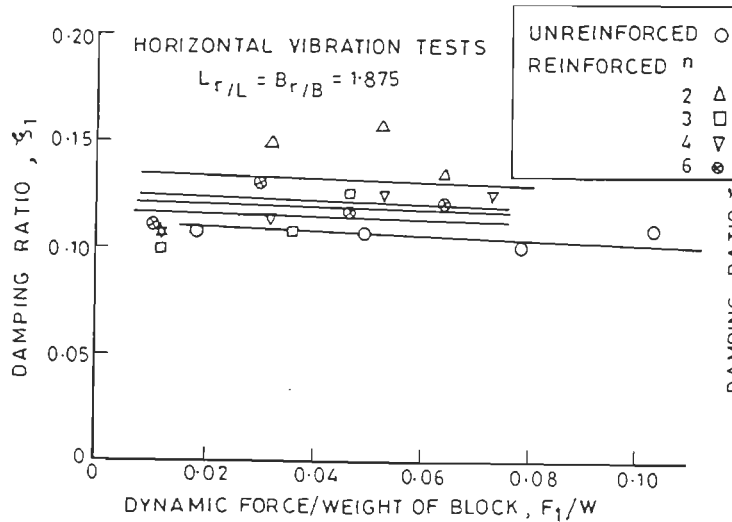


FIG. 4-56 DAMPING RATIO VERSUS F_1/W

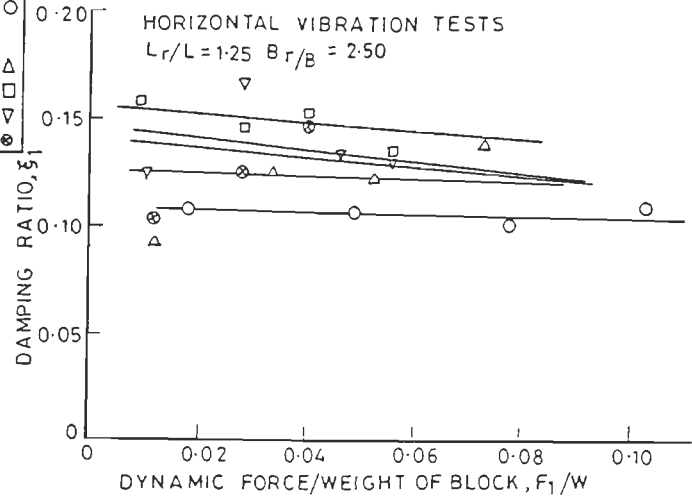


FIG. 4-57 DAMPING RATIO VERSUS F_1/W

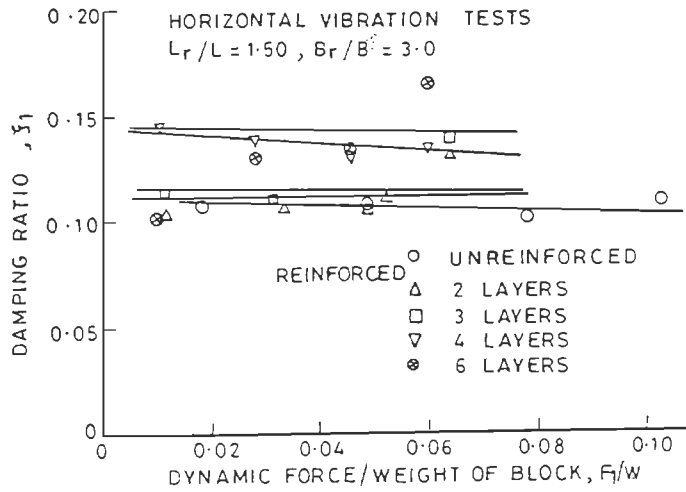


FIG. 4-58 DAMPING RATIO VERSUS F_1/W

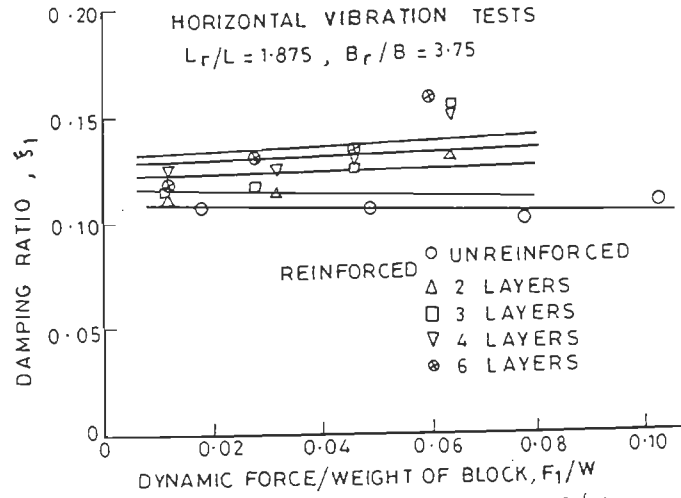


FIG. 4-59 DAMPING RATIO VERSUS, F_1/W

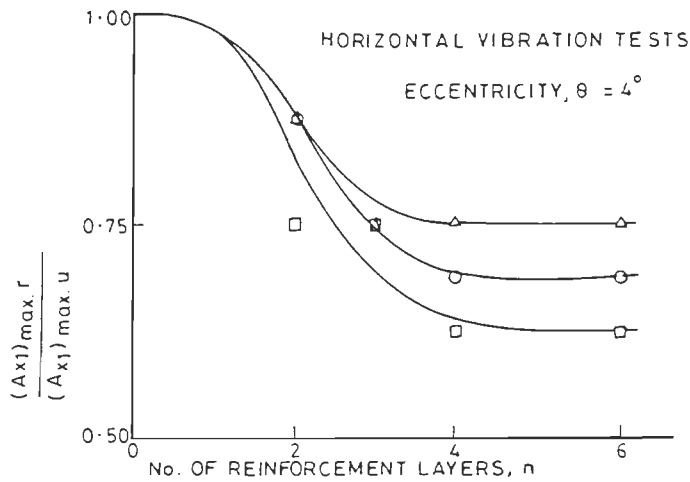


FIG. 4-60 AMPLITUDE REDUCTION FACTOR VERSUS n

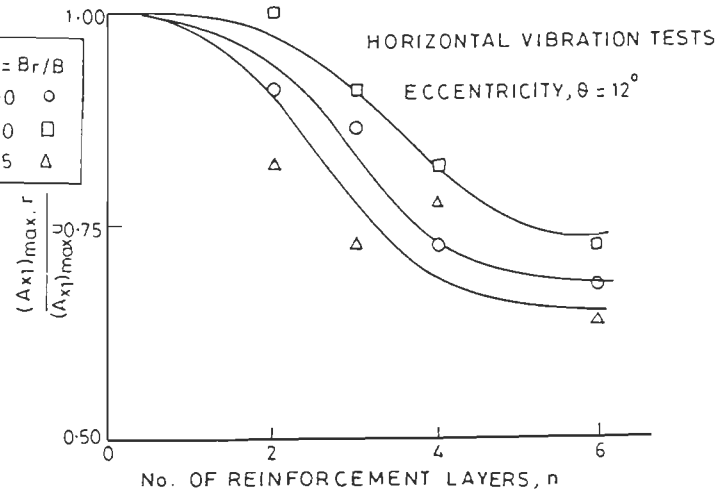


FIG. 4-61 AMPLITUDE REDUCTION FACTOR VERSUS n

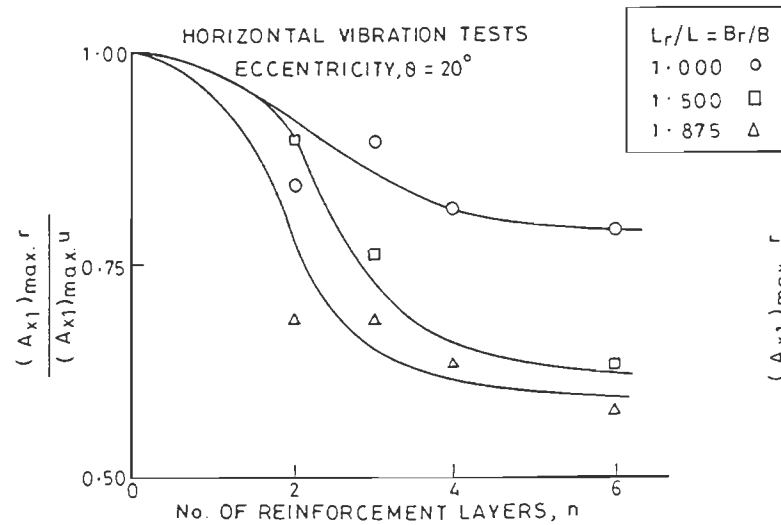


FIG. 4-62 AMPLITUDE REDUCTION FACTOR VERSUS n

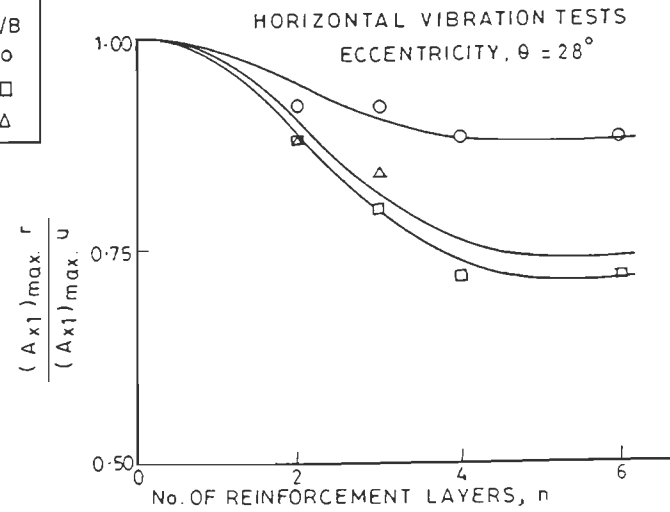


FIG. 4-63 AMPLITUDE REDUCTION FACTOR VERSUS n

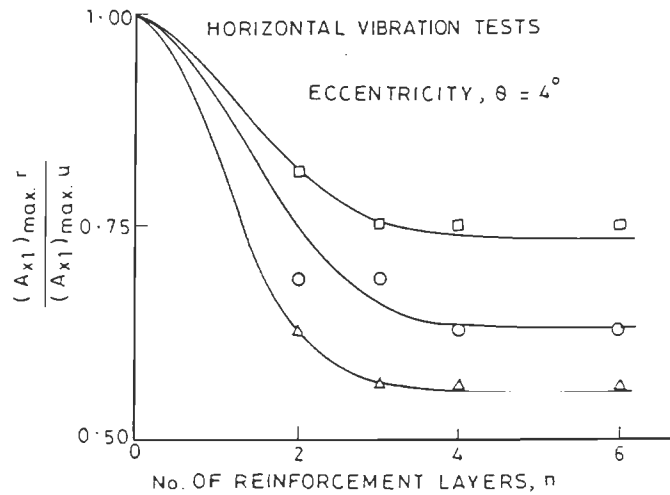


FIG. 4-64 AMPLITUDE REDUCTION FACTOR VERSUS n

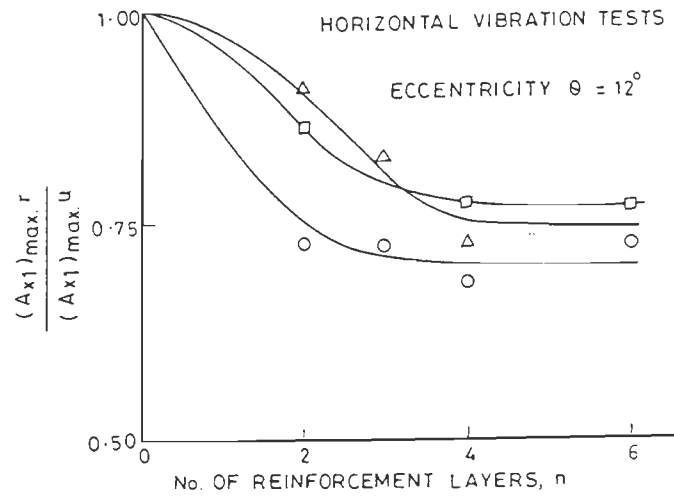


FIG. 4-65 AMPLITUDE REDUCTION FACTOR VERSUS n

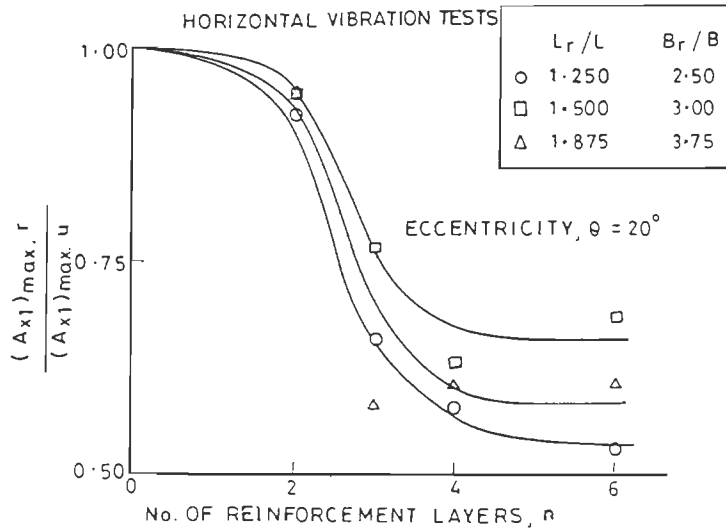


FIG. 4-66 AMPLITUDE REDUCTION FACTOR VERSUS n

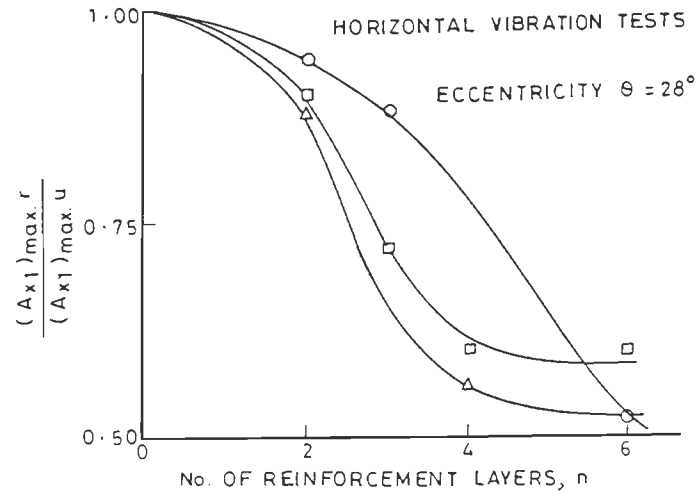


FIG. 4-67 AMPLITUDE REDUCTION FACTOR VERSUS n

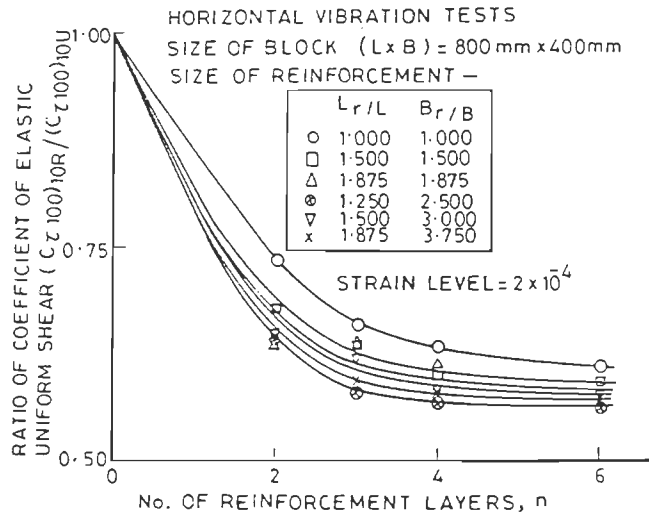


FIG. 4-68 $(C_{z100})_{10R} / (C_{z100})_{10U}$ VERSUS n

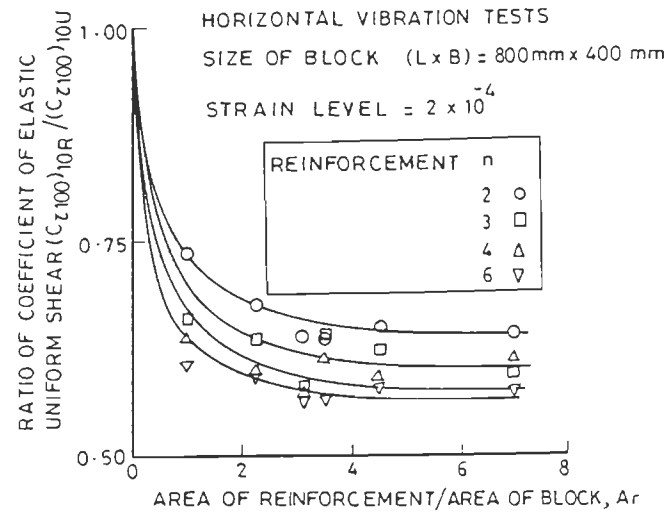


FIG. 4-69 $(C_{z100})_{10R} / (C_{z100})_{10U}$ VERSUS AREA RATIO, A_r

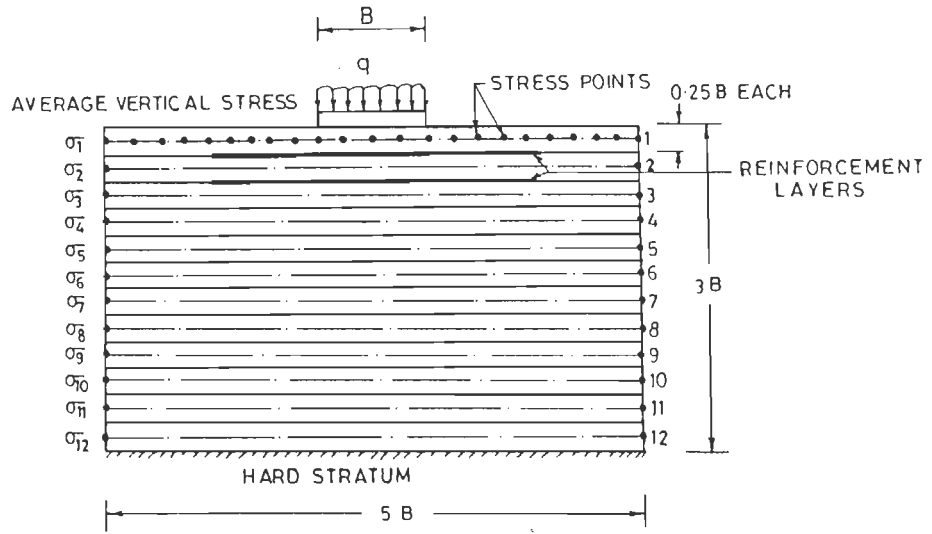


FIG. 4.70 SOIL-REINFORCEMENT LAYERED SYSTEM

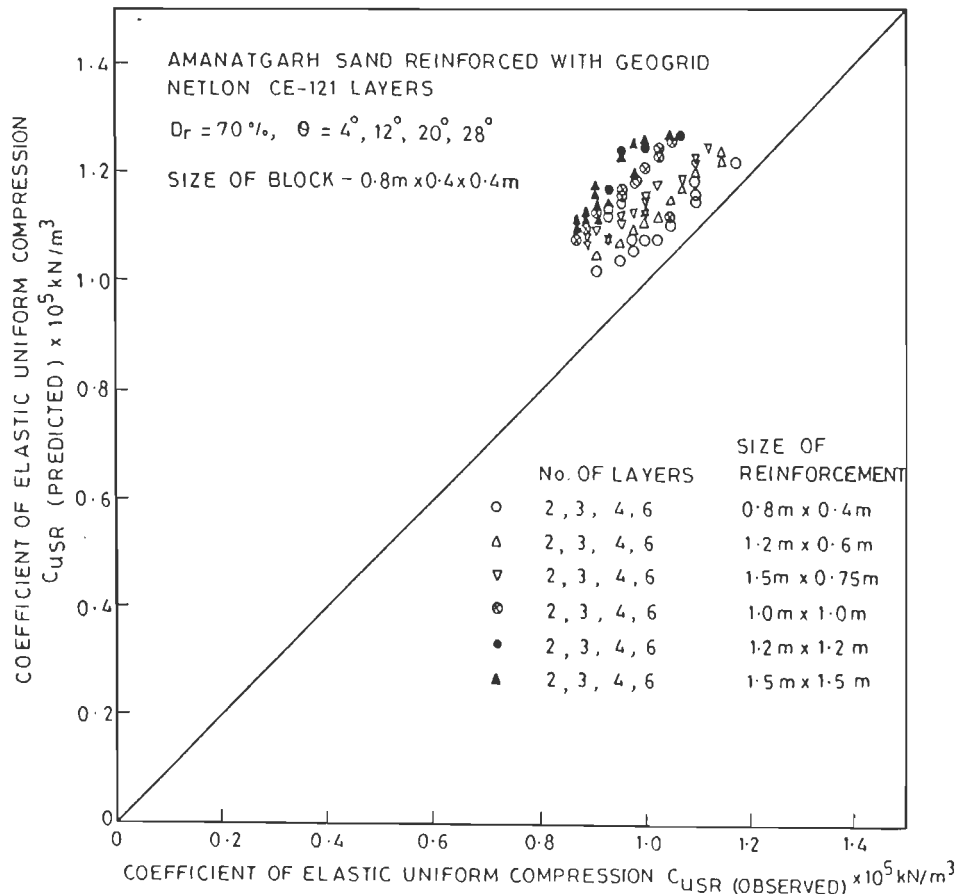


FIG. 4.71 EXPERIMENTAL VERSUS PREDICTED VALUES OF C_u IN VERTICAL VIBRATION TESTS

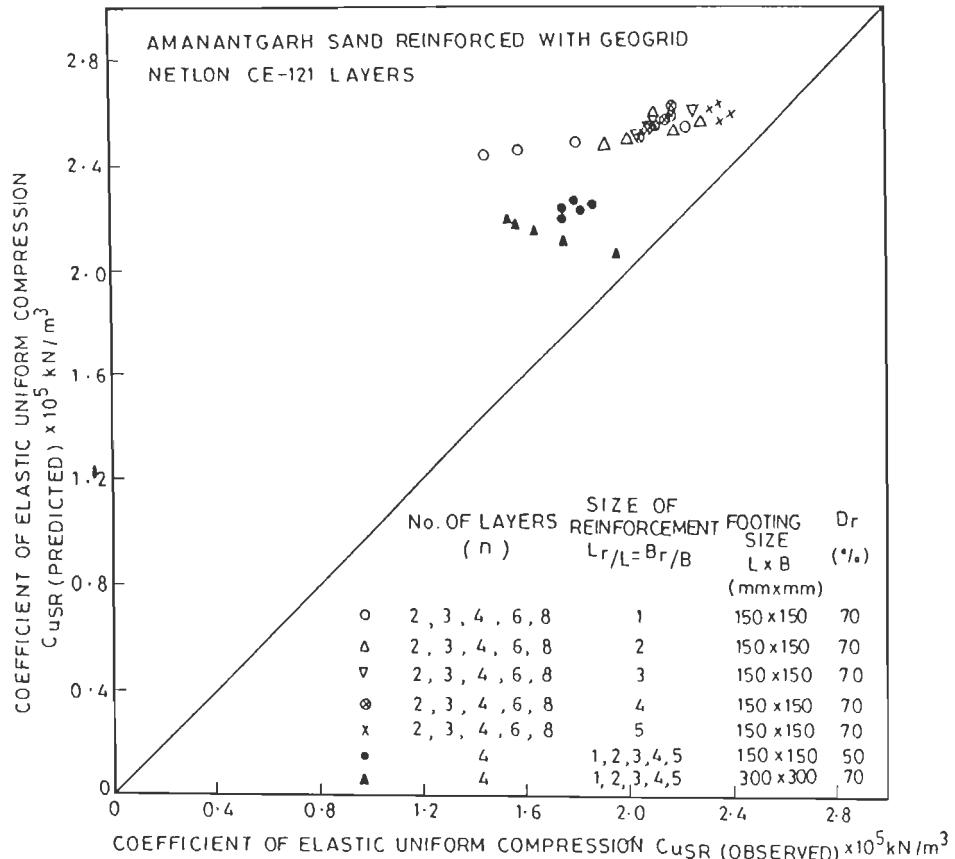


FIG. 4.72 EXPERIMENTAL VERSUS PREDICTED COEFFICIENT OF ELASTIC UNIFORM COMPRESSION IN CYCLIC PLATE LOAD TESTS

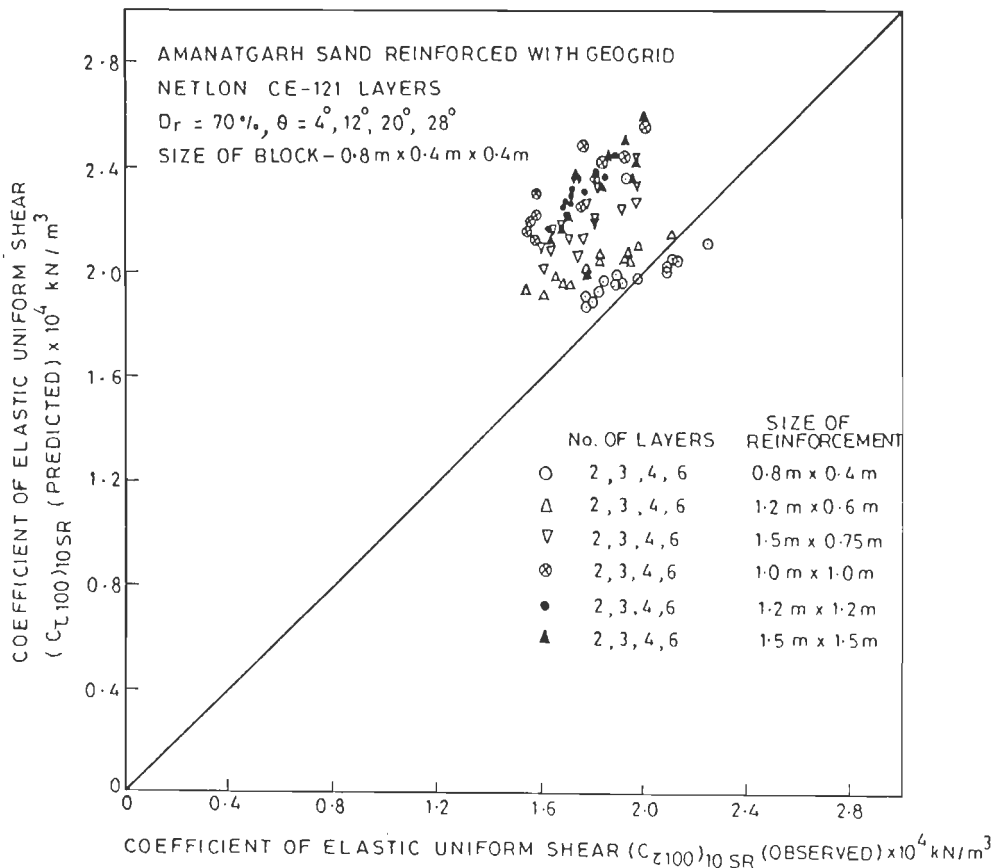


FIG. 4.73 EXPERIMENTAL VERSUS PREDICTED VALUES OF C_z — HORIZONTAL VIBRATION TESTS

CONCLUSIONS

The main conclusions of the experimental and analytical research work carried out, and reported in this thesis are as follows :

Cyclic Plate Load Tests

1. The ultimate bearing capacity of sand bed is improved upon reinforcing with geogrid layers. The improvement in ultimate bearing capacity is upto about four times depending upon the size and number of the reinforcement layers. There is greater improvement in the ultimate bearing capacity with increase in the number and size of reinforcement layers. For size of reinforcements greater than four times the footing width and the number of reinforcement layers more than six, the rate of improvement in ultimate bearing capacity is not significant i.e., the optimum benefit is obtained by providing this particular size and number of reinforcement layers.
2. The total settlements are reduced upto less than half upon providing geogrid reinforcements in sand bed. The reduction in the total settlement is more with increase in size and number of reinforcement layers. The optimum benefit is achieved by providing six geogrid layers of size four times the width of footing.
3. The coefficient of elastic uniform compression decreases maximum upto 45% upon reinforcing the sand bed, the decrease being more for larger number and smaller size of reinforcement layers, in general. However, the pressure range for which C_u values of reinforced sand beds are valid, are much higher than

that for the unreinforced sand bed. Beyond the ultimate bearing pressure the value of the coefficient of elastic uniform compression, C'_u of the reinforced sand bed is more than C'_u of unreinforced sand bed and normally increases with the increase in size and number of reinforcement layers. For the size of reinforcement twice the width of footing and four number of reinforcement layers, the C_u and C'_u are 81% and 55% of C_u of the unreinforced sand bed. The corresponding ultimate bearing capacities (pressure ranges of validity of C_u values) are 390 kN/m^2 and 700 kN/m^2 for reinforced and 160 kN/m^2 for unreinforced sand beds respectively. The associated strain levels are 9.5×10^{-3} and 25×10^{-3} for reinforced sand bed and 3.96×10^{-3} for the unreinforced sand bed.

4. The damping capacity of sand bed is improved upon reinforcing with geogrid layers. The improvement is more with increase in number and size of reinforcement layers. The optimum benefit is obtained for six geogrid layers of size four times the width of footing.

Vertical Block Vibration Tests

1. The maximum amplitude decreases by a maximum of about 43% when the sand bed is reinforced with geogrid reinforcements. The decrease in amplitudes is generally more with the increase in the size and number of reinforcement layers.
2. The resonant frequency is reduced by a maximum of about 14% for the reinforced sand beds. The decrease in resonant frequency is observed to be generally more with the increase in size and number of reinforcement layers.
3. With the increase in the excitation level of vertical vibrations of the block, the maximum amplitude increases whereas the resonant frequency drops slightly for the reinforced sand likewise the unreinforced sand.

4. The damping ratio, ξ of the reinforced sand bed is higher than that of the unreinforced sand bed and it increases generally with the increase in the size and number of the layers of geogrid. Also the damping ratio ξ , is observed to increase with F/W ratio (strain level) both for unreinforced and reinforced sand beds.
5. The coefficient of elastic uniform compression, C_u decreases by a maximum of about 26% depending upon the size and number of geogrid reinforcements. The decrease in the C_u value is less at higher strain levels. Also, there is a decrease in C_u with the increase in the dynamic force to weight of block, F/W ratio both for the unreinforced and reinforced sand beds. This is due to softening behaviour of soil with increase in strain level.
6. Upon comparing the C_u values obtained from vertical block vibration and cyclic plate load tests, the variation of C_u with strain level for reinforced sand bed is observed to be similar to that for unreinforced sand bed as reported in literature (Seed and Idriss, 1970). Further, it is observed that for strain levels less than 3%, the values of C_u for reinforced sand bed are less than those for the unreinforced sand bed; beyond which C_u for reinforced sand bed is higher than C_u for unreinforced sand bed. Thus, reinforcing effect of geogrid is not effective for strain levels less than 3% but must be considered for higher strain levels.

Horizontal Block Vibration Tests

1. The maximum amplitudes corresponding to the first and second modes of vibration decrease upto about 48% and 41% depending upon the size and number of the reinforcement layers. The decrease in maximum amplitude is generally more with the increase in the size and number of geogrid layers and is dependent upon excitation level also.

2. The resonant frequencies for the first and second modes of vibration decrease maximum by 28% and 20% for the reinforced sand beds, the decrease being more with the increase in the size and number of geogrid layers, in general.
3. The increase in excitation level of horizontal vibrations increases the amplitudes for the first and second modes of vibration with slight drop in the resonant frequencies corresponding to both the modes of vibration for the reinforced sand beds similar to the unreinforced one.
4. The damping ratios ξ_1 and ξ_2 for the first and second modes of vibration are different and generally increase with the increase in the size and number of reinforcement layers. The values of the damping ratios for the reinforced sand are higher than those for the unreinforced sand. ξ_1 and ξ_2 generally increase with increase in strain level.
5. The coefficient of elastic uniform shear is reduced by a maximum of about 48%, the decrease being more with the increase in size and number of reinforcement layers. With the increase in dynamic force to weight of block (F_1/W) ratio, the coefficient of elastic uniform shear decreases for the reinforced sand bed similar to the unreinforced sand bed. C_τ values are observed to decrease with the increase in strain level for both unreinforced and reinforced sand beds.
6. A comparison of the values of coefficient of elastic uniform compression, $(C_{u100})_{10}$ with the corresponding values of coefficient of elastic uniform shear, $(C_{\tau100})_{10}$ shows that $(C_{u100})_{10}/(C_{\tau100})_{10}$ ratio is 2.8 to 2.95 for unreinforced sand bed whereas it is 3.2 to 3.9 for the reinforced sand beds. Thus, the decrease in C_τ is more than the decrease in C_u for the similar geogrid reinforced sand beds.

Non-dimensional Correlations

The non-dimensional correlations have been developed to bring out the influence of different factors affecting the dynamic properties of reinforced sand. These correlations can be used for obtaining different parameters for design of foundations on reinforced sand beds subjected to cyclic and dynamic loads.

The non-dimensional correlations have been developed for

- (i) Coefficient of elastic uniform compression C_u , damping capacity ratio D_{cr} , BCR and SR in cyclic plate load tests.
- (ii) Coefficient of elastic uniform compression C_u , damping ratio ξ and amplitude reduction factor in vertical block vibration tests, and
- (iii) Coefficient of elastic uniform shear C_τ , damping ratio ξ_1 and amplitude reduction factor in horizontal block vibration tests.

Equivalent Parameters Analysis

Equivalent parameter analysis presented taking into account moduli of sand and geogrid and neglecting interface friction, predicts decrease in the coefficient of elastic uniform compression and coefficient of elastic uniform shear, upon reinforcing the sand bed with geogrid layers. The provision of geogrid reinforcements in sand beds improves the static strength characteristics, reduces amplitudes of vibration and increases damping with marginal reduction in coefficient of elastic uniform compression and coefficient of elastic uniform shear. The use of reinforced sand beds would provide an alternative for the design of foundations of machines, where the natural frequency of the foundation soil system may lie close to the operating frequency of the machine otherwise and the amplitudes exceed the permissible limits as demonstrated by design problem in 4.7. The maximum amplitude can be controlled and disturbance during starting and stopping of machine can be decreased.

RECOMMENDATIONS FOR FURTHER RESEARCH

The results of the investigations reported in this thesis have clearly established that the dynamic properties of dry sand are significantly changed upon reinforcing it with geogrid layers. The dynamic properties of geogrid reinforced dry sand beds in which the geogrids are placed in horizontal layers only, have been studied. The experimental techniques used are the cyclic plate load tests and the block vibration tests conducted on sand beds prepared in laboratory. Thus, there is need to carry out further research work on the following aspects:

1. To study the dynamic properties of soils reinforced with other type of reinforcing materials or a combination of reinforcing materials placed in vertical mode or a combination of vertical and horizontal modes under field conditions.
2. To study the dynamic properties of moist and saturated reinforced sands, clays and other types of soils.
3. To study the effect of the Poisson's ratio ν of the reinforcing materials on the dynamic properties of reinforced soils.
4. Development of analytical methods for determining dynamic properties of reinforced soils at high strain levels considering the mobilisation of the interface friction between the soil and reinforcement.
5. To conduct tests on prototype foundations for establishment of the results of laboratory experimental data.
6. More tests, particularly in the field, are needed to have definite conclusions and correlations.

REFERENCES

1. Adams, M.T., and Collin, J.G., (1997), "Large Model Spread Footing Load Tests on Geosynthetic Reinforced Soil Foundations", *Journal of Geotechnical and Geoenvironmental Engineering*, ASCE, Vol. 123, No. 1, pp. 66-72.
2. Ahmad, S., and Bharadwaj, A., (1991), "Horizontal Impedance of Embedded Strip Foundations in Layered Soil", *J. Geotech. Engg. Div., ASCE*, Vol. 117, No. 7, pp. 1021-1041.
3. Akai, et al., (1971), "Model Studies on Stress Distribution in Layered Systems", *Proc. JSCE*, 185, pp. 83-93.
4. Akinmusuru, J.O., and Akinbolade, J.A., (1981), "Stability of Loaded Footings on Reinforced Soil", *Journal of Geotechnical Engineering Division, ASCE*, Vol. 107, No. GT6, pp. 819-27.
5. Anandkrishnan, M., and Krishnaswamy, N.R., (1973), "Response of Embedded Footings to Vertical Vibrations", *ASCE J. Soil Mech. and Found. Div.*, Vol. 99, SM-10, 863-883.
6. Arnold, R.N., Bycroft, G.N., and Warburton, G.B., (1955), "Forced Vibrations of a Body on an Infinite Elastic-Solid", *J. App. Mech.*, pp. 391-400.
7. Awojobi, A.O., and Grootenhuis, P., (1965), "Vibration of Rigid Bodies on Semi-infinite Elastic Media", *Proc. Royal Soc. of London, Series A*, 287, pp. 27-63.
8. Awojobi, A.O., (1972), "Vertical Vibration of a Rigid Circular Foundation on Gibson Soil", *Geotechnique*, 22(2), pp. 333-343.
9. Babushanker, N., Ali, M., and Reddy, S.G., (1991), "Cyclic Load Tests on Sand", *IGC-1991, Surat, India*, Vol. 1, pp. 213-216.
10. Baidya, D.K., and Krishna, G.M., (1996), "Damping of Layered Soil System", *IGC-1996, Madras, India*, pp. 317-320.

11. Baranov, V.A., (1967), "On the Calculations of Excited Vibrations of an Embedded Foundation", *Voprosy Dynamiki i Prochnosti*, No. 14, Polytechnical Institute of Riga, pp. 195-209.
12. Barkan, D.D., (1962), "Dynamics of Bases and Foundations", McGraw-Hill Book Co., Inc. (translated), pp. 17-41.
13. Barkan, D.D., and Ilyichev, V.A., (1977), "Dynamics of Bases and Foundations", *Proc. 9th International Conference on Soil Mechanics and Foundation Engineering*, Tokyo, Vol. 2, p. 630.
14. Basavanna, B.M., (1975), "Bearing Capacity of Soil under Static and Transient Load", Ph.D. Thesis, University of Roorkee, Roorkee, India.
15. Basavanna, B.M., and Honagodu, H., (1984), "Effect of Static Stress on Some Dynamic Properties of Sand", *Indian Geotechnical Conference*, Vol. 1, pp. 47-51.
16. Basset, R.H., and Last, N.C., (1978), "Reinforced Earth Below Footings and Embankments", *Proc. Symposium on Earth Reinforcement*, ASCE, Pittsburgh, pp. 202-31.
17. Binquet, J., and Lee, Kenneth L., (1975a), "Bearing Capacity Tests on Reinforced Earth Slabs", *Journal of Geotechnical Engineering Division*, ASCE, Vol. 101, No. GT12, pp. 1241-55.
18. Binquet, J., and Lee, Kenneth L., (1975b), "Bearing Capacity Analysis of Reinforced Earth Slabs", *Journal of Geotechnical Engineering Division*, ASCE, Vol. 101, No. GT12, pp. 1257-76.
19. Boominathan, S., Senathipathi, K., and Jayaprakasam, V., (1991), "Field Studies on Dynamic Properties of Reinforced Earth", *Soil Dynamics and Earthquake Engineering*, Vol. 10, No. 8, pp. 402-6.
20. Borja, R.I., Wu, W.H., and Smith, H.A., (1993), "Non-linear Response of Vertically Oscillating Rigid Foundations", *J. Geotech. Engg. Div.*, ASCE, Vol. 119, No. 5, pp. 893-911.

21. Brandow, G.E., (1971), "Soil-Structure Interaction during Earthquake Excitations", Tech. Report No. 145, Deptt. of Civil Engg., Vol. 3, pp. C 9/1-C 9/19.
22. Bycroft, G.N., (1956), "Forced Vibrations of a Rigid Circular Plate on a Semi-infinite Elastic Space and on an Elastic Stratum", Phil. Trans., Roy. Soc. of London, Series A, 248, pp. 327-368.
23. Chae, Y.S., (1971), "Dynamic Behaviour of Embedded Foundation-Soil-Systems", Presented at 49th Annual Meeting, U.S., H.R.B.
24. Damy, J.R., and Casales, C.G., (1985), "Soil Stresses under a Polygonal Area Uniformly Loaded", Proc. XI Int. Conf. on Soil Mech. and Foundn. Engg., Vol. II, pp. 733-735.
25. Das Gupta, S.P., and Rao, N.S.V.K., (1978), "Dynamics of Rectangular Footings by Finite Element", J. Geotech. Engg. Div., ASCE, Vol. 104, No. GT5, pp. 621-637.
26. Dimbicki, E., (1986), "Bearing Capacity of Strip Foundation on Soft Soil Reinforced by Geotextiles", Proc. 3rd International Conf. on Geotextiles, Vienna, Austria, Vol. 2A/6, pp. 205-208.
27. Dobry, R., and Gazetas, G., (1986), "Dynamic Response of Arbitrarily shaped Foundations", J. of Geotechnical Engg. Div., ASCE, Vol. 112, No. 2, pp. 109-135.
28. Eastwood, W., (1953), "Vibrations in Foundations", The Struct. Engr., 31(1), pp. 82-93.
29. Edil, T.B., and Luh, G.F., (1978), "Dynamic Modulus and Damping Relationships for Sand", Proc. Conf. on Earthquake Engg. and Soil Dynamics, Geotech. Engg. Divn., ASCE Specialty Conference, Pasadena.
30. Fahoum, K., Aggour, M.S., and Amini, F., (1996), "Dynamic Properties of Cohesive Soils Treated with Lime", Journal of Geotechnical Engg., ASCE, Vol. 122, No. 5, pp. 382-389.

31. Fragaszy, R.J., and Lawton, E., (1984), "Bearing Capacity of Reinforced Sand Subgrades", *Journal of Geotechnical Engineering Division, ASCE*, Vol. 110, No. GT10, pp. 1500-11.
32. Gazetas, G., and Roesset, J.M., (1979), "Vertical Vibration of Machine Foundations", *ASCE Journal of Geotechnical Engineering Division*, Vol. 105, GT-12, pp. 1435-1454.
33. Gazetas, G., Dobry, R., and Tassoulas, J.L., (1985), "Vertical Response of Arbitrarily shaped Embedded Foundations", *J. of Geotechnical Engg. Div., ASCE*, Vol. III, No. 6, pp. 750-771.
34. Gazetas, G., and Tassoulas, J.L., (1987a), "Horizontal Stiffness of Arbitrarily Shaped Embedded Foundations", *J. of Geotechnical Engg. Div., Div., ASCE*, Vol. 113, No. 5, pp. 440-457.
35. Gazetas, G., and Tassoulas, J.L., (1987b), "Horizontal Damping of Arbitrarily shaped Embedded Foundations", *J. of Geotech. Engg. Div., ASCE*, Vol. 113, No. 5, pp. 458-475.
36. Gazetas, G., (1991), "Formulas and Charts for Impedance of Surface and Embedded Foundations", *J. Geotech. Engg. Div., ASCE*, Vol. 117, No. 9, pp. 1363-1381.
37. Gladwell, G.M.L., (1968), "Forced Tangential and Rotatory Vibration of a Rigid Circular Disc on a Semi-infinite Solid", *Proc. International J. Engg. Sci.*, 6, pp. 591-607.
38. Gucunski, N., and Peek, R., (1993), "Vertical Vibrations of Circular Flexible Foundations on Layered Media", *Soil Dynamics and Earthquake Engg.*, Vol. 12, pp. 183-192.
39. Guido, V.A., Chang, D.K., and Sweeney, M.A., (1986), "Comparison of Geogrid and Geotextile Reinforced Earth Slabs", *Canadian Geotechnical Journal*, 23: pp. 435-40.

40. Guido, V.A., and Squerciati, J., (1994), "Dynamic Plate Loading Tests on Geogrid Reinforced Subgrades", Proc. XIII International Conference on Soil Mechanics and Foundation Engineering, New Delhi, India, Vol. III, pp. 1283-86.
41. Gupta, B.N., (1972), "Effect of Foundation Embedment on the Dynamic Behaviour of Foundation Soil System", *Geotechnique*, 32, No. 1, pp. 129-137.
42. Hadjian, A.H., and Ellison, B., (1985), "Equivalent Properties for Layered Media", *Soil Dynamics and Earthquake Engineering*, Vol. 4, No. 4, pp. 203-209.
43. Hardin, B.O., (1965), "The Nature of Damping in Sand", *Journal of Soil Mechanics and Foundations Division, ASCE*, 91 (SM1), pp. 63-97, Part 1.
44. Hardin, B.O., and Black, W.L., (1966), "Sand Stiffness under Various Triaxial Stresses", *Journal of Soil Mechanics and Foundations Division, ASCE*, 92 (SM2), pp. 27-42.
45. Hardin, B.O., and Black, W.L., (1969), "Closure to Vibration Modulus of Normally Consolidated Clays", *Journal of Soil Mechanics and Foundations Division, ASCE*, 95 (SM-6), pp. 1531-37.
46. Hardin, B.O., and Drnevich, V.P., (1972a), "Shear Modulus and Damping in Soils, Measurements and Parameter Effects", *Journal of Soil Mechanics and Foundations Division, ASCE*, 98 (SM-6), pp. 603-624.
47. Hardin, B.O., and Drnevich, V.P., (1972b), "Shear Modulus and Damping in Soils, Design Equations and Curves", *Journal of Soil Mechanics and Foundations Division, ASCE*, 98 (SM-7), pp. 667-692.
48. Hardin, B.O., (1978), "The Nature of Stress-Strain Behaviour of Soils, State-of-the-Art Report, ASCE, Specialty Conference on Earthquake Engineering and Soil Dynamics, Pasadena, CA, Vol. 1, pp. 3-90.
49. Haroon, M., Shah, S.S., and Pandey, S., (1990), "A Study on Behaviour of Annular Footings Resting on Geotextile Reinforced Sand", Proc. IGC-90, Bombay, India, Vol. 1, pp. 65-68.

50. Hausmann, M.R., (1976), "Strength of Reinforced Soil", Proc. 8th Australian Road Research Board Conf., Perth.
51. Hoadley, P.J., (1985), "Measurement of Dynamic Soil Properties", Analysis and Design of Foundations for Vibrations, Editor – Moore, P.J., Oxford and IBH Publishing Co., New Delhi, pp. 349-420.
52. Hryciw, R.D., and Thomann, T.G., (1993), "Stress-History-Based Model for G^* of Cohesionless Soils", Journal of Geotechnical Engg. Div., ASCE, Vol. 119, No. 7, pp. 1073-1093.
53. Hsieh, T.K., (1962), "Foundation Vibrations", Proc. I.C.E., 22, pp. 211-25.
54. Huang, C.C., and Tatsuoka, K., (1990), "Bearing Capacity of Reinforced Horizontal Sandy Ground", Geotextiles and Geomembranes, 9 : pp. 51-82.
55. IS:2720 (Part XIV)-1983, "Indian Standard Method of Test for Soils- Determination of Density Index (Relative Density) of Cohesionless Soils", Indian Standards Institution, Manak Bhawan, New Delhi, India.
56. IS:1498-1970, "Classification and Identification of Soil for General Engineering Purposes", Indian Standards Institution, Manak Bhawan, New Delhi, India.
57. IS:5249-1977, "Indian Standard Method of Test for Determination of Dynamic Properties of Soil", Ist Revision, Indian Standards Institution, New Delhi.
58. IS:6403-1981, "Indian Standard Code of Practice for Determination of Bearing Capacity of Shallow Foundations", Ist Rev., Indian Standards Institution, Manak Bhawan, New Delhi, India.
59. IS:1888-1982, "Indian Standard Method of Load Test on Soils", 2nd Rev., Indian Standards Institution, Manak Bhawan, New Delhi, India.
60. Ishihara, K., (1971), "Factors Affecting Dynamic Properties of Soils", Proc. 4th Asian Reg. Conf. on Soil Mech. & Foundn. Engg., Bangkok, Vol. 2.
61. Iwasaki, T., and Tatsuoka, F., (1977), "Dynamic Soil Properties with Emphasis on Comparison of Laboratory Tests with Field Measurements", Proc. World Conf. on Earthquake Engg., 6th, New Delhi, Vol. 1, pp. 153-158.

62. Jaky, J., (1948), "Pressures in Silos", II International Conf. Soil Mech. Foundn. Engg. Vol. I, p. 103.
63. Jones, C.J.F.P., (1985), "Earth Reinforcement and Soil Structures", Butterworths and Co. Ltd., London.
64. Johnson, G.R., Christiano, P., and Epstein, H.I., (1975), "Stiffness Coefficients for Embedded Footings", ASCE J. Geotech. Engg. Div., Vol. 101, No. GT8, pp. 789-900.
65. Kagawa, T., and Kraft, L.M., (1981), "Machine Foundations on Layered Soil Deposits", Proc. Tenth International Conf. Soil Mech. & Foundation Engg., Stockholm, Vol. 3, pp. 249-252.
66. Kaldjian, M.J., (1969), "Discussion of Design Procedures for Dynamically Loaded Foundations", ASCE, J. Soil Mech. & Found. Div., Vol. 95, SM-1, pp. 364-366.
67. Karasudhi, P., Keer, L.M., and Lee, S.L., (1968), "Vibratory Motion of a Body on an Elastic Half Plane", J. App. Mech., ASME, 35E, p. 698.
68. Kazuya Yasuhara, and Kazutoshi Hirao, (1988), "Mattress Foundation by Geogrid on Soft Clay Under Repeated Loading", Proc. International Geotechnical Symposium on Theory and Practice of Earth Reinforcement", Fukuoka, Japan, pp. 251-56.
69. Khan, A.K., Purkayastha, R.D., and Pise, P.J., (1992), "Effect of Testing Methods on Dynamic Properties of Soil", IGC-1992, Vol. 1, pp. 379-382.
70. Khing, K.H., Das, B.M., Puri, V.K., Yen, S.C., and Cook, E.E., (1994), "Foundation on Strong Sand Underlain by Weak Clay with Geogrid at the Interface", Geotextiles and Geomembranes, 13 : pp. 199-206.
71. Lavania, B.V.K., and Mukherjee, S., (1984), "Dynamic Soil Parameters and Other Studies for Tehri Dam (Part-2)", EQ 84-10, Deptt. of Earthquake Engg., University of Roorkee, Roorkee, India.
72. Lopes, F.R., and Ribeiro, A.T.F., (1985), "Vibration Tests for the Analysis of Machine Foundations", Proc. XI ICSMFE, Sanfrancisco, Vol. 2, pp. 899-902.

73. Luco, J.E., and Westmann, R.A., (1968), "Dynamic Response of a Rigid Footing Bonded to an Elastic Halfspace", *J. App. Mech.*, ASME, 35E, p. 697.
74. Luco, J.E., and Westmann, R.A., (1971), "Dynamic Response of Circular Footings", *J. Engg. Mech. Div.*, ASCE, Vol. 97, EM-5, p. 1381.
75. Lysmer, J., and Richart, F.E.Jr., (1966), "Dynamic Response of Footings to Vertical Loading", ASCE, *J. Soil Mech. and Found. Div.*, Vol. 92, SM-1, pp. 65-91.
76. Lysmer, J., and Kuhlemeyer, R.L., (1969), "Finite Dynamic Model for Infinite Media", ASCE *J. Engg. Mech. Div.*, Vol. 95, EM-4, pp. 859-877.
77. Meek, J. W., and Wolf, J.P., (1994), "Cone Models for Embedded Foundation", *J. Geotech. Engg. Div.*, ASCE, Vol. 120, No. 1, pp. 60-80.
78. Moore, P.J., (1985), "Design of Shallow Foundations : Analysis and Design of Foundations for Vibrations", Editor – Moore, P.J., Oxford & IBH Publishing Co., New Delhi, pp. 267-308.
79. Murray, R.T., Carder, D.R., and Krawczyk, J.V., (1979), "Pull-out Tests on Reinforcements Embedded in Uniformly Graded Sand Subject to Vibration", *Seventh European Conference on Design Parameters in Geotechnical Engineering*, London, Vol. 3, pp. 115-20.
80. Nagendra, M.V., and Sridharan, A., (1981), "Response of Circular Footings to Vertical Vibrations", ASCE *J. Geotech. Engg. Div.*, Vol. 107, GT.7, pp. 989-995.
81. Nagendra, M.V., and Sridharan, A., (1982), "Stiffness Coefficients of Elastic Medium", *J. of Geotechnical Engg. Div.*, ASCE, Vol. 108, No. GT4, pp. 661-668.
82. Navarro, C., (1992), "Vertical Radiation Damping for a Circular Footing Resting on a Simple Layered Half-Space", *Soil Dynamics and Earthquake Engg.*, Vol. 11, pp. 249-253.
83. Nayfeh, A.H., and Serhan, S.J., (1989), "Vertical Vibration of Machine Foundations", *J. of Geotech. Engg.*, ASCE, Vol. 115, No. 1, pp. 56-74.

84. Novak, M., (1970), "Prediction of Footing Vibrations", J. of SMFD, ASCE, Vol. 96, No. SM3, pp. 837-861.
85. Novak, M., and Beredugo, Y.O., (1972), "Vertical Vibration of Embedded Footings", ASCE, Journal of Soil Mechanics and Foundation Division, Vol. 98, SM-12, pp. 1291-1310.
86. Ohsaki, Y., and Iwasaki, R., (1973), "On Dynamic Shear Modulus and Poisson's Ratio of Soil Deposits", Soils and Foundations, 13 (4) : pp. 61-73.
87. Omar, M.T., Das, B.M., Puri, V.K., Yen, S.C., and Cook, E.E., (1994), "Bearing Capacity of Foundation on Geogrid Reinforced Sand", Proc. XIII International Conference on Soil Mechanics and Foundation Engineering, New Delhi, India, pp. 1279-82.
88. Pak, R.Y.S., and Guzina, B.B., (1995), "Dynamic Characterization of Vertically Loaded Foundations on Granular Soils", Journal of Geotechnical Engineering, ASCE, Vol. 121, No. 3, pp. 274-286.
89. Patel, N.M., and Paldas, M., (1983), "Cyclic Load Tests on the Reinforced Foundation Sand Beds", Proc. VIII European Conference on Soil Mechanics and Foundation Engineering, Helsinki, pp. 527-30.
90. Petrovski, J.T., (1975), "Evaluation of Soil Structure-Interaction Parameters from Dynamic Response of Embedded Footings", Proc. 5th European Conf. on Earthquake Engg., Istanbul, Paper No. 43.
91. Poulos, H.G., and Davis, E.H., (1974), "Elastic Solutions for Soil and Rock Mechanics", John Wiley & Sons, Inc., New York, p. 17.
92. Prakash, S., Basavanna, B.M., and Arya, A.S., (1968), "Report on Soil Characteristics for Heavy Duty Forging Hammer Foundation of Hindustan Aeronautics Ltd.", School of Earthquake Engg., University of Roorkee, Roorkee, India.
93. Prakash, S., and Gupta, M.K., (1971), "Report on Dynamic Properties of Soil for Diesel Power House Nakodar", Earthquake Engg. Studies, School of Research and Training in Earthquake Engg., University of Roorkee, Roorkee, India.

94. Prakash, S., and Puri, V.K., (1977), "Critical Evaluation of IS:5249-1969", Indian Geotechnical Journal, Vol. 7, No. 1, pp. 43-56.
95. Prakash, S., Ranjan, G., Saran, S., Ramaswamy, G., and Vijayvargiya, R.C., (1979), "In-Situ Tests for Forge Hammer Foundation Design", International Symp. on In-situ Testing of Soils, Rocks and Performance of Structures, Sarita Prakashan, New Delhi, Vol. 1, pp. 270-276.
96. Prakash, S., and Puri, V.K., (1981), "Dynamic Properties of Soils from In-Situ Tests", J. of Geotechnical Engg. Divn., ASCE, Vol. 107, No. GT7, pp. 943-963.
97. Prakash, S., (1981), "Soil Dynamics", McGraw-Hill Book Co., New York.
98. Prakash, S., and Puri, V.K., (1988), "Foundations for Machines-Analysis and Design", John-Wiley and Sons Inc., New York.
99. Puri, V.K., Chae, J.A., and Das, B.M., (1991), "Cyclic Load Resistance of Vertically Reinforced Sand Subgrades", Proc. II International Conference on Recent Advances in Geotechnical Earthquake Engineering and Soil Dynamics, St. Louis, Missouri, Paper No. 1-47, pp. 125-30.
100. Quinlan, P.M., (1953), "The Elastic Theory of Soil Dynamics", Symposium on Dynamic Testing of Soils, ASTM-STP No. 156, pp. 3-34.
101. Ramaswamy, S.V., and Srinivasan, S.P., (1996), "Viscoelastic Analysis of Reinforced Soil Bed", Indian Geotechnical Conference (IGC-96), Madras, India, Vol. 1, pp. 422-25.
102. Ranjan, G., Saran, S., Kumar, S., and Vijayvargiya, R.C., (1978), "Embedment Effect on Dynamic Response of Footings", VI Symp. on Earthquake Engg., University of Roorkee, Vol. 1, pp. 193-198.
103. Ranjan, G., and Kumar, K., (1989), "Dynamic Elastic Constants for Hydel Power House Site at Rajpura, Punjab", GEP-GR-208, Civil Engg. Deptt., University of Roorkee, Roorkee, India.

104. Ray, P.R., and Woods, R.D., (1988), "Modulus and Damping due to Uniform and Variable Cyclic Loading", *Journal of Geotech. Engg.*, ASCE, Vol. 114, No. 8, pp. 861-76.
105. Reissner, E., (1936), "Stationare Axialsymmetrische durchteine Schuttelnde Masse erregte Schwingcmgen eines homgenen elastische Halbraumes, *Ing.-Archiv*, 7(6), pp. 381-96.
106. Richart, F.E. Jr., and Whitman, R.V., (1967), "Comparison of Footing Vibration Tests with Theory", *ASCE J. Soil Mech. and Found. Div.*, Vol. 93, SM-6, pp. 143-168.
107. Richart, F.E. Jr., Hall, J.R. Jr., and Woods, R.D., (1970), "Vibrations of Soils and Foundations", Prentice-Hall, Inc., Englewood Cliffs, New Jersey.
108. Richart, F.E., Jr., (1977), "Dynamic Stress-Strain Relations for Soils, State-of-the-Art Report, Proc. International Conf. on Soil Mech. and Foundn. Engg., 9th, Tokyo, Vol. 2, pp. 605-612.
109. Richart, F.E., Jr., (1989), "Foundation Dynamics - 1987", *The Art and Science of Geotechnical Engg. at the Dawn of Twenty-First Century*, Prentice-Hall, Inc., Englewood Cliffs, New Jersey.
110. Robertson, I.A., (1966), "Forced Vertical Vibration of a Rigid Circular Disc on a Semi-Infinite Elastic Solid", *Proc. Comb. Phil. Soc.*, 62, p. 547.
111. Saha, S., and Chattopadhyaya, B.C., (1984), "Evaluation of Dynamic Soil Parameters", *Proc. VIII Regional Conference for Africa on Soil Mech. and Foundation Engg.*, Harare, pp. 115-122.
112. Saran, S., and Talwar, D.V., (1978), "Laboratory Investigations of Reinforced Earth Slabs", *Symposium on Engineering -Behaviour of Coarse Grained Soils, Boulder and Rock*, Hyderabad.
113. Saran, S., and Vijayvargiya, R.C., (1979), "Dynamic Behaviour of Embedded Foundation", *International Symp. on In-Situ Testing of Soils and Rocks and Performance of Structures*, U.O.R., Roorkee, India, pp. 336-370.

114. Saran, S., (1990), "Soil Investigations and Recommendations for a Hammer Foundation at B.H.E.L., Haridwar", GEP-SS-303, Civil Engg. Deptt., University of Roorkee, Roorkee, India.
115. Savinov, O.A., (1955), "Machine Foundations", (in Russian), Leningrad.
116. Saxena, Suren, and Alsaïdi, H., (1990), "Seismic Analysis of Geotextile Reinforced Embankment", Proc. Ninth Symposium on Earthquake Engineering (9SEE-90), Roorkee, India, Vol. 1, pp. 5-33-5-40.
117. Seed, H.B., and Idriss, I.M., (1970), "Soil Moduli and Damping Factors for Dynamic Response Analysis", Report No. 70-10, E.E.R.C., Berkley, California.
118. Seed, H.B., Wong, R.T., Idriss, I.M., and Tokimatsu, K., (1986), "Moduli and Damping Factors for Dynamic Analysis of Cohesionless Soils", Journal Geotech. Engg. Divn., ASCE, 112 (GT-11), pp. 1016-32.
119. Shankaran, B., (1991), "Effect of Size and Type of Reinforcement on Bearing Capacity of Reinforced Sand", Proc. IGC-91, pp. 95-99.
120. Shekhter, O. Ya., (1948), "Consideration of Inertial Properties of Soil in the Computations of Vertical Forced Vibrations of Massive Foundations", NII, Symposium 12, Moscow : Vibratratsi Osnoviniy i Fundamentov.
121. Shewbridge, S.E., and Sousa, J.B., (1991), "Dynamic Properties of Reinforced Sand", Journal of Geotechnical Engineering Division, ASCE, Vol. 117, No. 9, pp. 1402-22.
122. Silver, M.L., and Seed, H.B., (1971), "Deformation Characteristics of Sands under Cyclic Loading", J. Soil Mech. and Foundation Division, ASCE, Vol. 97, No. SM8, pp. 1081-1098.
123. Sitharam, T.G., and Raghavendra, H.B., (1995), "Nonlinear Finite Element Analysis of Reinforced Soil Beds", Proc. Indian Geotechnical Conference (IGC-95), Bangalore, India, Vol. 1, pp. 119-22.
124. Sridharan, A., Nagendra, M.V., and Chinnaswamy, C., (1981), "Embedded Foundations under Vertical Vibration", ASCE J. Geotech. Engg. Div., Vol. 107, GT-10, 1429-1434.

125. Sridharan, A., Srinivasa Murthy, B.R., and Singh, H.R., (1988), "Shape and Size Effects of Foundations on Bearing Capacity of Reinforced Soil Beds", Indian Geotechnical Conference, IGC-88, Vol. 1, pp. 205-10.
126. Sridharan, A., Baidya, D.K., and Raju, D.M., (1990a), "Analog Solutions for Design of Machine Foundations", Soils and Foundations, Vol. 30, No. 4, pp. 53-62.
127. Sridharan, A., Gandhi, N.S.V.V.S.J., and Suresh, S., (1990b), "Stiffness Coefficients of Layered Soil Systems", Journal of Geotechnical Engineering, ASCE, Vol. 116, No. 4, pp. 604-624.
128. Srinivasa Murthy, B.R.S., Sridharan, A., and Singh, H.R., (1993), "Analysis of Reinforced Soil Beds", Proc. Indian Geotechnical Journal, Vol. 23(4), pp. 447-58.
129. Stokoe, K.H. II, and Richart, F.E. Jr., (1974), "Dynamic Response of Embedded Machine Foundation", JGED, ASCE, Vol. 100, No. GT4, pp. 427-447.
130. Sung, T.Y., (1953), "Vibrations in Semi-infinite Solids due to Periodic Surface Loading", Symposium on Dynamic Testing of Soils, ASTM-STP, No. 156, pp. 35-68.
131. Talwar, D.V., (1981), "Behaviour of Reinforced Earth in Retaining Structures and Shallow Foundations", Ph.D. Thesis, Deptt. of Civil Engineering, University of Roorkee, Roorkee, India.
132. Taylor, D.W., (1948), "Fundamentals of Soil Mechanics", Asia Publishing House, Bombay.
133. Temel Yetimoglu, Jonathan, T.H. Wu., and Ahmet Saglamer, (1994), "Bearing Capacity of Rectangular Footings on Geogrid-Reinforced Sand", Journal of Geotechnical Engineering Division, ASCE, Vol. 120, No. 12, pp. 2083-99.
134. Terzaghi, K., and Peck, R.B., (1967), "Soil Mechanics in Engineering Practice", John Wiley and Sons, Inc., New York.

135. Triantafyllidis, Th., and Prange, B., (1988), "Rigid Circular Foundation : Dynamic Effect of Coupling to the Half-Space", *Soil Dynamics and Earthquake Engg.*", Vol. 7, No. 1, pp. 40-52.
136. Ulrich, C.M., and Kuhlemeyer, (1973), "Coupled Rocking and Lateral Vibrations of Embedded Footings", *Canadian Geotechnical Journal*, Vol. 10, No. 2, pp. 145-160.
137. Valliappan, S., Favaloro, J.J., and White, W., (1977), "Dynamic Analysis of Embedded Footings", *J. Geotech. Engg. Div., ASCE*, Vol. 103, No. GT-2, pp. 129-133.
138. Veletsos, A.S., and Verbic, B., (1973), "Vibration of Viscoelastic Foundations", *International J. Earthquake Engg., Struct. Div.*, 2, p. 87.
139. Verma, B.P., and Char, A.N.R., (1986), "Bearing Capacity Tests on Reinforced Sand Subgrades", *Journal of Geotechnical Engineering Division, ASCE*, Vol. 112, No. 7, pp. 701-6.
140. Vidal, H., (1966), "La Terre Armee", *Annales de l'Institut Technique du Batiment et des Travaux Publics*, pp. 888-938.
141. Vijayvargiya, R.C., (1980), "Dynamic Behaviour of Embedded Block Foundation", Ph.D. Thesis, University of Roorkee, Roorkee, India.
142. Waas, G., and Lysmer, J., (1972), "Vibrations of Embedded Footings in Layered Media", *Proc. Symp. on Application of FEM in Geotechnical Engg.*, Vicksberg, Miss.
143. Warburton, G.B., (1957), "Forced Vibration of a Body upon on Elastic Stratum", *J. Appl. Mech., Trans. ASME*, 24, pp. 55-58.
144. Wong, H.L., and Luco, J.E., (1985), "Tables of Impedance Functions for Square Foundations on Layered Media", *Soil Dynamics and Earthquake Engg.*, Vol. 4, No. 2, pp. 64-81.
145. Wong, H.L., and Luco, J.E., (1986), "Dynamic Interaction Between Rigid Foundations in a Layered Half-Space", *Soil Dynamics and Earthquake Engg.*, Vol. 5, No. 3, pp. 149-158.

146. Woods, R.D., (1978), "Measurement of Dynamic Soil Properties", Proc. Conf. on Earthquake Engg. and Soil Dynamics, Geotech. Engg. Divn., ASCE Specialty Conference, Pasadena, pp. 91-178.
147. Yoshinori, Nii, (1987), "Experimental Half-Space Dynamic Stiffness", J. of Geotech. Engg. Div., ASCE, Vol. 113, No. 11, pp. 1359-1373.
148. Youssef, Z.T., (1995), "Investigations of Plane-Frame-Footing-Reinforced Soil Interaction", Ph.D. Thesis, Deptt. of Civil Engineering, University of Roorkee, Roorkee, India.